A Lateglacial Plateau Icefield in the Monadhliath Mountains, Scotland: reconstruction, dynamics and palaeoclimatic implications

Clare Mary Boston

A thesis presented for the degree of
Doctor of Philosophy
in Geography
Queen Mary, University of London
April 2012

Abstract

The complex record of glaciogenic landforms and sediments in Britain relating to the last British-Irish Ice Sheet provides the opportunity to reconstruct former ice extents, ice dynamics, retreat patterns and examine their links to climate change. Yet in Scotland, as in the rest of Britain, a previously fragmentary approach to palaeoglaciological research has limited our understanding of glacier dynamics and their relationship to climate, particularly during the Last Glacial-Interglacial Transition.

The Monadhliath Mountains in the Central Scottish Highlands are dominated by an extensive plateau area that has received little research attention in the past. The few examples of research include work by British Geological Survey officers in the early 1900s and J.R. Young in the 1970s. These studies focussed primarily on the geomorphology and sedimentology of isolated valleys and therefore this PhD research provides the first systematic mapping of the region as a whole.

Results of remote and field mapping demonstrate that two coalescent plateau icefields, together covering an area of c. 280 km^2, occurred over the southwest and central sector of the Monadhliath Mountains during the Younger Dryas. Equilibrium line altitudes calculated for the icefield are of comparable magnitude to those reconstructed for nearby Younger Dryas ice masses, such as in Drumochter and Creag Meagaidh, but indicate slightly lower precipitation in the Monadhliath Mountains. ELAs of individual outlet glaciers rise steeply from west to east across the plateau, indicating a strong local precipitation gradient.

Significant variations in the geomorphology on the plateau and within outlet valleys allowed an examination of former thermal regime and differences in ice dynamics during retreat. In-depth analysis of moraine retreat patterns enabled a detailed insight into palaeoglaciological controls on deglaciation for the first time, concluding that valley morphology and gradient were the most influential factors on the retreat dynamics of the plateau icefield.

Acknowledgements

First and foremost, I would like to acknowledge the amazing support and guidance I have received from my primary supervisor Sven Lukas. His expertise, advice and enthusiasm have helped shape this PhD into what it is, but I am also very thankful to Sven for allowing me the freedom to take it in my own direction. I would like to thank him for the many enlightening discussions over the last three years, his help with fieldwork, and reading any written work at an incredible speed. I am also grateful to my second supervisor Simon Carr for his input and support, particularly for reading through the final drafts of this thesis with such a quick turnaround and for reminding me about the 'bigger picture'.

I am indebted to Jon Merritt for lending me BGS aerial photographs and for allowing me to complete a large proportion of the aerial photograph mapping at the BGS in Edinburgh. Thanks also to Andrew Finlayson for looking after me on the occasion that Jon was away. I would also like to thank a number of people for their helpful advice and discussions over the last few years that have in some way contributed to this thesis: Amanda Ferguson, Bethan Davies, Harold Lovell, Stephanie Mills, Danni Pearce, Vicky Brown, Stephen Livingstone, Simon Lewis, Mark Tarplee, Will Hughes, Iestyn Barr, Michelle Daniel, Jon Merritt, Andrew Finlayson, Tom Bradwell, Jez Everest, Dave Evans and David Jarman, to name but a few.

Fieldwork was an integral part of this PhD and I couldn't have done it without the help of a long list of field assistants. A big thank you therefore goes to everyone who helped me with fieldwork over the course of this PhD: Ricky Stevens, Niall Lehane, Amanda Ferguson, Bethan Davies, Alison Boston, Jennifer Lodwick, Adam Wallace, Sam Kent, Matt Frith, Will Hughes, Marcus Hatch, Danni Pearce and Simon Lewis. Your assistance and companionship was invaluable!

I would also like to thank the estate owners in the Monadhliath Mountains for allowing me to undertake fieldwork on their land. In particular, I would like to thank James Willink and the other owners of the Killin Estate for their permission to undertake some coring by Loch Killin, Graham Mabon at the Pitmain Estate for driving me to the top of the Dulnain catchment (and kindly picking me up again at the end of both days!), and Sandy Dey at the Coignafearn Estate for allowing me to drive as far as my car was capable of going along the estate track. I would also like to thank the Glendoe Hydroscheme engineers, particularly Richard Appleby, Angus Speirs and Julius Wallace for their assistance and co-operation in allowing me to undertake fieldwork around Glen Doe and Stronelairg whilst the hydroscheme was still being built. In particular, for giving me a 'tour' of the soon-to-be reservoir and intakes on the Monadhliath

plateau, driving me to the top of Glen Doe, and providing a number of photographs, some of which are displayed in this thesis.

Thanks to Simon Dobinson in the QM lab for providing field equipment and adhering to a number of strange requests over the years such as drainpipes, bags of sand, sinks to wash rocks and copious amounts of extra large sample bags. His ease of dealing with last minute requests made preparing for fieldwork much easier. Thank you also to all the admin and IT staff in the School of Geography for helping this PhD run smoothly.

To the members of Room 104, thanks for making our office such a friendly, yet productive work environment. I will really miss our chats, discussions, moans and attempts not to eat too many biscuits in one go!

This research was funded by a NERC Algorithm Studentship and small grants are gratefully acknowledged from the QRA, RSGS, University of London Central Research Fund, IAS and UKPN towards fieldwork in Scotland, conference attendance and a trip to Svalbard.

Last, but definitely not least, I'd like to thank all my friends and family for their support and encouragement over the last few years. For attempting to understand my PhD, listening to my 'glacial chats' and being there when the going got tough. You've contributed to this PhD more than you think!

For my family
Paul, Mavis and Alison

Contents

Abstract **2**
Acknowledgements **3**
Table of Contents **6**
List of Figures **9**
List of Tables **13**

Chapter 1: Introduction **14**
1.1 Introduction and Rationale 14
1.2 Aims and Objectives 16
1.3 Thesis Structure 16

Chapter 2: The Monadhliath Mountains: Contextual and Conceptual Frameworks **18**
2.1 Study Area 18
2.2 Pre-Quaternary Geology 19
2.3 Previous Quaternary Research in the Monadhliath Mountains 21
2.3.1 Regional overview 21
2.3.2 Ice sheet retreat from the LGM 27
2.3.3 Younger Dryas glaciation in the Monadhliath Mountains 34
2.3.4 Summary of previous Quaternary research in the study area 40
2.4 The Plateau Icefield Landsystem 41
2.4.1 Plateau icefield dynamics 42
2.4.2 Geomorphological signature of plateau icefields 44
2.4.3 Implications of plateau ice on equilibrium line altitudes 46
2.4.4 Synthesis 47
2.5 Chapter Summary 48

Chapter 3: Methods **50**
3.1 Geomorphological Mapping 50
3.1.1 Field mapping 52
3.1.2 DEM-based mapping 53
3.1.3 Aerial photographs 62
3.14 Geomorphological map production 68
3.2 Sedimentology of Glaciogenic Deposits 69
3.2.1 Lithofacies associations 70
3.2.2 Clast morphology 71
3.2.3 Clast macrofabrics 73
3.3 Chapter Summary 74

Chapter 4: Geomorphological and Sedimentary Evidence for Glaciation in the Monadhliath Mountains **76**
4.1 The Western Monadhliath Mountains 78
4.1.1 Glen Shesgnan 78
4.1.2 Glen Chonnal 80
4.1.3 Glen Turret and adjoining areas 82
4.1.4 Glen Buck 86
4.1.5 Culachy Forest 88
4.1.6 Interpretation of the geomorphological evidence in the western Monadhliath Mountains 91
4.2 The Northern Monadhliath Mountains 94
4.2.1 Glen Tarff 94
4.2.2 Glen Doe 96
4.2.3 Glen Brein 97
4.2.4 Carn Easgainn Bàna – Carn Dubh Plateau 99
4.2.5 Glen Killin 103

4.2.6 Interpretation of the geomorphological and sedimentary evidence in the northern Monadhliath Mountains 123
4.2.7 Synthesis of the geomorphological and sedimentary evidence for a former lake in the area around Loch Killin 133
4.3 The Eastern Monadhliath Mountains 135
4.3.1 Upper River Findhorn 135
4.3.2 Upper River Dulnain 140
4.3.3 Glen Mòr 142
4.3.4 Interpretation of the geomorphological and sedimentary evidence in the eastern Monadhliath Mountains 144
4.4 The Southern Monadhliath Mountains 146
4.4.1 Gleann Chaorainn and Gleann Beinne 146
4.4.2 Gleann Fionndrigh 148
4.4.3 Gleann Ballach 150
4.4.4 Gleann Lochain 153
4.4.5 Gleann Madagain 155
4.4.6 Glen Markie 156
4.4.7 Glen Talagain 159
4.4.8 Coire Iain Oig and Glen Gilbre 161
4.4.9 Glen Mhoraire and Glen Luaidhe 163
4.4.10 Coire nan Laogh and Corrie Yairack 164
4.4.11 Interpretation of the geomorphological and sedimentary evidence in the southern Monadhliath Mountains 167
4.5 Summary of the Geomorphological and Sedimentary Evidence within the Monadhliath Mountains 170

Chapter 5: Plateau Icefield Reconstruction 175
5.1 Establishing a Relative Chronology for Glacial Events 175
5.1.1 Morphostratigraphical criteria 176
5.1.2 The relative age of glacial events in the Monadhliath Mountains 179
5.2 Younger Dryas Glacier Reconstruction 182
5.2.1 Glacier profile modelling 183
5.2.2 Younger Dryas glacier reconstruction in the western Monadhliath Mountains 188
5.2.3 Younger Dryas glacier reconstruction in the eastern Monadhliath Mountains 192
5.2.4 Younger Dryas glacier reconstruction in the central Monadhliath Mountains 198
5.2.5 3D reconstruction of the Younger Dryas Monadhliath Icefield 201
5.3 Last Glacial-Interglacial Transition events prior to the Younger Dryas 205
5.4 Younger Dryas Climate in the Monadhliath Mountains 209
5.5.1 Equilibrium line altitude reconstruction 209
5.5.2 Palaeoprecipitation reconstruction 214
5.5.3 Summary 220
5.5 Examination of the Former Dynamics of the Monadhliath Icefield 221
5.5.1 Variations in thermal regime across the Monadhliath Icefield 221
5.5.2 Ice margin retreat patterns 227
5.6 Chapter Summary 241

Chapter 6: Younger Dryas Glaciation in the Monadhliath Mountains and Implications for the Plateau Icefield Landsystem 245
6.1 Timing of Maximum Glacial Extent 247
6.2 Regional Palaeoclimatic Inferences 249
6.3 An Assessment of Modern Analogues for the Monadhliath Icefield 254
6.4 Insights from the Monadhliath Mountains into Plateau Icefield Landsystems 254
6.5 Chapter Summary 262

Chapter 7: Summary and Conclusions **264**
7.1 Production of a Systematic Glacial Geomorphological Map of the Monadhliath Mountains 264
7.2 Identification of a Relative Chronology for Glacial Events in the Monadhliath Mountains 265
7.3 Younger Dryas Plateau Icefield Reconstruction and Palaeoclimatic Implications 268
7.4 Contribution to the Plateau Icefield Landsystem 269
7.5 Future Work 272
7.6 Conclusion 274

References **275**

Appendix I **Sleeve on back cover**
A Map of Place Names in the Study Area

Appendix II **Sleeve on back cover**
The Glacial Geomorphology of the Monadhliath Mountains

List of Figures

Chapter 2

Fig. 2.1. Topographic map of the Central Scottish Highlands and the study area……. 19
Fig. 2.2. Generalised map of the geology of the Monadhliath Mountains and vicinity…. 20
Fig. 2.3. NGRIP $\delta^{18}O$ curve between 17 and 10 ka (Rasmussen *et al.*, 2006; Ballantyne & Stone, 2011)……. 22
Fig. 2.4. Approximate locations of previous major studies in the Monadhliath Mountains…… 22
Fig. 2.5. Reconstructed configuration of the British and Irish ice sheets during deglaciation from 16 ka to 15 ka BP (Clark *et al*., 2010)……..... 24
Fig. 2.6. Reconstruction of the configuration of the Western Cairngorm Ice Cap and Strathspey Glacier between 16.6 and 13.6 ka BP (Everest & Kubik, 2006)…… 24
Fig. 2.7. Younger Dryas ice masses in Scotland (Sissons, 1979d; Golledge *et al*., 2008). 26
Fig. 2.8. Modelled Younger Dryas ice extent in the Monadhliath Mountains (Golledge *et al*., 2008)……. 27
Fig. 2.9. Ice-dammed lakes and corresponding ice margin positions in the Monadhliath Mountains (Charlesworth, 1955)……. 29
Fig. 2.10. Geological map of Raitts Burn, Strathspey (Phillips & Auton, 2000)……..... 31
Fig. 2.11. Glacial and glaciofluvial landforms within Glen Banchor and the area around Raitts Burn (Young, 1978)……. 32
Fig. 2.12. Sequence of glacial advance into Glen Roy and Glen Spean (Palmer *et al*., 2010)……. 36
Fig. 2.13. Approximate limits of a Younger Dryas ice cap to the northeast of Glen Turret (Johnson-Ferguson, 2004; Benn & Evans, 2008)…… 39
Fig. 2.14. The relationship between summit breadth and height above the firn line for viable plateau icefield development (Manley, 1955; Rea *et al*., 1998)…… 43
Fig. 2.15. Schematic diagram of a plateau icefield landsystem (Rea & Evans, 2003)……. 44
Fig. 2.16. Altitudinal shifts in ELA as a function of the percentage of plateau area to total combined area (Rea & Evans, 2003)……..... 47

Chapter 3

Fig. 3.1. Digitised versions of two geomorphological maps drawn in the field for Coire Easgainn and Glen Odhar……..……... 54
Fig. 3.2. Example of the ORI, DSM and DTM products from the NEXTMap dataset…. 55
Fig. 3.3. Relief-shaded models from the NEXTMap DSM for Corrie Yairack using azimuths of 45° and 315°…… 57
Fig. 3.4. Geometric artefacts associated with IFSAR data acquisition (Clark, 1997)…… 58
Fig. 3.5. ORI and DSM NEXTMap products of Loch Dubh demonstrating the lost of data due to the effects of shadow, foreshortening and layover…… 59
Fig. 3.6. Examples of mapping produced in ESRI ArcGIS using relief-shaded models created from the NEXTMap DSM……... 61
Fig. 3.7. Illustration of the effect of relief displacement (Lillesand *et al*., 2008)…….. 63
Fig. 3.8. Hand-drawn aerial photograph overlays of geomorphological features in Coire Easgainn and Gleann Fionndrigh……. 64
Fig. 3.9. An example of the georectification process in Erdas Imagine…… 67
Fig. 3.10. Flowchart to summarise the approaches and processes involved in geomorphological map production……. 69
Fig. 3.11. Lithofacies codes used in this research (Evans & Benn, 2004)…….. 71

Chapter 4

Fig. 4.1. Map showing the division of the study area into the western, northern, eastern and southern sectors……... 76
Fig. 4.2. Legend for geomorphological maps found throughout Chapter 4……. 77
Fig. 4.3. The geomorphology of Glen Shesgnan…….. 79

Fig. 4.4. Photograph showing ridges on the western side of Coire Shesgnan and an area of deep stream incision in the valley bottom……..... 80
Fig. 4.5. The geomorphology of Glen Chonnal…….. 81
Fig. 4.6. The geomorphology of Glen Turret and Coire an t-Sìdhean……. 82
Fig. 4.7. Photographs showing mounds and ridges, terraces and fans within Glen Turret……..... 83
Fig. 4.8. The geomorphology of upper Glen Buck……..... 86
Fig. 4.9. Photograph showing closely spaced mounds and ridges in Coire Larach…..... 87
Fig. 4.10. The geomorphology of the Culachy Forest area……..... 89
Fig. 4.11. Photographs showing conical mounds and ridges in Glen Lagan a' Bhainne… 90
Fig. 4.12. The geomorphology of the upper Tarff catchment…… 94
Fig. 4.13. Photograph showing talus slopes, high-level terraces and river terraces in Glen Tarff…….. 95
Fig. 4.14. The geomorphology of the upper part of Glen Doe…….. 96
Fig. 4.15. The geomorphology of the upper part of Glen Brein…… 97
Fig. 4.16. Photographs showing a prominent ridge at the entrance to Glen Brein and small mounds on the eastern valley side of Glen Brein…… 98
Fig. 4.17. The geomorphology of the area around the Carn Easgann Bàna – Carn Dubh plateau…….. 100
Fig. 4.18. Photographs showing ridges and channels in Coire Dubh Cùil na Creige and exposed bedrock on the valley floor……. 100
Fig. 4.19. Photographs showing ridges and channels in Coire Easgainn……. 102
Fig. 4.20. Clast shape and roundness data from Section AE1, Coire Easgainn…… 102
Fig. 4.21. The geomorphology of the area around Loch Killin…… 104
Fig. 4.22. Section sketch and annotated photographs of the principle units found within Section LK1, Glen Killin…….. 106
Fig. 4.23. Clast shape and roundness data for sample LK1, Section LK1, Glen Killin… 108
Fig. 4.24. Sketch of the principle units found within sections LK2a and LK2b, Glen Killin…….. 109
Fig. 4.25. Clast shape and roundness data for sample LK2, Section LK2b, Glen Killin... 111
Fig. 4.26. Lower hemisphere equal area stereonets and a ternary plot for a-axis and a/b plane clast macrofabrics from LFA 5, Section LK2b, Glen Killin…… 112
Fig. 4.27. Photographs showing an accumulation of sediment on the valley sides at the head of Glen Killin…… 113
Fig. 4.28. Photographs of a ridge at Stronelairg…… 114
Fig. 4.29. Section sketches of a ridge at Stronelairg…….. 115
Fig, 4.30. Clast shape and roundness data for samples STL1, STL2 and STL3 taken from the Stronelairg ridge……. 116
Fig. 4.31. Photographs of high-level terraces within Glen Odhar……. 117
Fig. 4.32. Annotated photograph of Section LKO2, Glen Odhar……. 118
Fig. 4.33. Annotated photograph of Section LKO3, Glen Odhar…… 119
Fig. 4.34. Photographs taken by Glendoe Hydroscheme engineers of excavations into a flat-topped hill on the plateau to the south of Glen Eich……..... 121
Fig. 4.35. Clast shape and roundness data for samples AE1, LK1, LK2, STL1, STL2 and STL3, alongside fluvial and rockfall control samples…… 125
Fig. 4.36. Co-variance plots showing the C_{40} index against the RA and RWR indices for clast shape and roundness samples…….. 125
Fig. 4.37. Fabric shape triangles with genetic envelopes for a-axis and a/b plane clast fabric measurements from LFA 5, Section LK2b……. 132
Fig. 4.38. Idealised model to show the advance of an ice lobe from the Ness basin into the Fechlin-Killin valley that created Glacial Lake Killin…… 134
Fig. 4.39. The geomorphology of the upper part of the Findhorn catchment…….. 136
Fig. 4.40. Photograph of ridges and mounds in the Findhorn Valley, south of Dalbeg…. 137
Fig. 4.41. The geomorphology of the plateau between Glen Markie, Glen Eskin and Glen Abhainn Crò Chlach…… 139
Fig. 4.42. The geomorphology of the upper Dulnain catchment…….. 141

Fig. 4.43. Photograph showing a large accumulation of sediment in the form of mounds and ridges in the upper part of the Dulnain catchment…….. 141
Fig. 4.44. The geomorphology of Glen Mòr…….. 142
Fig. 4.45. Annotated photograph showing a section within a terrace in Glen Mòr…… 143
Fig. 4.46. The geomorphology of Gleann Chaorainn and Gleann Beinne……. 147
Fig. 4.47. Photograph showing low relief ridges in Gleann Chaorainn…….. 148
Fig. 4.48. The geomorphology of Gleann Fionndrigh…… 149
Fig. 4.49. Photographs showing the geomorphology of Gleann Fionndrigh…….. 150
Fig. 4.50. The geomorphology of Gleann Ballach and Gleann Lochain…… 151
Fig. 4.51. Photographs showing a large ridge and a number of smaller ridges in Gleann Ballach, alongside extensive talus slopes…… 152
Fig. 4.52. Photograph of mounds and ridges within Gleann Lochain……. 154
Fig. 4.53. The geomorphology of Gleann Madagain…….. 155
Fig. 4.54. The geomorphology of Glen Markie…….. 157
Fig. 4.55. Photograph of ridges within Coire nam Beith……. 159
Fig. 4.56. The geomorphology of Glen Talagain…… 160
Fig. 4.57. The geomorphology of Coire Iain Oig and Glen Gilbre……. 162
Fig. 4.58. Mounds and ridges in the lower part of Glen Gilbe near the confluence with Coire Iain Oig…….. 163
Fig. 4.59. The geomorphology of Glen Mhoraire and Glen Luaidhe…….. 163
Fig. 4.60. The geomorphology of Coire nan Laogh and Corrie Yairack…… 165
Fig. 4.61. Photographs showing ridges and mounds within Corrie Yairack……... 166
Fig. 4.62. Idealised model to show the damming of drainage by regional ice in the Spey Valley, which created a lake in each of the Glen Banchor tributary valleys.….. 169
Fig. 4.63. Example locations in the study area where there is clear geomorphological evidence for the existence of a plateau icefield……... 171

Chapter 5

Fig. 5.1. Example output graph from the Benn and Hulton (2010) model…… 184
Fig. 5.2. Mathematical symbols used to define glacier surface profiles (Ng *et al*., 2010)…… 186
Fig. 5.3. Scatter plot of glacier relief (*H*) against *C** and glacier length…….. 188
Fig. 5.4. Younger Dryas glacier limits, western sector of the Monadhliath Mountains… 189
Fig. 5.5. Younger Dryas glacier limits, eastern sector of the Monadhliath Mountains…. 194
Fig. 5.6. Younger Dryas glacier limits, central sector of the Monadhliath Mountains…. 199
Fig. 5.7. Overlain minimum, average and maximum icefield reconstructions……. 203
Fig. 5.8. Reconstructed ‘average’ Younger Dryas Monadhliath Icefield……. 204
Fig. 5.9. Major outlet glaciers of the Monadhliath Icefield classed according to their ELA in groups of 50 m intervals…… 214
Fig. 5.10. Outlet glaciers of the Monadhliath Icefield, classed according to their thermal regime……. 226
Fig. 5.11. Illustration of the approach used to link chains of moraines together…… 227
Fig. 5.12. Former ice margin positions of outlet glaciers in the Monadhliath Mountains that produced recessional moraines……..... 229
Fig. 5.13. Styles of moraine crestline bifurcation found in the study area…… 230
Fig. 5.14. ‘Barcodes’ showing the distance between recessional moraines in sixteen outlet valleys in the Monadhliath Mountains…….. 231
Fig. 5.15. Ice margin positions during retreat overlain onto slope angles…….. 233
Fig. 5.16. The effect of bed slope on the horizontal distance moved by the ELA for the same vertical change…… 233
Fig. 5.17. Graphs to illustrate the effect of % plateau area, glacier area, glacier length and glacier aspect on the initial retreat type…… 234
Fig. 5.18. ‘Barcodes’ for each outlet glacier overlain onto the bed topography along the central flowline of each respective outlet glacier…….. 235
Fig. 5.19. Normalised hypsometric curves for the outlet glaciers at their maximum extents…….. 237

Fig. 5.20. Reconstructed outlet glaciers at their final retreat stage…… 238
Fig. 5.21. Graphs demonstrating the influence of glacier length and % plateau area change in ELA during retreat…… 240

Chapter 6

Fig. 6.1. Comparison between the Monadhliath Icefield reconstruction and predicted Younger Dryas ice extent by Golledge *et al*. (2008)…… 245
Fig. 6.2 Comparison of different precipitation-temperature relationships for Scottish Younger Dryas sites (Golledge *et al.*, 2010)…… 251
Fig. 6.3. Conceptual diagram of a polythermal plateau icefield landsystem…..…… 255
Fig. 6.4. Illustrative diagram showing ELA fluctuations over a number of years…….. 260

Appendix I

A Map of Place Names in the Study Area Sleeve on back cover

Appendix II

The Glacial Geomorphology of the Monadhliath Mountains Sleeve on back cover

List of Tables

Chapter 3

Table 3.1. A) Pixel size and horizontal accuracy for the NEXTMap ORI product. B) Spatial resolution and vertical errors for the DSM and DTM NEXTMap products……. 55

Table 3.2. RMSEs for the five geometric models tested to examine their suitability for georectifying the aerial photography overlays…….. 68

Table 3.3. Descriptive criteria used to define clast roundness in this study (Benn, 2004a)…… 73

Chapter 5

Table 5.1. Criteria used to define the limits of Younger Dryas outlet glaciers in the Monadhliath Mountains……. 180

Table 5.2. Ice thickness at major ice divides in the western sector, modelled using the Benn and Hulton (2010) and Ng *et al*. (2010) glacier surface profiles…….. 193

Table 5.3. Ice thickness at major ice divides in the eastern sector, modelled using the Benn and Hulton (2010) and Ng *et al*. (2010) glacier surface profiles……. 197

Table 5.4. Ice thickness at major ice divides in the central sector, modelled using the Benn and Hulton (2010) and Ng *et al*. (2010) glacier surface profiles…… 200

Table 5.5. Equilibrium line altitudes for the Monadhliath Icefield and major outlet glaciers……. 213

Table 5.6. Palaeoprecipitation values for the Monadhliath Icefield and major outlet glaciers at the ELA and sea level…….. 219

Table 5.7. Comparison between the AABR 1.9 ELAs for the average icefield at its maximum extent and the ELAs for retreated outlet glaciers…… 239

Chapter 6

Table 6.1. Comparison between Younger Dryas palaeoprecipitation and modern precipitation values for the Monadhliath Mountains and other sites in Scotland…….. 250

Table 6.2. Modern and Younger Dryas precipitation data in the eastern, central and western sectors of the Monadhliath Mountains…….. 252

Chapter 1
Introduction

1.1 Introduction and Rationale

In Britain, a complex record of Quaternary subglacial and ice-marginal landforms and sediments provides an excellent opportunity to reconstruct former ice flow patterns, basal thermal regime and associated flow dynamics. Palaeoglaciological reconstructions of the Laurentide and Scandinavian ice sheets, and the dating of these ice flow events, illustrate the potential use of the geomorphological and sedimentary record for enhancing our understanding of ice dynamics and North Atlantic environmental change (e.g. Hiscott *et al*., 2001). However, a previously fragmentary approach to research in Britain has resulted in large variations in its quality and density and has hindered the development of British-Irish Ice Sheet (BIIS) reconstructions (e.g. Boulton *et al*. 1977, 1985; Evans *et al*., 2005; Clark *et al*., 2010).

This is particularly true in Scotland where our understanding of the pattern of glacier fluctuations during and after ice sheet deglaciation is still limited in a number of areas. This region contains former ice accumulation and dispersal centres within which key evidence for constraining and understanding the extent, timing and dynamics of past glaciations is manifest in the geomorphological and sedimentary record. However, as in the rest of Britain, systematic research on regional landsystem variations is limited and as a result our understanding of the relationship of glacier fluctuations and dynamics to climatic reconstructions remains incomplete (Benn & Lukas, 2006).

In particular, events relating to the Last Glacial-Interglacial Transition (LGIT) and the Loch Lomond Stadial are poorly constrained due to this unsystematic approach, alongside a lack of suitable dating material. The Loch Lomond Stadial is equivalent to the Younger Dryas Stadial in Scandinavia and Greenland Stadial-1 (GS-1), as recorded in Greenland ice cores, which occurred between 12.9 and 11.7 ka b2k (before 2000; Rasmussen *et al.*, 2006; Lowe *et al*., 2008). The Younger Dryas is particularly important as it was a period of rapid climate change at decadal and centennial time scales (Anderson, 1997; Tarasov & Peltier, 2005; Lukas, 2011) and was the last time in Britain in which glaciers existed. As a result, the geomorphological and sedimentological record from this period is very well preserved (Lukas & Benn, 2006) and can therefore provide key evidence about glacier dynamics and their links to climate change. However, at present there are still large areas in Scotland that have not been investigated in detail and of which very little is known about the palaeoglaciology, making regional comparisons of glacier dynamics and palaeoclimate difficult.

The Monadhliath Mountains in the Central Scottish Highlands is one such area which has received very little research attention in the last 100 years. For the majority of the region, previous research is mostly limited to mapping by British Geological Survey (BGS) officers at the beginning of the 20th Century and by J.R. Young in the 1970s, both of which focused on the southern and eastern areas only. The only extensive body of research deals with the southwest corner around the area of Glen Roy (e.g. Sissons, 1978, 1979a; Sissons & Cornish, 1983; Peacock, 1986; Lowe & Cairns, 1991; Fabel *et al*., 2010; Palmer *et al*., 2010, 2012). Since no systematic mapping has ever been undertaken across the region as a whole, current understanding of ice mass fluctuations and dynamics in the area is very inconsistent and confined to major valley systems around the perimeter. A need for a re-investigation of the geomorphological evidence is exemplified by recent work in other areas of Scotland (e.g. Lukas, 2005a; Finlayson, 2006; Golledge, 2006, 2010; Bradwell *et al*., 2007, 2008; Lukas & Bradwell, 2010; Finlayson *et al*., 2011), which have instigated drastic re-interpretations of the field evidence, in part due to the fragmentary and inconsistent nature of previous research, but also necessitated by advances in glaciological knowledge during the last 30 years. In addition, whilst it is traditionally believed that ice masses did not build up in the Monadhliath Mountains during the Younger Dryas, recent modelling suggests that the central plateau area of the Monadhliath Mountains was sufficiently high and wide enough to support glaciation during this time (Hubbard, 1999; Golledge *et al*., 2008), therefore also advocating a need for a re-examination of the field evidence.

Since the Monadhliath Mountains consist of an upland area of dissected plateau, this also provides the opportunity to examine the role and dynamics of plateau ice in the region. Plateau icefields form important ice dispersal centres both at present and during glacial periods (Evans, 2010). Research on modern plateau icefields has demonstrated that they are able to sustain valley glaciers in their surrounding outlet valleys below the regional equilibrium line altitude, due to ice avalanching and redistribution of snow, a characteristic that has important implications for palaeoclimate and glacier mass-balance reconstructions (Rea *et al*., 1999). Their identification in the palaeoglaciological record is, however, problematic since plateau ice is often cold-based, leaving very little evidence for its existence following deglaciation (Rea & Evans, 2003). Despite large advances in our knowledge and understanding of plateau icefields since the 1980s, few studies have recognised plateau icefields in the palaeoglacial record (Dyke, 1993; McDougall, 2001; Vieira, 2008). As a result, limited research has been undertaken on plateau icefield dynamics during retreat, with respect to changes in thermal regime, ice-divide migration and the interaction between plateau icefields and ice sheets during the transition from regional to local glaciation. A detailed examination of the palaeoglacial record within the

Monadhliath Mountains therefore provides the opportunity to examine such plateau icefield dynamics.

1.2 Aims and Objectives

Against the background of extremely limited field data from the Monadhliath Mountains and the recent glaciological advances in our understanding of plateau icefields, the following aims and objectives for the research were identified.

There are two interlinked aims of this research. Firstly, to produce a systematic, regional geomorphological inventory of the palaeoglaciological record of the Monadhliath Mountains that can be used to construct a more robust relative chronology for glacial events in the region, which is currently lacking. Secondly, to reconstruct prominent ice-masses in the region that can be used to assess former regional climate patterns and to examine glacier dynamics particularly with respect to the plateau icefield landsystem. Specific objectives of this research are listed below:

Objective 1: To assess the evidence for ice masses of varying character in the Monadhliath Mountains during the LGIT.

Objective 2: To establish a chronology for glacial events during the LGIT.

Objective 3: To reconstruct the maximum extent, thickness and style of any prominent phases of glaciation in the study area.

Objective 4: To reconstruct palaeo-equilibrium line altitudes (ELAs) of the reconstructed ice mass(es), establish an estimate for palaeoclimate for the study area and examine its relationship to other contemporaneous ice masses in Scotland.

Objective 5: To examine the dynamics of the reconstructed ice mass(es) with particular focus on glacier dynamics during retreat within a plateau icefield landsystem.

1.3 Thesis Structure

The thesis is divided into seven chapters. This chapter has introduced the key conceptual frameworks and current knowledge gaps associated with the research. Chapter 2 examines the conceptual frameworks in further detail with respect to our current understanding of LGIT glacier fluctuations in the study area and the plateau icefield landsystem. Chapter 3 describes the key methods that were used to undertake geomorphological mapping and sedimentological

analysis in the study area. Chapter 4 is divided into four sections and describes the geomorphological and sedimentary evidence for the western, northern, eastern and southern parts of the study area, with an initial interpretation of this evidence at the end of each section. Chapter 5 is the main interpretation chapter and addresses the approach used to identify a relative chronology for glacial events in the region during the LGIT, introducing a more detailed and spatially coherent chronology, deals with the reconstruction of a plateau icefield during a renewed phase of glaciation and its associated ELA and palaeoprecipitation calculations, and examines plateau icefield dynamics during retreat. Chapter 6 discusses the results of Chapter 5 within the wider context, considering the implications of the research on the timing of glaciation and palaeoclimate during the Younger Dryas and how the research has contributed to our understanding of plateau icefield landsystems. The research is summarised within Chapter 7, which includes avenues for future research.

Chapter 2

The Monadhliath Mountains: Contextual and Conceptual Frameworks

The aim of this chapter is to describe the context for the study area in terms of its physical location, topography, pre-Quaternary geology, and the current state of our understanding of glacier fluctuations in the region during the LGIT and the plateau icefield landsystem. The latter two sections (Sections 2.3 and 2.4) also elaborate on and exemplify key concepts identified within Chapter 1, including: 1) the need for a systematic approach to geomorphological mapping following a previously fragmentary approach to research that has hindered regional simulations of glacier fluctuations and retreat patterns 2) the need for a re-investigation of the field evidence following major shifts in our understanding of ice sheet and plateau icefield dynamics; 3) the need for greater constraint on chronology within the palaeoglacial record; 4) the need for a greater understanding of plateau icefield dynamics during retreat and their interaction with regional ice during this time.

2.1 Study Area

The Monadhliath Mountains comprise of an upland area of plateau in the Central Highlands of Scotland, which is bounded to the north by the Great Glen and to the south by Strathspey. The region is located immediately to the northwest of the Cairngorm Mountains, to the north of Creag Meagaidh and to the northeast of the Ben Nevis Range (Fig. 2.1). Figure 2.1 also indicates the area of the region included in this research, which covers approximately 840 km^2. Beyond initial reconnaissance mapping, the research focussed on the area to the west of easting NH 76 and did not include the areas of Strathnairn and Stratherrick to the north of northing NH 18. However, high ground to the north of Glen Roy, in the west, coalesces with the main Monadhliath plateau area around Corrie Yairack and Glen Tarff and was therefore included in the study. A map with all place names used in this thesis can be found in Appendix I.

The plateau consists of rounded summits and is dissected by at least twenty-five main catchments. The area slopes downwards to the north and therefore the altitude of the plateau ranges from 900 m in the south, with individual summits as high as 945 m (Carn Dearg, NH 636 024), to 600 m in the north. As a result, the main watershed runs from west to east across the southern edge of the plateau, and this asymmetry is manifest in short, steep catchments on the south side of the plateau, with the majority of the plateau draining northwards or eastwards within large catchment areas. Valleys draining the plateau to the south tend to have steep backwalls separating the valley floor from the plateau above whilst catchments in the north gently rise onto the plateau, often with no backwall.

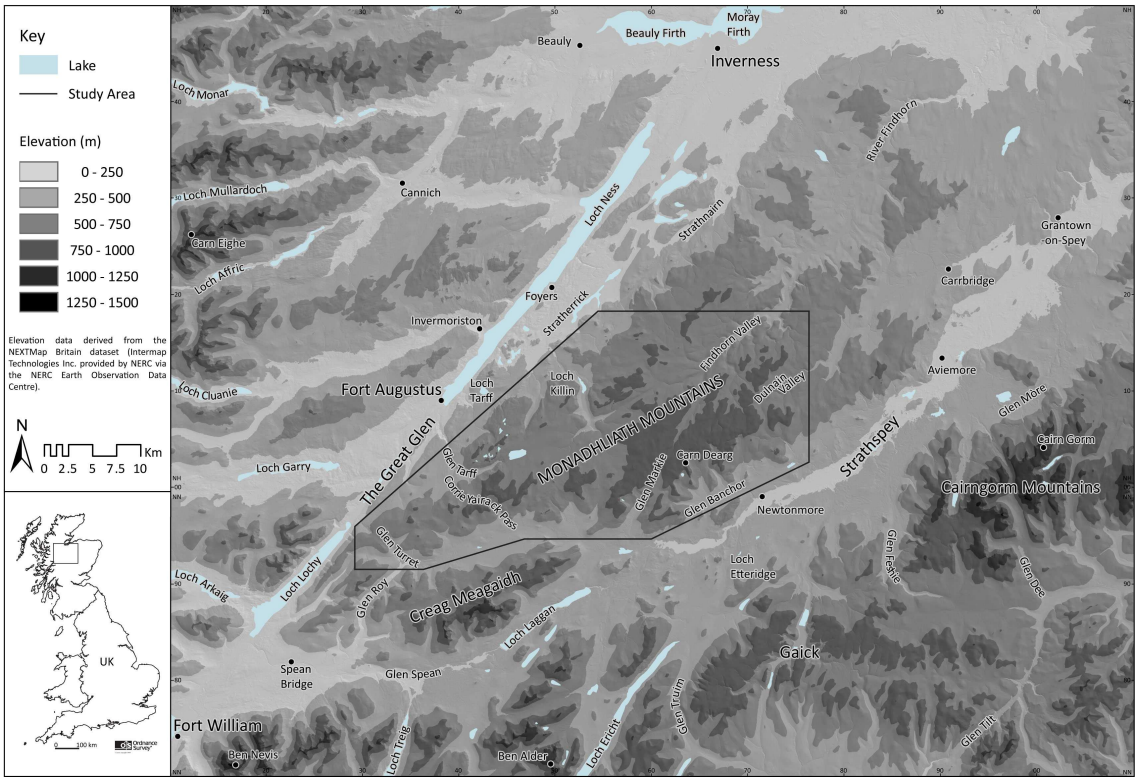

Figure 2.1. Topographic map to show the location of the Monadhliath Mountains in Scotland, within which the study area is outlined by a black box. Elevation data was derived from the NEXTMap Great Britain DTM and overlain on a hillshade model, also derived from NEXTMap (Intermap Technologies Inc. provided by NERC via the NERC Earth Observation Data Centre). UK Outline from Ordnance Survey © Crown copyright 2010.

2.2 Pre-Quaternary Geology

The Monadhliath Mountains are broadly situated between the Great Glen Fault to the north and the Highland Boundary Fault to the south and form part of the Grampian Highlands geological terrane. This region is dominated by the metamorphic Dalradian Supergroup and igneous rocks from the Caledonian Igneous Supersuite (Stephenson & Gould, 1995). The Monadhliath Mountains specifically (Fig. 2.2), are primarily underlain by various Late Precambrian psammites and semipelites belonging to the Grampian Group, within which the study area is dominated by the two oldest subgroups, the Glenshirra and Corrieyairack successions. Pelitic to semipelitic schists from the younger Appin Group are also exposed in Glen Roy (Phillips & Key, 1992) and the older Pre-Dalradian Central Highland Migmatite Complex outcrops to the north of Newtonmore and Kincraig, termed the Glen Banchor succession (Robertson & Smith, 1999; Smith *et al*., 1999; Strachan *et al*., 2002). This succession is composed predominantly of banded psammite, micaceous psammite and subordinate semi-pelite. Igneous intrusions of granite, microdiorite and granodiorite of predominately Silurian age also occur in the region, forming the Corrieyairack, Allt Crom and Findhorn plutons, as well as the Monadhliath Pluton, which occurs to the northeast of the study area and is not shown in Figure 2.2 (Stephenson & Gould, 1995).

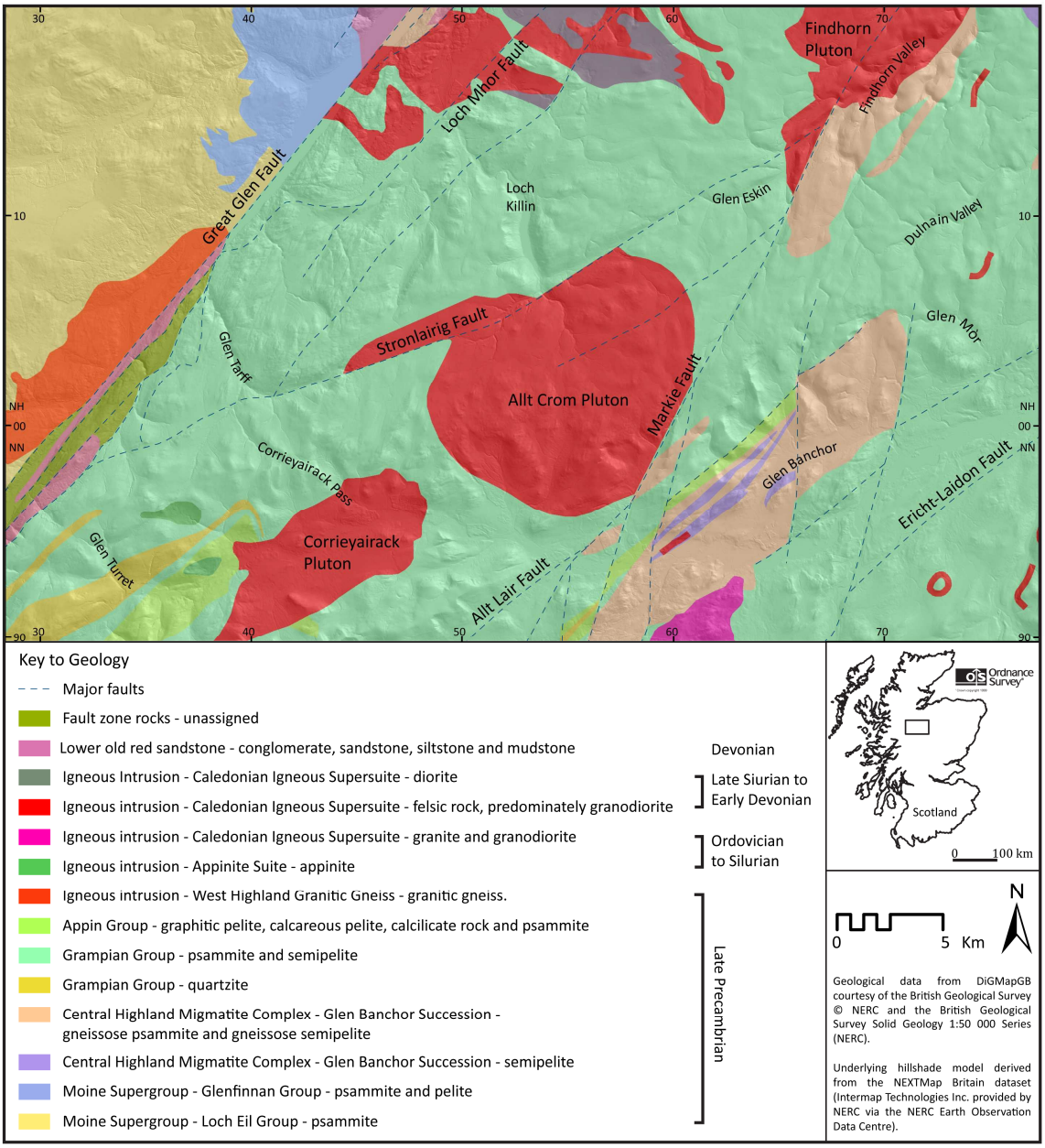

Figure 2.2. Generalised geology map of the Monadhliath Mountains and immediate vicinity. The key is arranged in stratigraphical order, although the precise stratigraphical position of the Central Highland Migmatite Complex and Moine Supergroup are unknown at present. Geological data from DigMapGB courtesy of the British Geological Survey © NERC and the British Geological Survey solid Geology 1: 50 000 Series (NERC). Underlying hillshade model derived from NEXTMap (Intermap Technologies Inc. provided by NERC via the NERC Earth Observation Data Centre). UK Outline from Ordnance Survey © Crown copyright 2010.

The parent sediments (protoliths) of these groups were deposited in shallow marine environments, where the Grampian Group protoliths were formed mainly from sandy shallow-marine shelf deposits during basin filling (Stephenson & Gould, 1995; Strachan *et al*., 2002). Isotopic evidence suggests that the Glen Banchor succession was migmatised by a tectonothermal event during the early Neoproterozoic at around 840-800 Ma (Highton *et al*., 1999; Strachan *et al*., 2002), whilst the low to medium-grade metamorphism within the Grampian Group appears to have occurred during the Caledonian (Robertson & Smith, 1999;

Smith *et al*., 1999; Strachan *et al*., 2002). The granitic intrusions that formed the Corrieyairack, Allt Crom and Findhorn plutons and other minor intrusions were emplaced after this tectonic activity (Stephenson & Gould, 1995).

Structurally, the Monadhliath Mountains are composed of a series of major folds that have been formed through three to four deformation events (Haselock *et al*., 1982; Haselock & Leslie, 1992; Stephenson & Gould, 1995). A number of major structural features occur, including the Geal Charn Ossain Steep Belt, the Eilrig Shear Zone, the Grampian Slide (Phillips *et al*., 1993; Strachan, 2002) and the Gairbeinn Slide, which separates the Glenshirra and Corrieyairack subgroups (Haselock *et al.*, 1982). The age of the slides is currently undetermined since there are problems in placing the occurrence of the slides within a time frame of between 750 Ma at the base of the Grampian Group and the peak of metamorphism at around 490 Ma, although the Eilrig Shear Zone is suggested to have occurred during the Caledonian Orogeny (Stephenson & Gould, 1995). Prominent faults in the region include the Markie and Stronlairg faults, which trend W-E and SW-NE respectively and converge in the upper part of the Findhorn Valley (Haselock *et al.*, 1982). These faults form two of the major valleys that dissect the Monadhliath plateau area and are most likely to have developed towards the end of the Caledonian Orogeny (Stephenson & Gould, 1995). Very little geological activity has occurred in the region since the Caledonian, forming a major hiatus between this time and the Quaternary, which is described below.

2.3 Previous Quaternary Research in the Monadhliath Mountains

This section summarises previous research in the Monadhliath Mountains and surrounding area relating to the LGIT. The section will identify the key research findings that are relevant to this PhD research and aims to inform the reader of the current understanding of LGIT glacier fluctuations and dynamics in the region. The review is written in the context of the chronological framework identified from the Greenland ice-core record (Fig. 2.3) (Rasmussen *et al*., 2006; Lowe *et al*., 2008), and, based on available absolute dates, attempts to provide some chronology for events in the region, despite the majority of previous studies lacking clear chronological constraints. The approximate areas covered by previous research are shown in Figure 2.4, which highlights the fragmentary nature of current knowledge in the Monadhliath Mountains.

2.3.1 Regional overview

Very little is currently known about ice sheet dynamics in the Monadhliath Mountains during the Last Glacial Maximum (LGM). NEXTMap DEMs show a clear contrast between ice-moulded bedrock on the southern summits of the Monadhliath massif, interpreted by Hughes *et*

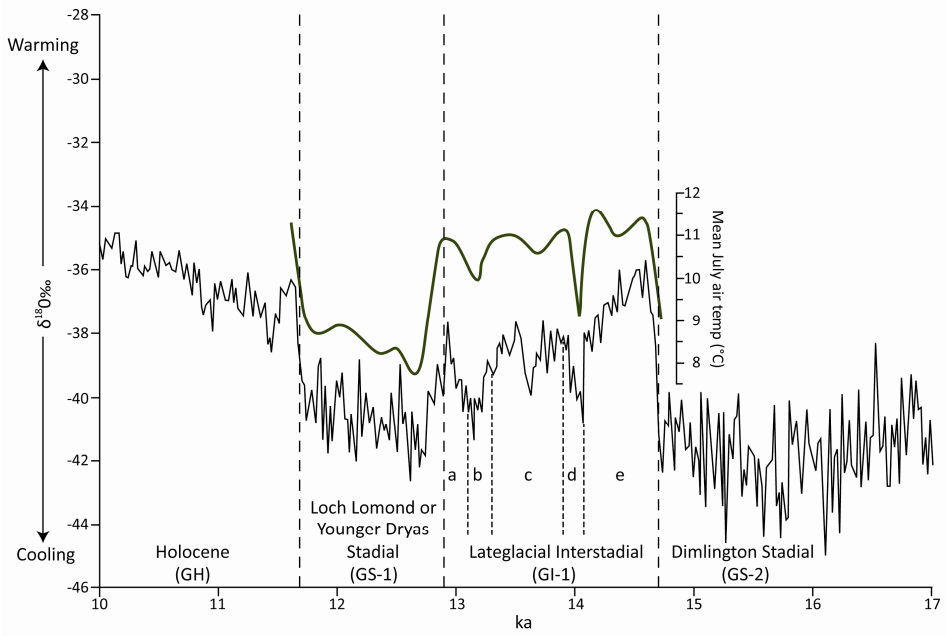

Figure 2.3. NGRIP $\delta^{18}O$ curve between 17 and 10 ka (Rasmussen *et al*., 2006), showing the ice core stages proposed by Lowe *et al*. (2008) and estimated mean July temperatures from chironomid assemblages in SE Scotland in green (Brooks & Birks, 2000), which were visually matched to the NGRIP ice core data by Ballantyne and Stone (2011). Figure adapted from Ballantyne and Stone (2011).

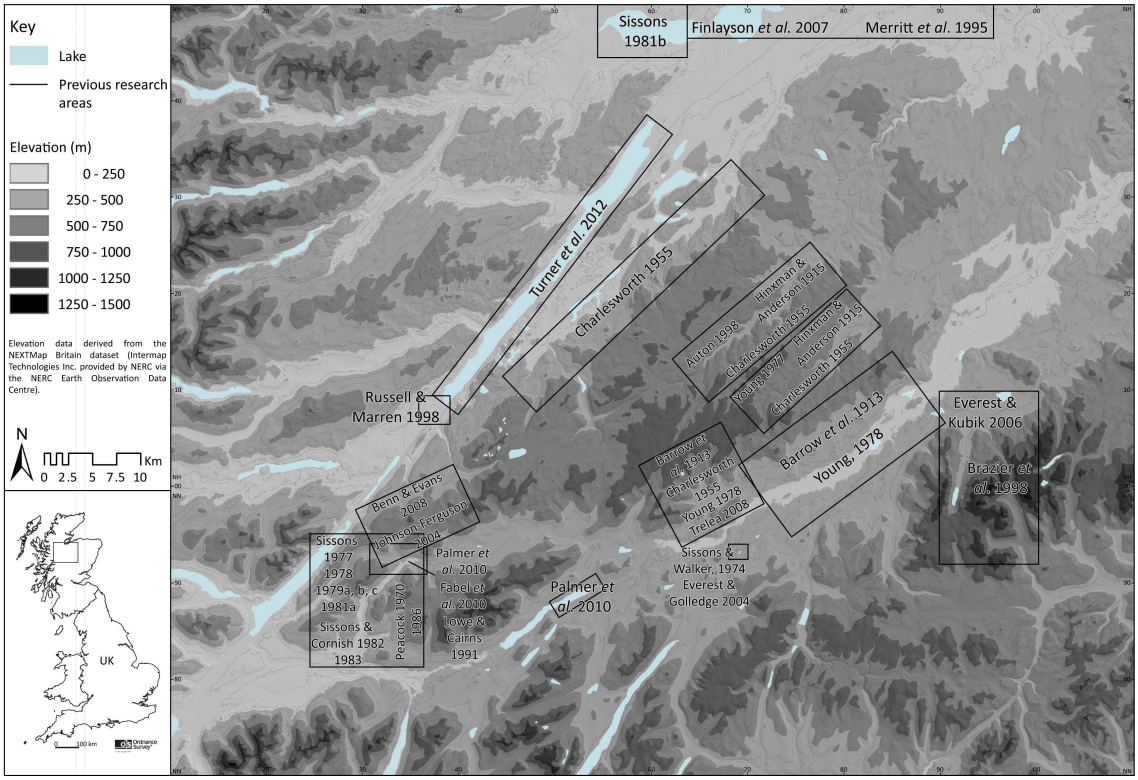

Figure 2.4. Topographic map of the study area showing the approximate location, and area of coverage, of major studies that have previously been undertaken in the Monadhliath Mountains, or are relevant to the current research. Elevation data was derived from the NEXTMap Great Britain DTM and overlain on a hillshade model, also derived from NEXTMap (Intermap Technologies Inc. provided by NERC via the NERC Earth Observation Data Centre). UK Outline from Ordnance Survey © Crown copyright 2010.

al. (2010) as crag and tail features, and the unmodified interior of the central plateau. This has led several researchers familiar with the area to suggest that slow moving, possibly cold-based ice over the Monadhliath plateau was surrounded by two zones of fast-flowing ice, possibly ice streams, in the Great Glen and Strathspey that both flowed northeastwards towards the Moray Firth (Hinxman & Anderson, 1915; Merritt *et al*., 1995; J.W. Merritt, pers. comm., 2008; M. Krabbendam, pers. comm., 2011). However, the interactions between the different zones are currently unknown and it is unclear whether the Monadhliath Mountains acted as an independent ice dispersal centre at any stage during the last glaciation.

The majority of the research previously undertaken in the Monadhliath Mountains has focussed on the dynamics of major ice lobes in the region during ice sheet retreat. However, there has been no regional assessment of ice sheet retreat dynamics and as a result current knowledge and understanding is both spatially and temporally fragmented, where the majority of previous research lacks any form of chronological framework (e.g. Barrow *et al*., 1913; Hinxman & Anderson, 1915; Charlesworth, 1955; Young, 1977, 1978; Phillips & Auton, 2000) (Fig. 2.4). More recent studies have attempted to establish a more robust chronology for deglacial events in the surrounding region based on absolute dates linked to the Greenland ice core record (e.g. Merritt *et al*., 1995; Everest & Golledge, 2004; Everest & Kubik, 2006; Finlayson *et al*., 2007; Clark *et al*., 2010), but in the absence of any reliable absolute dates in the Monadhliath Mountains relating to this period, there is still a large amount of uncertainty regarding the timing of deglaciation and oscillations during retreat.

Current understanding of retreat patterns in eastern and central Scotland suggests that deglaciation in Strathspey was already well advanced by 16 ka (Fig. 2.5) (Clark *et al*., 2010) and that Loch Etteridge in the Spey Valley to the south of the Monadhliath Mountains (Fig. 2.1) was ice free by ca. 15.8 to 15.5 ka BP based on radiocarbon dates (13 150 ± 350 ^{14}C yr BP (Sissons & Walker, 1974; Walker, 1975) and 12 930 ± 40 ^{14}C yr BP (Everest & Golledge, 2004)). This evidence provides a key constraint on the timing of deglaciation in the region of the Monadhliath Mountains. Further research in Strathspey by Everest and Kubik (2006) on the northern fringe of the Cairngorm Mountains (Fig 2.4) found evidence for a major stillstand during the separation of the Strathspey Glacier from local Cairngorm glaciers, which caused ice-dammed lakes to form in between the Strathspey and Cairngorm ice lobes that could have existed for up to 1000 years (Fig. 2.6) (Brazier *et al*., 1996, 1998; Everest & Golledge, 2004). Everest and Kubik (2006) tentatively postulated that this event occurred after Heinrich Event 1 based on optically stimulated luminescence (OSL) dates, cosmogenic surface exposure dating (SED) (Everest & Golledge, 2004) and the requirement of ice-free conditions at Loch Etteridge by 15.8 to 15.5 ka BP.

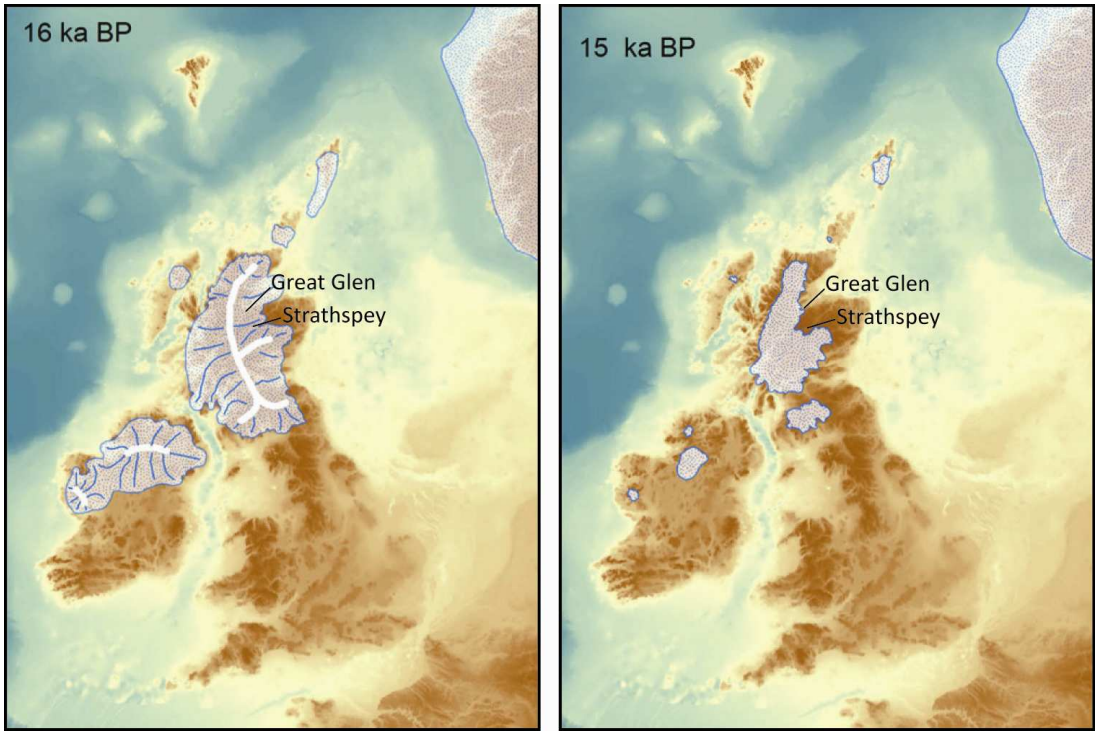

Figure 2.5. Reconstructed configuration of the British and Irish ice sheets during deglaciation from 16 ka to 15 ka BP, showing earlier deglaciation in the Strathspey compared to the Great Glen. Adapted from Clark *et al.* (2010, p. 23).

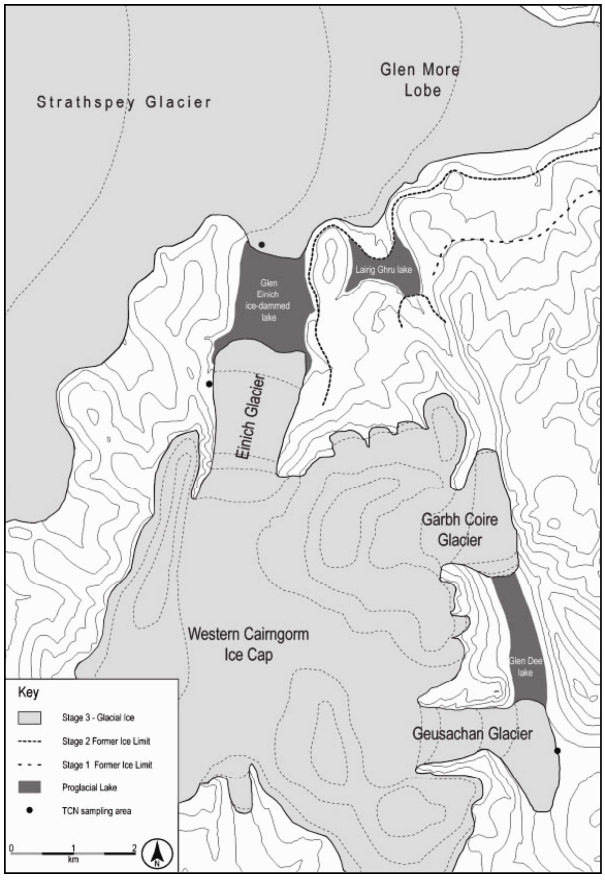

Figure 2.6. Reconstruction of the configuration of the Western Cairngorm Ice Cap and Strathspey Glacier, which is estimated to have occurred after 16.6 ka BP. The figure includes earlier margins of the Strathspey glacier and the location of ice-dammed lakes that occurred between the ice lobes. The location of this figure is shown in Figure 2.4. From Everest and Kubik (2006, p. 99).

To the north of the study area in the Great Glen, the nearest dates available to constrain the timing of deglaciation are found immediately north of Inverness. In this area, there is evidence for two ice sheet oscillations in the Moray Firth during retreat. The first, the Elgin Oscillation, has been suggested to have occurred before 15 ka due to the presence of fauna within proximal raised glaciomarine sediments found inside the oscillation limit, which have been correlated to the 'Errol Beds' in eastern Scotland, dated to between 13 000 and 14 000 ^{14}C yr BP (Merritt *et al*., 1995, 2003a; Peacock, 1999; Finlayson *et al*., 2007). The second oscillation, the Ardersier Oscillation is argued to predate the beginning of the Lateglacial Interstadial (GI-1; 14.7 to 12.9 ka b2k; Rasmussen *et al*., 2006; Lowe *et al*., 2008) based on the occurrence of sediments from GI-1 and the Younger Dryas (GS-1) found inside the limits of the oscillation (Smith, 1966; Peacock & Wilkinson, 1995; Merritt *et al*., 1995; Finlayson *et al*., 2007). These dates suggest that ice within the Great Glen remained more extensive for longer than in Strathspey, although both the dates stated above are minimum dates for ice-free conditions and there are no dates to constrain the timing of deglaciation within the Great Glen itself.

As well as the lack of a clear chronostratigraphic framework in the region, research on Late Devensian ice sheet retreat has also been hindered by the influence of different ideas and paradigms over the last century, making comparison between already fragmented studies very difficult. The most striking example of this is the way in which glaciogenic landforms have been interpreted in Strathspey, where early researchers (e.g. Barrow *et al*., 1913; Hinxman & Anderson, 1915; Charlesworth, 1955) predominantly interpreted geomorphological features as evidence for an active, oscillatory retreating ice margin (similar to the recent work by Everest and Kubik, 2006), whilst J.R. Young in the 1970s favoured a style of retreat dominated by ice stagnation. Following a paradigm shift back to an oscillatory style of glacier retreat, Young's (1977, 1978) interpretation of numerous eskers in the Spey and Dulnain valleys may now be questionable, as has been shown in other areas of Scotland, where Huddart (1999) re-interpreted 'eskers' in Dumfriesshire as dissected ice-contact outwash (*cf.* Evans *et al*., 2005).

The most chronologically well-constrained part of the study area is to the southwest in the area around Glen Roy and relates to the Younger Dryas or GS-1 (Fig. 2.3). During this stadial, ice lobes from the West Highland Ice Cap advanced into Glen Roy and Glen Spean, damming drainage and creating a series of lakes (Sissons, 1979a, b, c). A Younger Dryas age for this event is suggested by pollen stratigraphy (Macpherson, 1978; Lowe & Cairns, 1991) and SED that indicates that the lake shorelines were abandoned between 11.5 ± 1.1 ka and 11.9 ± 1.5 ka (Fabel *et al*., 2010). Further constraint is provided by Palmer *et al*. (2010, 2012) who suggest, based on the varve record in Glen Roy and Glen Spean, that the lakes were in existence for a

total for 515 years and argue that this occurred late in the Younger Dryas based on correlation with the GRIP ice core record.

In the rest of the Monadhliath Mountains, there is very little published evidence for glaciation during the Younger Dryas, although the existence of small, isolated glaciers has previously been suggested by Young (1978), Sissons (1979d) and Auton (1998) (e.g. Fig. 2.7A). This previous research was very much shaped by the alpine glacier paradigm in which reconstructions of small former ice masses were mainly depicted as corrie or valley glaciers. Therefore the presence of a large expanse of plateau that could have acted as a major source area for these small valley glaciers was overlooked (Section 2.4). In addition, the absence of formal glacier reconstructions and/or the lack of dating control has resulted in these areas being neglected in recent depictions of Younger Dryas ice extent in Scotland (e.g. Golledge *et al*., 2008; Benn & Evans, 2010) (Fig. 2.7B). Furthermore, palaeoglaciological reconstructions and palaeoprecipitation calculations in other areas of Scotland, such as the Grampians (Sissons & Sutherland, 1976), Drumochter (Benn & Ballantyne, 2005), Creag Meagaidh (Finlayson, 2006), Sutherland (Lukas & Bradwell, 2010), Skye (Ballantyne, 1989), Arran (Ballantyne, 2007a), Harris (Ballantyne, 2007b) and Mull (Ballantyne, 2002a) suggest that a strong precipitation gradient existed from southwest to northeast across Scotland. This gradient would have led to reduced precipitation rates in the northeast by 70-80% compared to the southwest (Golledge *et al*., 2008; Golledge, 2010), restricting glacier growth in the east due to more arid conditions. These findings have reinforced a perception that only small ice masses, if any, were able to form in the Monadhliath Mountains during the Younger Dryas.

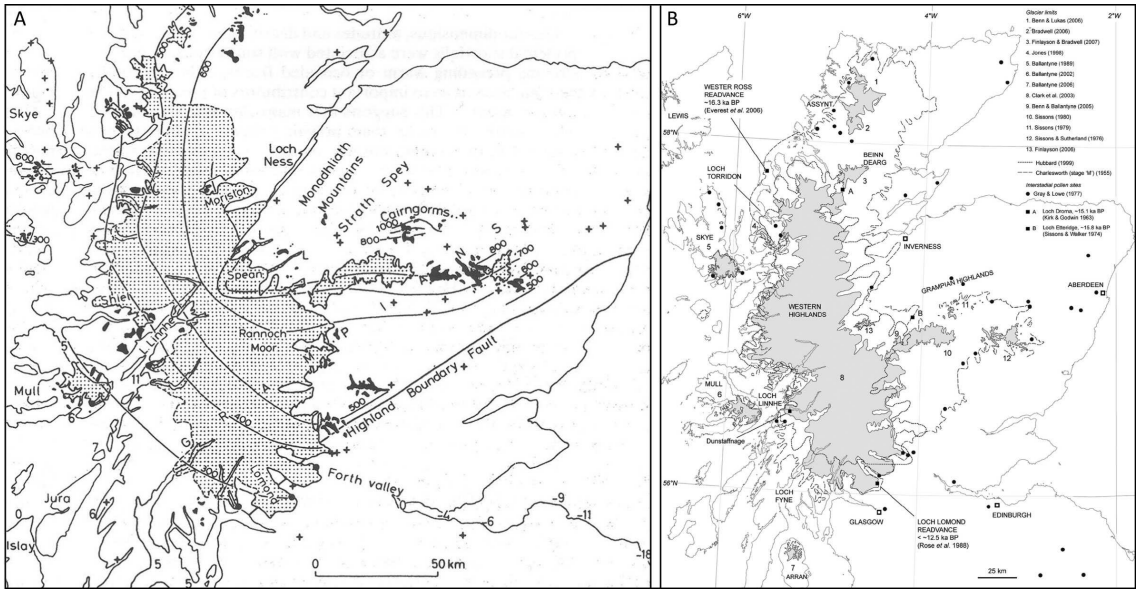

Figure 2.7. Younger Dryas ice masses in Scotland from A) Sissons, 1979d, p. 201 and B) Golledge *et al.*, 2008, p. 890. Note the presence of two small valley glaciers in the Monadhliath Mountains in A) but their absence in B).

However, recently there has been renewed interest in the Monadhliath Mountains, in part aided by a greater understanding of plateau icefield dynamics (see Section 2.4) and by a renewed interest in glacial geomorphology (see Section 3.1). Recent research (e.g. Johnson-Ferguson, 2004; Trelea, 2008; Benn & Evans, 2008) has identified isolated evidence for the presence of Younger Dryas ice masses in the southeast and west of the area (Fig. 2.4). To add to this, thermomechanical glacier modelling by Golledge *et al*. (2008) indicated that the area of plateau in the centre of the Monadhliath Mountains was sufficiently high and wide enough to support glaciation during the Younger Dryas (Fig. 2.8). The model consistently produced an icefield over this area under a range of climatic parameters, suggesting that further empirical studies are required to test these model results.

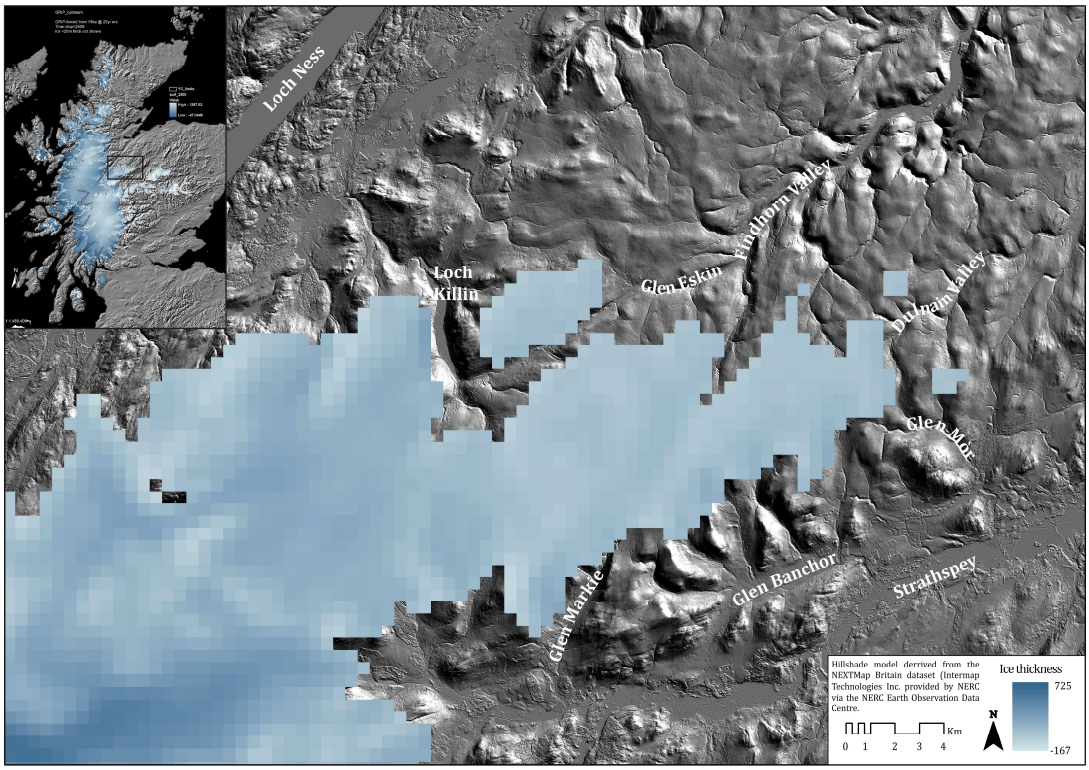

Figure 2.8. Modelled Younger Dryas ice extent in the Monadhliath Mountains from an 'optimum fit' 500 m resolution three-dimensional thermomechanical ice-sheet model that was constrained by field evidence in other areas of Scotland. Adapted from Golledge *et al.* (2008).

The fragmented nature of previous research in the Monadhliath Mountains makes it difficult to review systematically and chronologically. The following sections therefore provide a detailed description of previous studies by location, but an attempt is made to link the research chronologically, where possible, to ice-core stages proposed by Lowe *et al*. (2008) (Fig. 2.3).

2.3.2 Ice sheet retreat from the LGM

Dulnain and Findhorn Valleys

Following the chronological framework outlined above, the Findhorn and Dulnain valleys are likely to have been one of the first areas of the Monadhliath Mountains to deglaciate, potentially

forming part of an unzipping corridor as ice retreated southwestwards around the Monadhliath massif, as depicted in the deglaciation model by Clark *et al*. (2010) (Fig. 2.5). However, the role of possible plateau ice in the Monadhliath Mountains is unknown and likewise the dominance of local versus regional ice in these valleys is unclear, meaning that locally sourced ice could have remained in these valleys whilst Strathspey and the Great Glen became ice-free.

This juxtaposition of local and regional ice has been deliberated by previous authors and has resulted in a division of opinions. Charlesworth (1955) described the retreat of the Dulnain Glacier towards the Spey and Findhorn watersheds based on prominent channels at the head of the Dulnain Valley around Carn Sgùlain and Bruach nan Imirichean (in square NH 7008), which he argued demonstrated that the Dulnain Glacier was sourced by ice on the plateau to the west. Hinxman and Anderson (1915), however, whilst acknowledging independent glaciers in the Findhorn and Dulnain, contended that the same channels around Carn Sgùlain and Bruach nan Imirichean documented meltwater drainage at the margin of the Findhorn Glacier that for a time flowed eastwards towards the Spey Valley, demonstrating the changing dominance of the three glaciers over time. Young (1977) on the other hand, following the alpine paradigm, suggested that due to the absence of any source corries at the head of the Dulnain, ice only existed in the Dulnain when the Strathspey Glacier was thick enough to cross the Spey-Dulnain watershed, supported by significant streamlining of summits along the watershed.

Within the Dulnain Valley itself, there are other clear differences in the interpretation of the geomorphology. Charlesworth (1955) identified numerous moraines and spillways, which he interpreted as evidence for blocking of drainage within tributary catchments that had already become ice-free along the sides of the Dulnain Glacier (Fig. 2.9). Hinxman and Anderson (1915) also noted these former channels, but related the features mainly to ice-marginal drainage, rather than spillways from ice-dammed lakes. Alternatively, Young (1977) argued that the SW-NE orientation of these channels and their development across interfluves indicated they were formed by subglacial meltwater. Young (1977) also identified eskers around Caggan (square NH 8116), which are probably the same features that Charlesworth (1955) interpreted as moraines.

In the Findhorn Valley, the above authors made similar arguments regarding the source and relative dominance of the Findhorn Glacier as described above. Yet despite the Findhorn Valley representing a major drainage pathway from the centre to the east of the Monadhliath Mountains, with relatively good accessibility, very little research has been undertaken. Hinxman and Anderson (1915) present a comprehensive description of the upper Findhorn Valley up to Dalbeg (NH 655 132), but impart little about the area upstream of this point.

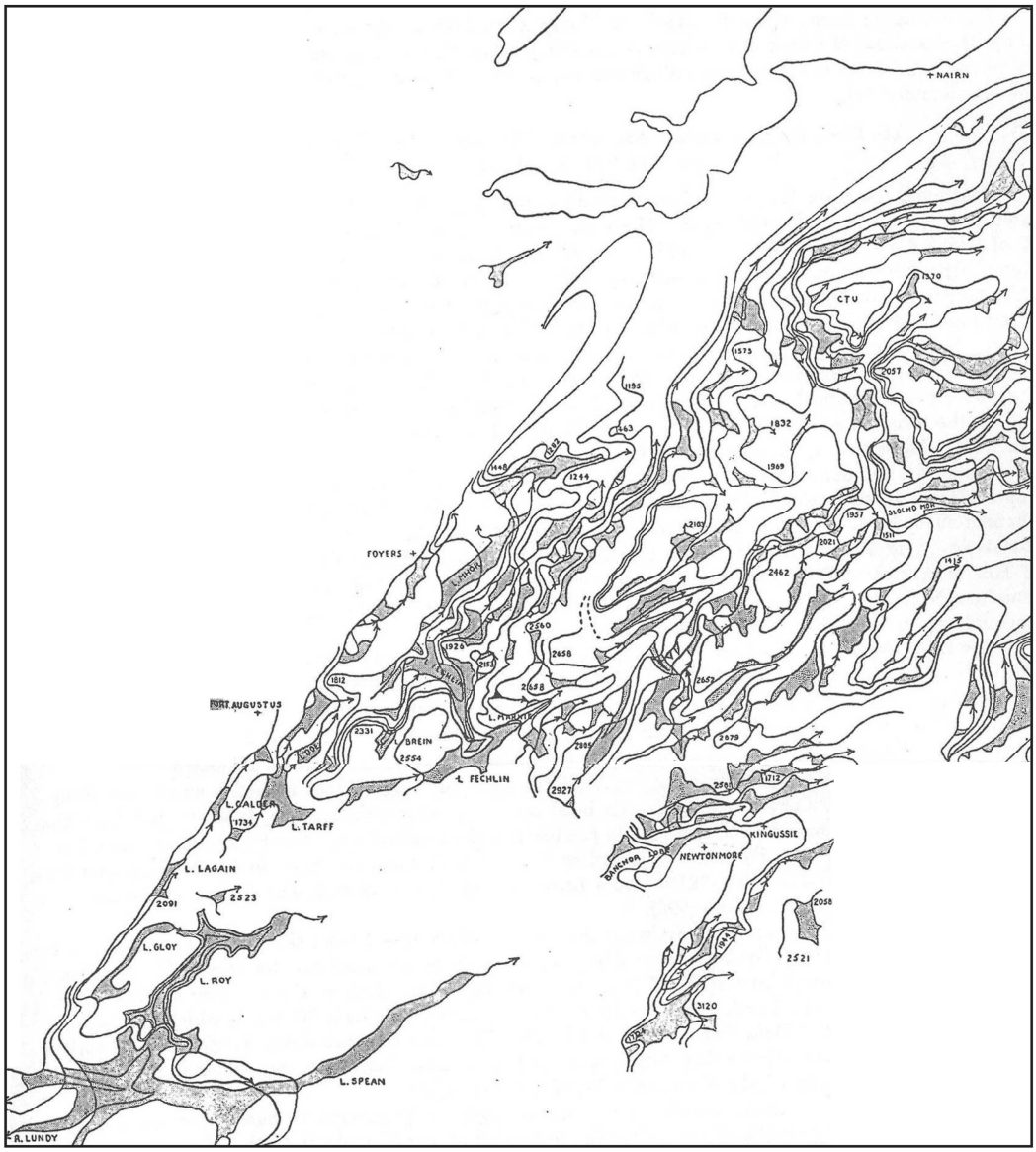

Figure 2.9. Ice-dammed lakes and corresponding ice margin positions identified by Charlesworth (1955) in the Monadhliath Mountains. The majority of the lakes are most likely associated with ice sheet deglaciation, but the figure also includes ice-dammed lakes in Glen Roy and Glen Spean that were later assigned to the Younger Dryas (Section 2.3.3). Adapted from Charlesworth (1955, p. 810).

These authors focused predominantly on the large number of former meltwater channels that cross the hillsides on both sides of the Findhorn Valley, which they related to ice marginal drainage that recorded a lowering of the ice surface during retreat. Charlesworth (1955) also noted little about the upper area of the Findhorn catchment, instead focussing on the interactions of the Moy, Kylachy and Findhorn ice lobes just upstream of Tomatin. The author's illustration of ice-dammed lake distribution in the area (Fig. 2.9), however, suggests ponding of drainage occurred in many of the tributary valleys to the upper Findhorn Valley during ice retreat.

The most detailed assessment of the geomorphology of the Findhorn Valley was by the British Geological Survey in 1998. Rapid reconnaissance mapping by Auton (1998) identified contrasting geomorphology in the upper and middle parts of the Findhorn catchment. In the

upper part, the geomorphology is dominated by moraines, screes, valley side benches and large glaciofluvial fans at the mouths of tributary valleys, whilst thick sequences of till and glacial outwash sands and gravels are found further downstream (Auton, 1990). The identification of numerous moraines by Auton (1998) is in contrast to the research by Hinxman and Anderson (1915, p.82) who stated that "moraines are remarkably scarce in the upper part of the Findhorn basin".

Auton (1998) proposed three types of moraine in the upper Findhorn Valley based upon their location and morphology. He associated types 2 and 3 to stages of active recession of the Findhorn Glacier from the LGM, linking them to the ice-marginal drainage channels identified by Hinxman and Anderson (1915) on the plateau on either side of the valley. Type 3 moraines form patches of mounded topography in isolated areas on the southern side of the Findhorn Valley from just downstream of Dalbeg (square NH 6613) to Dalmigavie (square NH 7419) and on the western side of the lower part of the Elrick Burn Valley (square NH 6713). Type 2 moraines were argued to be slightly younger since they possess a more defined morphology and form lenticular ridges between Coignafearn Lodge (square NH 6815) and Dalbeg (square NH 6513). This evidence suggests that a major glacier occupied the Findhorn Valley during deglaciation towards the end of the Dimlington Stadial, yet it is still unclear whether this glacier was sourced by local plateau ice or by regional ice that crossed the Spey and Dulnain watersheds from the south.

Strathspey

The next area likely to have deglaciated, or that deglaciated simultaneously to the Dulnain and Findhorn valleys, is the Spey Valley, which was ice-free at least as far south as Loch Etteridge (Fig. 2.1) by ca. 15.8 to 15.5 ka BP (Everest & Golledge, 2004; Everest & Kubik, 2006). The Spey Valley has received considerable research attention, where a variety of landform-sediment assemblages document the retreat of the former Strathspey Glacier. As discussed above, Everest and Kubik (2006) provide evidence for a major stillstand of the Strathspey Glacier, which created a series of ice-dammed lakes between the southern edge of the Spey Valley and valley glaciers radiating northwards from the Cairngorms massif near Glen More (see also Brazier *et al.*, 1998). Similar evidence for an active, oscillating ice margin is also found further west immediately to the south of the Monadhliath Mountains, where Phillips and Auton (2000) describe glaciolacustrine sediments and debris flow deposits produced by oscillations of the northern margin of the Strathspey Glacier during LGM retreat.

Phillips and Auton (2000) identified six gently sloping benches in the lower part of the Raitts Burn valley, a south flowing tributary to the north of the Spey Valley, that were dissected by

arcuate channels (Fig. 2.10). Sections within the benches revealed a sequence of poorly-sorted, matrix-supported gravels beneath a unit of deformed sand, silt and clay laminations, overlain by a weakly stratified diamicton. Using micromorphology, these authors identified varves within the laminated unit and therefore suggested that it was deposited in an ice-dammed lake that was in existence for approximately 600 years. They argued that a subsequent advance of an ice-margin, sourced in the southwest, overrode the lake sediments causing several phases of deformation, including ductile shearing, hydrofracturing, fluidization, tight folding, thrusting and brittle microfaulting within the unit. Phillips and Auton (2000) related the deposition of the lower part of the overlying diamicton unit to this ice advance due to further evidence for deformation, but suggested due to its friable nature that the upper part was deposited by subaerial ice-contact debris flows during ice retreat. Based on the location of Raitts Burn with respect to Glen More, it seems probable that this lake formation and re-advance occurred at a similar time to, or shortly after, the stillstand suggested by Everest and Kubik (2006).

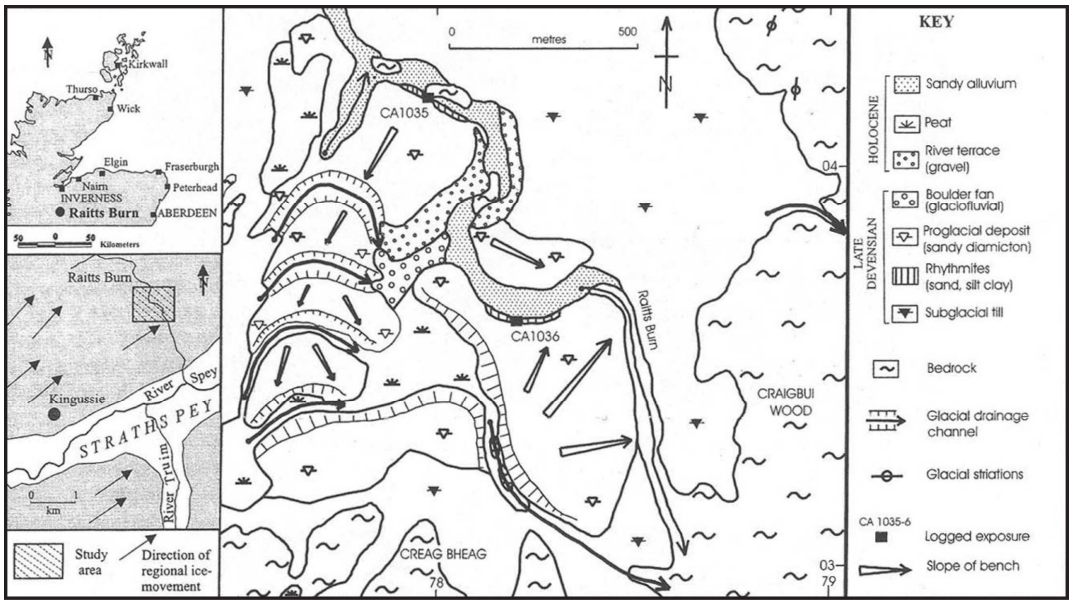

Figure 2.10. Geological map of Raitts Burn, illustrating deposits and landforms relating to the margin of the Strathspey Glacier during deglaciation. Taken from Phillips and Auton (2000, p. 280).

Further evidence for ice-dammed lakes has been proposed within the tributary valleys of Glen Banchor, a short valley that runs parallel to the main Spey Valley. In this area, deep channels have been cut across the interfluves between these tributary valleys. The altitude at which the channels are cut steadily decreases from west to east and the channels lead into pronounced ridges across the floors of Gleann Ballach and the Allt a' Chaorainn and Allt na Beinne catchments. Barrow *et al*. (1913) interpreted the channels as ice-marginal features that were created by drainage at the margin of the Spey Glacier following blockage of drainage across the mouths of the tributary valleys and this idea was also proposed by Charlesworth (1955) (Fig. 2.9). Barrow *et al*. (1913) did not interpret the ridges across Gleann Ballach and Gleann Beinne specifically, but suggested that the series of ridges that emanate from a gully to the west of Gleann Chaorainn were deposited

glaciofluvially by water draining into an ice-dammed lake. Young (1978), however, proposed an alternative argument, interpreting the ridges as eskers and therefore assigning the interfluve channels to a subglacial origin, similar to his interpretation of channels found within the Dulnain (Fig. 2.11). These two entirely different scenarios are the products of a large shift in paradigms, and under our current knowledge and understanding of modern glacial environments the former interpretation seems more plausible. Further discussion on the origin of these features and evaluation of these previous interpretations is found in Sections 4.4.11 and 5.3.

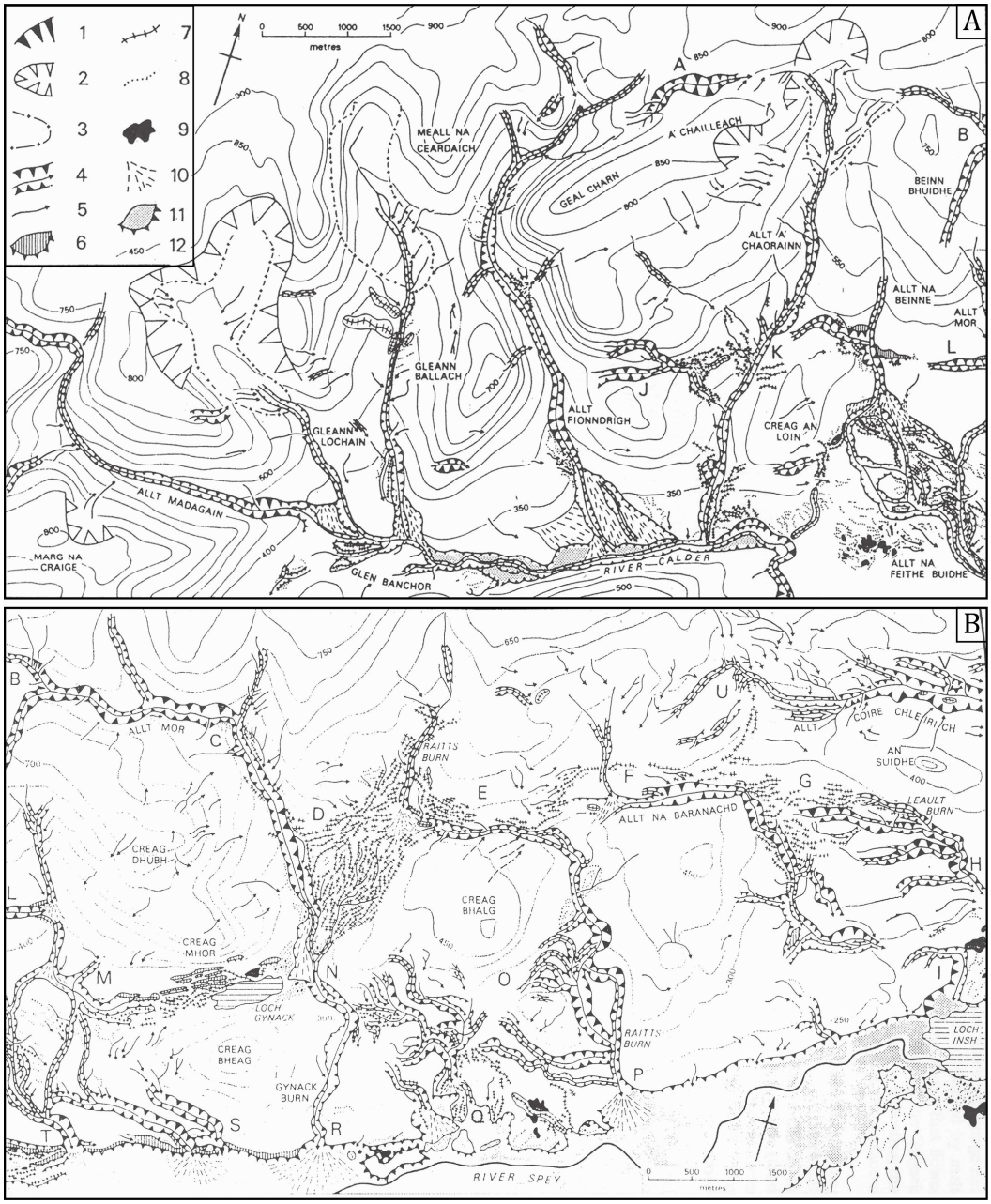

Figure 2.11. Geomorphological map illustrating glacial and glaciofluvial landforms identified by Young (1978) within A) Glen Banchor and B) the area around Raitts Burn. Key: 1 = Major break of slope; 2 = Corrie; 3 = Moraine limit; 4 = Major meltwater channel; 5 = Meltwater channel; 6 = Kame terrace; 7 = Esker; 8 = Kame ridge; 9 = Kettle hole; 10 = Alluvial fan; 11 = Alluvial terrace; 12 = Contours in metres. Taken from Young (1978, pp. 82 & 85).

Other features in the Spey Valley have also been associated with wide ranging interpretations, suggesting both active retreat and ice stagnation. Hinxman and Anderson (1915) interpreted hollows in the otherwise relatively flat plain of glaciofluvial sediments around Boat of Garten as kettle holes, indicative of areas of ice stagnation during ice retreat. However, in other areas Hinxman and Anderson (1915) suggested more active ice retreat, where they mapped large areas of lateral moraines within Glen Gynack and the Allt na Beinne, Allt Mòr and Raitts Burn valleys. In contrast, mapping by Young (1978) in the same area shows a complex arrangement of eskers and meltwater channels related to subglacial drainage patterns (Fig. 2.11). Since these features were mapped alongside kame terraces, kettle holes and alluvial fans in other parts of the Spey Valley, Young (1978) suggested that they indicated an overall process of ice stagnation during retreat.

The Great Glen

Following the model for deglaciation suggested by Clark *et al*. (2010) and radiocarbon dates to the north of Inverness (Merritt *et al*., 1995), the Great Glen is likely to have become ice-free later than Strathspey. During this retreat, Charlesworth (1955) proposed that early ice retreat on the hills to the east of Stratherrick allowed the formation of a series of ice-dammed lakes within the eastern tributary catchments of the Allt Mòr (in square NH 6224), the Allt Uisgan an t-Sidhein (square NH 6020), the Aberchalder Burn (square NH 5619), the River E (square NH 5216), the River Fechlin (square NH 4914), the Allt Breineag (square NH 4712), the Allt Doe (square NH 4107) and the River Tarff (square NH 3805) (Fig. 2.9). Charlesworth (1955) stated that drainage of these lakes was initially to the northeast into the River Nairn and then later into the Ness Basin. More specifically, the author described the formation of a large lake within the Fechlin (or Killin) Valley that was caused by the advance of a lobe of the Ness Glacier into the Fechlin Valley. This ice lobe impounded a large lake that drained over a col at 642 m at the top of Glen Markie into the River Eskin at the head of the Findhorn Valley. In order for the lake drainage to occur at this location, it implies that the Findhorn Glacier had already disappeared at a time when there was still a large ice lobe in the Great Glen, perhaps resolving some of the uncertainty regarding the survival of local ice from the Monadhliath plateau (this is discussed further in Section 5.3).

Geophysical surveys by Turner *et al.* (2012) provide the first investigation of the glaciolacustrine record within Loch Ness. Using seismic surveys and bathymetric data, these authors identified De Geer moraines at the northern end of the loch, a pronounced moraine orientated across the width of the basin at Foyers, other smaller hummocky moraines, proglacial sediments and jökulhlaup deposits. Using this information, Turner *et al*. (2012) proposed a model to explain the depositional history of Loch Ness following retreat from the LGM. The

authors proposed that the margin of the Ness Glacier terminated in water throughout retreat within the Ness Basin due to raised sea levels prior to glacioisostatic uplift. In the northern part of the glen they suggested that the Ness Glacier formed a lightly grounded or potentially floating ice shelf, but subsequently retreated to a more grounded position by Foyers, where a major moraine that now divides the basin in two was deposited. Turner *et al.* (2012) interpreted this moraine as evidence for a major stillstand. Furthermore, the authors suggested that subsequent retreat of the ice lobe was dynamic and also punctuated by stillstands and oscillations, which deposited the smaller hummocky moraines. At present the relationship between this record of deglaciation in the Ness Basin and ice-dammed lake formation at the southern margin of this ice lobe has not been established and will be examined further in Section 5.3. The only constraint on timing of the deglaciation in the Ness Basin is from pollen stratigraphy within Loch Tarff, near the southern end of Loch Ness, which contains Lateglacial pollen (Pennington *et al*., 1972), indicating that this area was ice-free by the Younger Dryas.

There is no published data describing the retreat of LGM ice in the western Monadhliath Mountains, perhaps partly a result of removal of evidence by a subsequent glacial advance during the Younger Dryas, or research attention being focussed on the Younger Dryas only in this area, as described below.

2.3.3 Younger Dryas glaciation in the Monadhliath Mountains

Glen Roy and western Monadhliath Mountains

As discussed in Section 2.3.1, the most documented area relating to Younger Dryas glaciation in the region is to the west of the Monadhliath Mountains in Glen Roy. The recognition that the 'parallel roads' of Glen Roy represent former lake shorelines of an ice-dammed lake was first established in the mid 19th Century during the emergence of glacial theory by early workers such as Agassiz (1840), Jamieson (1863) and Prestwich (1879). Since this time, the area has become one of the most documented areas in Scotland, in particular due to extensive work by J.B. Sissons and other co-workers during the late 1970s and early 1980s (e.g. Sissons, 1977a, 1978, 1979a, b, c, 1981a; Sissons & Cornish, 1982, 1983). These researchers established that the advance of ice lobes from the West Highlands Ice Cap into Glen Roy, Glen Spean and Glen Gloy impounded a series of lakes in these valleys, which formed a succession of shorelines. This event was assigned to the Loch Lomond Stadial, later correlated to the Younger Dryas, based on the almost continuous moraine limit between the radiocarbon dated Menteith moraine, near Loch Lomond, and the glacier limits in Glen Roy (Sissons, 1979a), alongside pollen stratigraphy from within the glacier limits that presented a chronology from the end of the Loch Lomond Stadial into the Middle Flandrian (Macpherson, 1978; Lowe & Cairns, 1991). More recently, the abandonment of the lake shorelines has been dated to the latter part of the Younger

Dryas using SED (Fabel *et al.*, 2010) and a floating varve chronology from the lake sediments has been matched to the latter part of the Younger Dryas (or GS-1) using oxygen isotope data from the Greenland ice-core record (Palmer *et al*., 2010, 2012; MacLeod *et al*., 2011).

Sissons (1977a, 1978) identified a sequence of events to explain the different altitudes of the lake shorelines in Glen Spean, Glen Roy and Glen Gloy due to the use of different drainage pathways (Fig. 2.12). Initial advance of the Spean Glacier blocked drainage within Glen Spean and caused a lake to form in glens Roy and Spean that drained to the northeast of Glen Spean at an elevation of 260 m over the Pattack-Mashie col, causing a lake shoreline at 260 m to form (Fig. 2.12A). Continued advance of the Spean Glacier into Glen Roy and also towards Roughburn in Glen Spean, separated the Roy and Spean lakes and caused the lake in Glen Roy to rise to 325 m, the level at which water was able to drain over a 325 m col between glens Roy and Laggan. At the same time, during this rising sequence, an intermediate lake would have formed in Caol Lairig at 297 m, which drained over a 297 m col into Glen Roy. A lobe of the Garry Glacier also advanced into Glen Gloy, damming drainage and causing a 355 m lake level to occur, where water escaped into the 325 m lake in Glen Roy over a col between glens Gloy and Turret at an elevation of 355 m (Fig. 2.12B). Further advance of the Spean Glacier into Glen Roy blocked off the 325 m Roy-Laggan col and caused the lake level in Glen Roy to rise to 350 m where it drained to the north via a 350 m col between glens Roy and Spey (Fig. 2.12C). During glacier retreat this sequence would have occurred in reverse. The relative contributions of the rising and falling lake levels to the final shoreline morphologies remain unclear (*cf.* Sissons, 1978; Fabel *et al*., 2010), however. SED on bedrock taken from the shorelines has confirmed a Younger Dryas age for their formation, indicating an age of between 11.5 ± 1.1 ka and 11.9 ± 1.5 ka BP for their final abandonment (Fabel *et al*., 2010). These authors suggest that erosion is likely to have occurred during both the rising and falling sequences.

An estimate of the length of time for which the lakes existed was recently proposed by Palmer (2008) and Palmer *et al*. (2010, 2012) (see also MacLeod *et al*., 2011), who used micromorphology to construct a varve chronology for the rising and falling sequences. These authors examined sections within the Glen Turret Fan and the Burn of Agie Fan in Glen Roy and sampled a core extracted from the northeastern end of Loch Laggan in Glen Spean. Palmer (2008) and Palmer *et al*. (2010) correlated the varve sequences at the three sites to produce a Lochaber Master varve chronology (LMVC), which was used to estimate the duration of the various lake levels, using changes in varve thickness to identify changes in lake level. The 260 m lake is estimated to have existed for a minimum of 191 years during the rising sequence. This stage was followed by the formation of the 325 m lake in Glen Roy, which was in

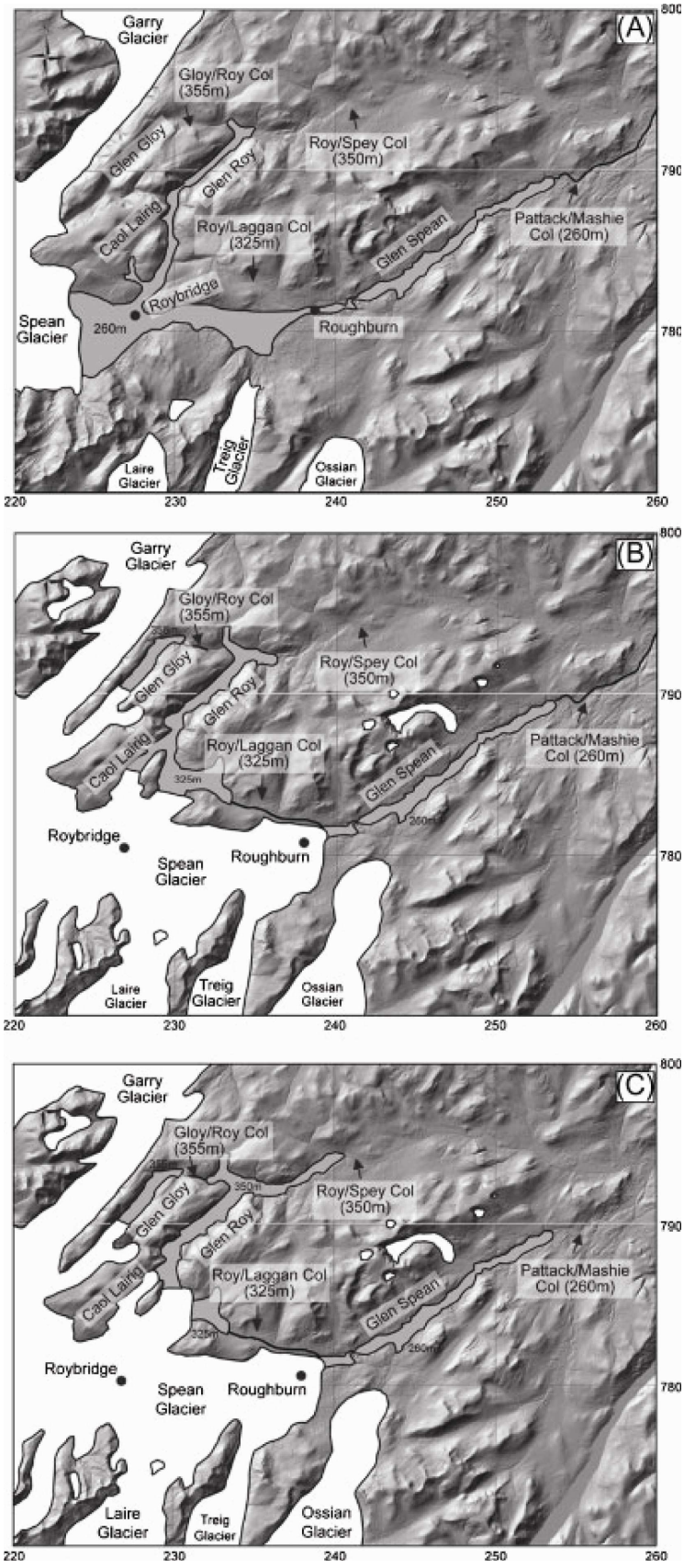

Figure 2.12. Sequence of glacial advance into Glen Roy and Glen Spean that caused the damming of drainage within these two valleys and created the 260 m lake level in Glen Spean, the 297 m lake level in Caol Lairig, the 355 m lake level in Glen Gloy and the 260 m, 325 m and 350 m lake levels in Glen Roy. Further explanation of these events is found in the text. Taken from Palmer *et al.* (2010, p. 583). Hillshade model derived from the NEXTMap Britain data set from Intermap Technologies Inc.

existence for a minimum of 112 years. The 350 m lake existed for a minimum of 116 years before lake levels began to fall, which was recognised in a change to thinner varves. The authors state that the 325 m and 260 m lakes of the falling sequence existed for a minimum of 96 years, but there are difficulties differentiating between the two stages, suggesting that either the 260 m lake did not persist for very long, or that the final part of the sequence is missing from the varve record.

Palmer *et al*. (2010) used these findings to estimate advance and retreat rates of the Spean Glacier by measuring the distance that the glacier was required to advance in order to form each higher lake level. The results indicate that the Spean Glacier may have advanced at an average rate of 41.9 ma^{-1} in Glen Roy from its 260 m to 325 m lake level position, and at an average rate of 13.4 ma^{-1} to its 350 m position. In Glen Spean the glacier was estimated to have advanced to its maximum position at Roughburn at an average rate of 37.0 ma^{-1}. Retreat rates may have been as high as 80.8 ma^{-1} owing to the effect of a calving margin. Palmer *et al*. (2010) also estimated the annual erosion rates required to form the 260, 325 and 350 m shorelines, estimated at 0.050, 0.069 and 0.097 ma^{-1} respectively, based on mean widths measured by Sissons (1978) and the duration of the lakes.

Sissons (1977a, 1979a, b, c) argued that the drainage of the lakes in Glen Spean and Glen Roy occurred catastrophically as a jökulhlaup into the Great Glen. This has been confirmed by the interpretation of sediments within the Auchteraw terrace near Fort Augustus as compatible with jökulhlaup deposition (Russell & Marren, 1998), alongside the presence of a thick layer of gravel in the Beauly Firth (Sissons, 1981b). More recent research in the Ness Basin also found sediments to support a jökulhlaup at the end of the Younger Dryas (Turner *et al*., 2012).

The sequence of events within Glen Gloy and Glen Turret, a tributary valley at the head of Glen Roy has been subject to a rigorous debate since the late 1970s and is of most relevance to this research. Initial research by Sissons (1978, 1979a) suggested that the maximum limit of the ice lobe that advanced into Glen Gloy was defined by moraine mounds around NN 2891, in accordance with Peacock (1970). This limit was incorporated into the sequence of events, proposed by Sissons (1977a, 1978) to produce the 355 m shoreline in Glen Gloy during both the advance and retreat stages. However, subsequent mapping of the fans and terraces in the upper part of Glen Roy led Sissons and Cornish (1983) to propose that the gravels that make up a substantial proportion of the Turret Fan were deposited as ice-contact glacial outwash sediments within the 260 m lake, which required the ice lobe within Glen Gloy to have advanced further, over the col at the head of the Allt a' Chomlain catchment and into Glen Turret. These authors argued that as the lake levels rose to the 325 and 350 m levels, the Gloy lobe rapidly retreated

back into Glen Gloy, allowing deposition of the overlying laminated silt and clay unit on the Turret Fan and the formation of the 355 m lake shoreline within Glen Gloy.

This hypothesis was heavily disputed by Peacock (1986), who argued that the gravels within the Turret Fan were deposited subaerially as bedload within shallow, ice-proximal, braided channels. Based on the morphology of the fan and associated moraines, Peacock (1986) also suggested that the fan had been deposited by the advance of a glacier in Glen Gloy over the Gloy-Chomlain col, but argued that the most likely scenario in which a glacier sourced from the west could have deposited the Turret Fan was at a time when the main Glen Roy valley was ice free and was most likely during ice retreat from the LGM.

Lowe and Cairns (1991) argued against this hypothesis, using a pollen stratigraphy for the upper part of Glen Roy. These authors extended the pollen chronology identified by Macpherson (1978) and also included new sites such as the Turret Bank site and the Gloy-Turret col. The oldest pollen assemblages found within both these successions related to the early Flandrian and importantly, no Lateglacial pollen was recovered. Lowe and Cairns (1991) used this evidence to argue that the ice advance that deposited the Turret Fan occurred during the Loch Lomond Stadial, therefore supporting Sissons and Cornish's (1983) hypothesis. However, the base of the sequence at the Turret Bank site was not recovered since sand deposits at a depth of around 8 m could not be penetrated. The authors also admitted that Lateglacial deposits at the Gloy-Turret site could have been removed by water flowing over the col from the ice-dammed lake in Glen Gloy.

In order to provide an alternative solution to the debate in Glen Turret, recent studies have suggested the existence of a small plateau icefield around the summits of Carn Dearg, Carn Leac and Corrieyairack Hill to the northeast of Glen Roy, which sourced an outlet glacier within Glen Turret (Johnson-Ferguson, 2004; Benn & Evans, 2008) (Fig. 2.13). Evidence for this ice cap is provided by moraines and meltwater channels in all of the major valleys radiating from this area. Benn and Evans (2008) linked this ice cap morphostratigraphically to the Younger Dryas using evidence found within a section at the head of Glen Turret, at the mouth of the Allt Teanga Bige tributary (NN 329 944). The section consists predominantly of a unit of laminated silt, which is interbedded with smaller layers of sand, gravel and diamicton (Benn & Evans, 2008). Benn and Evans (2008, p.160) interpreted the sediments as having been deposited subaqueously as "mass flows, turbidites and rain-out deposits", similar to a previous interpretation by Peacock (1986) of this feature. This interpretation indicates that the section was in close proximity to a glacier margin further upstream within the Allt Teanga Bige catchment at the same time that the 350 m lake was in existence. The upper 3 m of the section

consists of a massive clast- and boulder-rich diamicton that Benn and Evans (2008) interpreted as a subaerially deposited moraine, suggesting a minor advance of the Teanga Bige glacier occurred following lake drainage within Glen Turret.

Benn and Evans (2008) proposed a model for the sequence of Younger Dryas events in Glen Turret that incorporated elements of all previous models (e.g. Sissons & Cornish, 1983; Peacock, 1986; Peacock & Cornish, 1989; Lowe & Cairns, 1991). They suggested that an early advance of a local ice cap centred over the Carn Dearg – Corrieyairack Hill culminated in the Turret outlet glacier reaching the mouth of Glen Turret and depositing the Turret Fan subaerially (Fig. 2.13). Subsequent advance of the Spean Glacier into Glen Roy eventually blocked drainage in Glen Roy. As lake levels rose, calving accelerated at the terminus of the Turret Glacier, and caused rapid retreat to the head of Glen Turret where it was able to stabilise and the thick sequence of glaciolacustrine sediments was deposited in the 350 m lake (Fig. 2.12C). A small minor advance following an initial drop in the 350 m lake level deposited the moraines on top of the glaciolacustrine sediments, before final retreat of the icefield. The presence of this icefield and its relationship to events within Glen Turret has, however, been disputed by Peacock (2009).

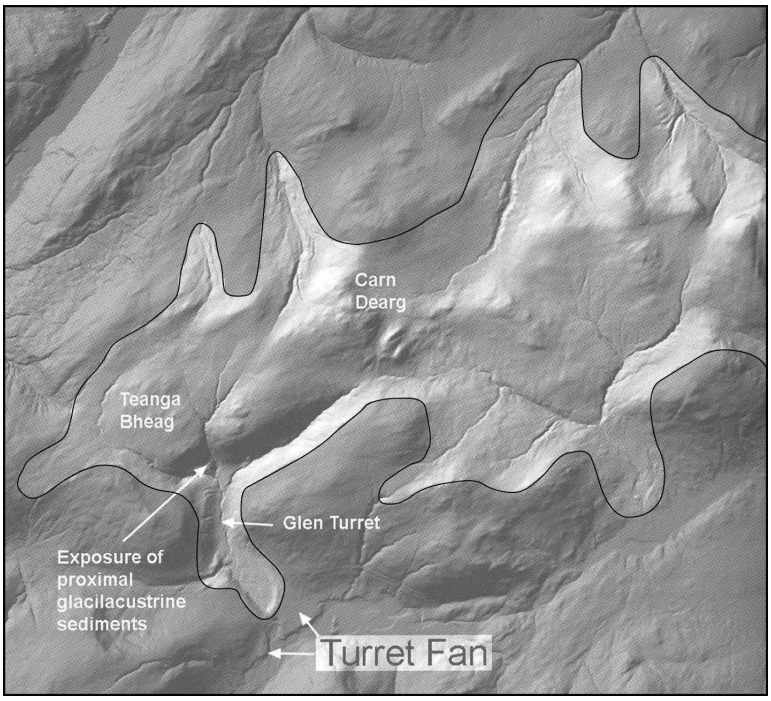

Figure 2.13. Approximate limits of a Younger Dryas ice cap in the area to the northeast of Glen Turret, as identified by Johnson-Ferguson (2004) and Benn and Evans (2008). The ice cap is overlain onto a NEXTMap image from Intermap Techologies Inc. From Benn and Evans (2008, p.160), but ice cap limits delineated in black by the current author.

Central to eastern Monadhliath Mountains

Very little evidence for Younger Dryas glaciation has previously been documented in the central to eastern Monadhliath Mountains, and where the existence of glaciers has been

suggested, no detailed glacier reconstructions have been published. This is most notable in Glen Banchor, where Young (1978) correlated the shape and form of moraines within Gleann Lochain, Gleann Banchor and Gleann Chaorainn to that of moraines of Loch Lomond Stadial age in Glen Spean and Drumochter (Fig 2.11). Whilst there are no published field maps or detailed accounts in this area by Sissons, two small glaciers are shown in several small-scale illustrations of Loch Lomond Stadial ice extent in Scotland by Sissons (e.g. Sissons, 1974a, 1979d, 1983) (Fig 2.7A). From the shape of the glaciers and their approximate location, the two glaciers appear to be located within Gleann Lochain and Gleann Ballach, agreeing with Young (1978). Recent research by Trelea (2008) in the Glen Banchor tributaries also indicated the presence of Younger Dryas glaciers in the Glen Banchor tributary valleys and this has been recently confirmed through a set of presently unpublished Younger Dryas dates on moraines within these valleys (D.M. Gheorghiu & D. Fabel, pers. comm., 2011).

The only other evidence for Younger Dryas glaciation in the Monadhliath Mountains that has previously been described is from the upper part of the Findhorn Valley. Here, Auton (1998) identified three types of moraine based on their morphology. Types 2 and 3 were suggested to have formed during deglaciation from the LGM (Section 2.3.2), but Type 1 was interpreted as Loch Lomond Stadial in age based on the similar morphology and 'freshness' to other Loch Lomond Stadial moraines in Scotland. In support of this assertion, Auton (1998) suggested that extensive scree slopes, which indicate intense periglacial conditions, were only present outside the limits of the Type 1 moraines. These features have been noted in other areas of Scotland to only occur outside the limits of Younger Dryas glaciation (e.g. Sissons, 1972, 1979d; Sissons & Grant, 1972; Thorp, 1981, 1986; Ballantyne & Harris, 1994; Curry, 2000) (See Section 5.1). Auton (1998, p.6) tentatively suggested that these moraines provided evidence for "small glaciers in the head water tributaries of the Findhorn catchment" during the Loch Lomond Stadial, but neglected to acknowledge the presence of a large area of plateau to the south of the Findhorn Valley, which could have sourced these glaciers.

2.3.4 Summary of previous Quaternary research in the study area

Previous research in the Monadhliath Mountains, although generally limited compared to other areas of Scotland, has produced detailed maps of glaciogenic features relating to Late Devensian retreat within the Spey, Findhorn and Dulnain valleys (e.g. Barrow *et al*., 1913; Hinxman & Anderson, 1915; Charlesworth, 1955; Young, 1977, 1978). This includes views on the relative dominance of local and regional ice in the Dulnain, Findhorn and Spey valleys and evidence for ice-dammed lakes in numerous tributaries to the Great Glen and Spey Valley. However, interpretations made about ice dynamics during retreat are wide ranging, influenced by dominant paradigms at the time. As a result, the geomorphology of these areas requires a

detailed re-examination, at a level similar to that undertaken by Phillips and Auton (2000) in Raitts Burn, which currently provides the only thorough examination of events during ice retreat within that part of the Spey Valley. This research and that by Everest and Kubik (2006) in the Cairngorm Mountains, as well as Turner *et al*. (2012) in the Great Glen importantly suggests that ice retreat from the LGM was punctuated by a series of oscillations and still-stands rather than ice stagnation, as previously envisaged (Young, 1977, 1978).

The most researched and chronologically well-constrained part of the study area is to the west of the Monadhliath Mountains in Glen Roy, where advance of the West Highlands Ice Cap into Glen Spean and Glen Roy is constrained to the Younger Dryas by pollen stratigraphy, varve chronology and SED (Lowe & Cairns, 1991; Palmer *et al*., 2010, 2012; Fabel *et al*., 2010). The debate over the genesis of the Turret Fan, towards the head of Glen Roy and the extent of the Gloy Glacier during the Younger Dryas still remains unresolved, however (*cf.* Palmer *et al*., 2008; Peacock, 2009). The most recent addition to this debate is by Benn and Evans (2008) who suggest an alternative, local source of ice for the glacier that deposited the Turret Fan in order to resolve at least some of this dispute, although there is clearly a need for further investigation into the age and dimensions of this icefield.

Several studies have indicated the presence of small ice masses in the Monadhliath Mountains during the Younger Dryas (e.g. Young, 1978; Sissons, 1974a, 1979d, 1983; Auton, 1998; Johnson-Ferguson, 2004; Benn & Evans, 2008; Trelea, 2008). However, many of these studies were influenced by the 'alpine glaciation' paradigm and there are no published detailed reconstructions of these ice masses. As a result, few have been formally acknowledged in descriptions and maps of Scottish Younger Dryas extent (e.g. Golledge *et al*., 2008; Golledge, 2010; Benn & Evans, 2010) and the presence of a substantial plateau area in the Monadhliath Mountains as a source area for a Younger Dryas icefield has been overlooked. Indeed, recent modelling of Younger Dryas ice masses in Scotland suggested that the occurrence of ice masses in the Monadhliath Mountains during the Younger Dryas may have been centred on the Monadhliath plateau and were more extensive that the current published evidence suggests (Golledge *et al*., 2008). Due to the central role of plateau areas in the Monadhliath Mountains, the current state of research on plateau icefields is reviewed in detail below.

2.4 The Plateau Icefield Landsystem

From previous research in the Monadhliath Mountains, as outlined above, it is clear that the role of potential local plateau ice in the overall deglacial chronology of the region following the LGM, and its relative dominance compared to regional ice, is uncertain. Furthermore, the research outlined above indicates the potential existence of a plateau icefield during the

Younger Dryas (e.g. Benn & Evans, 2008; Golledge *et al*., 2008), but as yet no relative or absolute chronology for glacier fluctuations within the area has been established and the extent of Younger Dryas ice in the region remains indefinite. In light of this currently elusive role of plateau ice, a comprehensive understanding of the plateau icefield landsystem is required in order to identify whether such a landsystem exists in the palaeoglacial record and to inform further interpretations about glacier dynamics. The following sections therefore review the plateau icefield landsystem with regards to plateau icefield dynamics during a glacial cycle, geomorphological evidence for plateau icefields in the palaeo-record, and the effect of the presence of plateau ice on equilibrium line altitudes (ELAs). The section also identifies areas in which further research is required.

2.4.1 Plateau icefield dynamics

Plateau icefields play an important role as independent ice dispersal centres both during glacial periods and at present, where they can be considered long-term glacial landsystems that continue to exist within warmer interglacial periods, unlike the majority of ice sheets (Rea & Evans, 2003; Evans, 2010). Plateaux, although previously argued to have been areas of refugia during glacial periods, are now recognised to provide ideal areas for glacier growth and expansion, often ahead of ice sheet advance into a region. As a result, plateau icefields often occur close to the margins of ice sheets, both in modern (e.g. Greenland) and palaeo-settings (e.g. Ellesmere Island), and therefore not only exist as independent glacier systems but also have the potential to influence the configuration of initial ice sheet advance into a region and patterns of ice sheet retreat, as is likely to have occurred in the Monadhliath Mountains during the build up and retreat of the BIIS (Section 2.3). Glaciation of plateau areas can therefore be divided into two distinct episodes; that of a local to regional plateau icefield, where the distribution of ice is strongly determined, alongside climatic factors, by the size and altitude of the plateau; and larger scale ice sheet cover, where the underlying topography has a much smaller influence on the direction of ice flow (Rea & Evans, 2003).

An important aspect of plateau icefields, as outlined above, is that at the onset of glaciation, local plateau icefields will develop ahead of any regional ice. Since they often lie above the regional glaciation level, they will collect snow earlier than any lower lying corries. However, at the same time, Manley (1955) noted that the narrower the summit, the higher it needs to be above the regional firn line to maintain snow cover. The relationship is demonstrated in Figure 2.14A, where Manley (1955) used examples, primarily from Norway, to estimate the relationship between the breadth of the summit (measured in the direction of the prevailing wind) and the height of the summit above the firn line required for plateau icefield glaciation to occur. This relationship was subsequently tested by Rea *et al*. (1998), who added additional

area-altitude data from a number of glaciated and unglaciated summits in north Norway. These authors found that although the additional points supported the existence of a relationship between the summit breadth and plateau height above the firn line, a more complex relationship occurred, with one unglaciated plateau plotting above the curve and a number of glaciated plateaux plotting below it (Fig. 2.14B), although delayed response to climatic amelioration following the end of the Little Ice Age (LIA) could have skewed the additional dataset.

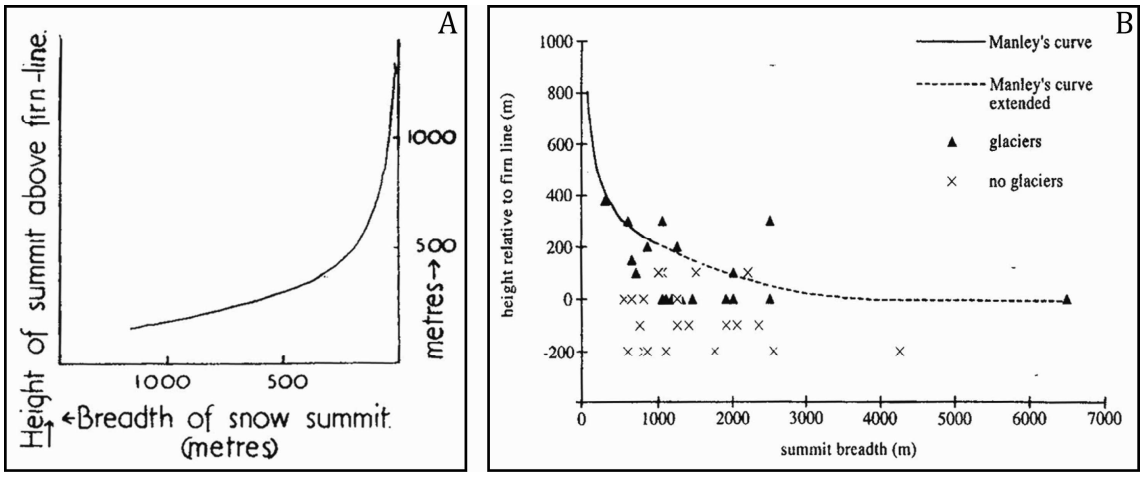

Figure 2.14. A) Manley's curve showing the relationship between summit breadth and height of the summit above the firn line, required for viable plateau icefield development. Taken from Manley (1955, p. 455). B) Glaciated and non-glaciated summit heights plotted against an extended version of Manley's original curve. Taken from Rea *et al*. (1998, p. 36).

Since lower temperatures are required to support glaciation on narrower summits, generally at a greater height above the firn line, ice on narrow summits is often cold-based ice, whilst warmer ice resides on lower, wider plateau areas (Rea & Evans, 2003). In addition, Dyke (1993) suggested that if icefields develop on permafrost of which the ice thickness in the accumulation area is thinner than the depth of the permafrost, the icefield will be entirely cold-based, whilst thicker plateau icefields can reach the pressure melting point (PMP), e.g. Øksfjordjøkelen (Gellatly *et al*. 1988; Rea *et al*. 1998), due to greater ice thickness. Icefield thermal regime is also controlled by bed slope angles, where ice is likely to remain cold-based on ground with low slope angles due to low strain rates within the ice (Rea *et al*., 1998). Strain rates often increase towards the plateau margins as slope gradients increase, allowing cold-based ice to reach the PMP, leading to sliding and enabling subglacial erosion (Rea & Evans, 2003; Evans, 2010).

As regional ice advances into areas of localised plateau glaciation, plateau icefields are likely to initially exert a control on ice flow directions, but will eventually become overwhelmed with the dominant flow direction of the regional ice, which is usually parallel to major valley systems (Rea *et al*., 1998). In the early stages of full glacial conditions, ice on the plateau may remain or become cold-based, due to low annual air temperatures, and Sugden (1968) discusses how fast-flowing ice streams situated within an ice sheet can effectively erode pre-existing valleys and

breach watersheds, whilst cold-based ice immediately adjacent can preserve a pre-existing landscape, such as in the Cairngorm Mountains. However, an increase in ice thickness can allow the PMP to be reached, instigating glacial erosion (Rea & Evans, 2003). At this stage the geomorphological signature of regional trunk valleys becomes overprinted on the plateau icefield palaeoglacial record and erratics may be brought onto the plateau from further afield (Rea *et al*., 1998; Rea & Evans, 2003).

During ice sheet decay the underlying topography will exert an increasing control on ice distribution and flow direction, as thinning occurs. Depending on the nature of climatic amelioration, the style of glaciation may revert back to localised plateau icefield dispersal centres (e.g. Clark *et al*., 2000). At present there is little research on plateau icefield dynamics and configurations during decay from full glacial conditions and as a result, this remains an area of limited understanding and knowledge. Nonetheless, the transition from local or regional to larger scale ice cover and back to local scale glaciation on the plateau can lead to a palimpsest landscape containing a range of geomorphological signatures.

2.4.2 Geomorphological signature of plateau icefields

A variety of erosional and depositional features can be produced by plateau icefields depending on thermal regime and the extent of ice cover. If these factors vary spatially and temporally, a complex glacial landsystem is created (Fig. 2.15). Recognition of landforms generated by plateau icefields is essential for accurate reconstructions of ice masses in formerly glaciated regions and these features will be discussed below with reference to their associated thermal regime.

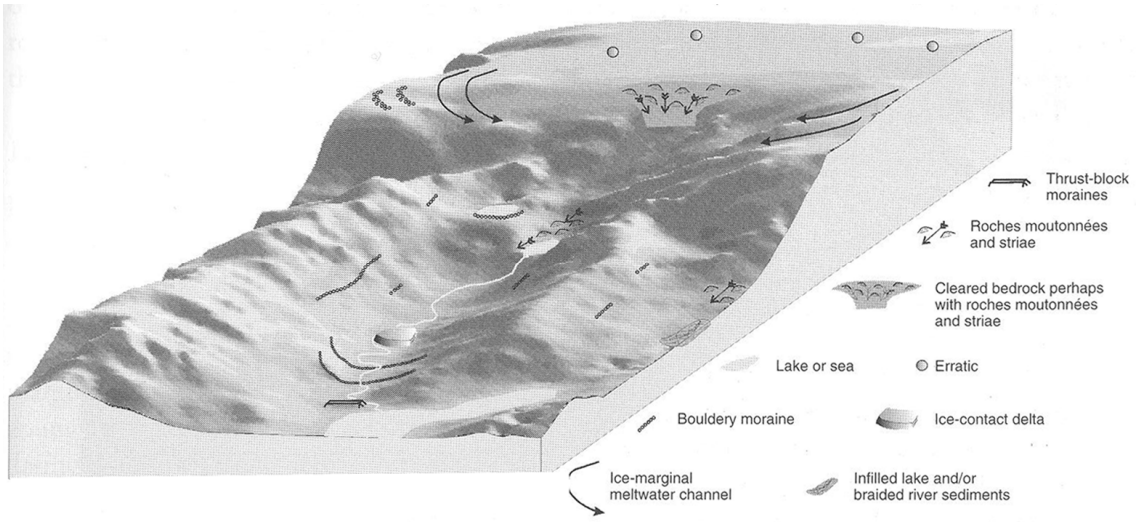

Figure 2.15. Schematic diagram illustrating the glaciogenic landforms produced by a plateau icefield landsystem. Taken from Rea and Evans (2003, p. 423).

Cold-based ice is non-erosive and ice movement is predominantly through ice creep (Benn & Evans, 2010) and therefore under this thermal regime the plateau ice leaves very little evidence

for its existence. This phenomenon is exemplified on plateaux in Norway, where it has been demonstrated that blockfields, felsenmeer, weathered bedrock and periglacial features have survived intact beneath cold-based plateau ice (Dahl, 1966; Whalley *et al*., 1981; Gellatly *et al.*, 1988; Kleman, 1994; Rea *et al*., 1996), which has been recently supported by SED (Stroeven *et al.*, 2002; Sugden *et al*., 2005; Phillips *et al*., 2006). The potential of cold-based plateau ice to preserve older features has resulted in many plateaux being interpreted as nunataks located above the upper surface of ice sheets in the past. For example, extensive work by C.K. Ballantyne in Scotland on the thickness of the last British-Irish Ice Sheet interpreted high-level weathering limits as periglacial trimlines that delineated the maximum altitude of the ice surface (*cf.* Ballantyne *et al*. 1998 and references therein). Recently, this work has been revised by numerous researchers, including Ballantyne (Phillips *et al*., 2008; Ballantyne & Hall, 2008; Ballantyne, 2010a), who demonstrated, using SED, that these trimlines may instead represent englacial thermal boundaries. The lack of clear geomorphological features relating to cold-based plateau ice is one of the major reasons why plateau icefields in the palaeoglaciological record are difficult to recognise and why in the past, an 'alpine' model of former glaciation has dominated, leaving former plateau icefields largely unrecognised (e.g. in the Lake District, *cf.* McDougall, 2001).

In the palaeoglaciological record, the only evidence for the occurrence of a former plateau icefield is often in the outlet valleys, as described below. However, lateral meltwater channels can occur at the margins of cold-based ice, where meltwater cannot flow subglacially since the ice is frozen to its bed and is therefore directed around the margins of the ice, incising lateral channels (England, 1986; Ó Cofaigh *et al*., 1999, 2003; Atkins & Dickinson, 2007). These meltwater channels can be found on the plateau itself and can also document the margins of ice flowing from the plateau into outlet valleys. If plateau ice was entirely cold-based, lateral meltwater channels may provide the only means of identifying the existence of a former plateau icefield (Dyke, 1993; Rea & Evans, 2003).

If ice on the plateau is cold-based, it may be able to reach PMP at the plateau margins, due to increased basal stress and strain heating, caused by an increase in bed gradient as the ice flows over the plateau edge, leaving erosional features, such as striated bedrock or roches moutonnées (Rea & Evans, 2003) (Fig. 2.15). The effects of strain heating and the juxtaposition of warm and cold-based ice are exemplified in work by Dyke (1993) on the Late Wisconsinan ice caps in the Canadian Arctic Archipelago. Dyke (1993) identified two landscape zones, a central zone, which exhibited very little glacial modification, and an outer zone containing erosional and depositional features, related to an icefield with a cold-based centre and a warm-based periphery. Under a static ice cap, the inner zone is usually warm-based, where ice is thickest

and the ice becomes cold-based as it thins towards the margins. Dyke (1993) related the reversed zonation found to a combination of lower air temperatures at higher altitude over the central zone and the effects of strain heating at the margins. He argued that in the central area the ice cap would have been cooled by the downward movement of cold firn and little to no horizontal flow, resulting in virtually no strain heating. Beyond the centre, as horizontal flow increased, along with strain heating, the effect of firn refrigeration would have been diminished, allowing the ice to reach PMP. Dyke (1993) also suggested that, since the central zone of no erosion was still present in the geomorphological record, the warm-based zone did not migrate inwards during deglaciation, signifying that retreat was likely to have been accompanied by an expansion of the cold-based ice towards the margins, potentially due to overall glacier thinning.

Predominantly warm-based plateau icefields are generally restrained to lower, larger plateau areas, such as Øksfjordjøkelen in Norway. Plateau ice at or above the PMP is able to erode the plateau surface and can remove pre-existing regolith or blockfields, leaving striated and streamlined bedrock and forming moraines on the plateau, as has been observed following the retreat of Øksfjordjøkelen (Gellatly *et al*., 1988). In some cases these erosional landforms can also be used as palaeo-flow indicators; ice flowing radially from the centre of the plateau indicates a former local icefield, whilst parallel suites of landforms signify larger scale ice sheet cover (Rea & Evans, 2003). Till cover on plateau surfaces is usually thin, however, due to relatively short distances over which plateau ice is able to erode and transport material (Rea & Evans, 2003).

Evidence of former glaciation in the outlet valleys is often similar to those for valley glacier landsystems, including, striated bedrock, streamlined bedforms, moraines, meltwater channels, erratics and glaciofluvial and glaciolacustrine sediments (Fig. 2.15). Careful assessment of the geomorphological evidence is therefore required to differentiate between valley and plateau icefield landsystems, where the majority of evidence may be constrained to the outlet valleys.

2.4.3 Implications of plateau ice on equilibrium line altitudes

Whilst a lack of evidence for plateau icefields often makes their identification in the palaeo-record difficult, the addition of plateau ice to glacier reconstructions has important implications for ELA calculations and therefore regional climate calculations. The contribution of ice from plateau icefields to glaciers in the surrounding valleys can significantly shift reconstructed ELAs to higher elevations due to the increase in ice volume at higher altitudes on the plateau. This upwards shift is therefore greater for larger areas of plateau ice and can also be exaggerated if a narrow gully connects the main valley to the plateau, as the difference in elevation between the plateau and the outlet valley will be greater (Rea *et al.*, 1999; Rea & Evans, 2003). Figure 2.16 shows the rise in altitudes for Accumulation Area Ratio (AAR) ELAs calculated for ice

masses when the contribution of plateau ice is included. The figure clearly demonstrates that the larger plateau areas will cause a greater rise in ELAs and this is most apparent for the more extensive Younger Dryas outlet glaciers.

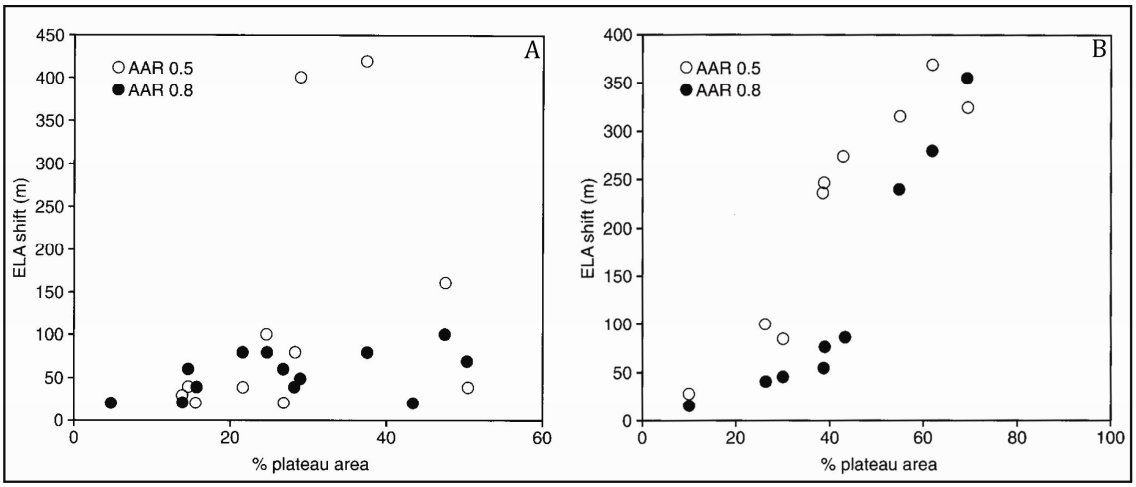

Figure 2.16. Altitudinal shifts in ELA as a function of the percentage of the plateau area to the total combined area, for accumulation area ratios of 0.5 and 0.8, for A) Little Ice Age maximum glaciers in Lyngen, Norway and B) Younger Dryas outlet glaciers in Øksfjordjøkelen, Norway. Taken from Rea and Evans (2003, pp. 429 & 431).

Rea *et al.* (1999) also demonstrated that the presence of plateau ice has a sustaining effect on outlet glaciers, where Fauldalsbreen and Goverdalsbreen in the Lyngen Alps, Norway, exist as substantial outlet valley glaciers, despite the whole of their valley components residing below the regional firn line. Rea *et al*. (1999) suggested that these outlet valley glaciers will respond rapidly to changes in climate, in that climate amelioration will cause plateau ice to shrink away from the plateau edges, resulting in detachment of the valley part of the glacier from its source area, leading to rapid ice decay, whilst small increases in winter precipitation and/or decreases in temperatures will allow outlet glaciers to expand rapidly. In the palaeoglacial record, McDougall (1998, 2001) argued that the sustaining effect of plateau ice allowed relatively extensive glaciers to exist in the Lake District during the Younger Dryas, providing a much simpler explanation than the three individual snowfall intensity zones concocted by Sissons (1980) to explain their erroneously low ELAs in comparison to other smaller ice masses in the region. The work by McDougall (1998, 2001) highlighted the importance of identifying plateau icefields in the palaeoglacial record and signified a significant move away from the alpine paradigm, towards an acknowledgement that plateau areas are likely to have provided significant source areas for many ice masses, despite evidence for their existence often remaining elusive.

2.4.4 Synthesis

Current literature on modern plateau icefields is at present restricted to a relatively small number of studies mainly in Norway and Arctic Canada. However, this work has established

the plateau icefield as an individual glacial landsystem with its own unique geomorphic signature, identified the role of cold-based ice in the preservation of pre-existing landforms, and observed the sustaining influence of plateau ice on the existence of outlet valley glaciers (*cf.* Rea & Evans, 2003).

However, these studies have predominantly focussed on establishing the characteristics of contemporary plateau icefields and/or their retreat from Little Ice Age or Younger Dryas positions (Gellatly *et al*. 1988; Evans, 1990; Rea *et al*. 1998; Evans *et al*. 2002). There are still very few palaeoglaciological studies (e.g. Dyke, 1993; McDougall, 2001; Fjellanger *et al*., 2006; Vieira, 2008; Brown, 2009) that have recognised the presence plateau icefields in currently unglaciated regions, despite an increased awareness of plateau icefields. In addition, and to an even greater extent, the dynamics of such palaeo-icefields have been very much neglected, with respect to spatial and temporal changes in thermal regime (*cf.* Dyke, 1993; Fjellanger *et al*., 2006), debris transport pathways (*cf.* Evans, 2010), ice divide migration and retreat dynamics. Therefore despite large advances in our understanding of plateau icefields during the 1990s and early 2000s, plateau icefield dynamics still remain relatively unknown, compared to those of other glacial landsystems.

2.5 Chapter Summary

This chapter has described the physical characteristics of the Monadhliath Mountains and has reviewed the literature pertinent to the study area. The limited and fragmented nature of previous Quaternary research in the region highlights the current lack of a clear chronostratigraphical framework within which to frame glacier fluctuations, retreat patterns and dynamics. In order to rectify this situation, it is apparent that a more systematic approach to geomorphological mapping, alongside the use of relative and absolute dating techniques is required. Following major shifts away from the ice stagnation and alpine glaciation paradigms, due to increases in our understanding of ice sheet and plateau icefield dynamics, a re-interpretation of the geomorphological evidence previously examined is also likely to be necessary.

In particular, the relative inactivity of plateau icefields and paucity of geomorphological evidence has previously led to substantially less research attention on this glacier system than others, resulting in a more limited understanding. A corollary of this is that the presence of plateau ice during ice sheet deglaciation and within smaller ice mass reconstructions has often been previously neglected, leading to erroneous glacier reconstructions and palaeoclimate calculations (e.g. Sissons, 1980; Ballantyne, 1990). Furthermore, limited knowledge on the interaction of plateau ice with regional ice during deglaciation and the dynamics of the plateau icefield system itself during retreat hinders both our understanding of former ice sheet retreat patterns and has

implications for our understanding of the future behaviour of modern plateau icefields (e.g. Giesen & Oerlemans, 2010). The Monadhliath Mountains therefore provides an important study area in which to firstly investigate the role of plateau ice in the region during the LGIT, and secondly, to examine the dynamics of such ice. The following chapter will describe the methods used to elucidate these broader problems/questions.

Chapter 3

Methods

This chapter describes the methods used in this research to address the objectives and significant knowledge gaps identified in Chapters 1 and 2. The key methods were geomorphological mapping, through remote sensing and field mapping, and sedimentological analysis. Details of additional methods used for further analysis of the geomorphological evidence such as morphostratigraphy, 2D glacier profile modelling, equilibrium line altitude and palaeoprecipitation calculations are not included in this chapter since they relate to the interpretation of geomorphological evidence described in Chapter 4 and are therefore described in the appropriate sections within Chapter 5. The following two sections now discuss the approaches used for geomorphological mapping and sedimentological analysis in detail.

3.1 Geomorphological Mapping

The main approach used was geomorphological mapping, since this provided a means of assessing the glacial geomorphology of the region systematically. The mapping was carried out using a combination of remotely-sensed data and fieldwork to provide a holistic approach to data collection and landform identification. The aim of the geomorphological mapping was to produce a detailed geomorphological map as one of major products of the research that would 1) address the issues arising from a previously fragmented approach to research as outlined in Chapter 2, 2) enable reconstruction of ice masses relating to the LGIT, and 3) allow an examination of glacier retreat dynamics.

Geomorphological mapping is a fundamental tool for assessing the characteristics of a particular landscape and the processes that have shaped the landscape (Hubbard & Glasser, 2005). As a consequence, the analysis of geomorphological evidence has been used as an approach for reconstructing former ice masses for over 150 years (e.g. Barrow *et al*., 1913; Hinxman & Anderson, 1915; Sissons, 1974b, 1979a; Ballantyne, 1989; Clark *et al*., 2006; Coleman & Carr, 2008; Livingstone *et al.*, 2008, 2010a, b, 2012; Lukas & Bradwell, 2010; Carr *et al*., 2010; Clark *et al*., 2010; Finlayson *et al*., 2011). More recently, geomorphological evidence has been used as an important constraint for numerical models (e.g. Hubbard, 1999; Gollege & Hubbard, 2005; Gollege *et al*., 2008; Evans *et al*., 2009). Geomorphological data is usually recorded on a geomorphological map, both as a means of presenting the data and in order to assess the spatial relationships between features. Varying approaches to geomorphological mapping have developed over time and are described below, focusing on developments in glacial geomorphological mapping in Britain.

Traditionally, geomorphological mapping has been undertaken through intensive field mapping (e.g. Close, 1867; Goodchild, 1875; Kendall, 1902; Trotter, 1929; Hollingworth, 1931; Raistrick, 1933; Rose & Letzer, 1977; Mitchell & Riley, 2006). This field mapping provided information on glacier flow directions from erratic trains (e.g. Peach, 1909; Hinxman *et al*., 1923), erosional features (e.g. Peach & Horne, 1981; Hinxman & Anderson, 1915; Wilson *et al*., 1935) and subglacial bedforms such as drumlins (e.g. Hollingworth, 1931; Rose & Letzer, 1977; Mitchell & Riley, 2006), alongside evidence for maximum ice positions, stillstands and retreat patterns (e.g. Hinxman & Anderson, 1915; Benn, 1989; Benn *et al*., 1992; Lukas & Benn, 2006).

The widespread availability of aerial photography since the 1950s has provided consistent aerial views of surface topography and aided geomorphological mapping by providing data for areas that were otherwise inaccessible or difficult to map on foot. Field mapping is often combined with mapping from aerial photographs, which has resulted in a number of detailed maps on the glacial geomorphology of discrete areas in Britain (e.g. Wilson & Evans, 2000; Benn & Ballantyne, 2005; Lukas & Lukas, 2006a, b; Sahlin & Glasser, 2008; Brown *et al*., 2011). However, the time-consuming nature of detailed field and aerial photograph mapping has meant that in the past many areas in Britain were subject to more rapid aerial photograph mapping in order to cover larger areas (e.g. Sissons, 1974b, 1977b).

The development of satellite-based remote sensing in the 1970s and subsequent advances in remote sensing technologies, have enabled time-efficient and cost-effective geomorphological analysis of large areas at increasingly higher resolutions. A further advantage of satellite imagery is its digital format, which enables surface morphology to be investigated over a range of scales and has been particularly advantageous for identifying landform patterns over large areas that may be indistinguishable within the field or at larger scales (Clark, 1997). As a result, remote sensing has revolutionised the way formerly glaciated landscapes are viewed and understood, and has been at the forefront of new conceptual models, such as changes in ice sheet flow direction over time, ice marginal asynchroneity and the preservation of older landforms (e.g. Boulton & Clark, 1990; Clark, 1997; Salt & Evans, 2004; Stokes *et al*., 2008; Livingstone *et al*., 2008; Hughes *et al*., 2010).

However, despite these advances, research on the British-Irish Ice Sheet (BIIS) has lagged behind that of the Fennoscandinavian and Laurentide ice sheets (Evans *et al*., 2005). Although all three approaches to geomorphological mapping have produced a large amount of information on many glacial features, there are still areas in Britain, such as the Monadhliath Mountains, that have not been mapped systematically in any detail (Section 2.3). In addition, the quality of

the information available at present varies over different areas and has often been moulded by the key academic paradigms at the time of mapping, causing difficulties in the integration of datasets produced by different authors over varying timescales, as exemplified by previous research in the study area (Section 2.3) (*cf.* Clark, 1997; Evans *et al*., 2005; Clark *et al*., 2004; 2006; Greenwood *et al*., 2007).

Consequently, the BRITICE project was initiated to re-invigorate glacial geology and geomorphology-based studies in Britain (Clark *et al*., 2004; Evans *et al*., 2005). This coincided with the addition of the NEXTMap Great Britain™ (NEXTMap from hereon) dataset to the pool of remotely-sensed imagery, following its original commission for Norwich Union in 2003 (NEODC, 2012). This data has contributed significantly since this time to our understanding of the palaeogeography of the BIIS due to its high spatial resolution (5 m) and widespread availability. NEXTMap, alongside other forms of remote sensing and field mapping, has facilitated some progress towards reducing variations in previous research and has enabled new maps of subglacial bedforms and retreat patterns of the last BIIS and Younger Dryas ice masses to be produced (e.g. Bradwell *et al*., 2007; Golledge, 2007; Greenwood & Clark, 2008; Livingstone *et al*., 2008, 2010a, b; Sahlin & Glasser, 2008; Hughes *et al*., 2010; Clark *et al*., 2010; Finlayson *et al*., 2011;).

As implied above, geomorphological mapping has a long tradition of using a combined approach of remote sensing and field mapping (e.g. Young, 1978; Sissons, 1979a; Ballantyne & Wain-Hobson, 1980; Sissons & Cornish, 1983; Benn & Ballantyne, 2005; Lukas & Lukas, 2006a, b; McCormack *et al*., 2008; Brown *et al*., 2011; Finlayson *et al*., 2011). Following this approach, research in this PhD was carried out through field mapping and two sets of remotely sensed data: NEXTMap and aerial photographs. These approaches are described in detail below.

3.1.1 Field mapping

Field mapping involves walking across the area to be mapped and recording landforms onto a topographic base map, usually at a scale of 1:10,000 (Mitchell & Riley, 2006; Rose & Smith, 2008). The starting point of most field maps is to draw in breaks of slope (Savigear, 1965), which often need to be viewed from several perspectives in order to be accurately represented on the map (Mitchell & Riley, 2006). This is referred to as a *morphological* map, which describes the morphology of the landscape, but with no interpretation. Once a morphological map of the main breaks of slope has been created, more detail can be added within this framework and by interpreting features, to produce a *geomorphological* map (Mitchell, 1991). Often, however, the process is not as 'artificial' as described above and primary landforms are

grouped and interpreted at an early stage of mapping, at least subconsciously. There is no standard key for geomorphological maps, with authors usually creating their own codes (e.g. Mitchell, 1991; Lukas & Lukas, 2006a, b; Evans *et al.*, 2006a; Sahlin & Glasser, 2008; Lovell *et al*., 2011), although the symbols for some features such as breaks of slope and meltwater channels usually remain very similar (Hubbard & Glasser, 2005).

The accuracy of field maps, alongside being guided by the skill of the cartographer to place landforms in the correct position and at the right orientation and scale, is also a function of the map scale. A pencil line has a thickness of between 0.2 and 0.5 mm on a field map and will therefore represent a thickness of between 2 and 5 m on a 1:10,000 scale map, rendering the map accurate to this level only. This means that not all the information that can be seen in the field can be mapped, even at a large scale such as 1:10,000 and therefore some element of generalisation is required. The level of generalisation is very subjective and again, often determined by the skill of the cartographer (Dorling & Fairbairn, 1997).

In this study fieldwork was undertaken over two field seasons in 2009 and 2010 for a total of 12 weeks. The field maps were drawn at a scale of 1:10,000 onto enlarged photocopied 1:25,000 Ordnance Survey (OS) topographic maps (Fig. 3.1). Features such as moraines, meltwater channels, outwash terraces, alluvial fans, river terraces, exposed bedrock, rock slope failures (RSF), prominent erratics, breaks in slope and periglacial features, were mapped onto the topographic maps. The location of features was guided by 'landmarks' such as river bends, confluences and large mounds or ridges that could be identified using contours on the OS maps. A Garmin eTrex Venture HC handheld GPS, with an accuracy of ± 3 m, was used occasionally to verify locations. Reconnaissance maps derived from NEXTMap were also consulted during the field mapping in order to both verify the position and scale of landforms, and to make sure features identified remotely were not missed in the field, particularly where the genetic interpretation of a landform was ambiguous on NEXTMap. The following sections give a background to the remotely-sensed information used in part to aid this field mapping.

3.1.2 DEM-based mapping

The NEXTMap dataset was acquired by Intermap Technologies between 2002 and 2003 using airborne interferometric synthetic aperture radar (IFSAR). IFSAR works by sending out a pulse of microwave energy and then recording the return signal. Two parallel antennae are attached to the underside of the survey aircraft, which send out a signal obliquely rather than vertically downwards. Both the time taken for the signal to return and the nature of the echo are recorded independently (Clark, 1997; Intermap Technologies, 2004). Waves arriving at the two antennae, A and B, are often out of phase due to the waves striking the antennae independently.

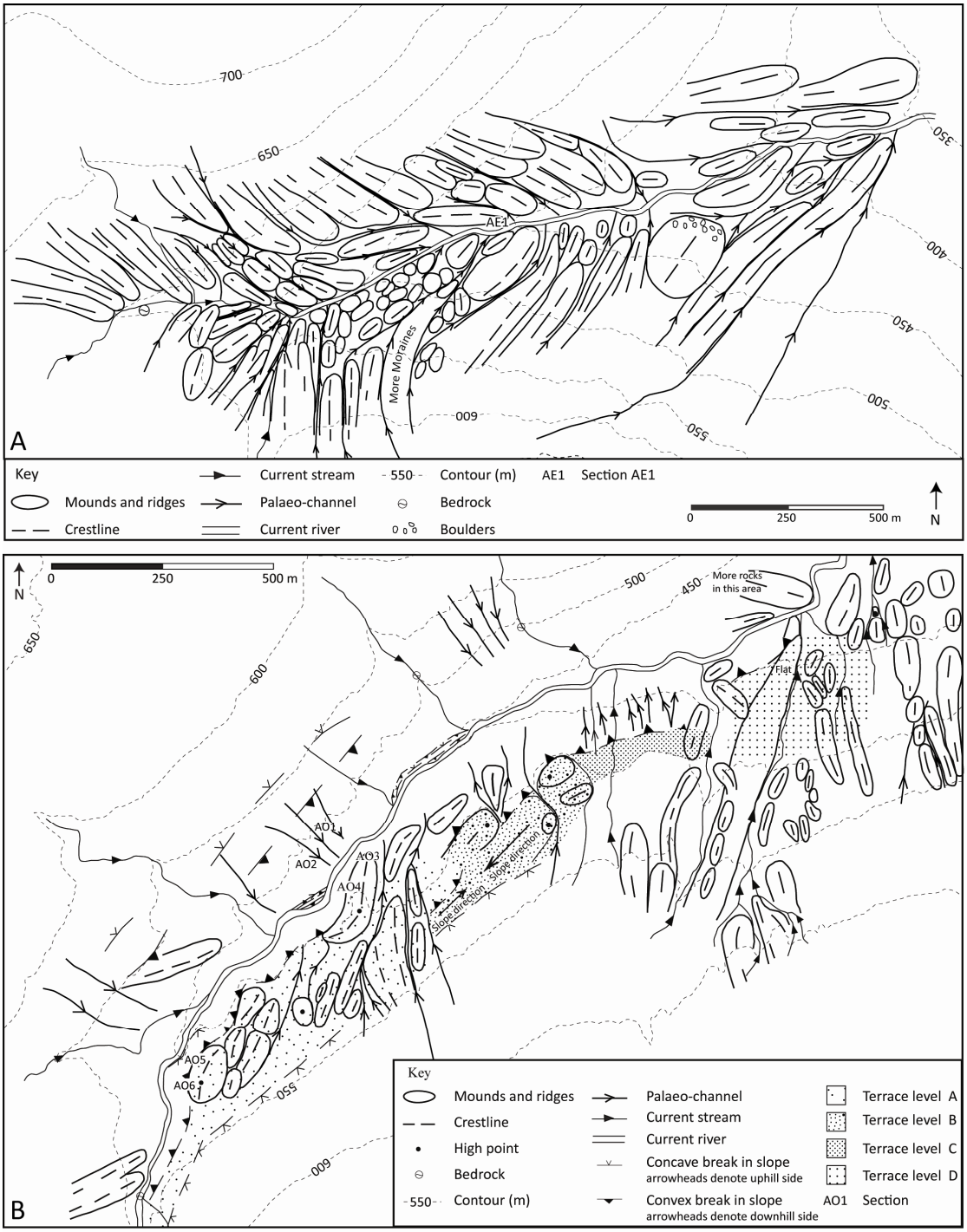

Figure 3.1. Digitised versions of two geomorphological maps drawn in the field for: A) Coire Easgainn, B) Glen Odhar.

This resultant phase difference is used alongside the independent topographic information from each antenna to obtain the altitude and x, y coordinates of the target, where the return signals are digitally combined to artificially enhance the resolution of the image (Intermap Technologies, 2004).

Several products are available within the NEXTMap dataset, but the three core products are the orthorectified radar image (ORI), the digital surface model (DSM) and the digital terrain model (DTM) (Fig. 3.2). The ORI is a greyscale image that is visually similar to that of a black and

white aerial photograph. The image has a pixel size of 1.25 m and a horizontal accuracy of 2 m root mean square error (RMSE) (Table 3.1; explanation below). Roads, field boundaries, rivers and lakes can be clearly identified on the ORI image and due to the oblique viewing angle of the sensor, shadows are created, allowing variations in elevation to be visually detected (Intermap Technologies, 2004). However, in areas of low textural contrasts, geomorphological features such as moraines can be hard to distinguish (Chen & Rose, 2008).

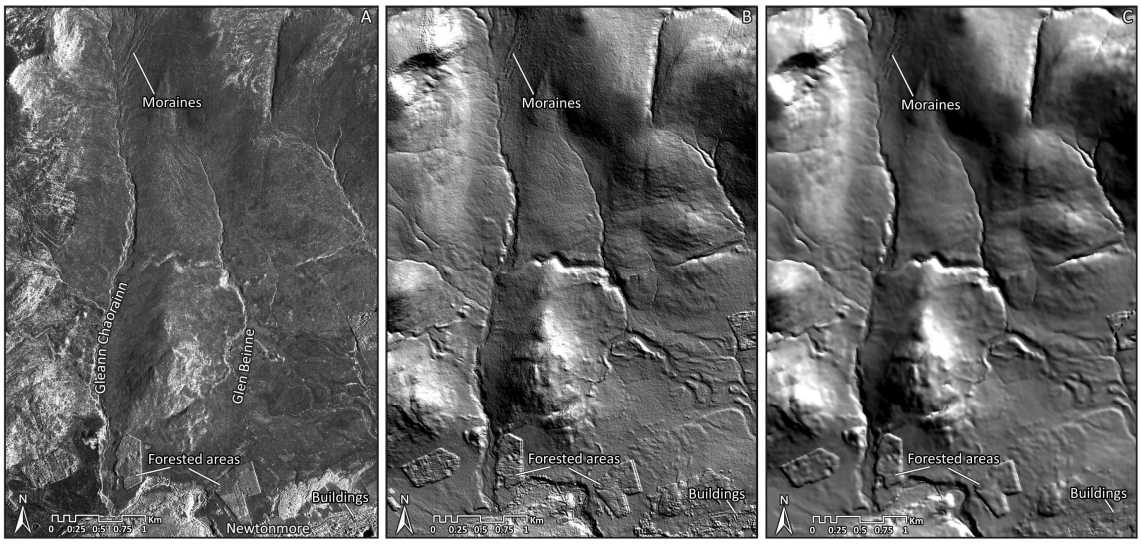

Figure 3.2. Example of the A) ORI, B) DSM and C) DTM products from the NEXTMap dataset, where the DSM and DTM products are shown as relief-shaded models. The images show the northern edge of Newtonmore, Gleann Chaorainn and Glen Beinne in the southeast of the study area. Moraines are clearly visible towards the top of Gleann Chaorainn on the ORI and DSM, but are less visible on the DTM. Trees and buildings have been removed to an extent on the DTM, but their boundaries are still clearly visible. NEXTMap ORI, DSM & DTM from Intermap Technologies Inc. provided by NERC via the NERC Earth Observation Data Centre.

Table 3.1. A) Pixel size and horizontal accuracy (RMSE and CE(95)) for the NEXTMap ORI product, where CE(95) = circular error and denotes the radial distance within which 95% of the errors occur. B) Spatial resolution and vertical errors associated with the DSM and DTM NEXTMap products, where 95% denotes the vertical distance within which 95% of the errors can be found. Intermap Technologies (2004) and NEODC (2012).

A	Product	Pixel Size (m)	RMSE (m)	CE (95) (m)
	ORI	1.25	2	4

B	Product	Spatial resolution (m)	RMSE (m)	95% (m)
	DSM	5	1	2
	DTM	5	1	2

The DSM provides a geo-referenced topographic model of the earth's surface and represents the first surface that the radar strikes, thereby including buildings, vegetation and roads (Fig. 3.2). The spatial resolution is 5 m and the image has a vertical accuracy of 1 m RSME (Intermap Technologies, 2004; NEODC, 2012) (Table 3.1). The DTM is also a geo-referenced topographic model, but features such as buildings and trees have been digitally removed to leave a representation of the bare earth only (details of this process are described later in this

section) (Fig. 3.2). The DTM also has a spatial resolution of 5 m and a vertical accuracy of 1 m RMSE (Intermap Technologies, 2004; NEODC, 2012) (Table 3.1).

Table 3.1 displays the specifications for the ORI, DSM and DTM. These specifications compare favourably with other DEMs, such as Landmap, OS Panorama®, OS Profile® and LiDAR (Light Detection and Ranging), where NEXTMap possesses the second highest spatial resolution and vertical accuracy, second only to LiDAR. Intermap Technologies specifies the vertical accuracy of the DSM and DTM products and the horizontal accuracy of the ORI using statistical measures. The accuracies they present represent the upper limit based on moderately sloped terrain and therefore the errors on steeper topography, such as in the Monadhliath Mountains, may be greater due to a number of artefacts, which are discussed further below.

The RMSE is the standard error normally quoted by the mapping industry (Dorling & Fairbairn, 1997; Intermap Technologies, 2004). However, the 95%, 90% and 68% confidence levels, which are often associated with the RMSE, cannot be used unless the mean error is equal to zero. Experiments by Intermap Technologies found that the mean error was often offset from zero, and that the errors were not normally distributed. Therefore Intermap Technologies not only report the RMSE, but also the 95% confidence level. For example, the DSM is quoted as having 1 m vertical accuracy RMSE, but a 95% confidence level of 2 m, meaning that 95% of the vertical errors will be within 2 m of the actual elevation value. Similarly, for the ORI, 95% of the x or y errors are within a 4 m radius (Intermap Technologies, 2004) (Table 3.1).

The DSM and DTM have no fixed illumination and therefore an exhaustive number of viewing images can be created by varying the direction (azimuth) and elevation angle of the light source through the relief-shading model (Chen & Rose, 2008). This gives it a large advantage over satellite imagery such as Landsat, which has a fixed illumination. Changing the direction of the light source allows different features to be accentuated (Smith & Clark, 2005). The solar elevation angle also has a significant effect on the relief-shaded image produced. High illumination angles highlight lee slopes and produce limited textural and tonal variation, whilst low illumination angles produce large shadows, concealing lee slopes. An angle of 30° is recommended by several authors as a balance between the two extremes, where the shadows are used to enhance topographic features (Chen & Rose, 2008; Hughes *et al*., 2010). Hughes *et al.* (2010) also suggest using a vertical exaggeration of four or five times in order to enhance features further.

Whilst the ability to alter the illumination direction on the relief-shaded model is one of the great advantages of NEXTMap, the selection of the illumination direction also introduces bias.

The selection of a light source direction that is the same as the direction of the lineaments will suppress them. Conversely, lineaments that are perpendicular to the light source will be enhanced (Clark & Meehan, 2001; Smith & Clark, 2005; Smith & Wise, 2007; Hughes *et al*., 2010; Brown *et al*., 2011) (Fig. 3.3). This can also sometimes over-emphasise the apparent size of some features, creating 'artificial' lineaments (Smith & Clark, 2005). In order to restrict this azimuth biasing, Smith and Clark (2005) recommend that each area should be viewed using at least two illumination directions, with one parallel and one perpendicular to the main lineament direction. Hughes *et al*. (2010) also recommend the use of a relief-shaded model with the sun angle overhead at 90º.

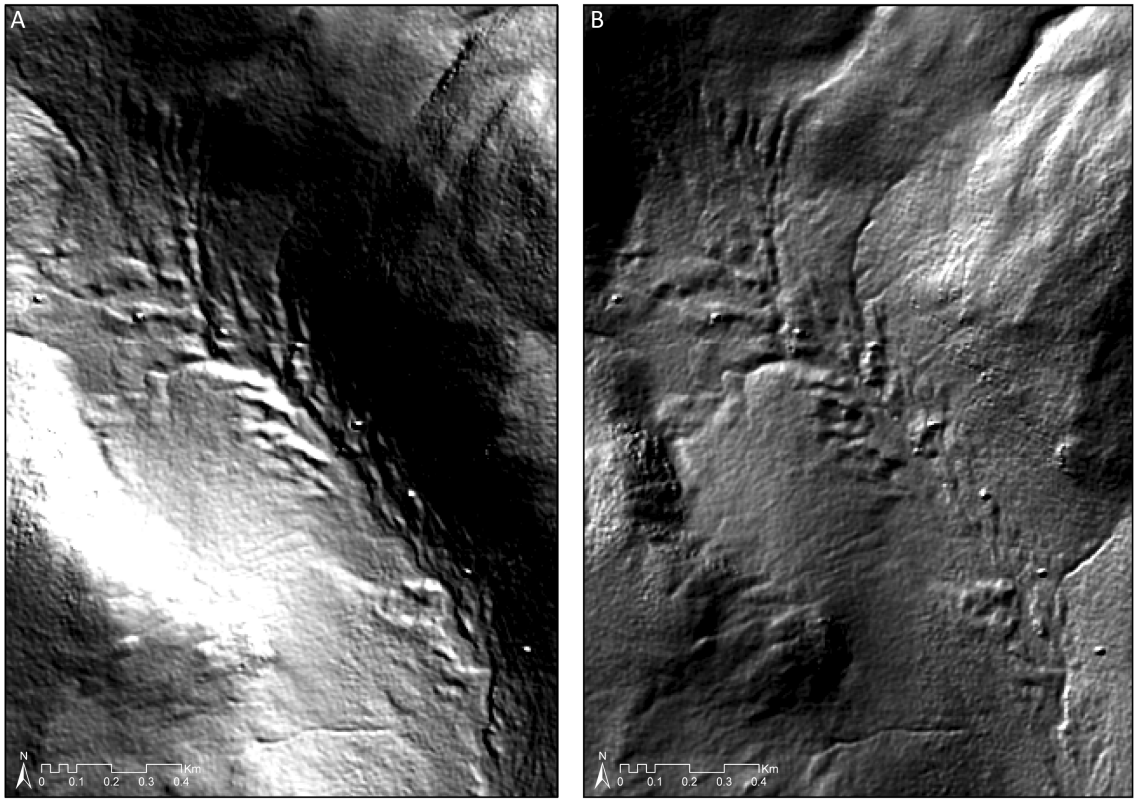

Figure 3.3. Relief-shaded models from the NEXTMap DSM showing Corrie Yairack in the study area using azimuths of A) 45° and B) 315°. The two models demonstrate the significant differences in the appearance of landforms in the valley when the artificial illumination is set at different directions. NEXTMap DSM from Intermap Technologies Inc. provided by NERC via the NERC Earth Observation Data Centre.

Both the DSM and DTM can also be used in surface analysis applications within ArcGIS, to calculate slope angle, aspect, contours and area, and to identify watersheds, which were all used in later analysis in this research. However, a number of artefacts and other factors affecting accuracy have to be taken into account when dealing with these data sources and are considered in detail below.

Artefacts

Artefacts occur within an IFSAR image due to the way the data is collected. These can be classified as 'geometric', 'sensor' and 'phase unwrap' types. Geometric artefacts are particularly common in mountainous areas, such as the Monadhliath Mountains, and are therefore described in more detail (Fig. 3.4). Foreshortening will occur in mountainous areas due to the oblique viewing angle of the sensor. This is because the radar will reach a point on higher terrain earlier than if that point had the same x and y coordinates at a lower elevation. This causes the length of the foreground slope to become compressed, whilst causing background slopes to be lengthened (Clark, 1997) (Fig 3.4a). Layover is a severe form of foreshortening in which the mountaintops become incorrectly positioned in relation to their base due to the tops of the mountains being closer to the sensor than the low ground in front of them (Intermap Technologies, 2004) (Fig 3.4b). Foreshortening and layover in NEXTMap products are corrected during the orthorectification process by stretching high terrain back into the correct position. This can cause a blurred region where the stretching has occurred (Intermap Technologies, 2004) and this is visible on some steep slopes in the study area (Fig. 3.5).

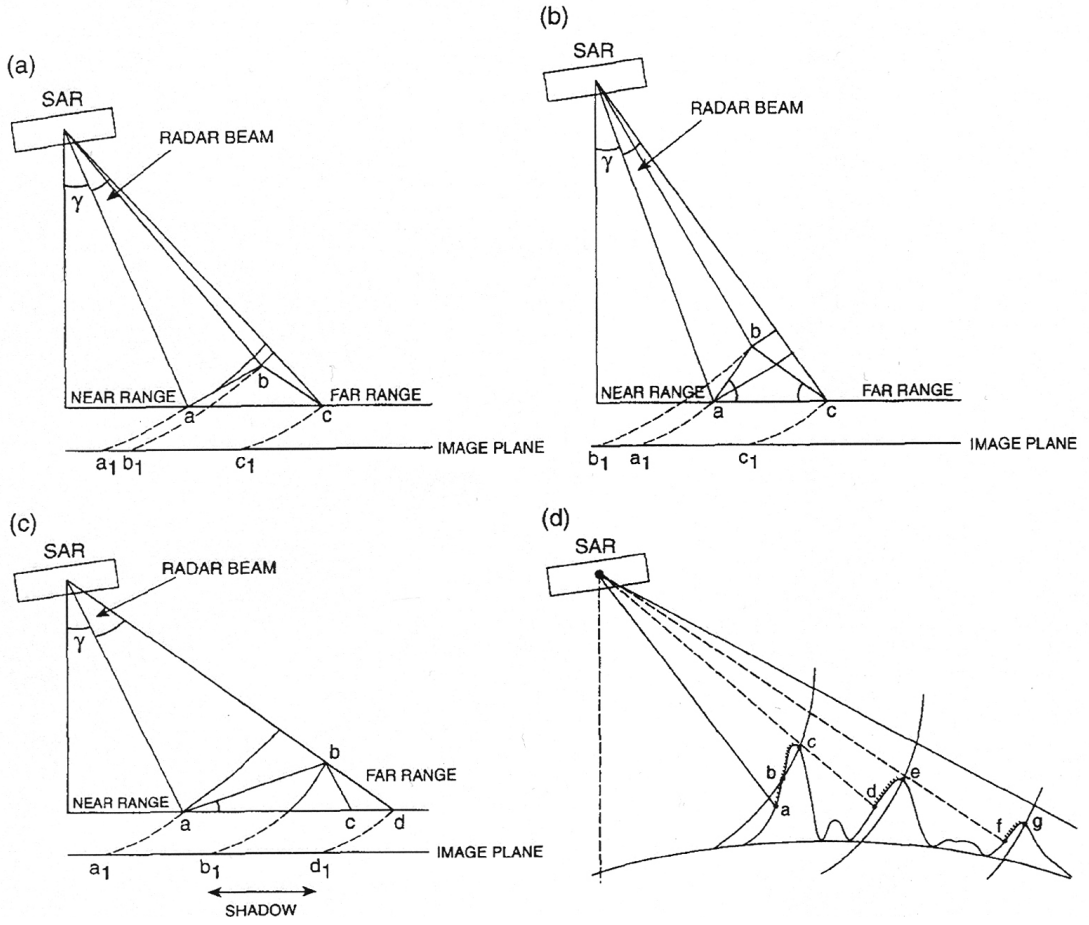

Figure 3.4. Geometric artefacts that are associated with IFSAR data acquisition and are particularly common in mountainous environments: (a) Foreshortening – ab becomes compressed to a1b1, whilst bc becomes lengthened to b1c1; (b) Layover – b1 becomes position incorrectly compared to a1; (c) Radar shadow – Location c is not recorded due to shadow between b and d; (d) Over a mountainous region of varying terrain, a combination of foreshortening, layover and radar shadow will occur. Taken from Clark (1997, p. 1082).

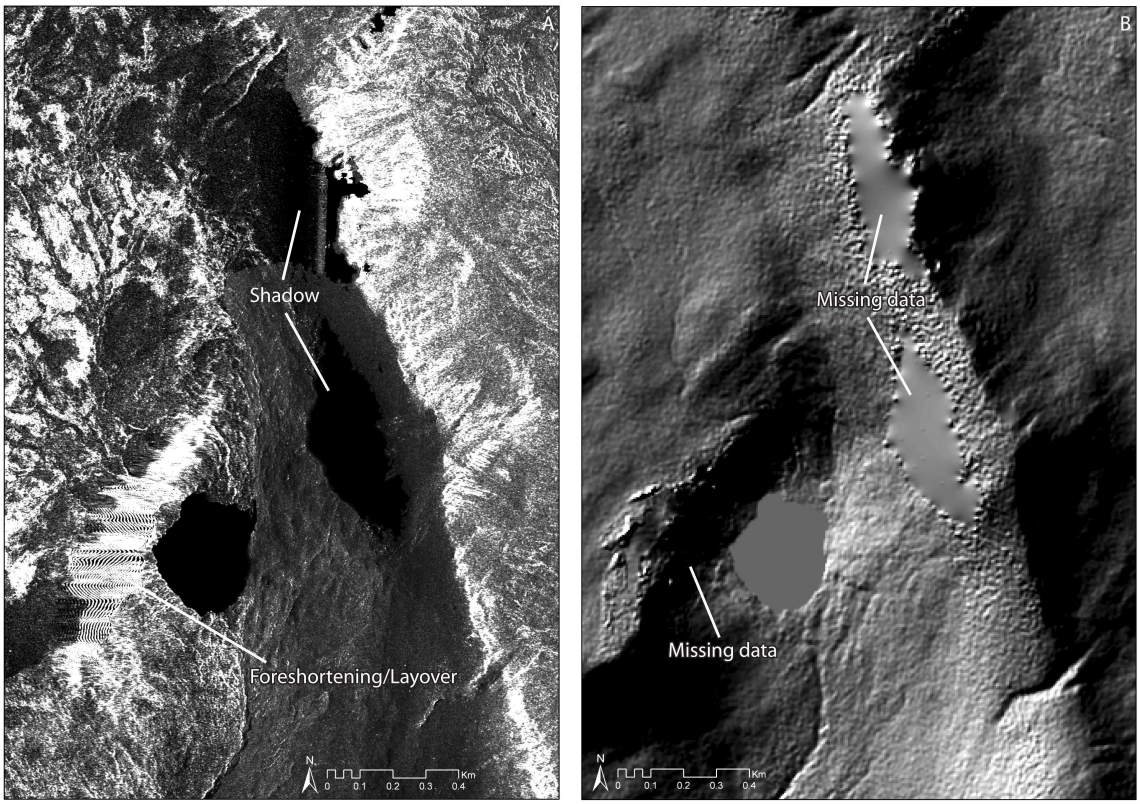

Figure 3.5. A) ORI and B) DSM NEXTMap products centred on Loch Dubh at the head of Gleann Lochain, demonstrating the loss of data due to the effects of shadow and either foreshortening or layover on steep slopes in the study area. NEXTMap DSM from Intermap Technologies Inc. provided by NERC via the NERC Earth Observation Data Centre.

In other parts of mountain areas, information will be lost on the leeside of slopes, away from the sensor, where high ground prevents the radar beam from reaching the lower ground beneath it (Fig. 3.4c). Larger radar shadows will occur in the far range of the sensor than in the near range, due to the oblique viewing angle (Campbell, 2002). Although additional data can be added when all the geometric information is merged, sometimes the shadowed area will remain as a void dark area on the image. This effect is found to varying degrees on some of the steep slopes in the Monadhliath Mountains (Fig. 3.5).

Factors affecting accuracy

The surface representation at a particular location on the DSM is a combination of all the elevations within a square footprint (radar 'integration footprint') that is about 50% larger than the 5 m posting. Therefore the DSM will not represent features of different elevations that are smaller than this spacing, such as a tree or a ditch, since their elevation will be combined with other elevations within this square (Intermap Technologies, 2004). This means that glaciogenic features such as very small moraines, river terraces, kettle holes, erratics, trimlines and meltwater channels may not be seen or easily identified from the DSM, as observed by several authors (e.g. Smith *et al*., 2006; Hughes *et al*., 2010; Brown *et al*., 2011). Therefore, although NEXTMap and other airborne and satellite imagery have had a large impact on

geomorphological mapping at the small and intermediate scales, they have not been able to fully supersede aerial photograph and field mapping at larger scales. These latter methods still possess higher spatial resolutions and are therefore invaluable for detailed geomorphological mapping (Hubbard & Glasser, 2005).

Trees and vegetation should be digitally removed in the production of the DTM, but an area of trees that has a radius of greater than 50 m in all directions will not be removed. This is because the software used to do this samples what it believes to be bare earth elevations from points within and around the trees. If the trees are too densely spaced and/or cover too large an area, the software will use lower parts of the canopy to derive an incorrect bare earth elevation (Intermap Technologies, 2004). As a result, the DTM often performs poorly in forested areas (Dowman *et al.*, 2003) and this was apparent in many areas in the study area (e.g. Fig. 3.2).

Mapping from NEXTMap

NEXTMap provided an important tool for the initial geomorphological assessment of the Monadhliath Mountains. The whole region covers an area of about 1500 km^2 and therefore NEXTMap was extremely valuable for reconnaissance mapping of the region. The ability to instantaneously alter the viewing scale from small- (<1:50,000) to medium- (1:10,000 – 1:50,000) to large-scale (1:5,000 – 1:10,000) allowed for a very flexible approach to mapping and enabled localised, detailed mapping to be placed within a regional context, as well as maintaining a systematic mapping approach (*cf.* Clark, 1997).

The DSM was used rather than the DTM as the majority of the study area was not forested. A few areas of trees occur, such as in Glen Buck and Coire an t-Sìdhean, but they were often still visible on the DTM due to the dense cover of trees and therefore the DTM was not any more useful for identifying glaciogenic features in these areas than the DSM. As a result it meant that these areas could not be mapped with great confidence using NEXTMap. The DSM was visualised using a relief-shaded model with a sunlight angle set at 30º, as recommended by Chen and Rose (2008) and Hughes *et al.* (2010). Since there was no main lineament direction, up to six azimuths were used (0°, 45°, 135°, 180°, 225°, 315°), with the dominant two being 45° (NE) and 315° (NW). The effects of foreshortening, layover and shadow meant that it was difficult to identify features on or at the base of a number of steep valley sides, but in general these artefacts did not cause too many problems for landform identification.

Mapping using NEXTMap was undertaken in *ESRI ArcMap*, using the Editor toolbar to create sets of polylines and polygons, each representing a different geomorphological feature (Fig. 3.6). NEXTMap was particularly useful for identifying large meltwater channels,

moraines, outwash terraces and river terraces, alongside bedrock structure. This mapping facilitated the identification of key research locations to be focused on in the field and using aerial photographs. However, as discussed above, it was found that smaller moraines and river terraces, could not be easily depicted in NEXTMap, due to both the coarseness of the resolution and often also azimuth biasing (Fig. 3.6E), since the exact shape of a feature was frequently unclear.

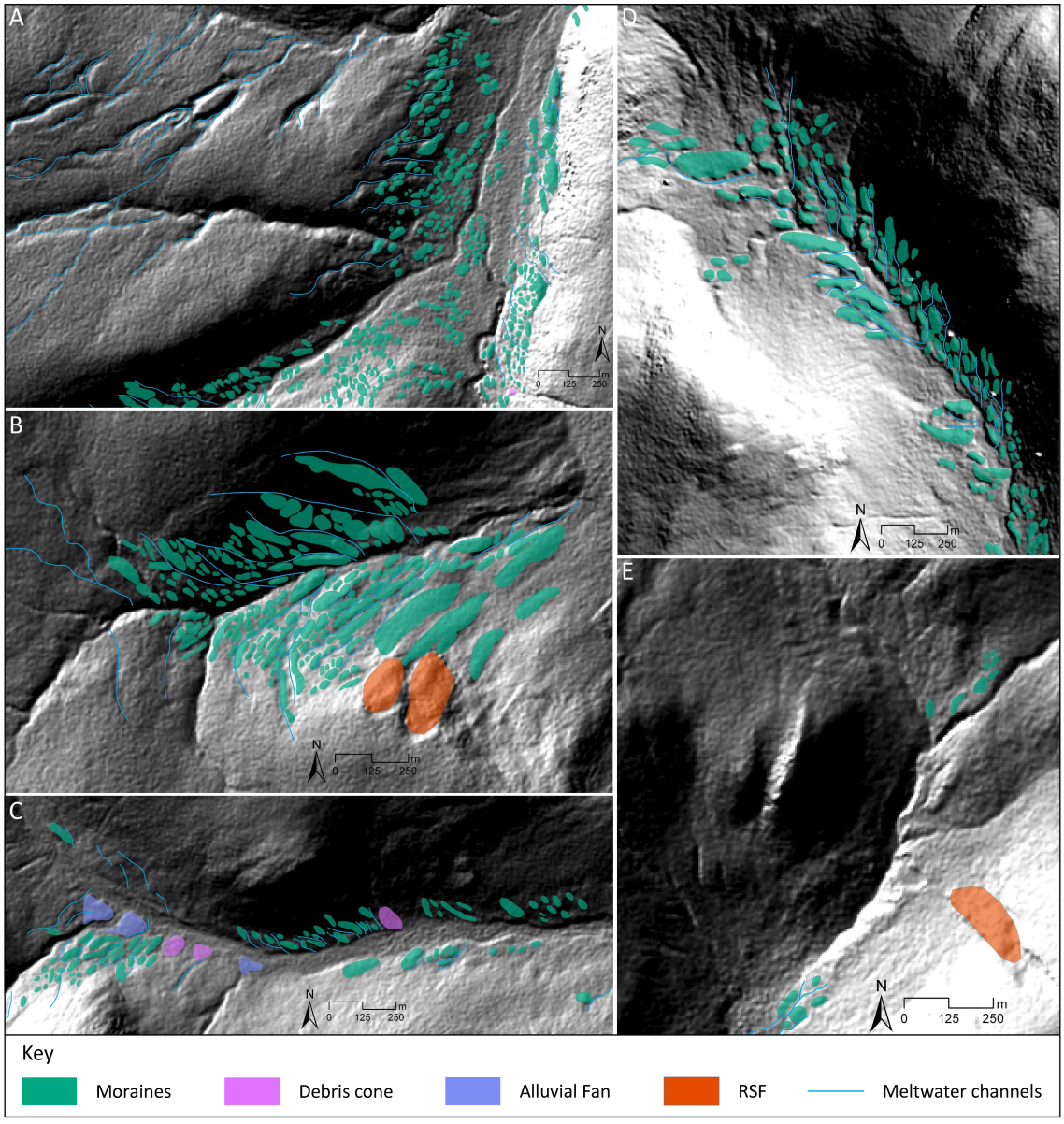

Figure 3.6. Examples of mapping produced using relief-shaded models created from the NEXTMap DSM in: A) the upper part of the Findhorn Valley, B) Coire Easgainn, C) Gleann Madagainn, D) Corrie Yairack, E) Gleann Fionndrigh. A) illustrates how meltwater channels were very visible from the relief-shaded model. Other features such as rock slope failures (RSF), alluvial fans and large debris cones were also identifiable from the DSM. However, whilst larger moraines were clearly recognisable within some valleys, E) demonstrates that although moraines were found in Gleann Fionndrigh during field mapping and the topography on the relief-shaded model appears mounded, only the larger moraines could be mapped with confidence, since the 5 m NEXTMap resolution restricted precise positioning of many of the smaller, closely spaced moraines. The spatial pattern of these moraines is shown within Figure 3.8. NEXTMap DSM from Intermap Technologies Inc. provided by NERC via the NERC Earth Observation Data Centre.

3.1.3 Aerial photographs

Aerial photographs have a sufficiently high spatial resolution (1-4 m; Smith *et al*., 2006) that many small glaciogenic landforms can be recognised and they are therefore still used extensively for large-scale mapping (e.g. Jansson, 2005; Lukas, 2005a; Lukas & Lukas, 2006a, b; Sahlin & Glasser, 2008; Brown *et al*., 2011). Two types of aerial photograph exist, oblique and vertical. The latter, where the camera axis is positioned vertically, are predominantly used for geomorphological mapping and are focused on here. Photographs are taken as a series of parallel strips, which usually have an endlap of 60%, with flight paths overlapping sideways by about 30-40% (Lillesand *et al*., 2008). This enables pairs of photographs (stereopairs) to be viewed in stereo, which eases the identification and interpretation of landforms in the photograph (Hubbard & Glasser, 2005; Lillesand *et al*., 2008). The stereoscopic effect is caused by the two different viewing angles of the same area (known as parallax) and can be seen using a stereoscope (Lillesand *et al*., 2008). Vertical heights within the 3D visualisation produced by the stereoscope can also often appear exaggerated due to the distance between our eyes being much smaller than the distance at which the stereopairs are taken (Hubbard & Glasser, 2005). The amount of exaggeration is determined by the ratio between the flying height and the air base (distance on the ground between photo centres) (Lillesand *et al*., 2008).

Limitations

Aerial photographs, or maps derived directly from aerial photographs, cannot be directly overlain onto topographic maps or DEMs since they possess varying degrees of geometric distortion. These are mainly in the form of relief displacement and scale variations across the image (Lillesand *et al*., 2008). Relief displacement is similar to the foreshortening and layover artefacts that occur with the NEXTMap products in that it occurs because of the different distances on varied terrain between the terrain and the camera lens. However, because the camera is positioned vertically over the ground, rather than obliquely, as for NEXTMap, it results in higher altitude relief appearing to 'lean away' radially from the centre of the photograph. This is most apparent at the edges of the photograph, whereas very little will occur in the centre, where the camera is directly overhead (Gibson, 2000; Campbell, 2002; Lillesand *et al*., 2008) (Fig. 3.7).

Variations in scale are also caused by differences in the elevation of the terrain. Terrain at higher elevations is closer to the camera lens and the same sized feature will therefore appear larger at higher elevations. As a result, a number of scales occur within the same aerial photograph (Gibson, 2000; Lillesand *et al*., 2008). Scale variation can also be caused by the aircraft tilting during the acquisition of photographs, causing one side of the image to be closer to the camera lens than the other (Gibson, 2000; Campbell, 2002).

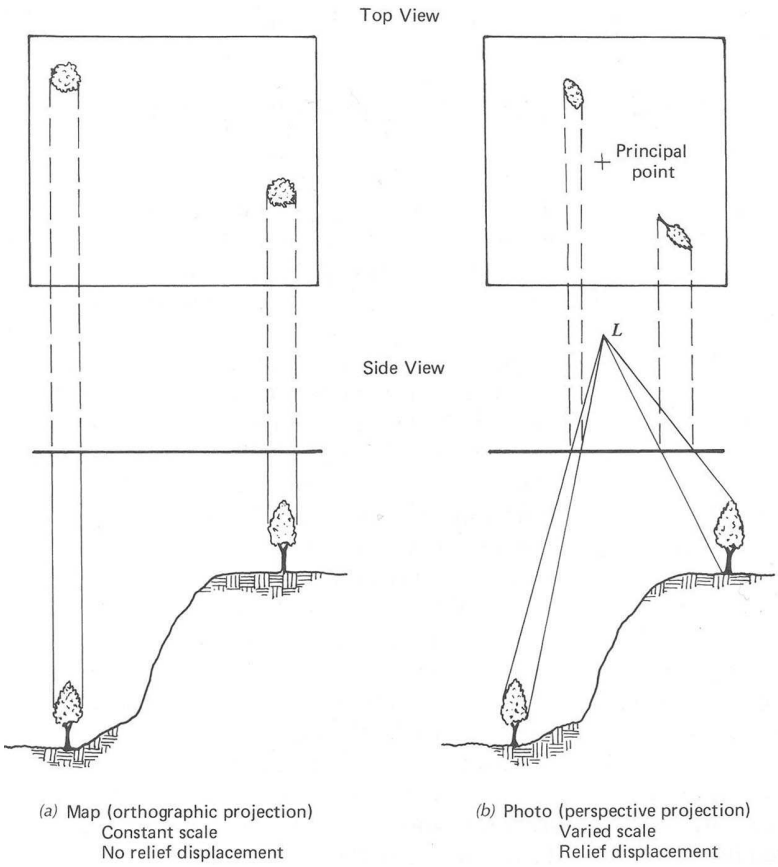

Figure 3.7. The projection of trees as viewed from above, on a) a map (orthographic projection) and b) an aerial photograph (perspective projection), which shows the effect of relief displacement. Taken from Lillesand *et al*. (2008, p.139).

Several authors have noted that, in some areas, the tonal contrasts on aerial photographs are not distinct enough to enable detailed geomorphological mapping (Benn *et al*., 1992; Smith & Wise, 2001; Mitchell & Riley, 2006). This could be caused by a number of factors, including a lack of shadows if the photographs were taken around midday, particularly in summer, or due to an effect called vignetting in which less light reaches the camera lens from the peripheral areas, compared to the centre, causing a dark rim to form around the edge (Campbell, 2002). However, other researchers have been able to produce high quality glacial geomorphological maps using aerial photographs (e.g. Lukas & Lukas, 2006a, b; Sahlin & Glasser, 2008), demonstrating that there are large variations in the quality of aerial photographs sets between different flight years.

Mapping from aerial photographs

Geomorphological maps were produced using two sets of aerial photographs held at the British Geological Survey (BGS). Aerial photographs at a scale of approximately 1:24,000 were part of the *All Scotland Survey* flown in 1988 and 1989, whilst the other set consisted of approximately 1:27,000 scale photographs that were commissioned by the Ordnance Survey in 1963. The two sets generally covered different areas, although there was some overlap between the two, with tonal contrast much higher on the *All Scotland Survey* set. The photographs were viewed in

stereo using a mirror stereoscope with 3 times magnification. Individual landforms were drawn onto acetate, which was overlain on one of the aerial photographs (Fig 3.8). Field maps and previous mapping from NEXTMap were referred to frequently during the production of the aerial photograph overlays in order to ensure a robust and consistent interpretation of the landforms. Although the quality of the aerial photographs was generally good, there were variations and, in some areas, features were difficult to define due to the effects of vignetting and low tonal contrasts. In these cases NEXTMap and the field maps were relied on more heavily in the final map production stages (Section 3.1.4).

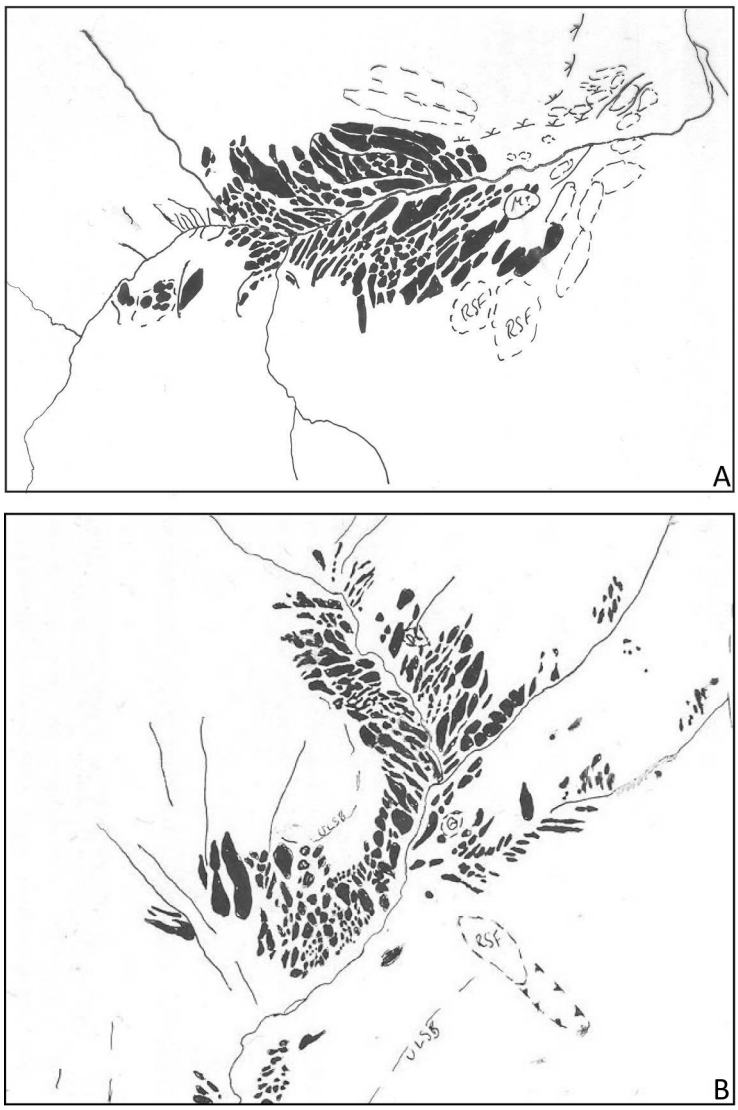

Figure 3.8. Hand-drawn aerial photograph overlays of geomorphological features in A) Coire Easgainn and B) Gleann Fionndrigh, prior to geometric correction and digitisation. B) shows the extensive occurrence of small closely spaced moraines at the head of Gleann Fionndrigh that could not be mapped satisfactorily using a relief-shaded model from the NEXTMap DSM (Figure 3.6).

Georeferencing and Orthorectification

Aerial photographs, or the mapping overlays derived from them, need to be georeferenced or orthorectified to remove the geometric distortions described above before they are used in the production of final geomorphological maps. Georectification is the term applied to a process of

transforming, or warping, an aerial photograph to fit a local coordinate system. The end result is an image that has been corrected horizontally with x and y coordinates, but is still likely to have some height distortion, which will be most extreme in mountainous areas (Aber *et al*., 2010; Morgan *et al*., 2010). During orthorectification the aerial photograph is draped over a DEM to derive elevations (z coordinates), correcting it both horizontally and vertically. This process therefore produces a more accurate result than georectifying, but consequently is also more complex and the accuracy of the final product is dependant on the accuracy of the DEM used (Channel Coastal Observatory, 2011).

There are various methods that have been used in previous glacial geomorphological research to georeference and/or orthorectify aerial photographs, or the maps derived from aerial photographs. These vary from manually re-drawing features identified on aerial photographs onto topographic maps (e.g. Young, 1978; Ballantyne, 2002a, 2007a,b; Benn & Ballantyne, 2005), to visually manipulating aerial photograph-derived mapping overlays (e.g. Lukas, 2005a; Sahlin & Glasser, 2008) to orthorectification of digitised aerial photographs using a DEM (Brown *et al*., 2011), although many studies do not specify their method of georeferencing or orthorectification (e.g. Sissons, 1979a; Bradwell, 2006; Stokes *et al*., 2008). In this research, the aerial photographs were not available digitally and therefore a new approach was undertaken in which the aerial photograph-derived map overlays were corrected geometrically.

There are numerous software programs available that are capable of carrying out geometric orthorectification and georeferencing, which include *ESRI ArcMap* and *Erdas Imagine*. Within these programs different geometric models are used to transform aerial photographs. ArcMap uses a *polynomial model* (three orders), *spline transformation* and *adjust transformation*. Erdas Imagine has a wider range of geometric models available, several of which were identified as having the potential to correct the aerial photograph overlays, including the *polynomial model* (infinite number of orders), a *direct linear transform model* (DLT) and a *projective transform model*, and so Erdas Imagine was used to carry out the georectification process.

The polynomial model has been used in previous research to georeference aerial photographs (e.g. Hughes *et al*., 2006). The model uses a polynomial equation to specify the amount and style of transformation that an uncorrected image undertakes (Gibson & Power, 2000). Any polynomial order can be used, where the equation is linear for a first order polynomial, quadratic for a second order, cubic for a third order and so on (Gibson & Power, 2000; Hughes *et al*., 2006). This method does not use a DEM and therefore only corrects in the x and y dimensions. However, higher order polynomial models are powerful enough to correct more complex distortions (Hughes *et al*., 2006). In general, the higher the order of polynomial the

more accurate the transformation, although higher order polynomial models require more ground control points (GCPs; see below), longer computing time and can cause larger errors in areas away from the GCPs (Gibson & Power, 2000). The DLT model is specifically designed for orthorectifying images taken from aerial cameras. The model requires a DEM, thus enabling a z coordinate to be calculated in addition to x and y, and so can correct for relief displacement, unlike the polynomial model. The projective transform model also includes a reference DEM to produce a z coordinate and therefore also corrects for relief displacement, but is more powerful than the DLT model.

All these models require ground control points (GCPs). These are easily identifiable points on the ground that can be located on both the DEM and aerial photograph. Hughes *et al*. (2006) define GCPs as either hard or soft points. Hard points consist of features such as road intersections and fences, which have sharp edges or corners. Soft points include the centre points of trees or the edges of rock outcrops. Hard points are favoured over soft points, but in order to include enough GCPs for some of the models to be effective, soft points may also need to be used (Hughes *et al*., 2006). The number of GCPs required depends on the geometric model used. For the polynomial model a minimum of three are required for a first-order transformation, but twenty-two are required for a fifth-order model (Gibson & Power, 2000). A minimum of six GCPs is required for the DLT model, but these need to be spread out across the photograph with variations in all three planes (x, y, z) in order for the model to work effectively (Nagelhout & Hofstee, 2011). Whilst there is a general consensus that GCPs should be evenly distributed across the image, a compromise often has to be made, as less favourable GCPs may need to be used in order to gain a good distribution (Gibson & Power, 2000; Campbell, 2002).

Following geometric correction using the models outlined above, the image needs to be re-sampled in order to re-assign new pixel values and enable it to be visualised. Cubic convolution, which uses a weighted average of the nearest 16 pixels, was used here, as it is a frequently used re-sampling method (Campbell, 2002; e.g. Hughes *et al*., 2006) and creates a smoother final image than the bilinear interpolation or nearest neighbour methods (Hughes *et al*., 2006). However, its complexity compared to the other two methods means that computational time is longer and more GCPs are required (Gibson & Power, 2000; Campbell, 2002).

In order to establish the best geometric model to use, a comparison was undertaken between the polynomial model, the DLT model and the projective transform model following the method described here. The scanned aerial photograph overlays were cropped in *Adobe Photoshop* into smaller sections of each valley and saved as TIFFs in preparation for distortion correction in

Erdas Imagine. The three models, including 3rd, 4th and 5th orders for the polynomial model, were tested using aerial photograph mapping from several valleys. As many GCPs as possible were selected from each aerial photograph map, such as river junctions, tight river bends, end or centre points of moraines and edges of river terraces, and linked to the same place on a NEXTMap ORI (Fig. 3.9). An ORI was chosen as the reference image due to its similar visual appearance to an aerial photograph, which meant that GCPs could be easily identified. The same GCPs were used for all the models and the RMSEs for each location and model are shown in Table 3.2.

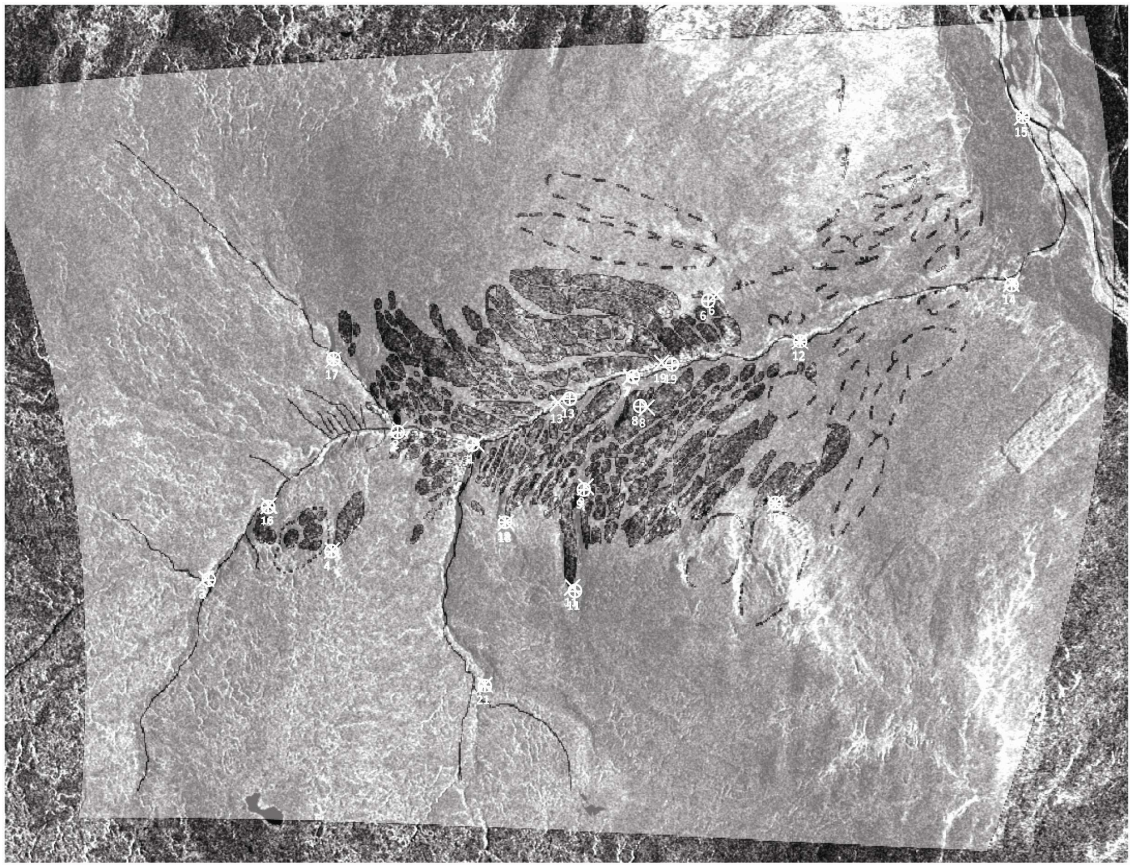

Figure 3.9. An example of the georectification process in Erdas Imagine, showing the aerial photograph overlay for Coire Easgainn overlain on the NEXTMap ORI after georectification using a 3rd order polynomial model. The GCPs used in this process are also shown in the figure, where each cross represents a GCP on the aerial photograph overlay and the 'target' (circle with a cross in it) marks the corresponding GCP on the ORI. This shows that, whilst the majority of GCPs match well, there are some minor differences in the positioning at some of them. NEXTMap ORI from Intermap Technologies Inc. provided by NERC via the NERC Earth Observation Data Centre.

The results of Table 3.2 show that some models performed better than others at different locations. This variation generally corresponds to the range of elevations over which the mapping was carried out. The polynomial model produced the lowest RMSEs for areas only containing small variations in elevation, i.e. when landforms were confined to the valley floor and lower parts of the valley sides. This was potentially because there was not enough variation in the elevations of the GCPs for the DLT and projective transform models to work effectively. There was little improvement in RMSEs by increasing the polynomial order, and so the 3rd order

model was deemed to be the most appropriate, as it provided a good balance between model complexity and a low RMSE. For maps that covered a larger range of elevations, particularly where landforms were mapped both in valley bottoms and on adjacent plateaux, the DLT and projective transform models often produced better results.

Table 3.2. RMSEs for the five geometric models that were tested to examine their suitability for georectifying the aerial photograph overlays.

	RMSE for each Method (m)					
Site	**Polynomial 3rd**	**Polynomial 4th**	**Polynomial 5th**	**DLT**	**Projective**	**Best visually**
Corrie Yairack	7.50	7.42	7.82	6.26	6.35	DLT
Corrie Easgainn	5.33	5.33	5.20	55.09	7.49	Polynomial
Coire an Eich	3.89	3.90	3.90	4.21	4.52	Polynomial
Corrie Dubh CnaC	5.13	5.09	5.08	5.79	5.92	Poly or DLT
Dalbeg Findhorn	4.67	4.67	4.67	4.47	4.40	DLT
Glen Odhar 1	4.74	4.79	4.94	5.31	5.36	Polynomial
Glen Odhar 2	7.20	7.18	8.35	Unsolvable	8.73	Projective T
Dalbeg Coignafearn 1	5.36	5.62	5.25	10.81	4.66	Polynomial
Dalbeg Coignafearn 2	4.69	4.69	4.67	41.64	4.68	Projective T
Gleann Fionndrigh	5.54	5.43	6.02	485.41	8.76	Polynomial
Plateau GMACC 1	4.24	4.13	4.03	27.99	4.46	Poly or Proj
Plateau GMACC 2	4.76	4.78	4.78	26.69	7.97	Polynomial
Gleann Chaorainn	3.30	3.30	3.30	3.92	3.99	Poly of DLT
Corrie Iain Oig	2.71	2.71	2.71	9.90	2.60	Polynomial

Therefore, for the remaining overlays, the model used varied depending upon which one produced the lowest RMSEs and fit best visually, although, in general, the 3rd order polynomial model was used predominantely. In order to minimise RMSEs, GCPs with high individual errors were removed if the GCP was likely to be inaccurate. For example, if the GCP was located on a stream bend, it could have changed position since the acquisition of the aerial photograph (Gibson & Power, 2000). However, the error in some cases was a function of the ability of the model to match individual GCPs. Therefore, although taking out all GCPs above a threshold RMSE, as suggested by some authors (e.g. Gibson & Power, 2000; Brown, 2009), would have decreased the RMSE, it would not have improved the match and could have made it worse (*cf*. Hughes *et al*., 2006). As a result, some GCPs with seemingly high errors were retained and the georectified image was accepted when it visually matched the underlying ORI, particularly where moraines and other landforms matched, rather than the current streams, which, as stated above, could have changed position. The average RMSE for all orthorectified maps was 4.54 m.

3.1.4 Geomorphological map production

The georectified aerial photograph overlays were used to produce the final geomorphological map. This was because the aerial photographs had a higher spatial resolution than NEXTMap, which enabled small features to be identified and they were more accurate in terms of landform position, orientation, shape and size than the field mapping. However, in order to reach this

stage, an iterative process involving several consultations of all three mapping approaches was used (Fig. 3.10). The NEXTMap DSM and aerial photographs were consulted prior to and during fieldwork and the mapping from NEXTMap was then updated following fieldwork. NEXTMap and the field maps were referred to frequently during the production of the aerial photograph overlays and the final maps. *Google Earth* was also consulted repeatedly during this process and was often very helpful in combination with NEXTMap.

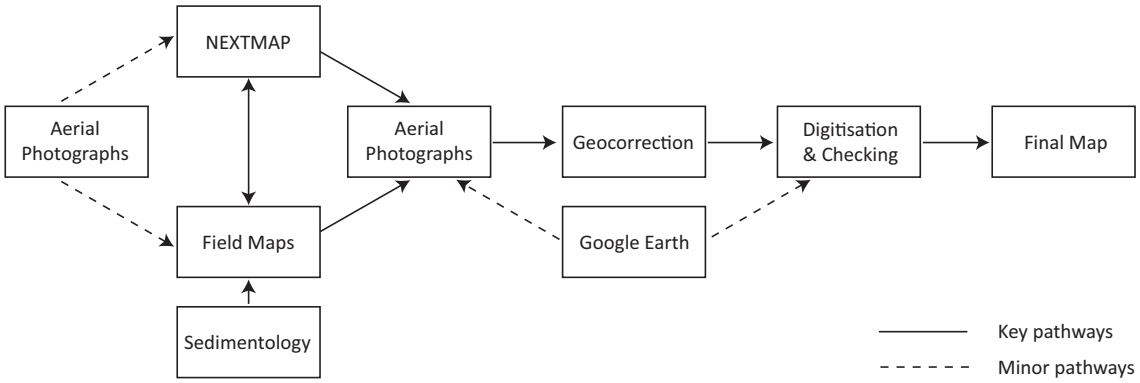

Figure 3.10. Flowchart to summarise the approaches and process involved in geomorphological map production and the relative contributions of each form of mapping to the final map.

To create the final geomorphological maps, each georectified overlay was imported as a new layer into ArcMap and overlain on top of the NEXTMap DSM relief-shaded model. The aerial photograph overlays were then compared with the DSM and the features mapped from the DSM as a further check on accuracy. A contour layer, created in ArcMap from the NEXTMap DTM, was then overlain on the aerial photograph overlay layer and the image was exported out of ArcMap into *Adobe Illustrator*. In this program, the overlay was digitised and any minor changes to the mapping were made, such as small adjustments to moraine position and the re-alignment of streams to the more recent NEXTMap DSM if meander migration had occurred.

3.2 Sedimentology of Glaciogenic Deposits

Sedimentological analysis was used in combination with the geomorphological mapping to aid landform identification and assess the processes involved in forming such landforms. However, the availability and accessibility of suitable sections was limited in the study area and therefore sedimentology was only used in a discrete number of areas.

The examination and analysis of sediments within glaciogenic landforms can provide valuable information on the processes that occurred during their formation. As a result, geomorphology is often combined with sedimentology to provide a more thorough analysis of a landscape and the processes that have shaped it (Benn & Evans, 2010). A sedimentological approach can lead to more robust interpretations regarding the genesis of a landform if a number of possible interpretations exist based on its geomorphology alone (equifinality, e.g. Bennett, 1999; Benn &

Lukas, 2006; Mills *et al.*, 2009). Interlinked within this, sedimentology can help to understand how particular landforms are formed and can assist interpretations about glacier dynamics (e.g. Lukas, 2005a, b, 2007a, 2012; Benediktsson *et al*., 2008; Evans, 2009; Hiemstra *et al*., 2009; Evans, 2010; Lukas *et al*., 2012). In both capacities, the study of processes occurring in modern glacial environments is critical to enable interpretations in former glacial settings to be made (Benn & Lukas, 2006).

In the present study area, the number of natural exposures that were easily and safely accessible were low. As a result, sediment descriptions in this research are limited and often made from a distance. However, several sections near Glen Killin were examined in detail. These natural exposures were enlarged to permit a more extensive and detailed examination of the sediments. The sections were logged on squared paper, using a tape measure hung vertically from the top of the section and 1 m markers horizontally to maintain proportions. Key units were drawn first, before further detail was added. The sections were assessed for structural characteristics, sediment architecture, compaction, sorting and texture, bed contacts, unit geometry and colour, using criteria described in Evans and Benn (2004) and grouped into lithofacies associations (Section 3.2.1). Bedding directions were measured within sand units, and clast morphology and macrofabrics were measured within diamictons, using methods outlined in Sections 3.2.2 and 3.2.3.

3.2.1 Lithofacies associations

The term ‘lithofacies’ is used to describe a sediment body with similar physical characteristics, architecture and bed contacts. Lithofacies can be collated into groups of sediment units that display unique characteristics that represent a particular depositional environment, which are known as lithofacies associations (LFAs) (Evans & Benn, 2004). Once LFAs have been identified, their physical characteristics, architecture and relationship to other LFAs can be considered in order to formulate a robust interpretation of the overall depositional environment. In this thesis, lithofacies and lithofacies associations are used to describe the sediments found and to organise the units into groups that have undergone similar sedimentary processes. The characteristics of each lithofacies were recorded using a slightly modified version of codes established by Miall (1978), Eyles *et al*. (1983), Maizels (1993), Krüger and Kjær (1999) and summarised by Evans and Benn (2004) (Fig. 3.11).

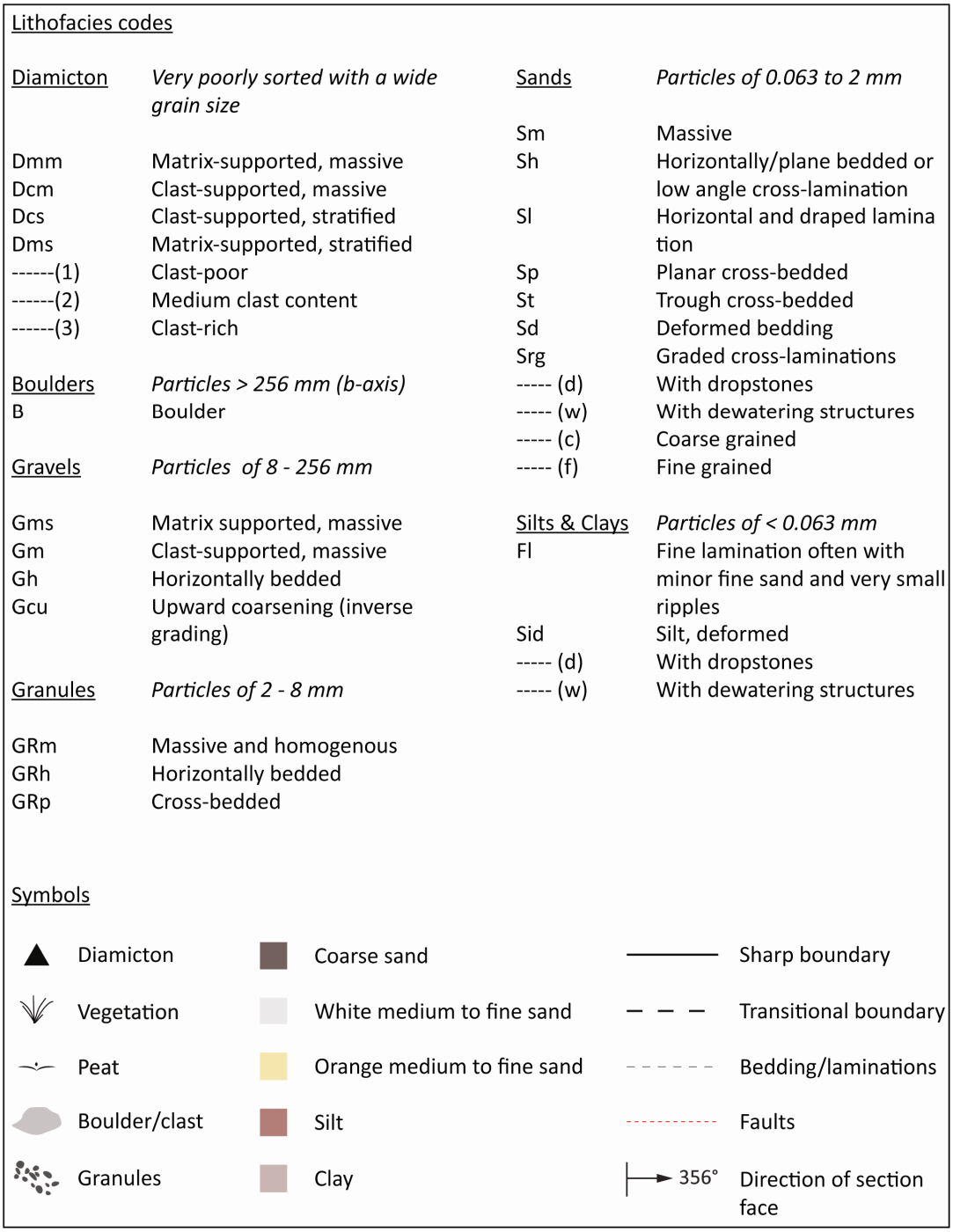

Figure 3.11. Lithofacies codes used in this research. Adapted from Evans and Benn (2004).

3.2.2 Clast morphology

Clast morphology, i.e. the shape and the relative roundness of clasts, is an important tool for examining the mode of transport, such as subglacial, englacial, supraglacial and fluvial, that a clast has been subject to following separation from the bedrock source, and can be used to aid genetic interpretations of particular lithofacies (Benn, 2004a). In order to make reliable interpretations based on clast morphology, samples, known as control samples, are taken from different environments where the transport history can be unequivocally established such as streams and scree slopes following guidelines by Benn (2004a). Samples should be taken using

the same lithology, since different lithologies respond differently to erosional processes (Benn & Ballantyne, 1994; Benn, 2004a; Lukas *et al*., in press) and a grain size of 35 – 125 mm is recommended since clast shape can be influenced by clast size (Benn & Ballantyne, 1994; Benn, 2004a). A sample of 50 clasts is also recommended in order to produce statistically significant results (Benn, 2004a).

In this research, control samples were taken from streams and areas where rockfall had occurred, in addition to the sections under investigation. Samples of 50 psammite clasts were taken, since this is the main lithology in the study area (see Section 2.2). The recommended clast size range of 35 – 125 mm was used, although it was sometimes necessary to include some clasts just outside the lower end of this range due to the dominant size of the clasts available.

Clast shape was quantified by measuring the three orthogonal axes of a clast: a (longest), b (intermediate) and c (shortest) leading to three possible clast shape end members: 1) a cube, where a = b = c, 2) a rod, where a >> b = c, and 3) a disc where a = b >> c (Benn, 2004a). Most data points lie somewhere between these end members and therefore clast shape data is best suited to being displayed on triangular plot. Although a number of variations of ternary diagrams have been previously suggested to display clast shape data (e.g. Sneed & Folk, 1958; Hockey, 1970; Ballantyne, 1982; Hofmann, 1994), a version of the Sneed and Folk (1958) diagram, devised by Graham and Midgley (2000) for *Microsoft Excel*, was used to present all clast shape data in this research. The clast shape data was also assessed using the C_{40} index (Benn & Ballantyne, 1993), where samples with a high degree of 'blockiness' have a higher c:a ratio. Using this index, Ballantne (1982) demonstrated that actively transported subglacial clasts can be differentiated from passively transported englacial and supraglacial clasts by examining the percentage of clasts that have a c:a ratio of ≤ 0.4.

Although several approaches for categorising clast roundness have been suggested (e.g. Krumbein, 1941; Powers, 1953; Benn & Ballantyne, 1994), in this study the descriptive criteria outlined by Benn (2004a) were used (Table 3.3). Clast roundness was then assessed using the RA index, which expresses the percentage of angular and very angular clasts in a sample (Benn & Ballantyne, 1994) and the RWR index, which denotes the percentage of rounded and well-rounded clasts (Benn, 2004a; Benn *et al*., 2004). These two indices were then plotted against the C_{40} index to allow covariance analysis (Benn & Ballantyne, 1994), where the RA index is best for discriminating between supraglacially and subglacially transported clasts and the RWR index between fluvial and subglacial transport (Lukas *et al*., in press). This approach has allowed discrimination between different transport paths in a number of previous studies (e.g.

Benn & Ballantyne, 1994; Lukas, 2005b, 2007b; Midgley *et al.*, 2007; Kellerer-Pirklbauer, 2008; Evans, 2010; Evans *et al*., 2010a; Lukas *et al.*, 2012, in press).

Table 3.3. Descriptive criteria used to define clast roundness in this study. From Benn (2004a, p. 81).

Class	Description
Very Angular (VA)	Edges and faces unword; sharp, delicate protuberances
Angular (A)	Edges and faces unworn
Sub-angular (SA)	Faces unworn, edges worn
Sub-rounded (SR)	Edges and faces worn but clearly distinguishable
Rounded (R)	Edges and faces worn and barely distinguishable
Well Rounded (WR)	No edges or faces distinguishable

3.2.3 Clast macrofabrics

Clast macrofabrics are employed to examine the processes involved in the deposition of sediments and have also been used to establish ice flow directions (Benn, 2004b). Although the value of this approach has previously been questioned (Bennett *et al*., 1999), a growing body of research suggests that, as long as limitations to the data are recognised and it is used alongside other sedimentological techniques, clast macrofabrics can provide additional information for genetic interpretations (e.g. Larsen & Piotrowski, 2003; Evans & Hiemstra, 2005; Li *et al.*, 2006; Evans *et al*., 2007, 2010b; Evans & Thomson, 2010) The majority of research has focussed on the orientation of the a-axis, which will rotate when subjected to an applied stress (Benn, 1994; Hooyer & Iverson, 2000; Benn, 2004b). However, Evans *et al*. (2007) recently advocated the use of the a/b plane as an alternative to avoid some of the problems associated with using the a-axis, which can align transverse to flow. Instead, the a/b plane is suggested to dip in a direction that is parallel to ice flow more readily than the a-axis, producing stronger fabrics (Li *et al.*, 2006; Evans *et al.*, 2007). For comparison with the majority of previous fabric data, but in light of this newer body of research, both a-axis and a/b plane fabrics were undertaken in this study for a sample size of 50 clasts with a:b ratios of $\geq$ 1.5:1 and within the recommended size-range of 35-125 mm (Benn, 2004b; Evans *et al.*, 2007). The sample area was kept as small as possible (~ 0.2 x 0.2 m), under the constraints of finding 50 clasts of the correct size and shape.

Data was plotted on lower hemisphere equal-area contoured stereonets using the Stereo32v1.0.3 program (Duyster, 2011), which provided a means of presenting both the orientation and dip of each clast. Eigenvectors and eigenvalues (Mark, 1973, 1974) were also calculated using Stereo32, further details of which are found in Benn (1994). Eigenvalues can be used to describe the shape of the fabric. When the data points are distributed evenly within a sphere, the fabric is known as isotropic ($S_1 \approx S_2 \approx S_3$). If the data is evenly distributed around a circle ($S_1 \approx S_2 \gg S_3$) it is identified as a planar girdle and if all the data lies approximately parallel ($S_1 \gg S_2 \approx S_3$) it is know as a linear cluster (Benn, 1994).

The position at which fabric data plots (usually on a tertiary diagram) on the continuum between these three end members can be used to examine the depositional environments using reference data from samples of known origin (e.g. Benn, 1995; Benn & Evans, 1996; Benn, 2004b; Evans *et al*., 2007). The isotropy and elongation indices are calculated alongside the tertiary plots, which can also be used to examine the depositional environment. The isotropy index (I) is calculated using $I = S_2/S_1$ and ranges from 0, where the data is organised to a single plane or axis, and 1, where the observations exhibit perfect isotropy. The elongation index (E) = $1-(S_2/S_1)$, where 0 indicates that the data has no preferred orientation and 1 signifies that all the observations are parallel (Benn, 1994).

3.3 Chapter Summary

This chapter has reviewed the two key methods used for data collection in this research, namely geomorphological mapping and sedimentological analysis. Geomorphological mapping was the key method used to achieve the aims and objectives set out in Chapter 1. This was undertaken using two forms of remotely-sensed data, NEXTMap and panchromatic aerial photographs, alongside a 12-week field campaign spread over two field seasons. Using the three different approaches to mapping allowed for a holistic approach in which the advantages of each method could be combined to produce a detailed and accurate geomorphological map, with robust genetic interpretations.

NEXTMap was particularly advantageous for reconnaissance mapping and the identification of interesting sites that could be targeted for more detailed investigation in the field. However, the resolution of NEXTMap, although high in comparison to other remotely-sensed datasets, often did not allow for the recognition of smaller landforms, such as some moraines. Additionally, the boundaries of features were often difficult to identify clearly for accurate mapping purposes due to azimuth biasing. Field mapping therefore provided the most robust means of interpreting landforms, but difficulties in accurately positioning features on the fieldslips meant that the final geomorphological maps were drawn using aerial photographs, which had a higher spatial resolution, but required relief distortion and variations in scale to be corrected for. The fieldslips and NEXTMap were consulted during the production of the final map to ensure consistency between the three approaches and to check the accuracy of the aerial photograph maps after they had been georectified in Erdas Imagine. Google Earth was also consulted during the production of the final geomorphological map since it provided an additional means by which to check landform identification.

Sedimentological analysis was used alongside geomorphological mapping, within the constraints of section availability, to provide additional information of landform genesis and the processes involved in landform deposition. The main sedimentological techniques used were

section logging, description and the grouping of sedimentary units into lithofacies and lithofacies associations. At some sections, analysis of clast morphology, macrofabrics and bedding dip and orientation was also undertaken to provide further information about debris transport pathways, depositional environments and the direction of ice flow or water movement.

These two methods are well-established approaches used to assess the characteristics of formerly glaciated areas, the processes that shaped these areas and to reconstruct the dynamics of former glaciers. Previous studies based on geomorphological mapping, especially since the acquisition of the NEXTMap Britain dataset, have provided significant information on maximum ice positions, ice flow directions, glacier dynamics, retreat patterns and depositional environments during retreat (e.g. Bradwell *et al*., 2007; Golledge, 2007; Greenwood & Clark, 2008; Livingstone *et al.*, 2008, 2010a, b, 2012; Sahlin & Glasser, 2008; Hughes *et al*., 2010; Finlayson *et al*., 2011). The combination of geomorphological mapping and sedimentological analysis has been shown to be particularly effective, where an understanding of the spatial patterns of ice flow and ice-marginal positions during retreat can be combined with details on the depositional environments and processes of landform formation (e.g. Lukas, 2005a, b; Benn & Lukas, 2006; Evans, 2010; Livingstone *et al*. 2010b, c, d). It is perceived that using this approach in the current research will aid landform interpretation and will enable not only an assessment of the spatial distribution of glaciogenic landforms, but also a greater understanding of the processes involved in landform deposition, thus enabling the objectives outlined in Chapter 1 to be fulfilled. The following chapter, Chapter 4, describes the results of this geomorphological and sedimentological analysis. Details of the methods used to analyse these results are described in Chapter 5.

Chapter 4

Geomorphological and Sedimentary Evidence for Glaciation in the Monadhliath Mountains

Chapter 4 describes and synthesises the landforms and lithofacies associations found within the western and central upland areas of the Monadhliath Mountains, covering the area defined as the study area in Figure 3.1. This chapter is divided into four sections based upon four geographic areas within the study area, which are shown in Figure 4.1. These are: *the western Monadhliath Mountains* (Section 4.1), *the northern Monadhliath Mountains* (Section 4.2), *the eastern Monadhliath Mountains* (Section 4.3), and *the southern Monadhliath Mountains* (Section 4.4). Each section contains a description of the glacial and periglacial geomorphological and sedimentological evidence found within individual glens, which is followed by an initial interpretation and synthesis of the evidence. The wider significance of these findings will be discussed in Chapter 5.

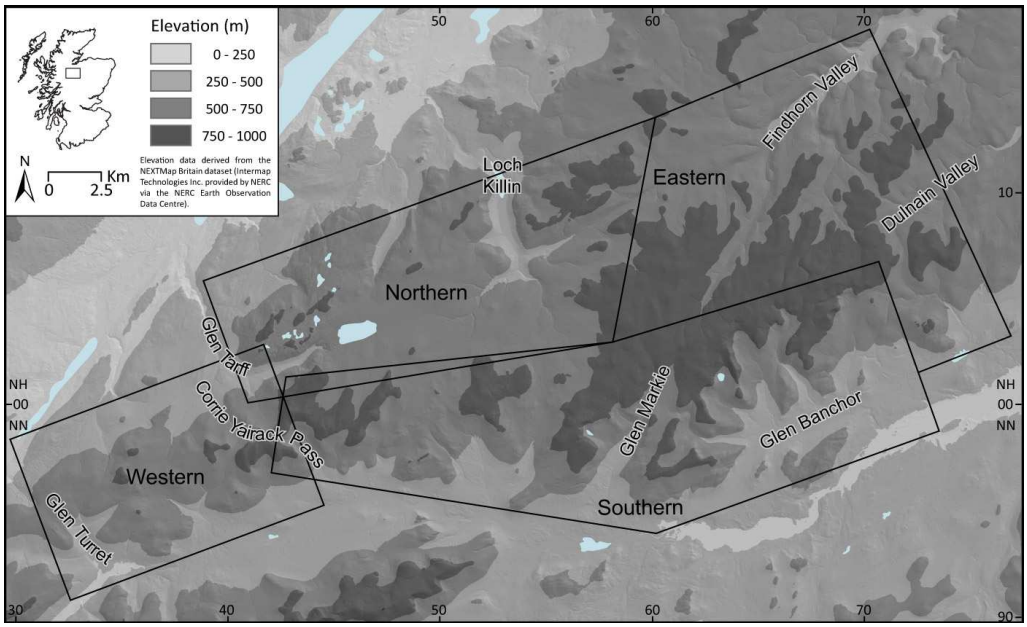

Figure 4.1. Map showing the division of the Monadhliath Mountains into the western, northern, eastern and southern sectors, as described in the text above. Elevation data was derived from the NEXTMap Great Britain DTM and overlain on a hillshade model, also derived from NEXTMap (Intermap Technologies Inc. provided by NERC via the NERC Earth Observation Data Centre). UK Outline from Ordnance Survey © Crown copyright 2010.

The geomorphological evidence is described with as little interpretation as possible to allow transparency as to how key landforms in the study area were interpreted. The terms *mounds* and *ridges* are used to describe depositional features that are generally less than 100 m wide and 50 m high, with rounded to sharp crestlines. *Mounds* describe features with rounded to oval bases, whilst *ridge*s are more elongate. The term *channel* is used to describe an erosional feature that forms a continuous trough into sediment or bedrock. *Terraces* are used to describe raised

features with extensive, relatively flat upper surfaces, although there may be a slight slope in a particular direction. The term *river terrace* is used to describe raised, relatively flat areas that are immediately next to a stream or river. Although this term is interpretative, it is used in order to immediately distinguish these types of terrace from other terraces. *Fans* are used to describe masses of sediment that spread out laterally, broadening in a downstream direction from a central channel at stream junctions. The term *scarp* is used to describe a steep cliff that is often not very extensive and occurs above a large accumulation of rock-fall material. Other terms that are used less often in the description are interpretative and include *debris cones*, *blockfields*, *solifluction lobes*, *frost-shattered bedrock* and *talus slopes*, following descriptions and definitions by Ballantyne (1984) and Ballantyne and Harris (1994).

The geomorphology of the majority of the upland valleys in the Monadhliath Mountains is dominated by mounds, ridges and channels, alongside other features such as talus slopes, debris cones, fans, extensive river terraces and large terraces that are over 20 m high in several valleys. Geomorphological features on the central plateau area are comparatively sparse, although some mounds, ridges and channels are found in addition to areas of blockfields, solifluction lobes and frost-shattered bedrock on the higher summits. Geomorphological maps are interspersed throughout this chapter within the appropriate sections and a key to these maps is shown in Figure 4.2 below. Since these maps correspond to the site descriptions, the features are represented as described above. A fully interpreted geomorphological map of the whole region can be found in Appendix II, which corresponds to interpretations at the end of each section in this chapter and within Section 5.1. A map of all place names is shown in Appendix I.

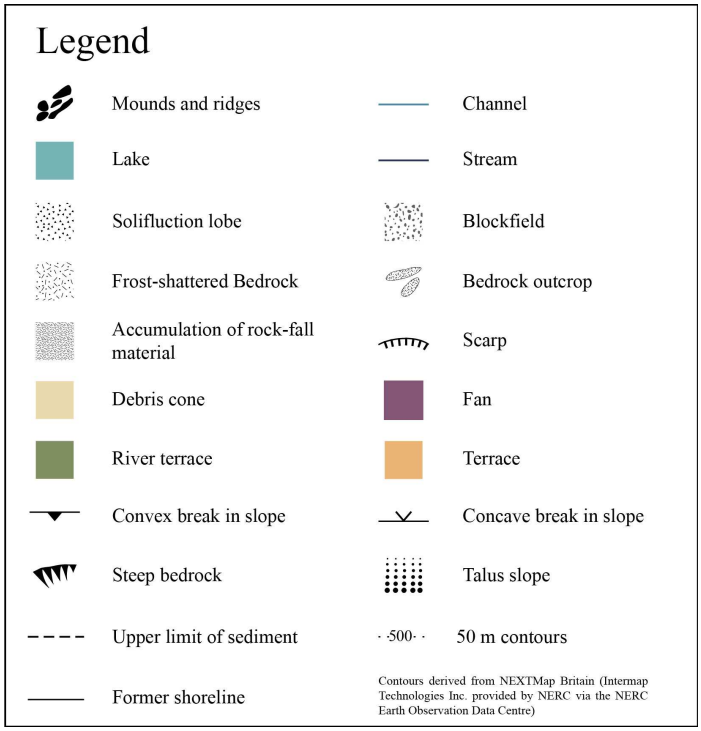

Figure 4.2. Legend for geomorphological maps found throughout Chapter 4.

There was an uneven distribution of natural sediment exposures across the region and therefore descriptions of sediment exposures cannot be presented at every site. The most extensive sedimentary analysis was carried out in the area around Loch Killin (northern sector) where there were an unusually large number of natural exposures. This allowed a detailed examination of the sedimentary characteristics of landforms within this area (Section 4.2.5), which was assessed within a geomorphological context to enable a better understanding of the depositional environment.

4.1 The Western Monadhliath Mountains

The western Monadhliath Mountains comprise an area to the west of the main plateau of approximately 110 km^2. In this area, north, south and west facing valleys are connected by an area of upland which ranges in height between 600 m in the west to 800 m in the east, with individual summits of up to 884 m (Figs. 3.1 and 4.1). Previous work in this area is mainly restricted to the vicinity around Glen Roy (e.g. Sissons, 1977a, 1978, 1979a; Sissons & Cornish, 1982, 1983; Peacock, 1986; Peacock & Cornish, 1989; Lowe & Cairns, 1991; Johnson-Ferguson, 2004; Benn & Evans, 2008; Fabel *et al*., 2010; Palmer *et al*., 2010) (Section 2.3).

4.1.1 Glen Shesgnan

Glen Shesgnan is a south-facing valley at the head of the River Spey, which is fed by three small corries to the south of Carn Leac (884 m, NN 407 978), namely Coire Shesgnan, Coirean Caol and Coire Cùil (Fig. 4.3). Large isolated, sporadically spaced mounds, up to 10 m high, are present in the lower parts of the valley, just upstream of its confluence with the River Spey. Occasional streams and former channels are positioned in between these mounds and a large, approximately 3 m high, river terrace occurs on either side of Shesgnan Burn, inset by the current river terrace.

The large river terrace continues upstream, until it ends abruptly directly upstream of the confluence with Allt Cùil (NN 421 957). At this point a semi-arcuate ridge occurs on the outside of both Shesgnan Burn and Allt Cùil. The ridge on the eastern side is more sharp-crested than that on the west, but both are fairly narrow, measuring around 30 m across. These ridges are not, however, the most downstream ridges with this morphology and a further two are present on both sides immediately downstream.

Above the confluence with Allt Cùil, the topography flattens out and the current river terrace widens slightly. Further upstream the slope becomes steeper again and from this point upwards, to the top of Coire Shesgnan, the central stream has incised deeply into the underlying substrate. Allt Caol and other streams and former channels have also incised deeply in this area. No

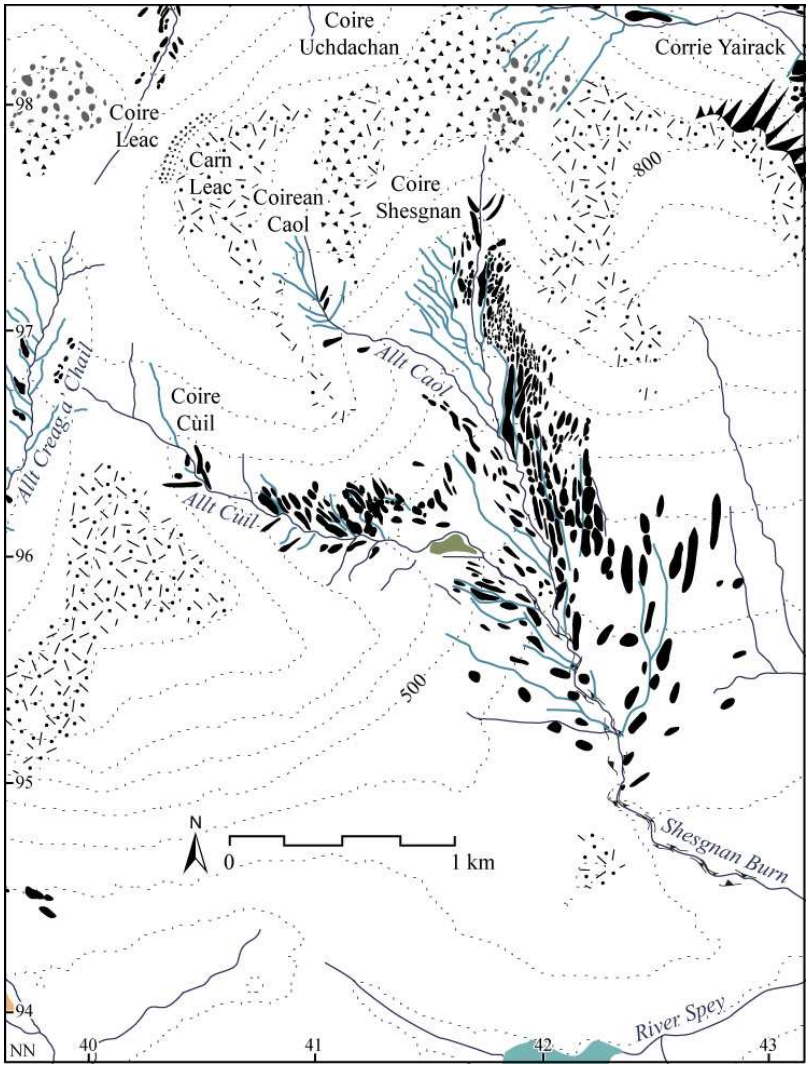

Figure 4.3. The geomorphology of Glen Shesgnan (see Fig. 4.2 for key).

bedrock is observed to outcrop within the sides of the channels and incision appears to have occurred into a 10 to 15 m thick sequence of unconsolidated sediment (Fig. 4.4).

Narrow (width ≤ 30 m) ridges occur on the eastern side of Shesgnan Burn in this area and continue upstream until they meet the eastern valley side of Coire Shesgnan. Where they meet the valley side, they are highly dissected, forming chaotically spaced mounds, which continue towards the top of Coire Shesgnan. The original pattern of ridges is still visible, however, when viewed from upstream and directly overhead.

Ridges also occur on the western side of Shesgnan Burn, where they are predominantly more subdued than those on the eastern side (Fig 4.2). The lower ridges curve towards Coirean Caol at their upstream ends, whilst those further upstream, alongside a large number of channels, trend obliquely across the slope in an upvalley direction towards the western valley side of Coire Shesgnan. There are a limited number of subdued arcuate ridges within Coirean Caol, which are intersected by former channels.

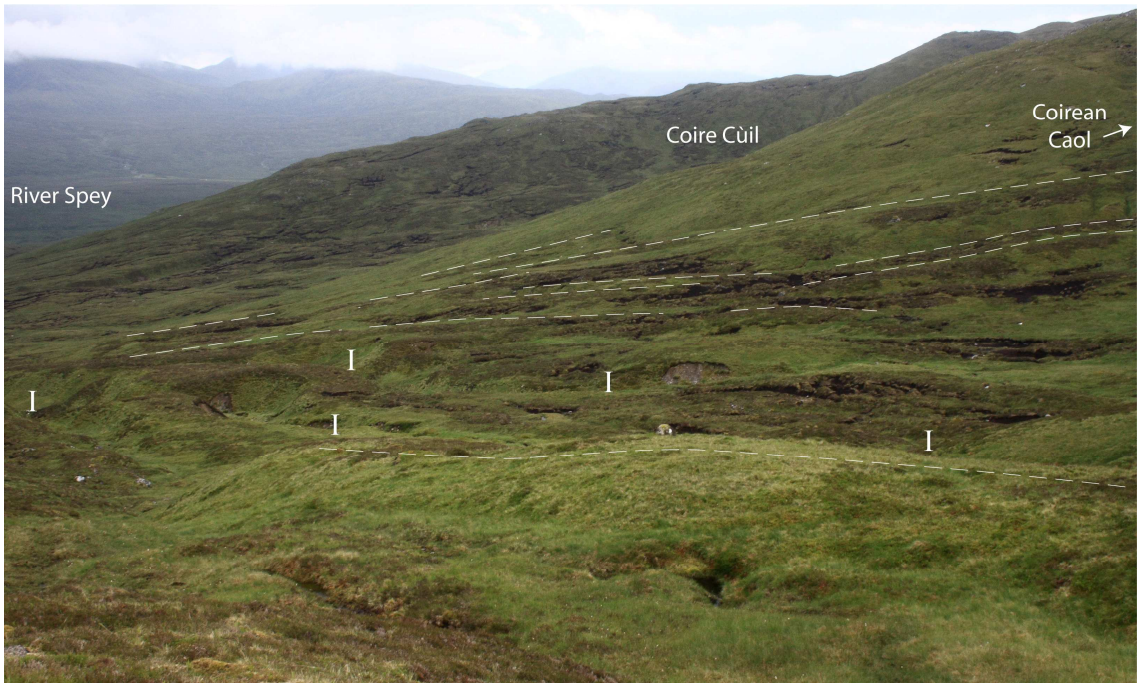

Figure 4.4. Ridges on the western side of Coire Shesgnan, the crestlines of which are highlighted by white dotted lines, and an area of deep stream incision in the valley bottom (I). The photograph was taken from the eastern valley side of Coire Shesgnan looking southwestwards.

Small, narrow (width ≤ 20 m), subdued mounds and ridges are also found within Coire Cùil, to the west of Coire Shesgnan and Coirean Caol. They occur throughout the whole of the corrie, but are most apparent on the northern valley side near the confluence with Coire Shesgnan and at the top of the corrie, where it connects with the Allt Creag a' Chail catchment. In both places well-defined former channels border the ridges. The Allt Cùil has incised to form a V-shaped channel, although in some places the channel widens and a small river terrace is observed.

4.1.2 Glen Chonnal

The Allt Chonnal stream flows south-southeast into the head of the River Roy to the west of the Shesgnan Burn catchment. It is fed by three tributaries: Allt Dubh, which drains an east-southeast facing catchment and by Allt Poll-gormack and Allt Creag a' Chail, which converge within a predominantly south-facing valley (Fig. 4.5).

Large (10 m high) landforms occur in the lower part of the valley, just upstream of where it converges with Glen Roy. These features take the form of terraces with a mounded surface in some areas that have, in places, been dissected by former channels. The upper surface of all these features is around 350 m. The slope steepens immediately upstream of these features, and wide, but relatively low-profile, ridges with rounded crestlines and widths of 50-70 m, occur on both valley sides. These ridges are located on top of a major river terrace within which the current river terrace is inset.

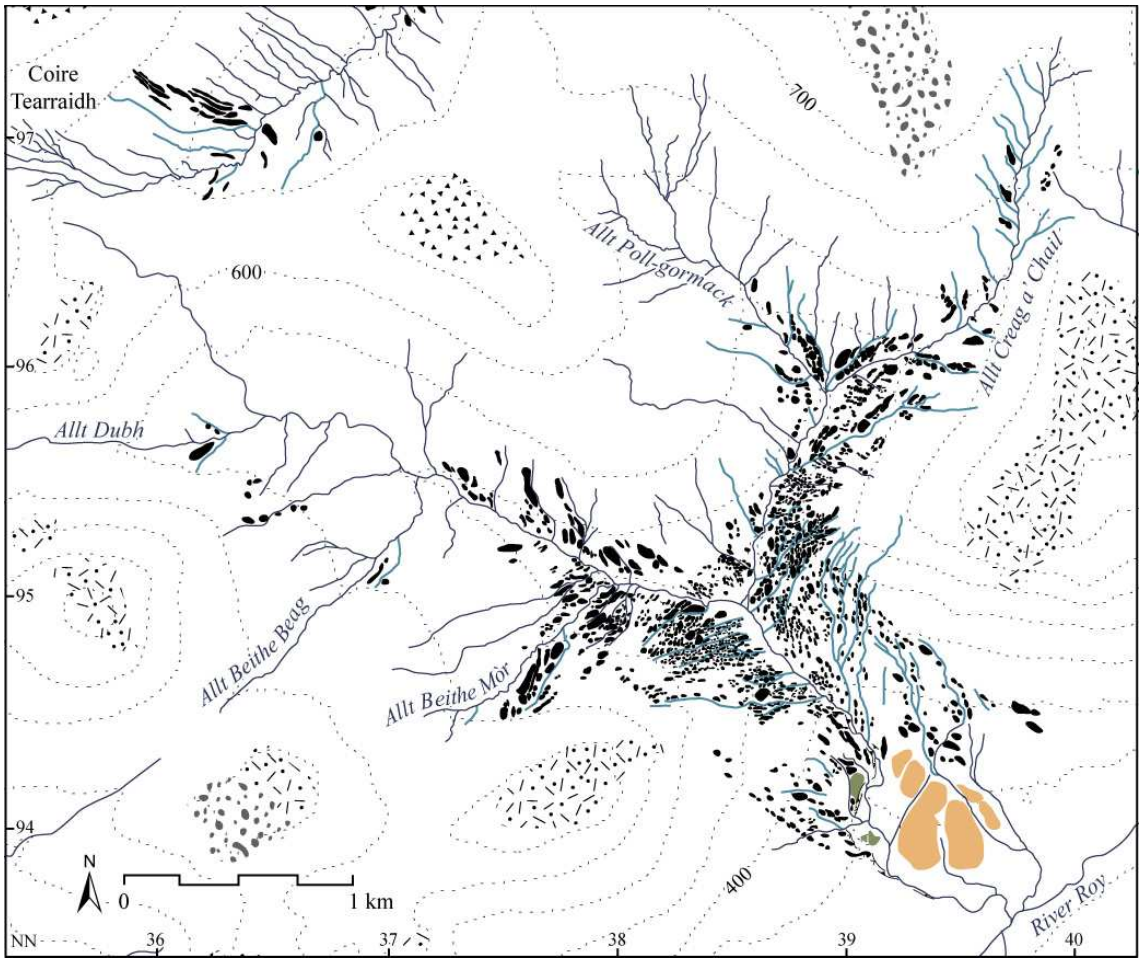

Figure 4.5. The geomorphology of Glen Chonnal (see Fig. 4.2 for key).

At grid reference NN 389 945 the major river terrace ends and both valley sides become covered by densely spaced small mounds and ridges. These mounds and ridges are not as broad as the ridges downvalley, usually measuring less than 30 m across and are dissected by a dense network of well-developed channels. The mounds and ridges continue upstream on both valley sides into the Allt Dubh and Allt Poll-gormack - Allt Creag a' Chail catchments.

By Allt Dubh, the mounds and ridges continue only a little way upstream on the southwestern side and upstream of the Allt Beith Mòr tributary (NN 380 950) there are very few. On the southwestern side, the mounds and ridges are often subdued, although larger, sharper-crested ridges are also present. On the northeastern valley side, ridges are aligned obliquely upvalley and continue towards the Allt Beithe Beag confluence (NN 371 955), but the steeper gradient on this side of the valley has caused many of them to be heavily dissected by channels trending directly downslope. The upper portion of the Dubh basin is relatively featureless, although some isolated channels, mounds and ridges do occur.

Mounds on the eastern side of Glen Chonnal that lead into the Allt Poll-gormack - Allt Creag a' Chail catchment have a slightly more chaotic hummocky appearance than those on the western side

and within the Dubh basin. An interconnecting series of former channels occurs between the mounds, with key channels delineating a coherent spatial pattern around former ridges, when viewed from overhead. The mounds are better preserved on the eastern side of the valley compared to the west, where downslope trending channels have dissected them, particularly further upstream. On the eastern side, the mounds continue upwards, beyond the confluence of Allt Poll-gormack and Allt Creag a' Chail, but do not continue much further beyond this area and channels, orientated directly downslope, become more dominant. A few isolated, obliquely trending ridges are, however, observed in the upper areas of both the Allt Poll-gormack and Allt Creag a' Chail catchments.

4.1.3 Glen Turret and adjoining areas

Glen Turret is a south-facing tributary valley of Glen Roy to the west of Glen Chonnal. Three streams, the Allt Teanga Bige, Allt Teanga Mòire and Allt Eachach, drain the plateau to the north of the valley and coalesce at the head of Glen Turret (Fig. 4.6). A fourth stream, Allt a' Chòmhlain, drains a basin to the west of Glen Turret and joins the River Turret about half way down the valley. The valley was flooded by Lake Roy during the advance of the Spean Glacier from the west into Glen Roy during the Younger Dryas (see Section 2.3). Two of the three lake shorelines found within Glen Roy, at 325 and 350 m, can be seen along the valley sides of Glen Turret.

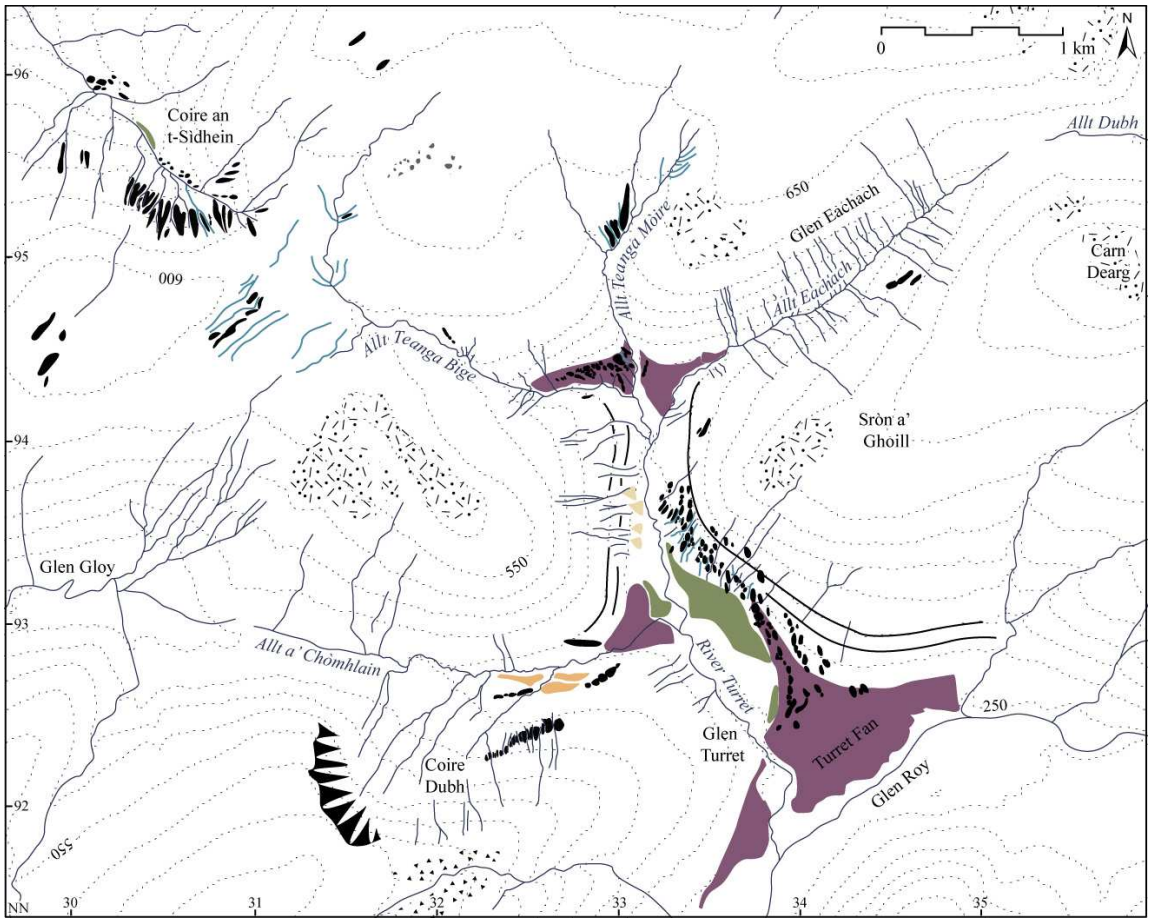

Figure 4.6. The geomorphology of Glen Turret and Coire an t-Sìdhean (see Fig. 4.2 for key).

A large fan, known as the Turret Fan, with a height of up to 30 m along the downstream edge and a surface elevation of 255 to 265 m, has developed at the mouth of Glen Turret, constraining the River Turret to the western valley side. Several rounded mounds are present on top of the fan at the northern end and can be joined to form two arcuate lines that curve downvalley in the centre. These chains of mounds can be followed onto the eastern valley side, where they form rounded ridges that continue obliquely up the valley side (Fig 4.7A). Numerous streams flowing from Sròn a' Ghoill have significantly dissected these mounds and ridges, causing difficulties in identifying their true orientation.

Figure 4.7. A) Mounds and ridges on top of the Turret Fan, crestlines of which are marked with a white dashed line. These features continue upwards across the eastern valley side of Glen Turret. Photograph taken from the Allt a Chòmhlain fan looking eastwards. B) Terraces (T) within the Allt a' Chòmhlain catchment, the large ridge (R) at the mouth of Allt a' Chòmhlain and dissected mounds (M) by Coire Dubh. Photograph taken from the northern side of the Allt a' Chòmhlain valley towards the southeast. C) Obliquely trending mounds and ridges (R) on the eastern valley side of Glen Turret, crestlines of which are highlighted by white dashed lines. Photograph taken northwestwards from the eastern valley side of Glen Turret, with the Allt Teanga Bige fan and section in the background. D) Large fan at the mouth of the Allt Teanga Bige as it enters Glen Turret. The section described in the text is marked by an 'S'. Photograph taken from the southern side of the Allt Teanga Bige catchment looking northeastwards.

Upstream from the fan, the lower part of the valley forms a wide flat basin, the downstream end of which is approximately 10 m lower than the elevation of the top of the fan. The River Turret is unconstrained within this area forming a braided river channel. Abandoned channels and several river terraces document the migration of the channel across the valley floor.

A second large fan, with a maximum elevation of 325 m occurs at the mouth of the Allt a' Chòmhlain basin as it joins Glen Turret (NN 932 929). The fan is more extensive on the northern side, where the top consists of a horseshoe-shaped ridge, with a depression in the centre. A second fan emerges to the north between the main fan and the valley side. Directly behind the fan(s), a

large ridge trends obliquely across both valley sides in an upslope direction. On the northern side, this is the only ridge that occurs, but at least two more occur on the valley floor to the south. Two terraces, at elevations of 318 and 325 m, are found inside these ridges next to the stream, which flows in a deep v-shaped channel at least 15 m below (Fig. 4.7B). Above these terraces, a large accumulation of sediment occurs higher up on the southern valley side, which has been heavily dissected by streams flowing from the escarpment above to form several discrete mounds. This sediment leads upvalley to Coire Dubh where a number of pronounced stream channels flow directly down the valley side to Allt a' Chòmhlain.

About half way up Glen Turret, upstream of the confluence with Allt a' Chòmhlain, at NN 333 933, the valley narrows significantly where the river becomes constrained to a single channel in the centre in between steep valley sides. The lower halves of both valley sides are covered with a thick accumulation of sediment. On the western side, deep channels, orientated directly downslope, have developed in this material, forming large broad ridges in between. Immediately upstream of the Allt a' Chòmhlain confluence (NN 934 929), both the 325 and 350 m Lake Roy shorelines can be seen cut into the sediment, but they become lost in the central section due to the deep channels. The 350 m shoreline re-appears again near the Allt Teanga Bige.

There are also a large number of predominantly downslope-trending channels on the eastern valley side, but unlike on the west, in the area between the elevations of 280 and 370 m, the channels trend more obliquely downslope across the valley side and smaller pronounced ridges occur in between and parallel to the channels (Fig. 4.7C). In the lower part of the valley side, towards the floor, the channels then turn to flow more directly down the valley side again. The 350 m lake shoreline can be seen faintly above the area of ridges, but the 325 m shoreline is absent.

At the head of Glen Turret, large fans occur at the mouths of Allt Eachach and Allt Teanga Bige. By Allt Eachach, a large fan occurs at an elevation of just over 330 m, with a smaller terrace at an elevation of 350 m further upstream. Opposite the 350 m fan, three prominent ridges occur, which stop abruptly at roughly the same height, slightly above the 350 m shoreline.

Upstream of the fans, the Glen Eachach forms a narrow v-shaped valley, with numerous small streams flowing down both valley sides from the plateau above. Whilst most streams flow directly down the slope of the valley sides, some of them are diverted as they near the valley bottom and flow obliquely downvalley, despite no obvious cause for this diversion. A limited number of ridges also occur on the southern valley side and can be traced upvalley, very faintly, towards the northern flank (NN 355 952) of Carn Dearg (768 m).

The central of the three streams at the head of Glen Turret, Allt Teanga Mòire, drains the central part of the plateau to the north of Glen Turret and flows down a steep backwall into the main valley. As the stream enters Glen Turret, a small fan emerges, which coalesces with the 330 m fan at the mouth of Allt Eachach. The Allt Teanga Mòire has cut into this fan to produce a lower terrace on its eastern side. An arcuate ridge occurs on top of the main fan and appears to link to a faint ridge on the eastern side of Allt Teanga Mòire that continues obliquely up the valley side. Further upstream, on the plateau, several other ridges and channels occur around the two tributaries that source the Allt Teanga Mòire.

A large fan also occurs at the head of Glen Turret to the east of Allt Teanga Mòire (Fig 4.7D). This feature is located on the northern valley side where Allt Teanga Bige joins the main valley (NN 330 944). The feature is partly flat-topped at an elevation of around 350 m but a ridge also occurs on top of the feature. This ridge curves arcuately towards the northern valley side, with others occurring immediately upstream of them. A large number of deeply incised channels trend down both valley sides at a very slightly oblique angle further upstream, with more ridges in between.

The stream has excavated a large section within the fan and beneath the ridge. The section has a total height of around 30 m, but there is a large amount of slumping in the lower half. The lowermost non-vegetated part consists of diamicton, but the unit is still slumped and therefore the structure of the diamicton cannot be recognised. Above this unit there is a layer about 30 cm thick of laminated clay, followed by a consolidated matrix-supported diamicton showing fissility. This is capped by a clast-supported diamicton. This section has previously been described by Benn and Evans (2008), who found a similar sequence (Section 2.3.3).

Coire an t-Sìdhein to the west of the Allt Teanga Bige catchment and is a small northwest-facing corrie, situated below the southwest corner of the plateau to the north of Glen Turret. The backwall and southwest valley side are characterised by densely spaced, sharp-crested ridges, with deeply incised channels in between them that trend almost directly downslope. Channels are also superimposed on these ridges and trend perpendicular to the original orientation of the ridges. However, some of the ridges, particularly towards the top of Coire an t-Sìdhean do not have deep channels around them or superimposed on them. On the northeastern valley side, some ridges occur that trend more obliquely across the valley side. There is no river terrace in the upper part of Coire an t-Sìdhean and the stream resides within a v-shaped channel. Further downstream, a river terrace begins at around NN 306 955.

4.1.4 Glen Buck

Glen Buck is a large northeast-trending valley that runs parallel to Loch Oich in the Great Glen. Very large ridges occur across the valley sides throughout the lower part of Glen Buck, whilst within the heads of the smaller tributary basins, upstream of the confluence of Allt Innis Shim and Allt na Larach (NH 338 000) and to the north of Glas Charn (791 m; NN 354 978) in Coire Charn and Coire Eilrig, small, closely spaced ridges and mounds occur separated by an often anastomosing network of channels (Fig. 4.8).

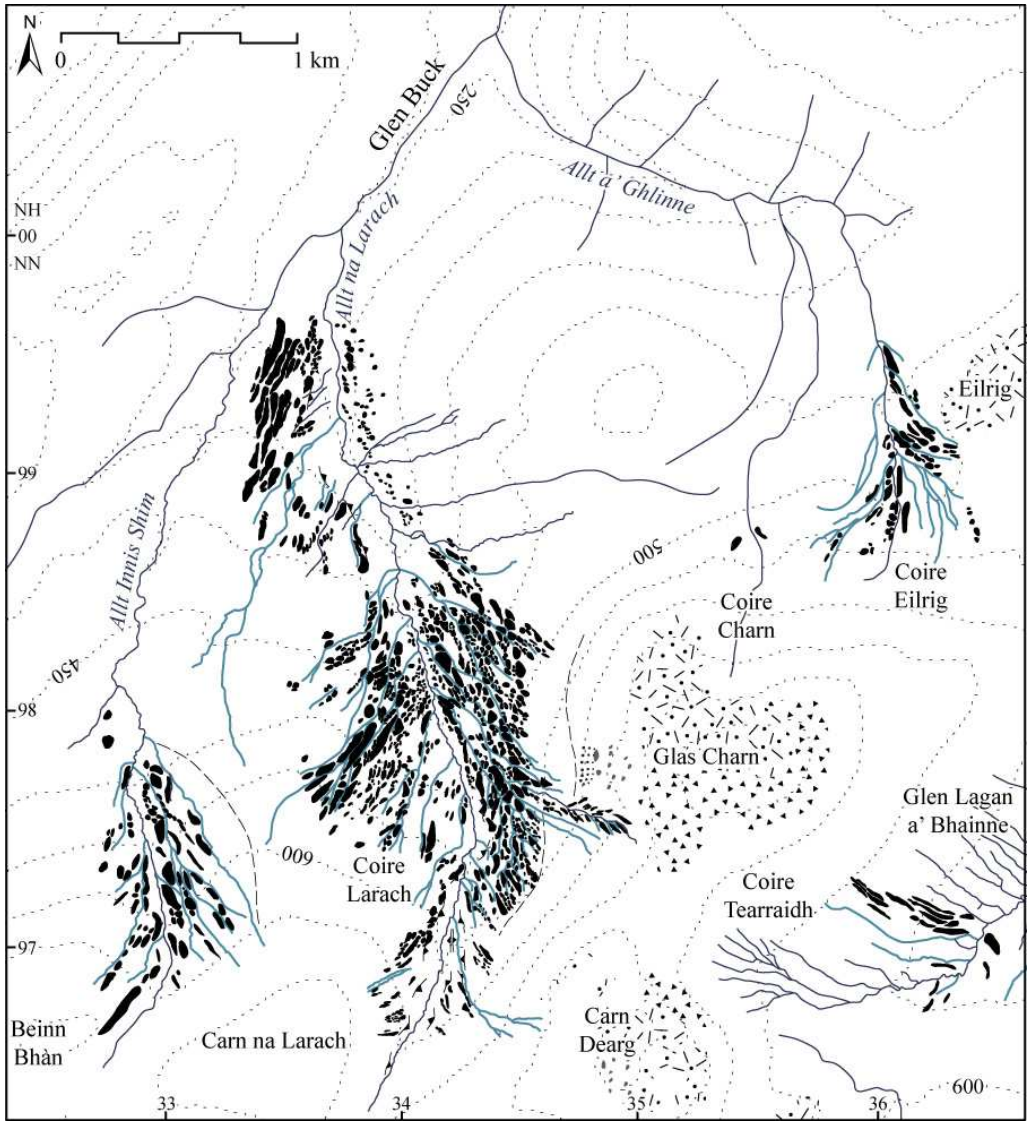

Figure 4.8. The geomorphology of upper Glen Buck (see Fig. 4.2 for key).

The main tributary is the Allt na Larach, which flows from Coire Larach into Glen Buck at the confluence with the Allt Innis Shim to the west. Immediately upstream of this confluence, the shape of the lower part of Coire Larach is asymmetrical, with the western valley side being much steeper initially compared to the eastern side. However, whilst the eastern valley side remains the same gradient upslope, the western side flattens to a broad area in between Allt na Larach and Allt Innis Shim that gently slopes downstream. A large number of ridges and mounds occur on both valley sides and their morphology reflects this asymmetry. On the

western side, the ridges are fairly wide and show a low profile on the flatter area, but form distinct ridges with deep gullies on either side, on the steep section by the river. Conversely, on the eastern valley side, they occur as densely spaced mounds, some of which are large and relatively sharp-crested.

1.4 km upstream of the Larach-Innis Shim confluence, the valley steeply slopes upwards for 300 m before flattening out into a broader, flatter basin within which there has been much less stream incision than further downstream. There is a clear transition in the landscape in this uppermost part of the valley. The vegetation changes from trees, grass, heather and fern to tougher grasses and heather. The number of individual mounds and ridges also increases and they are generally smaller in area, but often taller than those lower down and more sharp-crested. In addition, very few boulders were observed on either the mounds or ridges, both in this area or further downstream.

There is a clear upper limit to an accumulation of sediment on the eastern side below Glas Charn and Carn Dearg (817 m; NN 349 967), which merges into the mounded topography below (Fig 4.9). A small area of talus also occurs immediately above the drift limit below Glas Charn. Gullying occurs in the area between Glas Charn and Carn Dearg, but the gullies are less incised below the upper boundary of the sediment accumulation, compared to above it. On the western valley side such a distinguishable upper limit of ridges or sediment is not present, but a well-formed channel can be followed upwards, across the northern flank of Carn na Larach (746 m; NN 334 966), which delineates a subtle boundary between ridges that are heavily dissected by channels and smoother, more subdued ridges further downstream.

Figure 4.9. Closely spaced mounds and ridges in Coire Larach, with a distinct upper boundary below Glas Charn (dashed line) and a small accumulation of talus (T) on the slope above. Photograph taken from the eastern side of Coire Larach towards the west.

Towards the plateau, the valley narrows and the current stream has incised into diamicton by over 20 m. A number of inset ridges, which trend almost parallel to the Allt na Larach, occur on the eastern side in close proximity to it and each other. Although the ridges are separated by shallow channels that are also orientated nearly parallel to the current stream, they appear to form part of a large terrace that gently slopes downstream.

Coire Innis Shim is a small, north-facing pseudo cirque that occurs to the west of Coire Larach below the plateau between Beinn Bhàn (712 m; NN 320 965) and Carn na Larach (746 m; NN 335 966). The cirque leads straight up onto the plateau and there is no backwall. It is dominated by a number of deep channels, which flow obliquely downslope and turn arcuately towards the centreline as they reach it. In between some of the channels there are ridges. Much fewer channels occur beyond NN 329 978 and at this point the Allt Innis Shim channel widens slightly. Additional river terraces do not occur until further downstream, however.

The Allt a' Ghlinne tributary joins the Calder Burn within Glen Buck further downstream from the Allt Innis Shim-Allt na Larach confluence and is fed by two tributary basins, Coire Eilrig and an unnamed pseudo cirque which both occur on the north-facing side of Glas Charn (NN 354 983 and NN 361 986). For the purposes of this thesis, the unamed cirque is referred to as Coire Charn from now on. Within this cirque, two small arcuate ridges are identified, one on either side of the central stream, about 200 m from the base of the backwall. Several stream channels occur both upstream and downstream of these ridges, but whereas the upstream channels are arcuate, those downstream follow the main gradient of the slope.

Coire Eilrig neighbours Coire Charn to the east and connects with Glen Lagan a' Bhainne on the eastern side. Stream channels are a dominant feature within the corrie, trending obliquely downslope, but becoming slightly more arcuate immediately before joining the central stream. Several ridges also occur in between the stream channels and lead up onto the northeastern and southwestern flanks of Glas Charn and Eilrig respectively.

4.1.5 Culachy Forest

Three tributary basins, Glen Lagan a' Bhainne, Glen Uchdachan and Coire na Cèire, drain into the upper part of Glen Tarff from the area known as the Culachy Forest and are described below (Fig. 4.10). Since Glen Tarff itself begins further to the north and east it is described in Section 4.2.

Glen Lagan a' Bhainne comprises a northeast trending valley that joins Glen Uchdachan just over 1 km upstream of its junction with Glen Tarff. At the confluence with Glen Tarff, a small

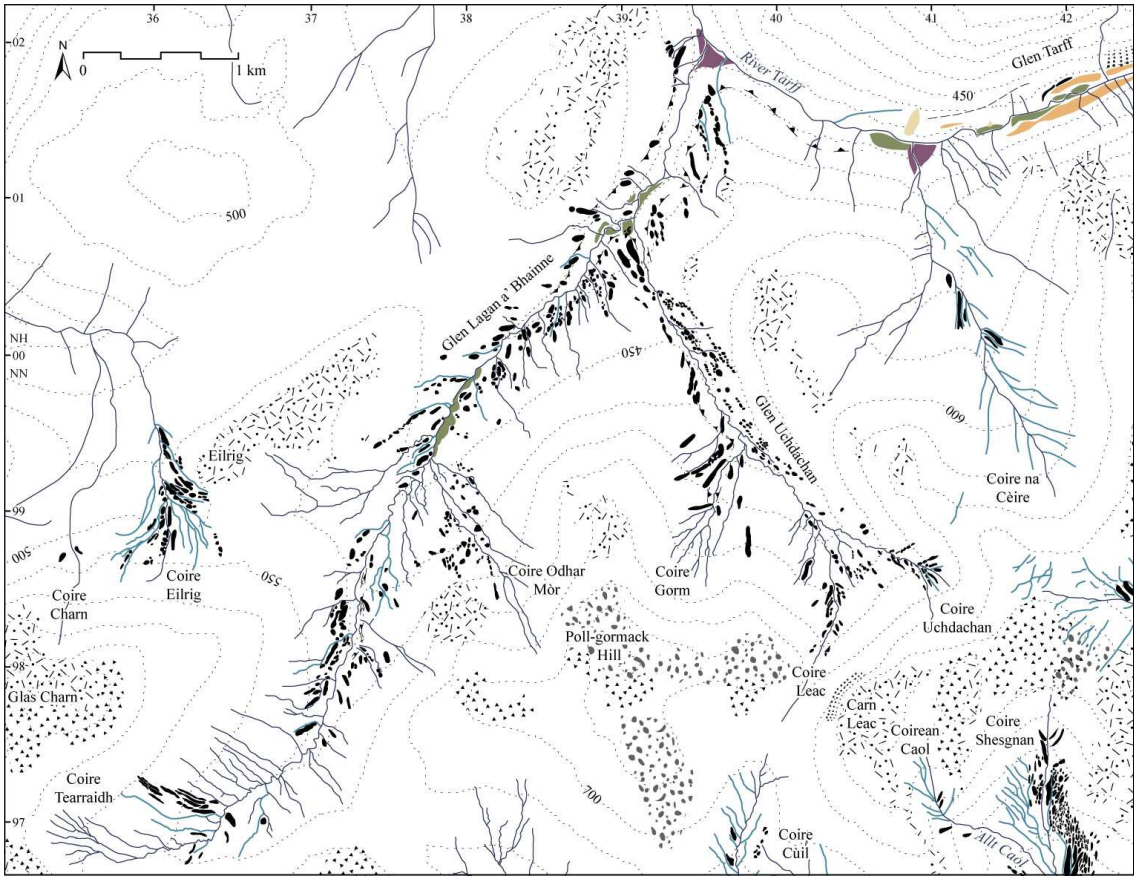

Figure 4.10. The geomorphology of the Culachy Forest area, including Glen Lagan a' Bhainne, Glen Uchdachan and Coire na Cèire (see Fig. 4.2 for key).

fan emerges from the mouth of the Lagan a' Bhainne – Uchdachan stream. Large, rounded ridges, which are about 5 m in height and up to 60 m wide, occur on both sides of the Lagan a' Bhainne - Uchdachan stream around its confluence with the River Tarff and trend obliquely upwards across the valley sides. On the western valley side, the ridges form part of the steep gorge-like sides of the river and are deeply incised by channels. Conversely, on the eastern side, the ridges occur on flatter ground above the lower, steeper sides.

Upstream, a number of large conical mounds (~ 10 m high) occur (Fig. 4.11A) around the confluence of Allt Coire Uchdachan and Allt Lagan a' Bhainne (NH 391 009). The river has incised deeply into the bedrock by 10 to 15 m at this location and an exposed section above the bedrock reveals a unit of laminated sands that are about 1 m thick. The exposure is inaccessible and the remaining section obscured by slumping, but the sand unit appears to be bounded below by gravel and above by diamicton, although this cannot be confirmed. This section occurs below a fragment of a higher-level terrace, on which some ridges occur. On the northern valley side a terrace remnant is found at a significantly lower altitude than that on the southern side, with a track running over the top of it at present.

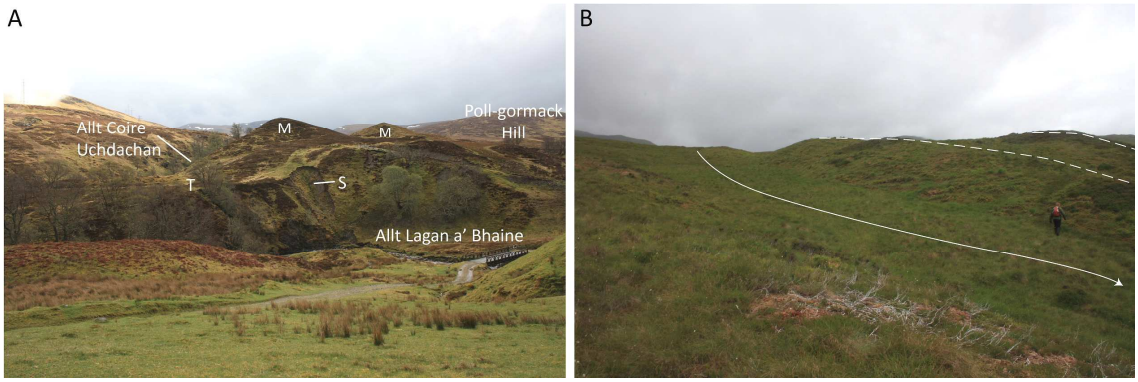

Figure 4.11. A) Conical mounds (M) by the confluence of Allt Lagan a' Bhainne with Allt Coire Uchdachan, with a high-level terrace (T) and the section described in the text (S). Photograph taken from the northwestern valley side towards the southeast. B) Smaller ridges found upstream of the Lagan a' Bhainne – Uchdachan confluence (crestlines highlighted by a white dashed line), with a person for scale in a large channel between them, highlighted by a white arrowed line. Photograph taken on the southern side of the Lagan a' Bhainne catchment looking approximately upstream.

Ridges and mounds also occur upstream in the main part of Glen Lagan a' Bhainne (Fig. 4.11B). These features occur mainly on the southern valley side and tend to be fairly broad with rounded crestlines, but much smaller than those further downstream, with a maximum height of around 5 m. The valley widens upstream of the Allt Coire Uchdachan confluence to approximately 1 km across, to form a gently downstream sloping basin. The stream is located towards the northwestern valley side and has caused considerable incision. It is bounded by steep sides to the northwest, but more gently-sloping sides to the southeast, which contain small terrace fragments in several places. The ridges and mounds on the southeastern side tend to only occur in fairly close proximity to the current stream. Whilst there are fewer ridges on the northern valley side in this part of the valley, a large number of obliquely trending channels occur on the steep slopes next to Allt Lagan a' Bhainne.

Ridges and mounds become more numerous on the northwestern side opposite Coire Odhar Mòr (NN 378 993) and mainly occur as longer ridges. A thick accumulation of sediment can be seen within Coire Odhar Mòr due to intensive erosion by several former stream channels. These channels are generally orientated downslope, parallel to the central stream, but turn more arcuately across the slope immediately before they meet the central stream. Ridges occur in between some of the channels. At the head of Glen Lagan a' Bhainne, within Coire Tearraidh (NN 355 970), several long, thin ridges are present on the northern side of the stream, which are interspersed with former channels.

Glen Uchdachan is located immediately to the east of Glen Lagan a' Bhainne, coalescing with it about 1 km upstream from the confluence with Glen Tarff. It is a northwest-facing valley that forms part of the Corrieyairack Pass between Carn Leac (884 m; NN 407 978) and Glen Tarff. Headed by Coire Uchdachan, the valley is asymmetrical in shape, with steep valley sides to the

northeast, but a more gently sloping valley floor to the west, which leads up to two corries, Coire Leac and Coire Gorm. The current stream flows within a narrow channel, which has deeply incised into sediment on the southwestern side, so that the sloping valley floor is raised by up to 40 m above the height of the stream**.** Small sections within the sediment reveal that it is mainly composed of diamicton.

Small mounds occur about 500 m upstream of the Lagan a' Bhainne – Uchdachan confluence on the northeastern side, which are organised into several lines that trend obliquely upwards across the valley side. Some subdued ridges also occur on the southwestern valley side that have been dissected by Allt Coire Uchdachan to form a steep cliff. Varyingly shaped mounds and ridges are also found within the three tributary corries. Deep channels occur between them, which dominate the landform assemblage. A trimline is observed below Carn Leac (NN 404 978), where a talus slope abruptly stops on the hillslope at a height of 735 – 745 m.

The third main catchment in the area is Coire na Cèire, which is a north-facing corrie located on the southern side of Glen Tarff and connected to a smaller corrie to the west. Coire na Cèire is linked to the plateau by a relatively shallow, gently sloping backwall. The valley is dominated by a large number of small channels with a few subdued ridges, which are orientated obliquely across the valley floor.

4.1.6 Interpretation of the geomorphological evidence in the western Monadhliath Mountains

The majority of mounds and ridges within the western Monadhliath valleys are distributed to form arcuate or chevron shaped chains, which are orientated obliquely downslope across the valley sides. Their morphology varies from sharp-crested ridges or conical mounds to subdued features with rounded crestlines, with dimensions varying between 5 to 10 m in height and 20 to 70 m in width. Based on their dimensions and spatial organisation, these features are interpreted as moraines, following interpretations of similar features in other areas of Scotland (e.g. Benn, 1992; Benn *et al*., 1992; Bennett & Boulton, 1993a, b; Wilson & Evans, 2000; Lukas, 2005b; Benn & Ballantyne, 2005; Lukas & Benn, 2006; Finlayson, 2006; Ballantyne, 2007a, b; Finlayson *et al*., 2011) (see geomorphological map in Appendix II). Most moraines are latero-frontal, since they curve arcuately across the valley floor, although some that trend obliquely downslope across the valley side only are interpreted as lateral. The moraines are thus interpreted to represent former ice-marginal positions following Bennett and Boulton (1993a, b), Benn and Lukas (2006) and Lukas and Benn (2006). A more detailed discussion of this interpretation is found in Section 4.5.

Channels that occur in between and parallel to the chains of moraines are interpreted as former ice-marginal meltwater channels due to their orientation and position among the moraines

(Benn & Lukas, 2006; Lukas & Benn, 2006; Greenwood *et al*., 2007). Channels that do not occur in between moraines, but are also orientated obliquely or arcuately across the valley sides and/or the valley floor in a downslope direction are also interpreted as former ice-marginal meltwater channels (Greenwood *et al*., 2007), where meltwater flowed around former glacier margins (Ò Cofaigh *et al*., 1999; Atkins & Dickinson, 2007). These channels therefore also delineate former ice-marginal positions. Channels that are orientated directly downslope, with no association to moraines, are not interpreted as of glacial origin and are instead interpreted as gullies cut into unconsolidated sediment.

Whilst the majority of valleys contain mounds, ridges and channels that are confidently interpreted as moraines and former ice-marginal meltwater channels, there are some exceptions, most notably within Coire an t-Sìdhean. The southwestern valley side within the upper part of this corrie is characterised by densely-spaced, sharp-crested ridges separated by deep channels. These ridges and channels are orientated parallel to the slope rather than obliquely across, as would be expected for moraines. These features are therefore interpreted as having been formed through the downcutting of streams on either side of them (i.e. through gullying). The occurrence of these gullies indicates that a large accumulation of sediment is present on this valley side. On the northeastern valley side, however, there are a number of mounds and ridges that are orientated more obliquely downwards across the slope, alongside ridges at the top of Coire an-t Sìdhean that do not have deep channels around them, indicating that they were not formed through gullying. These features are therefore interpreted as moraines.

Gullying has also had a large effect on the morphology of the eastern and western valley sides in Glen Turret and in the adjoining Coire Dubh. The apparent ridges on both the eastern side of Glen Turret and in the main part of Coire Dubh are interpreted as having formed through gullying on either side due to the broad, almost flat-topped nature of most of the ridges. This opposes an earlier view by Chen and Rose (2008) that the ridges in Coire Dubh are flutes, where gullying is preferred here as a simpler explanation. Immediately to the east of the gullies in Coire Dubh, however, there are at least one, if not two, coalescent ridges of sediment that have been dissected by a large number of small streams flowing down the hillside. These ridges are interpreted as former lateral moraines that have been subsequently dissected by gullying. Small obliquely trending ridges also occur on the eastern side of Glen Turret, which are separated by obliquely trending channels that are initially orientated parallel to the ridges, but turn to continue more directly downslope nearer to the valley floor. These ridges are interpreted as former latero-frontal moraines due to their orientation. However, their dissected nature and the orientation of the channels on the lowest part of the valley side indicate that gullying has subsequently modified these moraines and this has been attributed to snowmelt erosion elsewhere (e.g. Lukas, 2003; Benn & Lukas, 2006).

Coire Innis Shim, Coire na Cèire, Coire Eilrig, Coire Odhar Mòr and the upper area of Coire Larach and Coire Shesgnan are dominated by ice-marginal meltwater channels, that trend obliquely or arcuately across the valley floor. Ridges often occur in between and parallel to these channels, but not all the ridges are interpreted as moraines since some have been formed through the downcutting of two closely spaced meltwater channels to leave a remnant of the former surface as an apparent 'ridge'. Ridge-like features in these valleys were only interpreted as moraines if the landform stood out as a depositional feature above the former surface. The number of features interpreted as moraines varies between these valleys. In Coire na Cèire most of these features are interpreted as remnants of the former surface, whilst in Coire Innis Shim and Coire Eilrig, most are interpreted as moraines.

Other features found in the valleys in the western part of the Monadhliath Mountains include the terraces at the mouth of Glen Chonnal and the fans within Glen Turret. The large fan at the mouth of Glen Turret has previously been interpreted to be both a subaqueous ice-contact fan, related to development of the 260 m lake (Sissons & Cornish, 1982, 1983), and a subaerial glaciofluvial fan (Peacock, 1986). The present research did not examine the sediments within the fan and therefore cannot add to the debate at this stage. However, the origin of the Turret Fan in terms of the chronology of events is discussed further in Section 5.2.2. Fans also occur at the mouths of the Allt a' Chòmhlain, Allt Teanga Bige, Allt Teanga Mòire and Allt Eachach catchments. The surface elevations of the Allt a' Chòmhlain and lower Allt Eachach - Allt Teanga Mòire fans are 325 m and indicate that they relate to the 325 m lake, alongside a 325 m terrace behind the Allt a' Chòmhlain fan. The surface of the remaining fans at the mouth of the Allt Teanga Bige and Allt Eachach catchments is at 350 m, demonstrating their association with the 350 m lake level in Glen Roy. Diamictic sediments within the Teanga Bige fan are interpreted as subaqueous debris flow deposits, whilst the moraines on top indicate a glacial advance over the subaqueous fan, following lake drainage, in agreement with Benn and Evans (2008) (Section 2.3.3). The same interpretation is therefore used to explain the formation of the fans that emanate from the Teanga Mòire and Eachach catchments. The large terraces at the mouth of Glen Chonnal also have upper surfaces at an elevation of 350 m and are interpreted as remnants of a former (glacio)fluvial fan associated with the 350 m lake. Further discussion on the association of the fans to the evidence for glaciers found within both Glen Chonnal and Glen Turret is provided in Section 5.2.2.

To summarise, the landforms found within the valleys of the western Monadhliath Mountains provide strong evidence for the former presence of glaciers in the valleys. This evidence is predominantly in the form of moraines and ice-marginal meltwater channels, which in many valleys, such as Glen Chonnal, Coire Larach, Coire Innis Shim and Glen Lagan a' Bhainne, continue towards the plateau due to the lack of backwall, suggesting that the glaciers were

sourced by plateau ice. Other features such as accumulations of sediment on the valley sides are also apparent in some valleys such as Glen Turret and Coire Larach. The moraines change in morphology up valley, often changing from either large isolated mounds or ridges with rounded crestlines to smaller, more densely spaced moraines with sharper crestlines. Meltwater channels also become more densely spaced in the upper parts of the valleys and the number of river terraces decreases upvalley, with abrupt changes in Glen Shesgnan and Glen Chonnal. These differences will be examined further in Section 5.1.

4.2 The Northern Monadhliath Mountains

The area of the northern Monadhliath Mountains described in this section comprises the catchments that drain the main plateau in the Monadhliath Mountains to the north, in addition to Glen Tarff, the only valley to face west from the plateau (Figs. 3.1 and 4.1). The plateau elevation in this area is between 600 and 800 m OD and the region covers an area in the order of 160 km^2. No previous glacial geomorphological or sedimentological research has been conducted in this area.

4.2.1 Glen Tarff

The River Tarff drains a large proportion of the western part of the central Monadhliath plateau. Throughout the valley the river flows through a narrow, steep-sided valley. In the lower part of the valley this forms an impressive narrow gorge, but the valley widens slightly just downstream of the Lagan a' Bhainne - Uchdachan confluence, forming a deep, steep-sided trough, which continues until a jagged bedrock backwall leads to the plateau (Fig. 4.12).

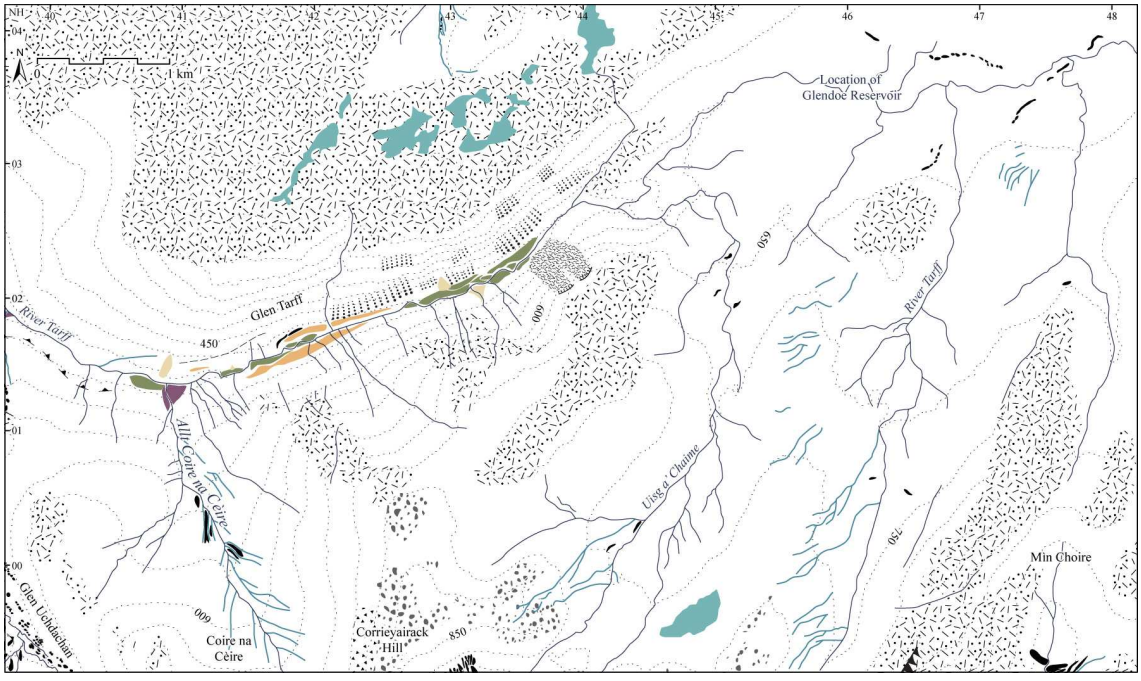

Figure 4.12. The geomorphology of the upper Tarff catchment (see Fig. 4.2 for key).

Once the valley widens into a trough, thick accumulations of sediment on the valley sides are observed. On the southern valley side below Coire na Cèire (NH 411 012) the thick sediment accumulations have been heavily incised by channels orientated directly downslope. As these channels reach the valley floor, some become orientated slightly more obliquely across the valley side. On the opposite valley side a large accumulation of sediment also occurs at the base of the slope, the upper boundary of which gradually rises further upstream.

Further upstream (NH 430 022), the northern valley side is dominated by thick talus, which covers the whole of the valley side, reaching the valley floor (Fig. 4.13). On the southern side a significant number of downslope trending channels occur in unconsolidated sediment. A sequence of river terraces also occurs on either side of the River Tarff in this area and these terraces continue downstream, although becoming more fragmented towards the confluence with Allt Coire na Cèire. Towards the top of Glen Tarff, at NH 439 021, a scarp occurs at the top of the southern valley side. A large lobe of rocky material occurs below this scarp that extends to the valley floor. Almost immediately upstream of this feature the backwall begins, which has been dissected by three tributary streams. All three, particularly the northernmost and southernmost are fairly well incised into the exposed bedrock. The northernmost stream has also incised into a large accumulation of sediment that sits within the bedrock channel. A number of isolated mounds and ridges occur on the plateau within the Tarff catchment and are shown on Figure 4.12.

Figure 4.13. Talus slopes (marked), high-level terraces (T) and river terraces (RT) on the northern side of Glen Tarff. Photograph taken from the southern side of Glen Tarff, immediately to the east of the Allt Coire na Cèire tributary, looking northeastwards.

4.2.2 Glen Doe

The upper part of Glen Doe forms a wide, open slope between Carn Doire Chaorach (530 m; NH 409 049) and Creag Coire Doe (704 m; NH 436 066) (Fig. 4.14). The valley floor is composed of a thick accumulation of sediment, which Allt Doe has incised into by over 20 m. A section was examined on the northern bank of Allt Doe (NH 423 060) in which the lowest part consisted of large boulders resting in a gravel matrix, above which a massive sand occurred that contained patches of diamicton and gravelly sand. Further upwards patches of sand, silt and diamicton were present, with gradational boundaries between them. Much further upwards in the section, alternating units of clast-rich, matrix-supported diamicton and clast-supported diamicton were observed.

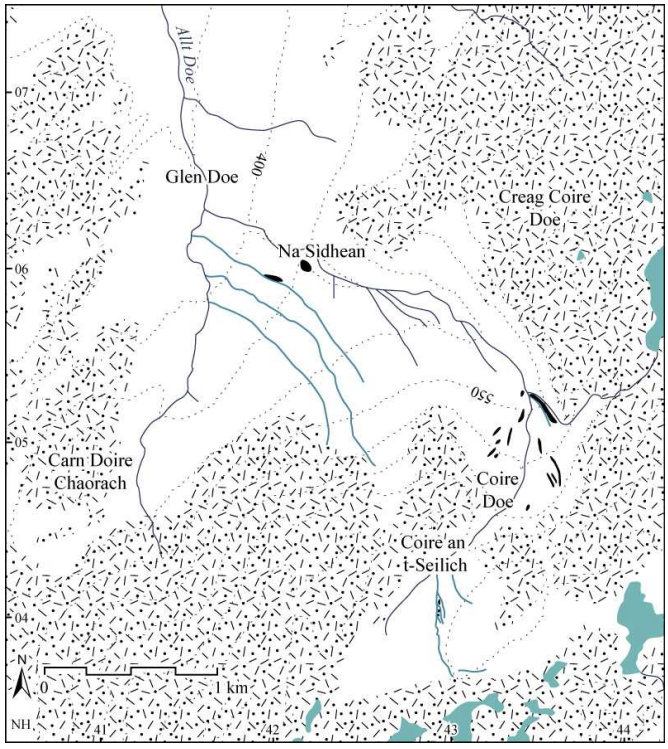

Figure 4.14. The geomorphology of the upper part of Glen Doe (see Fig. 4.2 for key).

Several other streams curve arcuately downslope to join another tributary stream flowing from near Carn Doire Chaorach. These streams have previously also caused deep incisions by between 5 to 10 m, to reveal several sections of diamicton. Apart from these channels, the majority of the valley floor forms a smooth, gently sloping terrace, with the exception of two isolated conical mounds that occur at similar elevations of 435 and 450 m and both on the edge of streams. The larger of the two occurs on the southern side of Allt Doe and is named locally as Na Sìdhean (NH 422 060).

The valley narrows dramatically as it reaches Coire Doe. At the mouth of Coire Doe the stream flows at a similar elevation to the surrounding topography, with a very small river terrace on either side, but further upstream, the stream becomes confined again within a narrow channel cut into soft sediments. At the same point as the stream morphology changes, a small arcuate

ridge occurs on the eastern valley side, which curves round towards the backwall, continuing as an accumulation of sediment on the backwall. This laterally continues upwards towards two small channels cut into the bedrock, which may be controlled structurally. Other small ridges are present upstream, but are relatively subdued and seem to merge into the surrounding terrace into which the stream has incised. Coire Doe leads into Coire an t-Seilich through a narrow passage, about 350 m long, within which small narrow ridges and channels are observed on the eastern side and lead up on to the hillside above.

4.2.3 Glen Brein

Glen Brein is located to the north of the central plateau area and trends north-northeastwards. The lower part of the valley is wide and open, with steep, bedrock sides to the east only, whilst the upper part forms a fairly narrow trough with steep sides that have rocky outcrops towards the top (Fig. 4.15). The head of the valley narrows further as it reaches the plateau and the gradient increases, although no distinct backwall is present.

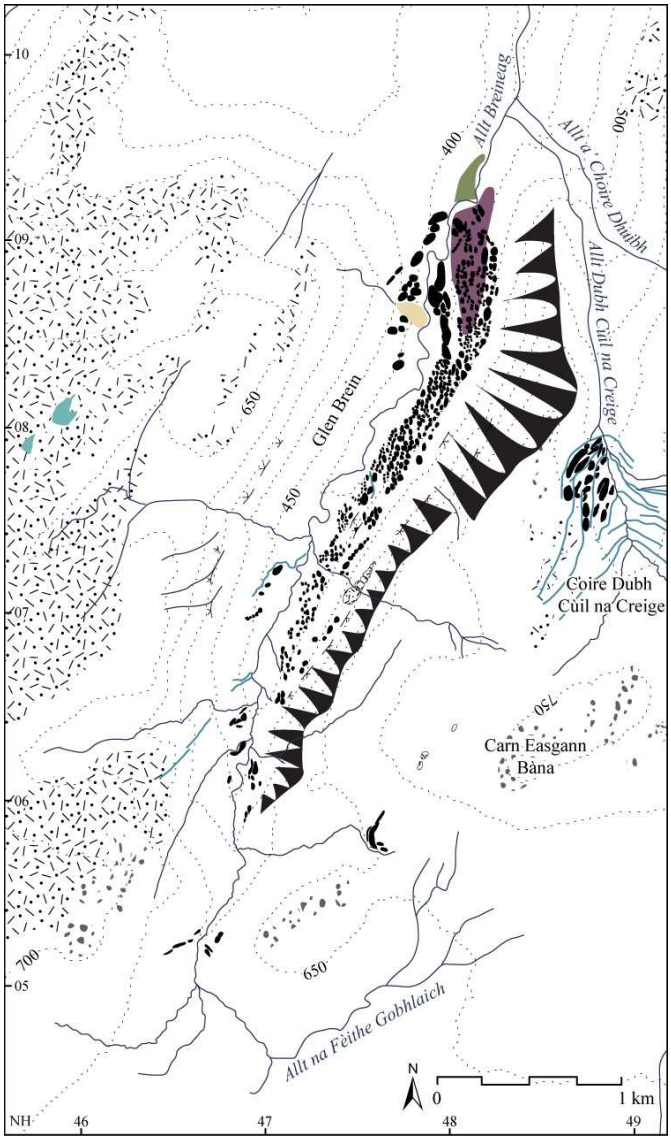

Figure 4.15. The geomorphology of the upper part of Glen Brein (see Fig. 4.2 for key).

At the entrance to the upper part of the valley, a large raised area, 10 to 20 m in height, with a width of 180 m and a length of over 650 m occurs to the east of the stream. The feature has a hummocky surface, the distal slope of which is covered by numerous boulders. This feature is formed of subdued mounds which sit above and also merge into a terrace. Immediately upstream of this feature, a significant ridge, < 10 m high and ~ 45 to 60 m wide, occurs that is orientated obliquely across the valley floor (Fig 4.16A). This ridge bifurcates in places and is separated from the raised mounded area by a large channel. Some subdued ridges also occur on the western valley side, although it is comparatively sparse of features compared to the eastern side.

Figure 4.16. A) Prominent ridge and channel at the entrance to the upper part of Glen Brein, with the ridge crestline indicated by a white dashed line and the channel by a white arrowed line. Photograph taken by the fan at the mouth of the valley looking upstream. B) Small mounds on the eastern valley side of Glen Brein, with steep bedrock above. Photograph taken looking down valley from about midway up the narrow part of Glen Brein.

Upstream of this area, the eastern valley side is covered in small (< 5 high and ~ 25 m wide) and sharp-crested mounds that are organised into chains that trend obliquely down valley (Fig. 4.16B). Whilst the mounds are mainly confined to the valley side a few also occur on the

valley floor, which consists of an alluvial outwash plain with a meandering gravel bed river. There are no large river terraces within this part of Glen Brein, although some small fragments of terraces are present in places, particularly on meander bends. Several more distinct terraces are observed, however, downstream of the raised mounded area at the mouth of the upper sector of the valley.

Very few mounds or ridges occur on the western valley side for about 1 km upstream of the mouth of the upper part of the valley. At NH 474 081, however, a large accumulation of sediment occurs, which continues upstream to the head of the valley. This sediment has been heavily gullied by streams flowing directly down the valley sides, but some channels are orientated more obliquely downvalley and in places prominent ridges occur that are orientated parallel to these channels. As the gradient steepens and the valley narrows at the head of the valley, ridges occur on both sides. Ridges are also found on the plateau above Glen Brein around the Allt na Fèithe Gobhlaich (NH 467 049) and to the southwest of Carn Easgann Bàna (779 m; NH 475 058).

4.2.4 Carn Easgann Bàna – Carn Dubh plateau

An area of high ground occurs between the Brein and Killin basins, which is drained by a number of smaller catchments (Fig. 4.17). The most westerly is the Allt Dubh Cùil na Creige, which flows northwards from the plateau, immediately to the east of Glen Brein, within a steeply sloping, narrow valley. Small, subdued ridges, separated by former channels are present upstream of the confluence of Allt Dubh Cùil na Creige with Allt Breineag (NH 488 085). The stream has incised by about 1 to 2 m in this area into a laterally extensive terrace that appears to surround the subdued ridges.

Where the valley reaches the plateau, it widens out, the terrace is no longer present and a number of small, but relatively sharp-crested ridges are found on the western valley side. Former channels occur around these ridges and continue upwards where they have cut into the side of a bedrock outcrop (NH 485 073) (Fig. 4.18A). Channels also occur on the eastern valley side, but there are very few ridges in between them. A small area of smoothed psammite bedrock is exposed on the valley floor at NH 489 078, within which quartz veins are raised above the psammite surface by 1 to 1.5 cm (Fig 4.18B).

Immediately to the northeast of Coire Dubh Cùil na Creige and to the west of Carn Dubh (762 m), the small, gently sloping, west-northwest-facing basin of Coire Dubh occurs (NH 495 086). No ridges occur within Coire Dubh, although there are some prominent channels towards the very top, which trend obliquely downslope and converge at the same point

on opposite sides with the central stream. There are no river terraces along the entirety of the Allt a' Choire Dhuibh, but it becomes more greatly incised beyond the lip of Coire Dubh where the slope dramatically steepens.

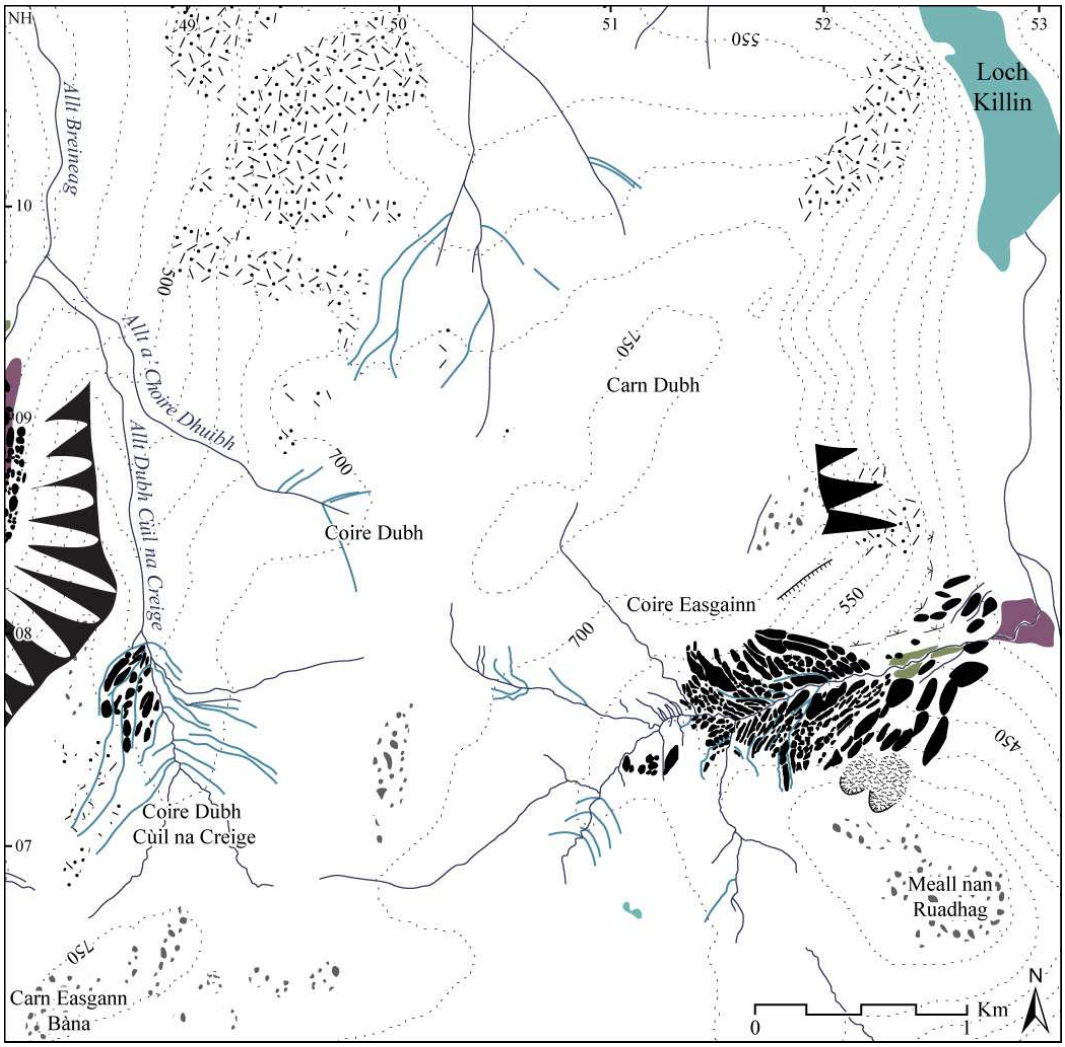

Figure 4.17. The geomorphology of the area around the Carn Easgann Bàna – Carn Dubh plateau (see Fig. 4.2 for key).

Figure 4.18. A) Ridges (crestlines marked with white dashed lines) and channels (white arrowed lines) within the upper part of Coire Dubh Cùil na Creige. Photograph taken on the eastern valley side looking southwestwards towards Carn Easgann Bàna. B) Exposed bedrock on the valley floor of Coire Cùil na Creige. Lens cap in the centre for scale.

Two small pseudo corries occur to the east of Coire Dubh and to north of Carn Dubh (762 m; NH 513 093). Several channels occur within the upper parts of both corries, with some ridge-like remnants of the former slope occurring in between them particularly in the western corrie. The outer two channels within both corries are orientated more obliquely downslope, but the remaining channels generally trend directly down the slope of the valley sides. Downstream of the point where the outer two oblique channels meet the central streams the landscape is much less dominated by channels. In addition, the central streams become more deeply incised and river terraces have developed, particularly along the western stream.

Coire Easgainn is the most easterly valley located on the Carn Easgann Bàna plateau that coalesces with Glen Killin (Fig. 4.17). The geomorphology within this small hanging valley is dominated by small ridges that trend obliquely downslope across the valley side and lead up onto the plateau. These ridges are closely spaced and sharp-crested, with well-developed channels in between them, but are generally less than 10 m high and 15 to 25 m wide. Former channels also flow around the northwestern flank of Meall nan Ruadhag (NH 518 073) into Coire Easgainn (Fig 4.19A).

Two prominent ridges, approximately 20 m in height and one with a very sharp crestline, occur approximately halfway down the valley at NH 521 078 and can be linked together across the valley (Fig. 4.19B). A natural sediment section, caused by stream erosion occurs parallel to the stream and perpendicular to the ridge crestline on the northern valley side. The section consists of a friable, clast-supported diamicton with a sandy matrix. At the upstream end of the section, the clast size varies within the diamicton, with some areas containing mainly smaller clasts, around 20-80 mm a-axis, whilst other areas contain predominantly larger clasts of over 100 mm a-axis. Discontinuous sand stringers, of a different colour to the main matrix, also occur in this area of the section, which are orientated horizontally to sub-horizontally. Large boulders occur only at the top of the upstream part of the section. By contrast, at the downstream end, very large boulders also occur within the clast-supported diamicton throughout the whole of this part of the section, where there is a clear divide between the upstream and downstream halves of the section in terms of clast size. Clast shape and roundness measurements were taken on 50 psammite clasts from within the upstream half of the section and are shown in Figure 4.20. This sample (AE1) has a C_{40} index of 48, an RA index of 62 and an RWR index of 0.

Down-valley of these sharp-crested ridges, further ridges become more subdued and much wider in cross-section, with a curved to flat-topped morphology, compared to the sharp-crested appearance of ridges further upstream. The river terrace morphology remains the same between the two areas, however, and a large river terrace does not occur until slightly further downstream

Figure 4.19. A) Ridges (white dashed lines) and channels (white arrowed lines) on the southern valley side of Coire Easgainn, the latter of which originate on the plateau and continue into the corrie. Photograph taken from the northern valley side towards the southwest. B) Prominent sharp-crested, arcuate ridges and channels within Coire Easgainn, with crestlines highlighted by the white dashed lines and channels by arrowed white lines. 'AE1' indicates the location of the section examined. Photograph taken from the northern valley side looking downstream towards the southeast.

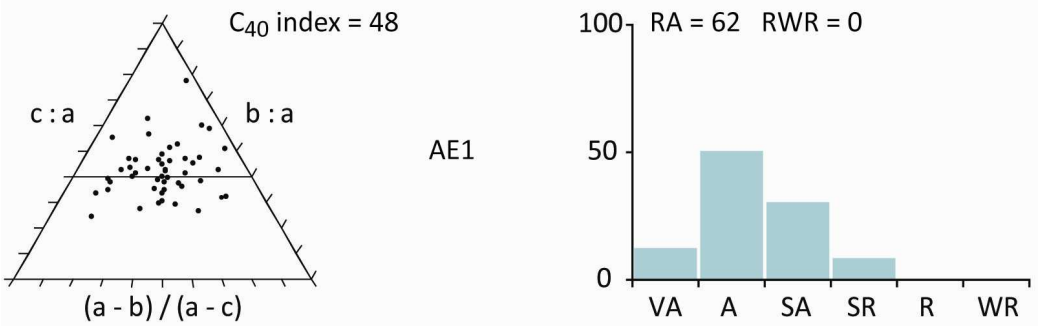

Figure 4.20. Clast shape and roundness data for the sample of 50 psammite clasts taken from Section AE1 within a prominent moraine in Coire Easgainn.

at NH 523 078. At this point there are no clearly defined ridges and topography consists of subdued mounds and ridges that appear streamlined in a direction parallel to the central stream. In addition to the mounds and ridges, a raised flat area, which has a large accumulation of boulders on the distal slope, occurs immediately downstream of the pronounced ridges on the southern valley side.

A large scarp occurs at the top of the northern valley side, which has a large amount of material on the valley side below it, and continues down to the valley floor. This material makes up significant portion of the ridge-like hummocky topography found downstream of the ridges and mounds on the northern side. Two smaller arcuate scarps also occur at the top of the southern valley side, which both have lobes of rocky sediment below them to about one third of the way down the hillside. Again, this rocky sediment occurs downstream of the main area of ridges and mounds.

4.2.5 Glen Killin

Glen Killin is a north-trending valley, bounded to the north by Garrogie Lodge and to the south by Stronelairg Lodge. Loch Killin occupies the northern half of the valley, whilst the southern half consists of the flood plain of the River Killin, within which significant fluvial aggradation has occurred. The River Killin is fed by three main tributaries, Allt Odhar, Allt Coire an Eich and Glenmarkie Burn, and joined by Allt Easgainn further downstream. The geomorphology in the area around the Killin basin is shown in Figure 4.21 and is reported below, alongside several detailed sediment descriptions.

Loch Killin is constrained to the north by a large accumulation of unconsolidated sediment, which is breached in the centre by the River Fechlin exiting Loch Killin. The feature has an undulating surface, which slopes slightly downstream and is continuous along on both sides of the loch, merging with the valley sides after about 0.5 to 1 km upstream of the start of the River Fechlin. The feature is also more extensive to the east of Loch Killin, where it has been dissected by Allt Mharconaich (NH 533 109). Downstream of this area a large flat terrace occurs at NH 521 119, which is over 10 m in height above the current river.

Section LK1 is located within the large accumulation of sediment on the western bank of the River Fechlin at NH 524 113. Three lithofacies associations are identified at LK1 and are shown in Figure 4.22. These are named LFA 1, LFA 2 and LFA 3 and are described below.

- **LFA 1** – The majority of the section, between the relative heights of 0 to 9.5 m, is composed of LFA 1. This lithofacies association is composed of several units of gravel and sand and capped by a clast supported diamicton. The boundaries between units are sharp, often scoured and rarely horizontal. The lowest lithofacies is a gravel, which is

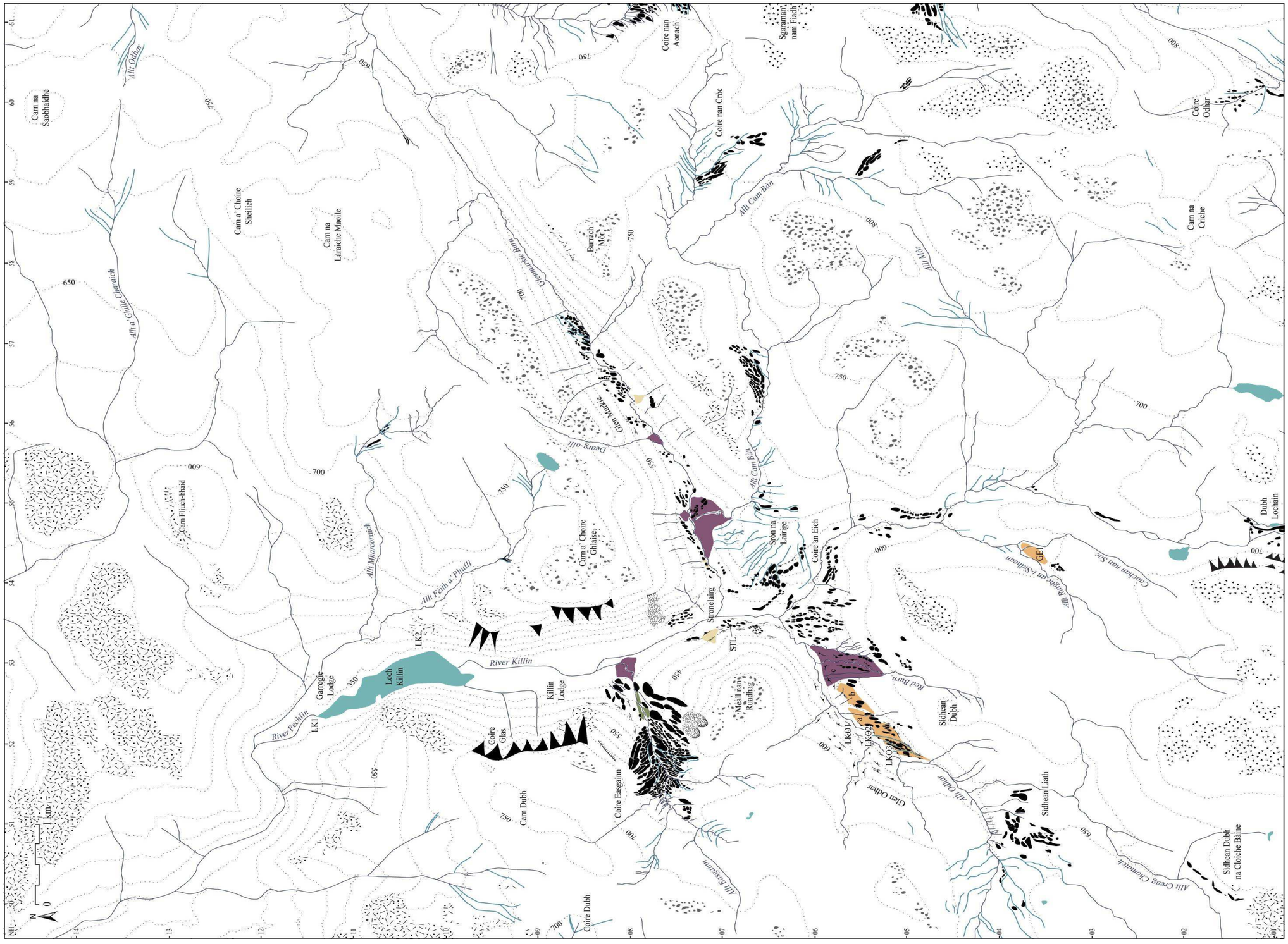

Figure 4.21. The geomorphology of the area around Loch Killin (see Fig. 4.2 for key). The locations of sections LK1, LK2, STL, LKO1, LKO2, LKO3 and GE1, described in the text, are indicated here.

supported by a sandy matrix and contains a mixture of clast sizes with larger clasts of between 50 and 100 mm a-axis. The gravel is generally massive, but has some faint stratification. It occurs repeatedly upwards in the section, with large variations in thickness laterally. In the lower gravel unit, small, elongate lenses of laminated sand and clay that are orientated near to the horizontal occur sporadically. These lenses are not found in the gravel units higher in the section. The interbedded units of sand are discontinuous and occur as large lenses within the gravel, suggesting that the gravel is a more continuous body of sediment, although this could not be established due to large areas of slumping.

The large lenses of sand are composed of a number of units with different bedding structures and are well compacted. The majority of units are planar cross-bedded, but the angle of the bedding, grain size and/or colour varies between units. Other units contain trough cross-bedding. Lenses of granules also occur sporadically within these large sand lenses, which are generally orientated to match the bedding of the surrounding sand. Larger patches of granules also occur in and around the lowermost and uppermost sand lens. By the lowermost lens, an undulating clay vein, 10 mm thick, runs through these granules and across the top of the sand lens. Similar fine sand veins run through a unit of granules at the top of the uppermost sand lens.

The second lowest sand unit contains slightly folded bedding in some units. Small lenses of lighter coloured sand also occur within one sand unit. The third highest sand lens has a vertical boundary with the gravel lithofacies on its northern side, although its continuity to the south and upwards in the section could not be determined due to slumping. Ball and pillow and flame structures occur in the lower parts of this lens, whilst a unit of heavily folded and faulted, discontinuously laminated sand occurs towards the top of the lens. More flame structures occur above this lithofacies, within the overlying sand unit. Laminations within the uppermost sand lens are gently folded, but the disturbance is less than in the lens below.

Five bedding plane measurements were taken from the sand units, the locations of which are shown in Figure 4.22A. The three measurements were taken from the lowest sand lens in the section and show a consistent direction of dip between 008º and 012º (perpendicular to the strike), with dips between 15º and 23º. The two measurements taken from the sand lens above also show consistent dip directions between 355º and 356º, although the dips vary from 15º to 32º. Clast shape and roundness was also measured on a sample of 50 psammite clasts from the lower gravel unit, the location of which is marked on Figure 4.22A and results of which are shown in Figure 4.23. The C_{40}, RA and RWR indexes for this sample are 24, 0 and 12 respectively.

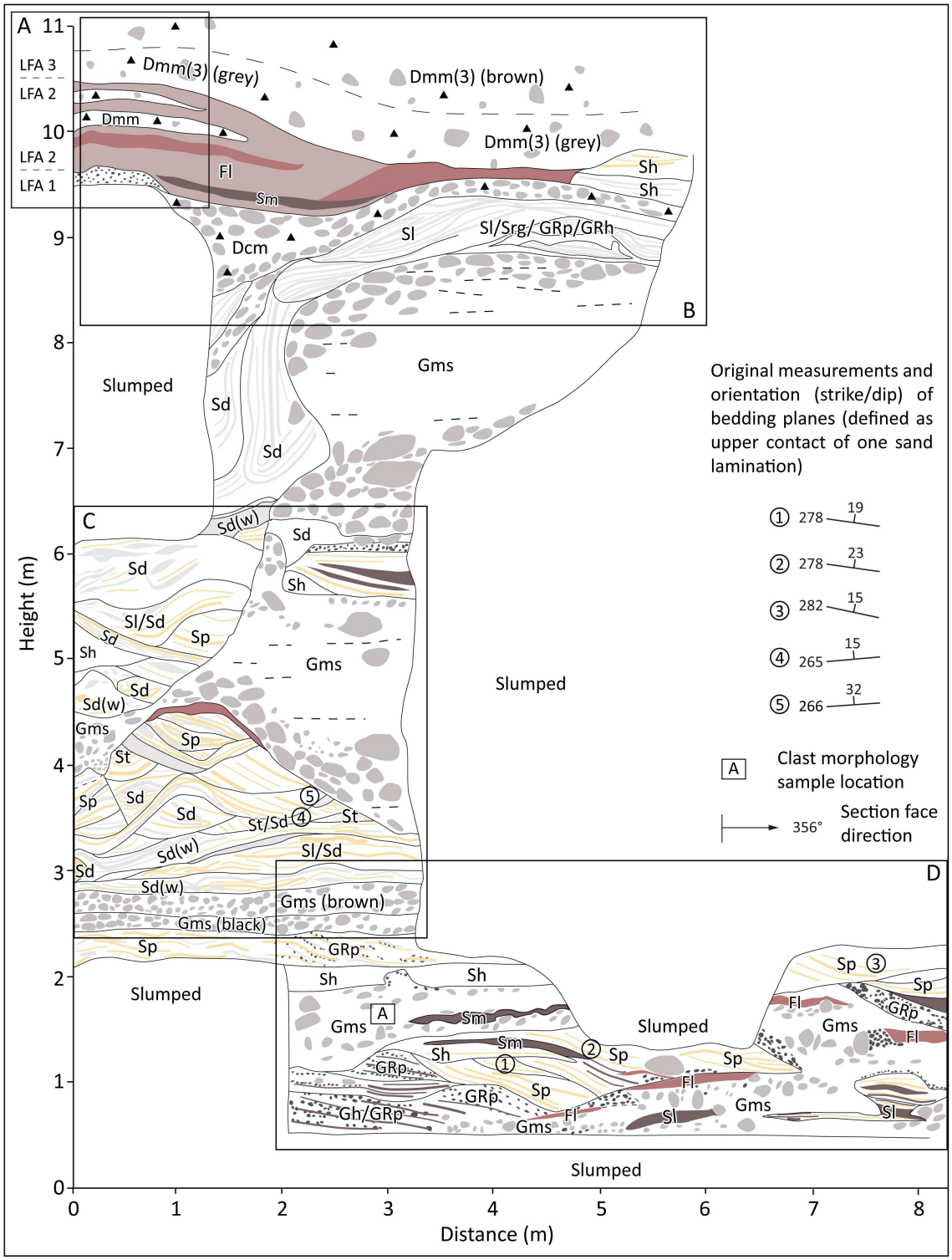

Figure 4.22A. Sketch of the principle units found within Section LK1, including lithofacies association boundaries. The circled numbers represent the locations at which bedding plane measurements were undertaken, the values of which are also shown on the figure. The boxed letter A indicates the location at which the sample for clast morphological analysis was taken. The large boxes A to D indicate where annotated photographs in Figure 4.22B were taken. A key to the lithofacies codes and colours used is found in Figure 3.11 in Section 3.2.

Figure 4.22B. Annotated photographs from LK1, locations of which are marked on Figure 4.22A. A) Upper south section. B) Upper north section. C) Middle section. D) Lower section.

- **LFA 2** – LFA 2 is found towards the top of the section between heights 9.5 and 10.5 and consists predominantly of laminated clay. Slumping obscures the majority of the boundary between LFA 2 and LFA 1, but the northern end of the section reveals a sharp boundary between lenses of clay and sand within LFA 2 and the underlying clast-supported diamicton within LFA 1. The main body of clay within the lithofacies association is formed of fine, discontinuous laminations. Numerous lenses of massive diamicton and deformed, laminated sand occur within the clay, where the sand lenses are generally more elongate than the diamicton lenses. The

boundaries between the lenses and the surrounding clay vary from gradational to sharp. Clasts occur within some of the upper parts of the clay lithofacies. Laminations are draped on top of these clasts and are observed to bend below some of them. The upper contact between this clast-rich clay and the overlying grey diamicton is gradational.

- **LFA 3** – The sequence is capped by LFA 3, which consists of two clast-rich massive diamictons. The first diamicton is approximately 0.3 m thick, is grey and has a finer matrix than the overlying brown diamicton, which contains more sand. The boundary between the two diamictons is sharp in some places and more gradational in others. The brown diamicton occurs at the top of the section and is weathered, with intrusions of roots from the overlying thin (< 1 m) layer of peat.

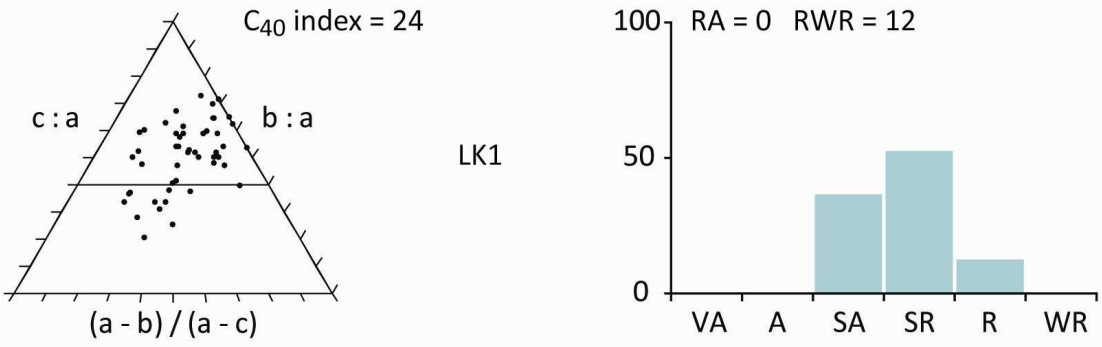

Figure 4.23. Clast shape and roundness data for sample LK1 taken from the lower gravel unit within Section LK1 (location indicated on Figure 4.22A).

A second section, LK2 (NH 534 101) is located in a man-made roadside section to the east of Loch Killin and 1.2 km south of LK1. The section is located in approximately the same area that the large accumulation of sediment described above merges with the eastern valley side. The section is divided into two parts due to a thick accumulation of slumped material in the middle of the section that was too extensive to remove manually. LK2a is located at the northern end of the section between 3 and 7.5 m above the road, whilst LK2b is located at the southern end of the section between 3 and 7 m above the road. Despite their close proximity, the nature of the sediment within the two sections is different, suggesting lateral discontinuity of the units described, at least along a north-south axis. The section was examined over two summer field seasons in 2009 and 2010. Excessive slumping during the 2009/10 winter meant that different structures within the sand units were observed during the second season. Three lithofacies associations are identified in the section; LFA 1, LFA 4 and LFA 5, using coding continued from Section LK1 and are described in upwards order (Fig. 4.24).

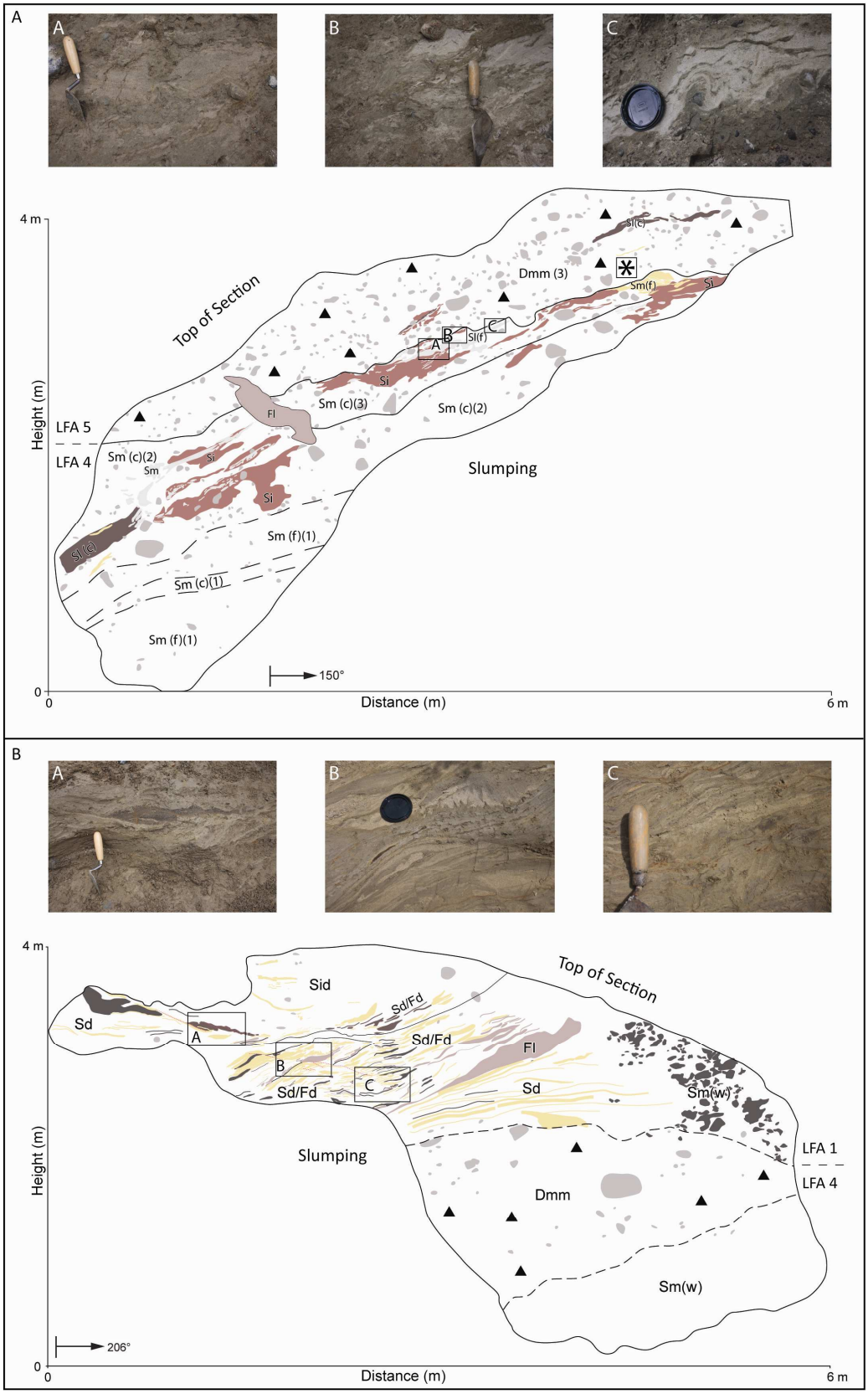

Figure 4.24. Sketch of the principle units found within sections A) LK2a and B) LK2b, showing the boundaries between LFA 4 and LFAs 1 and 5. Boxed letters mark the locations at which the inset photographs were taken. The boxed star marks the location at which the LK2 sample was taken to measure clast shape and roundness and clast macrofabric measurements were carried out. A key to the lithofacies codes and colours used is found in Figure 3.11 in Section 3.2.

- **LFA 4** – This lithofacies association occurs within the lower part of LK2a and LK2b and is composed of units of massive sand, with lenses of silt and sand, alongside a unit of massive diamicton at LK2b. At LK2b, the lowest unit is a massive sand, which shows no clear bedding, but is patchy in colour due to faint lenses of darker sand. A clast-poor overconsolidated massive grey diamicton, with a maximum thickness of 0.7 m overlies this sand. Its upper boundary is undulating and grades into a unit of laminated sand (LFA1). At LK2a, the massive sand is composed of alternating units of fine and coarse sand, with gradational boundaries between each unit. Outsized clasts, with a-axes ranging from 10 to 200 mm, occur within the lower two units, but are not in high density.

  In the upper unit of coarse sand, however, clasts are abundant, frequently with a-axes of 200 mm and over. Large lenses of silt occur within the unit, which contain very few clasts compared to the surrounding sand. The boundary between the silt and sand is gradational and the lenses pinch and swell, exhibiting a pseudo boudin structure. Associated with these silt lenses are smaller, wispy lenses of white sand that occur both within the silt lenses and within the surrounding clast-rich coarse sand. These sand lenses are more attenuated and also exhibit a pinch and swell shape, with more clearly formed boudins. The surrounding silt has also been squeezed into some of the boudinaged sand lenses, such as in photograph A of Figure 4.24A. In another area the sand lenses are folded asymmetrically folded around a clast, as in Figure 4.24A, photograph C.

  The massive, clast-rich sand unit that surrounds the silt and sand units has a gradational boundary with the overlying diamicton in LFA 5, but the boundary predominantly occurs at the upper boundary of the main body of silt and sand lenses. However, at the northern end of the section, an approximately 300 mm thick unit of laminated clay, with some laminated silt and sand, intrudes diagonally downwards in a southerly direction into the upper part of LFA 4 from the overlying LFA 5.

- **LFA 1** – LFA 1 forms the majority of LK2b. The section consists predominately of sand and is described in an upwards order. The lower unit of sand consists of discontinuous laminations of medium to coarse sand, silt and clay of varying colour from orange to grey. This unit also contains pods and lenses of sand and clay at the southernmost end. A thin band of silt separates this sand unit from a second unit that contains more deformation structures, which increase upwards. Within this unit, discontinuous, contorted laminations of predominantly sand, but also clay and silt

occur, as in photograph C in Figure 4.24B. Other structures also occur, including clay folds, sand lenses and pods, and an area of symmetrically folded sand, which protrudes into a silt layer above (see photograph B, Figure 4.24B). Small normal faults, which dip in a southerly direction, also occur in this unit. The unit progressively grades into a body of silt, which contains deformed sand and silt lenses. A sharp, scoured boundary separates this unit from the overlying diamicton (LFA 5).

- **LFA 5** – LFA 5 consists of a stratified, grey diamicton, which predominantly overlies LFA 4 in LK2a, but also occurs above LFA 1 in LK2b, although is mainly slumped in this area so structures are not visible. The diamicton is clast-rich and contains fine sand partings that separate the layers of diamicton. Larger sand and silt lenses also occur within the diamicton, which are highly attenuated. Most boundaries are gradational, but one sand lens has a loaded boundary with the surrounding silt. The upper 0.5 m of the diamicton is light brown, weathered and includes intrusions of roots from the overlying peat.

Clast macrofabrics and clast morphology measurements were taken from LFA 5 on a sample of 50 psammite clasts, the location of which is marked on Figure 4.24A. The clast shape and roundness data are shown in Figure 4.25, where the C_{40} index is 30, the RA index is 6 and the RWR is also 6. Stereonets and fabric shape triplots for the clast macrofabrics are shown in Figure 4.26. A-axis measurements show some clustering of a-axis dip in a southwest direction, with a secondary cluster in a southeast direction. The a/b plane measurements indicate that the a/b planes dip more steeply than the a-axes and are predominantly orientated in a northwest to northeast direction. Eigenvalues calculated for the a-axis measurements are S1= 0.4448, S2 = 0.3644, S3 = 0.1903, with an isostropy index of 0.43 and an elongation index of 0.18. For the a/b plane measurements, the eigenvalues are S1 = 0.5077, S2 = 0.2497, S3 = 0.2426, with isostropy and elongation indexes of 0.48 and 0.51 respectively. These are plotted in Figure 4.26 on a fabric shape triplot.

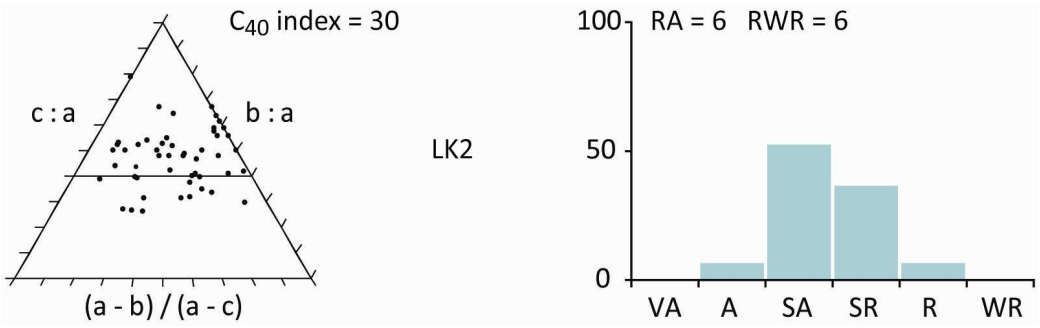

Figure 4.25. Clast shape and roundness data for sample LK2 taken from LFA 5 at Section LK2 (location indicated on Figure 4.24A).

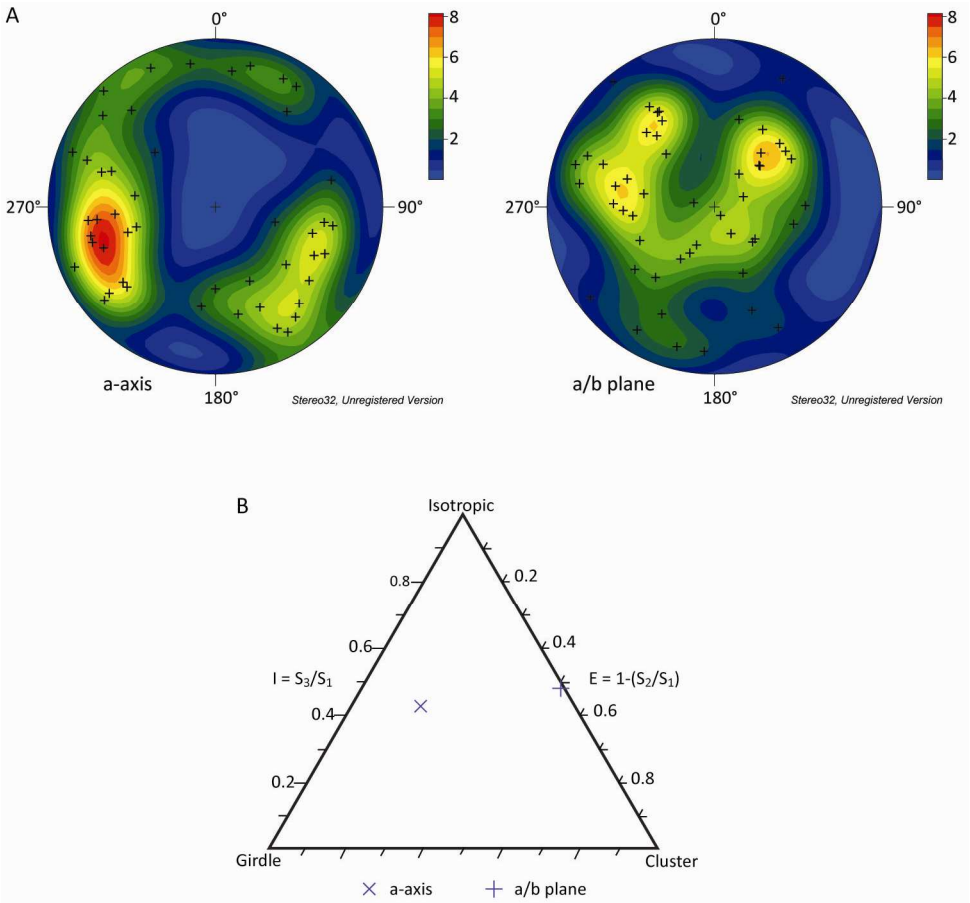

Figure 4.26. A) Lower hemisphere equal area stereonets and B) ternary plot, showing the fabric shape for a-axis and a/b plane clast macrofabrics from LFA 5, Section LK2b (location marked on Figure 4.24A).

Between Killin Lodge (NH 526 091) and Stronelairg Lodge (NH 536 069), the valley floor south of Loch Killin consists of a broad flood plain with surface vegetation of reeds and grasses. The River Killin is a braided gravel bed river, with one or two main threads, which is currently located in the central to eastern area of the valley floor. The presence of unvegetated gravel and abandoned channels highlights the migratory nature of the river and indicates that it is likely to have wandered across the whole of the flood plain. The flood plain slopes very gently upstream, until 0.5 km north of the head of the valley, when the gradient increases.

The valley sides to the south of Loch Killin are very steep and bedrock is exposed on the upper half to third of the slopes. Rockfall material is abundant on the lower portions of the valley sides in several areas, forming an extensive veneer of large angular boulders on the slopes. A straight scarp occurs at the top of the flank of Carn a' Choire Ghlaise on the eastern valley side (NH 538 077). Below this scarp, two lobes of rocky debris occur which reach almost to the valley floor.

Thick sequences of sediment occur on the lower halves of the valley sides. Deep downslope orientated channels have formed below Corrie Glas (NH 520 095), an east-facing pseudo cirque,

immediately north of Killin Lodge, to reveal a thick accretion of diamicton of at least 10 m, whilst on the opposite side, the aforementioned rockfall material covers underlying sediment ridges to create a chaotic hummocky topography. Towards the head of the valley, a mounded accumulation of sediment is found on both valley sides (Figs. 4.21 & 4.27). These two masses of sediment are different to those found further down the valley, in that an upper and downvalley limit can be identified that are at similar heights and positions to each other across the valley. Downstream of these accumulations, sediment on the valley sides has a smoother appearance with no channels cut into it. The sediment on the eastern side forms a series of faint lateral ridges, which rise upwards slightly to the south. On the western side, lateral ridges can also be identified, but are fainter than those on the east. Here, the mass of sediment generally rises steadily in an upstream direction, forming a terrace with mounds and ridges on it at the mouth of Allt Odhar. At NH 534 070, a debris cone, produced by a small stream flowing from the plateau above, has formed on top of the sediment accumulation.

Figure 4.27. Accumulation of sediment on A) the eastern and B) western valley sides at the head of Glen Killin, where crestlines of ridges are highlighted by the white dashed lines. 'R' indicates the position of lobes of rockfall on the eastern valley side, 'SA' indicates the position of the sediment accumulation on the western side, 'M' indicates the terrace with mounds and ridges on it by Stronelairg and 'RT' highlights the current river terrace. Photograph A was taken from the western valley side by Stronelairg, looking northeastwards, and photograph B taken on the eastern valley side towards the west.

Sediments within a ridge located on the western valley side accumulation, at NH 535 068 opposite Stronelairg Lodge, were examined (Figs. 4.28 & 4.29). The track-side section revealed exposed sediments along the entire length of the ridge, facing southeastwards at the upvalley section to eastwards on the central to downvalley side of the ridge. The ridge crestline is

Figure 4.28. Photographs of the ridge at Stronelairg, viewed from A) upstream, looking southwards and B) from downstream looking northwards.

orientated at 194-014°. Three lithofacies associations were identified within this moraine and are described below.

- **LFA 6** – LFA 6 occurs on the southeast-facing side of the section and consists of a firm, clast-supported, massive diamicton. The visible part of the unit is around 0.5 m thick, but its lower boundary is obscured by a thick accumulation of slumped material.

- **LFA 7** – LFA 7 overlies LFA 6 on the southeast-facing side and is separated from it by a gradational boundary. LFA 7 is less firm than LFA 6. The lithofacies association consists of a diamicton that varies between being matrix-supported and stratified to clast-supported and massive. Long, thin sand lenses occur frequently within the diamicton, where laminations within the sand are gently folded and some proto-boudinage occurs. Bedding plane measurements of three of these sand lenses have dips between 12° and 28° and strikes between 182° and 226°. The upper 0.5 m of the diamicton is orange-brown, indicative of weathering.

- **LFA 8** – A friable massive diamicton occurs on the eastwards facing side of the section. The diamicton varies between areas that are clast-supported and those that are matrix-supported. Sand lenses also occur within the diamicton, but the bedding within them is generally less folded than within LFA 7. Bedding plane measurements of two of these sand lenses have dips of 22° and 22° and strikes of 221° and 166° respectively.

The average direction of dip of the five sand lenses measured within the proximal and distal sides is 295°. In addition, clast shape and roundness samples were taken from all three lithofacies associations and are displayed in Figure 4.30. All samples consisted of psammite and although a sample of 50 was taken from LFA 6 (STL1), samples STL2 and STL3, from LFAs 7

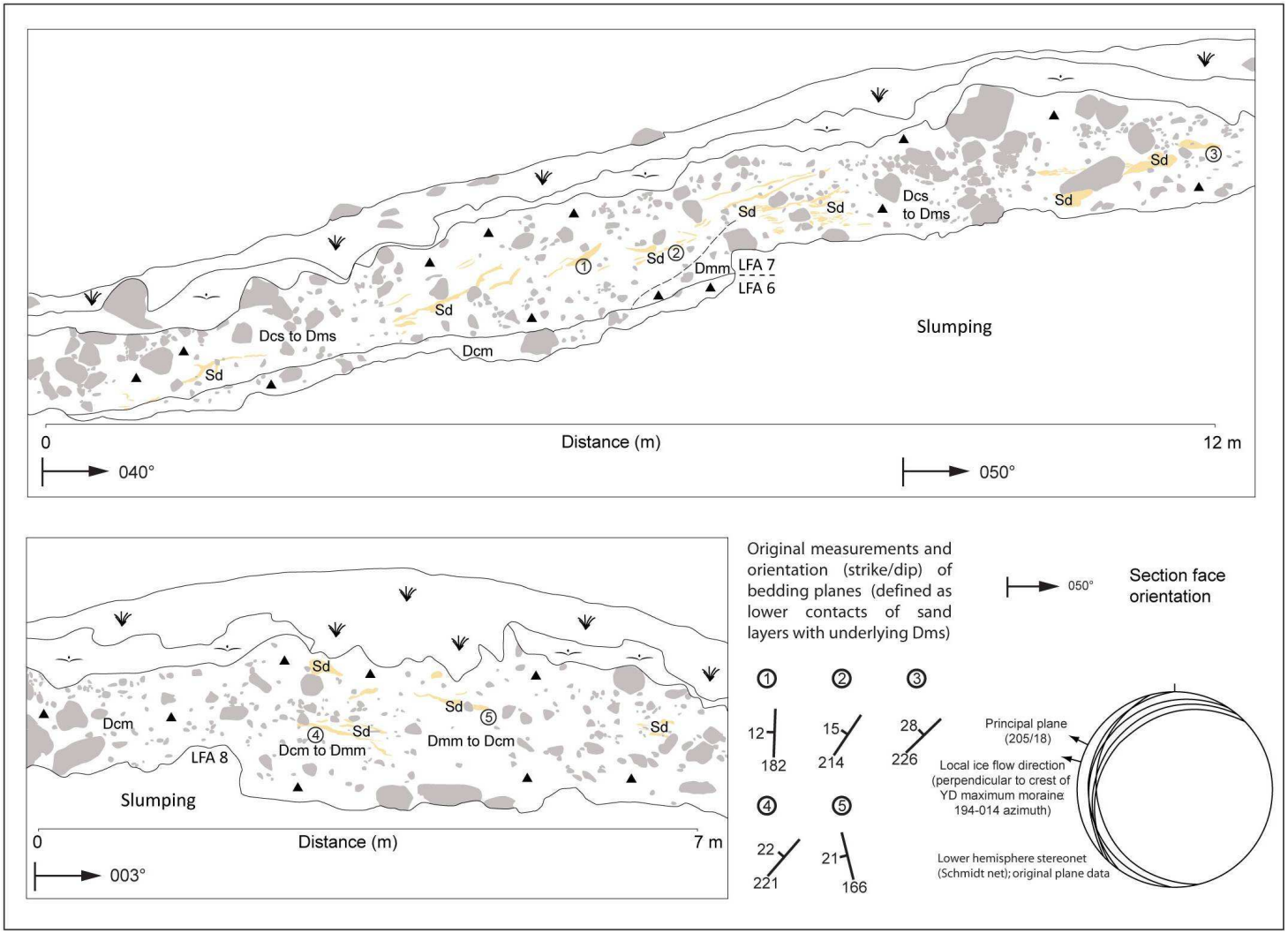

Figure 4.29. Section sketches of the upstream and downstream sides of the ridge at Stronelairg, including strike and dip measurements of sand lens bedding planes. A key to the lithofacies codes and colours used is found in Figure 3.11 in Section 3.2.

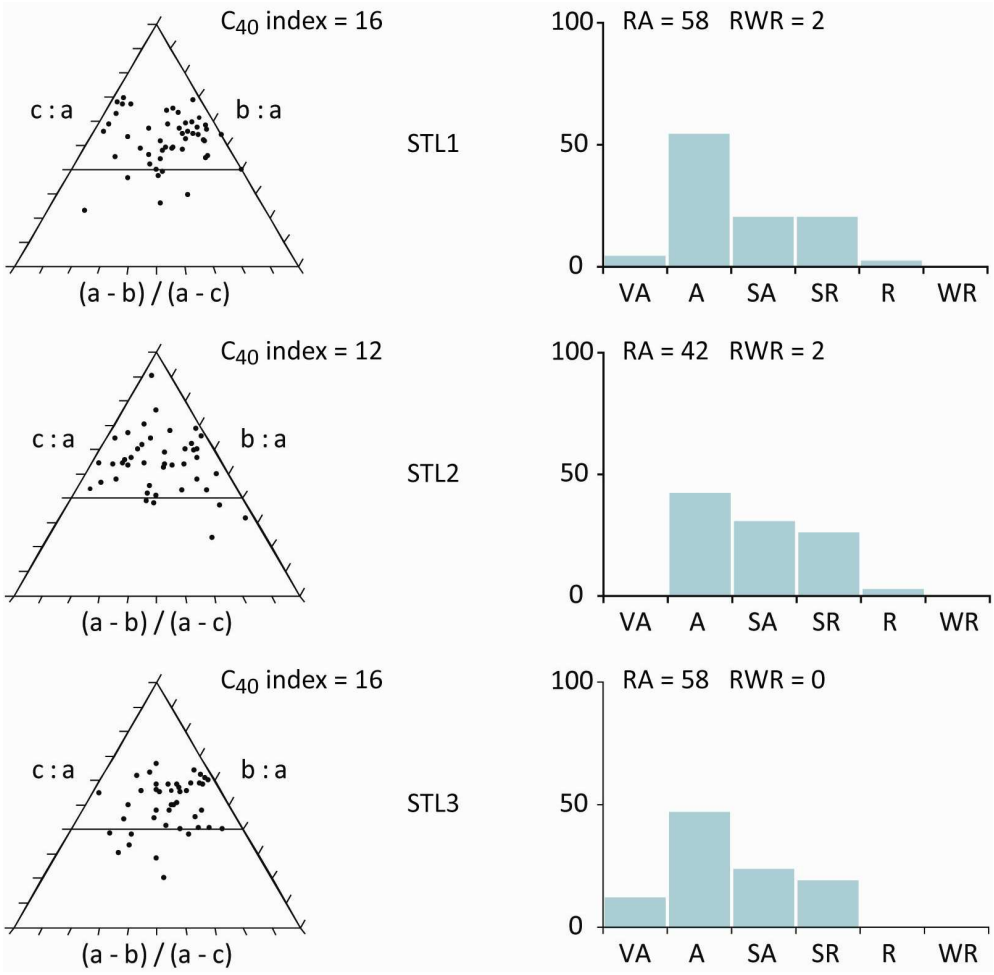

Figure 4.30. Clast shape and roundness data for samples STL1, STL2 and STL3 taken from LFAs 6, 7 and 8 respectively within the ridge at Stronelairg.

and 8 respectively, consisted of 43 clasts due to misidentification of some clasts as psammite in the field. The sample from LFA 6 (STL1) has a C_{40} index of 16, an RA index of 58 and an RWR index of 2. C_{40}, RA and RWR indexes for LFA 7 (STL2) are 12, 42 and 2 respectively and for LFA 8 (STL 3) are 16, 58 and 0 respectively.

Glen Odhar

Allt Odhar is the most easterly of the three tributaries and flows within a SW-NE trending valley. Large amounts of sediment are found within this valley on both sides and the incidence of a number of very large sections (up to 50 m in height) allows the valley to be described in terms of both the geomorphology and sedimentology. Unfortunately, lack of accessibility due to the river and the consolidated, vertical nature of the sections meant that no detailed sedimentological work could be undertaken and sediment descriptions are limited to observations from a distance.

Greater river erosion on the northwestern valley side has resulted in only fragments of the sediment accumulations remaining on this side, compared to the sediment on the southeastern

side that forms a broad terrace with ridges, mounds and former channels on its surface. The shape of these mounds varies from conical to oval to very elongate ridges, with some very sharp crestlines.

The terraces begin immediately east of Sìdhean Dubh at NH 515 045, where the valley widens following a change in orientation from east to north. The sediment masses begin at roughly the same altitude on both valley sides (~550 m), but the southeastern terrace, labelled 'a', soon drops to around 480 m, at 950 m downstream, compared to the altitude of 530 m at the corresponding point on the north-western side (Figs. 4.21 & 4.31). The height of the southeastern terrace rises, however, soon after this point, to an elevation of 518-520 m, which matches the upper limit of sediment on the opposite side. This terrace is labelled 'b' and has been deeply incised by two channels to create two near conical-shaped mounds and an intermediary flatter section (Fig. 4.31). The terrace continues for only 250 m before terminating and giving way to a lower-level fan surface at an elevation of 490 m ('c'). This fan continues, whilst steadily sloping both downstream and towards the stream, for around 500 m before merging with the valley side. There is no equivalent sediment accumulation on the northern valley side at this point. On the southern valley side, between fan 'c' and Allt Coire an Eich, further mounds and ridges, with channels occurring in between them, trend obliquely downslope.

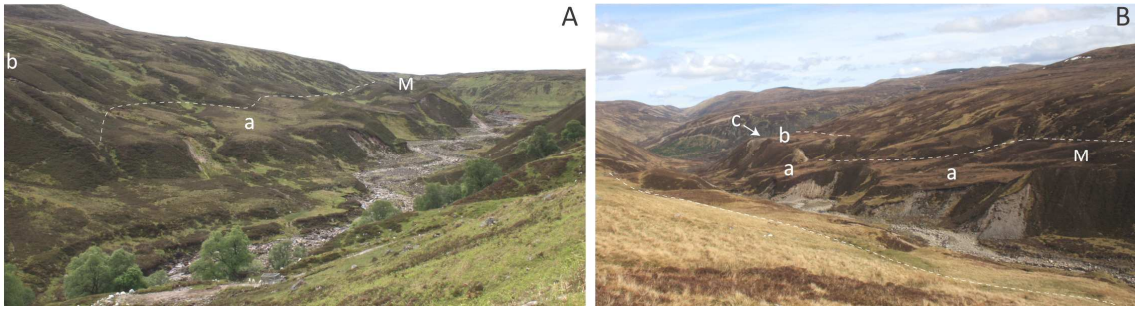

Figure 4.31. Terraces on the southeastern valley side of Allt Odhar viewed from the northern valley side looking A) upstream showing terrace 'a' and the start of terrace 'b' and B) downstream showing terraces 'a' and 'b', and the position of fan 'c'. 'M' indicates the position of a number of particularly prominent mounds and ridges on terrace 'a'.

The northwestern side of Allt Odhar has been severely eroded, producing two large sections, which are up to 50 m in height. Both sections (LKO1) (NH 521 055) reveal a succession of sediments that occur within all the sections examined and are grouped together as LFA 9 following on from previous coding:

- LFA 9 – LFA 9 consists of alternating units of massive to stratified, matrix-supported diamicton, which contains areas of densely packed clasts. In other areas, a series of large boulders occurs, which are all embedded at the same level.

The sedimentology of two sections, cut by the river within terrace 'a', on the southeastern valley side (Figs. 4.32 & 4.33) are described with reference to the lithofacies associations found, starting with the lowest unit first and using the same coding as at previous sections:

Section LKO2 (NH 522 055):

- **LFA 10** - The lowest lithofacies within LFA 10 consists of a large, open fold of laminated sands and silts. A layer of fine gravel that coarsens upwards overlies this unit. The geometry of this unit also follows the shape of the fold in the sand unit below.

- **LFA 9** - A sharp boundary separates LFA 10 from a unit of predominantly stratified, matrix-supported diamicton, with at least two clear downstream-dipping layers of clast-supported diamicton and large boulders.

- **LFA 11** - A sharp boundary occurs between LFA 9 and an overlying clast-supported diamicton. This boundary coincides almost exactly with the boundary between the terrace level and the overlying mound under which Section LKO2 is located.

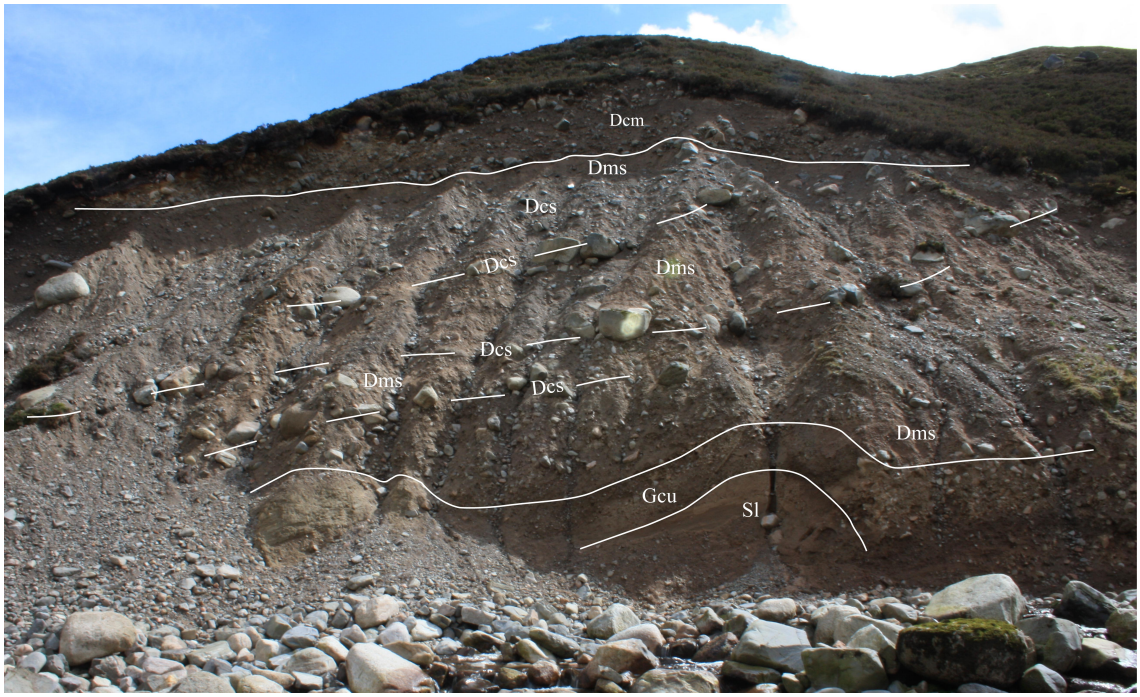

Figure 4.32. Annotated photograph of Section LKO2. The large boulder in the centre is about 0.5 m in horizontal diameter. A key to the lithofacies codes used is found in Figure 3.11 in Section 3.2.

Section LKO3 (NH 519 051):

- **LFA 9** – Section LKO3 consists predominantly of a massive, matrix- to clast-supported diamicton, with some areas containing horizontally continuous layers of gravel. Towards the top of the section the diamicton is faintly stratified and matrix supported.

- **LFA 10** - A laterally continuous, 2 to 3 m thick unit of horizontally laminated sands or silts occurs about two thirds up in the section, interbedded between LFA 9. A line of boulders occurs immediately below it in the central part of the section.

- **LFA 12** – LFA12 consists of a unit of planar cross-bedded gravels that occurs at the top of the section towards the centre. This lithofacies association is not laterally continuous across the whole section and possesses a concave lower boundary with the underlying LFA 9.

A further section is found beneath the same ridge slightly further upstream, which demonstrates the lateral continuity of LFA 10 in this area, although the top of the section is obscured here.

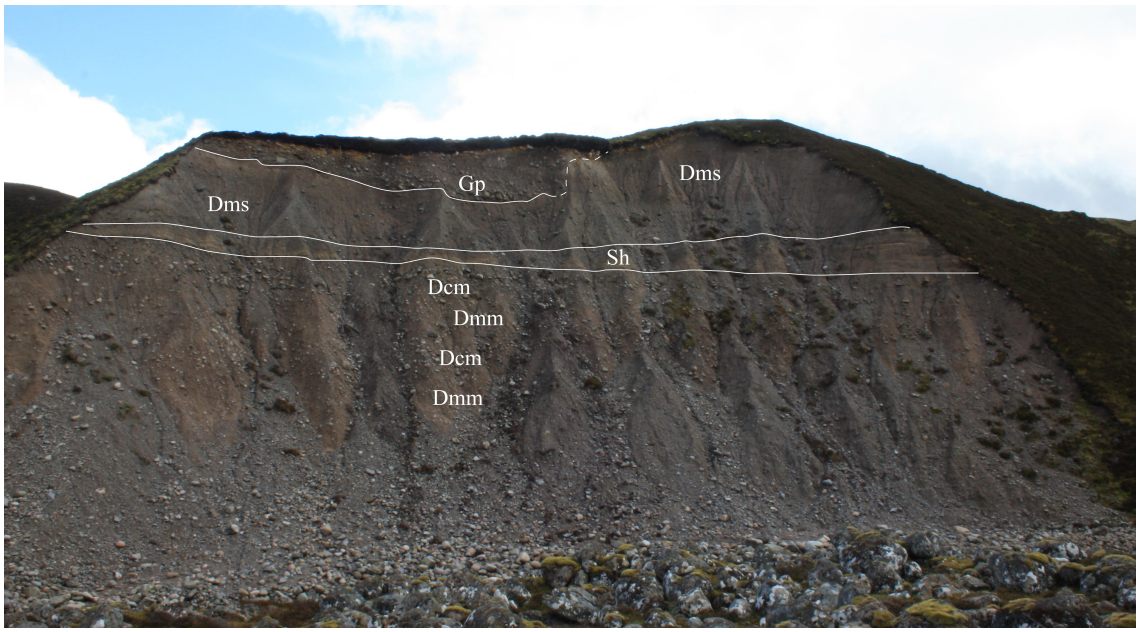

Figure 4.33. Annotated photograph of Section LKO3. The section is over 20 m high. A key to the lithofacies codes used is found in Figure 3.11 in Section 3.2.

An area of large mounds and ridges is also found on the plateau in an area called Sìdhean Liath, immediately to the southwest of Glen Odhar at NH 510 038. These mounds and ridges have a similar morphology to the ridges found further downstream within Glen Odhar and the rest of the study area, but lack any spatial pattern, where they are orientated at random and appear to bear no relationship to each other. The composition of these ridges was examined through some shallow excavations on the top of them since there were no natural sections. These small excavations revealed that at least the upper parts of the ridges are formed of a sandy diamicton containing mainly psammite and granite clasts. Boulders of granite were also found on the surface of these features. A longer ridge is also observed further onto the plateau in between the Allt Creag Chomaich and Sìdhean Dubh na Cloiche Bàine, which has been dissected into a number of smaller ridges and mounds.

Coire an Eich

The neighbouring valley to the east of Glen Odhar is Coire an Eich, which is the central and smaller of the three valleys at the head of Glen Killin. A limited number of ridges occur in this valley compared to Glen Odhar and Glen Markie (Fig. 4.21). The most notable of these are two sets of large ridges on the south and northwestern valley sides close to the confluence with Allt Odhar. These ridges are orientated across the valley sides, with a slight trend downslope. They are delineated further by channels, particularly those on the northwestern side. However, additional channels, orientated directly downslope and nearly perpendicular to these channels, have dissected some of the northwestern ridges into several large (> 10 m high), and in some cases conical, mounds.

Former channels, parallel to those that demarcate the ridges on the southwestern flank of Sròn na Lairige, continue further up onto the top of that hill. These channels originate from a fairly flat area on the top of Sròn na Lairige and increase in depth as the slope steepens forming ridges in between them. Small sections at varying heights on Sròn na Lairige reveal a thick succession of sand on the top of Sròn na Lairige. The lower-most section exposes at least 2 m of very firm grey sand. The sand generally appears massive, although an iron band picks out a bedding plane dipping at 20° northwards. All other sections expose sediments that are closer to the surface and reveal an orange to yellow sand, which contains varying amounts of clasts of 100 mm or less, with most being below 50 mm. The sand is also well compacted and difficult to dig into in most sections.

Whilst the stream generally has no river terraces around it, occasional fragments of a larger terrace, which sits about 10 m above the current stream occur. Track-side cuttings on the eastern hillslopes above the valley, and above one of the larger terrace fragments, show that the sand found on Sròn na Lairige continues up further onto the plateau. Sediments in these sections consist of a lower unit of grey laminated silt, interbedded with coarse orange laminated sand and containing sporadic discontinuous patches and lenses of gravel. The unit bedding dips northwards and appears relatively undisturbed, although there are some small normal faults. A grey diamicton occurs beneath the sand, but the nature and exact location of the boundary could not be verified due to slumping. A diamicton also overlies the sands, separated by a sharp boundary. This diamicton is clast rich, dark brown and merges into the overlying peat.

Further onto the plateau, excavations for the Glendoe Hydro Scheme exposed a large area of sand and gravel in between Allt Ruighe an t-Sìdhean and Caochan nan Sac, immediately upstream of where these two streams converge (NH 544 036) (Section (GE1). The feature was a flat-topped hill, which was roughly 5-10 m higher than the streams on either side and

consisted of an upwards sequence of clay, steeply dipping sands, gravel, sand and gravel (J. Wallace, pers. comm., 2009). A large proportion of the sediments were extracted from the area (60,000 cubic metres of sand; J. Wallace, pers. comm., 2009) before the start of the current research, but photographs taken by hydroscheme engineers in 2007 (Fig. 4.34A) and 2008 (Figs. 4.34B & C) and a personal communication with J.W Merritt (2008) confirm the presence of this sequence of sediments.

Figure 4.34. Photographs taken by Glendoe Hydroscheme engineers of excavations into a flat-topped hill on the plateau to the south of Glen Eich. A) Section GE1 showing LFAs 13 and 14. B & C) Section GE2 showing LFA 15. Photographs courtesy of the Glendoe Hydroscheme. A key to the lithofacies codes used is found in Figure 3.11 in Section 3.2.

One photograph shows steeply dipping laminated sands interbedded with finely bedded units of medium to fine gravels (Section GE1). This unit is assigned to LFA 13 and is separated from

the overlying unit by a very sharp boundary. This unit consists of coarse gravels within a sandy matrix, which displays some crude horizontal stratification and is named LFA 14. Two photographs document the upper part of the succession (Section GE2) (Fig. 4.34B & C), although the relationship between sections GE1 and GE2 is unknown. In these photographs, a horizontally laminated unit of sand occurs below a unit that varies in composition between gravels and massive sand, although a continuously sharp boundary divides the two lithofacies associations. These two units are assigned to LFA 15. Further onto the plateau, a number of chaotically spaced mounds occur immediately upslope of this flat-topped hill.

Glen Markie

Ridges and mounds occur throughout the lower half of Glen Markie, particularly on the northern valley side (Fig. 4.21). They vary quite significantly in their shape and size, from subdued to prominent ridges or mounds, to areas of hummocky topography. Most of these features are confined to the valley floor or the lowest parts of the valley sides, but a few isolated large ridges occur orientated across the higher parts of the valley sides.

The fluvial morphology also varies significantly throughout the valley. Immediately upstream of where Glenmarkie Burn joins the River Killin the stream is deeply incised down to bedrock. A fan occurs upstream of this point on the southern side, emanating from the tributary stream Allt Cam Bàn (NH 548 074). A much smaller fan, in terms of both breadth and height, also emerges from a small stream on the northern valley side, almost opposite the Cam Bàn fan. Other fans occur further up the valley at the mouths of Dearg-allt, and a stream flowing southwards, east of Burrach Mòr (827 m; NH 583 084). Further upstream the gradient of the valley floor decreases and the valley widens, allowing the stream to meander. There are no significant river terraces in this area. In the upper half of the valley, it narrows to a v-shape (NH 572 086), before widening again to an area of deep stream incision with several fragments of a large terrace, approximately 10 m in height.

Carn a' Choire Ghlaise to Carn na Saobhaidhe

The area between Carn a' Choire Ghlaise (778 m; NH 547 087) and Carn na Saobhaidhe (811 m; NH 600 144) forms a high area of plateau, dissected by a number of small streams and several rounded summits to the northeast of Glen Killin (Fig. 4.21). Due to time constraints, field mapping was not undertaken in this area and the description that follows is from aerial photographs, NEXTMap and Google Earth. Low profile ridges with rounded crestlines and obliquely trending channels occur towards the top of the Allt Fèith a' Phuill (within square NH 5409) and Allt Mharconaich (square NH 5510) catchments (Fig. 4.21). In these valleys the most downstream ridge is demarcated by a prominent stream channel and beyond this point the

central stream widens slightly, although this does not coincide with the development of additional river terraces, which tend not to occur until further down valley. In addition, several small obliquely trending channels occur in the upper parts of the Allt a' Ghille Charaich (square NH 5913) and Allt Odhar (square NH 6113) catchments, alongside an unnamed catchment to the east of Carn a' Choire Sheilich (square NH 5712).

4.2.6 Interpretation of the geomorphological and sedimentary evidence in the northern Monadhliath Mountains

The geomorphological evidence in the northern part of the Monadhliath Mountains is very similar to that of the western Monadhliath Mountains, where the landscape is dominated by mounds, ridges and channels, particularly in the upper parts of valleys that lead towards the plateau, such as in Glen Brein, Coire Dubh Cùil na Creige, Coire Easgainn, Glen Odhar, Coire an Eich and the Allt Cam Bàn catchment (Appendix II). Following arguments made in Section 4.1.6, ridges and mounds are predominately interpreted as moraines (e.g. Benn, 1992; Bennett & Boulton, 1993a, b; Benn & Ballantyne, 2005; Lukas 2005b; Finlayson *et al*., 2011). Channels that trend obliquely downslope, often between moraines are interpreted as ice-marginal channels (Benn & Lukas, 2006; Greenwood *et al*., 2007), whilst channels orientated directly downslope are interpreted as gullies. A large variation in the number and density of moraines occurs in each valley, where valleys such as Glen Brien and Coire Easgainn contain a large number of densely spaced moraines, whilst few occur in Glen Doe and Glen Eich. This will be discussed further in Sections 5.3 and 5.5. The morphology of the moraines is less variable, however, that in the western area.

A number of scarps with large accumulations of sediment below them were identified within this part of the study area. These are all interpreted as rock slope failures (RSF), following criteria by Jarman (2006). In Glen Tarff, a large RSF is recognised on the southern valley side towards the head of the valley (NH 438 022) and is interpreted as an arrested to sub-cataclasmic RSF (Holmes, 1984; D. Jarman, pers. comm., 2009). Smaller RSFs are recognised on both valley sides of Coire Easgainn; on the northern valley side the feature is interpreted as an arrested to sub-cataclasmic RSF (NH 522 087), whilst two small adjoining RSFs at NH 525 072 on the southern side are identified as sub-cataclasmic (D. Jarman, pers. comm., 2009). A sub-cataclasmic RSF is also recognised on the eastern side of Glen Killin at NH537078 (D. Jarman, pers. comm., 2009). The lobe of sediment that extends down the hillside from this RSF stops just above subtle ridges on the western valley side that are interpreted as lateral moraines.

Geomorphological and sedimentary evidence at sites around Loch Killin that are of particular interest is now discussed below.

Coire Easgainn

Following the interpretation above, the sharp-crested ridges within Coire Easgainn are interpreted as moraines, whilst the channels in between them are interpreted as ice-marginal meltwater channels. The corrie has no backwall and moraines and meltwater channels begin on the plateau and continue into the corrie, clearly indicating that ice in the corrie was sourced from the plateau above. This spatial distribution of moraines and meltwater channels is particularly apparent on the southern side of the corrie.

A large section cut by the Allt Easgainn into a moraine on the northern side shows that this moraine is composed of a friable, clast-supported diamicton, which contains very large boulders (particularly on the distal side) and fine sand laminations on the proximal side. A clast shape and roundness sample (AE1) from the proximal part of this moraine has a C_{40} index of 48, an RA index of 62 and a RWR index of 0 (Figs. 4.20 & 4.35). Co-variance plots of the C_{40} index against the RA and RWR indexes (Fig. 4.36) show that the C_{40} index is of a similar magnitude to that of both the rockfall and fluvial control samples, but the RA index distinguishes the sample from both the fluvial and rockfall samples.

The rockfall samples provide a proxy for supraglacial material, whilst clasts of a subglacial origin are likely to have similar RA values to the fluvial samples, but different RWR values. Figure 4.36 shows that the angularity of the clasts is greater than is usually found for subglacial samples (e.g. Ballantyne & Benn, 1994; Benn, 2004a; Benn & Lukas, 2006), since the RA value is higher than that of the fluvial samples. This therefore indicates that the proximal part of the moraine is composed primarily of supraglacial material, which is supported by the value of zero for the RWR index. A supraglacial origin is also suggested for the distal side of the moraine, which contains large boulders that are argued to have originally fallen onto the glacier surface from the valley sides and subsequently fallen from the glacier margin to build up the moraines as an ice-contact scree slope (Boulton & Eyles, 1979*;* Small, 1983; Owen, 1994; Evans & Benn, 2010). In this setting, the sand laminations found within the proximal part of the moraine may represent episodic deposition by sheet wash influenced by variations in debris supply and water content (Krzyszkowski & Zielinski 2002; Lukas, 2005a, b). The significant height (20 m) of the moraine compared to others in the corrie (< 10 m) indicates that the ice-margin remained at this position for a substantial amount of time in order to build up this height. However, the highly friable nature of the diamicton throughout the section indicates that a later glacier advance did not override the moraine (*cf.* Lukas 2005b).

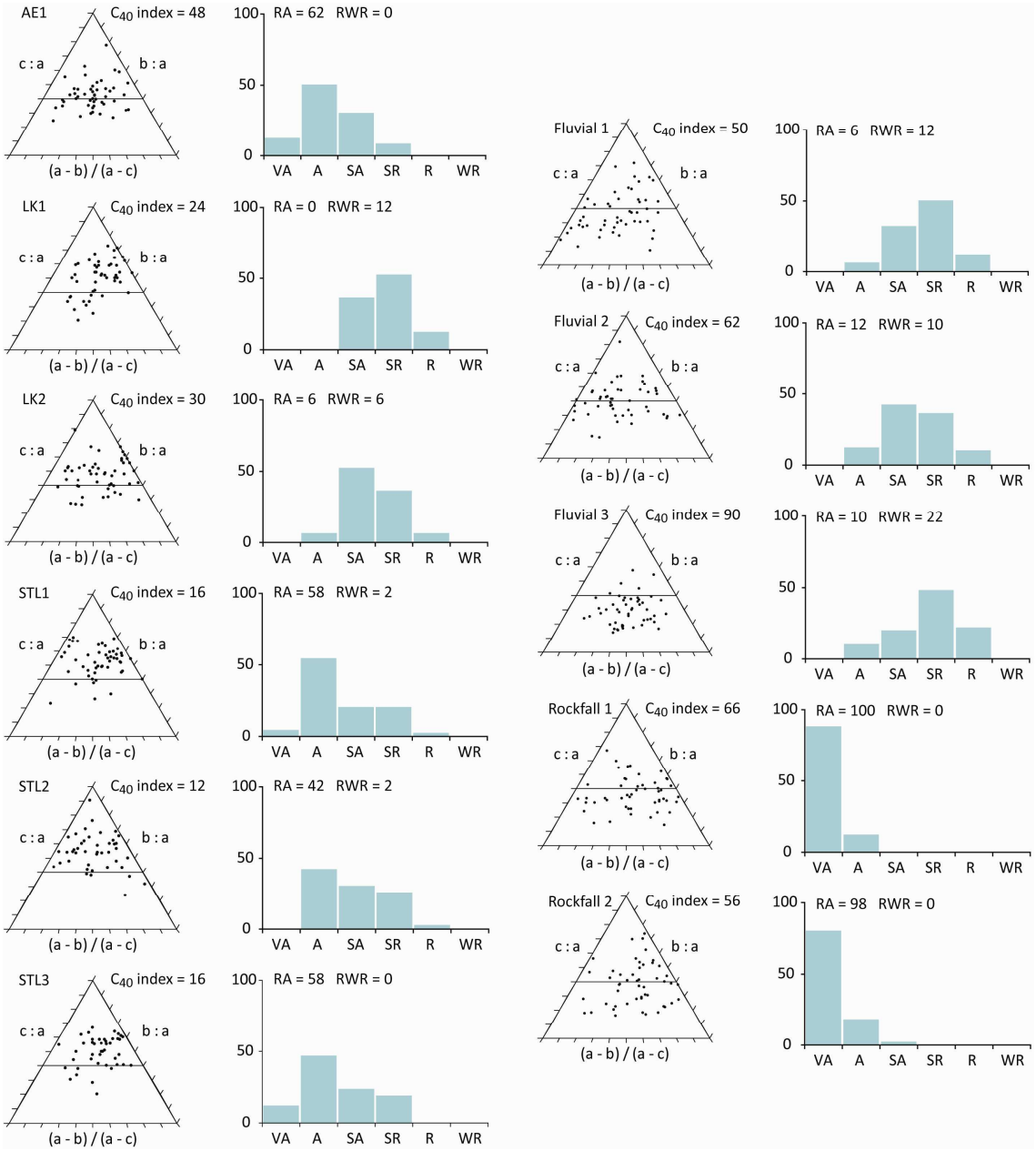

Figure 4.35. Clast shape and roundness data for psammite clasts from samples AE1, LK1, LK2, STL1, STL2 and STL3, alongside fluvial and rockfall control samples.

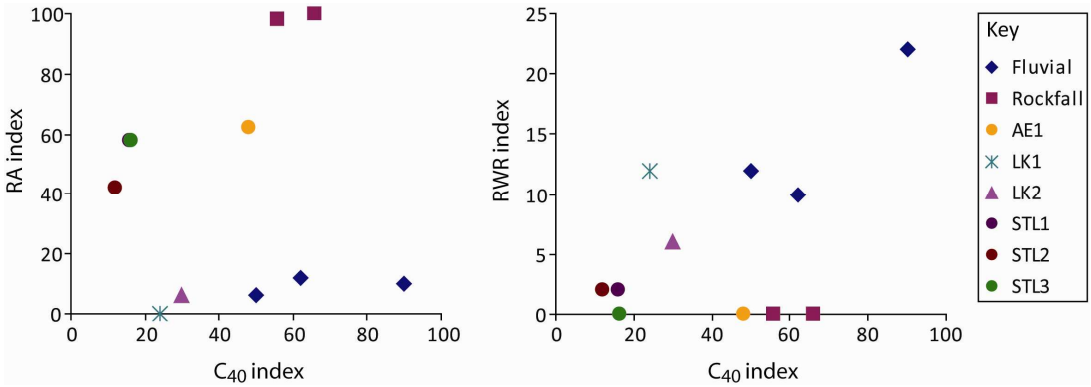

Figure 4.36. Co-variance plots showing the C_{40} index against the RA and RWR indices for clast shape and roundness samples on psammite clasts, including the control samples from fluvial and rockfall locations in the study area. NB. The data point for sample STL1 is hidden behind the STL3 data point for the RA index.

Stronelairg

The sedimentary and structural characteristics of sediments found within a moraine at Stronelairg (NH 535 068) were also examined and three lithofacies associations were identified. LFA 6 occurs on the proximal side of the moraine and consists of a firm, clast-supported, massive diamicton. It is overlain by LFA 7, which is less firm than LFA 6 and consists of a diamicton that varies between matrix-supported and stratified to clast-supported and massive, with gently folded sand lenses that occur frequently. LFA 8 is a friable massive diamicton found on the distal side of the moraine. This diamicton varies between areas that are clast-supported and those that are matrix-supported, with some sand lenses.

The presence of sand lenses within LFAs 7 and 8, alongside the variable nature of the diamicton indicates that these lithofacies were deposited as discrete debris flow units (Lawson 1982, 1989; Benn, 1992; Lukas, 2005a, b), where the sand lenses represent periods of sheet wash controlled by changes in debris and water content (Krzyszkowski & Zielinski, 2002; Lukas, 2005a, b). The orientation of the dip of the sand lens bedding planes to the west and northwest is consistent with the interpretation of sedimentation within an ice-contact fan, as has been previously recognised in other ice-marginal moraines (e.g. Zielinski & van Loon, 2000; Krzyszkowski & Zielinski, 2002; Lukas, 2005a, b; Reinardy & Lukas, 2009; Evans *et al*., 2010a; Lukas & Sass, 2011; Lukas *et al*., 2012). Variations in the orientation of the bedding planes are explained by the formation of the moraine through the coalescence of a number of small debris fans, where individual bedding plane measurements include variations in the dip of these smaller fans.

The compacted nature of LFA 7 compared to the friable nature of LFA 8 indicates partial overriding of the ice-contact fan on the proximal side during a minor readvance of the ice-margin (*cf*. Lukas, 2005b). This is supported by the gentle folding within the sand lenses in LFA 7 that does not occur in the sand lenses within LFA 8. Whilst the dips of the sand lenses in both LFAs 7 and 8 are steeper than often found on fan surfaces (e.g. Kjær *et al*., 2004; Lukas, 2005b; Lukas & Sass, 2011), the gentle folding within the sand lenses suggests that only minor disturbance within the sediments has occurred. This evidence is therefore interpreted to indicate some subglacial deformation with a limited amount of proglacial deformation following interpretations of similar structures made by Lukas (2005b).

C_{40} indexes for psammite clasts taken from the three lithofacies are between 12 and 16 and are much lower than that of AE1 suggesting a subglacial origin (e.g. Benn & Ballantyne, 1994; Benn, 2004a; Benn & Lukas, 2006) (Fig. 4.30). On the basis of clast roundness, the samples can be distinguished from both the rockfall and fluvial control samples based on their RA and RWR indices (Fig. 4.36). The Stronelairg samples are similar in angularity to the Easgainn moraine

sample, therefore also indicating a predominantly supraglacial pathway for the sediments within the Stronelairg moraine. The lower C_{40} index, however, suggests that there is probably some subglacial component, which is supported by the slightly lower RA values and higher RWR values than from the Easgainn moraine. This interpretation differs from that of Lukas (2005a, b; Lukas & Benn, 2006), who found that the material deposited in ice-contact fans examined in the Northwest Highlands, Scotland had a far greater subglacial component, and therefore potentially indicates less re-working of pre-existing sediment in the Monadhliath Mountains. The similarity of all three samples, particularly those taken from LFAs 6 and 8 indicates that similar material was deposited throughout the moraine; the only difference being that LFA 6 was deposited earlier and later overridden.

Glen Odhar

Ridges and mounds found on the plateau above the main part of the Odhar valley are not oriented obliquely or arcuately downslope and do not form any spatial pattern, despite having a similar morphology and composition to landforms that are interpreted as moraines in the rest of the study area. These features are therefore interpreted as moraines that were formed during ice stagnation by the dumping of supraglacial and englacial material, following previous interpretations of similar features on the Isle of Skye (Benn, 1992; Benn *et al*., 1992). Mounds upstream of the flat-topped hill in Glen Eich were also interpreted in this way. These features provide evidence for the existence of ice on the plateau above Glen Odhar and Glen Eich.

The sedimentology of the sections within ridges in the main part of Glen Odhar also suggests that not all of the obliquely trending ridges found on top of the terraces can be interpreted as moraines. The morphology of these features varies in shape from conical mounds to elongate ridges, which often possess sharp crestlines. Although the spatial distribution of these ridges is consistent with an interpretation that the mounds are latero-frontal moraines (Benn, 1992; Bennett & Boulton, 1993a, b; Wilson & Evans, 2002; Lukas, 2005b; Lukas & Benn, 2006), the composition of the two ridges, exposed at the top of sections LKO2 and LKO3, is different. Massive, clast-supported, diamicton (LFA 11) occurs within the ridge at LKO2, with a sharp boundary with LFA 9 below, corresponding to the height of the terrace. At LKO3, however, there is no clear boundary separating sediments in the terrace from sediments that form the ridge. Part of the ridge consists of stratified, matrix-supported diamicton (LFA 9), which is the same as within the majority of the terrace, whilst the other portion is composed of planar cross-bedded gravels (LFA 12).

Massive, clast-supported to matrix-supported diamictons have been well documented within moraines (e.g. Benn, 1992; Lukas 2005a, b; Evans *et al*., 2010a; Lukas, 2012; Lukas *et al*., 2012; Stronelairg and Easgainn moraines in this research) and therefore the ridge containing LFA 11 is

interpreted as a moraine due to its sedimentology, morphology and orientation. However, the planar crossed-bedded gravel (LFA 12) that forms the ridge at LKO3 is more typical of a channel-fill deposit due to its trough-shaped lower boundary (e.g. Reineck & Singh, 1975; Benn & Evans, 1993). This suggests that a former stream existed in the area that now forms part of the ridge, before stream migration and subsequent stream erosion occurred to produce the current ridge as it is now seen. This indicates the ridge at LKO3 is not a depositional feature, but represents a remnant of a former terrace level that has subsequently been eroded by streams. The continuation of LFA 9 from the terrace into the ridge supports this argument. Since the orientation of the channel that has formed the ridge is obliquely trending in the upstream part and becomes increasingly arcuate as it reaches a more central position in the valley, it is interpreted as an ice-marginal channel (Ó Cofaigh *et al*., 1999; Atkins & Dickinson, 2007; Greenwood *et al*., 2007). The two different interpretations for the formation of the ridges at sections LKO2 and LKO3 suggests that the other ridges that occur on top of the Glen Odhar terrace could have formed in either of these two ways, although this cannot be tested due to a lack of available sections.

The terrace itself is composed predominantly of a massive to stratified matrix-supported diamicton (LFA 9) with horizontal to sub-horizontal continuous units of gravel and downstream dipping lines of large boulders. This downslope stratification and heterogeneity, which consists of areas of sorted and non-sorted material, is characteristic of the laminar flow of sediments containing a high water content, and is compatible with downslope resedimentation through cohesive debris flows (Eyles *et al*., 1988). Subglacial till is discounted as an interpretation due to this downslope stratification and the lack of features indicative of a high stress environment such as shear planes and deformation structures.

The occurrence of LFA 10, a unit of laminated sand and fine gravel, interbedded with LFA 9 suggests that episodic periods of higher energy mass flows were interspersed with periods of flowing water (Church & Gilbert, 1975; Reineck & Singh, 1975; Krzyszkowski & Zielinski, 2002). As well as terrestrial deposition during moraine formation (e.g. Zielinski & van Loon, 2000; Krzyszkowski & Zielinski, 2002; Lukas, 2005a; Reinardy & Lukas, 2009; Evans *et al*., 2010a; Lukas & Sass, 2011; Lukas *et al*., 2012), debris flow deposits have also been described within other depositional environments including during paraglacial reworking of glacial sediments (Jackson *et al.*, 1982; Eyles *et al*., 1988; Owen, 1989; Ballantyne, 2002b, c) and subaqueously within proglacial lakes (Lunkka & Gibbard, 1996; Benn, 1996; Bennett *et al*., 2002; Johnsen & Brennand, 2006; Reitner, 2007; Hornung *et al*., 2007; Winsemann *et al*., 2009).

Although paraglacial resedimentation of valley-side sediments following deglaciation is a plausible explanation for the terraces (e.g. Ballantyne & Benn, 1994; Ballantyne, 2002b, c;

Iturrizaga, 2008), the morphology of the terraces and their sedimentary architecture does not indicate paraglacial deposition. In a paraglacial environment, debris flow material usually moves down the valley sides towards the centre as a series of coalescent debris cones, with sediment moving in both the upstream and downstream directions (Ballantyne, 2002b, c). This is not reflected in the Glen Odhar terraces, where the geomorphology does not prescribe to a debris cone shape and the exposed sections show the sediments dipping in a downstream direction only.

Subaqueous debris flows can form a large component of glaciolacustrine environments and thick diamictic sequences have been documented in other upland areas (e.g. Benn, 1996; Bennett *et al*., 2002; Johnsen & Brennand, 2006; Reitner, 2007; Hornung *et al*., 2007). Laminated sand and gravel facies are also well documented within former glaciolacustrine environments (e.g. Cheel & Rust, 1982; Bennett *et al*., 2002; Krzyszkowski, 2002; Hornung *et al*., 2007; Winsemann *et al*., 2007a, b) and the juxtaposition of stratified diamicton and horizontally laminated sands and gravels provides strong evidence for the presence of a former lake in Glen Odhar (Lunkka & Gibbard, 1996; Benn, 1996; Reitner, 2007). The deposition of debris flow units suggests that the sediment was deposited as a subaqueous grounding-line fan, therefore indicating that a glacier was in contact with the lake in the upper part of Glen Odhar (Benn, 1996; Lunkka & Gibbard, 1996; Benn & Evans, 2010).

Glen Eich

Further evidence for the existence of a lake is found within the neighbouring catchment of Glen Eich, where a flat-topped hill occurs on the plateau in between the Allt Ruighe an t-Sìdhean and Caochan nan Sac streams. The feature is composed of four lithofacies associations (LFAs 13 – 16). The lowermost, LFA 13, comprises steeply dipping laminated sands, which are interbedded with finely bedded units of medium to fine gravels. In combination with the overlying unit of horizontally bedded coarse gravels (LFA 14), these two units are interpreted as deltaic deposits typical of a Gilbert-type delta succession (Postma, 1990; Benn & Evans, 2010). LFA 13 is characteristic of deltaic foresets, deposited through avalanching of sediment down a fan slope and documenting the infill of a lake basin, whilst the topsets within LFA 14 record deposition within a subaerial fluvial system following emergence of the delta above the level of the lake (e.g. Nemec, 1990; Benn & Evans, 1993; Nemec *et al*., 1999; Johnsen & Brennand, 2006; Winsemann *et al*., 2007a). The horizontally laminated sand, massive sand and gravels in LFA 15 are also interpreted to record deposition within a subaerial fluvial system, where alternating sand and gravel deposition suggests migratory stream flow (Reineck & Singh, 1975; Miall, 1977, 1985). The large amounts of sorted sediment on the plateau indicate the existence of a nearby glacier as a source for this sediment. In the same way, sand on Sròn na Lairige is also interpreted to have been deposited during the existence of the lake and subsequent glaciofluvial activity, although the

available sections were not large enough to examine any structures and therefore further differentiation between subaqueous and subaerial deposition is not possible at present.

Loch Killin

Sections LK1 and LK2 are located to the north and east of Loch Killin, respectively, beneath a large undulating accumulation of sediment. LFA 1 is found within both sections and consists of interbedded units of sand and gravel, with some lenses of silt and clay within the sand units, although no gravel units are found at LK2. The sorted nature of each unit indicates that they are fluvial in origin (Reineck & Singh, 1975; Miall, 1977, 1985), where alternating areas of trough cross-bedding and horizontal bedding within the sands suggests migratory stream flow, with episodic higher energy events that deposited the gravels (Collinson & Thompson, 1989). This interpretation is consistent with the sediments being deposited either terrestrially or as part of a subaqueous outwash fan (e.g. Cheel & Rust, 1982; Bennett *et al*., 2002; Hornung *et al*., 2007; Winsemann *et al*., 2007a, b). Bedding plane data collected in the lower part of the LK1 section indicates that stream flow occurred in a general northerly direction, with dip directions of individual units varying between 355º and 012º (Fig. 4.22). Clast shape and roundness data also support a fluvial transport history for the lower sand units, with RA and RWR indexes of 0 and 12 respectively (Figs. 4.23, 4.35, 4.36). The C_{40} index is, however, lower than that of the fluvial control samples, potentially suggesting an inherited subglacial signal.

Evidence for both ductile and brittle deformation in the sand lenses within LFA 1 increases with increasing height within both sections, indicating a greater intensity or disturbance upwards at both sites. Ball and pillow and flame structures within LFA 1 at LK1 indicate high pore water pressure and fluidization due to applied pressure to the unit (Philips *et al*., 2002, 2007), which is corroborated by evidence for compression through folding and faulting in other areas and has led to deformed and discontinuously laminated sand units. The overall architecture of LFA 1 at LK1 confirms that the site has been subject to intense disturbance and glaciotectonism, where steeply dipping to near vertical boundaries between some of the units (i.e. the large sand and gravel units towards the centre of the section) indicate that individual units or parts of units have been tectonically elevated or overturned within the section (van der Wateren, 2003; McCarroll & Rijsdijk, 2003). At LK2, the intense folding and faulting of sand, silt and clay units in the middle part of the section also suggests that the section has been subjected to compression (McCarroll & Rijsdijk, 2003), where normal faults indicate that pressure was applied from the north. Overall, the architecture and deformation structures within LFA 1 indicate that following deposition, the sediments were subject to proglacial to subglacial glaciotectonism.

At section LK1, LFA 1 is overlain by laminated clay that contains discontinuous lenses of diamicton and sand. This clay is discontinuously laminated, with laminations that bend beneath and over the top of some clasts within it. Due to the deformation of these laminations around the clasts, the clasts are interpreted as dropstones, indicating that the LFA 2 was deposited subaqueously within a lake (e.g. Powell, 2003; Evans & Thomson, 2010), and imply that a glacier margin was in close proximity. The presence of lenses of diamicton corroborates this assertion, suggesting a nearby glacier margin from which episodic high energy events were sourced, possibly through debris 'dumping' events by icebergs (e.g. Benn, 1989, 1996; Powell, 2003; Reitner, 2007). The compacted nature of the clay, elongation of sand and diamicton lenses and the discontinuity of laminations within the clay suggests that the lake sediments were later overriden by a subsequent glacial advance.

The sequence at LK1 is capped by LFA 3, which consists of two massive diamictons. The lower diamicton is interpreted as a subaqueous debris flow unit due to the lack of structures within it and its gradational boundary with the underlying clay (Eyles, 1983). This sequence from LFA 2 to LFA 3 suggests a transition from a low energy lake environment, which allowed fines to settle out, to a higher energy environment in which debris flows occurred, suggesting an increase in glacier proximity. The upper diamicton within LFA 3 is interpreted as a weathered version of the lower diamicton due to its close proximity to the surface, the presence of roots indicating pedogenosis and the change to a brown colour, which suggests the oxidation of ferric ions (Madgett & Catt, 1978).

At section LK2, a second lithofacies association, LFA 4 is identified at both below and a similar height stratigraphically to LFA 1, although slumping has obscured the majority of the boundary between the two units. LFA 4 consists predominantly of alternating units of massive fine and coarse sand that are massive in the lower part of the section, but at LK2a, contain increasing proportions of large lenses of silt and wispy white sand, which have been attenuated and boudinaged to varying degrees. The original depositional environment of the sands is interpreted as subaqueous due to the lack of bedding structures within the sand and diamicton units (Cheel & Rust, 1982). The boundinage and attenuation found within sand and silt lenses in the upper parts of the lithofacies demonstrates that the unit has been subject to shear stress, indicative of subglacial deformation (Benn, 1996; Boulton *et al*., 2001; McCarroll & Rijsdijk, 2003), suggesting glacial overriding following deposition, in line with evidence found within LK1.

LFA 5 overlies both LFA 1 and LFA 4 at section LK2 and consists of a stratified diamicton containing fine sand partings and larger, highly attenuated sand lenses. The lithofacies is interpreted as a subglacial glaciotectonite due to the highly attenuated nature of the sand lenses

within it and fine sand partings, both of which have been excavated from the underlying sand units (Boulton *et al*., 2001; Phillips, 2002, 2007; Evans *et al*., 2006b; Ó Cofaigh *et al*., 2011). The C_{40} index of 28 and RA and RWR indices of 6 support a subglacial origin for LFA 5, as shown in Figures 4.35 and 4.36. Figure 4.36 indicates that the LK2 sample contains more rounded clasts than the rockfall control samples, but the clasts are not as rounded as the fluvial control samples, indicative of subglacial erosion. The C_{40} index for the LK2 sample is lower than that of the fluvial and rockfall samples, demonstrating that the sample is less 'blocky', also pointing towards a subglacial origin.

The clast macrofabrics are less conclusive than the clast morphological data, since the fabrics are fairly weak and fabric shapes for both the a-axis and a/b plane measurements do not fit within previously identified envelopes for depositional processes (Fig. 4.37) However, although weak, the clast fabrics do support a general direction of ice flow from approximately north to south as indicated by the direction of normal faults within LFA1 at Section LK2b. a/b planes generally rotate parallel to the direction of ice flow under shear stress, with the planes dipping towards the direction of stress, similar to imbricated clasts in fluvial settings (Evans *et al*., 2007), which suggests ice flow from the north to northeast. The a-axis usually aligns parallel to ice flow and therefore indicates ice flow to the southwest or southeast, in accordance with the a/b plane data.

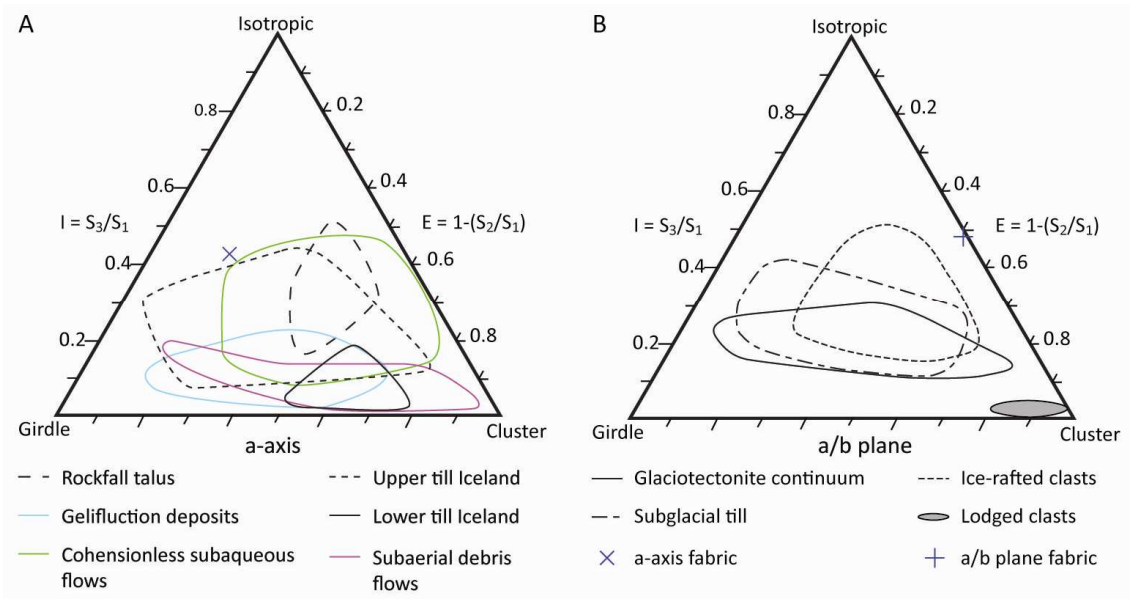

Figure 4.37. Fabric shape triangles for A) a-axis and B) a/b plane fabric measurements from LFA 5, Section LK2b, displaying envelopes for sediments with different genetic histories compiled from data from Dowdeswell and Sharp (1986) Benn (1994, 1995), Evans and Benn (2004), Evans *et al.* (2007, p. 116).

The a-axis fabric plots just outside the envelope for the upper till horizon of subglacial tills in Iceland (Dowdeswell & Sharp, 1986, in Benn, 1994), which were interpreted as having high pore water pressures which allowed clasts to rotate freely in all directions (Benn 1994, 1995), which is consistent with evidence for high water pressures in the underlying LFA 1 through

dewatering structures in the sand. The attenuation of sand lenses within LFA5, indicative of high strain rates (e.g. Boulton *et al*., 2001), is not incompatible with a weak a-axis fabric, since several authors argue that a weak a-axis fabric can occur in highly-strained deformation tills (e.g. Hicock & Dreimanis, 1992; Hart, 1994; Benn, 1995; Benn & Evans, 1996). However, other research suggests that strong fabrics should always develop under high strain rates (e.g. Hooyer & Iverson, 2000; Larsen & Piotrowski, 2003) and Evans *et al*. (1998) found that weaker a/b plane fabrics were indicative of lower cumulative strain rates within a glaciotectonite at Loch Quioch, Scotland. This discrepancy is difficult to resolve for the strain history of LFA 5 with only one clast macrofabric measurement, particularly since strain has been found to be highly variable within glaciotectonites (Evans *et al*., 1998, 2006b, 2007). Therefore, whilst the results of the clast fabric measurements are encouraging, more samples need to be taken from a number of areas within LFA 5 in order to understand the depositional environment further.

4.2.7 Synthesis of the geomorphological and sedimentary evidence for a former lake in the area around Loch Killin

Sediments interpreted as representing subaqueous deposition within former glaciolacustrine environments are found in the main Killin Valley within sections LK1 and LK2, in Glen Odhar and on the plateau immediately to the south of Glen Eich. The occurrence of a flat-topped hill containing Gilbert-type deltaic sediments at the latter provides evidence for the altitude of the former lake level in this area, at the boundary between subaqueous and subaerial deposition (LFAs 13 and 14). Although the exact altitude of this boundary could not be determined here, the Glendoe Hydroscheme photographs indicate that the boundary occurred only a few metres below the surface of the flat-topped hill, of which the NEXTMap DEM indicates a surface altitude of approximately 646 m. Whilst it is possible that the flat-topped hill was an isolated feature, representing a small lake on the plateau within a stagnating ice margin (*cf*. Livingstone *et al*., 2010c, e), the presence of a 642 m col between Glen Markie, and Glen Eskin (NH 599 101) that corresponds with the height of the subaqueous/subaerial boundary suggests that an extensive lake could have existed in the area. This argument is supported by the presence of a thick succession of subaqueously deposited diamicton in Glen Odhar, an extensive area of sand on Sròn na Lairige and subaqueously deposited sand and clay with sections LK1 and LK2.

The existence of such a lake was previously suggested by Charlesworth (1955) who argued that it was formed by the damming of the River Fechlin by the Ness Glacier during ice sheet deglaciation (Section 2.3.2). Figure 4.38 shows that the margin of this lobe of ice would have been positioned at the head of the Killin Valley in order for lake water to drain over the Markie-Eskin col, rather than northwards around the eastern margin of the ice into neighbouring valleys

to the east of Glen Killin. This ice margin position is similar to that suggested by Charlesworth (1955) (Fig. 2.9).

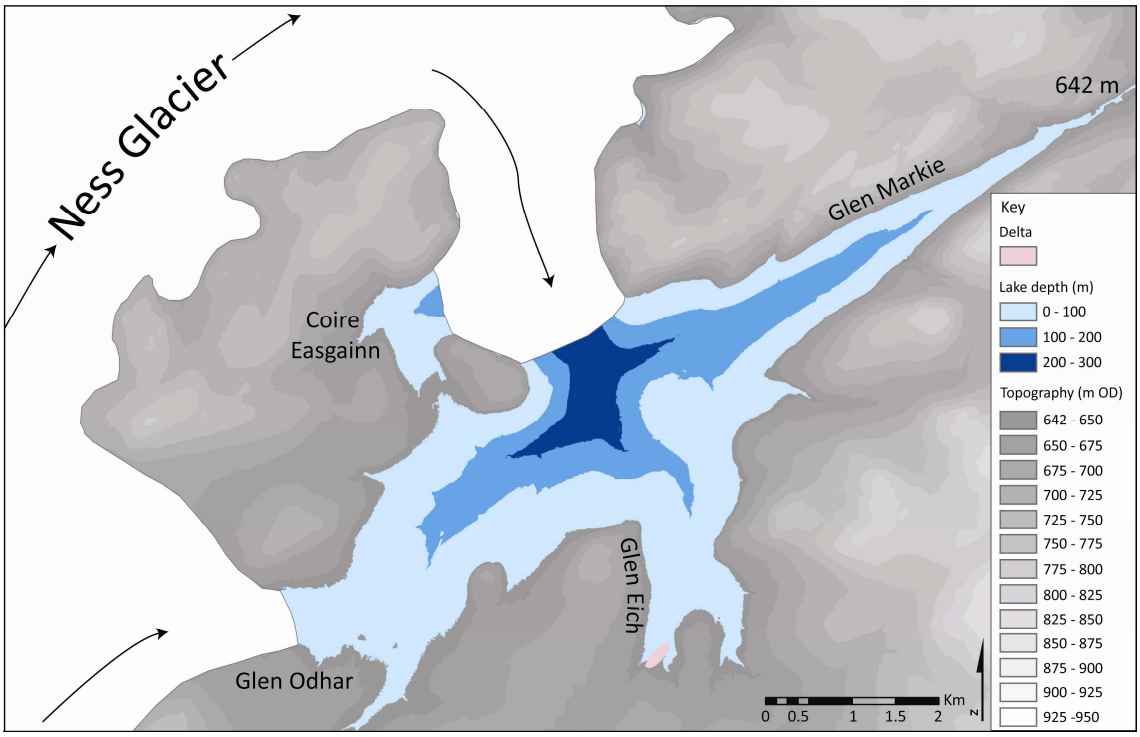

Figure 4.38. Idealised model to show the advance of an ice lobe from the Ness basin into the Fechlin-Killin valley, which dammed local drainage, creating Glacial Lake Killin that reached a maximum level of 642 m. Arrows denote approximate ice flow directions. Note: ice margins of the Ness Glacier are approximate and it is assumed that the parabolic surface of the glacier would prohibit lake drainage over the glacier surface (*cf.* Stokes & Clark, 2004).

Using the sedimentological evidence collected from the sections around Glen Killin, a sequence of events associated with the creation of Glacial Lake Killin is proposed. Sand and gravel deposited at the base of LK1 are interpreted as glaciofluvial outwash sediments, from which palaeocurrent data indicates water flow in a northwards direction suggesting that they were sourced from a nearby glacier to the south. Increasing evidence for glaciotectonism upwards in the section suggests an advancing glacier margin. Although there are no structural indicators in the exposed part of the section at LK1, normal faults and clast macrofabrics at LK2 indicate a glacier advance from the north. Fine lacustrine sediments and subaqueous debris flow deposits at the top of the LK1 section indicate that a lake formed in front of the advancing glacier margin, supporting an advance of a glacier margin from the north.

Continued advance of ice into the Killin Valley is recorded in the sediments at LK2, which show a transition from a subaqueous to subglacial environment, manifest in increasing levels of glaciotectonism upwards in the sequence, which is capped by a laminated diamicton containing attenuated, boudinaged and folded sand lenses. It is likely that during the advance of this ice lobe from the north, local ice to the south was forced to rapidly retreat due to increasing lake

levels in the valley. During initial lake formation, the lake would have been able to drain to the northeast around Carn Fliuch-bhaid (NH 551 129), controlled by the height of the ice margin. Further advance of the ice lobe, however, to the head of the Killin Valley would have dammed drainage to the 642 m level, where the lake was forced to drain over the 642 m col into Glen Eskin at the head of the Findhorn Valley.

During the existence of the maximum lake level, the delta was formed on the plateau and the majority of the subaqueous debris flow sediments in Glen Odhar also formed during this time. The interpretation of these sediments as a subaqueous grounding-line fan indicates that ice was present in the upper part of the Odhar catchment. This is depicted as regional ice in Figure 4.38, but it is likely that some local plateau ice was also present in order to source the deltaic deposits in the Eich catchment. The occurrence of moraines on top of the subaqueous sediments in Glen Odhar indicates that a glacier subsequently advanced down the Odhar Valley some time after lake drainage. This is discussed further in Chapter 5.

4.3 The Eastern Monadhliath Mountains

The area of the eastern Monadhliath Mountains included in this study is approximately 135 km^2 and covers the upper parts of the River Findhorn and River Dulnain valleys, alongside Glen Mòr to the southeast and its two tributary catchments, Glen na Gearra and Glen Unaig (Fig. 4.1). These glens drain the eastern side of the main plateau, which ranges from 700 to 900 m OD, to the northeast, east and southeast respectively. Previous research in the area was undertaken by Hinxman and Anderson (1915), Charlesworth (1955), Young (1977) and Auton (1998) in the Findhorn and Dulnain valleys (Section 2.3).

4.3.1 Upper River Findhorn

The River Findhorn is sourced in the Monadhliath Mountains and drains a substantial part of the main plateau area. The river flows northeastwards, eventually entering the Moray Firth at the village of Findhorn. The description presented here focuses only on the area upstream of Coignafearn (Fig. 4.39) (Appendix I). This upper part of the Findhorn Valley consists of a deep, low gradient glacial trough that mainly trends northeastwards. A large river terrace occurs throughout the majority of the valley downstream of Dalbeg and is particularly apparent on the southern valley side, which is often inset by smaller river terraces. Three large fans emanate from the three main tributary valleys on southern side; the Allt Deamhaidh, Allt Coire Challich and Elrich Burn catchments; and several river terraces have developed beside each stream. Isolated rounded ridges occur across the valley sides in this area. Mature talus slopes are present on the valley sides and several areas of the northern valley side are covered in rockfall.

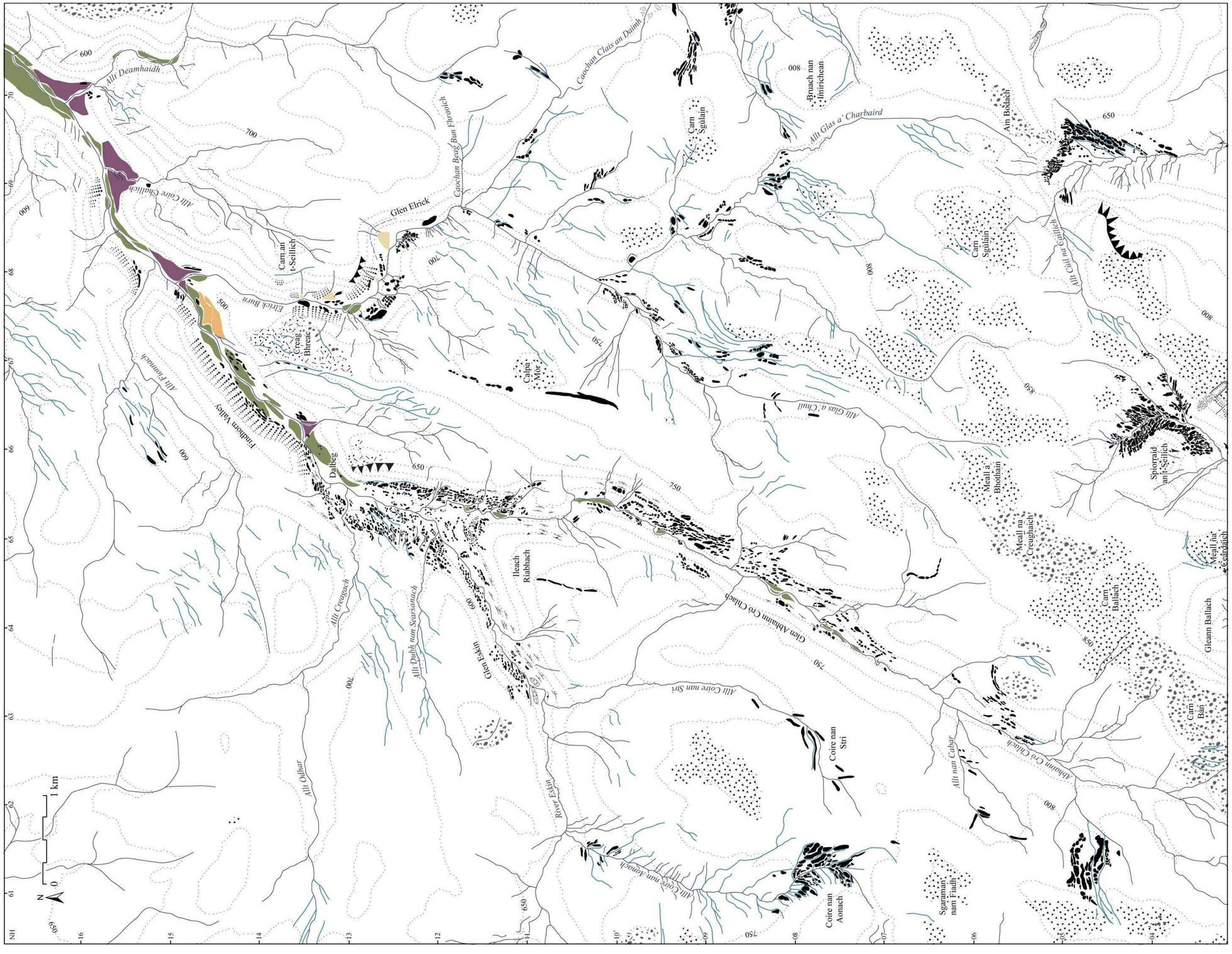

Figure 4.39. The geomorphology of the upper part of the Findhorn catchment (see Fig. 4.2 for key).

Ridges and mounds become less isolated upstream of NH 674 147. These features are most prominent in an area on the northern valley side, where small rounded ridges occur that are approximately 5 m high and have a network of channels in between them. The ridges are heavily covered in talus from an extensive talus slope on the valley side that reaches the valley floor both upstream and downstream of the ridges. The ridges occur on top of, or are surrounded by, a prominent 5 m high river terrace. Sporadic mounds and ridges also occur on the southern valley side in this area.

Further upstream, at around NH 660 134, the river terrace that surrounds the ridges on the northwestern side gradually disappears, although there is no abrupt end point. Upstream of this area, closely spaced rounded mounds occur on the northern side. These are mirrored by very small, less that 20 m in diameter, rounded mounds on the southeastern side. The mounds on the northern side continue upstream on a low sloping area at the base of the valley side, which is separated from the steeper part of the valley side by a small channel. Upstream of the Allt Creagach tributary stream (NH 655 130) the mounds continue, covering both the valley floor and the valley side to the top. They are very sharp-crested and both heavily composed of and covered in boulders, with a network of well-formed channels in between them.

Small rounded mounds or ridges less than 5 m high, also occur on the southeastern valley side opposite Dalbeg (NH 657 131) and continue upstream. A little further upstream, three large (> 10 m) lateral ridges are present at the base of the valley side between Dalbeg and the Eskin – Abhainn Crò Chlach confluence (Fig. 4.40). The ridge crestlines are orientated nearly parallel to the valley side with a large channel separating each ridge from the valley side. Other smaller, sharp-crested, mounds occur on the valley side and the valley floor in this area and continue into the Eskin and Abhainn Crò Chlach basins. These mounds are also found in the area in between the two catchments but are more subdued in this area.

Figure 4.40. Ridges and mounds on the eastern side of the Findhorn Valley south of Dalbeg, with crestlines highlighted by white dashed lines. Photograph taken on the west side of the valley towards the east.

The mounded topography that covers the whole of the western side of the Findhorn valley terminates soon after the valley turns a corner into the Eskin catchment. However, smaller mounds and ridges begin again at NH 648 118 on the lower part of the northern valley side. Similarly the mounded topography on the southeastern side of the Glen Eskin merges into a series of faint lateral benches on the valley side. Lateral benches, small mounds and ridges are present in the valley up to the Allt Coire nan Stri tributary (NH 632 108). At this point two large bedrock ridges occur on either side of the River Eskin, with large channels separating them from their respective valley walls. Upstream of this point very few other features occur and the valley sides are largely steep and smooth, although large accumulations of sediment can be seen on them upstream of the Allt Coire nan Aonach tributary at NH 616 106.

The plateau area in between Glen Markie (Killin), Glen Eskin and Glen Abhainn Crò Chlach consists of several rounded summits, dissected by small valleys (Fig. 4.41). Mounds and ridges were noted in a number of these glens using aerial photographs and Google Earth imagery, but have not been verified in the field. Small low profile ridges are present within Coire nan Aonach (within square NH 6108), Coire nan Stri (square NH 6207), Coire Cam nan Cròc (square NH 5907) by Allt Cam Bàn (squares NH 5606 and NH 5905) and to the southeast of Sgaraman nam Fiadh (squares NH 6104 and NH 6105). There are also a large number of small channels that trend obliquely downslope between the ridges within these valleys and the head of the Allt Mòr catchment (square NH 5704). In addition, a large thin (5 m high and 30 m wide) north-trending ridge occurs on Ileach Bhàn (NH 645 107) that is broken up into five segments (Figs. 4.39 & 4.41).

To the east of this plateau area, the Abhainn Crò Chlach valley is located along a fault, forming a generally straight southwest-northeast trending valley that dissects the eastern part of the central plateau. Most of the valley is v-shaped, with a few 4-5 m high river terrace fragments occurring sporadically along the valley floor. Where sections are available the terraces are composed of clast-supported gravels and boulders, but bedrock is also exposed beneath some terraces. The mounds and ridges in the Findhorn Valley continue into Glen Abhainn Crò Chlach, where they are sharp-crested and clearly delimited by prominent channels. These features are present up to two thirds up the valley side and continue up to a bedrock spur just over 1 km from the Eskin - Abhainn Crò Chlach confluence. Further upstream numerous lateral benches occur on the southeast valley side. These continue for the majority of the length of the valley, but the continuity of individual benches is often difficult to trace. Very few benches occur on the northwest valley side, although extensive gullying in several areas indicates the presence of large accumulations of sediment.

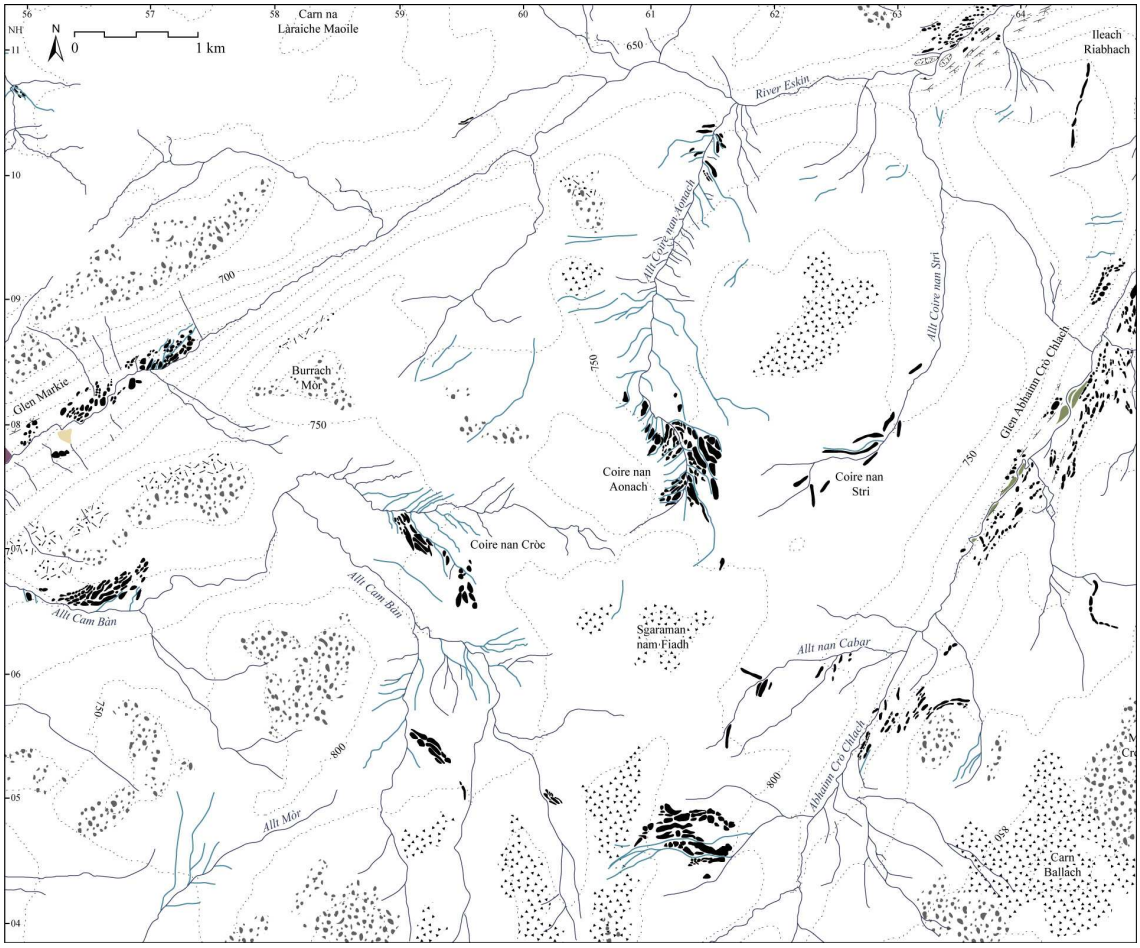

Figure 4.41. The geomorphology of the plateau between Glen Markie, Glen Eskin and Glen Abhainn Crò Chlach (see Fig. 4.2 for key).

Elrick Burn is a tributary of the River Findhorn that joins downstream of Dalbeg and is sourced from the convergence of several streams that drain the plateau to the east of Abhainn Crò Chlach (Fig. 4.39). In the plateau areas above Elrick Burn all the streams reside within v-shaped channels and no river terraces are present. Numerous downslope channels dissect the valley sides upstream of the confluence of Elrick Burn with Caochan Beag Bun Fhraoich at NH 688 118, and indicate the presence of large amounts of sediment on the valley sides. A few obliquely trending ridges occur in this area, but the landscape is mainly dominated by channels. In particular, several deep channels are present on the southeastern flank of Calpa Mòr (814 m; NH 669 109). These channels trend obliquely downwards across the hillside towards the middle to lower part of Glen Elrick. In addition, they all lead upslope towards a large, 10 m high ridge, which occurs on the central part of the plateau to the north and south of Calpa Mòr on the watershed between the Abhainn Crò Chlach and Elrick Burn catchments. This ridge is broken up into several mounds, apart from at the southernmost end where it forms a continuous ridge for nearly 2 km.

Downstream of Caochan Beag Bun Fhraoich (NH 686 119) a series of short downslope-trending channels appear on the western valley side by Elrick Burn and a series of subdued ridges occur

on the eastern side. The valley is v-shaped up to where it turns towards the west and opens out slightly. In this area, two heavily dissected and subdued ridges of sediment can be seen less than half way up the northeastern valley side, which trend gently downslope across the valley side. Chaotic mounds are found on the inside of this bend, which are dissected by channels in between them that flow almost directly downslope. These mounds continue to occur for a short distance downstream from the bend, but become increasing dissected by small channels.

Further downstream on the southwestern valley side, there is a 10 m high ridge that has been deposited across the valley side, with a well-developed channel immediately upslope of it that separates the ridge slightly from the valley side (NH 675 126). Beyond this ridge, a drift limit that is heavily dissected by downslope trending channels is observed at roughly the same altitude. This limit can be faintly traced further downstream, although it is greatly obscured by a thick talus slope on the eastern flank of Creag Bhreac (679 m; NH 674 136). On the opposite valley side, a significant amount of rockfall has fallen from the slopes below Carn an t-Seillich (NH 684 135), producing a thick talus slope. Occasional mounds are found at the base of the valley side and are covered by the rockfall material. These mounds occur on top of a river terrace, although no clear start to the terrace is observed further upstream.

Mature talus slopes occur on both sides of the remaining lower portion of the valley. At the confluence of Elrick Burn with the River Findhorn, a large fan is present. This fan consists of a number of river terraces and former river channels and is bounded to the east by a ridge on the lower part of the valley side.

4.3.2 Upper River Dulnain

The River Dulnain drains a large proportion of the southeastern part of the Monadhliath Mountains, eventually flowing into the River Spey just beyond Dulnain Bridge. This research examined the upper part of the catchment area, upstream of NH 718 094 (Fig. 4.42).

The River Dulnain begins at the confluence of four tributary streams to the east of Bruach nan Imirichean (NH 701 078). Closely spaced mounds and ridges occur in this area, which are prominent and sharp-crested on the southeastern side, but have more rounded crestlines on the northwestern side. Well-developed channels surround these ridges and also occur across the eastern side of Bruach nan Imirichean. The mounds and ridges form a large accumulation of sediment on the northwestern valley side, the upper limit of which steadily decreases in elevation in a downstream direction (Fig. 4.43). Beyond this limit the valley sides have a smoother surface. The limit of the sediment corresponds approximately to the start of a large river terrace, although the terrace begins inside a few of the downstream-most ridges. On the

eastern side the terrace is not so pronounced and a wide ridge with a rounded crestline occurs on the valley side just above it.

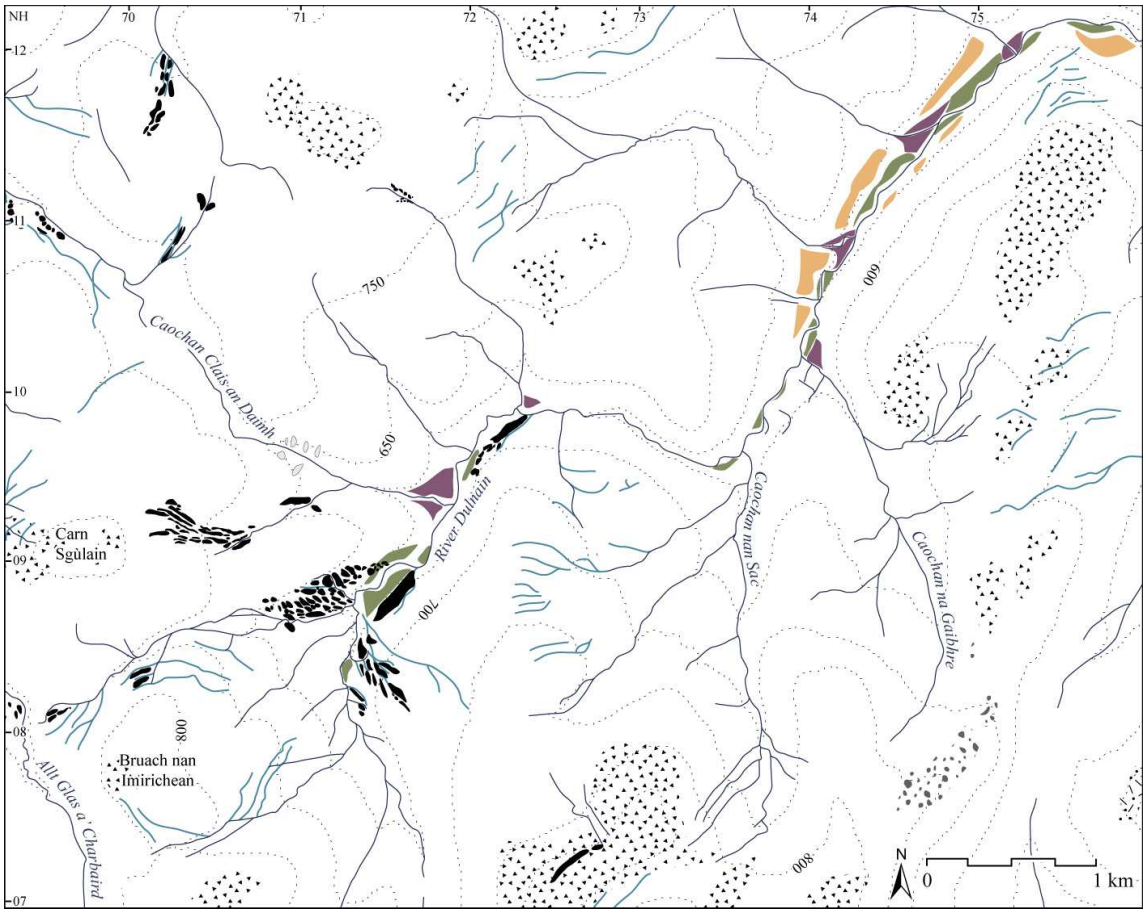

Figure 4.42. The geomorphology of the upper Dulnain catchment (see Fig. 4.2 for key).

Figure 4.43. A large accumulation of sediment in the form of mounds and ridges on the northwestern valley side of the upper part of the Dulnain catchment. Crestlines of ridges are marked by the dashed white lines and 'T' indicates the location of a major river terrace. Photograph taken looking northeastwards from Bruach nan Imirichean.

Ridges are also found in a small tributary catchment to the River Dulnain, which occurs immediately to the north of the area described above (NH 705 092). These ridges are very low

profile with small channels in between them and occur predominantly on the northern side of the central stream. Further downstream in the Dulnain Valley, fragments of a major river terrace occur, alongside a higher level terrace that occurs mainly on the western valley side. There are few ridges in this part of the Dulnain Valley, but fans emanate from most tributary streams as they join the River Dulnain.

4.3.3 Glen Mòr

Glen Mòr is located on the southern edge of the Monadhliath Mountains and begins to the south of the Dulnain catchment, trending southeastwards to Kingussie in the Spey Valley. The valley itself is fairly wide, but Allt Mòr flows within a deep, narrow channel that has been cut into a 25 m high terrace of unconsolidated sediments, indicating that the valley has been filled by a considerable amount of sediment (Fig. 4.44). Fragments of at least two river terraces occur on either side of the Allt Mòr inside the channel it has created in the higher-level terrace.

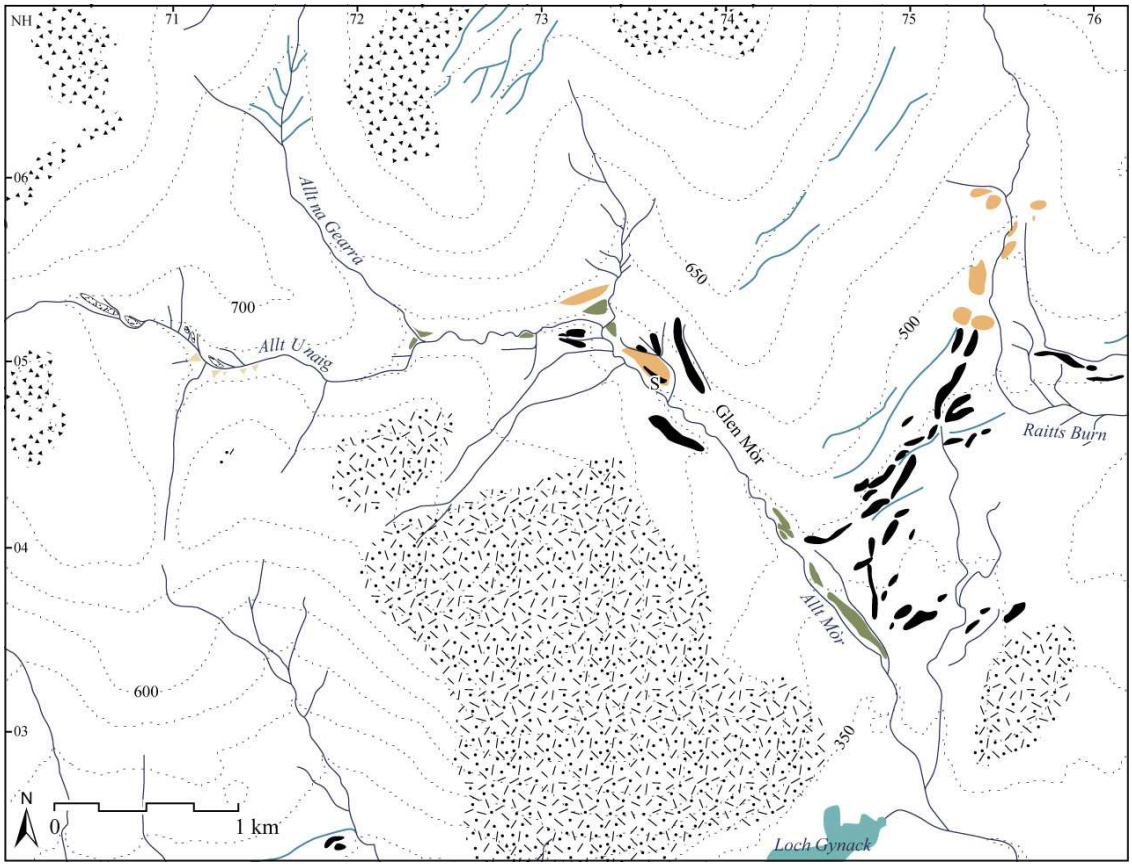

Figure 4.44. The geomorphology of Glen Mòr (see Fig. 4.2 for key). The section in Figure 4.45 is marked by an 'S'.

A number of large (10 m high) ridges occur on top of the high terrace on both sides of Allt Mòr. Ridges also occur on the valley sides, which trend obliquely down valley. Sections excavated by the stream reveal some of the sediments within the terrace. One section, in particular, exposes the sediments within both the terrace and ridge above it (NH 736 049) (Fig. 4.45). The section contains the same lithofacies as the terrace in Glen Odhar in the Killin catchment and

therefore the same lithofacies associations are used and described below in an order from lowest to highest.

- **LFA 9** – The lower part of the section consists of an interbedded clast-rich, matrix-supported diamicton and clast-supported diamicton, which show some faint stratification in a downstream direction. Clasts vary in size from gravel to boulder size and appear to be roughly arranged in layers within the diamicton.

- **LFA 10** – LFA 10 is separated from LFA 9 by a sharp boundary. It consists of a unit of horizontally laminated sand that is no more than 1 m thick. This sand occurs at a similar level to the top of the terrace on which the ridge above it is located.

- **LFA 11** - This lithofacies association forms the ridge and is composed of a clast-supported diamicton. The unit contains clasts of a similar size to LFA 9 except none of the larger boulders. There is some faint horizontal bedding within the unit and a small discontinuous layer of laminated sand is observed at the most downstream end. It is separated from the underlying LFA 10 by a sharp boundary.

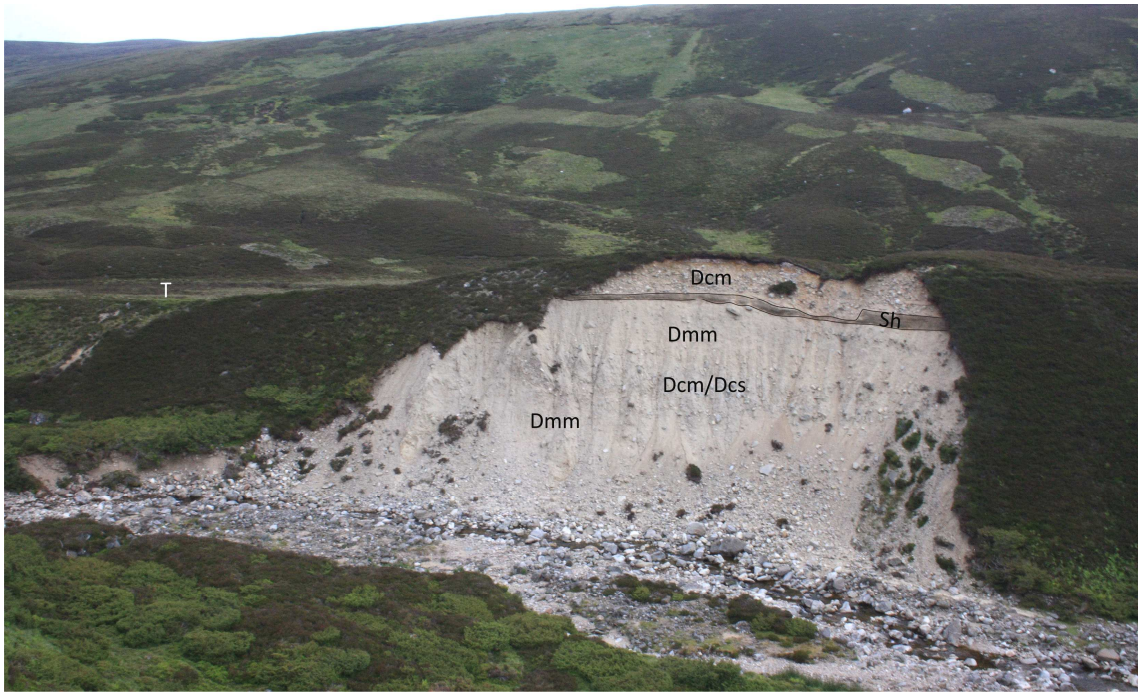

Figure 4.45. Annotated photograph showing a section in a terrace within Glen Mòr, revealing LFAs 9 to 11. A key to the lithofacies codes used is found in Figure 3.11 in Section 3.2 and the 'T' indicates the terrace level. Obliquely trending ridges can also be seen on the valley side behind the section.

Further upstream, the valley divides in two where the two tributary streams, the Allt na Gearra and the Allt Unaig join. Allt na Gearra flows southwards from the watershed with the Dulnain catchment. The upper part of the valley contains several small channels, but there are no mounds or ridges. These channels trend more obliquely downslope than those in the lower portion of the

valley, which are orientated parallel to the valley slope. The current stream is small and has incised very little throughout most of the valley. There are also no river terraces throughout most of it, although the stream is more deeply incised towards the confluence with Allt Unaig and where the surface slope steepens, a small river terrace (~ 1 m in height) occurs.

The other tributary is the Allt Unaig, which flows from west to east, from the watershed with Gleann Chaorainn (NH 701 052). Several large, bedrock-cored ridges occur in the upper part of Gleann Unaig that have formed through stream erosion. The Allt Unaig has also caused significant incision in the main valley. The current stream is very small compared to the width of the incision and is banked on either side by a low (<0.5 m) grassy terrace. This is continuous throughout Gleann Unaig, but as the gorge widens downstream, the terrace becomes higher compared to the stream. By the time the stream reaches the confluence with Allt na Gearra, the terrace is more substantial, although is still not particularly high (~ 1 m). The change in river terrace height is gradual and no significant change in river terrace size or number occurs. A significant number of well vegetated, relict debris cones emanate from the gullies on the valley sides, particularly on the southern side.

4.3.4 Interpretation of the geomorphological and sedimentary evidence in the eastern Monadhliath Mountains

The geomorphological evidence in the eastern Monadhliath Mountains is similar to that of the western and northern parts of the region (Appendix II). Therefore following arguments made in Section 4.1.6, the majority of ridges and mounds are interpreted as lateral and latero-frontal moraines and obliquely trending channels are interpreted as ice-marginal meltwater channels (Benn, 1992; Benn *et al.*, 1992; Bennett & Boulton, 1993a, b; Lukas, 2005a; Greenwood *et al.*, 2007; Finlayson *et al*., 2011).

Two long ridges are also found on the plateau on either side of the Findhorn Valley, near Calpa Mòr and Ileach Bhàn, which are both orientated almost directly northwards. These ridges have been previously interpreted by Hinxman and Anderson (1915) as moraines, but were later interpreted as eskers by the British Geological Survey (2004). The ridges are both positioned along watersheds and are straight rather than sinuous. These features, combined with the occurrence of a large number of channels (see below), indicate the presence of ice on the plateau above the Findhorn Valley. Eskers are unlikely to have developed on the highest ground since any subglacial meltwater is likely have been routed towards topographic lows on the plateau. The ridges are therefore interpreted here as lateral moraines that document the margins of the Findhorn Glacier as it became constrained within the Findhorn Valley.

There are also a large number of deep channels that trend SW-NE across the plateau on both sides of the Findhorn Valley. These channels have profiles that steadily decrease in a northeast direction indicative of ice-marginal rather than subglacial meltwater drainage (Greenwood *et al*., 2007). These channels are therefore also interpreted as documenting the position of the margin of the Findhorn Glacier as it flowed from the plateau into the Findhorn Valley, which supports the interpretation of the large ridges on the plateau as lateral moraines and further provides evidence of plateau ice.

Ice-marginal meltwater channels are a dominant feature of the landscape in this area of the Monadhliath Mountains, where they are also found on the plateau above Elrick Burn and on Bruach nan Imirichean at the head of the Dulnain Valley. All these features were interpreted as ice-marginal meltwater channels based upon their downslope trending profiles (Greenwood *et al*., 2007). Moraines occur more sporadically in the Elrick and Dulnain catchments and are less well preserved. In several areas in the Elrick Burn catchment, accumulations of sediment occur on the valley sides forming mounds with channels in between them. The edges of the mounds are not well defined, however, with no clear spatial pattern and the channels in between them are often orientated directly downslope rather than obliquely. These areas of sediment are interpreted as areas of former moraines that have been subject to intense paraglacial activity in the form of downslope movement of sediment and gullying by streams (Ballantyne, 2002b, c, 2008).

No moraines are found in the Allt na Gearra and Allt Unaig catchments, although obliquely trending channels at the head of Glen na Gearra are interpreted as ice-marginal meltwater channels. No glaciogenic landforms are found in Glen Unaig, but the steep bedrock sides suggest that the Allt Unaig was previously much larger than the current stream.

The section at Glen Mòr reveals a very similar sequence to that found in Glen Odhar in the northern sector of the study area (Section 4.2.5). The section reveals a stratified, matrix-supported, clast-rich diamicton (LFA 9), which is separated by a sharp boundary from a unit of horizontally laminated sand (LFA 10), which forms the upper surface of the terrace. The ridge is composed of a clast-supported diamicton (LFA 11), which is separated from LFA 10 by a sharp boundary at the same elevation as the base of the ridge. Since the section occurs in a very similar setting to the sections within Glen Odhar, both in terms of the geomorphology and the location in the valley, the same interpretation is applied here. The geomorphology and sedimentology at Glen Mòr therefore provides evidence for deposition of the terrace within a glaciolacustrine environment, where LFA 9 was formed through subaqueous cohesive debris flows that were sourced subglacially as a subaqueous grounding-line fan from a glacier at the head of Glen Mòr (Benn, 1996; Lunkka & Gibbard, 1996; Johnsen & Brennand, 2006; Reitner, 2007). The

horizontal sand unit, LFA 10, is interpreted to have formed through subaqueous fan deposition, indicating a change in energy environment and possible retreat of the glacier (Cheel & Rust, 1982; Krzyszkowski & Zielinski, 2002; Bennett *et al*., 2002; Hornung *et al*., 2007). The extent of this lake is uncertain, but based on the location of the glaciolacustrine sediments, the lake surface is likely to have been at an altitude of between 550 and 600 m. As at Glen Odhar, the ridge on top of the terrace is interpreted as a latero-frontal moraine based on its morphology, orientation and composition of clast-supported diamicton, indicating a subsequent glacial advance over the lake sediments (*cf.* Benn & Evans, 1993; Reitner, 2007).

4.4 The Southern Monadhliath Mountains

The southern sector of the Monadhliath Mountains comprises the remaining valleys in the study area that drain the central plateau area to the south and cover an area of approximately 195 km^2. The elevation of the plateau varies between 650 to 900 m, with summits of between 911 and 945 m in the southeast corner, north of Glen Banchor. Previous research in this area is restricted the area around Glen Banchor (Barrow *et al*., 1913; Young, 1978).

4.4.1 Gleann Chaorainn and Gleann Beinne

Gleann Chaorainn is a south-facing, 5 km long valley, which is connected to the southeast corner of the Monadhliath plateau by a steep backwall at its northern end and converges with Glen Banchor to the south (Fig. 4.46). 5-10 m high ridges occur towards the downstream end of the valley, to the south of Creag na h-lolare (815 m; NH 672 010). These ridges lie roughly parallel to each other and trend obliquely down the valley sides in an upstream direction. The ridges are heavily strewn with boulders and small natural sections indicate they are composed of sandy material.

A staircase of two to three river terraces occurs in this area and continues upstream until after the confluence with Allt Tom Dubh a' Ghobhlaich at NH 693 020, where the stream has eroded into a large fill of sediment to form a 15 m deep channel. Fragments of a smaller river terrace, about 1 m high, occur within this channel. Further upstream, the valley floor becomes less deeply incised and consists of a gently sloping terrace. Sections excavated by the river reveal that the terrace is composed of a grey diamicton overlain by a thin veneer of peat.

In the upper part of Gleann Chaorainn low relief (~ 3 m) ridges trend obliquely downvalley on the eastern side of the valley floor (Fig. 4.47). Prominent channels occur between these ridges, but have also dissected the ridges into smaller mounds and ridges. The ridges become increasingly dissected further upstream, where they are confined to the eastern and northern edges of the valley floor immediately below the backwall. Boulders of both psammite and granite occur sporadically on the surface of these ridges.

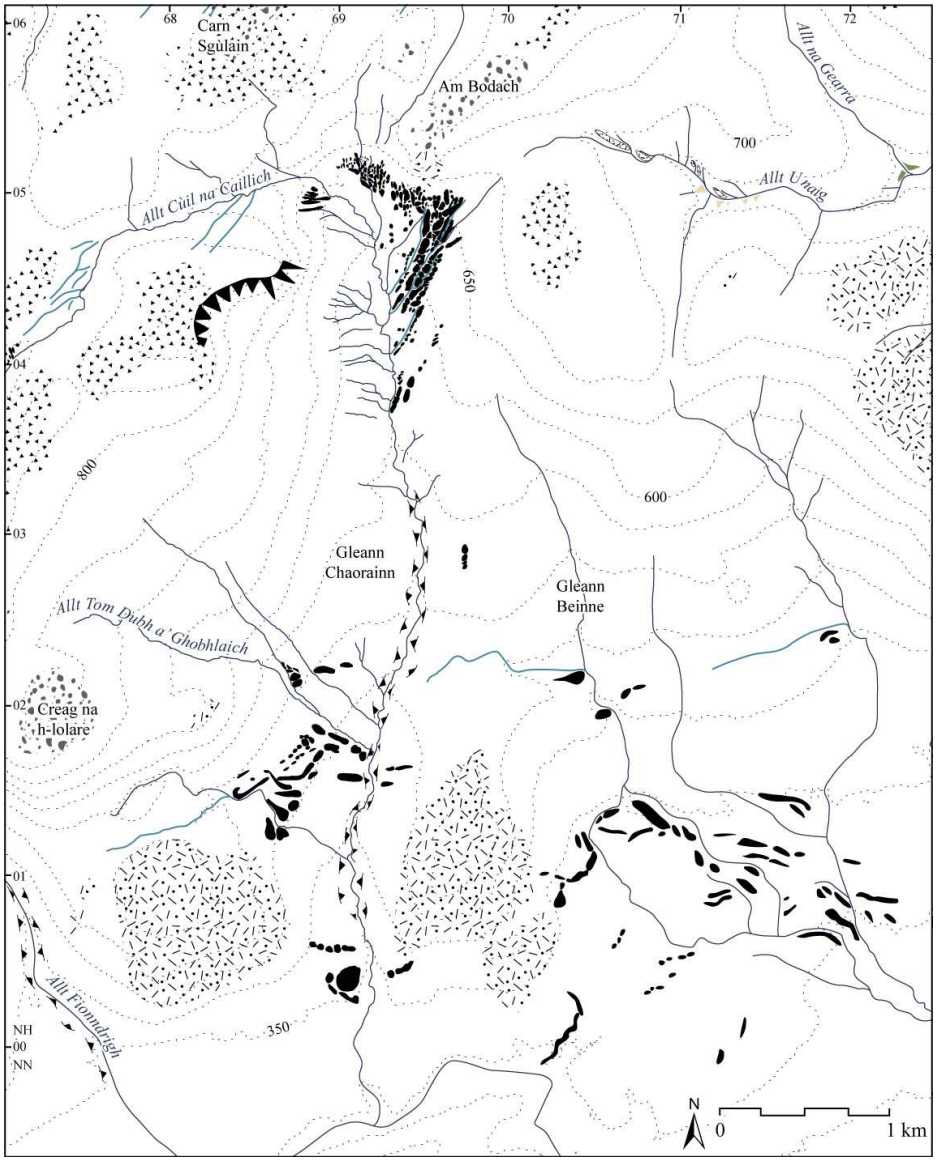

Figure 4.46. The geomorphology of Gleann Chaorainn and Gleann Beinne (see Fig. 4.2 for key).

Areas of blockfield and solifluction lobes occur on the plateau on Carn Sgùlain (920 m; NH 684 059) and Am Bodach (820 m; NH 697 055) immediately to the north of Gleann Chaorainn. At least three anastomosing channels, which trend obliquely downstream across the valley side, also occur on the plateau immediately to the west of Allt Cùil na Caillich.

Gleann Beinne is a small catchment that occurs to the east of Gleann Chaorainn and is connected to it via a deep channel cut into the higher ground in between the two catchments. Few features occur upstream of this channel, but a large ridge occurs immediately to the south of it that is orientated perpendicular to the main slope of the valley. A number of sinuous 10 m high ridges occur in the lower part of Gleann Beinne, immediately to the north of Newtonmore, which widens out at this point to coalesce with the neighbouring catchment to the east. These ridges are orientated across the mouth of the Beinne catchment, but progressively lower in

altitude from west to east. Several areas of flat ground are located in between these ridges and the upslope side of Gleann Beinne to the north.

Figure 4.47. View from the Monadhliath plateau looking southeastwards into Gleann Chaorainn, showing low relief ridges in the middle-ground of the photograph (R to R) and exposed bedrock (Br) and talus (Ta) to the left on the slope below Am Bodach.

4.4.2 Gleann Fionndrigh

Gleann Fionndrigh is a predominantly south-facing valley, which flows from Meall na Creughaich (906 m; NH 655 055) towards Glen Banchor (Fig. 4.48). A large river terrace (10-15 m in height above the current river) is present continuously along the lower part of the valley (Fig. 4.49A) and a thick talus slope exists on the eastern valley side. A few subdued mounds and ridges also occur on the terrace and the lower parts of the valley sides in this area. The river terrace ends abruptly at NH 663 017. This coincides with the end point of a large, heavily dissected ridge, on the western valley side, which slopes downstream across the valley side (Fig. 4.49B). A number of mounds also occur on the valley floor on the eastern side. These mounds are spatially organised into several lines and can be followed upwards onto the eastern valley side. Upstream of this point, there is initially no river terrace and the stream resides in a narrow gorge with steep sides to the west, formed of sediment. A few subdued mounds occur in this area on the eastern side, but significant rockfall below Geal Charn (889 m; NH 669 031) has obscured some features here. On the western side, two very large (~ 15 m high) mounds are located on the top of the steep-sided sediment bank, which forms a relatively flat area of ground in between Gleann Fionndrigh and Gleann Ballach. One of these mounds is conical in shape, whilst the other is formed of at least two rounded coalescent mounds.

Further upstream, the valley widens slightly and fragments of a river terrace occur. Mounds and ridges are present on both valleys sides in this area, but are less clearly defined and have a more ambiguous spatial pattern than further downstream. A large accumulation of sediment occurs on the western valley side, which is heavily dissected by downslope trending channels. On the

opposite valley side, a downslope termination of a thick talus slope is observed below Geal Charn at an altitude starting at 615 and ending at 670 m in an upstream direction. The lower boundary of this talus slope coincides with approximately the same altitude that the upper boundary of a sediment accumulation occurs.

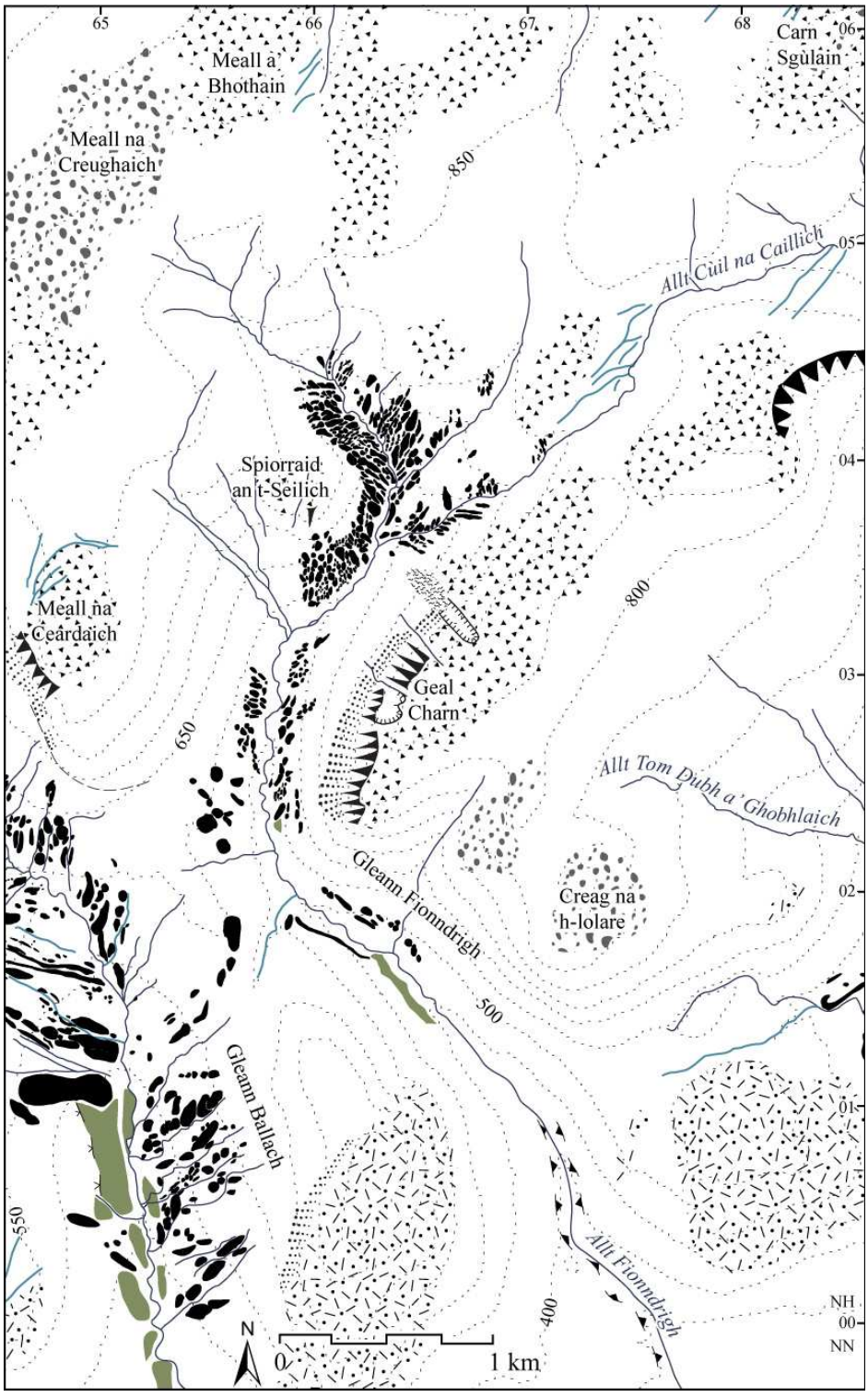

Figure 4.48. The geomorphology of Gleann Fionndrigh (see Fig. 4.2 for key).

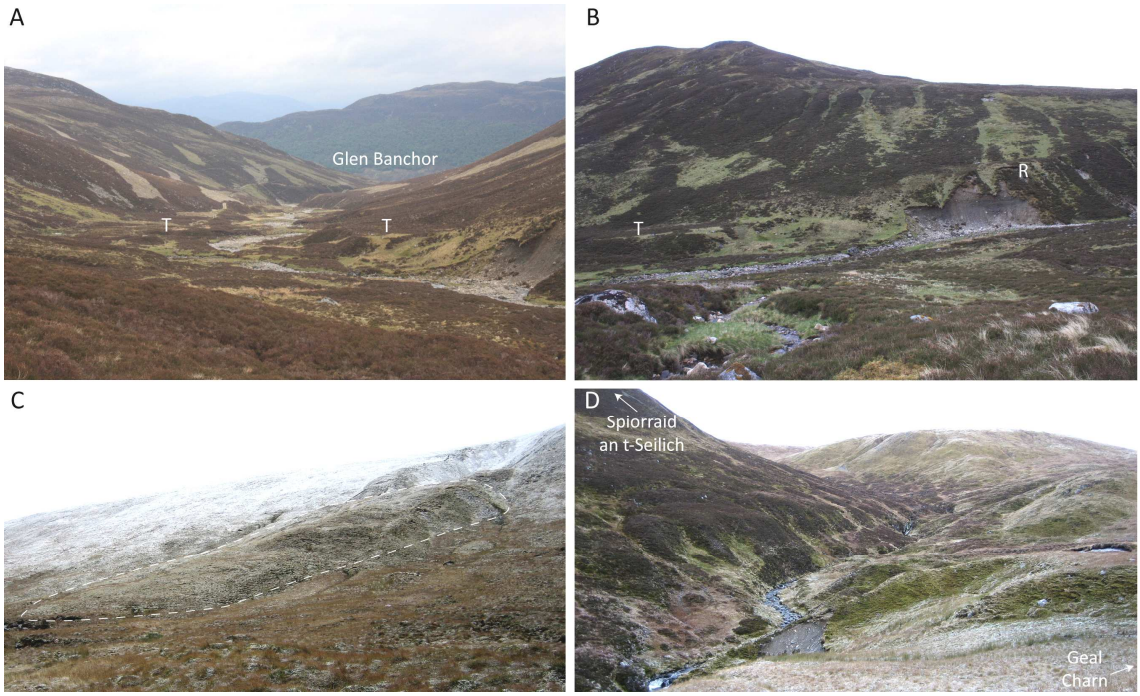

Figure 4.49. Gleann Fionndrigh: A) Photograph of the lower part of the valley, taken looking downvalley, showing major river terraces (T), particularly on the right hand side. B) Photograph of a major river terrace (T) on the left, which merges with a ridge (R) of sediment on the valley side to the right. Photograph taken on the eastern valley side looking southwestwards. C) Photograph of a large lobe of sediment (outlined by a white dashed line) that emanates from a scarp at the top of the hillside on the eastern valley side. Photograph taken on the eastern valley side towards the northeast. D) The upper part of the valley upstream of Spiorraid an t-Seilich, showing closely spaced mounds and ridges on both valley sides. Photograph taken on the eastern valley side looking northwards upvalley.

At Spiorraid an t-Seilich (NH 660 039), the valley narrows again and below it, the western valley side becomes covered in small, densely-spaced mounds. On the eastern side, a large bench of sediment slopes downstream. The upstream part of this bench has been disturbed by a large lobe of material that begins further up the valley side below a scarp and large, deep scar in the valley side (Fig. 4.49C). Upstream of this feature, small, closely spaced mounds occur on both sides of the valley (Fig. 4.49D). The mounds are dissected by numerous interconnecting channels, which enable a clear chevron-shaped pattern of adjoining mounds to be deciphered. Although the mounds occur on both sides, they are better preserved on the western valley side where a distinct upper limit is present.

4.4.3 Gleann Ballach

Mounds and ridges occur throughout the length of Glen Ballach, which is a south-facing valley to the north of Glen Banchor and is separated from the plateau by a steep backwall (Fig. 4.50). In the lower part of the valley, the mounds and ridges are very subdued and barely distinguishable. A large laterally extensive river terrace is present in this portion of the valley and culminates as a fan at the confluence with the streams from Gleann Lochain and Gleann Madagain.

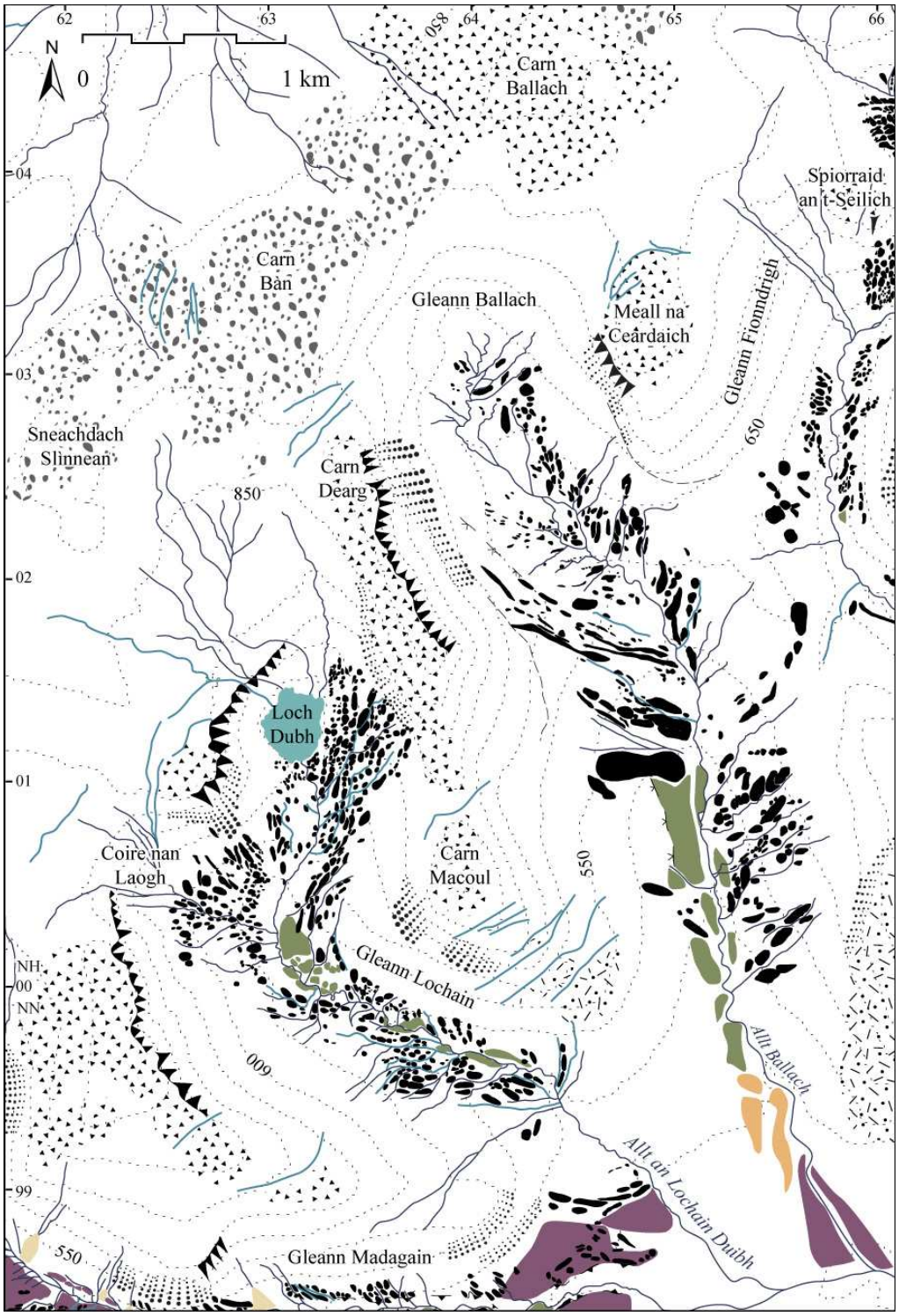

Figure 4.50. The geomorphology of Gleann Ballach and Gleann Lochain (see Fig. 4.2 for key).

About half way up the valley, a 30 m high ridge occurs on the western valley side, which is divided into two main parts and a third smaller part (Fig. 4.51A). The two main ridges are flat-topped, the upper part at a height of 550-560 m and the lower part at 510 m. The ridge is disproportionately larger than any other features in the valley and is orientated perpendicular to the main valley slope, rather than obliquely like the ridges upstream of it. The third, smaller part is composed of laminated sand, which is folded and faulted to varying degrees.

Figure 4.51. A) Photograph of a large ridge (R) on the western side of Gleann Ballach that is orientated perpendicular to the valley slope, with a major river terrace (RT) on the downstream side. B) The western valley side in the upper part of Gleann Ballach, showing the thick talus slope on the valley side and that the talus has been deposited on a ridge (R to R) running obliquely downslope across the base of the valley side. Both photographs were taken from the eastern side looking towards the northwest.

Upstream of this ridge, the valley contains a series of closely spaced arcuate ridges. On the western side, these are most apparent immediately upstream of the large ridge, whilst on the eastern side, the features are better preserved further up the valley. The ridges are relatively low in height (< 5 m), but show little slope degradation on their sides. A change in river terrace morphology also occurs upstream of the large ridge, where the pronounced terrace ends immediately to the south of the most downstream arcuate ridge. Upstream of this point, only a small river terrace is present. Further upstream, in the upper part of the valley, on the eastern side of the valley floor, the topography becomes more mounded, with individual mounds harder to define.

Directly below and leading up onto the plateau, a distinct trimline is present on both sides of the valley. On the eastern valley side there is an abrupt downslope termination of a thick talus slope, which leads upwards to a former channel. This channel leads around the back of Meall na Ceardaich (879 m; NH 649 031) and is connected to several former channels that flow eastwards into Gleann Fionndrigh at NH 651 036. On the western side a similar periglacial trimline occurs, where a thick talus slope terminates at an upslope termination of sediment. Here, material from the talus slope has continued to roll a little way onto the top of the sediment accumulation. This movement of talus is seen along much of the western valley side, where talus material has also accumulated along the distal sides of the ridges further downstream (Fig. 4.51B).

4.4.4 Gleann Lochain

Gleann Lochain is a predominantly southeast trending valley that flows into the western end of Glen Banchor (Fig. 4.50). Based on its morphology, the valley is divided into an upper and lower part. The lower part consists of a trough-shaped southeast trending valley with steep bedrock sides, whilst the upper section consists of a south-facing hanging cirque. A small loch, Loch Dubh occurs within this cirque, behind which a steep backwall separates it from a gently sloping plateau area above.

Mounds and ridges are a dominant feature within Gleann Lochain and occur in both the lower and upper parts. They begin at the mouth of the valley, where two arcuate ridges occur on the southern side of the Allt an Lochain Duibh (NN 649 989). In the lower valley, the mounds and ridges are very large, up to 10 m high, with rounded crestlines and are better preserved along the southern valley side (Fig. 4.52). On the northern side, hummocky accumulations of sediment are present in a number of places, which are covered by extensive downslope movement of sediment and rockfall. A well-defined river terrace occurs throughout the whole of the lower part of the valley. The terrace is generally about 1 to 1.5 m high and sporadically inset with lower terrace fragments.

Towards the head of the lower valley, a large marshy basin has formed, confined by a large arcuate ridge that curves downstream across the valley floor on the southwestern side. Two river terraces occur in this area, the highest of which is 3 to 4 m higher than the current stream and fragmented. The large ridge, which confines this area, bifurcates and breaks up in several places into a series of smaller mounds. The ridge merges with the valley side, so that only a crestline of about 1 m in height is visible, whilst on the other side of the ridge, by the stream, lobes of sediment from the ridge have moved downwards onto the terrace below.

Figure 4.52. Mounds and ridges in the lower part of Gleann Lochain with rounded crestlines. Photograph taken from the southern valley side looking northwestwards.

Higher lateral benches occur upslope of this ridge and can be followed upstream and across Coire nan Laogh (NH 625 005), although the topography becomes very undulating and chaotic in appearance. These benches cannot be traced any further upstream beyond Coire nan Laogh and the hummocky terrain does not occur on the western valley side between Coire nan Laogh and Loch Dubh either.

In the upper section of Gleann Lochain, closely spaced mounds and ridges occur mainly on the southeastern side of Loch Dubh. These features have rounded crestlines, but their lateral extent is more clearly defined than those in the lower part of the valley that merge into the underlying topography. Channels occur around the mounds and ridges by Loch Dubh and only a small river terrace, approximately 1 m high, surrounds the current stream. This river terrace disappears once the slope steepens towards the main part of Gleann Lochain.

A thick talus slope is observed on the eastern valley side of Loch Dubh, directly above the mounds and ridges. The talus culminates at the uppermost ridge, although at the southern end of the talus there is some overlap between the two, where talus material overlies the upper ridge. The downslope limit of this talus slope can be traced upstream towards the plateau above Loch Dubh, where it continues as a solifluction lobe on the slopes below Carn Dearg (945 m; NH 635 024). The edge of the solifluction lobe then connects with a deep channel, which curves around the northern edge of Carn Dearg into Gleann Ballach.

4.4.5 Gleann Madagain

Gleann Madagain is a predominantly east-facing valley that joins the upper part of Glen Banchor by Strath an Eilich (Fig. 4.53). A large fan occurs at the mouth of Gleann Madagain on both sides of the stream, which continues inside the valley as a large terrace that is up to 20 m high. Fragments of a lower 5-10 m high terrace also occur on the northern valley side. The stream is relatively unconfined within this lower part of the valley and is able to meander across a relatively wide valley floor, where another small 1 m high river terrace has developed.

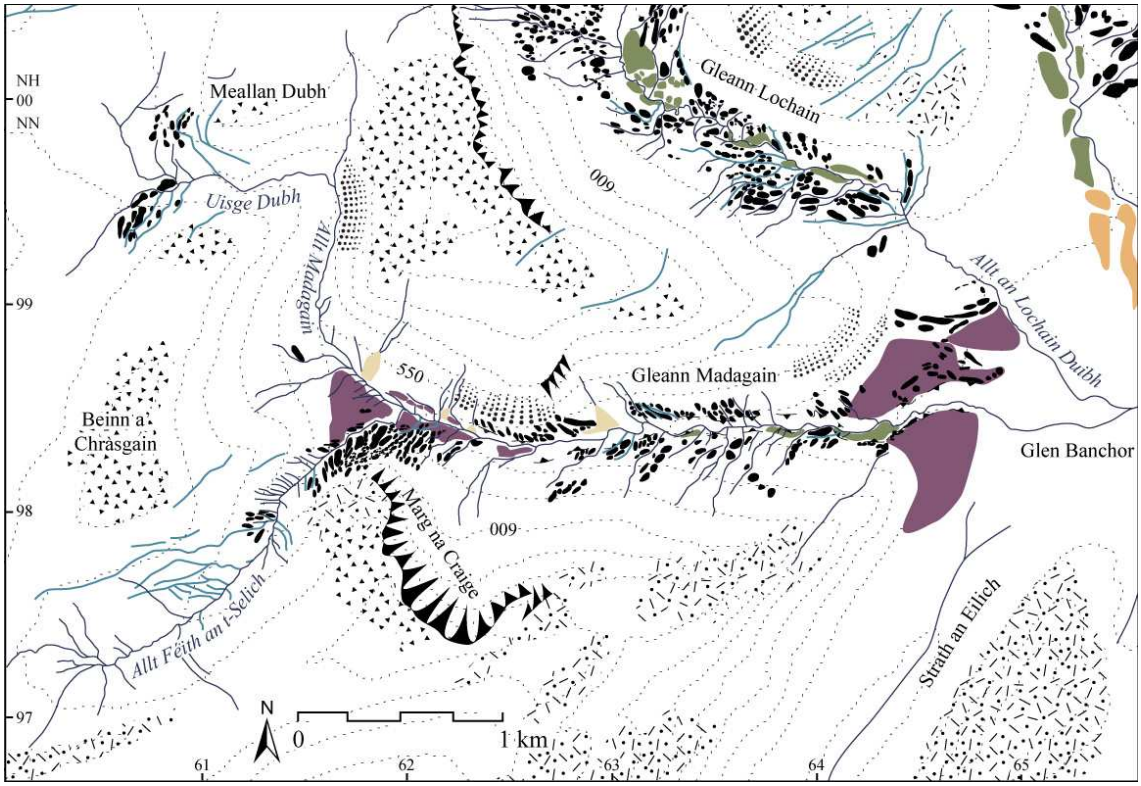

Figure 4.53. The geomorphology of Gleann Madagain (see Fig. 4.2 for key).

Mounds and ridges also occur throughout the lower part of the valley. Most have fairly subdued crestlines and a number of them, particularly on the southern valley side, are very subdued. On the northern side there are clusters of more prominent mounds, with rounded crestlines.

The mounds and ridges change in morphology to the east of the confluence of Allt Féith an t-Selich with Allt Madagain at NN 620 984, where they become closely-spaced, smaller mounds and ridges that are better defined, although their crestlines are still rounded. These mounds form chains that curve up into the Allt Féith an t-Selich valley and continue for a little way upstream. However, after a short distance, downslope trending channels become the more dominant feature and only a few sporadic ridges and channels that trend obliquely across the slope of the valley can be seen.

On the western side of the Allt Féith an t-Selich, at NN 618 984, some mounds occur, but they are not as clearly formed as those on the eastern side, partly due to the presence of a fan which emerges from Allt Féith an t-Selich at the confluence. The fan is also present on the eastern side of the stream, forming a raised flat area between the small, densely-spaced mounds and the valley floor. Smaller fans also emerge from streams flowing down from Marg na Craige, and these fans, alongside the Féith an t-Selich fan, have subsequently been incised to produce several small river terraces in this area.

Upstream of the confluence with Allt Féith an t-Selich there are no river terraces and there is a large amount of sediment of the valley sides which forms an undulating topography. Further upstream, the valley narrows to a v-shape and a large number of boulders occur in this area. On the eastern side the source is a talus slope slightly further up the valley side, whilst there are crags at the top of the western side, although no talus slope in between.

The upper part of Allt Madagain at NN 608 997 forks into two tributary streams; Uisge Dubh, which flows eastwards from the plateau and another that flows southwards to the east of Meallan Dubh (796 m; NH 614 001). A number of small ridges are visible towards the lower part of the stream to the east of Meallan Dubh, where it flows down the main valley side. Accumulations of sediment are also visible on the valley sides within the Uisge Dubh catchment. On the northern side this can be followed obliquely upvalley to a small lateral ridge, which then leads into a channel that curves round the western flank onto the plateau. On the southern valley side, the boundary is not as clear, but can be faintly traced at a similar altitude to that on the northern side towards Beinn a' Chràsgain (828 m; NN 606 981).

4.4.6 Glen Markie

Glen Markie is a southwest trending valley, which is guided by a fault and continues directly into Glen Abhainn Crò Chlach on the other side of the plateau. The valley is fairly broad until Creag an Fhìr-eòin (739 m; NN 590 997), where it narrows to a v-shape, with steep sides of 100 m to over 200 m in height. The valley is v-shaped for 3 km before it widens out onto the plateau. The Markie catchment is described in four separate parts here: first the main valley, followed by three corries, Coire Odhar, Coire nam Beith and Coire an Lochain, that are located above the main valley on the western side (Fig. 4.54).

In the main Glen Markie valley, a large ridge occurs about one third of the way up on the western valley side at NN 578 971. The ridge is orientated perpendicular to the main valley axis, but appears to stem from ridges with very rounded crestlines that trend obliquely down the valley side in an upstream direction and emanate from a series of channels to the south of Beinn

Sgiath (887 m; NN 567 981). Erosion by Markie Burn has exposed a large section, where much of the lower part is vegetated, but the upper half is visible. The lower vegetation-free part is slightly slumped, but a clast-rich diamicton is visible, which is equivalent to LFA 9 found in other sections within the study area. The upper half of the section is more visible and shows a laminated sand unit, which is slightly deformed and is assigned to LFA 10.

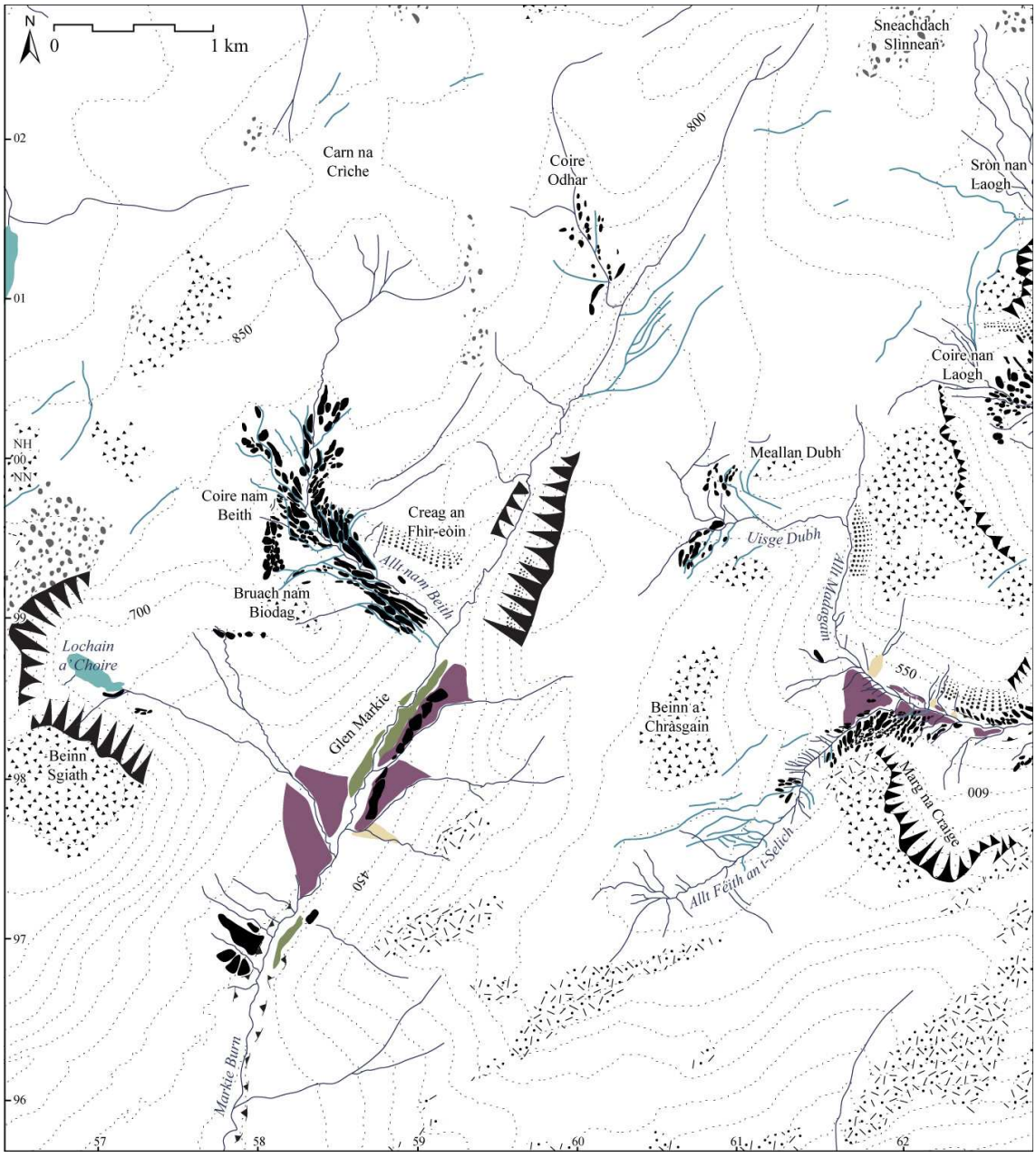

Figure 4.54. The geomorphology of Glen Markie (see Fig. 4.2 for key).

A staircase of at least two river terraces is found along the whole of the main part of the valley. Two large and almost coalescent fans emanate from two streams on the eastern valleys sides to form an additional, higher terrace level on that side. Large ridges, up to 10 m in height, with very rounded to subdued crestlines, also occur on the eastern valley floor and merge into the higher terrace.

Glen Markie narrows to a deep, steep-sided, v-shaped valley upstream of the confluence with Allt nam Beith. Rocky outcrops occur at the top of the eastern valley side and also at various points on the side itself, with areas of thick talus in between. Further upstream the valley narrows further and shallows. Several obliquely trending streams can be seen in this area on both sides of the valley, with one in particular on the western side that flows around the outside of a ridge that is orientated nearly parallel to the central stream. Upstream of the confluence with Allt Odhar a number of channels occur on the eastern side and flow parallel to the central stream, curving upwards onto the plateau. A particularly deep channel is observed curving around the hillside to the south of Sneachdach Slinnean (919 m; NH 621 028) joining with other channels trending eastwards towards Sròn nan Laogh (NH 628 016) and Loch Dubh.

Coire Odhar (within square NH 5902) is a southeast facing catchment that flows into the upper part of Glen Markie. Mapping of this area was done remotely using Google Earth imagery and NEXTMap. Closely spaced mounds and ridges occur within this valley, alongside a number of channels that are located between the mounds and ridges and trend obliquely downslope. No river terraces are observed in the corrie.

Coire nam Beith is located to the southeast of Coire Odhar and forms a small hanging valley above Glen Markie. Long, narrow (25 to 35 m wide), sharp-crested ridges are abundant within this valley and constrain the Allt nam Beith to a narrow channel. On the steep slopes above the confluence of Allt nam Beith with Markie Burn, the ridges are orientated almost directly downvalley. These ridges are well developed on the southwestern valley side only, with only a few very subdued mounds and ridges on the northeastern side. The inner two ridges on the southwestern side (those closest to Allt nam Beith) have very sharp crestlines, whilst the crestlines on the outer ridges are more subdued.

Further upstream, towards the head of the corrie, the ridges trend more obliquely downslope and occur on both sides, forming a closely spaced chevron pattern, with channels in between them. A very distinct ridge of sediment has been deposited along the southern half of the backwall and this ridge continues onto Bruach nam Biodag (NN 581 991), where it forms a flat area at the same altitude (Fig. 4.55). The distal side of the flat area is heavily strewn with large boulders and ends on the southern side of Bruach nam Biodag. Downslope of this area in the neighbouring corrie, a small, dissected, arcuate ridge occurs which is connected to the higher ground to the south and north of Bruach nam Biodag by former channels. Within Coire nam Beith, the ridge of sediment does not continue further downstream beyond Bruach nam Biodag, but several channels emerge from this point.

Figure 4.55. Ridges (crestlines indicated by a white dashed line) and channels (white arrowed line) within Coire nam Beith, including a large ridge located across the backwall of the corrie and connected to Bruach nam Biodag on the left. Photograph taken on the northeastern valley side towards the west.

At the northern end of the backwall, the large ridge leads up onto the plateau, where it tapers out. Other ridges, which have been deposited inside this large one, continue upwards onto the plateau. The ridges on the plateau are small and subdued, and occur on either side of the stream draining the southern area of Carn na Crìche (862 m; NH 585 020), with channels in between them.

To the south of Coire nam Beith, Lochain a' Choire (NN 570 986) occurs which is situated within a well-developed southeast facing corrie, located on the western valley side above Glen Markie. Several small ridges occur on the southern valley side and river terraces do not develop until much further downstream, towards the confluence with Markie Burn.

4.4.7 Glen Talagain

Glen Talagain is a predominantly south-facing valley that is connected to the central southern part of the plateau by a gently sloping backwall (Fig. 4.56). It merges with Blackcorrie to the west and Coire nan Dearcag to the east. Ridges of 5 to 10 m in height occur mainly in the lower portion of the valley. These ridges are closely spaced, with rounded crestlines. They are orientated slightly arcuately downvalley, but their general orientation is more across the valley than obliquely downslope. Ridges and mounds also occur on the downstream side of a small bedrock hill (518 m; NN 535 967) and these are clearly orientated across the valley side.

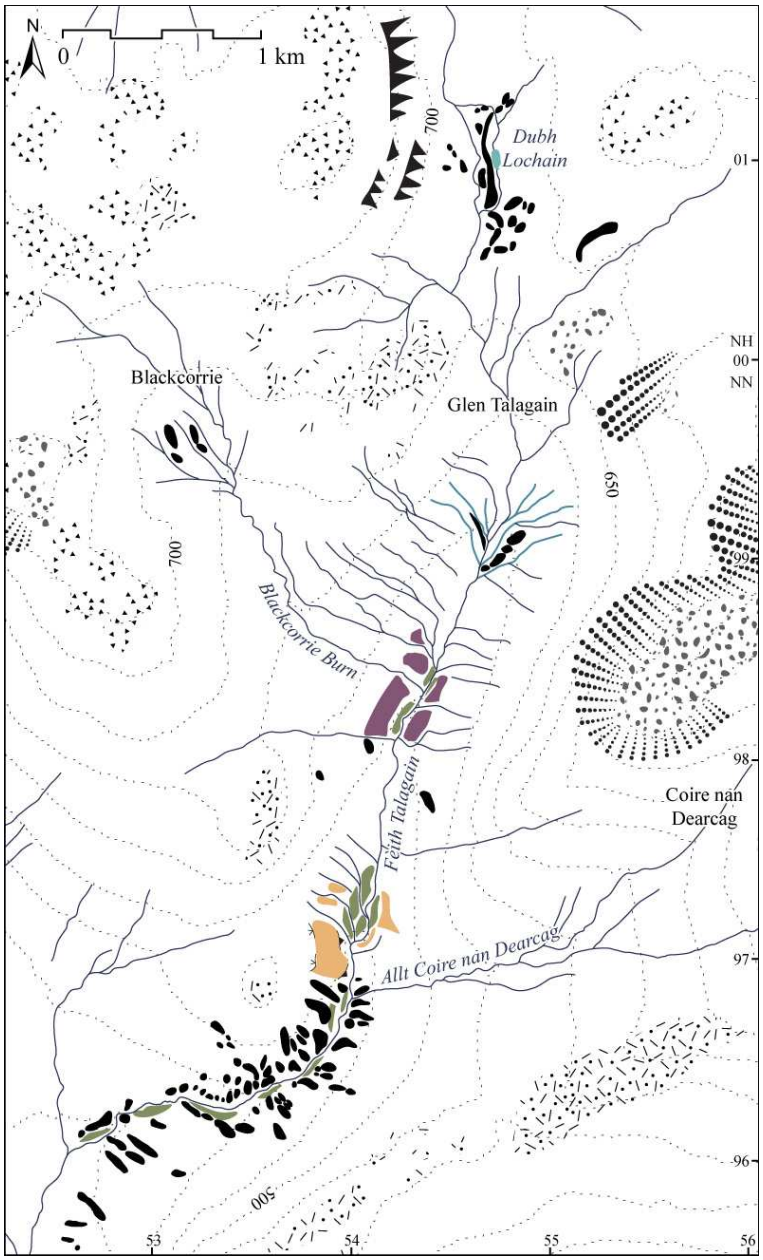

Figure 4.56. The geomorphology of Glen Talagain (see Fig. 4.2 for key).

In this part of the valley, the stream is constrained to a narrow channel and the valley is almost v-shaped, although fragments of a roughly 2 m high terrace occur in places. The valley widens out significantly upstream of the confluence with Allt Coire nan Dearcag and a river terrace and a higher level terrace occur in this area. Ridges and mounds also occur in this area, although they are very subdued and merge into the valley floor and sides. A 10 m high fan is located at the mouth of Blackcorrie Burn, where it joins Fèith Talagain (NN 543 984). The fan merges with other terraces in the valley on the downstream side, but ends more abruptly upstream.

Upstream of the fan, no river terraces occur and there is very little incision by the stream. The topography in this area is mounded, with a high quantity of boulders scattered on the valley floor. Some of these boulders are very large (over 2 m in height) and have been frost-shattered.

There is no clear boundary to the sheet of boulders, but they do not occur in such large quantities once the Blackcorrie Burn fan is reached. Whilst the topography is mounded, no clear mounds or ridges can be deciphered within it. From the NEXTMap hillshaded DSM, the topography has a 'ribbed' appearance, but this pattern was not visible in the field. On the aerial photographs, the ribbed appearance seems to result from dissection of the terrain by downslope trending channels.

On the plateau, above Glen Talagain, a series of ridges occur around Dubh Lochain (NH 546 010). Those closest to the plateau edge are mainly orientated east-west, but further onto the plateau a long ridge trends north-south. The ridges are covered in large sub-angular to angular boulders and have heights of approximately 6 m.

4.4.8 Coire Iain Oig and Glen Gilbre

Coire Iain Oig is found at the head of a south-facing valley (Fig. 4.57). It has a steep backwall directly to the north of it, but to the west, the gradient is lower and the cirque connects directly onto the plateau. The lower part of the valley below the corrie is wide and has a fairly shallow gradient. A continuous 1-2 m high river terrace occurs in this area. Where the eastern valley side becomes steeper, a few subdued ridges occur across the valley side. Opposite, the western side is dominated by deep channels, which are orientated directly downslope, although there are also fainter channels that run more obliquely across the slope.

Towards the lower part of the corrie, the river terrace merges with a 3 to 4 m high fan, which emerges from Allt a' Choire Ghuirm as it joins Allt Coire Iain Oig (NN 516 982). Just downstream of the Allt a' Choire Ghuirm, a very large, broad ridge, at least 10 m high and over 100 m across occurs on the eastern valley side. The Allt a' Choire Chuirm fan is located across the front of this large ridge but ends a short distance upstream. The terrace on the western side of the stream is also part of this fan.

Other large, broad ridges occur upstream of the Allt a' Choire Ghuirm, which have mounded surfaces and are all separated by large channels. The most downstream ridges are orientated obliquely downstream, but a clear spatial pattern is lost in the upper part of the corrie. In particular, two ridges are orientated in opposite directions on the lower part of the backwall, one obliquely downstream and one obliquely upstream. A few ridges also occur on the western valley side, but the transition between depositional ridges and apparent ridges that are formed by incision of the channels on either side is gradual and therefore the downslope limit of ridges is difficult to distinguish.

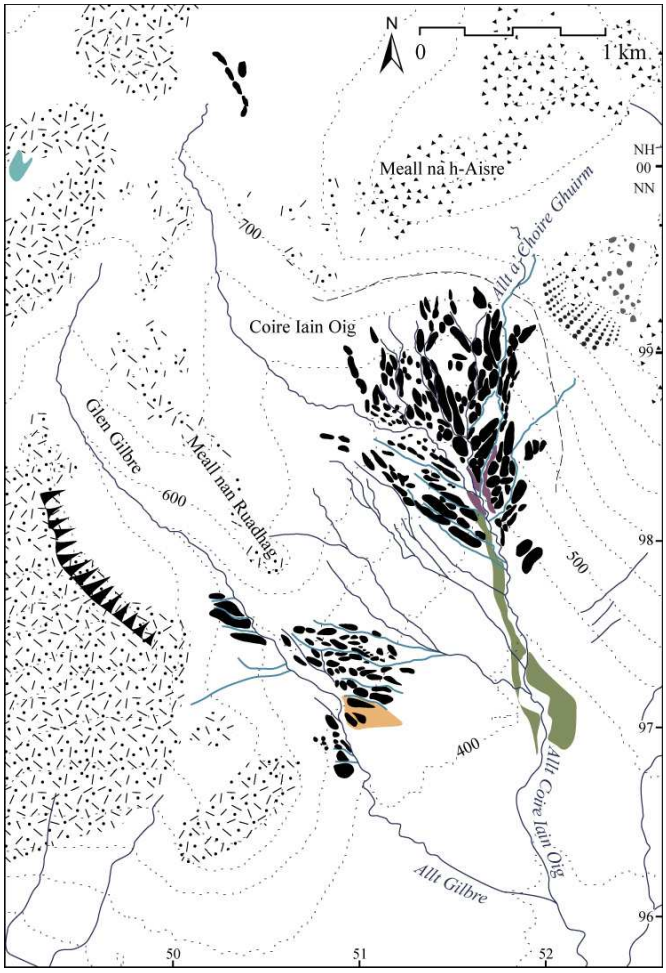

Figure 4.57. The geomorphology of Coire Iain Oig and Glen Gilbre (see Fig. 4.2 for key).

To the west of the main part of the corrie, the ridges end suddenly and beyond this point only a few small obliquely orientated channels on the valley floor and sides. A long sinuous ridge occurs on the plateau above Coire Iain Oig. The ridge is of a similar morphology to those on the plateau above Glen Talagain (Section 4.4.7).

Glen Gilbe is located to the west of Coire Iain Oig and trends southeast, later merging with the Iain Oig catchment to the south of Meall nan Ruadhag (NN 520 961) (Fig. 4.57). The lower part of the valley is dominated by a series of mounds and ridges, which run across both the western and eastern valley sides in a west-east orientation (Fig. 4.58). These ridges are up to 10 m high with rounded crestlines and have channels flowing between them. The ridges are located on a 10 m high terrace and a second, smaller river terrace is present on either side of Allt Gilbe in the same area. Immediately upstream of these ridges, the valley becomes v-shaped where the stream has cut a narrow gorge into bedrock. The valley opens out again towards the top into a small cirque. The valley floor and sides are smooth and there are no river terraces, although a few stream channels are present, which flow obliquely downslope. The cirque has a gently sloping backwall, which leads up onto an area of exposed bedrock on the plateau.

Figure 4.58. Mounds and ridges in the lower part of Glen Gilbe near the confluence with Coire Iain Oig. Photograph taken from the western side of the Gilbe catchment looking towards the southeast.

4.4.9 Glen Mhoraire and Glen Luaidhe

Glen Mhoraire originates in the central southern part of the Monadhliath plateau, immediately to the west of Glen Gilbe. The valley is orientated towards the southwest and therefore joins the Spey Valley much further upstream than Glen Gilbe (Fig. 4.59).

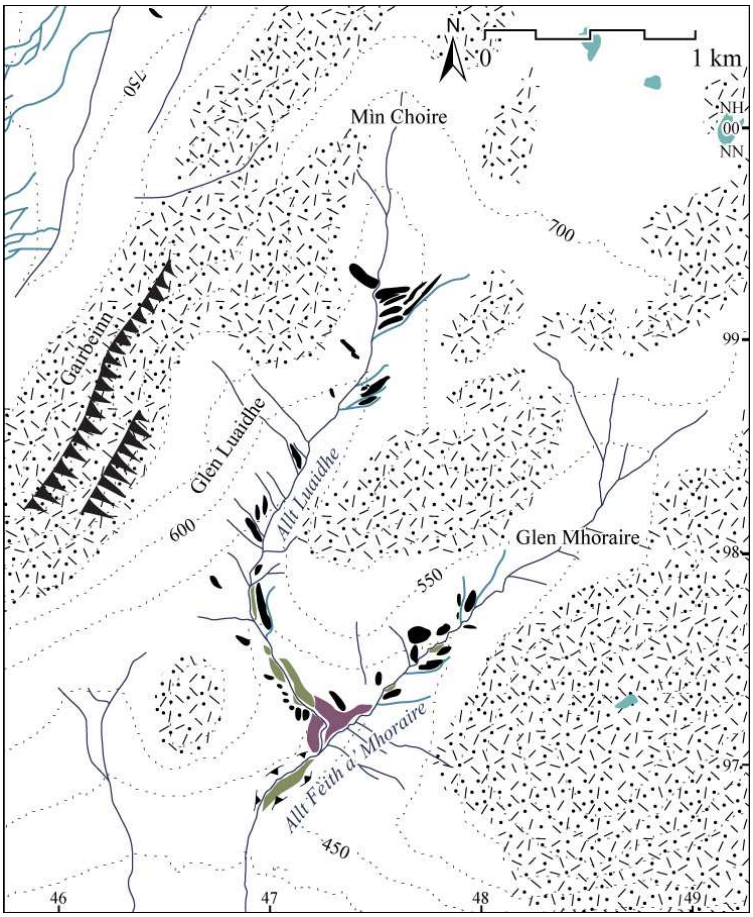

Figure 4.59. The geomorphology of Glen Mhoraire and Glen Luaidhe (see Fig. 4.2 for key).

The Allt Fèith a' Mhoraire flows within a fairly well incised channel in the lower parts of the valley and some small terrace remnants occur inset within the steep sides that bound the channel. Slightly further upstream, more terrace fragments develop as the stream widens out. Ridges that are over 50 m across with rounded crestlines occur in this area of the valley. The ridges are not densely spaced, appearing sporadically within the valley, where they are fairly subdued and often merge into the valley sides or floor. No mounds or ridges are present in the upper half of the valley and the valley sides are smooth. In this area the stream narrows to a singular downward incision with only one terrace, but the change from several terraces is gradual.

Glen Luaidhe is a south-facing valley, located immediately to the east of Gairbeinn (896 m; NN 460 985), which coalesces with Glen Mhoraire to the south (Fig. 4.59). There are a number of ridges in the lower part of Glen Luaidhe. Some of the ridges are relatively large, particularly near the confluence with Allt Fèith a' Mhoraire, where one has a height of 10 to 15 m. They possess either rounded crestlines or are fairly subdued. A river terrace is present in this lower part of the valley and a fan occurs at the confluence with Allt Fèith a' Mhoraire.

Slightly further upstream, as the valley turns towards the north-northeast, the stream width narrows and the stream flows through a bedrock gorge about 1.5 to 2 m deep. Upstream of this section, the stream widens again and is similar to the lower part of the valley, with the valley floor forming a terrace 1 to 2 m above the stream. A set of subdued ridges occurs about two thirds of the way up the valley, but aside from these the valley sides are very smooth. The stream narrows upstream of this point, where there is little incision and no river terraces are present.

4.4.10 Coire nan Laogh and Corrie Yairack

Coire nan Laogh sits at the head of a predominantly south-facing valley to the east of Corrie Yariack (Fig. 4.60). In the lower part of the valley, the Allt a' Mhill Ghairbh flows over steep terrain in which it has incised a little, but no river terraces have developed. Further upstream, as the slope gradient lowers, closely-spaced ridges with rounded crestlines occur that continue upstream as the valley turns towards the east. Aside from a pair of ridges, no other ridges are found in this upper part of the valley. Some channels that flow obliquely down the hillside are observed, however. Several ridges can be found at NN 460 998 on the other side of the 755 m col above Coire nan Laogh, which trend obliquely downslope towards the north.

Corrie Yairack resides at the head of a large south-southeast facing valley that originates at the southwest corner of the main plateau. The corrie is bounded to the northwest by a steep

backwall and possesses steep valley sides in the upper part to the east and west, all with weathered bedrock outcrops (Fig. 4.60). However, in between these steep areas, the northeast and west sides of the corrie are lower in altitude, with lower gradients, no exposed bedrock and connect to flatter plateau areas above.

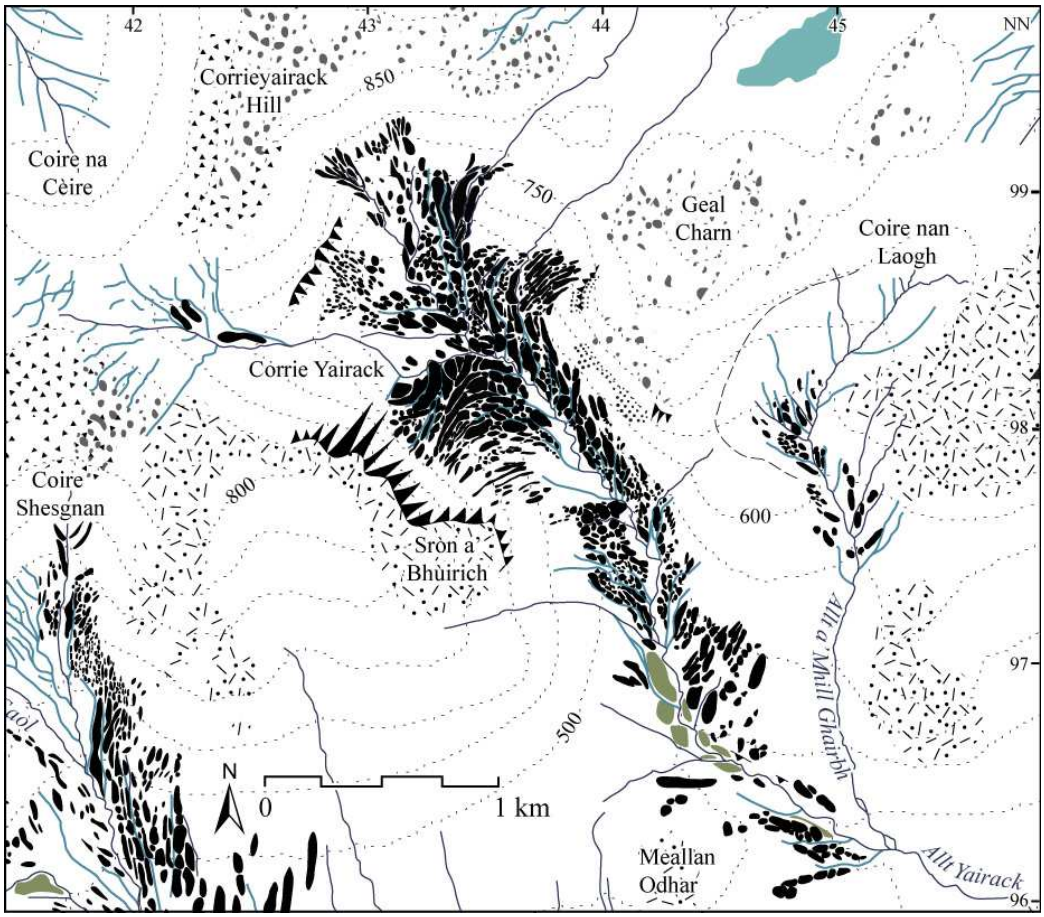

Figure 4.60. The geomorphology of Coire nan Laogh and Corrie Yairack (see Fig. 4.2 for key).

In the lower part of the valley, just over 1 km from the confluence of Allt Yairack with the River Spey, several large ridges occur, of which one is over 20 m high and 80 m across (Fig. 4.61A). These ridges have very rounded crestlines and are significantly larger than any other ridges in the valley. An extensive river terrace is present in this area and has formed around these ridges. This river terrace continues upstream where more ridges and mounds are located. These features are subdued, with rounded crestlines, and a clear spatial pattern is often difficult to decipher, particularly on the western side of the stream, where the features tend to merge into the terrace.

About 1.5 km further upstream, the ridges and mounds change in morphology to densely spaced, sharp-crested ridges that trend obliquely across the valley sides and floor in a downslope direction, with well-defined channels located between them (Fig. 4.61B). This type of ridge occurs throughout the rest of the valley, upstream of this point. The change in

morphology does not, however, occur on both valley sides at the same time. The ridges on the eastern valley side change morphology first from very subdued ridges to narrow, well-preserved, sharp-crested ones. Mounds and ridges on the west side remain subdued for a further 350 m upstream before more sharp-crested ridges occur. These ridges still lack a clear spatial pattern, however, compared to those on the eastern side, which trend obliquely upslope. The river terrace morphology also changes in this area, at the point where the sharp-crested ridges occur on the eastern valley side and the large extensive terrace does not continue any further upstream.

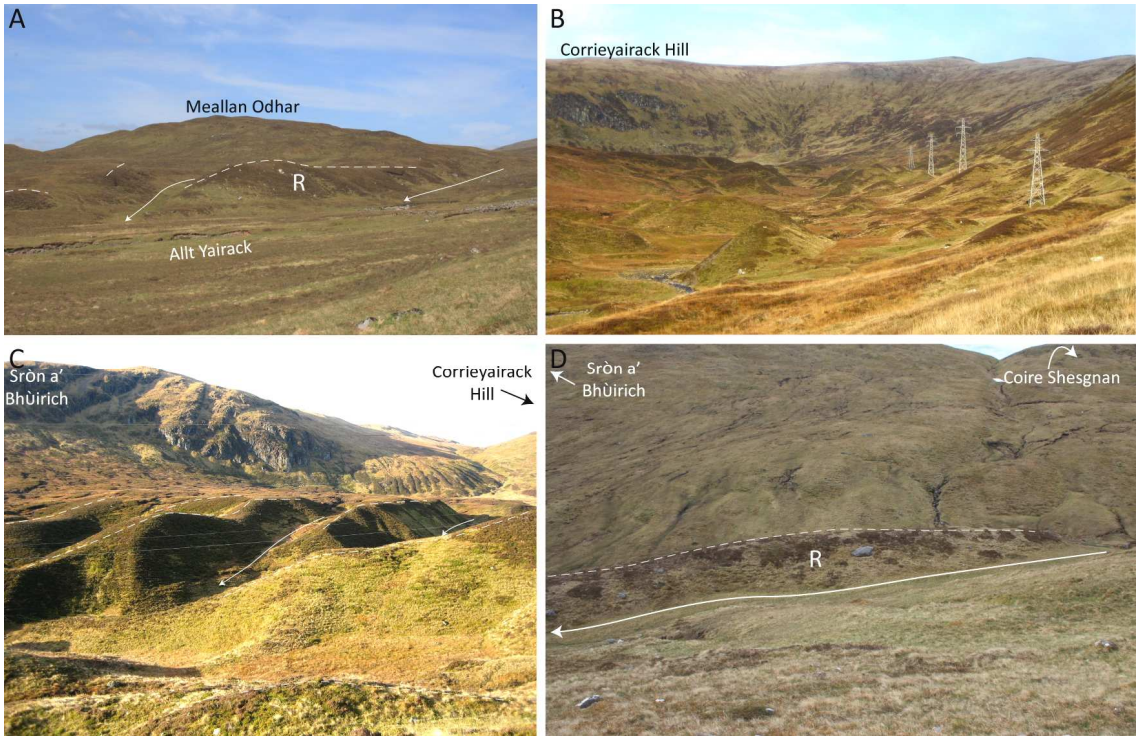

Figure 4.61. A) A 20 m high ridge (R) in the lower part of Corrie Yairack. Its crestline and those of smaller neighbouring ridges are indicated by a white dashed line, whilst a white arrowed lines denote channels between these ridges. Photograph taken from the northern valley side looking westwards. B) Smaller 10 to 15 m high mounds and ridges in the upper part of Corrie Yairack, pilons for scale. Photograph taken looking northwards upstream. C) Sharp crested ridges (crestlines are highlighted by white dashed lines) and channels (white arrowed lines) on the western side of Corrie Yairack that merge into a raised relatively flat area. Photograph taken on the eastern valley side towards the northwest. D) Ridge (R; crestline indicated by a white dashed line) and channel (white arrowed line) on the plateau above Corrie Yairack. Photograph taken on the northern valley side looking southwards.

Upstream of this area, ridges continue on the eastern side only for 350 m before ridges re-occur on the western side. The combination of ridges on both sides produces a chevron-shaped pattern. The ridges on the western side are 10 to 15 m in height and sharp-crested, but stem from a high flat area that slopes gently down towards the stream and is faintly dissected by small channels (Fig. 4.61C). In the area at the head of the corrie, further topographic highs occur that have been heavily dissected by streams and within which mounds and ridges can be identified.

On the plateau to the west above Corrie Yairack, three ridges occur, with channels between them (Fig. 4.61D). Immediately above these ridges, a number of southwest-northeast trending deep channels are clearly visible on the plateau. Other channels are observed on the eastern plateau edge above Corrie Yairack.

4.4.11 Interpretation of the geomorphological and sedimentary evidence in the southern Monadhliath Mountains

The south-facing valleys of the Monadhliath Mountains contain the most wide-ranging geomorphological evidence in the region (Appendix II). Mounds and ridges are found in the majority of valleys, but their morphology, spacing, quantity and orientation varies greatly within the valleys. Following arguments made in Section 4.1.6, the majority of the mounds and ridges are interpreted as moraines (e.g. Benn, 1992; Bennett & Boulton, 1993a, b; Lukas, 2005b; Finlayson *et al.*, 2011). Channels that trend obliquely downslope are interpreted as ice-marginal channels (Greenwood *et al.*, 2007), whilst other channels that trend directly downslope are interpreted as gullies. Evidence that the ice in the southern valleys was sourced by ice on the plateau to the north is found in the occurrence of moraines on the plateau above Glen Talagain, Coire Iain Oig and Corrie Yairack, a moraine on the backwall of Coire nam Bieth that leads onto the plateau, and meltwater channels and a distinct downslope limit of a talus slope and solifluction lobe at the head of Gleann Ballach and Gleann Lochain.

Most variation between moraines occurs in this part of the study area, where variations in morphology, spacing and quantity occur. Sharp-crested and/or closely-spaced moraine mounds and ridges are found within the upper parts of the Chaorainn, Fionndrigh, Ballach, Lochain, Madagain, Markie, Iain Oig, Luaidhe, Laogh and Yairack catchments, whilst broader, often subdued moraines that are spaced further apart are found in the lower parts of these valleys and within Glen Mhoraire.

The other variation in the mounds and ridges is in terms of orientation. Mounds and ridges found in the lower part of Glen Gilbre are orientated west-east, across the slope of the valley, rather than obliquely down valley. The features are interpreted here to have formed as lateral moraines by a glacier in the Spey Valley due to their orientation obliquely across the northern side of the Spey Valley in a downvalley direction. This interpretation also explains the formation of a number of the mounds and ridges that occur across the lower part of Glen Talagain immediately to the east of Glen Gilbre, particularly those ridges that are located on the southwestern side of the small bedrock knoll. However, ridges and mounds further upstream are orientated more obliquely down Glen Talagain and are therefore interpreted as moraines that were formed by a locally sourced glacier in Glen Talagain. This combination of moraines of

different orientations suggests that a complex interplay between the Strathspey Glacier and the Talagain Glacier occurred. Similarly, ridges in the lower part of Gleann Beinne are interpreted as lateral moraines deposited by the Strathspey Glacier. Channels that occur in between these moraines are interpreted as ice-marginal channels, since their profiles lower in altitude in a downstream direction following the gradient of the Spey Valley (Greenwood *et al*., 2007).

Other ridges that occur in the southern Monadhliath Mountains that are not orientated obliquely across the valley sides in a downstream direction are found in Gleann Ballach, Gleann Chaorainn and Gleann Markie. The ridge in Gleann Ballach is orientated across the valley floor, perpendicular to the stream and at least the lower segment is composed of horizontally bedded sands that show some folding and faulting. The sediments within this ridge are very similar to those within a ridge in the lower part of Glen Markie. Both these ridges are located on the western valley sides, like the ridges in Gleann Chaorainn and all three sets of features emanate from channels that are cut across their respective western interfluves. These channels also occur across the interfluves to the west of Gleann Fionndrigh and Gleann Beinne and all become lower in altitude from west to east.

Evidence for the northern margin of the Strathspey Glacier flowing across the lower slopes of the southern Monadhliath Mountains at Glen Gilbre, Glen Talagain and Gleann Beinne, indicates drainage in the Monadhliath valleys was probably blocked by this ice, creating a series of lakes, similar to those identified on the southern side of the Spey Valley in the Cairngorms (Brazier *et al*., 1998; Everest & Golledge, 2004; Everest & Kubik, 2006) (Section 2.3). The channels that cut across the interfluves to the north of Glen Banchor are therefore interpreted as lake overflow channels that were formed as water flowed from one ice-dammed lake to the other across the interfluves in a west to east direction, similar to previous interpretations by Barrow *et al*. (1913) and Charlesworth (1955). This would have resulted in a maximum lake level of 730 m in Gleann Lochain, 555 m in Gleann Ballach, 526 m in Gleann Fionndrigh and 471 m in Gleann Chaorainn. An idealised diagram of the relationship between the lakes and interfluve channels is shown in Figure 4.62, which also indicates an approximate margin for the Strathspey Glacier at the time when these lakes would have been in existence, although it is unknown whether the maximum level of each lake was reached contemporaneously.

In line with this interpretation, the broad ridges within Gleann Ballach and Glen Markie are interpreted as remnants of subaqueous fans that emanated from these overflow streams as they entered each respective lake, as suggested by Barrow *et al.* (1913). This interpretation is supported by the laminated sand composition of the ridges, which is typical of deposition on a low gradient fan surface, where sediment loading is likely to have caused the varying amounts

of deformation (McCarroll & Rijsdijk, 2003). The flat-topped morphology of the upper two segments of the ridge in Gleann Ballach suggests that these features are former deltas. This is supported by the correspondence between the surface of the higher ridge segment (550-557 m) and the 555 m Ballach-Fionndrigh col. The lower remnant may represent a subsequent lower lake level.

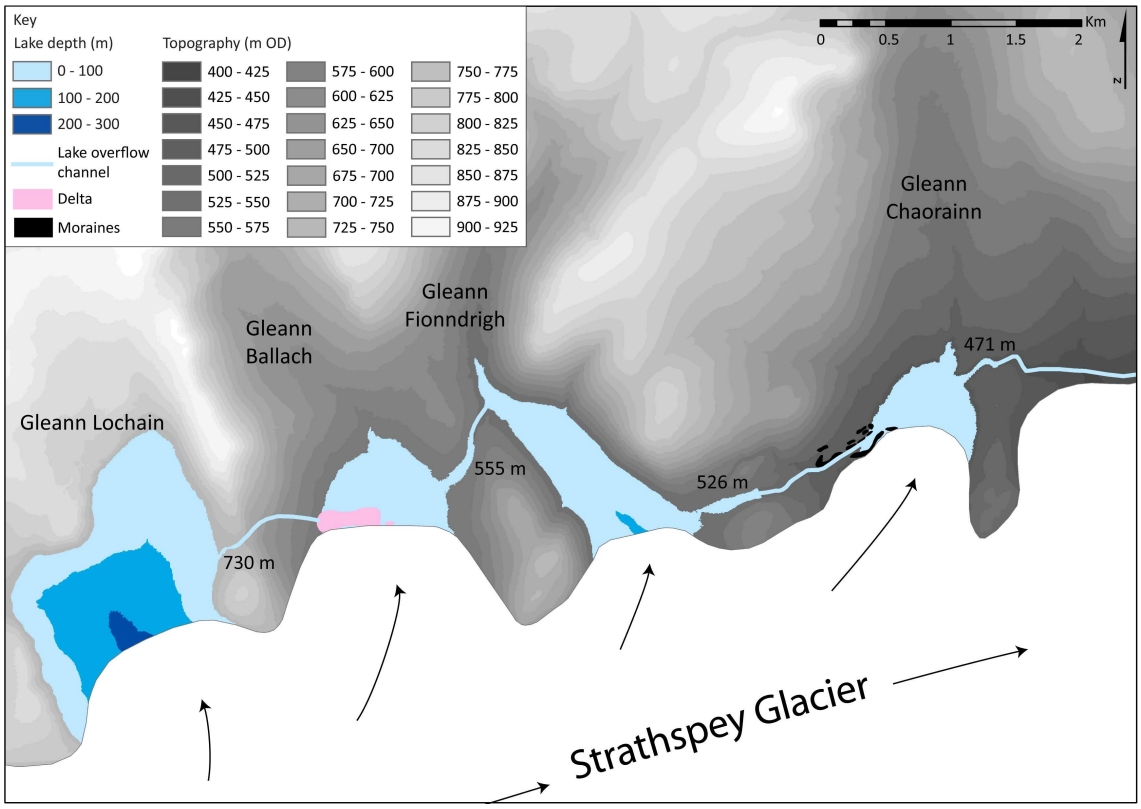

Figure 4.62. Idealised model to show the damming of local drainage by regional ice in the Spey Valley, which created a lake in each of the Glen Banchor tributary valleys. Lake levels at their maximum depth were controlled by the height of overflow channels which drained from west to east into the neighbouring valley. Arrows denote approximate ice flow directions. Note: ice margins of the Strathspey Glacier are approximate and it is assumed that the parabolic surface of the glacier would prohibit lake drainage over the glacier surface (*cf.* Stokes & Clark, 2004).

The origin of the ridges in Gleann Chaorainn is more ambiguous since they are sharp-crested and trend obliquely down the valley side in an upstream direction. Without further sedimentological work, it is unclear whether they also represent remnants of a more extensive fan surface (Barrow *et al.*, 1913), or whether they are latero-frontal moraines that document advance of part of the Spey Glacier into Gleann Chaorainn, although the latter is favoured here due to their morphology and orientation.

Other geomorphological features in the southern valleys of the Monadhliath include the fans found at the mouths of Gleann Lochain and Gleann Madagain and those emanating from tributary streams within Gleann Madagain and Coire Ian Oig. The fans that emanate from the tributary streams are interpreted as alluvial fans based on their dissemination laterally on either

side of a stream. The fans at the valley mouths in Glen Banchor are interpreted a ice-contact fans since they are an order of magnitude larger than any of the alluvial fans found in the study area and emanate from prominent moraines. The scarp and accumulation of sediment found on the eastern valley side of Gleann Fionndrigh at NH 667 033 is interpreted as a cataclasmic RSF following criteria by Jarman (2006). This feature has previously been recognised as an RSF by Holmes (1984) and D. Jarman (pers. comm., 2009) who also identified an arrested RSF immediately to the south of the main cataclasmic RSF.

4.5 Summary of the Geomorphological and Sedimentary Evidence within the Monadhliath Mountains

Moraines

The majority of mounds and ridges found within the study area are interpreted as moraines since a clear spatial pattern is observed in which adjacent mounds and ridges can be joined to form chains that trend obliquely downvalley, often curving arcuately towards the valley centre line (Appendix II). This spatial pattern has been observed in many other upland areas of Scotland in which the landforms have been interpreted as moraines (e.g. Benn, 1992; Benn *et al*., 1992; Bennett & Boulton, 1993a, b; Wilson & Evans, 2000; Lukas, 2005a, b; Benn & Ballantyne, 2005; Lukas & Benn, 2006; Finlayson, 2006; Ballantyne, 2007a, b; Finlayson *et al.*, 2011).

These moraines are found predominantly within the valleys surrounding the plateau, but a small proportion are also found on the plateau surface, where they either form chevron shaped recessional patterns within small, proto-valleys on the plateau, or form long ridges often either on the watersheds between catchments or around the sides of small summits on the plateau. The fact that moraines and meltwater channels in many of the valleys continue onto the plateau, alongside the occurrence of moraines on the plateau (e.g. Fig. 4.63A), provides clear evidence for the existence of a plateau icefield that provided a significant source area for glaciers within the outlet valleys. This is supported by the morphology of many of the valleys, which have no backwall separating them from the plateau, and therefore evidence for glaciation within these valleys necessitates that the plateau was the source area for these ice masses (e.g. Fig. 4.63B). In addition, support for the existence of a plateau icefield is also found in the south-facing Glen Banchor tributaries in the southeast corner of the study area, where sharp downslope limits of talus and solifluction lobes indicate the position of the former ice surface (see Section 5.2 for more discussion on this) and indicate, in conjunction with meltwater channels at the plateau margin, that glaciers in these valleys were fed by plateau ice, despite having steep backwalls (e.g. Fig. 4.63C).

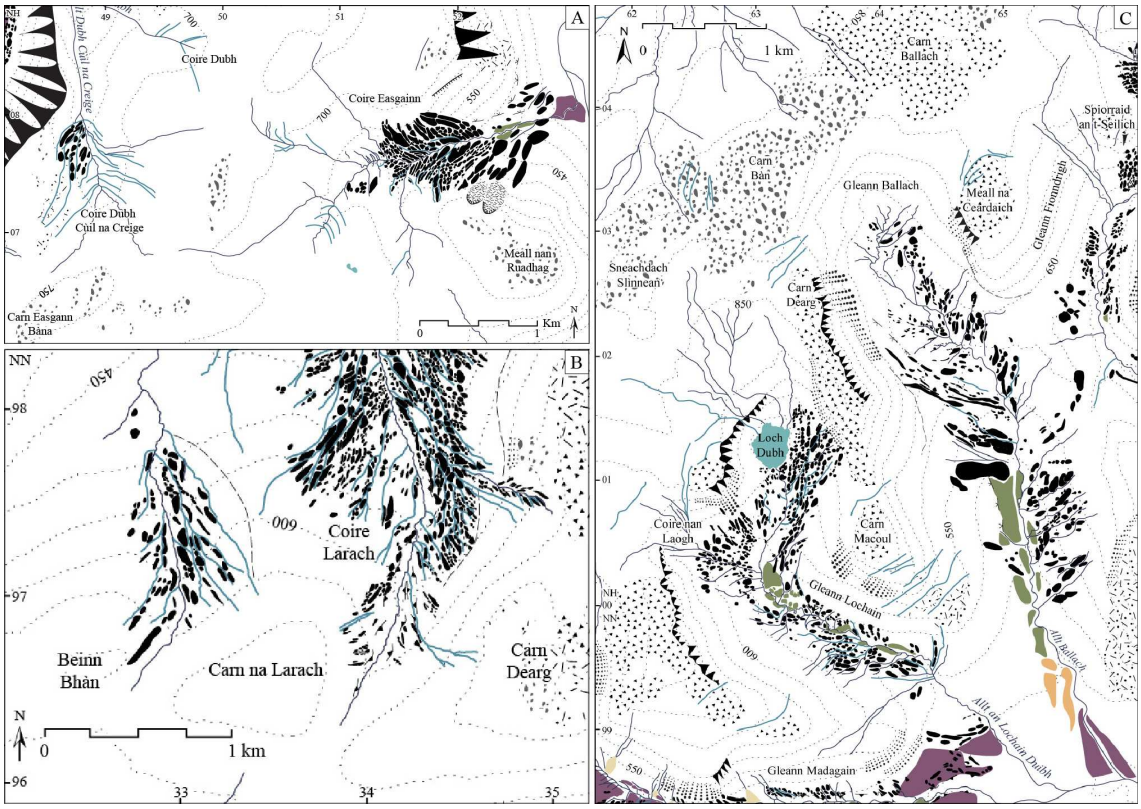

Figure 4.63. Example locations in the study area where there is clear geomorphological evidence for the existence of a plateau icefield (see Fig. 4.2 for key). A) Coire Dubh Cùil na Creige and Coire Easgainn in the northern Monadhliath Mountains, where moraines and meltwater channels continue from the valley onto the plateau, with no backwall separating these valleys from the plateau. B) Coire Innis Shim and Coire Larach in the western part of the study area, which have no backwalls, making it impossible to reconstruct ice within the valley without connecting it to the plateau. C) Gleann Lochain and Gleann Ballach in the southeastern part of the study area, where sharp lower limits of solifluction lobes and talus slopes that lead into meltwater channels at the plateau margin, particularly around Meall na Ceardaich, indicate that the former ice surface continued onto the plateau to the north. Whether the higher ground of Carn Bàn and Carn Ballach to the north was covered by plateau ice is unclear at this stage, however, and is discussed further in Section 5.2.

The morphology of the moraines changes significantly within many of the valleys, particularly those on the southern side of the plateau, where moraines in the lower parts of the valleys are generally larger in terms of base area, possess rounded crestlines and are sometimes up to 20 m in height, although are also often subdued, whilst those in the upper parts of the valleys are smaller (5 to 10 m high), more closely spaced and have sharper crestlines. This will be discussed further in Sections 5.1 and 5.2.

A number of mechanisms have been evoked to describe the processes involved in the deposition of small, closely spaced moraines in Scotland, which are often known as Scottish 'hummocky moraine'. These moraines have previously been interpreted as 1) the product of ice stagnation (e.g. Sissons, 1979d; Sissons & Sutherland, 1976), 2) the product of englacial thrusting (e.g. Bennett *et al*., 1998) and 3) a series of ice-contact fans (e.g. Lukas, 2005b; Benn & Lukas, 2006). These three processes have important implications for the use of chains of moraines in Scotland as

representative of former ice-marginal positions. Their history in terms of research on Scottish moraines is therefore briefly described below.

The mechanism of ice stagnation gained popularity in the 1970s and 1980s in order to explain the 'chaotic' nature of many of the Younger Dryas moraines found in Scotland (e.g Sissons, 1974a, b, c, 1979d; Sissons & Sutherland, 1976; Young, 1977, 1978). However, several authors have since demonstrated that there is a spatial pattern to most areas of hummocky moraines (e.g. Benn, 1992; Benn *et al*., 1992; Bennett & Boulton 1993a, b; Lukas & Benn, 2006), although accepting that localised stagnation may still have occurred in some areas (Benn *et al*., 1992). This work suggested ice retreat of an active margin, where moraines represented former ice-marginal positions. More recently, however, a group of researchers have argued that Scottish 'hummocky moraine' was formed by the meltout of englacial debris septa, in which basal material had been translocated upwards through thrusting, a process which is seen in many, often surging polythermal glaciers in Svalbard (e.g. Bennett, 1996; Hambrey *et al*., 1997; Bennett *et al*., 1998). An important corollary of this research was that the moraines did not represent former positions of the ice-margin. Lukas (2005a, b, 2007a) argued against this mechanism for 'hummocky moraine' formation in Scotland based on detailed examination of the sediments within moraines in the Northwest Highlands of Scotland. This sedimentary analysis suggested that the moraines were composed of interbedded diamictons and sorted sediments representative of deposition in terrestrial ice-contact fans, similar to those examined by Benn (1992) on the Isle of Skye. This research therefore found no support for the 'englacial thrusting' model and favoured moraine deposition at the margins of an actively retreating glacier (Lukas & Benn, 2006; Benn & Lukas, 2006).

The sedimentology of two moraines was examined in this present research. The Stronelairg moraine is interpreted to have formed as a terrestrial ice-contact fan, similar to those examined by Lukas (2005a, b) in the Northwest Highlands (Section 4.2.6). Clast shape and roundness data indicate, however, that there is less of a subglacial component within the sediments in the Stronelairg moraine than was found in moraines in the Northwest Highlands. Furthermore in the second moraine examined in Corrie Easgainn, clast shape and roundness data indicated that this moraine is composed predominantly of supraglacial material that is likely to have been 'dumped' at the ice-margin (e.g Boulton & Eyles, 1979*;* Small, 1983; Owen, 1994; Evans & Benn, 2010). Therefore the two moraines examined here also do not support a process of moraine formation through englacial thrusting due to their structural characteristics and a lack of subglacial material. It is perceived that similar models of deposition can be applied to other moraines in the study area, due to their similar morphology, although further sedimentological work is required to test this assumption. In addition, active glacier retreat is favoured since there is evidence at Stronelairg for

a minor glacier readvance that overrode the lower part of the section. Evidence for ice stagnation is only found in a few small areas on the plateau (Appendix II), where the mounds and ridges were oriented in a number of directions and could not be joined to form chains of moraines. Therefore, apart from in these areas, moraines in the study area are argued to represent former ice-marginal positions and can be linked together to reconstruct these positions (e.g. Benn, 1992; Benn *et al.*, 1992; Bennett & Boulton, 1993a, b; Golledge & Hubbard, 2005; Lukas & Benn, 2006; Finlayson, 2006; Finlayson *et al.*, 2011).

Ice-marginal meltwater channels

A large number of ice-marginal meltwater channels are identified in the study area based on either their location in between moraines, where they trend obliquely down the valley side, often curving arcuately towards the valley centre line, or their downslope trending profiles following criteria by Greenwood *et al*. (2007). Former ice-marginal channels identified in the same way are also found in valleys that contain few moraines and on the plateau, where they often form several sets of deep channels (Appendix II). A substantial number of ice-marginal meltwater channels on the plateau are found in the eastern part of the study area within the Findhorn, Elrick and Dulnain catchments. The large number of meltwater channels in this area and the rest of the study area indicates that ice-marginal drainage was a significant component of the former ice masses in the region and this will be discussed further in Section 5.5.

Fluvial landforms

A number of alluvial fans are recognised within the study area, which often surround areas of moraines, such as in Gleann Madagain, Corrie Iain Oig and Glen Markie (Killin) (Appendix II). Particularly impressive alluvial fans occur at the mouths of three tributaries to the River Findhorn. Debris cones, which emanate from small streams on the valleys sides are also visible within several catchments. River terraces are a particularly prominent feature in the study area and occur within a large number of valleys, although prominent river terraces are generally limited to the lower parts of the valleys only, however (Appendix II).

Periglacial features

Periglacial features such as blockfields and solifluction lobes are apparent on many of the plateau summits in the study area, particularly on the area of high ground to the north of the Lochain, Ballach, Fionndrigh and Chaorainn catchments in the southeastern part of the study area (Appendix II). The majority of features do not have distinct lower boundaries, although clear lower boundaries were observed on solifluction lobes on the plateau above Gleann Lochain and Gleann Ballach. Thick talus slopes occur on a number of valleys in the study area, some of which extend to the valley bottom, such as in Glen Tarff and the lower parts of the Findhorn Valley and

Glen Elrick. Other thick talus slopes end abruptly part way down the valley sides and this is particularly apparent in Gleann Fionndrigh, Gleann Ballach and Gleann Lochain.

Rock slope failures

Several significant rock slope failures (RSF) are recognised in the study area, the majority of which are around Loch Killin and are classed as sub-cataclasmic (Appendix II). A large sub-cataclasmic RSF is also found towards the head of Glen Tarff, in addition to a substantial catclasmic RSF in the upper part of Gleann Fionndrigh in the southeast of the study area. These RSFs have previously been identified by D. Jarman (pers. comm., 2009) in combination with research by Holmes (1984).

Glaciolacustrine landforms and sediments

Evidence for the existence of former ice-dammed lakes in the study area is found within Glen Turret, Glen Killin and the Glen Banchor tributary valleys. In Glen Turret, this evidence is in the form of former lake shorelines on the valley sides and subaqueous ice-contact fans at the head of the valley (Appendix II). Sediments were not examined within the Turret Fan, however, and it is therefore still unclear whether this feature represents a terrestrial or subaqueous ice-contact fan. A wide range of lake sediments occurs in the area around Glen Killin and represents deposition as a subaqueous grounding-line fan, subaqueous outwash fans and a Gilbert-type delta. These sediments document the advance of a lobe of regional ice from the Ness basin into the Killin-Fechlin Valley and the formation of a 642 m lake. Geomorphological and sedimentary evidence for former lakes in the Glen Banchor tributaries and Glen Markie indicates that drainage in these valleys was blocked by the Strathspey Glacier. Channels were created across the interfluves between these valleys and controlled the level of the lakes, which all drained eastwards into their neighbouring valleys, depositing subaqueous fans (possibly deltaic) within Glen Ballach and Glen Markie. Other ice-contact fans and large ridges are recognised in the study area, but these features cannot be assigned to a subaqueous or terrestrial origin until further sedimentological work has been undertaken.

Synthesis

The glaciogenic landforms identified in this chapter, and their spatial distribution, provide compelling evidence for the existence of a plateau icefield in the Monadhliath Mountains and damming of local drainage by regional ice in the Great Glen and Strathspey. The overprinting of landforms in Glen Odhar and Glen Mòr, and variations in moraine morphology within individual valleys, indicates that the geomorphological and sedimentary evidence presented here represents more than one glacial event. A relative chronology for these glacial events is identified within Chapter 5. Chapter 5 subsequently focuses on the reconstruction of a plateau icefield from the most recent phase of glaciation, calculates ELAs and palaeoprecipitation for this icefield, and examines icefield dynamics, with respect to thermal regime and glacier retreat patterns.

Chapter 5

Plateau Icefield Reconstruction

Chapter 5 focuses on the reconstruction former ice masses in the Monadhliath Mountains relating to the LGIT, particularly focussing on local plateau icefield reconstruction and subsequent analysis, based on the geomorphological and sedimentary evidence described in Chapter 4. Section 5.1 describes the approach used to identify a relative chronology for glacial events in the region in the absence of published absolute ages. Here, morphostratigraphy is used to identify glacier limits of a similar age, allowing reconstruction of approximately contemporaneous maximum limits of a plateau icefield during the most recent phase of glaciation. Section 5.2 deals with the reconstruction of a plateau icefield based on the glacier limits identified in Section 5.1. Two glacier surface profile models are used to provide minimum and maximum boundaries for a range of realistic ice thicknesses on the plateau where geomorphological evidence is lacking, enabling an 'average ice thickness' plateau icefield to be reconstructed. Section 5.3 introduces a more detailed and spatially coherent chronology for deglacial events from the LGM based on the geomorphological and sedimentary evidence within Chapter 4. This section also discusses the interaction between plateau ice and regional ice during this time. Former equilibrium line altitude (ELA) and palaeoprecipitation calculations for the reconstructed icefield from the most recent phase of glaciation are carried out in Section 5.4 for both the plateau icefield as a whole and major outlet glaciers. The final section, Section 5.5, examines the dynamics of the reconstructed plateau icefield based on the geomorphological evidence. This includes retreat dynamics based on moraine retreat patterns and spacing, an approach that has not been undertaken in such detail before, and plateau icefield thermal regime.

5.1 Establishing a Relative Chronology for Glacial Events

As discussed in Chapter 4, the geomorphological evidence found in the Monadhliath Mountains varies both between valleys and between the lower and upper parts of individual valleys. In the lower parts of the valleys, the moraines usually have wide base areas and can be up to 20 m in height, although many form subdued features with rounded crestlines. By comparison, moraines in the upper parts of the valley are smaller (< 10 m high), with sharper crestlines and are usually more closely spaced. Large river terraces tend to occur in the lower parts of the valley only and are observed to end abruptly within a number of valleys. Other features such as ice-marginal meltwater channels and periglacial features also vary within and between valleys in terms of quantity and extent. This evidence suggests that the landforms within many of the valleys were not formed contemporaneously and may document more than one glacial event.

The only published absolute dates in the study area are in Glen Roy (Section 2.3.3). In this area, the final abandonment of the shorelines formed in Glen Roy is dated to between 11.5 ± 1.1 ka and 11.9 ± 1.5 ka using cosmogenic nuclide exposure dating (Fabel *et al.*, 2010). A floating varve chronology from Glen Roy indicates that Glen Roy was flooded for 515 years placing the advance of the Spean Glacier into Glen Roy at ca. 12 165 a BP in the latter half of the Younger Dryas (Palmer *et al*., 2010, 2012).

In the absence of any published dates in the remainder of the study area, a relative chronology for glacial events in the Monadhliath Mountains was established using morphostratigraphy. Morphostratigraphy uses "the spatial relationship between individual landforms to assign them to events or periods" (Lukas, 2006, p.721; Hughes, 2010). By this it is meant that the overprinting or juxtaposition of landforms, alongside the assessment of changes in landform associations over a particular area, can be used to establish a relative sequence of events. This approach, whilst not always formally acknowledged, has been used as a relative dating tool in a large proportion of former ice mass reconstructions in the UK (e.g. Sissons, 1974b; Ballantyne, 2002a, 2007a, b; Benn & Ballantyne, 2005; Finlayson, 2006; Lukas, 2006; Lukas & Bradwell, 2010; Finlayson *et al.*, 2011). Even in areas where there is some absolute dating, it is usually impractical to ascertain absolute dates for every glacier or outlet lobe limit within a particular area, and therefore a common approach has been to correlate ice limits to a chronologically well-constrained ice limit based upon morphostratigraphy (e.g. Lukas & Bradwell, 2010; Finlayson *et al*., 2011).

Lukas (2006) used this approach to identify a set of geomorphological criteria that can be used to specifically test whether a particular landsystem is of Younger Dryas age. This was based upon contrasting sediment-landform associations found inside and outside prominent glacier limits which have been dated to the Younger Dryas in areas of Upland Britain (e.g. Sissons, 1974c; Benn & Ballantyne, 2005; Bradwell, 2006; Lukas & Bradwell, 2010). Criteria include moraines, river terraces, glaciofluvial landforms, glacially transported boulders, sediment-covered slopes, talus slopes, areas of periglacial activity and palaeoshorelines in areas near the coast (Lukas, 2006). Those criteria used to identify a relative chronology in the Monadhliath Mountains are discussed below in order of relevance for the study area.

5.1.1 Morphostratigraphical criteria

Moraines

A clear contrast has been observed in several areas of Scotland between sharp-crested moraines, which are relatively narrow, closely spaced and often dissected inside dated Younger Dryas limits and moraines outside of these limits, which tend to have more rounded crestlines and are

often wider and higher, although also sometimes subdued due to extensive degradation (e.g. Sissons, 1974b, c, 1979d; Robinson & Ballantyne, 1979; Ballantyne, 1988, 1989; Brown, 1993; Benn & Ballantyne, 2005; Lukas, 2005a; Finlayson *et al.*, 2011). In particular, the landform assemblage of Scottish 'hummocky moraine', which is widespread in upland areas of Scotland, has often been associated with deposition during the Younger Dryas (e.g. Sissons, 1967, 1974b, c, 1977b, 1979e; Sissons *et al*., 1973; Ballantyne & Wain-Hobson, 1980; Ballantyne, 1989, 2002a; Lowe & Walker, 1997; Wilson & Evans, 2000; Benn & Lukas, 2006; Finlayson, 2006; Lukas & Bradwell, 2011). However, it has also been demonstrated that the formation of Scottish 'hummocky moraine' is not restricted to the Younger Dryas (e.g. Clapperton *et al.* 1975; Clapperton & Sugden, 1977; Everest & Golledge, 2004; Everest & Kubik, 2006) and therefore the presence of hummocky moraine should not be used as the only criterion to assign a Younger Dryas age to landforms.

River terraces

River terraces form as a response to a change in conditions such as discharge, sediment load and transport capacity (Knighton, 1998; Gurnell *et al.*, 1999) and are intrinsically controlled by climate. Typically, during warm interglacial periods, vegetation cover and soil development can confine rivers to a single channel. During times of high discharge the river spills onto the floodplain and little incision is caused to the channel bed (Murton & Belshaw, 2011). In contrast, during cold conditions, flashy discharges occur due to snowmelt, periods of heavy rainfall, reduced vegetation cover and discontinuous permafrost, which cause both incision and aggradation, often in the form of cut and fill structures (Maddy *et al*., 1998; Murton & Belshaw, 2011). In addition, in areas immediately downstream of glaciers, sediment load will be higher, causing higher levels of aggradation than during interglacials. The transition between warm and cold, and cold and warm periods has been suggested as a mechanism for creating the long staircases of river terraces, although there is some debate over the exact mechanisms that drive the change from incision to aggradation (Maddy *et al*., 1998; Bridgland & Westaway, 2008; Murton & Belshaw, 2011).

Due to these climatically driven changes in the fluvial system, a contrast is often found between areas that were glaciated during the Younger Dryas and those that remained ice-free. Since the Younger Dryas was the last period in which major river terrace development occurred, major river terraces are not usually found in areas that were glaciated during the Younger Dryas, since cover by ice prevented river terrace development. This relationship between the location of a dated Younger Dryas glacier limit and the start of a large river or outwash terrace has been observed regularly in Scotland (Sissons *et al*., 1973; Sissons, 1974b, c, 1979d; Benn & Ballantyne, 2005; Finlayson *et al*., 2011) and can therefore be used to identify Younger Dryas glacier limits in areas

where no dates are available. However, some large outwash terraces have been observed to start slightly inside end moraines relating to the Younger Dryas limit due to continued terrace formation during the initial stages of deglaciation (Sissons, 1974a). In addition, further caution is required in some areas, since the relationship can occasionally break down due to palaeo-lake formation and drainage, variations in slope gradient and changes in sea level in areas near the coast (Lukas, 2006). A 3 m high terrace, known as the Main Holocene Terrace, has also been observed in many Scottish valleys, particularly in the eastern Grampians, which is related to floodplain aggradation at ca. 2.5 ka BP (Ballantyne & Whittington, 1999; Ballantyne, 2008).

Meltwater channels

Small meltwater channels have regularly been observed within dated Younger Dryas limits in several areas of Scotland, whilst beyond these limits, channels are often much larger and deeper (e.g. Sissons *et al*., 1973; Sissons, 1974b, c). These smaller meltwater channels often relate to ice-marginal positions of former Younger Dryas ice masses (Benn & Lukas, 2006), compared to ice-marginal and subglacial channels created by a retreating ice sheet, where much larger quantities of water were involved (e.g. Greenwood *et al*., 2007; Livingstone *et al*., 2010c). Sissons (1974a) suggests that this contrast is not as strong in western Scotland, since the Younger Dryas glaciers were larger.

Sediment-covered slopes

Several authors document the occurrence of thick accumulations of sediment on slopes inside dated Younger Dryas limits, particularly compared to areas downstream or above these Younger Dryas limits (e.g. Sissons, 1974b; Thorp, 1986; Ballantyne, 1989, 2002a; Gray & Coxon, 1991). This distinct accumulation of sediment is argued by Ballantyne (2002a) to be a result of the re-working of pre-existing sediment by Younger Dryas glaciers that was deposited originally during the LGM. This sediment accumulation, often known as the 'drift limit', usually has an upper boundary, which has been previously used to delineate former Younger Dryas glacier surfaces (e.g. Ballantyne & Wain-Hobson, 1980; Gray, 1982; Thorp, 1986; Ballantyne, 1989, 2002a; Gray & Coxon, 1991; Hughes, 2002; Benn & Ballantyne, 2005).

Periglacial deposits

The Younger Dryas is the most recent period in which severe periglacial conditions prevailed in Britain in ice-free areas (Ballantyne & Harris, 1994). As a result, although some periglacial processes still occur today in upland areas, most large periglacial features are believed to have formed during the Younger Dryas (Sissons, 1979d; Ballantyne, 1984, 1991, 1998; Ballantyne & Harris, 1994). Therefore the presence of major periglacial features can be used to identify areas that were outside the limits of Younger Dryas glaciation (Sissons, 1972, 1974b; Sissons &

Grant, 1972; Lukas, 2006; Ballantyne, 2007a, b; Finlayson *et al*., 2011). In particular, thick, mature talus sheets and thick solifluction lobes have been noted to be more extensive outside of dated Younger Dryas limits (e.g. Sissons, 1972, 1979d; Thorp, 1986; Ballantyne & Harris, 1994; Hinchcliffe *et al*., 1998; Curry, 2000).

Glaciofluvial landforms and sediments

Glaciofluvial landforms and sediments have been well associated with the retreat and decay of the Late Devensian ice sheet, usually in the form of large outwash terraces, kames and eskers (e.g. Auton, 1990; Young, 1974, 1978; Brown, 1993; Thomas & Montague, 1997). However, no such landforms and sediments have been observed within the limits of dated Younger Dryas glaciers, since the glaciers were smaller and usually in more upland locations dominated by glaciogenic features such as moraines and meltwater channels (e.g. Sissons *et al*., 1973; Sissons, 1974b, c, 1977b; Lukas & Bradwell, 2010).

Glacially transported boulders/erratics

Previous research has noted that large spreads of boulders often occur inside dated Younger Dryas limits and particularly at the Younger Dryas glacier limits themselves (e.g. Sissons, 1974a, 1977b, 1979d; Gray, 1982; Thorp, 1986; Benn, 1992; Gray & Coxon, 1991). This pattern of deposition has been observed at maximum limits of modern glaciers and has been associated with the toppling and sliding of boulders from the glacier surface (e.g. Sharp, 1984; Benn & Evans, 2010). Boulder spreads are not exclusively indicative of a Younger Dryas age, however, and like all other criteria must be used in combination with the other lines of evidence.

5.1.2 The relative age of glacial events in the Monadhliath Mountains

Using the criteria outlined above, the geomorphological evidence provides a strong indication that the most recent phase of glaciation in the Monadhliath Mountains occurred during the Younger Dryas, due to a similar morphological signature to other dated Younger Dryas sites in Scotland. This is manifest in the clear contrast in landform-sediment assemblages within the upper and lower parts of the majority of outlet valleys that surround the central plateau. The strongest evidence for this is found in the change in moraine morphology, which in many valleys coincides with the termination of a major river terrace. In addition, a combination of other factors, such as meltwater channels, periglacial trimlines, sediment covered slopes and in one valley, a boulder spread, provide further evidence that the landform-sediment assemblages in the upper parts of most valleys relate to formation during the Younger Dryas. This convergence of many lines of evidence enables Younger Dryas limits to be identified in most outlet valleys, although also recognises the absence of Younger Dryas ice in others. A grid reference for the Younger Dryas limit in each outlet valley is displayed in Table 5.1, alongside the geomorphological criteria used

Table 5.1. Criteria used to define the limits of Younger Dryas outlet glaciers in the Monadhliath Mountains.

Valley	Grid ref.	Change in moraine morphology	Lateral moraines	Drift limits	Termination of a major river terrace	Meltwater channels	Sharp boundary to talus sheet	Sharp boundary to solifluction lobe	Boulder Spread	Circumstantial evidence from neighbouring valleys
Ballach	NH 652 013	√	√	√		√	√	√		
Beith	NN 592 989	√	√		√					
Bhothain Dulnain	NH 713 064					√				√
Brien	NH 481 093	√								
Ceire	NH 409 012	√				√				√
Chaorainn	NH 693 037	√	√		√			√		
Charn	NN 355 987	√				√				
Chonnal	NN 389 946	√	√		√		√			
Chonnal Dearg	NN 354 939					√				√
Chonnal Bheinne	NN 373 937					√				√
Doe	NH 434 054	√				√				
Dubh	NH 497 086					√				√
Dubh C na C	NH 488 079	√	√		√	√				
Dubh Mor 1	NH 509 102					√				√
Dubh Mor 2	NH 504 099					√				√
Dulnain	NH 716 090	√		√	√	√				
Dulnain Daimh	NH 712 096					√				√
Dulnain Sgùlain	NH 707 093					√				√
Easgainn	NH 523 078	√	√		√	√				
Eilrig	NN 360 995	√				√				
Elrick	NH 679 127	√		√	√	√				
Elrick Dubha	NH 702 120					√				√
Elrick Icean 1	NH 717 112					√				√
Elrick Icean 2	NH 713 110					√				√
Findhorn	NH 661 135	√	√		√	√				
Findhorn Odhar	NH 616 135					√				√
Findhorn Searsanach	NH 634 122					√				√

Table 5.1. *continued.*

Valley	Grid ref.	Change in moraine morphology	Lateral moraines	Drift limits	Termination of a major river terrace	Meltwater channels	Sharp boundary to talus sheet	Sharp boundary to solifluction lobe	Boulder spread	Circumstantial evidence from neighbouring valleys
Fionndrigh	NH 665 017	√		√	√		√			
Gearra	NH 716 060					√				√
Ghille Charaich	NH 586 136				√	√				√
Gilbre	NN 494 988					√				√
Gloy	NN 309 939					√				√
Iain Oig	NN 517 979	√			√	√				
Innis Shim	NN 329 978	√				√				
Killin	NH 534 077	√		√						
Killin Laraiche	NH 575 116					√				√
Killin Mharconaich	NH 556 110					√				√
Killin Phuil	NH 543 094					√				√
Killin Sheilich	NH 578 126				√	√				√
Lagan a' Bhaine	NH 388 007	√			√					
Laogh	NN 451 975	√		√		√				
Larach	NN 340 985	√		√	√	√				
Lochain	NH 632 006	√			√		√	√		
Markie	NH 603 004	√				√				√
Min Coire	NN 475 990	√				√				√
Shesgnan	NN 421 958	√	√		√					
Sidhean	NN 305 955	√		√	√					
Talagainn	NN 544 985				√	√			√	
Tarff	NH 445 027									√
Turret Bige	NN 330 943	√								√
Turret Eachach	NN 336 944									√
Turret Mòire	NN 331 944	√								√
Uchadachan	NH 392 004	√	√		√					
Yairack	NN 443 970	√	√		√	√	√			

at each site to determine the Younger Dryas limit and where available, the lateral margins of such a glacier. These limits are discussed further in Sections 5.2.2 to 5.2.4.

These Younger Dryas limits and the geomorphological evidence found inside them indicate that a substantial plateau icefield occurred in the Monadhliath Mountains during the Younger Dryas, following arguments made for a plateau icefield rather than valley style of glaciation made in Section 4.5. The dimensions of this plateau icefield are reconstructed below in Section 5.2. This evidence for Younger Dryas glaciation in the upper parts of the outlet valleys indicates that landform-sediment assemblages in the lower parts relate to a phase of glaciation that occurred prior to the Younger Dryas. These features are interpreted to relate to a stage of deglaciation that occurred following the LGM and a sequence of LGM deglacial events is discussed in Section 5.3.

5.2 Younger Dryas Glacier Reconstruction

Younger Dryas masses in the Monadhliath Mountains are now reconstructed since this was the most recent phase of glaciation and therefore the geomorphological evidence provides the most complete record for this time period. Following identification of Younger Dryas limits within each outlet valley (Table 5.1), outlet glaciers were reconstructed in *ESRI ArcGIS* using lateral moraines, meltwater channels, drift limits and periglacial trimlines, where available, to delimit the lateral margins (see also Table 5.1). In the majority of cases extrapolation between ice-marginal features was used to reconstruct these margins, mirroring one side of the valley to the other if geomorphological evidence was lacking. The aim was to recreate a symmetrical glacier tongue, with lateral margins that steadily increased in altitude at a gradient set by any ice-marginal features available. There are a number of problems with this kind of approach, as discussed by Ng *et al*. (2010), most importantly that the glacier reconstruction is guided to an extent by what the researcher regards as being 'realistic'. However, in valleys where there was a good constraint on the Younger Dryas limit and the lateral margins, this approach provided a relatively quick way of reconstructing the former outlet glaciers.

However, the thickness of ice on the plateau itself was difficult to constrain due to a lack of geomorphological evidence that could provide clear, unequivocal evidence for ice thickness. Extensive areas of blockfield occur on the tops of a number of summits (Appendix II), yet the lower boundaries of these features could not be used to identify the former upper limit of ice on the plateau for the following reason. Blockfields are generally accepted to be relict features that may have formed as far back as the Neogene (Nesje, 1989; Rea *et al*., 1996; Whalley *et al.*, 1997, 2004; André, 2003; Marquette *et al*., 2004; Sumner & Meiklejohn, 2004; Fjellanger *et al.*, 2006; Paasche *et al*., 2006) and are likely to have been modified by physical weathering, such as frost wedging under periglacial conditions during the Quaternary (Ballantyne, 1998, 2010b). Therefore,

the extensive blockfields on some of the summits of the Monadhliath Mountains would not have formed on ice-free summits during the Younger Dryas alone. The presence of blockfields on the higher summits in the study area therefore suggests that these locations have not been subject to extensive periods of glacial erosion during both the Younger Dryas and earlier phases of glaciation. This indicates that the blockfields were either covered and protected by cold-based ice (e.g. Whalley *et al*., 1981; Gellatly *et al*., 1988; Kleman, 1994; Rea *et al*., 1996; Fjellanger *et al*., 2006; Ballantyne, 2010a) or remained as nunataks above the plateau icefield (e.g. Ballantyne, 1997; Ballantyne *et al*., 1997). The lower limits of the blockfields could therefore either represent the upper limit of warm-based Younger Dryas ice (e.g. Ballantyne, 1997; Ballantyne *et al*., 1997), an englacial thermal boundary between warm-based ice at lower elevations and higher altitude cold-based ice during the Younger Dryas (e.g. Goehring *et al*., 2008), a relict trimline protected by cold-based ice during the Younger Dryas, or simply the lower limit of blockfield formation that was also protected by cold-based Younger Dryas ice and previous ice masses. The preservation of pre-Younger Dryas landforms on the plateau, such as the delta to the south of Glen Killin, suggests that ice on the plateau was cold-based (see Section 5.5 for further discussion), and therefore the lower limit of the blockfield cannot be assumed to represent the altitude of the plateau icefield surface during the Younger Dryas.

Meltwater channels and isolated moraines curve around several of the plateau summits. However, these features could not be used to delineate maximum ice thickness since they could equally relate to ice-marginal positions during retreat, or may be older features that have been preserved below cold-based ice. Solifluction lobes are also widespread on many of the plateau summits (Appendix II). The majority of these features do not have linear lower boundaries, however, indicating that they do not represent the upper limit of the former plateau icefield surface. In addition, many of these features are thin, with low risers at their furthest extent indicating their formation during the Holocene only (Ballantyne, 2008). This means that the majority of solifluction lobes could not be used to delineate the maximum thickness of Younger Dryas plateau ice. However, thick solifluction lobes leading onto the plateau on the eastern valley sides of Gleann Lochain and Gleann Ballach and on the northern flank of A' Chailleach, to the west of Gleann Chaorainn have linear lower boundaries and thick risers and were therefore used to demarcate the upper ice surface in these areas. Evidence here provided a robust constraint on ice thickness that could be extrapolated to neighbouring areas in combination with a modelled approach, as described below.

5.2.1 Glacier profile modelling

In order to constrain ice thickness on the plateau and to test the assumption that all the outlet glaciers were connected to ice on the plateau above them, particularly in valleys with steep

backwalls, two glacier surface reconstruction models were used. These models were used to provide maximum and minimum elevation boundaries for the plateau ice surface from which an average surface could be taken. The first model is presented by Benn and Hulton (2010) in a comprehensible spreadsheet format that is available online. The model is a 'perfectly plastic' flowline model, which is adapted from Nye (1951, 1952) and van der Veen (1999), and various versions of this model have been previously used in glacier reconstructions (e.g. Schilling & Hollin, 1981; Locke, 1995; Rea & Evans, 2007; Carr & Coleman, 2007; Vieira, 2008). The Benn and Hulton (2010) version of this model is designed particularly for glacier reconstructions where geomorphological evidence for ice thickness is lacking and the authors specifically highlight its use for defining otherwise unconstrained ice surfaces on plateau icefields. Inputs to the model are bed topography and ice surface elevations, where known along the glacier centre line. A shape factor (f) is also required to estimate the effect of lateral drag from the valley sides and is defined as:

$$f = \frac{A_r}{H\rho^*} \quad (1)$$

where A_r represents the cross-sectional area of the glacier, H is the ice thickness and ρ^* is the perimeter of the cross section at a given point on the glacier.

Basal shear stress is then altered to initially constrain the modelled profile to the known ice surface elevations before being used to extrapolate the profile to areas where geomorphological evidence is absent (Fig. 5.1).

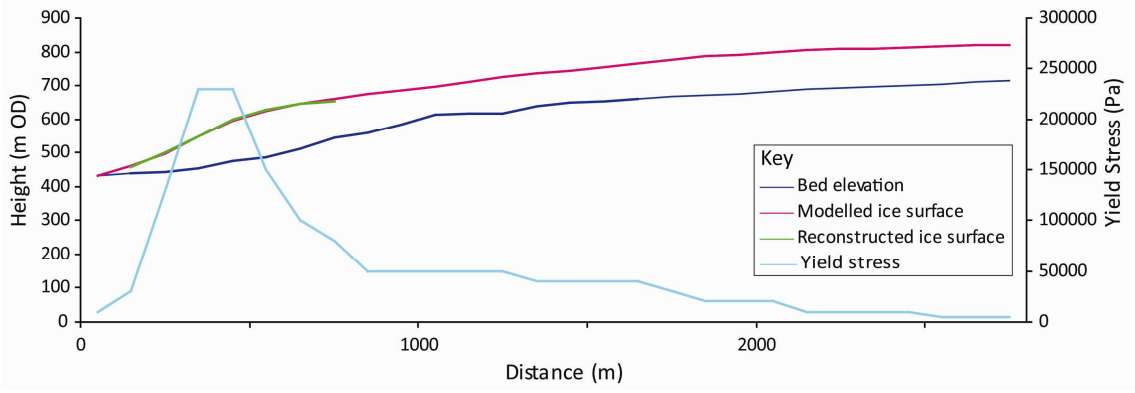

Figure 5.1. Example output graph from the Benn and Hulton (2010) model showing how the shear stress can be varied to fit the geomorphological evidence and then extracted further up glacier.

A key aspect of the model is that it assumes that the modelled glacier behaves in a 'perfectly plastic way', i.e. the ice will not deform until the driving stress reaches the yield stress (van der Veen, 1999). The driving stress cannot rise above the yield stress as it is assumed that once the yield stress is reached, the surface profile will continuously adjust (van der Veen, 1999; Benn &

Evans, 2010). Therefore the perfect plasticity model assumes that the driving stress will always equal the yield stress and therefore the basal shear stress will also equal the yield stress (Benn & Evans, 2010). For valley glaciers, this assumption is unrealistic due to frictional drag caused by the valley sides, although the use of a shape factor can go some way to alleviating this problem. More importantly, the model does not account for the thermal regime or the proportion of forward motion that can be attributed to basal sliding. Both of these factors may have a significant affect on the surface profile and therefore the yield stresses calculated may deviate substantially from the actual shear stresses (Benn & Hulton, 2010). For example, basal drag is reduced if sliding occurs and therefore a lower yield stress should be used in the model if some of the forward motion of the glacier is believed to be attributed to sliding, which will result in a lower glacier profile (van der Veen, 1999).

The main problem with the model is the wide range of shear stresses that can be used to create the ice surface profile. In modern valley glaciers basal shear stresses are generally estimated to range between 50 and 150 kPa (Benn & Evans, 2010). There is a large difference in the heights of the modelled surface profiles that are produced using the lower and upper extremes of this range and therefore the valley topography often causes a greater constraint on the scope of possible ice surface elevations than using the 50 to 150 kPa range. To overcome this problem, in this research, shear stresses of a similar magnitude to those in the constrained part of the glacier were used to extrapolate the glacier surface reconstruction into unconstrained areas. The shear stresses were increased slightly if the topography steepened and lowered if the gradient decreased, including an adjustment to zero near the ice divide (Benn & Hulton, 2010). The Benn and Hulton (2010) model was therefore used with most confidence to reconstruct the minimum and maximum surface elevations of the upper parts of outlet glaciers that were well-constrained for the majority of their profile.

An additional problem with the model is that it is based on a single valley glacier or plateau icefield outlet glacier, whereas in this study area, several tributary glaciers and/or a large source area on the plateau often contribute to each outlet glacier. The model does not account for additional fluxes of ice along the profile that will contribute to the surface profile and therefore, the use of the model in this study was restricted to the less complex glacier outlets.

The second model used in this research was devised by Ng *et al*. (2010) in order to alleviate some of the reconstruction problems encountered using an extrapolative approach and assumptions that are made using a typical modelling approach, as above. These authors examined variations in the curvature of modern glacier surface profiles and established an envelope within which realistic glacier profiles may fall. Using the Nye (1951, 1952) equation,

the authors define the parabolic surface profile of a glacier as:

$$h(x) = C\sqrt{x} \tag{2}$$

and the constant C as: $C = \left(\frac{2\tau_0}{\rho g}\right)^{\frac{1}{2}}$ (3)

where x is the horizontal distance from the ice margin in an up-glacier direction, h is the height above the glacier margin, τ_0 is the basal shear stress, ρ is the ice density and g is gravitational acceleration.

This equation describes the surface profile of a glacier that rests on a flat bed, rather than on a slope, but is favoured by Ng *et al*. (2010) to overcome the problem of extrapolating the bed topography from beneath modern glaciers. The constant C describes how 'stiff' the flow of ice is and this value increases with ice stiffness. Polar glaciers are therefore expected to have a higher C value than those near the equator, but other factors such as ice velocity, thickness, subglacial hydrology and bed topography can also affect the value of C (Ng *et al*., 2010).

Ng *et al*. (2010) calculated C for surface profiles from 200 ice masses by extracting each glacier's maximum height and length using the equation below, where C^* describes the whole of the glacier profile.

$$C^* = \frac{H}{\sqrt{L}} \tag{4}$$

A second value of C ($\tilde{C}$) was also calculated to 'best fit' equation 2 to the glacier profile, using a least-squares method to minimise vertical errors in h (see Figure 5.2).

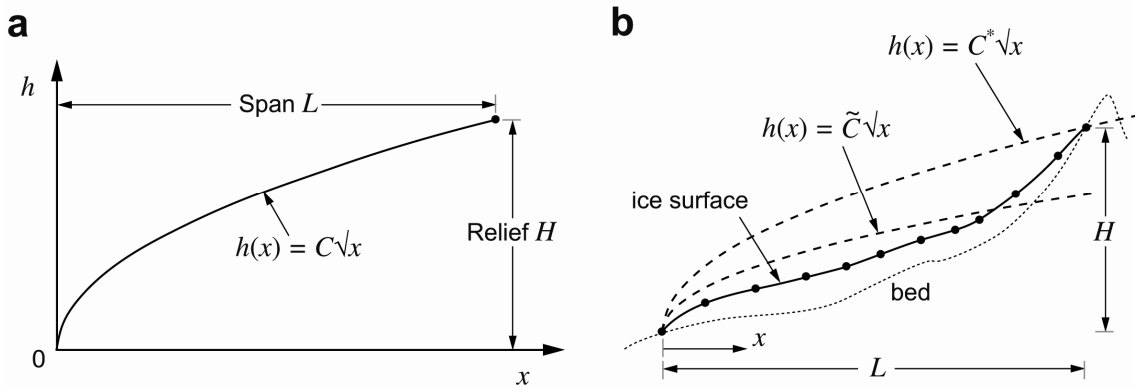

Figure 5.2. Mathematical symbols used to define glacier surface profiles for a) the parabolic surface of a glacier as defined by Nye (1951, 1952) from equation 2. b) diagram to illustrate the use of C^* and $\tilde{C}$ to best fit the parabola to the surface profiles sampled by Ng *et al*. (2010). Taken from Ng *et al*. (2010, p. 3242).

The authors then used the range of $C*$ and $\tilde{C}$ values found on the modern dataset to define minimum values for $C*$ and $\tilde{C}$ based upon glacier length, since the influence of bed topography on the *C* values was shown to increase as glacier length decreased, causing higher values of *C*. The authors specified that the minimum value for $C*$ within valley glaciers is 5.2 $m^{1/2}$ and demonstrated that this can be used to identify the minimum ice surface height at the ice divide. This approach is therefore very useful for testing whether a col will feasibly be submerged by ice and the minimum height of the ice above the col if this is the case.

This approach was therefore also used in order to examine the thickness of plateau ice in the Monadhliath Mountains and to test whether some glaciers were connected to the plateau ice. However, the lengths of the outlet glaciers in the study area are relatively small and therefore lie at the lower end of the range of glacier lengths in the dataset used by Ng *et al*. (2010), where *C* values are severely affected the bed topography. As a result, for the majority of outlets, the minimum value of 5.2 $m^{1/2}$ for *C** produced ice profiles that did not reach the height of the col despite geomorphological evidence clearly indicating the presence of ice over some cols. In other areas, where either the valley gradient was low, or the majority of the outlet catchment was on the plateau, the minimum *C** value of 5.2 $m^{1/2}$ produced an unrealistically high minimum surface profile, suggesting a potential lack of comparable modern analogues in the Ng *et al*. (2010) dataset.

In order to investigate these problems further, the original modern analogue dataset was acquired from one of the authors (I.D. Barr, pers. comm., 2011). This data was plotted on a scatter graph in a way that could encompass both the glacier length and the *C** value, but also the relief of the glacier (Fig. 5.3). Appropriate minimum, maximum and 'typical' *C** values were then identified from the scatter plot individually for each outlet glacier investigated that were of similar magnitudes. A range of ± 50 m either side of the glacier relief and ± 30% of the glacier length were used to define the envelope in which the *C** values were chosen from. Whilst this is potentially a very crude method of selecting appropriate *C** values, it provided a quick method of doing so and more realistic minimum and maximum *C** values for each outlet glacier. However, the location of the glaciers within the modern analogue dataset was not considered and therefore differences in the thermal regime between the modern and reconstructed glaciers were not taken into account, which could account for the wide range of ice surface elevations that were still reconstructed for some outlets. A larger dataset would be required, however, to take this into account and potentially constrain the range of *C** values further.

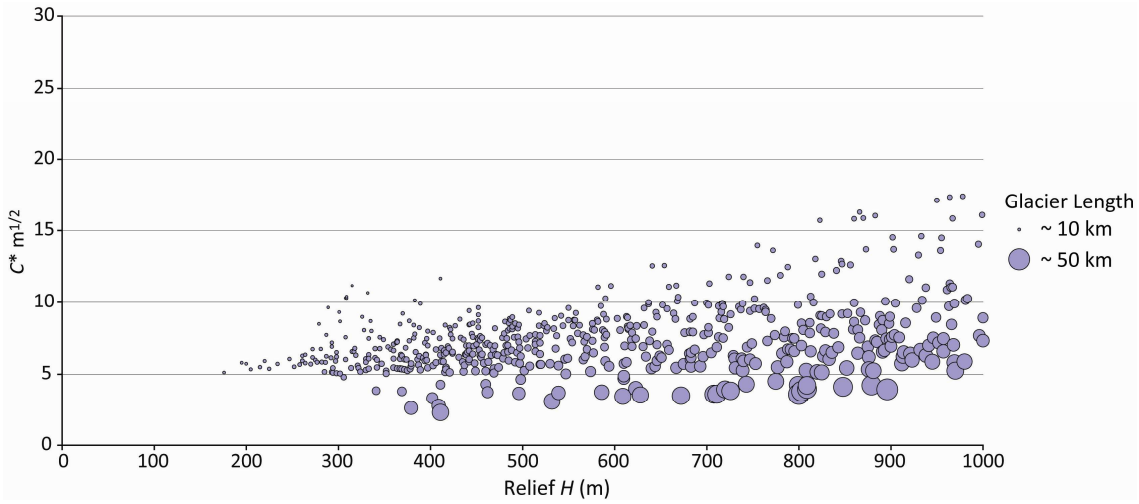

Figure 5.3. Scatter plot showing the glacier relief (*H*) against *C**, where the size of the data points corresponds to the length of the glacier. Data from Ng *et al*. (2010).

Sections 5.2.2 to 5.2.4 describe the reconstruction of the Younger Dryas outlet glaciers and estimations of plateau icefield thickness using a combination of the extrapolative approach and the two models described above. For this purpose the Monadhliath Mountains are divided into the western, central and eastern sections, so that the connection across the ice divide between north and south flowing outlet glaciers could be assessed. Since the central section contains the least geomorphological evidence to constrain ice thickness on the plateau, this is described last, so that inferences could be made from the better-constrained western and eastern sections.

5.2.2 Younger Dryas glacier reconstruction in the western Monadhliath Mountains

Younger Dryas glacier limits

Younger Dryas glacier limits were identified within all outlet valleys in the western Monadhliath Mountains. Criteria for defining these limits is listed in Table 5.1 and the location of the limits is shown in Figure 5.4. A change in moraine morphology from broad rounded moraines to sharp-crested densely spaced moraines was identified within all major valleys apart from Coire na Cèire, where the landscape was predominately dominated by meltwater channels. The most unambiguous evidence for a Younger Dryas glacier limit was found in glens Chonnal and Shesgnan, where the change in moraine morphology corresponded with the start of a major river terrace, in the lower part of the valleys, although in Glen Shesgnan it occurred inside the first few moraines. In Coire Larach, Glen Lagan a' Bhainne and Glen Uchdachan the change in moraine morphology was more gradual, but the Younger Dryas limit was identified where each valley became significantly more incised by the central stream in a downvalley direction, which corresponded with the change in moraine morphology. Younger Dryas limits in Coire Innis Shim, Coire Charn, Coire Eilrig and Coire na Cèire were identified at the point downvalley where closely spaced, small ice-marginal meltwater channels stopped occurring and the central stream either widened slightly or became more deeply incised. In the majority of these corries

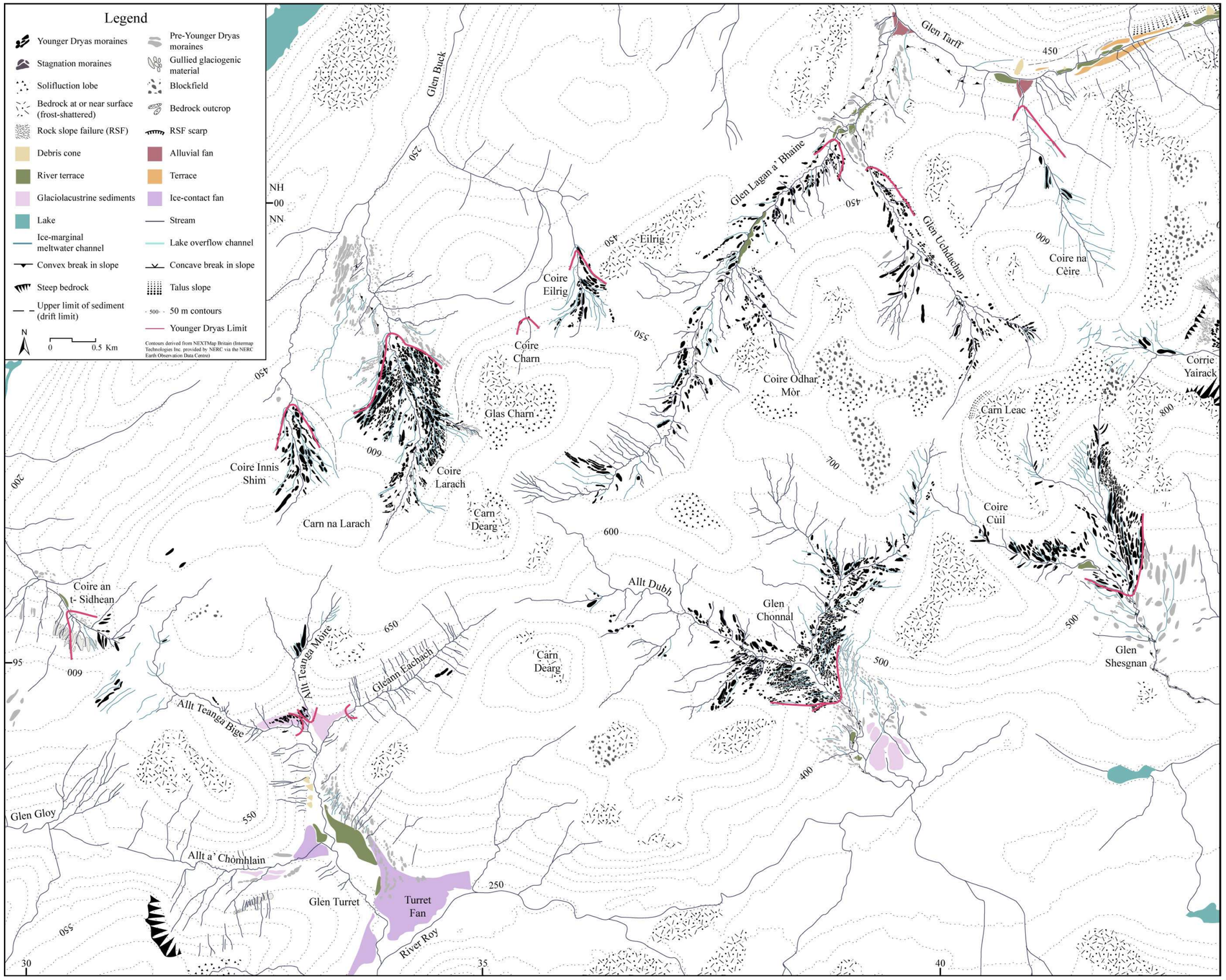

Figure 5.4. Younger Dryas glacier limits, marked by a red line, that were identified by morphostratigraphy for the western sector of the Monadhliath Mountains.

this also corresponded with the absence of any moraines further downstream. A Younger Dryas limit was difficult to identify in Coire an t- Sìdhean due to significant gullying on the valley sides and therefore the change in the number of river terraces did not correspond with the downstream termination of small sharp-crested moraines, which was much further upslope.

In Glen Turret, identification of a Younger Dryas limit was also complicated and reflects the fact that previous research has also been divided in terms of the age of glaciogenic features, such as the Turret Fan (Section 2.3.3). Sissons and Cornish (1982, 1983) argued that this fan was deposited subaqueously into the 260 m lake by an ice lobe that flowed from Glen Gloy into Glen Turret in the early part of the Younger Dryas before the formation of the 325 and 350 m lakes. This was supported by pollen stratigraphy in two cores taken from the Turret basin and the Gloy-Turret col, from which no Lateglacial pollen was recovered, indicating a Younger Dryas age (Lowe & Cairns, 1991). However, bedrock was not reached in the Turret basin and it is therefore possible that older pollen could exist below an impenetrable sand layer. In addition, older pollen could have been removed by water flowing over the Gloy-Turret col from the Gloy Lake (Lowe & Cairns, 1991). Alternatively, the Turret Fan has also been suggested to have been formed by an outlet lobe of a plateau icefield to the north of Glen Turret which advanced into Glen Turret during the early stages of the Younger Dryas (Benn & Evans, 2008) and also as an older subaerial landform that was formed by a glacier advance prior to the Younger Dryas (Peacock, 1986).

Geomorphological evidence in the Chonnal, Innis Shim and Larach catchments strongly indicates the presence of ice on the plateau areas to the north and east of Glen Turret, suggesting that an outlet lobe would have flowed into Glen Turret during the Younger Dryas, agreeing with Benn and Evans (2008). Several substantial river terraces occur in the lower part of Glen Turret, which forms a wide flat basin, whilst the upper part of the valley is much narrower, with the river constrained to a single channel. The moraines on the eastern valley side have slightly sharper crestlines in the upper part of Glen Turret than those further downstream, although all have been significantly modified by gullying. Morphostratigraphically, the change in the number of river terraces and the slight change in moraine morphology suggests that the lower part of Glen Turret was located outside the limit of Younger Dryas ice, whilst the upper part of the valley was inside the limit. However, the relationship between the river terraces is not straightforward in this valley as drainage of Lake Roy could have caused additional river terraces to form due to local base-level lowering that would have led to incision.

Placement of the Younger Dryas limit, either at the Turret Fan or further upstream where Glen Turret narrows, would mean that the terminus of the glacier would be at an altitude of 250 to 260 m. This elevation is significantly lower than the altitudes of any other Younger Dryas limits

identified in the western part of the study area, which range from 360 m to 470 m, suggesting that both of these potential limits could be unrealistically low. In order to achieve such a low altitude, it is possible that the Turret Glacier could have surged to its maximum position at the Turret Fan, either prior to lake formation or during the existence of the 260 m lake. Whilst this is plausible given evidence for the formation of extensive fans during glacier surges into water in modern glacial environments (e.g. Plassen *et al*., 2004; Ottesen & Dowdeswell, 2006; Ottesen *et al*., 2008), there is no other evidence such as flutes and crevasse-filled ridges, as would be expected in a surging glacier landsystem to support this assertion (Evans & Rea, 2003). Therefore, it is argued here that the Turret Fan and moraines within the main part of Glen Turret were deposited prior to the Younger Dryas, which is supported by the presence of older moraines outside the Younger Dryas limits within all neighbouring valleys (Appendix II). This also agrees with preliminary OSL ages that indicate that the Turret Fan is in part an older feature, although these results are not unproblematic (Lowick, 2005; S. Lowick, pers. comm., 2012). Moraines within the Allt a' Chòmhlian catchment and the Allt a' Chòmhlian fan are also assigned to an earlier phase of glaciation based on their rounded crestlines and degraded nature.

Following this interpretation, three Younger Dryas limits were identified at the head of Glen Turret, where three subaqueous grounding-line fans emanate from the Teanga Bige, Teanga Mòire and Eachach catchments, associated with deposition within the 325 m and 350 m lakes (Section 4.1.6). Moraines on top of the Teanga Bige and Teanga Mòire fans document an ice advance onto the fan surface, following lake drainage. This position is therefore argued to represent the maximum position of the ice lobes within Glen Turret, suggesting that these glaciers reached their maxima towards the end of the Younger Dryas, once the West Highlands Ice Cap had begun to retreat and lake levels in Glen Roy had dropped (see Section 6.1).

Outlet and plateau ice thickness

The area of plateau in between the outlet glaciers in the western Monadhliath Mountains is relatively narrow compared to the main central plateau area. However, all the outlet valleys in this area gently rise onto the plateau, with no backwalls separating the valleys from the plateau. Moraine retreat patterns clearly demonstrate glacier recession onto the central plateau areas, but there is little to constrain ice thickness at the maximum glacier extent in the majority of valleys. The evidence available is as follows: 1) Meltwater channels around the southwest side of Eilrig (NN 364 991), which outline the eastern margin of the Eilrig Glacier, also constrain the height of the Lagan a' Bhainne Glacier along the southern flank of Eilrig at below 530 m, whilst recessional moraines at the head of the valley suggest that the Lagan a' Bhainne Glacier was coalescent with the Larach Glacier over the 715 m col (NN 351 973). 2) An ice-marginal meltwater channel that joins the Larach and Innis Shim catchments indicates that the plateau ice

flowed over Carn na Larach (NN 335 966) and therefore had a surface altitude of over 745 m. 3) Downslope limits of talus slopes document the upper ice surface on the eastern flank of Glas Charn (NN 348 977) and the northeastern side of Carn Leac (NN 405 978), the latter of which indicates that the Uchdachan and Chonnal glaciers were coalescent over their 715 m col. 4) A drift limit on the southern flank of Carn Leac (NN 404 969) indicates the upper surface of ice flowing from the Chonnal catchment into Coire Cùil in the Shesgnan catchment (Fig. 5.4).

Key areas where there is no constraint on glacier thickness are across the Turret-Larach-Innis Shim ice divide (NN 335 965), the Turret Eachach-Chonnal Dubh ice divide (NN 353 957), the Larach-Lagan a' Bhainne ice divide (NN 351 973) and the Uchdachan-Ceire-Yairack-Shesgnan ice divides (NN 416 985). In order to constrain ice thickness in these areas further, the Benn and Hulton (2010) and Ng *et al.* (2010) models were used to evaluate possible minimum and maximum values altitudes for the ice surface across these divides, results of which are displayed in Table 5.2. The table indicates the maximum and minimum ice surfaces at each col calculated from both sides using both models, as well as a 'typical' value from the Ng *et al.* (2010) model. The table also displays the ice surface elevations that were used in the minimum, maximum and average icefield reconstructions based on a combination of the modelling results and the geomorphological constraints, which are explained within the notes section of Table 5.2.

5.2.3 Younger Dryas glacier reconstruction in the eastern Monadhliath Mountains

Younger Dryas glacier limits

For the purposes of examining plateau ice thickness across ice-divides in the eastern sector of the Monadhliath Mountains, the tributary valleys in Glen Banchor are included within this sector. Younger Dryas limits are identified within the Findhorn and Dulnain valleys, Glen Elrick, Glen na Gearra, Gleann Chaorainn, Gleann Fionndrigh, Gleann Ballach and Gleann Lochain using the criteria listed in Table 5.1 and are shown in Figure 5.5. The most conspicuous Younger Dryas glacier limits are found at the head of the Dulnain Valley and within Gleann Fionndrigh and Gleann Ballach, where a distinct change in moraine morphology coincides with the beginning of a major river terrace. In the Dulnain Valley, this also corresponds to an accumulation of sediment and gullied moraines on the northeastern valley side that have a clear upper boundary and end within 250 m of the start of the aforementioned river terrace. The upper parts of Gleann Lochain, Gleann Chaorainn and the Findhorn Valley also contain sharp-crested densely spaced moraines in contrast to larger moraines with rounded crestlines further downvalley. Whilst distinct river terraces do not begin immediately downstream of where the sharp-crested moraines terminate in these valleys, river terraces are found slightly further downvalley, supporting placement of the Younger Dryas limit at the outermost chain of sharp-crested moraines. There are very few obvious moraines within Glen Elrick, but the Younger

Table 5.2. Maximum, minimum and typical values for ice thickness at major ice divides in the western Monadhliath Mountains, modelled using the Benn and Hulton (2010) and Ng *et al*. (2010) glacier surface profiles. The table shows the average, minimum and maximum ice thickness values used in these locations based on the modelling and any geomorphological/topographic constraints as described in the notes section below. The units for *C** are $m^{1/2}$, LAB = Lagan a' Bhainne and No MA = No modern analogue.

No.	Ice Divide	Col grid ref	Col Height (m)	B&H Min (m)	B&H Max (m)	*C** Min	Ng Min (m)	*C** Typ	Ng Typ (m)	*C** Max	Ng Max (m)	Reconstructed icefields (m) Average	Min	Max
1	Larach centre - Turret	NN 335 965	691	753	790	7.0	693	8.0	740	8.7	774	763	753	774
2	Larach east - LAB	NN 351 973	715	731	775	7.3	675	8.2	714	9.9	789	761	747	775
3	LAB - Larach east	NN 351 973	715	747	801	3.8	667	5.3	782	5.4	790	761	747	775
4	Uchdachan - Ceire/Shesgnan	NN 415 987	787	839	886	6.0	764	6.7	805	8.3	898	848	837	856
5	Cèire - Yairack/Uchdachan	NN 419 987	763-87	----	----	6.9	725	7.8	773	9.6	869	845	837	857
6	Yairack - Cèire/Shesgnan	NN 419 985	787	858	945	5.1	755	6.1	812	7.3	881	848	837	857
7	Shesgnan - Uchdachan/Yairack	NN 417 982	838-45	----	----	6.7	785	7.8	841	8.8	891	848	840	856
8	Chonnal - Odhar Mòr LAB	NN 374 970	614	759	789	4.8	677	5.6	724	6.6	783	711	695	747
9	Chonnal Dubh - Turret Eachach	NN 353 957	572	694	734	No MA	----	No MA	----	No MA	----	715	708	725

No. Notes

1 Constrained to an extent by drift limit on eastern side of Carn Dearg.

2 Constrained by drift limit on eastern flank of Glas Charn.

3 Constrained by geomorphologcial evidence within Coire Larach.

4 Constrained by ice thickness at Shesgnan col.

5 Constrained by Yairack, Shesgnan and Uchdachan outlets.

6 Moraine retreat patterns in Coire Yairack indicate that Yairack Glacier was connected to plateau ice to the west.

7 Extrapolation from lateral moraines in Coire Shesgnan suggest ice did not flow over the 859 m summit to the east and the 879 m summit to the west of the col.

8 Models do not take into account that these are small tributaries that feed into the larger Chonnal and Lagan a' Bhainne glaciers. Thickness guided by geomorphology and neighbouring glacier profiles.

9 Guided by the altitude of frost-shattered bedrock on the two Carn Dearg summits to the north and south.

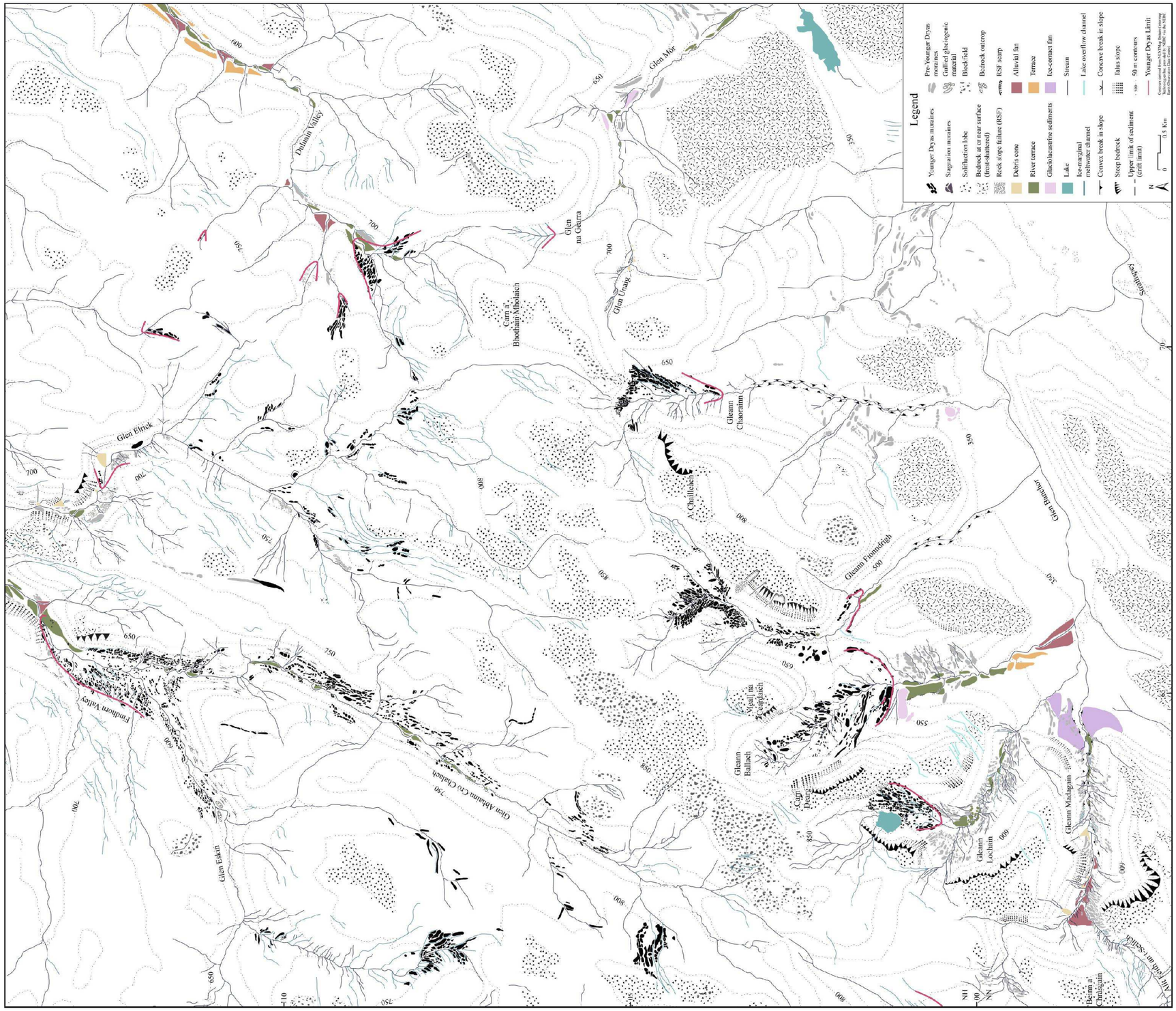

Figure 5.5. Younger Dryas glacier limits, marked by a red line, that were identified by morphostratigraphy for the eastern sector of the Monadhliath Mountains.

Dryas limit is identified where a small chain of moraines occurs on the northern valley side, beyond which a thick talus slope and river terrace begin almost immediately downstream, whilst the glacier limit can be traced upvalley by a drift limit and the upper limit of gullied glaciogenic material on the northeastern and southwestern sides respectively.

In Glen na Gearra, there is very little geomorphological evidence, other than some small ice-marginal meltwater channels. However, strong evidence for the existence of a Younger Dryas outlet glacier at the head of the River Dulnain requires that ice also flowed into Gleann na Gearra, due to ice thickness considerations for the Dulnain ice lobe. The margin of the Gearra Glacier is therefore interpreted to occur at the lowermost of the ice-marginal meltwater channels, which does coincide with a slight widening of the stream channel beyond this point. Glen Unaig comprises a deeply incised gorge that is much wider than the current stream. The valley shape, the absence of moraines, the occurrence of relict debris cones and the presence of a river terrace that continues throughout the length of the glen, becoming more significant further downstream, indicate that a glacier was not present in this glen during the Younger Dryas. It is located in close proximity to the Chaorainn Glacier (see above), which could have been a source for the large amounts of meltwater required to form the gorge. Similarly, moraines in Glen Mòr are not interpreted as relating to a Younger Dryas glacier advance due to the large rounded nature of the moraines and the presence of a river terrace that occurs inside the main river incision into the terrace and continues throughout the length of the valley. In addition, a large proportion of the source area for the Mòr Glacier is interpreted as being ice free during the Younger Dryas, since no evidence for Younger Dryas ice was found in Glen Unaig and the Younger Dryas Gearra Glacier is reconstructed to have only resided in the upper part of that glen. Therefore, the combination of this evidence suggests Glen Mòr also remained ice-free during the Younger Dryas and therefore moraines within the valley relate to an older glacial event that occurred after deposition of the terrace (discussed in Section 5.3).

In Gleann Madagain, moraines at the confluence of the Allt Féith an t-Seilich are similar in morphology to moraines that have been interpreted as Younger Dryas in age in the majority of the study area due to their close-spacing and the absence of a major river terrace in this area. However, the pattern of the moraines document ice retreat into the Allt Féith an t-Seilich catchment rather than further upstream in Glean Madagain, and, beyond this area, there are no moraines or meltwater channels in the upper part of Glean Madagain. The reconciliation of this source area with the plateau ice limit defined by the margins of the Lochain and Markie (Section 5.2.3) glaciers is difficult, since the area lies significantly south of the main plateau. This indicates that the moraines were deposited either during the Younger Dryas by an

isolated valley glacier or that they relate to an older phase of glaciation. Since a lack of plateau source area for an isolated glacier would result in a significantly lower ELA than any neighbouring glaciers, the latter is favoured here and a Younger Dryas glacier is not reconstructed in Gleann Madagain. However, the possibility still exists that plateau ice did occur during the Younger Dryas in the area around Beinn a' Chràsgain (828 m; NN 606 981), possibly connected to the main plateau icefield, but further examination of the geomorphological evidence alongside absolute dating of the moraines in Gleann Madagain is required to resolve this issue fully.

Outlet and plateau ice thickness

The lateral limits of the majority of outlets glaciers within the eastern sector of the Monadhliath Mountains are well constrained near the glacier margin, through a combination of lateral moraines (Findhorn, Elrick, Chaorainn and Lochain), ice-marginal meltwater channels (Findhorn, Elrick, Dulnain and Ballach), upper limits of sediment accumulations (Elrick, Dulnain, Fionndrigh and Ballach), downslope limits of thick talus slopes (Findhorn, Fionndrigh, Ballach and Lochain) and downslope limits of solifluction lobes (Chaorainn, Ballach and Lochain) (Fig. 5.5).

However, ice thickness over the high ground that divides the Findhorn and Elrick catchments from the Lochain, Ballach, Fionndrigh and Chaorainn catchments is difficult to establish and therefore a modelled approach was used to examine this further (Table 5.3). Areas of blockfield and solifluction lobes occur on these summits and, as discussed above, the lower boundaries of these features cannot be used to determine the upper ice surface as the blockfields could have been preserved beneath cold-based ice, and the solifluction lobes could have formed during the Holocene, since they do not have linear lower boundaries. There is also a large expanse of plateau to the north of this watershed, for which plateau icefield thickness is difficult to establish. South of Glen Elrick, there are numerous sets of ice-marginal channels that curve around the lower flanks of many of the small summits in this area, but these could not be used to delineate the upper limit of ice on the plateau, as they could document an ice-marginal position during retreat. In addition, solifluction lobes on these summits and others in the Findhorn catchment do not have sharp, linear boundaries and therefore cannot be used to identify the former ice surface. Minimum and maximum boundaries for ice thickness on the eastern part of the plateau were therefore established using the Benn and Hulton (2010) and Ng *et al*. (2010) models, whilst taking into consideration the geomorphological constraints, the results of which are displayed within Table 5.3.

Table 5.3. Maximum, minimum and typical values for ice thickness at major ice divides in the eastern Monadhliath Mountains, modelled using the Benn and Hulton (2010) and Ng *et al*. (2010) glacier surface profiles. The table shows the average, minimum and maximum ice thickness values used in these locations based on the modelling and any geomorphological/topographic constraints as described in the notes section below. The units for *C** are $m^{1/2}$ and No MA = No modern analogue.

No.	Ice Divide	Col grid ref.	Col Height (m)	B&H Min (m)	B&H Max (m)	*C** Min	Ng Min (m)	*C** Typ	Ng Typ (m)	*C** Max	Ng Max (m)	Reconstrcuted icefields (m) Average	Min	Max
1	Lochain - Findhorn	NH 625 030	915	896	944	6.0	871	6.5	898	7.8	966	920	896	944
2	Findhorn - Lochain	NH 625 030	915	--------	--------	3.5	857	4.3	945	4.8	999	920	896	944
3	Ballach - Findhorn	NH 638 039	875	850	927	5.7	825	6.6	876	7.9	949	915	890	940
4	Elrick - Fionndrigh	NH 675 057	880-911	--------	--------	No MA	--------	3.8	884	No MA	--------	915	886	944
5	Fionndrigh West - Findhorn/Elrick	NH 652 055	890-903	892	949	5.9	871	6.3	899	7.4	968	915	886	944
6	Fionndrigh East - Elrick	NH 675 057	853-884	876	912	5.3	839	5.7	868	6.5	924	895	885	930
7	Chaorainn West - Fionndrigh	NH 673 047	~865	897	923	5.1	828	6.0	876	6.8	919	875	865	895
8	Chaorainn East	NH 694 059	785-818	832	853	5.4	802	6.0	830	7.6	871	833	822	850

No.	Notes
1	Constrained by solifluction lobe to the east of Carn Dearg (945 m).
2	Constrained by geomorphological evidence in Gleann Lochain.
3	Constrained by meltwater channels and a solifluction lobe on Meall na Ceardaich (879 m).
4	Ice configuration too complex for Benn and Hulton (2010) model and not enough relief range for Ng *et al*. (2010) model.
5	Constrained to an extent by geomorphological evidence for ice thickness in Gleann Ballach and Gleann Chaorainn.
6	Constrained to an extent by geomorphological evidence for ice thickness in Gleann Ballach and Gleann Chaorainn.
7	Constrained by a solifluction lobe on the north eastern side of A' Chailleach and ice thickness in Gleann Fionndrigh.
8	Geomorphological evidence in Gleann Chaorainn and the Dulnain Valley suggests that ice did not flow over Carn a' Bhothain Mholaich (853 m).

5.2.4 Younger Dryas glacier reconstruction in the central Monadhliath Mountains

Younger Dryas glacier limits

Geomorphological evidence varies widely between valleys in the central sector of the Monadhliath Mountains, where the geomorphology of some valleys is dominated by small, densely spaced, sharp-crested moraines, such as in Glen Brien, Coire Easgainn, Corrie Yairack and Coire nam Beith, whilst other valleys contain widely spaced moraines with rounded crestlines only, i.e. Glen Talagain and Glen Mhoraire. As a result, conspicuous Younger Dryas limits were identified in Glen Brien, Coire Easgainn, Glen Killin, Coire nam Beith and Corrie Yairack only (Fig. 5.6). These were based on a clear change in moraine morphology, which often coincided with the start of a major river terrace (Table 5.1). In Glen Killin, the Younger Dryas limit was identified as a distinct accumulation of sediment and moraines that occurred on both valley sides. Younger Dryas limits were also identified within Glen Doe, Glen Markie, Coire Iain Oig, Glen Luaidhe and Coire nan Laogh based on similar criteria and the presence of ice marginal meltwater channels (Fig. 5.6; Table 5.1), although the limits were not as distinct as in the other valleys.

In Glen Talagain, a Younger Dryas limit was identified at NN 544 985, where two ice-marginal channels converge and a 10 m high fan emerges from Blackcorrie Burn. The glacier limit is supported by a few very subdued moraines at this location, a spread of boulders over this area, the absence of any river terraces and geomorphological evidence in the Killin catchment and Coire nam Beith that indicates that the area of plateau to the north of Glen Talagain would have had been covered by plateau ice during the Younger Dryas. The lack of backwall from the plateau into Glen Talagain and the relatively low level of the col between the Talagain and Killin catchments (688 m) suggests that plateau ice would have flowed into Glen Talagain during the Younger Dryas. Likewise a Younger Dryas limit is identified in Glen Gilbre based on a number of small ice-marginal meltwater channels, but supported by geomorphological evidence within the neighbouring Coire Ian Oig that suggests that ice was thick enough on the plateau to have also flowed into Glen Gilbre. Both these assertions are examined further in the section below using the two glacier surface models. A Younger Dryas limit was not identified within Glen Mhoraire due to the sparse distribution of subdued moraines with rounded crestlines and the lack of ice-marginal meltwater channels in the upper part of the valley. The configuration of plateau ice in this area, as reconstructed using the Iain Oig and Luaidhe outlet lobes also supports this interpretation that Younger Dryas ice was not present in Glen Mhoraire.

Outlet and plateau ice thickness

The lateral limits of the outlet glaciers in the central sector are predominantly not very well defined and therefore the models provide a key constraint on ice thickness in a number of areas (Table 5.4). Exceptions are in Coire Easgainn and Coire nam Beith, where ice-marginal

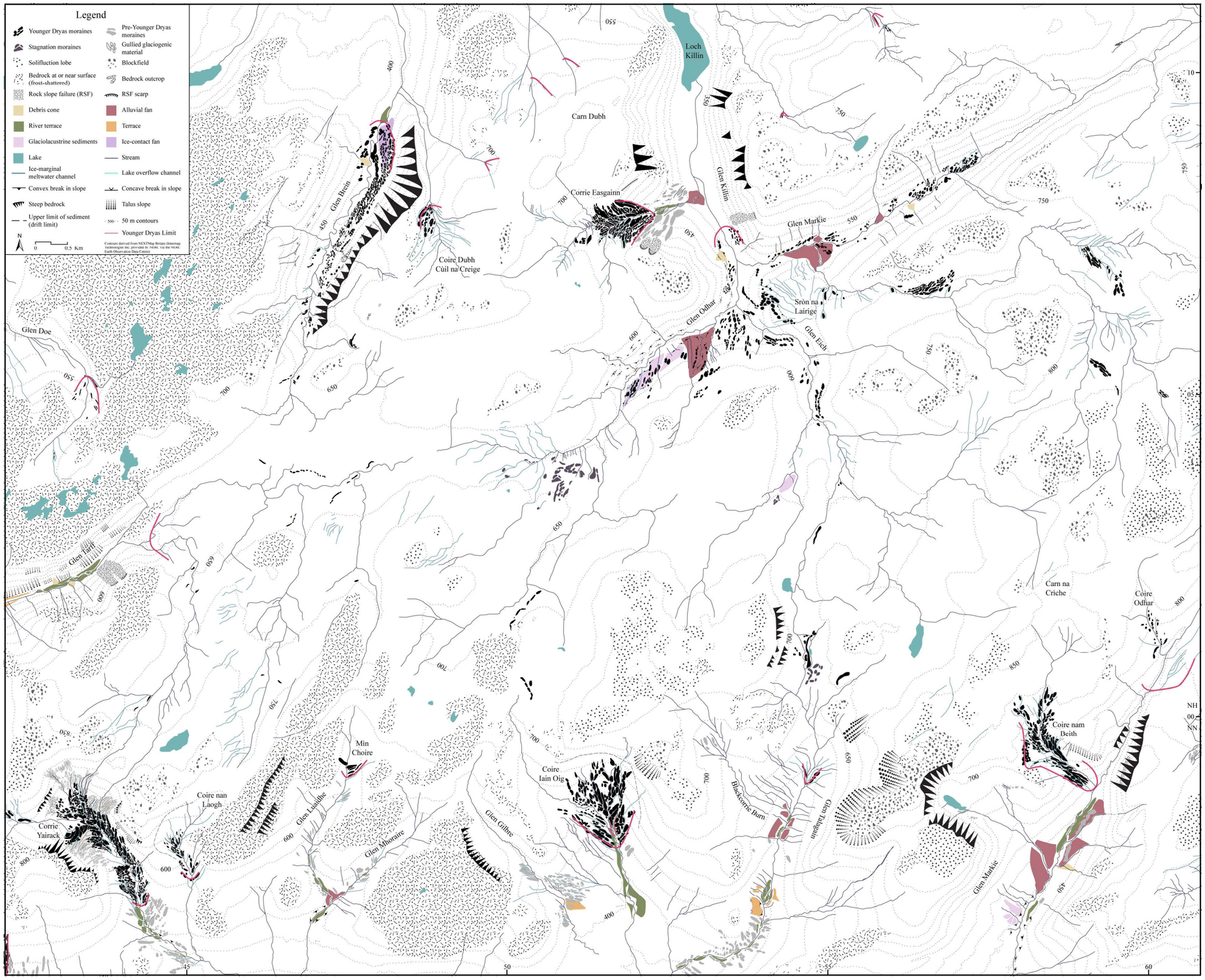

Figure 5.6. Younger Dryas glacier limits, marked by a red line, that were identified by morphostratigraphy for the central sector of the Monadhliath Mountains.

Table 5.4. Maximum, minimum and typical values for ice thickness at major ice divides in the central Monadhliath Mountains, modelled using the Benn and Hulton (2010) and Ng *et al*. (2010) glacier surface profiles. The table shows the average, minimum and maximum ice thickness values used in these locations based on the modelling and any geomorphological/topographic constraints as described in the notes section below. The units for *C** are $m^{1/2}$ and No MA = No modern analogue.

No.	Ice Divide	Col grid ref.	Col Height (m)	B&H Min (m)	B&H Max (m)	*C** Min	Ng Min (m)	*C** Typ	Ng Typ (m)	*C** Max	Ng Max (m)	Reconstrcuted icefields (m) Average	Min	Max
1	Brein - Tarff	NH 466 042	636	689	743	No MA	------	No MA	------	5.2	745	697	689	725
2	Easgainn - Carn Dubh	NH 500 075	748	781	820	5.1	706	5.4	723	6.3	772	793	781	815
3	Killin - Iain Oig	NH 504 008	707	------	------	3.8	683	4.5	745	5.3	819	793	763	816
4	Iain Oig - Killin	NH 504 008	707	763	816	4.8	717	5.1	735	5.6	765	793	763	816
5	Killin - Talagain	NH 546 015	688	------	------	3.8	651	4.5	709	5.2	766	754	725	776
6	Talagain - Killin	NH 504 008	688	715	776	No MA	------	No MA	------	No MA	------	754	725	776
7	Nam Beith - Carn na Crìche	NH 585 020	862	881	920	6.3	816	7.0	854	8.4	932	900	881	920
8	Laogh - Tarff	NN 457 990	756	787	824	5.2	768	5.4	776	6.0	801	805	787	824
9	Yairack East - Tarff	NN 440 993	777-803	816	841	6.0	768	6.8	809	7.7	855	825	816	851

No. Notes

1 Constrained to an extent by the configuration of ice in Glen Tarff.

2 Constrained by moraines and ice-marginal channels within Coire Easgainn.

3 Ice thickness based on the results of Benn and Hulton (2010) model for the Iain Oig Glacier and Ng *et al*. (2010) model for the Killin Glacier, which correspond well.

4 Ice thickness based on the results of Benn and Hulton (2010) model for the Iain Oig Glacier and Ng *et al.* (2010) model for the Killin Glacier, which correspond well.

5 Min ice surface possible is 725 m based on plateau topography & geomorphological evidence. Other ice surfaces guided by Benn & Hulton (2010) model for Talagain.

6 Min ice surface possible is 725 m based on plateau topography & geomorphological evidence. Other ice surfaces guided by Benn & Hulton (2010) model for Talagain.

7 Upper ice surface guided by Benn and Hulton (2010) model which fits inside the range identified using Ng *et al*. (2010).

8 Ice thickness based on the results of Benn and Hulton (2010) model, as Ng *et al*. (2010) model produces very thin ice over the col.

9 Moraines indicate that Yairack Glacier was sourced from the plateau to the east. Average glacier thickness is based on the lower limits of blockfield on both sides.

meltwater channels on both sides of Coire Easgainn document the margin of ice flowing from the plateau into the valley, whilst a lateral moraine across the backwall of Coire nam Beith constrains the upper ice limit at this location and indicates that ice flowed from the plateau into the corrie from the north. Ice-marginal meltwater channels within Glen Markie also delimit the eastern margin of the Markie Glacier, but its connection with the Beith Glacier to the west is unclear. In Glen Killin, the upper limit of the sediment accumulation can be followed upvalley into Glen Markie (Killin) on the eastern side and Glen Odhar on the western side, indicating that the Markie (Killin), Odhar and Eich tributary glaciers coalesced a short distance from the terminus. Ice-marginal meltwater channels on Sròn na Lairige also constrain ice thickness around this confluence to an extent, but there is little to constrain ice thickness further up any of these valleys. Finally, a small talus slope on the eastern side of Corrie Yairack and a drift limit in Coire nan Laogh provide some constraint on ice thickness in this area.

The Benn and Hulton (2010) and Ng *et al*. (2010) models were used to further examine the thickness of a number of the central sector ice lobes and to establish the thickness of plateau ice at ice divides. Of particular interest was the thickness of the Brein Glacier, its connection to plateau ice to the east and the upper surface of ice at the ice-divide with the Tarff Glacier (NH 466 042), the thickness of ice on the Carn Dubh plateau above Coire Easgainn (NH 500 075), ice thickness at the ice divide separating the Killin Glacier from the Talgainn and Iain Oig glaciers (NH 546 015 and NH 504 008), the upper ice surface across the Laogh - Tarff (NN 457 990) and Yairack - Tarff (NN 440 993) ice divides.

5.2.5 3D reconstruction of the Younger Dryas Monadhliath Icefield

The evidence described above indicates that the Younger Dryas Monadhliath Icefield consisted of two coalescent plateau icefields that occurred over the western and central plateaux in the Monadhliath Mountains. The icefield was reconstructed in ArcGIS using the Younger Dryas glacier limits identified from morphostratigraphy (Table 5.1, Figs. 5.4, 5.5, 5.6) and a combination of an extrapolated and modelled approach to reconstruct ice thickness in the outlet valleys and on the plateau. Where there was little geomorphological evidence to constrain ice thickness, minimum and maximum boundaries for ice thickness were established and an average ice thickness calculated (Tables 5.2, 5.3, 5.4). These ice thickness values were then used to produce a minimum, maximum and average reconstruction for the Monadhliath Icefield in order to try to quantify some of the uncertainty surrounding a large number of areas on the plateau.

Ice contours were drawn at 50 m intervals to depict ice thickness. The contours were hand drawn and their position estimated using the underlying topography, but some were also guided

by the surface profiles produced by the Benn and Hulton (2010) model, where ice thickness was particularly uncertain. Following the shape of contours on modern glaciers, the contours were drawn so that they curved downglacier in the estimated ablation zone and curved upglacier in the estimated accumulation zone, whilst more or less straight across in the zone around the estimated ELA. The estimated ablation and accumulation zones will have some bearing on the ELAs calculated, since the curvature of the contours controls the size of each area used to calculate the ELAs (see Section 5.4). However, this is a standard procedure for drawing glacier contours in reconstructions (e.g. Gray, 1982; Benn & Ballantyne, 2005; Carr & Coleman, 2007; Ballantyne, 2002a, 2007a, b; Lukas & Bradwell, 2010) and its influence on the calculated ELAs is likely to be minimal, as experimenting with straight contours has shown (I.D. Barr, pers. comm., 2011). In areas where the minimum, maximum and average reconstructions varied the contours were also drawn so that the maximum reconstruction contours depicted thicker ice than the average and minimum reconstructions. The minimum, maximum and average reconstructions are shown overlain on each other for comparison in Figure 5.7. The main areas of difference between the three reconstructions are on the high ground to the north of the Glen Banchor tributaries, the area to the south of the Killin Glacier limit and the plateau area above Glen Turret. The average reconstruction of the Younger Dryas Monadhliath Icefield covers an area of approximately 280 km^2 (Figure 5.8) and was used in subsequent calculations and analysis in Sections 5.4 and 5.5.

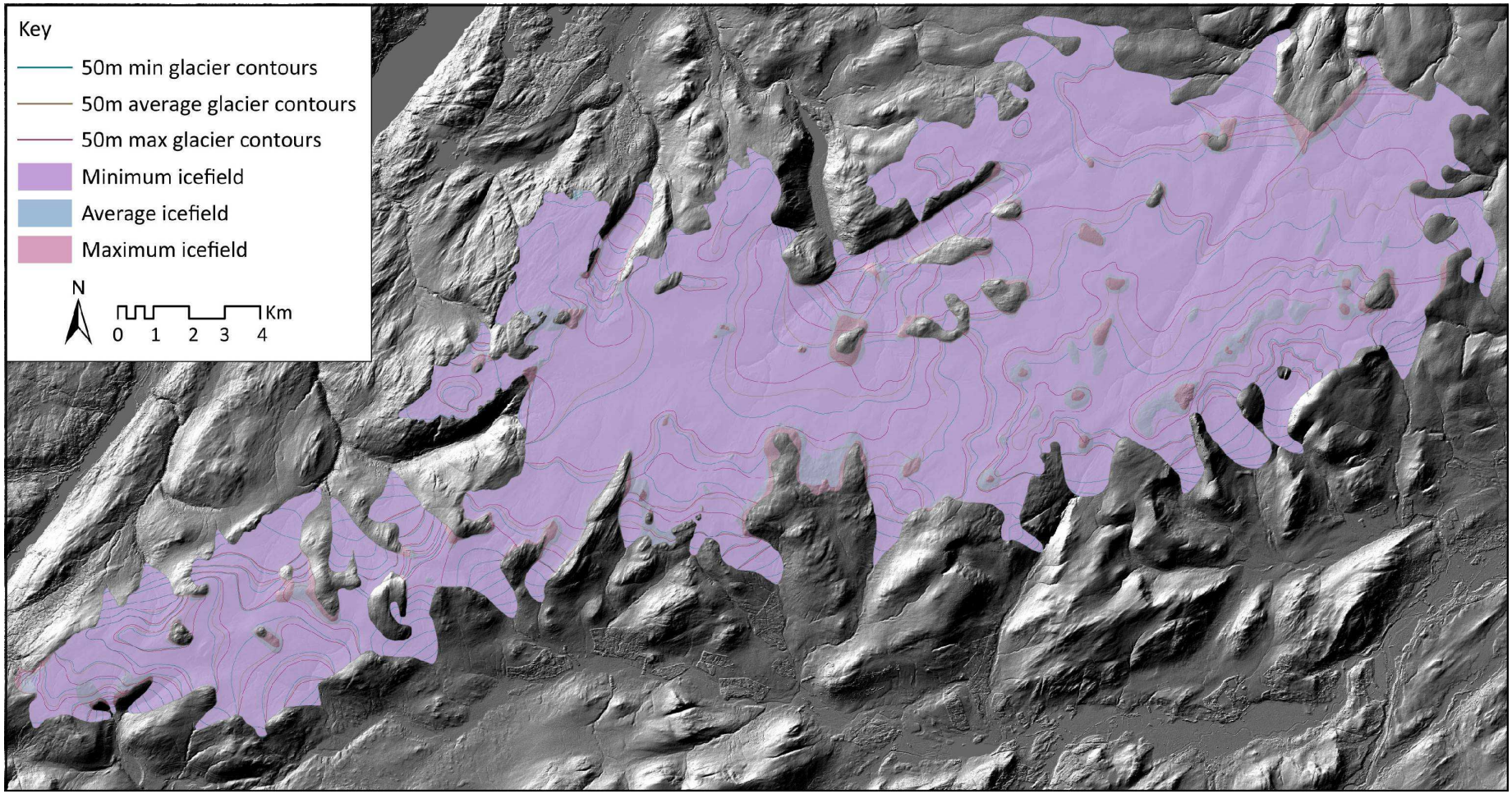

Figure 5.7. The minimum, average and maximum icefields, which were overlain on top of each other in order to illustrate the differences between the three reconstructions. NEXTMap DSM hillshade model from Intermap Technologies Inc. provided by NERC via the NERC Earth Observation Data Centre.

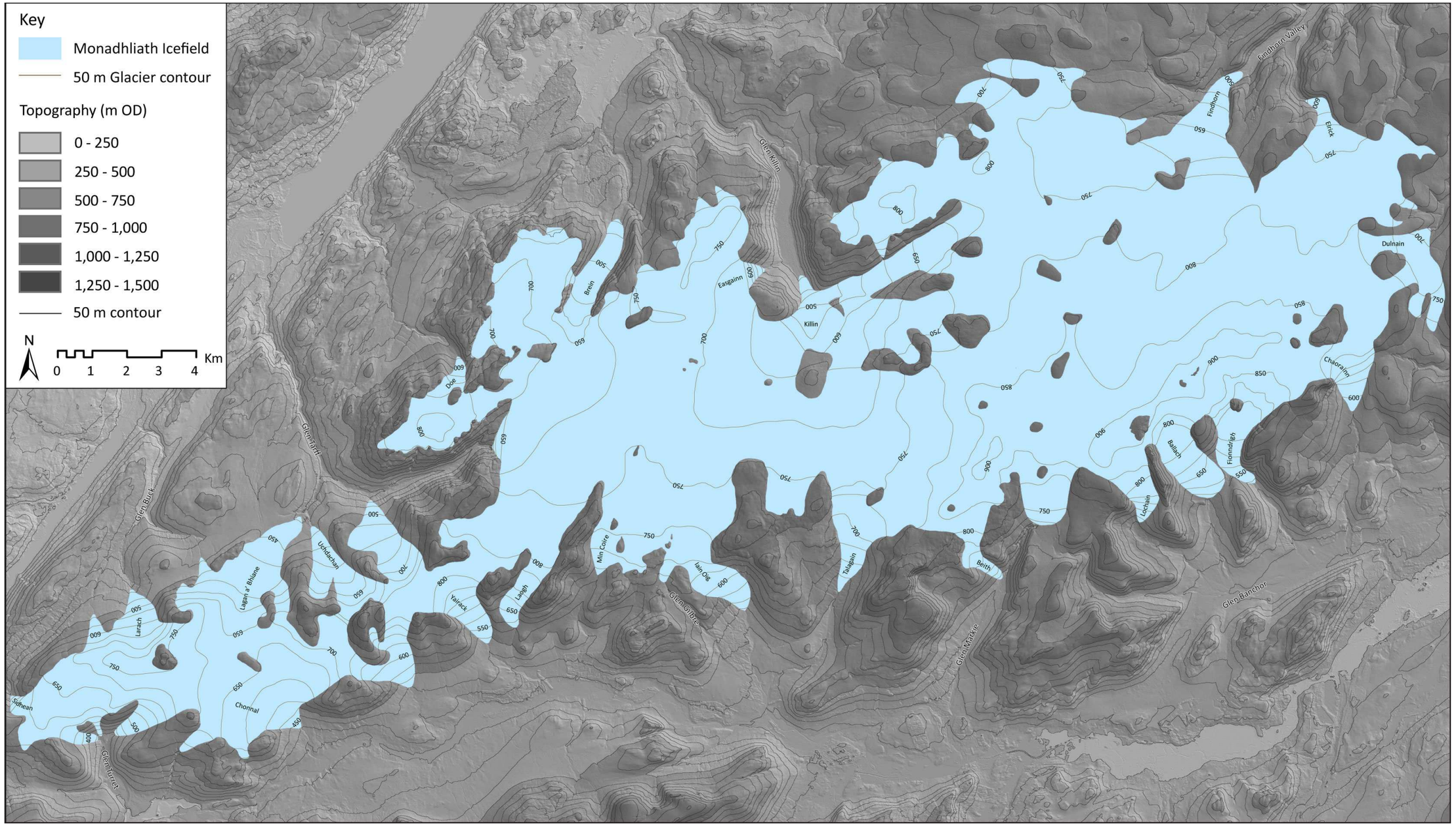

Figure 5.8. The reconstructed 'average' Younger Dryas Monadhliath Icefield, which covers an area of approximately 280 km^2. Elevation data was derived from the NEXTMap Great Britain DTM and overlain on a hillshade model, also derived from NEXTMap (Intermap Technologies Inc. provided by NERC via the NERC Earth Observation Data Centre).

5.3 Last Glacial-Interglacial Transition events prior to the Younger Dryas

Identification of the limits of a Younger Dryas icefield mid-way up the majority of valleys indicates that glaciogenic landforms in the lower parts of the Monadhliath valleys relate to an older phase of glaciation, which is argued here to have occurred during deglaciation from the LGM. A relative sequence for events relating to this time is discussed below and provides a chronological framework that now requires testing through absolute dating methods.

As discussed in Section 2.3, the current understanding of deglacial events in eastern Scotland suggests that regional ice retreated earlier in Strathspey than in the Great Glen (Fig. 2.5). This is indicated by radiocarbon dates on organic material from Loch Etteridge (13 150 ± 350 ^{14}C BP (Sissons & Walker, 1974; Walker, 1975) and 12 930 ± 40 ^{14}C BP (Everest & Golledge, 2004)) that indicate that the site was ice-free between 15 814 ± 603 and 15 536 ± 355 cal. yr BP (Everest & Kubik, 2006). The presence of lateral moraines and ice-marginal channels on the northern side of the Spey Valley to both the east and west of Glen Banchor (Section 4.4) indicates active retreat of the Stathspey Glacier in this area, as previously reported by Phillips and Auton (2000), who found evidence for an oscillating ice margin at Raitts Burn to the east of Glen Banchor.

At the same time, evidence described in Sections 4.3 and 4.4 demonstrates that this ice lobe dammed many of the southern valleys of the Monadhliath Mountains, creating a series of ice-dammed lakes within Glen Markie, Gleann Lochain, Gleann Ballach, Gleann Fionndrigh, Gleann Chaorainn, Gleann Beinne, Glen Mòr and possibly Glen Gilbre, Glen Iain Oig, Glen Talagain and Gleann Madagain. Evidence for the formation of these lakes is in the form of lacustrine sediments in many of the valleys and channels that occur across the interfluves of the Glen Banchor tributary valleys and document water exiting one lake into another in a direction from west to east (Section 4.4) (Fig. 4.62).

The formation of ice-dammed lakes within the southern tributary valleys indicates that at least the lower parts of these valleys were ice-free during this time. In Glen Mòr, bedding within the thick sequence of diamicton, interpreted as a succession of subaqueous debris flows within a grounding-line fan (Section 4.3.5), dips in a downvalley direction, suggesting that it was sourced from a local glacier that was still present in the upper part of Glen Mòr. Whether small local glaciers were also contemporaneous with the ice-dammed lakes in the other tributary valleys is unknown as there is no evidence in support of this, although subsequent glacial advances could have removed any evidence.

The formation of ice-dammed lakes at the margin of the Strathspey Glacier, with possible

interactions from local ice, depicts a similar scenario to that proposed by Everest and Kubik (2006) for deglacial events on the southern side of the Spey Valley, where glaciolacustrine sediments document unzipping of the regional ice in Strathspey from the local Cairngorms Ice Cap (Brazier *et al*., 1998; Everest & Golledge, 2004; Everest & Kubik, 2006). Everest and Kubik (2006) proposed, based on analysis of varves, that the ice-dammed lakes existed for up to 1000 years, suggesting the Strathspey glacier remained in a relatively stable position during this time before rapid deglaciation occurred to fulfil the required ice-free conditions at Loch Etteridge by ca. 15.8 to 15.5 ka BP. The close proximity of the Cairngorm ice-dammed lakes to those in Glen Banchor (< 25 km downvalley), suggests that the ice-dammed lakes in Glen Banchor formed at a similar time, or shortly afterwards. The deposition of a large volume of sediment into Gleann Ballach and the deeply incised nature of the majority of channels, suggests that the lakes were relatively stable features for a time. Research by Phillips and Auton (2000) on a sequence of varves by Raitts Burn immediately to the east of Glen Mòr, indicates that an ice-dammed lake was in existence in this valley for ca. 600 years, which provides an estimate for the length of time for which the Glen Banchor ice-dammed lakes existed. The down-valley location of Glen Banchor relative to Loch Etteridge also indicates that this area was ice free before ca. 15.8 to 15.5 ka BP.

Moraines overlying the glaciolacustrine terrace in Glen Mòr suggest that a readvance of the Mòr Glacier occurred after drainage of the ice-dammed lake. Based on morphostratigraphy, the moraines are interpreted as older than Younger Dryas in age (Section 5.2.3), indicating that a re-advance must have occurred following lake drainage, but prior to the Younger Dryas. If regional ice blocking drainage in Glen Mòr had retreated by ca. 15.8 to 15.5 ka BP, this potentially leaves up to 1000 years for an advance to occur before the climate rapidly warmed at the start of the Lateglacial Interstadial (GI-1; Fig. 2.3). Whilst it is possible that glacier advances also occurred during GI-1 (e.g. Bradwell *et al.*, 2008; Stoker *et al*., 2009), the end of GS-2 seems the most likely time for this readvance to have occurred, as suggested for the Wester Ross Readvance by Ballantyne and Stone (2011). Absolute dating is required to examine this further, however.

Further evidence for a readvance of local glaciers following deglaciation of regional ice in Strathspey is found in Gleann Madagain and Gleann Lochain, where a large number of moraines are found that document ice retreat into the heads of each valley, but were interpreted as older than Younger Dryas (Section 5.2.3). These moraines extend to the mouths of both valleys and an arcuate loop of moraines just outside Gleann Lochain indicates that the Lochain Glacier debouched into Glen Banchor as a piedmont lobe. These moraines must post-date the ice-damming event by the Strathspey Glacier since this regional ice would have been present in

the lower parts of Gleann Madagain and Gleann Lochain in order to dam drainage in the other Glen Banchor tributaries (Fig. 4.62). Moraines that are older than Younger Dryas also occur in the lower part of Gleann Ballach. However, the presence of the ridge of lacustrine sediments half way up the valley indicates that these moraines must have been deposited before the ice-dammed lake in Gleann Ballach was formed. The Gleann Ballach moraines are heavily dissected and less well preserved than those in Gleann Lochain and Gleann Madagain supporting this chronology. However, the configuration of the margin of the Strathspey Glacier that would be required to allow preservation of these features, yet form the ice-dammed lakes is unclear (see Fig. 4.62). In addition, it also seems anomalous that an advance of a similar magnitude to those in Gleann Lochain and Gleann Madagain did not occur in Gleann Ballach. This suggests that the configuration of ice on the plateau was different to that reconstructed for the Younger Dryas (Section. 5.2) and suggests a different climate or glacier dynamics during this period, possibly reflecting different ice accumulation centres on the plateau.

Evidence for an older more extensive plateau icefield than that reconstructed during the Younger Dryas is also found within a large proportion of the valleys in the Monadhliath Mountains, particularly those in the south of the study area. These moraines also document ice retreat upvalley towards the plateau, suggesting that as the regional ice retreated westwards through the Great Glen and Spey Valley, local plateau ice regained dominance in the region as an independent source area. In the majority of valleys, there are no clear end moraines, with exceptions in Gleann Madagain and Gleann Lochain, as discussed above, and therefore it is unknown whether the majority of moraines were deposited following a readvance of local outlet glaciers or whether some document continued retreat from the LGM only, following separation from regional ice. The Turret Fan, interpreted as older than Younger Dryas in this study (Section 5.2.2), and large moraines in other valleys, such as Corrie Yairack, Glen Luaidhe and Glen Elrick, indicate that there were at least major stillstands during retreat, if not readvances of all local glaciers.

To the contrary, evidence for the existence of extensive local glaciers prior to the Younger Dryas is not observed in the north-facing outlet valleys of Glen Doe, Glen Brien and Glen Killin. As in Strathspey, sedimentary evidence in the area around Loch Killin indicates that advance of an ice lobe from the Great Glen into Glen Killin blocked drainage and created a lake, as previously suggested by Charlesworth (1955) (Sections 4.2.5 to 4.2.7) (Fig. 4.38). The creation of the lake is argued to have been caused during a glacier advance rather than simply a stage of retreat due to evidence for glacier overriding and glaciotectonism of lacustrine sediments within Sections LK1 and LK2 (Section 4.2.6).

At its maximum, the lake level was 642 m and drained to the west over the col between Glen Markie (Killin) and Glen Eskin, submerging areas of the plateau immediately to the south of Glen Killin. A thick sequence of diamictic sediment within Glen Odhar and a Gilbert-type delta in the Eich catchment indicate the continued presence of ice on the plateau at the time the maximum lake level existed. The extensive area that the lake covered, however, indicates that ice on the Monadhliath plateau in this area was severely restricted, exemplified by the required absence of ice in the Findhorn Valley, in order to allow drainage of the lake through Glen Eskin. Reconstruction of the approximate dimensions and location of an ice lobe in Glen Killin that would be required to create a lake level of 642 m indicates that any remaining local plateau ice was probably confluent with the eastern margin of the Ness Glacier or may have been overwhelmed by this ice lobe (Fig. 4.38). The juxtaposition of local and regional ice in this area and the dominance of each remains an interesting avenue for future work in the region (Section 7.5).

Moraines found overlying the terraces within Glen Odhar are interpreted as Younger Dryas in age, unlike within Glen Mòr to the south. The absence of evidence for a readvance of local plateau ice in the period between lake drainage and the Younger Dryas, as at Glen Mòr, potentially suggests that either the climate or internal glacier dynamics in this area did not allow a local glacier readvance following lake drainage, probably as a result of diminished ice extent on the plateau. However, evidence for more extensive ice is found in Coire Easgainn and Coire Dubh Cùil na Creige and any later ice advance during the Younger Dryas may have removed evidence of a previous advance if it was less extensive (*cf.* Kirkbride & Brazier, 1998).

Bathymetric surveys from Loch Ness reveal that ice retreat in the Great Glen was punctuated by a number of stillstands and small readvances (Turner *et al*., 2012). Current understanding of ice sheet deglaciation in the area indicates that ice in the Great Glen may have survived for longer than that in the Spey Valley and a substantial lobe of ice may have still existed at 15 ka BP (*cf.* Clark *et al*., 2010). Damming of drainage in Glen Killin is therefore likely to have occurred later than on the southern side of Monadhliath Mountains. This asymmetric deglaciation of regional ice could explain the reason why there is no evidence for more extensive local glaciers in Glen Killin, Glen Brien and Glen Doe, since local glaciers here were unable to expand due to the continued presence of either regional ice or ice-dammed lakes.

However, alongside evidence for more extensive pre-Younger Dryas local glaciers in Coire Easgainn and Coire Dubh Cùil na Creige, there is similar evidence for extensive pre-Younger Dryas local glaciers in the north-facing valleys of Coire Larach and Glen Lagan a' Bhainne-Uchdachan. This is an area to the west of Glen Killin, from which regional ice in the Great

Glen would have retreated later, most likely causing ice dammed lakes in the tributary valleys, although no evidence was found to support this. Similar to the rest of the study area, it is unknown whether the pre-Younger Dryas moraines in these valleys were deposited following a readvance of local glaciers or whether they document continued ice retreat following separation from regional ice in the Glen Glen. A possible reason is that plateau ice in the western part of the study area became separate from ice on the main Monadhliath plateau and was able to act as an independent source area much later into the end of GS-2 and possibly into GI-1 (Fig. 2.3) than the main Monadhliath Icefield. This is supported by evidence for an early deglaciation of the Findhorn Valley in the east (drainage of Glacial Lake Killin) to suggest that deglaciation occurred asynchronously across the Monadhliath plateau from east to west, reflecting a similar pattern of deglaciation to that of the Scottish Ice Sheet.

5.4 Younger Dryas Climate in the Monadhliath Mountains

The reconstruction of a Younger Dryas plateau icefield in the Monadhliath Mountains allows inferences about regional palaeoclimate to be made. This exercise is not only useful for understanding past fluctuations in climate on a local to regional scale, but also provides a means of comparing the reconstructed ice mass with neighbouring ice-masses, in this case those in Creag Meagaidh (Finlayson, 2006), Drumochter (Benn & Ballantyne, 2005), the Cairngorm Mountains (Sissons, 1979e) and the central and southeastern Grampians (Sissons, 1972, 1974b), as well as those further afield in Scotland. The following two sections focus on ELA and palaeoprecipitation calculations based on the dimensions of the reconstructed Younger Dryas Monadhliath Icefield, which will then be used to discuss regional climate patterns in Section 6.2.

5.4.1 Equilibrium Line Altitude Reconstruction

The equilibrium line altitude (ELA) is the altitude on a glacier's surface at which accumulation is equal to ablation. The line is a partially theoretical construct since in reality it rarely occurs as a single line across the glacier surface at the same altitude (Oerlemans, 2001; Benn & Evans, 2010). However, the ELA provides a useful indication of the altitude at which mass balance on a glacier is equal to zero. As a result, the ELA is closely related to the glacier's annual net mass balance whereby, if this is positive, the ELA will be lower than the previous year and, conversely, if mass balance is negative, the ELA will be higher (Benn & Evans, 2010). If a glacier is in equilibrium with the climate it has a net mass balance of zero and its ELA is referred to as a steady-state ELA. However, the steady-state ELA could be argued to be almost entirely theoretical, since glaciers rarely have an annual mass balance of zero (Benn & Evans, 2010).

Due to this relationship with mass balance, the ELA is consequently very sensitive to variations

in winter precipitation (correlated to accumulation) and summer air temperature (correlated to ablation), and hence changes in the ELA provide an important indicator of fluctuations in local to regional climate (Benn & Evans, 2010). Although the altitude of the equilibrium line can be affected by local climate conditions, changes in mass balance have been found to correlate on a regional scale (Letreguilly & Reynaud, 1989), and therefore the ELA is used frequently in palaeo-glacier reconstructions as an important tool for examining regional palaeoclimate (e.g. Ballantyne, 2002a, 2007a, b; Benn & Ballantyne, 2005; Bakke *et al*., 2005a, b; Rea & Evans, 2007; Lukas & Bradwell, 2010; Finlayson *et al*., 2011). ELAs calculated for palaeo-glacier reconstructions are usually referred to as steady-state ELAs (Benn *et al*., 2005), since an assumption is made that the reconstructed glacier was in equilibrium with climate at the time it was at its maximum position. However, like the steady-state ELA itself, this is notional since it is unlikely that all glaciers reconstructed within a particular area were in equilibrium, as the maximum position could also represent a short-lived advance and because individual outlets are unlikely to have reached their maxima simultaneously.

A number of methods have been suggested to calculate the ELAs of former glaciers including Toe to Headwall Altitude Ratio (THAR), Maximum Elevation of Lateral Moraines (MELM), the Median Elevation of Glaciers (MEG), the Accumulation Area Ratio (AAR) (Porter, 1975; Torsnes *et al*., 1993; Benn & Lehmkuhl, 2000), the Area Weighted Mean Altitude (AWMA) (Sissons, 1974b) and the Area Altitude Balance Ratio (AABR) (Furbish & Andrews, 1984; Benn & Gemmell, 1997; Osmaston, 2005). The main three used in previous reconstructions of Younger Dryas glaciers in Scotland are AABR, AAR and AWMA. The AABR method is becoming increasingly used in preference to the AAR method since it takes into account both glacier hypsometry and incorporates different accumulation and ablation gradients through the use of a balance ratio. This gives it an advantage over both the AWMA and the AAR methods, which are static methods. Although the AWMA takes into account hypsometry by using areas between specific contour intervals, it assumes the same ablation and accumulation gradients. On the other hand, the AAR takes no account of hypsometry or the balance ratio (Osmaston, 2005) by assuming that "all parts of the accumulation and ablation areas contribute equally to the mass balance", whereas in reality net accumulation and ablation have been shown to both increase with distance from the ELA (Benn & Ballantyne, 2005, p. 588). As a result the AABR is currently considered the most reliable method for calculating palaeo-ELAs (Benn & Ballantyne, 2005; Osmaston, 2005; Rea, 2009). However, a key assumption it makes is that both the accumulation and ablation gradients are linear, which may cause errors if they were not linear, a factor that remains unknown in glacier reconstruction. The majority of accumulation and ablation gradients of glaciers within a dataset of sixty-six modern glaciers examined by Rea (2009) fulfilled this assumption, however, indicating that the assumption is likely to hold true

for the majority of reconstructed glaciers.

The AABR method can only be considered representative if an appropriate balance ratio is used (Rea, 2009). The balance ratio describes the relationship between the accumulation gradient and the ablation gradient, and for the AABR approach is defined as follows:

$$\mathrm{AABR} = \frac{b_{\mathrm{nab}}}{b_{\mathrm{nac}}} = \frac{Z_{\mathrm{ac}}A_{\mathrm{ac}}}{Z_{\mathrm{ab}}A_{\mathrm{ab}}} \quad (5)$$

where b_n is the net mass balance gradient for the accumulation ($_{ac}$) and the ablation areas ($_{ab}$), A is area and Z is the area-weighted mean altitude, which is measured positively from the ELA for both the accumulation and ablation areas.

The equation weights accumulation and ablation areas according to their distance from the ELA so that greater accumulation occurs with increasing altitude and greater ablation occurs with decreasing altitude away from the ELA (Rea, 2009). Glaciers with equal accumulation and ablation gradients will therefore have an area altitude balance ratio of 1, whilst glaciers in polar regions will have low balance ratios due to low ablation gradients and tropical glaciers, which have high ablation rates will have high AABRs (Benn & Gemmell, 1997; Benn & Lehmkuhl, 2000).

Previous palaeoglaciological research in Scotland has used AABRs of 1.67, 1.8 and 2.0 following Benn and Gemmell (1997), where a value of 2.0 was thought to be representative of maritime mid-latitude glaciers and 1.8 was representative of glaciers in Alaska (Furbish & Andrews, 1984), since mid- to high-latitude glaciers have previously been recognised as potential modern analogues for Scottish Younger Dryas glaciers (Benn & Gemmell, 1997). More recent work by Rea (2009) used a much larger database of modern glaciers to further investigate their balance ratios. Of the twenty-three mid-latitude maritime glaciers examined in the study, the average AABR was 1.9 ± 0.81, which coincidentally is close to the AABR of 2.0 previously used. Also, within this dataset, the ten glaciers from western Norway produced an average regional AABR of 1.5 ± 0.4. This AABR value may also be applicable for ELA reconstructions in Scotland since Norway has been suggested by Benn & Lukas (2006) as a potential modern analogue for Younger Dryas glaciation in Scotland. Critically, however, although the maximum extent of the icefield probably corresponds approximately to the coldest part of the stadial (see discussion in Section 6.1), ice build up is likely to have occurred in the more temperate earlier part of the stadial possibly commencing in GI-1 (Golledge *et al*., 2007; Bradwell *et al*., 2008; Coope & Rose, 2008), meaning that the suitability of the balance ratios identified above for Scottish Younger Dryas ice masses remains uncertain (*cf.* Lukas &

Bradwell, 2010).

Although the Rea (2009) dataset provides the most extensive range of balance ratios from a range of glacier types, the majority of these glaciers were in retreat, rather than in equilibrium or advancing as assumed for the maximum extent of reconstructed glaciers (Rea, 2009), which could introduce further errors in palaeo-ELA calculation. In addition, the errors on some of the AABRs for particular regions in the Rea (2009) dataset are significant. Critically, the error for the mid-latitude glacier AABR of 1.9 is ± 0.81, demonstrating the wide range of balance ratios found for glaciers at similar latitudes. In spite of these errors and uncertainties, the Rea (2009) dataset provides the largest number of balance ratios for mid-latitude and Norwegian glaciers at present and therefore provides the most representative AABRs for calculating AABR ELAs in the study area.

ELAs of the average Monadhliath Icefield reconstruction and its outlet glaciers were calculated using balance ratios of 1.67, 1.8, 2.0 as in previous studies, alongside 1.9 ± 0.81 and 1.5 ± 0.4 for mid-latitude and Norwegian glaciers respectively from the Rea (2009) dataset. ELAs were also calculated for the minimum and maximum Monadhliath Icefield reconstructions in order to consider the errors associated with each ELA value. Errors associated with the balance ratios of 1.9 ± 0.81 and 1.5 ± 0.4 were also taken into consideration using the minimum and maximum reconstructions. The ELAs are presented in Table 5.5 including the errors associated with them. ELAs calculated from a balance ratio of 1.9 ± 0.81 are considered the most representative ELAs, since this balance ratio encompasses all mid-latitude glaciers in the dataset, including the data from western Norway. The error range is also large, which means that the errors incorporate the ELAs calculated for the other balance ratios, providing the most all-encompassing value. Using this AABR value, the ELA for the average Monadhliath Icefield is 714 ± 25 m, calculated using areas within 50 m contour intervals. ELAs were also calculated for outlet glaciers that had an altitudinal range that spanned four or more 50 m contour intervals. The ELAs of outlet glaciers calculated using an AABR of 1.9 ± 0.81 range from 560 ± 20 m in the northwest to 814 ± 8 m in the southeast (Table 5.5).

ELAs were also calculated using the AAR and AWMA methods to enable comparison with previous studies in Scotland that have not used the AABR method (e.g. Sissons & Sutherland, 1976; Sissons, 1979d; Ballantyne & Wain-Hobson, 1980) and are also presented in Table 5.5. Following this previous literature, accumulation area ratios of 0.5 and 0.6 were used, since mid- to high-latitude glaciers without significant debris cover tend to have AARs within the range of 0.55 to 0.65 (Benn & Ballantyne, 2005). In the same way as for the AABR ELA, the ELAs were calculated using the average Monadhliath Icefield reconstruction, with the minimum and

Table 5.5. Equilibrium line altitudes for the Monadhliath Icefield and major outlet glaciers, calculated using the AABR, AAR and AMWA approaches. Errors are calculated from errors associated with the AABRs of 1.5 and 1.9 (Rea, 2009) and the maximum and minimum icefield reconstructions.

Glacier	AABR 1.5	AABR 1.67	AABR 1.8	AABR 1.9	AABR 2.0	AAR 0.5	AAR 0.6	AMWA
Western Valleys								
Sidhean	576 ± 14	573 ± 23	571 ± 20	570 ± 15	569 ± 20	562 ± 6	550 ± 15	586 ± 18
Innis Shim	654 ± 11	651 ± 1	648 ± 1	646 ± 20	644 ± 2	660 ± 0	635 ± 5	667 ± 2
Larach	631 ± 19	626 ± 6	623 ± 6	620 ± 31	618 ± 5	635 ± 10	605 ± 8	649 ± 7
Teanga Bige Turret	592 ± 15	589 ± 6	587 ± 5	585 ± 22	583 ± 6	590 ± 8	580 ± 13	604 ± 6
Teanga Mor Turret	648 ± 17	645 ± 9	643 ± 9	641 ± 24	640 ± 10	635 ± 15	622 ± 15	658 ± 10
Eachach Turret	634 ± 19	630 ± 5	627 ± 5	625 ± 28	622 ± 5	650 ± 12	630 ± 10	650 ± 7
Chonnal	636 ± 17	634 ± 10	632 ± 10	630 ± 23	629 ± 10	630 ± 18	610 ± 10	648 ± 10
Shesgnan	650 ± 20	646 ± 7	643 ± 7	640 ± 30	638 ± 8	635 ± 12	608 ± 7	666 ± 8
Charn	630 ± 14	628 ± 5	626 ± 5	624 ± 20	623 ± 5	615 ± 10	600 ± 10	642 ± 5
Eilrig	566 ± 14	563 ± 3	561 ± 3	560 ± 20	558 ± 3	550 ± 5	533 ± 7	580 ± 4
Lagan a Bhaine	580 ± 24	576 ± 9	572 ± 10	570 ± 34	568 ± 9	585 ± 20	535 ± 15	598 ± 11
Uchdachan	608 ± 17	604 ± 4	602 ± 4	600 ± 25	598 ± 4	595 ± 5	570 ± 1	624 ± 6
Ceire	629 ± 27	625 ± 12	622 ± 11	620 ± 36	618 ± 11	610 ± 7	580 ± 8	647 ± 13
Central Valleys								
Northern								
Tarff	725 ± 20	723 ± 14	722 ± 13	721 ± 24	719 ± 14	710 ± 8	695 ± 10	735 ± 12
Doe	712 ± 19	708 ± 10	706 ± 10	705 ± 26	703 ± 10	710 ± 15	695 ± 10	724 ± 11
Brein	657 ± 21	654 ± 10	651 ± 11	649 ± 29	647 ± 11	660 ± 15	648 ± 12	671 ± 10
Dubh C na C	722 ± 10	721 ± 5	720 ± 4	719 ± 13	718 ± 5	705 ± 5	695 ± 5	729 ± 11
Killin Dubh Mor 1	710 ± 7	708 ± 1	707 ± 0	706 ± 11	705 ± 0	695 ± 2	685 ± 0	719 ± 0
Killin Dubh Mor 2	732 ± 5	730 ± 0	728 ± 0	727 ± 10	726 ± 0	715 ± 0	705 ± 0	739 ± 0
Easgainn	697 ± 15	695 ± 9	693 ± 9	692 ± 21	691 ± 9	685 ± 10	677 ± 9	705 ± 10
Killin	725 ± 21	721 ± 11	719 ± 10	717 ± 29	715 ± 11	715 ± 13	700 ± 10	738 ± 11
Ghlaise Killin	757 ± 9	756 ± 2	755 ± 2	754 ± 12	753 ± 2	745 ± 0	737 ± 1	765 ± 3
Killin Phuill	755 ± 5	754 ± 0	753 ± 1	752 ± 8	752 ± 1	740 ± 3	730 ± 0	762 ± 1
Southern								
Yairack	726 ± 22	722 ± 7	718 ± 7	716 ± 32	713 ± 7	755 ± 3	730 ± 4	744 ± 9
Laogh	702 ± 21	699 ± 11	697 ± 10	695 ± 29	693 ± 11	700 ± 14	675 ± 10	715 ± 12
Min Coire	709 ± 24	707 ± 20	706 ± 20	705 ± 27	704 ± 20	690 ± 20	682 ± 22	717 ± 20
Gilbre	699 ± 13	698 ± 6	696 ± 6	695 ± 17	694 ± 7	687 ± 3	678 ± 2	706 ± 8
Iain Oig	659 ± 30	655 ± 16	652 ± 16	650 ± 40	649 ± 14	675 ± 10	635 ± 10	675 ± 19
Talagainn	683 ± 22	680 ± 12	677 ± 13	676 ± 29	674 ± 12	685 ± 15	675 ± 10	695 ± 14
Eastern Valleys								
Beith	780 ± 17	775 ± 5	772 ± 5	770 ± 27	768 ± 6	800 ± 5	785 ± 5	796 ± 6
Markie	822 ± 17	819 ± 8	817 ± 8	816 ± 24	814 ± 8	820 ± 10	795 ± 12	833 ± 9
Lochain	820 ± 28	816 ± 9	813 ± 19	811 ± 32	809 ± 19	835 ± 20	810 ± 20	835 ± 21
Ballach	750 ± 25	745 ± 14	741 ± 13	738 ± 36	736 ± 13	750 ± 10	725 ± 10	769 ± 15
Fionndrigh	794 ± 23	789 ± 13	786 ± 13	783 ± 34	781 ± 13	815 ± 15	787 ± 9	811 ± 14
Chaorainn	782 ± 19	778 ± 7	775 ± 7	773 ± 28	771 ± 7	795 ± 10	785 ± 5	798 ± 7
Findhorn	777 ± 16	774 ± 8	772 ± 8	770 ± 23	769 ± 8	765 ± 5	750 ± 5	789 ± 9
Elrick	798 ± 21	796 ± 16	794 ± 15	793 ± 26	792 ± 15	780 ± 20	767 ± 19	806 ± 15
Dulnain	743 ± 9	741 ± 3	740 ± 3	739 ± 13	738 ± 2	722 ± 2	712 ± 3	751 ± 3
Monadhliath Icefield	723 ± 16	719 ± 8	716 ± 7	714 ± 25	713 ± 8	720 ± 5	700 ± 5	739 ± 9

maximum reconstructions used to consider the errors associated with each ELA. The AWMA ELA for the whole Monadhliath Icefield is 739 ± 9 m, whilst the equivalent AAR ELAs are 720 ± 5 m and 700 ± 5 m for ratios of 0.5 and 0.6 respectively (Table 5.5).

The ELAs calculated for each glacier shown in Table 5.5 fall within a range of 10% of one another showing a reasonable level of agreement between the three methods, although the AWMA approach generally produced ELAs that were higher than those calculated using the AAR and AABR methods. Including errors, the ELAs calculated using the different methods

are largely indistinguishable. The ELAs calculated for the region show a range of altitudes from 560 ± 20 m to 816 ± 24 m for an AABR of 1.9 (Table 5.5). There is a clear rise from west to east across the Monadhliath Mountains, with a range of 560 – 646 m in the west, 649 – 754 m in the central sector and 738 – 816 m in the east for the 1.9 AABR ELA (Fig. 5.9). The highest ELAs were found on the southern side of the plateau and the lowest occur on the northern side, although the difference between the northern and southern ELAs is less pronounced than differences between the east and west. This suggests that conditions for glacier growth were more favourable on the west of the Monadhliath Mountains, which was close to the West Highlands Ice Cap.

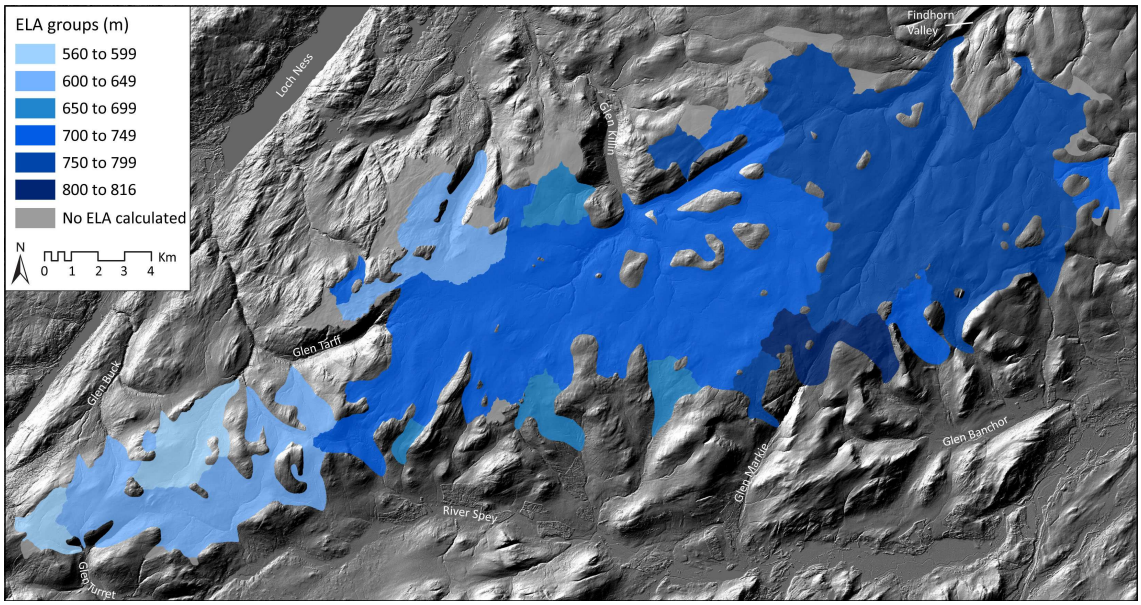

Figure 5.9. Major outlet glaciers of the Monadhliath Icefield classed according to their ELA in groups of 50 m intervals, showing a 'stepped' increase from the western to central to eastern sectors. NEXTMap DSM hillshade model from Intermap Technologies Inc. provided by NERC via the NERC Earth Observation Data Centre.

Since the AABR method is considered to be the most reliable, ELAs calculated using a BR of 1.9 ± 0.81 were used to calculate former precipitation in the area in the following section.

5.4.2 Palaeoprecipitation reconstruction

The link between annual precipitation and summer air temperatures at the ELA is such that in order to maintain a steady-state ELA, high ablation totals due to high air temperatures necessitate that precipitation totals must also be high in order to maintain a high mass flux through the ELA and keep the glacier in equilibrium (Benn & Evans, 2010). As precipitation levels decrease, regional ELAs tend to rise because lower temperatures are required to balance accumulation and ablation totals (Benn & Evans, 2010). Ohmura *et al.* (1992) examined the relationship between mean summer temperature and total annual precipitation at the ELA for 70 glaciers from mid- and high- latitudes, and developed an equation to describe this relationship:

$$P_a = 645 + 296T_3 + 9T_3^2 \quad (6)$$

Where P_a is the annual precipitation and T_3 is the mean summer temperature at the equilibrium line.

This relationship between temperature and precipitation at the ELA allows one of these variables to be calculated if an independent value is known for the other. It has been used extensively to derive palaeoprecipitation at the ELA of Younger Dryas glaciers in Scotland in combination with an independent temperature proxy, usually chironomids (e.g. Benn & Ballantyne, 2005; Lukas & Bradwell, 2010; Finlayson *et al*., 2011), superseding a previous function by Liestøl (1967) based upon glaciers in Norway alone. Some debate has arisen, however, over its suitability for palaeoclimatic reconstruction in Scotland (Dahl & Nesje, 1996; Dahl *et al*., 1997; Kaser & Osmaston, 2002; Benn *et al*., 2005; Evans, 2006; Braithwaite, 2008; Golledge *et al*., 2010). These authors have suggested that since the relationship between temperature and precipitation varies between geographic location due to differences in incoming radiation, and local factors such as aspect, wind direction and topography, the use of a global dataset cannot produce meaningful results at a regional to local level. The counter-argument to this is that by using a global dataset, any local variations are 'evened out', leaving the dataset more reliable than attempting to account for local variability in areas where no modern glacier data exists (Benn & Ballantyne, 2005; Lukas & Bradwell, 2010). Although more work is required in this field, in the absence of a more suitable equation, the Ohmura *et al*. (1992) relationship has consequently formed the basis for the majority of recent palaeoclimate reconstructions in Scotland.

As a first approximation of acknowledging the complexity introduced by changes in seasonality, however, a new function, specifically designed for Younger Dryas palaeoprecipitation calculations in Scotland, has recently been promoted by Golledge *et al*. (2010). At present, there is a discrepancy in the amount of precipitation suggested by palaeoglaciological reconstructions (e.g. Benn & Ballantyne, 2005; Lukas & Bradwell, 2010) and general circulation models (GCMs) (e.g. Björck *et al*., 2002; Jost *et al*., 2005), where the GCMs suggest a much drier climate. Golledge *et al*. (2010) suggest this inconsistency could be explained by an increase in continentality, caused by extensive sea-ice development in winter (Isarin *et al*., 1998; Isarin & Rensen, 1999), which is not accounted for by the Ohmura equation. This is supported by biological proxies and periglacial evidence that indicates that the annual temperature range in Scotland during the Younger Dryas was about 30°C. Golledge *et al*. (2010) therefore developed a function specifically for calculating precipitation at the ELAs of Younger Dryas glaciers in Scotland, based upon a model of the Scottish Younger Dryas ice cap, which incorporated Younger Dryas climate estimates from the Greenland ice core record and regional biological proxy data. The authors advocate that this new precipitation-temperature

function (eqn. 7) will provide a more realistic estimation of palaeoprecipitation in Scotland during the Younger Dryas and recommend its adoption into such studies.

This equation can be altered to account for neutral-, winter- and summer-type precipitation. Golledge *et al*. (2010) suggest that winter precipitation during the Younger Dryas in Scotland may have been reduced due to the presence of sea ice, compared to enhanced precipitation during the summer due to open water conditions. As a consequence a larger proportion of the precipitation falling on Scottish Younger Dryas glaciers may have fallen during the summer months and therefore would have been lost to ablation. The authors therefore recommend the use of the term effective precipitation, rather than total annual precipitation, in order to take this into account.

$$P = S(14.2T_3^2 + 248.2T_3 + 213.5) \quad (7)$$

Where S is the seasonality constant that takes into account different scenarios; S = 1 for neutral type, S = 1.4 for summer-dominated and S = 0.8 for winter-dominated precipitation seasonality. T_3 is the mean summer temperature at the equilibrium line.

Palaeoprecipitation for the Monadhliath Mountains was calculated using both the Ohmura *et al*. (1992) and the Golledge *et al*. (2010) equations. This enabled comparison with other studies that used the Ohmura equation and allowed comparison between the two methods. Two values for summer temperature at sea level of 8.5 ± 0.3° C (mean July temperature) and 6.4° C were used. 8.5 ± 0.3° C has been used by recent authors (e.g. Lukas & Bradwell, 2010), following the suggestion of Benn and Ballantyne (2005). The value is based on chironomid data from Whitrig Bog (125 m OD) and Abernethy Forest (220 m OD), which lie approximately 260 km southeast and 30-90 km east of the Monadhliath Mountains respectively. The chironomid data indicates that mean July temperatures for the coldest part of the Younger Dryas Stadial were 7.5° C at Whitrig Bog (Brooks & Birks, 2000, 2001) and 7.3°C at Abernethy Forest (S.J. Brooks, pers. comm., 2007, in Lukas & Bradwell, 2010). Using wet adiabatic lapse rates of 0.006-0.007°C m^{-1}, this corresponds to 8.2-8.3° C and 8.6-8.8° C at sea level respectively, which equates to a mean July temperature at sea level of 8.5 ± 0.3° C. As discussed for the ELA calculations, the use of a mean July temperature from the coldest part of the Younger Dryas is potentially at odds with a complex build-up history of Scottish Younger Dryas ice masses, which is likely to have started in more temperate conditions. This means that precipitation calculated using this temperature value could potentially underestimate precipitation totals, adding further uncertainty to these values.

The second value for mean summer temperature of 6.4° C is derived from modelling

experiments by Golledge *et al*. (2008). It is advocated by Golledge (2008) as an alternative value that takes into account the effects of localised cooling of air temperatures by glaciers (Khodakov, 1975; Braithwaite, 1980; Singh *et al*., 2000; Hughes & Braithwaite, 2008), unlike chironomid-derived temperatures that were derived from ice-free areas. This value has been used to calculate palaeoprecipitation by Finlayson *et al*. (2011) for the Younger Dryas Beinn Dearg Icecap in northern Scotland and is therefore included in this study for comparison.

In order to transform the mean July summer temperature of 8.5 ± 0.3° C into a mean summer temperature, as required by both the Ohmura *et al*. (1992) and Golledge *et al*. (2010) equations, equation 8 was used, as advocated by Benn and Ballantyne (2005) from analysis of meteorological data from Scotland and Scandinavia. This equation assumes that the current Scandinavian and Scottish summer climates are good analogues for summer climate in Scotland during the Younger Dryas. In the absence of any other data, however, this equation is used here and considered to be a reasonable approximation.

$$T_3 = 0.97T_J \quad (8)$$

where T_3 is the mean summer temperature and T_J is the mean July temperature.

An average wet adiabatic lapse rate of 0.0065 °C m^{-1} was then used to derive T_3 at the Monadhliath Icefield ELAs for both temperature values. The lower (0.006 °C m^{-1}) and upper (0.007 °C m^{-1}) adiabatic lapse rate boundaries, advocated in previous studies, were incorporated into the errors at a later stage. Although there are large uncertainties surrounding how representative these values are, they provide at least an approximation of likely adiabatic lapse rates.

Whilst the 6.4 °C value for summer temperature already accounts for the effect of air temperature cooling by glaciers, the 8.5 ± 0.3 °C value does not. In order to independently account for this cooling effect, Golledge *et al.* (2010) suggest that the following function can be used, based upon the length of the glacier:

$$\log\Delta T = 0.28L - 0.07 \quad (9)$$

where T is the temperature and *L* is the length the glacier.

This equation is derived from Khodakov (1975) who suggests that glaciers may reduce the surrounding air temperature by between 1.6-1.9°C for a glacier of 10-20 km in length. Alternatively, Golledge *et al.* (2010) combine equations 8 and 9, and taking adiabatic lapse rates

into consideration calculate mean summer temperatures at the ELA using the following equation:

$$T_3 = 0.97(T_J + 0.00205\Delta x - 0.00373\Delta y - 6.15\Delta z) - 1.10^{0.28\mathrm{Log}L - 0.07} \quad (10)$$

Where Δx, Δy and Δz are the differences (in kilometres) in easting, northing and altitude, respectively, from the site where T_J was derived to the study site and L is the length of the reconstructed glacier.

However, equations 9 and 10 cannot be used in the palaeoprecipitation calculations here, since the value of 8.5 ± 0.3 °C is an amalgamation of two chironomid sites and therefore eastings and northings can not be determined unless only one was used. In addition, even if a single temperature value was used, glacier length varies significantly across the Monadhliath Icefield and a single easting and northing value cannot be determined. Therefore, although the effects of localised air temperature cooling by glaciers is a significant factor that will affect the local glacier climate, it could not be quantified in this research for the 8.5 ± 0.3 °C mean July temperature. This factor is discussed further in Section 6.2.

Palaeoprecipitation values for the Monadhliath Icefield and outlet glacier AABR ELAs are displayed in Table 5.6. The precipitation at the 714 m ELA is taken as the 'average' precipitation value following arguments made in the section above. The minimum precipitation for the icefield was calculated using a 1.09 AABR ELA (lower error bracket of the AABR 1.9 ± 0.81) for the maximum icefield reconstruction, since this produced the highest ELA. The lower margin (8.2 °C) of the mean July sea level temperature of 8.5 ± 0.3 °C was used alongside the lowest adiabatic lapse rate (0.006 °C m^{-1}). Conversely, the maximum precipitation was calculated using a 2.71 AABR ELA from the upper boundary of the 1.9 ± 0.81 balance ratio from the minimum icefield reconstruction, using a mean July sea-level temperature of 8.8 °C and an adiabatic lapse rate of 0.007 °C m^{-1}. The use of the maximum icefield reconstruction for calculating the minimum precipitation values and vice versa will be discussed further in Section 6.4.

Errors were calculated from the larger of the differences between the maximum and minimum precipitation values and the average precipitation value. A standard error of ± 200 mm was added to this error to incorporate variations in the relationship between air temperature and ablation (Ohmura *et al*., 1992). Following the method outlined above, and incorporating these errors, average palaeoprecipitation of the Monadhliath Icefield is calculated at 1829 ± 491 mm a^{-1} at the 714 m ELA using the Ohmura curve and a mean July temperature at sea level of 8.5 ± 0.3° C. Using this temperature, values for summer-dominated, neutral and winter-dominated precipitation with an annual temperature range of 30° C are 1809

Table 5.6. Palaeoprecipitation values and errors for the Monadhliath Icefield and major outlet glaciers at their respective ELAs and at sea-level, calculated using the AABR = 1.9 ± 0.81 ELA. Palaeoprecipitation values for the Monadhliath Icefield are presented for both a mean July temperature at sea level of 8.5 ± 0.3° C (Benn & Ballantyne, 2005) and a summer sea level temperature of 6.4° C (Golledge, 2008). A mean July temperature at sea level of 8.5 ± 0.3° C only was used to calculate the palaeoprecipitation values for the major outlet glaciers. These glaciers are organised by area of the Monadhliath Mountains and from west to east within these groups.

Glacier	ELA	Effective Precipitation at the ELA				Effective Precipitation at Sea Level			
		Ohmura *et al.* (1992)	Golledge *et al*. (2010)			Ohmura *et al.* (1992)	Golledge *et al.* (2010)		
			Summer type ppt	Neutral type ppt	Winter type ppt		Summer type ppt	Neutral type ppt	Winter type ppt
Western Valleys									
Larach	620	2053 ± 498	2117 ± 498	1512 ± 491	1210 ± 433	1449 ± 432	1494 ± 509	1067 ± 421	854 ± 376
Teanga Bige Turret	585	2138 ± 472	2235 ± 576	1596 ± 468	1277 ± 415	1539 ± 413	1609 ± 487	1149 ± 405	919 ± 363
Teanga Mor Turret	641	2002 ± 482	2047 ± 585	1462 ± 475	1170 ± 420	1396 ± 413	1428 ± 484	1020 ± 403	816 ± 362
Eachach Turret	625	1988 ± 526	2027 ± 655	1448 ± 432	1158 ± 460	1436 ± 424	1478 ± 499	1056 ± 413	845 ± 371
Chonnal	630	2028 ± 479	2083 ± 581	1488 ± 472	1190 ± 418	1424 ± 412	1462 ± 483	1044 ± 402	836 ± 362
Shesgnan	640	2004 ± 497	2050 ± 605	1464 ± 489	1171 ± 432	1399 ± 427	1431 ± 502	1022 ± 416	818 ± 373
Lagan a Bhaine	570	2174 ± 502	2286 ± 617	1633 ± 498	1306 ± 438	1578 ± 445	1660 ± 528	1185 ± 434	948 ± 387
Uchdachan	600	2101 ± 481	2184 ± 587	1560 ± 476	1248 ± 421	1500 ± 419	1559 ± 494	1114 ± 410	891 ± 368
Central Valleys Northern									
Tarff	721	1812 ± 489	1787 ± 587	1277 ± 477	1021 ± 421	1209 ± 406	1192 ± 471	851 ± 393	681 ± 355
Brein	649	1983 ± 496	2020 ± 602	1443 ± 487	1154 ± 430	1377 ± 424	1403 ± 502	1002 ± 415	802 ± 372
Easgainn	625	1880 ± 479	1880 ± 577	1343 ± 469	1074 ± 415	1275 ± 402	1274 ± 468	910 ± 391	728 ± 353
Killin	717	1822 ± 501	1800 ± 603	1286 ± 488	1028 ± 430	1218 ± 417	1203 ± 485	859 ± 403	687 ± 363
Southern									
Yairack	716	1824 ± 525	1803 ± 648	1288 ± 520	1030 ± 456	1234 ± 435	1220 ± 519	872 ± 428	697 ± 382
Laogh	695	1873 ± 499	1870 ± 603	1336 ± 488	1069 ± 430	1268 ± 420	1266 ± 489	904 ± 406	723 ± 365
Iain Oig	650	1980 ± 523	2017 ± 639	1441 ± 513	1153 ± 451	1374 ± 450	1400 ± 529	1000 ± 435	800 ± 388
Eastern Valleys									
Beith	770	1699 ± 500	1633 ± 597	1167 ± 484	933 ± 427	1102 ± 408	1060 ± 472	757 ± 394	606 ± 355
Markie	816	1593 ± 496	1493 ± 588	1066 ± 477	853 ± 422	1007 ± 398	944 ± 454	674 ± 382	539 ± 345
Lochain	811	1605 ± 518	1508 ± 629	1077 ± 507	862 ± 445	1017 ± 424	956 ± 495	683 ± 410	546 ± 368
Ballach	738	1773 ± 519	1733 ± 625	1238 ± 504	990 ± 443	1171 ± 430	1146 ± 500	819 ± 414	655 ± 371
Fionndrigh	783	1668 ± 517	1593 ± 618	1138 ± 499	910 ± 439	1075 ± 421	1026 ± 484	753 ± 422	586 ± 363
Chaorainn	773	1692 ± 502	1624 ± 600	1160 ± 486	928 ± 429	1096 ± 410	1052 ± 472	751 ± 394	601 ± 355
Findhorn	770	1699 ± 490	1633 ± 585	1167 ± 475	933 ± 420	1102 ± 393	1060 ± 458	757 ± 377	606 ± 342
Elrick	793	1646 ± 499	1563 ± 599	1116 ± 485	893 ± 428	1054 ± 404	1001 ± 471	715 ± 394	572 ± 355
Dulnain	739	1770 ± 464	1730 ± 553	1236 ± 452	989 ± 402	1169 ± 382	1142 ± 440	815 ± 372	653 ± 337
Monadhliath Icefield (T_j = 8.5 ± 0.3 °C)	714	1829 ± 491	1809 ± 592	1292 ± 480	1034 ± 424	1224 ± 409	1211 ± 480	865 ± 400	692 ± 360
Monadhliath Icefield (T_3 = 6.4 °C)	714	1187 ± 371	963 ± 416	688 ± 354	550 ± 323	795 ± 324	645 ± 352	461 ± 308	369 ± 287

± 592 mm a^{-1}, 1292 ± 480 mm a^{-1} and 1034 ± 424 mm a^{-1} at the ELA respectively. Palaeoprecipitation was also calculated for major outlet glaciers using the mean July temperature of 8.5 ± 0.3° C and shows a decrease in precipitation from west to east, reflecting the rise in ELAs (Table 5.5). Precipitation values for the icefield calculated in the same way for the summer temperature of 6.4° C are significantly lower and are also presented in Table 5.6.

In order to compare the precipitation values with other studies the equivalent sea-level precipitation amounts were calculated. Since precipitation increases non-linearly with altitude, Ballantyne (2002a) devised a relationship to calculate the corresponding precipitation at different altitudes using:

$$P_{Z1} = P_{Z2}/(1+P^*)^{0.01(Z2-Z1)} \quad (11)$$

Where P_{Z1} and P_{Z2} are the amount of precipitation at altitudes Z1 and Z2. P^* is the proportional increase in precipitation per 100 m increase in elevation. Based on a dataset for Ben Nevis, which is approximately 30 km southwest of the study area, Ballantyne (2002a) showed that $P^* = 0.0578$ and this value is used here.

Values for equivalent sea-level palaeoprecipitation are also displayed in Table 5.6. The sea level equivalent precipitation for the Monadhliath Icefield is found to be 1224 ± 409 mm a^{-1} using the Ohmura *et al.* (1992) curve and 1211 ± 480 mm a^{-1}, 865 ± 400 mm a^{-1}, and 692 ± 360 mm a^{-1}, for the summer-, neutral- and winter-dominated precipitation types respectively using the Golledge *et al*. (2010) equation. Sea-level equivalent precipitation values for the major outlet glaciers show a significant decrease in precipitation across the Monadhliath Mountains from west to east, and from north to south, as expected from the rise in ELAs in the same direction, ranging from 1578 ± 445 in the northwest to 1007 ± 398 in the southeast using the Ohmura *et al.* (1992) equation.

5.4.3 Summary

Equilibrium line altitudes were calculated for the Monadhliath Icefield and the majority of its outlet glaciers using the AABR, AAR and AWMA methods. The AABR method is considered the most reliable since it takes into account glacier hypsometry and incorporates different accumulation and ablation gradients (Rea, 2009). Using an AABR of 1.9 ± 0.81, the ELA of the Monadhliath Icefield is calculated at 714 ± 25 m (Table 5.5). This value is considered the most appropriate for use in palaeoprecipitation calculations since the 1.9 AABR represents mid-latitude maritime glaciers (Rea, 2009), which have previously been suggested as modern analogues for Younger Dryas glaciation in Scotland (Benn & Gemmell, 1997; Benn & Lukas, 2006). ELAs of the outlet glaciers rise significantly from west to east across the plateau and to

a lesser extent from north to south, ranging from 560 ± 20 m in the northwest to 814 ± 8 m in the southeast using an AABR of 1.9 ± 0.81 (Table 5.5; Fig. 5.9).

Palaeoprecipitation is calculated as 1829 ± 491 mm a^{-1} at the 714 ± 25 m ELA using the Ohmura *et al.* (1992) curve and 1809 ± 592 mm a^{-1}, 1292 ± 480 mm a^{-1}, 1034 ± 424 mm a^{-1} at the ELA using the Golledge *et al*. (2010) function for summer, neutral and winter precipitation types respectively, all using a mean July summer temperature at sea level of 8.5 ± 0.3 °C (Table 5.6). These are equivalent to sea-level precipitation values of 1224 ± 409 mm a^{-1} (Ohmura *et al.*, 1992), 1211 ± 480 mm a^{-1}, 865 ± 400 mm a^{-1} and 692 ± 360 mm a^{-1} (Golledge *et al*., 2010; summer, neutral and winter type, respectively) (Table 5.6). Palaeoprecipitation values for the Monadhliath Icefield calculated using a summer temperature value of 6.4 °C are significantly lower and are also presented in Table 5.6. Precipitation values for the outlet glaciers reflect the differences in ELAs across the Monadhliath Icefield and show a decrease in precipitation of 500-700 mm a^{-1} at the ELA from west to east dependent on the calculation method used.

5.5 Examination of the Former Dynamics of the Monadhliath Icefield

In order to fully utilise the geomorphological evidence described in Chapter 4, the dynamics of the former Younger Dryas Monadhliath Icefield were examined in detail, in particular those relating to glacier retreat. A greater understanding of glacier dynamics and retreat patterns is important not only to provide further information on regional palaeoclimate (e.g. Benn & Lukas, 2006), but in terms of understanding how a particular glacial system, such as a plateau icefield, reacts to changes in climate and is influenced by its underlying topography. As discussed in Chapter 2, very few studies have reconstructed plateau icefields from the palaeoglacial record and little is known about spatial and temporal changes in thermal regime (*cf.* Dyke, 1993; Fjellanger *et al*., 2006), transport pathways (*cf.* Evans, 2010), ice divide migration and retreat dynamics. This current research therefore provides a unique opportunity to examine the retreat dynamics of a plateau icefield throughout the whole phase of retreat from its maximum position to final disappearance, a time period that can only be modelled on modern plateau icefields (e.g. Giesen & Oerlemans, 2010). The following sections therefore examine what factors control differences in thermal regime and ice margin retreat patterns across the Younger Dryas Monadhliath Icefield.

5.5.1 Variations in thermal regime across the Monadhliath Icefield

The following section reviews the geomorphological evidence for variations in thermal regime across the Monadhliath Icefield. On the plateau, geomorphological evidence for glaciation is constrained to latero-frontal moraines within a few small proto-valleys, long isolated lateral moraines and ice-marginal channels, stagnation moraines in isolated areas (Section 4.2.6) and

deltaic sediments above Glen Eich (Section 4.2.6), although the current presence of a thick layer of peat over the majority of the plateau may have obscured other geomorphological evidence. A relative chronology for events relating to the formation of features on the plateau is difficult to establish since other morphostratigraphic lines of evidence that are found in the outlet valleys are lacking, such as fluvial deposits, drift limits and clear trimlines. As discussed in Section 5.2, it is unclear whether the lower boundaries of periglacial features on the summits such as blockfields and solifluction lobes represent trimlines and hence the upper ice surface (e.g. Ballantyne, 1997; Ballantyne *et al*., 1997), whether they are older features that were covered by cold-based ice during the Younger Dryas (e.g. Whalley *et al*., 1981; Gellatly *et al*., 1988; Kleman, 1994; Rea *et al*., 1996; Fjellanger *et al*., 2006; Ballantyne, 2010a), or whether they are englacial thermal boundaries which separate warm-based ice from cold-based ice overlying the higher summits (e.g. Goehring *et al*., 2008).

Deltaic sediments on the plateau in the upper parts of the Glen Eich catchment are suggested in Section 4.2.6 to relate to an ice-dammed lake that formed prior to the formation of the Younger Dryas Monadhliath Icefield. The preservation of these features therefore indicates that the ice on the plateau, at least in this area, remained cold-based throughout this phase of glaciation. The occurrence of meltwater channels at the edge of the plateau above Gleann Ballach, which indicate ice-marginal rather than subglacial drainage (Rea & Evans, 2003), also suggests that ice on the plateau was predominantly cold-based (Dyke, 1993). This opens the possibility that other features on the plateau, such as the large isolated moraines above Glen Talagain & Corrie Iain Oig (see Section 4.4) and some of the larger meltwater channels are older and could have also been preserved beneath cold-based ice.

In other parts of the plateau, smaller closely spaced moraines and meltwater channels occur. These features are more confidently suggested to be of Younger Dryas age due to their morphology, close spacing and position in the source area of reconstructed Younger Dryas outlet glaciers (Section 4.3), although this interpretation has to remain less certain than those in the outlet valleys due to the lack of other morphostratigraphic evidence. Assuming a correct chronological placement of these features, however, they indicate that, during the final stages of retreat, plateau ice actively retreated into small proto-corries on the plateau. This occurred mainly between Glen Markie and the Eskin and Abhainn Crò Chlach catchments in the eastern sector of the Monadhliath Mountains, but also on the plateau above Coire Laogh, Glen Brein, Coire Easgainn and Corrie Yairack. This geomorphological evidence suggests that the ice on the plateau became more temperate at least during the final stages of retreat. A likely reason for this is that the topography in these areas forms proto-cirques and valleys in between summits on the plateau that could have captured snow transferred by wind from elsewhere, and/or shaded

any remaining ice, allowing glaciers to exist for longer at the end of the Younger Dryas in these areas (see also Section 5.5.2). This form of micro-relief on the plateau may have a more pronounced effect on plateau icefield dynamics than has previously been acknowledged.

The thermal regime of the plateau is therefore concluded to have been mainly cold-based, with blockfields, solifluction lobes, deltaic deposits, older moraines and older meltwater channels being preserved beneath the ice, as has often been argued for plateau icefields (e.g. McDougall, 2001). However, the geomorphological evidence implies that some areas became more temperate during deglaciation, indicating spatio-temporal changes in thermal regime. This mosaic of thermal regimes has previously been recognised beneath both plateau icefields and ice sheets by numerous authors including Dyke (1993), Rea *et al*. (1998), Evans *et al.* (2002), Hall and Glasser (2003), Kleman *et al*. (2008) and Evans (2010).

The greatest variations in geomorphological evidence occur in the outlet valleys. Of the fifty-three main outlet valleys, only seventeen have well-preserved, closely spaced recessional moraines. Glaciers in the remaining thirty-six outlet valleys were reconstructed based on the presence of ice-marginal meltwater channels and some, more sporadically spaced, moraines. Of these valleys, thirteen were dominated by lateral meltwater channels, but also contained moraines, whilst evidence for the remaining twenty-three outlet glaciers was based solely on the presence of lateral meltwater channels, abrupt changes in the number of river terraces and other circumstantial evidence that required ice to have been present (Section 5.2). While not every valley in other similarly-sized areas in Scotland contains moraines, the number of valleys without clear constructional glaciogenic landforms in the Monadhliath Mountains is certainly noticeable (*cf.* Lukas & Bradwell, 2010; Finlayson *et al*., 2011).

Research on modern glacial landsystems demonstrates that the formation of lateral meltwater channels is often associated with cold-based ice because cold-based ice prohibits drainage in subglacial positions and diverts it to the ice-margin (Rea & Evans, 2003). Nested lateral channels therefore document successive ice-marginal positions during retreat due to this meltwater flow around the frozen margin (England, 1986; Ó Cofaigh *et al.,* 1999; Atkins & Dickinson, 2007). This evidence has been used extensively to interpret the former thermal regimes of Quaternary glaciers and ice sheets as cold-based (e.g. Borgström, 1999; Dyke, 1993; Ó Cofaigh *et al.,* 1999; Hättestrand & Stroeven, 2002). However, Syverson and Mickelson (2009) argue that lateral meltwater channels can also be found at the margins of temperate glaciers and therefore the presence of these features is not solely indicative of cold-based glacier margins. Given the overwhelming evidence in this research, however, for a central cold-based area of the icefield on the plateau, it follows that some outlet glaciers also remained cold-based,

causing either little modification to the pre-existing landscape or producing a succession of nested lateral meltwater channels only. This interpretation is consolidated by the morphology and location of these reconstructed outlet lobes, which are usually thin and often reside in low gradient outlet valleys, with little altitudinal difference between the valley and the plateau, indicating that the glaciers would not have reached pressure melting point (Ó Cofaigh *et al*., 2003; Rea & Evans, 2003).

At the other end of the range of landsystems present in the Monadhliath Mountains are seventeen outlet valleys in which suites of closely spaced recessional moraines occur. The morphology of these moraines is very similar to other Younger Dryas moraines found elsewhere in Scotland, characterised by densely spaced mounds and ridges, sharp crestlines and crestline bifurcations (e.g. Benn, 1992; Benn *et al*., 1992; Bennett & Boulton, 1993a; Lukas, 2005a, b; Benn & Lukas, 2006; Finlayson, 2006; Finlayson *et al*., 2011). The presence of these moraines indicates that the glaciers were predominantly wet-based, at least in the marginal to sub-marginal zone, since they were able to entrain, transport and subsequently deposit sediment (Benn & Lukas, 2006; Evans, 2010). Moraine preservation following deposition was also high, suggesting that ice-marginal streams were unable to remove significant amounts of sediment from the margin, although (glacio)fluvial activity may have contributed to the dissection of the moraines into discrete mounds and ridges following deposition (Benn & Lukas, 2006).

The sedimentological characteristics of the moraine examined at Stronelairg (Sections 4.2.5 and 4.2.6) are very similar to moraines examined by Lukas (2005a, b) in the Northwest Highlands and by Benn (1992) and Benn *et al*. (1992) in Skye. These moraines are interpreted to have been deposited as terrestrial ice-contact fans composed of sheets of debris flow and glaciofluvial material. In the Northwest Highlands, Lukas (2005a, b) argued that the moraines were sourced supraglacially but by material that had previously been transferred from a subglacial position. Based on this evidence, Benn and Lukas (2006) suggested that glaciers in this region were polythermal, with a narrow zone of cold-based ice at the margin. They argued that englacial thrusting at the boundary between warm-based and cold-based ice was required to elevate the subglacial material to the glacier surface before deposition in the form of ice-contact fans. In the Monadhliath Mountains, however, although the moraines examined were interpreted to have formed as terrestrial ice-contact fans and 'dump' moraines, clast roundness data suggested that they were composed of a higher proportion of supraglacial material compared to the Northwest Highland moraines. Therefore the need for a frozen glacier margin in order to elevate a large proportion of subglacial material to the glacier surface is not required, although the slightly higher proportion of rounded clasts in the Stronelairg moraine suggests that some elevation of subglacial material may have occurred.

The remaining thirteen outlet glaciers that produced a landscape dominated by meltwater channels, but also some moraines, therefore lie on a continuum between cold-based basal conditions and predominantly warm-based conditions. This is due to the fact that, whilst ice-marginal drainage was still the dominant process in terms of landscape modification, the former outlet glaciers were able to entrain, transport and subsequently deposit sediment at their margins to varying extents. Reasons for the limited number of moraines are numerous and are discussed below.

1) There may have been low debris turnover due to a lack of debris entrainment, implying a cold thermal regime (Ó Cofaigh *et al*., 2003).
2) There could have been a lack of sediment readily available for re-entrainment (*cf.* Ballantyne, 2002b, c), although in most of the outlet valleys, stream exposures reveal thick diamictic deposits in the valley bottoms, indicating that a lack of available sediment was not a reason for the low number of moraines.
3) Moraines could have been deposited but not preserved due to the presence of buried ice, which can have a significant effect on postglacial landscape modification (Lukas, 2007a, 2011; Evans, 2009; Brook & Paine, 2011).
4) The glacial and fluvial systems were well-coupled and proglacial streams were able to immediately remove any sediment that was deposited at the ice margin (Benn *et al*., 2003; Lukas & Benn, 2006). This situation tends to occur within temperate valley landsystems, however, and the preservation of ice-marginal channels in the Monadhliath outlet valleys suggests that proglacial streams did not migrate across the glacier margin, which would be necessary in order to remove morainic material (Benn *et al*., 2003).
5) Slope steepness could be a cause of low moraine formation or preservation potential (see section 4.4.2). However, the majority of the outlet valleys had similar or slightly lower gradients than those outlet valleys that did have closely spaced recessional moraine sequences, implying that slope gradient in this sense was not a factor, although it could have had an effect on the glacier thermal regime as discussed above for cold-based glaciers.
6) Burial of small, particularly lateral, moraines by hillslope processes (e.g. Müller *et al*., 1983) could have caused moraines to no longer be clearly visible.
7) Burial of moraines by peat is possible if the moraines were small, causing valleys to 'appear' as if they contain very few moraines.

Of these factors low debris turnover (1) and/or low moraine preservation due to the presence of buried ice (3), burial by hillslope processes (6) and peat formation (7) are more likely reasons for the limited number of moraines in these outlet valleys. Both factors 1 and 3 are indicative of cold-based to polythermal conditions at the glacier bed (Ó Cofaigh *et al*., 2003).

As argued above, the range of geomorphological evidence found across the former outlet valleys of the Monadhliath Icefield suggests that the thermal regime of the glaciers within them lay on a continuum between cold-based, via polythermal to warm-based conditions. The spatial distribution of the range of thermal regimes found is shown in Figure 5.10. This figure demonstrates that the thermal regime of the Monadhliath Icefield outlet glaciers was related to their thickness, the size of the plateau source area and the gradient of the bed at the transition between the plateau and the outlet valley. The key control is glacier size, where the more temperate glaciers, which produced the extensive recessional moraine sequences, were generally thicker and often resided in deeper valleys. This also includes glaciers on the northern side of the plateau, which had large plateau catchment areas due to the asymmetric morphology of the Monadhliath plateau. As a result, the ice was able to reach pressure melting point due to the greater ice thickness (Dyke, 1993; Rea & Evans, 2003).

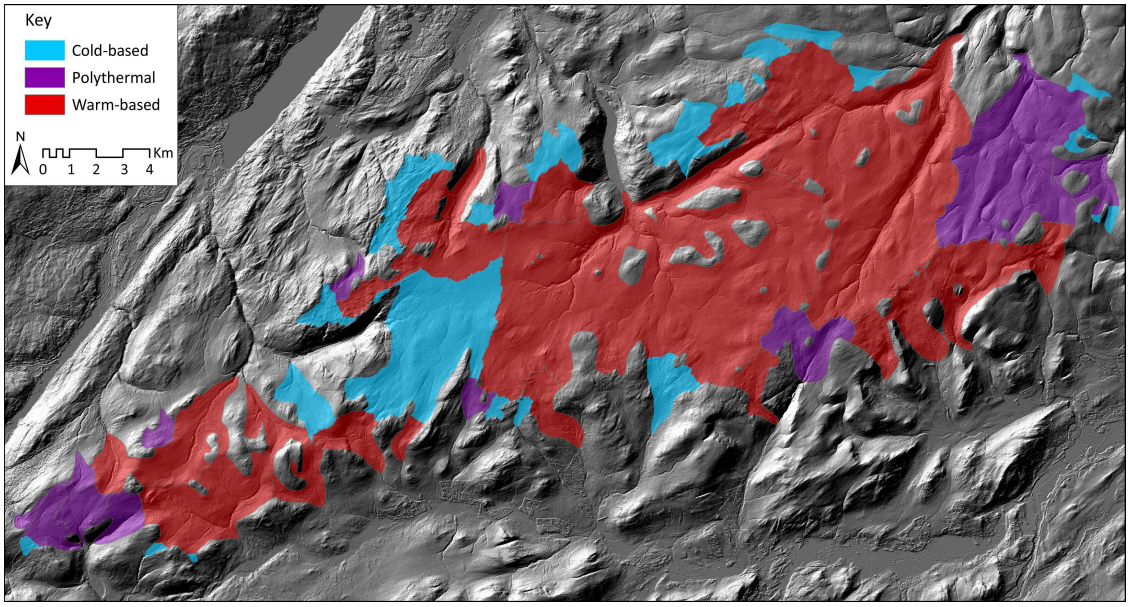

Figure 5.10. Outlet glaciers of the Monadhliath Icefield, classed according to their thermal regime. NB. This figure applies the thermal regime of each outlet glacier to the whole of its catchment and therefore does not also represent thermal regimes on the plateau. NEXTMap DSM hillshade model from Intermap Technologies Inc. provided by NERC via the NERC Earth Observation Data Centre.

The second control is bed slope, where glaciers that flowed in steeper outlet valleys or flowed over steeper backwalls were found to be more likely to be predominantly warm-based compared to outlet glaciers where there was less of a change in gradient from the plateau into the outlet valley. This is due to the increase in flow velocity as the gradient increases, allowing strain heating to occur and ice to reach pressure melting point (Rea *et al*., 1998; Evans *et al*., 2002; Rea & Evans, 2003; Evans, 2010). Differences in thermal regime of glaciers due to these factors have been observed in a variety of modern glacial environments from the Canadian Arctic (e.g. Dyke, 1993; Ó Cofaigh *et al*., 2003) to Norway (Rea *et al*., 1998; Evans *et al*., 2002; Rea & Evans, 2003) and Iceland (Evans, 2010).

Summary

Thermal regime on the plateau is suggested to have been predominately cold-based due to the preservation of older landforms. Younger Dryas moraines in other areas of the plateau, however, indicate that some of the plateau ice was warm-based, at least during retreat. This suggests a mosaic of thermal regimes on the plateau that changed spatially and temporally (Hall & Glasser, 2003). Thermal regime of the outlet glaciers is suggested to have lain on a continuum between cold-based outlets, for which the only geomorphological evidence is ice-marginal meltwater channels, and warm-based glaciers, which were able to entrain, transport and deposit sediment in the form of moraines at their margins. Differences in the thermal regimes of the outlet glaciers is argued to be controlled by: 1) the size of the glacier, where thicker glaciers were able to reach pressure melting point and 2) the bed slope, where glaciers that flowed down steeper terrain between the plateau and the outlet valley were able to reach pressure melting point through strain heating.

5.5.2 Ice margin retreat patterns

The patterns and spacing of recessional moraines within sixteen outlet valleys that contained a large number of moraines relating to glacier retreat during the Younger Dryas are analysed in this section. The main aims of this exercise are to examine the differences in retreat dynamics between valleys and to assess the influence of factors such as slope, aspect, glacier size, size of plateau source area, glacier hypsometry and valley morphology on the retreat dynamics. The only site that was excluded from this analysis was Coire Iain Oig, which also contains a number of large moraines and meltwater channels within the reconstructed Younger Dryas limits, but was not considered since the spatial pattern of moraines suggests a more complex depositional history.

An assessment of the retreat dynamics was achieved by linking chains of moraines together to re-create former ice-marginal positions, an approach that has been used by a number of previous authors (e.g. Benn, 1992; Benn *et al*., 1992; Bennett & Boulton, 1993a, b; McDougall, 2001; Lukas, 2003, 2005b; Golledge & Hubbard, 2005; Lukas & Benn, 2006; Finlayson, 2006; Finlayson *et al*., 2011), assuming that the moraines were formed in ice-marginal positions (Section 4.5). Figure 5.11 shows the approach used in linking the moraines together. Clearly identifiable chains of moraines, often defined by meltwater channels (not shown here due to the map scale), were linked together first, usually starting at the outermost margin. Reconstructed ice margins on the valley floor were extrapolated across the valley floor arcuately, following a projection set by the orientation of the moraine chain. Ice margins were joined from one side of the valley to the other when the extrapolated ice margin matched a similar ice margin on the opposite side that would create a symmetrical ice front.

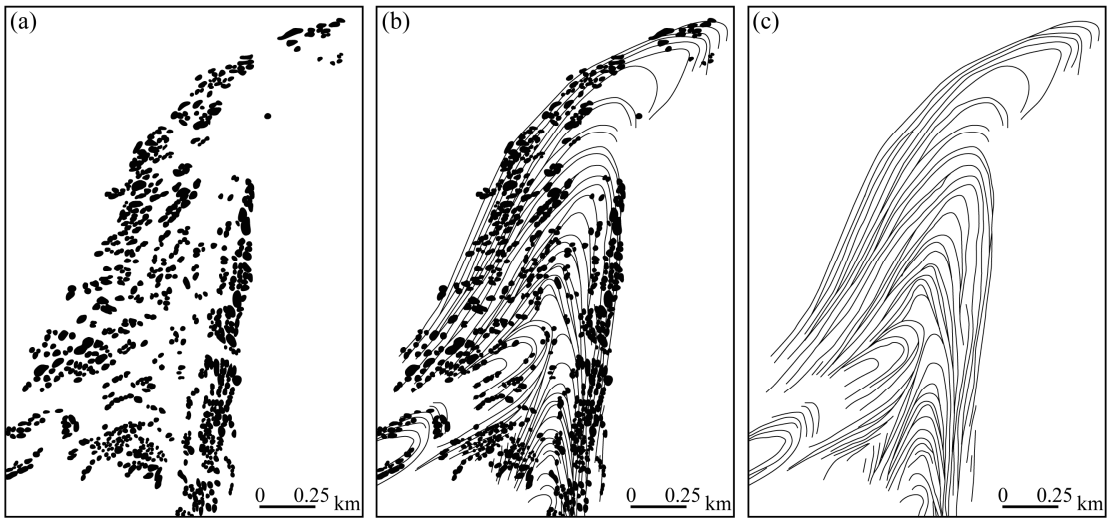

Figure 5.11. Illustration of the approach used to link chains of moraines together, using moraines in the Findhorn Valley near Dalbeg as an example. a) Mapped moraine mounds and ridges. b) Linkage of chains of moraines. c) Reconstructed ice margin positions.

The pattern and spacing of the reconstructed former ice fronts indicates that the outlet glaciers predominantly retreated towards their respective plateau source areas (Fig. 5.12). The only exceptions to this are the Ballach, Lochain, Shesgnan and Yairack glaciers, from which the pattern of moraines suggests that these glaciers disconnected from the plateau during the final stages of retreat, forming small corrie glaciers at the heads of their respective valleys.

Moraine crestline bifurcations occur regularly within the outlet valleys examined. Crestline bifurcation is caused by part of the ice margin retreating, whilst remaining stable in other areas. This process produces a new moraine at the new margin, which is adjoined to the original moraine in areas where the ice margin has remained stable. This creates a 'forked' moraine that has been observed in several modern and palaeoglacial settings (e.g. Benn & Lukas, 2006; Iturrizaga, 2008). Two forms of bifurcation can occur and are depicted in Figure 5.13. If the glacier length changes, but the thickness of the glacier thickness remains the same, a bifurcation will occur in the frontal part of the moraine (Fig. 5.13a). Alternatively, if the glacier thins, but its length remains the same, then a lateral bifurcation will occur (Fig. 5.13b). In the study area, of those outlet valleys that contained moraines with bifurcations, three bifurcation styles were identified; those that showed frontal bifurcations, those that exhibited lateral bifurcations, and those that displayed both frontal and lateral bifurcations.

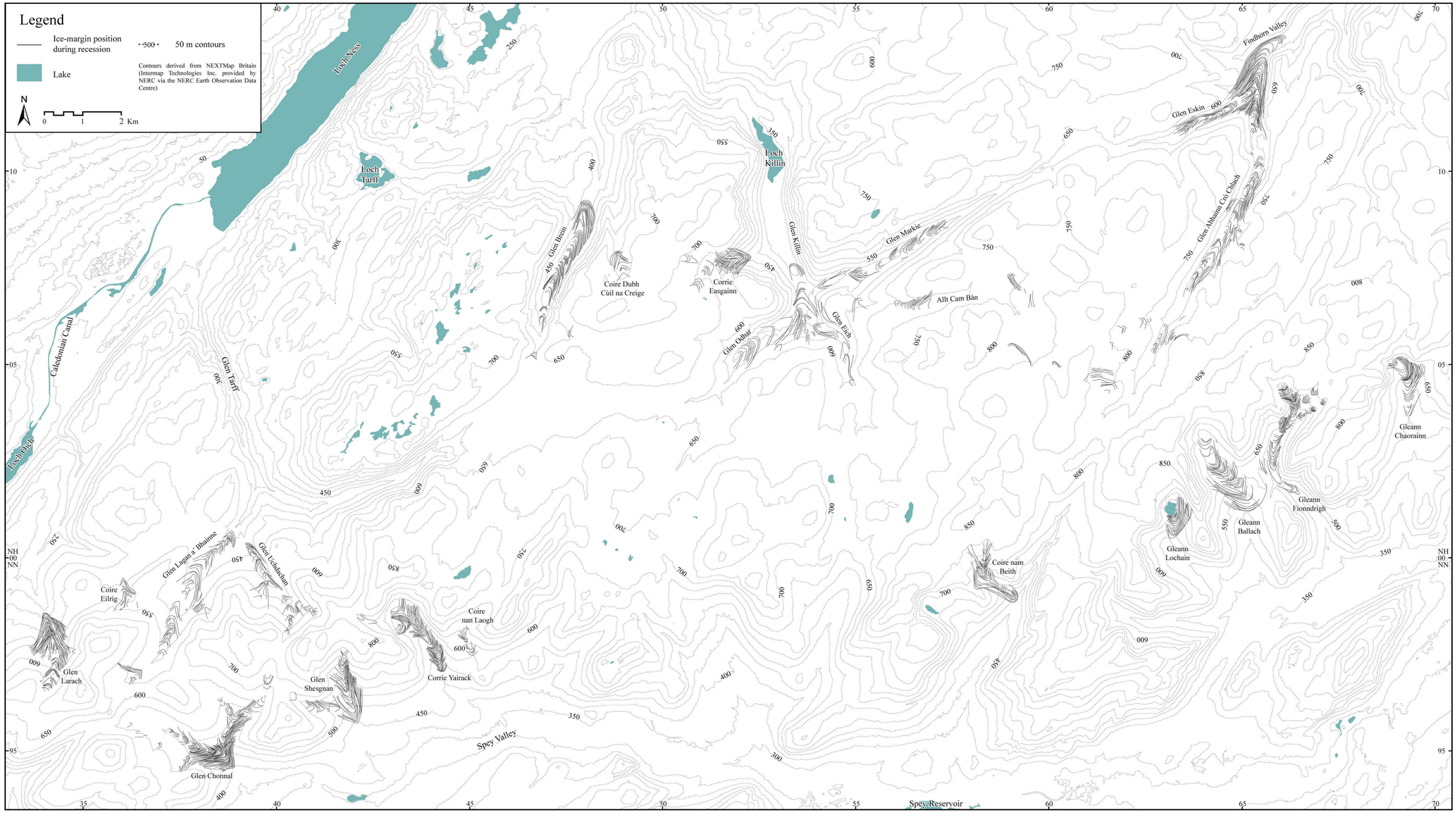

Figure 5.12. Ice margin positions for outlet glaciers in the Monadhliath Mountains that produced recessional moraines, including those for Coire Eilrig and Coire Dubh Cùil na Creige that were not used in the barcode analysis since they only contained a small number of moraines.

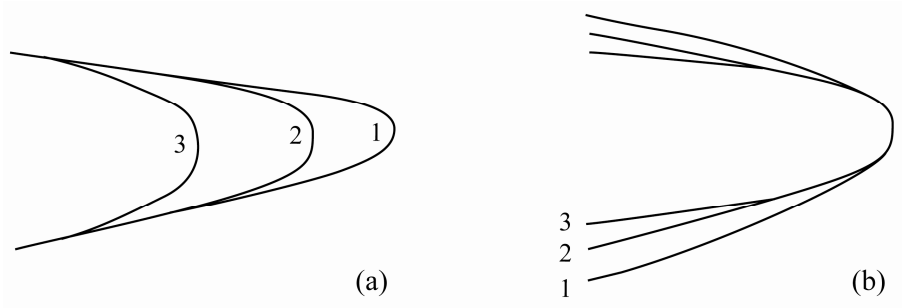

Figure 5.13. Style of moraine crestline bifurcation found in the study area. a) Frontal bifurcations, where ice thickness remains stable, whilst the glacier terminus retreats. b) Lateral bifurcations, where the glacier thins, but the terminus remains in the same position.

Together with the close spacing of former ice margins throughout the majority of the outlet valleys assessed, the presence of moraine bifurcations implies that the glaciers remained close to equilibrium during a large proportion of retreat and that this retreat would have been characterised by ice-marginal oscillations and stillstands. This oscillatory style of Younger Dryas glacier retreat has been identified in other areas of Scotland including Skye (Benn *et al*., 1992), Mull (Ballantyne, 2002a), the Northwest Highlands (Lukas & Benn, 2006), Arran (Ballantyne, 2007a), North Harris (Ballantyne, 2007b) and Beinn Dearg (Finlayson *et al*., 2011) where several of these authors identified that glacier retreat was characterised by minor advances and stillstands, indicative of glaciers with only slightly negative mass balances (Benn *et al*., 1992; Ballantyne, 2002a; Lukas & Benn, 2006). The recessional patterns found in the Monadhliath Mountains suggest similar glacier dynamics at least of the outlet glaciers that deposited extensive moraine sequences.

The spacing of the recessional moraines was assessed by measuring the distance between moraines along the former central flowline of the glacier. In order to represent the distances visually, the glacier centre line was straightened, whilst keeping distances the same, and a vertical line was used to represent each moraine at the junction of the moraine crestline and the flowline, creating a 'barcode' (cf. Lukas & Benn, 2006) (Fig. 5.14). The barcodes provide a quick, but effective means of assessing the differences in retreat dynamics between outlet glaciers, but account for frontal bifurcations only.

Initial retreat patterns

Using this approach, initial retreat patterns from the maximum glacier positions were examined first. The initial retreat patterns describe the early stages of retreat, documented by ice margin positions within the first ~ 1 km of the Younger Dryas limit. The initial retreat patterns were found to fall into three main types, which are also displayed in Figure 5.14. Former glaciers that exhibit retreat type 1 produced a succession of closely spaced moraine arcs just inside the maximum position, before retreating greater distances further up valley in an uninterrupted

Figure 5.14. 'Barcodes' showing the distance between recessional moraines in sixteen outlet valleys in the Monadhliath Mountains, organised into three initial retreat styles. The barcodes are organised according to major valley, with the retreat into tributary valleys defined by a split of the barcode onto a new line and the name of the tributary valley indented.

manner. Within retreat type 2, comparatively larger distances occur between ice-marginal positions immediately inside the maximum position, which decrease further up valley. Ice-marginal positions within type 3 are more evenly spaced throughout the valley.

These retreat types closely match the bifurcation styles identified above, where former ice margin positions within retreat type 1 are dominated by frontal bifurcations, within retreat type 2 are characterised by lateral bifurcations and within retreat type 3 contain both frontal and lateral bifurcations. The retreat type and the bifurcation style are intrinsically linked because if a glacier initially responds to climatic amelioration by thinning, whilst the terminus stays in the same position, a lateral moraine bifurcation will occur. A subsequent retreat of the glacier terminus is likely to cover a large distance in order to 'catch up' with the amount of glacier thinning. Conversely, if a negative mass balance is immediately translated to the position of the glacier terminus, whilst little overall thinning of the glacier occurs, frontal bifurcations and retreat type 1 will occur. Retreat type 3, where the terminus positions are more evenly spaced is linked to outlet valleys in which both styles of bifurcation were observed suggesting that the terminus and glacier thickness adjusted at a more similar rate during retreat.

Further examination of the bifurcation style and the patterns of retreat show that they are often closely linked to the morphology of the outlet valley, and in particular to the gradient of the valley floor along the glacier centre line. Former ice-marginal positions within wide, low-gradient valleys tend to contain chains of moraines with lateral bifurcations, which exhibit retreat type 2. Moraines within narrower valleys with steep valley sides often display retreat type 1 and frontal moraine bifurcations. Valley gradient in this group is more wide ranging, however. The differences between these two retreat types are most likely because wide low-gradient valleys will receive greater insolation due to less shadowing from the valley sides and therefore the response is distributed more areally in the form of glacier thinning, as well as changes in glacier length, compared to glaciers in narrow valleys, which mainly just exhibit changes in glacier length. The third type of retreat was found in outlet valleys that descend directly from the plateau with no backwall and which had a large plateau source area. These valleys display more evenly spaced retreat patterns, with both lateral and frontal moraine bifurcations, suggesting that the proximity to the plateau source area evens out the response of glacier termini.

Figure 5.15 shows the effect of changes in slope gradient on initial outlet glacier retreat. The figure demonstrates that moraine spacing is generally much closer on steeper slopes compared to that on lower gradient topography. This observation can be explained by the effect that a rising ELA will have on glaciers with different surface gradients. On topographically constrained glaciers, the glacier surface profile will mainly be controlled by the gradient of the

underlying topography. A small vertical rise in the ELA, of for instance 10 m, will cause a much larger increase in the size of the ablation area on a glacier with a low surface profile, compared to one with a much steeper gradient (Giesen & Oerlemans, 2010) (Fig. 5.16). Therefore this is likely to translate to a larger retreat distance of the terminus on flatter topography than on steeper slopes, where a much smaller increase in the ablation area occurs.

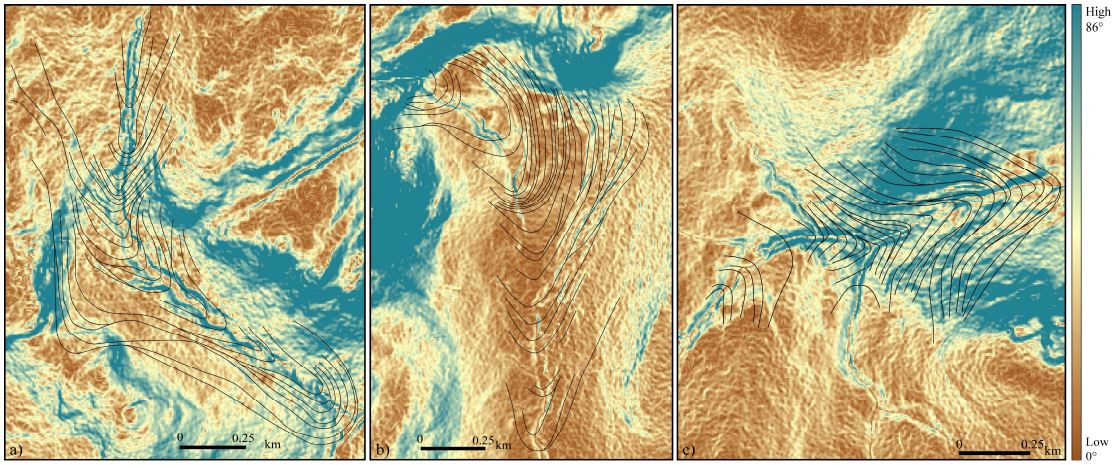

Figure 5.15. Ice margin positions during retreat for a) Beith Glacier, b) Chaorainn Glacier, c) Easgainn Glacier, overlain onto slope angles. The Beith Glacier displays initial retreat style 1 and is clearly influenced by slope, since ice margin positions are closer together on steeper slopes. The Chaorainn Glacier displays initial retreat style 2 and resides in a low gradient valley. However, as the glacier retreats towards the backwall the ice margin positions become closer due to the steeper gradient. The Easgainn Glacier resides in an outlet valley of relatively uniform steepness, but is closely linked to the plateau source area and displays initial retreat style 3. Slope data derived from the NEXTMap DSM (Intermap Technologies Inc. provided by NERC via the NERC Earth Observation Data Centre).

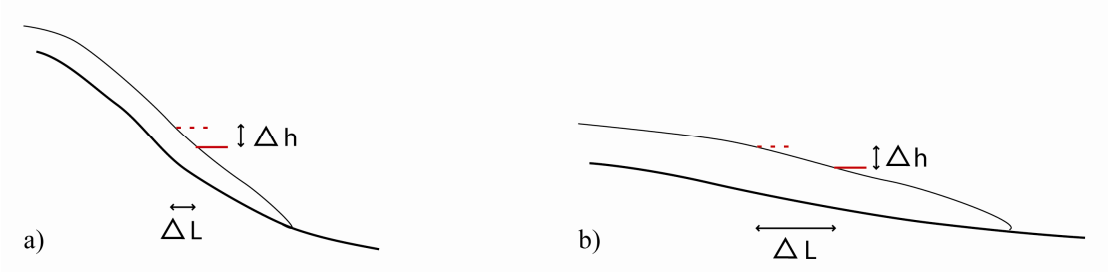

Figure 5.16. Diagram to show the effect of slope on changes in the position of the ELA relative to glacier length, where the same vertical rise in ELA will increase the size of the ablation area far more on a flatter glacier than on a steeper one. The solid red line represents the original ELA, the dotted red line represents the new ELA, Δ h is the change in ELA elevation and Δ L is the distance travelled by the ELA in a horizontal direction, which will eventually be translated into a glacier length change visible at the margin.

These results indicate that valley morphology has a large influence on the initial retreat dynamics of the outlet glaciers. During the initial phases of retreat, plateau source areas only appear to have had an effect on the moraine spacing and bifurcation style if the outlet glacier is small and closely linked to the plateau through the absence of a valley backwall. Other factors such as glacier area, % plateau area, glacier area, glacier length and aspect were also examined but found to have little effect on the initial retreat patterns (Fig. 5.17).

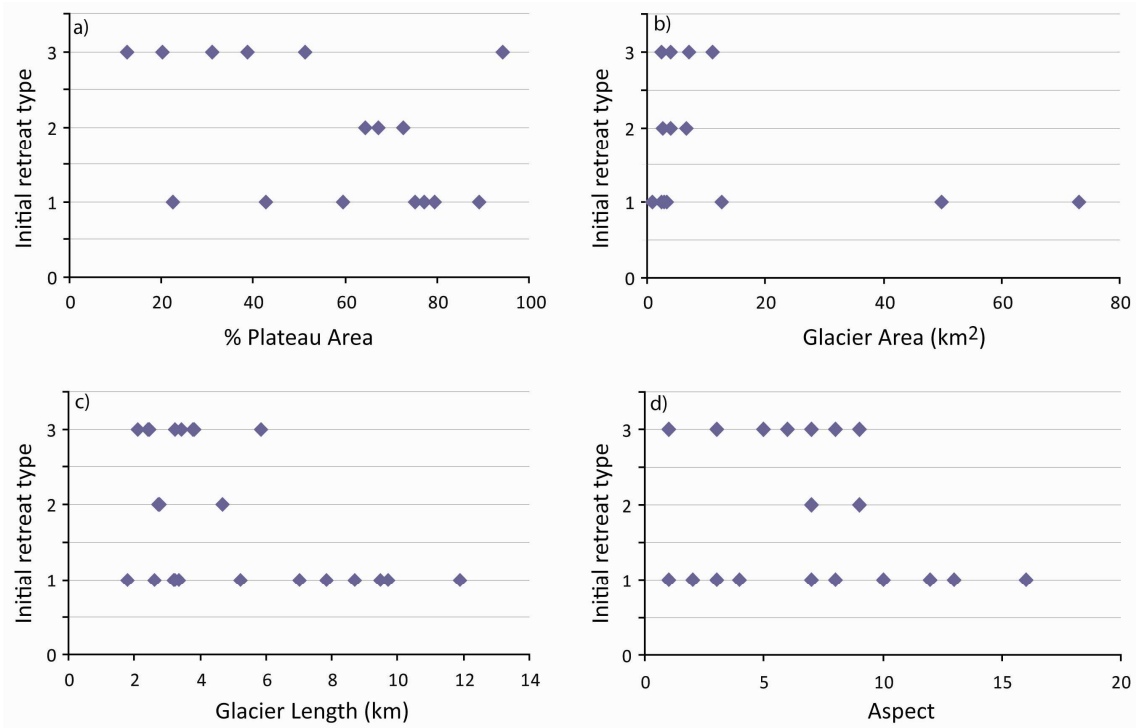

Figure 5.17. Graphs illustrating that a) % plateau area, b) glacier area, c) glacier length, d) glacier aspect (where 1 = north, 2 = north-northeast, 3 = northeast, 4 = east-northeast, 5 = east and so on) have no influence on the initial retreat type observed.

Overall retreat patterns

Examination of the effect of slope on moraine retreat patterns during the whole retreat phase also shows that the gradient of the glacier bed has a large influence of the retreat dynamics. Figure 5.18 shows the retreat barcodes in relation to the underlying topography along the central flowline of each outlet glacier investigated from the terminus up to the ice divide. The outlet valleys are grouped according to their overall retreat style, which is closely linked to outlet valley bed topography. Four styles have been identified:

1. Backwall (BW) – Outlet valleys in which moraine deposition stops close to the valley backwall, immediately before the glacier terminus retreats up the steep backwall slope and onto the plateau. These outlet valleys have very little plateau area (12 – 31 % of the total catchment area).
2. Plateau moraines (PM) – Outlet valleys in which moraines are found on the plateau. These are often a few isolated moraines that occur at much higher elevations than the majority of moraines in the main part of the valley. The majority of these valleys do not have steep backwalls and have large plateau source areas (in general, well over 50% of the total catchment area).
3. Plateau no moraines (PNM) – Outlet valleys that have large plateau source areas (over 50% of the total catchment area) but recessional moraines do not occur on the plateau.
4. Valley (V) – Outlet valleys in which the former glacier had a large plateau area at its maximum extent, but during retreat the proportion of plateau ice and outlet glacier ice

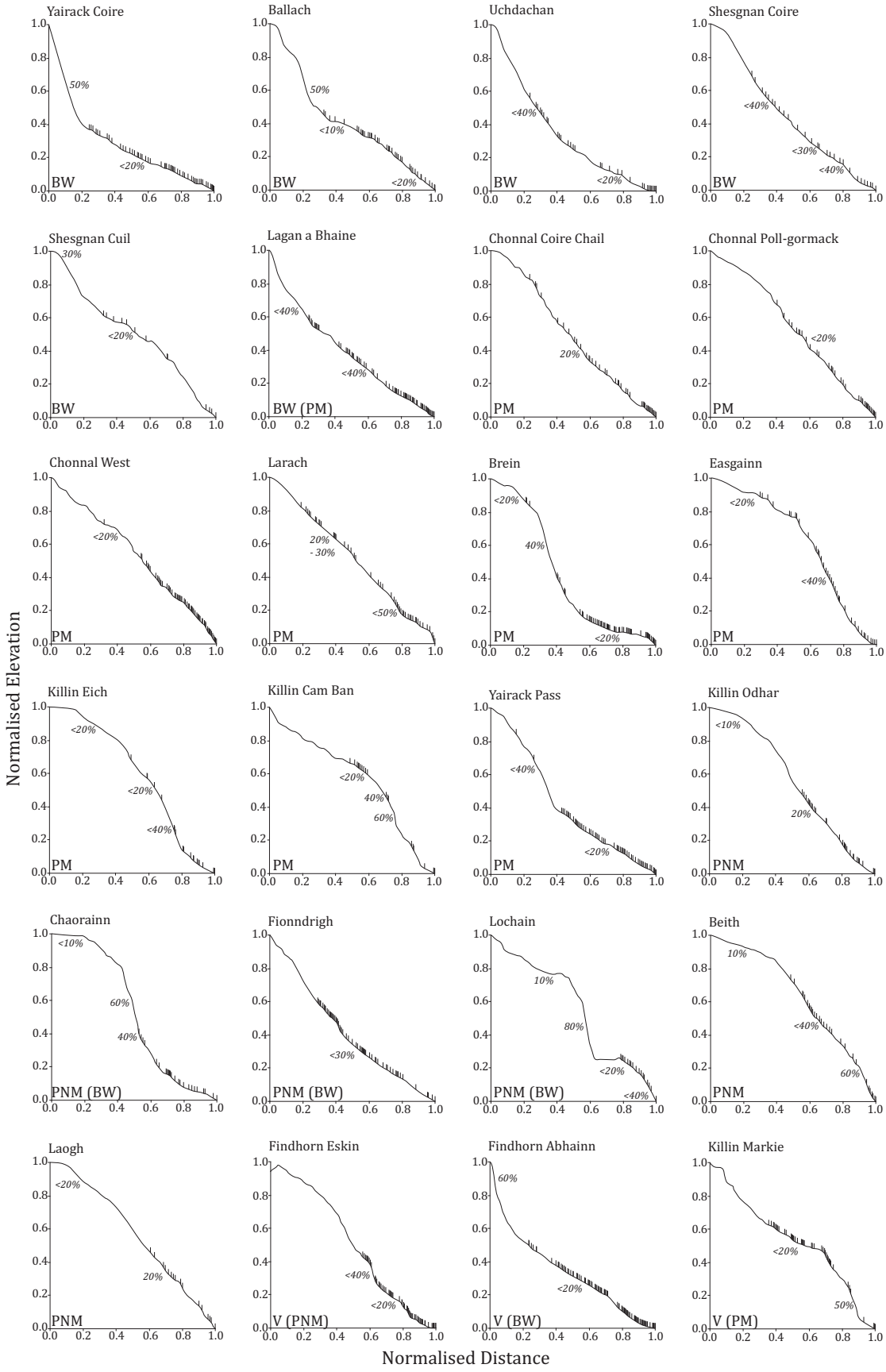

Figure 5.18. 'Barcodes' for each outlet glacier overlain onto the bed topography along the central flowline of each respective outlet glacier. The bed slope profiles are organised by overall retreat pattern groups as described in the text, where BW = backwall, PM = plateau moraines, PNM = plateau no moraines and V = valley. Where retreat patterns fit into more than one category the secondary group is shown in brackets. The gradient of the bed slope is indicated at key locations along each profile by the percentages in italics.

remained similar as the glacier retreated into the valley and plateau ice was lost simultaneously.

Some outlet valleys fall into two of these categories and this is also displayed in Figure 5.18. Of particular note is that outlet valleys with consistent gradients tend to have more evenly distributed moraines, whilst the density of palaeo ice-fronts in valleys with significant changes in gradient tends to vary to more widely. As discussed above, where the bed topography steepens during the early stages of glacier retreat, the palaeo ice margins generally become more closely spaced, such as in Gleann Fionndrigh, Coire nam Beith, Coire Easgainn and Coire Larach. However, moraines have not developed on slopes with gradients greater that 50%, such as in parts of Glen Cam Bàn, Glen Markie (Killin) and Glen Eich. The majority of changes in slope gradient occur where the outlet valley meets the plateau, manifest in an increase in slope gradient on the backwall before a decrease in slope gradient on the plateau. Very few moraines have been deposited in these areas, even at gradients of less than 50%, implying that this later stage of retreat was more uninterrupted than earlier on. This interpretation is supported by a lack of meltwater channels in these areas and by chaotic moraines on the plateau above glens Odhar and Eich, which document ice stagnation (Section 4.2.6). Exceptions, however, include Coire nam Cròc (Killin), Glen Cam Bàn (Killin), Glen Brein, the Coire Yairack Pass, Coire nam Stri (Eskin) and Coire nan Aonach (Eskin). These plateau areas tend to have slightly steeper gradients of 10-20% compared to other plateau areas with no moraines, which often have gradients of less than 10%.

In order to examine the effect of plateau areas on the retreat patterns further, the glacier hypsometry was examined. Hypsometry quantifies the shape of a glacier by describing the changes in glacier area with elevation. The response of a glacier to either climate control or external forcing can also be largely influenced by the glacier hypsometry, where glaciers which are 'bottom heavy' (i.e. where a large proportion of their area is at lower elevations) will respond very differently compared to a 'top heavy' glacier in which a large proportion of its area is at a higher elevation (Furbish & Andrews, 1984; Jiskoot *et al.*, 2009; Giesen & Oerlemans, 2010). Figure 5.19 shows the glacier hypsometry of each outlet glacier and demonstrates the sensitivity of the outlets within the latter stages of retreat, due to over 50% of the total glacier area often occurring in the upper 50% of elevations. At a number of glaciers, up to 95% of the total glacier area occurs within the upper 50% of elevations. This means that any rise in ELA at lower elevations (on the steep part of the hypsometric curve) will not cause a significant change in the relative proportions of accumulation and ablation areas, but once the flatter part of the hypsometric curve is reached, a small rise in ELA will result in a large area of the glacier becoming part of the ablation zone.

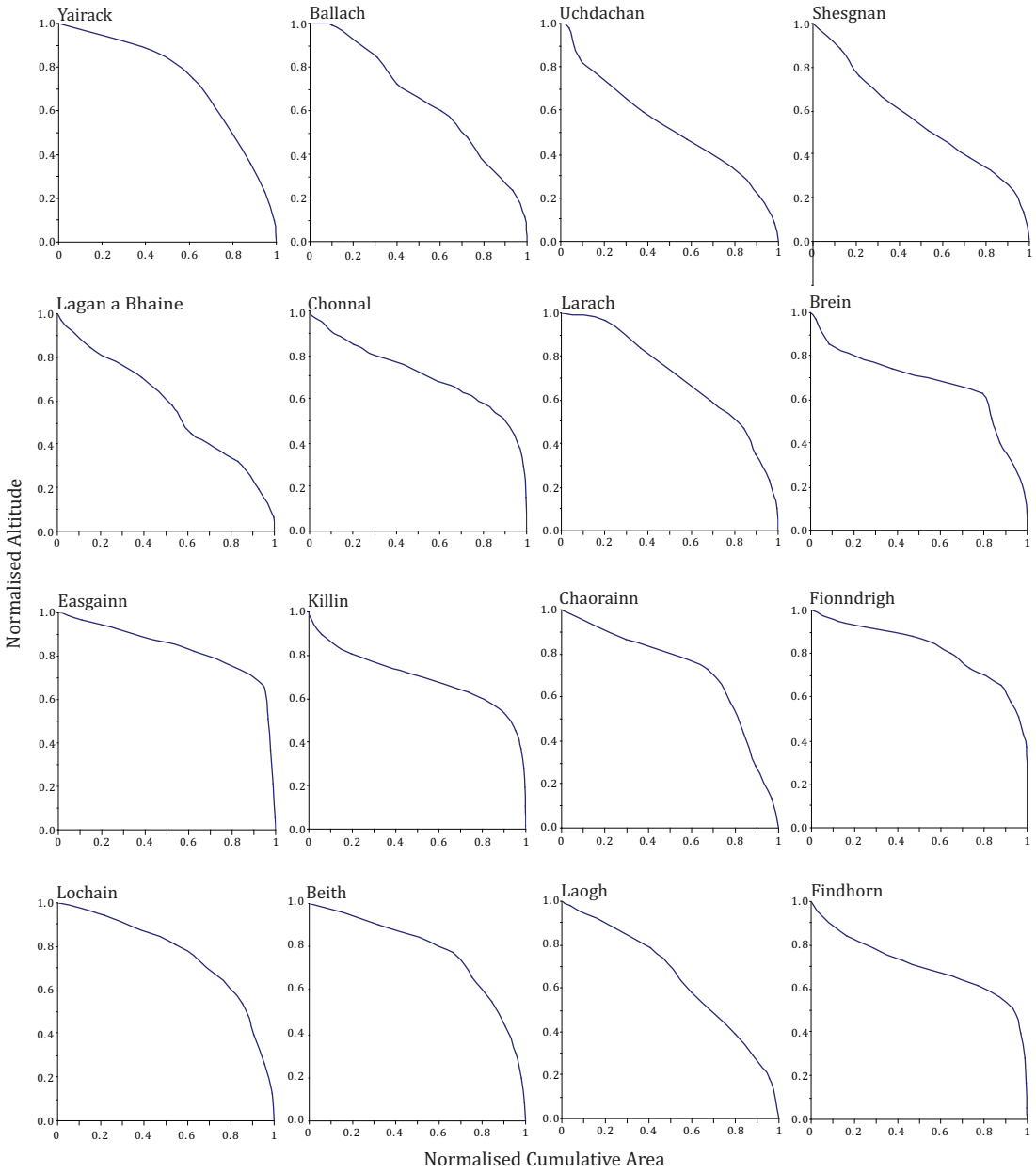

Figure 5.19. Normalised hypsometric curves for the outlet glaciers at their maximum extents.

This hypsometry goes some way to explaining the lack of moraines on the plateau since it predicts rapid and uninterrupted retreat once the ELA rises onto the flat part of the hypsometric curve. However, it is difficult to link glacier hypsometry at the maximum extent to the retreat patterns, since the shape of a glacier changes during retreat. For example, at its maximum extent, the Findhorn Glacier was sourced by a large area of plateau (Fig. 5.19), but moraine retreat patterns indicate that the glacier retreated into the Abhainn Crò Chlach valley, which continues into the centre of the plateau, connecting with Glen Markie in the south and splitting the higher ground of the plateau in two (Fig. 5.18). As the glacier retreated into this valley it also lost plateau source areas simultaneously. This means that the glacier hypsometry remained relatively similar throughout retreat, with the ELA not reaching the flatter part of the curve until much later in retreat than predicted by the hypsometric curve at the glacier's maximum extent.

There is some link between the initial retreat styles and the overall retreat groups in that a) the three outlet valleys with retreat style 2 have steep backwalls, but also no moraines on the plateau above the backwall (BW/PNM) and b) a number of the valleys which present retreat style 3 have moraines on the plateau (PM), most likely due to a lack of backwall between the plateau and the outlet valley. However, apart from this, there is little overall relationship between the initial retreat style, which is mainly controlled by outlet valley morphology, and the overall retreat patterns, which are more closely related to slope gradient over the whole catchment.

Change in ELA at the innermost ice-margin

The innermost ice fronts document the last stage during retreat at which moraines were formed and preserved at each outlet glacier. Beyond this point it is suggested that ice retreat was more continuous and uninterrupted. Using these innermost ice fronts, the outlet glaciers were reconstructed at this stage of retreat and are shown in Figure 5.20. The figure shows that the final ice fronts were reached asynchronously, particularly where neighbouring catchments do not match up across the ice divide. This demonstrates that some outlet glaciers began retreating more passively, without forming moraines, whilst neighbouring glaciers continued to retreat actively. The figure also shows which outlet glaciers became disconnected from the plateau or from their original ice divides.

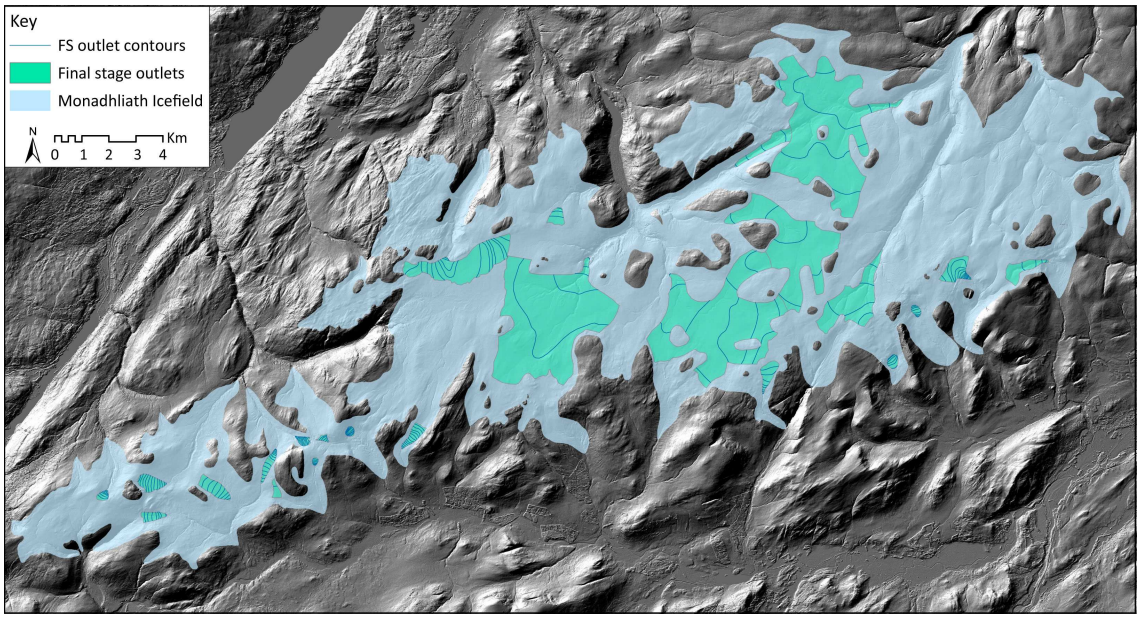

Figure 5.20. Reconstructed outlet glaciers at their final retreat stage (FS) (green), based on the innermost ice margin for which evidence has been preserved. These are contoured at 50 m intervals for the larger outlet glaciers and 10 m intervals for smaller ones. The final retreat stage glaciers are overlain on top of the average Monadhliath Icefield reconstruction for comparison (blue). NEXTMap DSM hillshade model from Intermap Technologies Inc. provided by NERC via the NERC Earth Observation Data Centre.

In order to assess these changes and differences between catchments further, the ELAs of the final retreat stage glaciers were calculated (Table 5.7). These glaciers are unlikely to have been

in equilibrium with the climate, since they represent a stage of retreat and therefore the assumption required for ELA calculations that they were in equilibrium (Section 5.4.1) is not valid in this instance. However, the calculation of these retreat stage 'ELAs' is useful as an exercise in understanding the dynamics of plateau icefield retreat. The ELA calculations reveal that a number of final stage ELAs are lower than their respective ELAs at their maxima. Three out of the four glaciers (Ballach, Lochain and Yairack) that disconnected from ice on the plateau have calculated ELAs that are significantly lower than their calculated ELAs at the maximum extent. The fourth glacier (Shesgnan) consisted of only a small percentage of plateau ice at its maximum extent, which probably explains why its retreat ELA rose. Interestingly, the moraine spacing does not alter dramatically within the Ballach, Lochain and Yairack outlet valleys in the area in which a disconnection from the plateau would have occurred. This suggests that factors such as ice avalanching, redistribution of snow and possibly shading from the backwall allowed these glaciers to exist well below the regional ELA (cf. Rea *et al*., 1999; Evans *et al.*, 2006a).

Table 5.7. Comparison between the AABR 1.9 ELAs for the average icefield at its maximum extent and the ELAs for retreated outlet glaciers at their final position of active retreat. The outlet valleys are grouped by area in the Monadhliath Mountains and within this organised from west to east.

Glacier	AABR 1.9 ELA	Retreat ELA	∆ ELA	Disconnect plateau?	Disconnect ice divide?
Western Valleys					
Larach	620	693	+73	No	No
Chonnal West	630	573	**-57**	No	No
Chonnal East Odhar	630	602	**-28**	No	No
Chonnal East Chail	630	701	+71	No	No
Shesgnan Cùil	640	684	+44	No	No
Shesgnan Coire	640	755	+115	**Yes**	**Yes**
Lagan a Bhaine	570	648	+78	No	In part
Uchdachan Leac	600	709	+109	No	No
Uchdachan Coire	600	741	+141	No	No
Northern Valleys					
Brein	649	665	+16	No	No
Easgainn	692	676	**-16**	No	In part
Killin Odhar	717	681	**-36**	No	No
Killin Eich	717	734	+17	No	No
Killin Cam Bàn	717	787	+70	No	No
Killin Markie	717	647	**-70**	No	In part
Eastern Valleys					
Findhorn Eskin	770	715	**-55**	No	No
Findhorn Abhainn Crò Chlach	770	822	+52	No	No
Southern Valleys					
Yairack Pass	716	766	+50	No	In part
Yairck Coire	716	633	**-83**	**Yes**	**Yes**
Laogh	695	733	+38	No	No
Beith	770	827	+57	No	**Yes**
Lochain	811	664	-147	**Yes**	**Yes**
Ballach	738	703	**-35**	**Yes**	**Yes**
Fionndrigh	783	847	+64	No	**Yes**
Chaorainn	773	835	+62	No	In part

A number of other glaciers are also found to have lower calculated ELAs following retreat. These glaciers all had large plateau source areas at their maximum extent and therefore the loss of an extensive area of plateau ice has paradoxically caused the calculated ELAs to decrease. The final retreat stage glaciers for which this has occurred are much larger than the glaciers for

which the calculated ELAs rose during retreat. The catchments of these glaciers tend to be formed of large plateau areas in which small depressions or proto-valleys occur, into which the glaciers retreated. This plateau morphology is found to be the key control on whether the calculated ELAs rose or fell during retreat. Figure 5.21 demonstrates that, similar to Figure 5.17 for the initial retreat patterns, factors such as glacier length and the % of the total area classed as plateau have little influence on the change in calculated ELA between each glacier's maximum and final stage configuration. Although the ELAs calculated here are only area-based estimates, as will be discussed further in Section 6.4, the final stage glaciers on the plateau for which the ELA estimate has lowered in altitude were most likely able to survive due to the redistribution of snow and some possible shading from higher ground on either side, in a similar way to the disconnected corrie glaciers (e.g. Ballach Glacier), meaning that their true ELAs were probably higher than calculated here. It is likely that uninterrupted retreat or ice stagnation occurred after these glaciers reached this stage and goes someway to explain the lack of moraines on large areas of the plateau, as well as the stagnation moraines on the plateau above Glen Odhar and Glen Eich (Section 4.2.6). These findings are discussed in greater detail in Section 6.4).

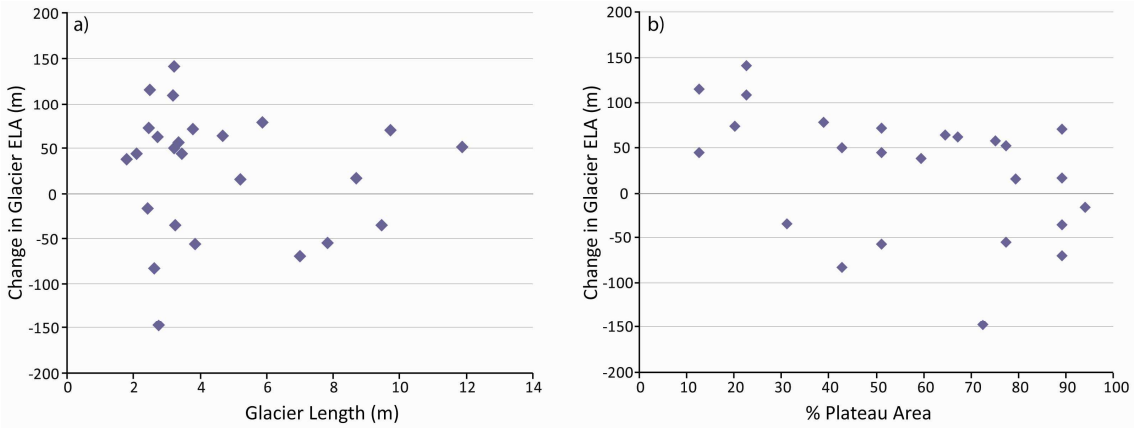

Figure 5.21. Graphs demonstrating that a) glacier length and b) % plateau area of the glaciers at their maximum extents have little influence on the change in glacier ELAs from the maximum extent to final stage of active retreat.

Summary

To summarise, reconstruction of palaeo-ice fronts in sixteen key outlet valleys demonstrates that these outlets retreated actively, with the retreat characterised by small advances and stillstands. Three initial retreat types were identified using the 'barcode approach' (Lukas & Benn, 2006), which are closely related to the style of moraine crestline bifurcation that occurred in each outlet valley. In turn, detailed analysis shows that the retreat type and bifurcation style are predominately controlled by outlet valley morphology and the gradient of the bed topography. This has added more certainty to the influence of dominant controls on plateau icefield outlet glacier retreat, which have not previously been examined in such detail and has wider implications for our understanding of plateau icefield dynamics on the whole.

Overall retreat patterns are also controlled by bed topography, where moraines do not develop on slopes with gradients greater than 50%. Glacier hypsometric curves, although highlighting the sensitivity of the plateau icefield system to retreat once the ELA rises onto the plateau, could not be linked to the retreat barcodes, owing to changes in the area of plateau ice during retreat.

Remnants of outlet glaciers reconstructed at the final stage of active retreat demonstrate that four glaciers became disconnected from the plateau, with a further five glaciers fully disconnecting from the original ice divide and five partly disconnecting. Many of the ELAs calculated for the retreat outlet glaciers are lower than the calculated ELAs of the glaciers at their maximum extent due to loss of plateau ice. These glaciers are likely to have been sustained through ice avalanching, capture of redistributed snow and/or shading from valley sides (cf. Rea *et al*., 1999), meaning that their true ELA was actually higher. Outlet glaciers that retreated onto the plateau, but had lower calculated ELAs than at their maximum, still had large catchment areas on the plateau, despite a substantial loss of plateau ice from the maximum, indicating that although their true ELA was probably higher, any subsequent retreat was probably uninterrupted, helping to explain the lack of moraines in the upper parts of these catchments. The finding that the retreat of some outlet glaciers onto the plateau caused a lowering of the calculated ELA has not been found on plateau icefields before and is potentially a 'special case' scenario owing to the undulating morphology of the Monadhliath plateau, characterised by small summits and proto-valleys. This phenomenon/potential problem will be discussed further in Section 6.4.

5.6 Chapter Summary

This chapter has concentrated on the reconstruction of plateau icefield glaciation in the Monadhliath Mountains during the LGIT, which included ELA and palaeoclimate calculations and an examination of plateau icefield dynamics for the most recent phase of glaciation. Section 5.1 established a relative chronology for glacial events in the Monadhliath Mountains using morphostratigraphy, and concluded that the most recent glacial event occurred during the Younger Dryas, with older features relating to retreat stages in the latter part of the Dimlington Stadial (GS-2). Younger Dryas glacier limits were established within outlet valleys using morphostratigraphical criteria, developed based on a large dataset of unequivocally dated Younger Dryas sites elsewhere in the UK (*cf.* Lukas, 2006). This includes a change in moraine morphology, a change in the number or magnitude of river terraces, a change in the number or size of ice-marginal meltwater channels, the absence of glaciofluvial features, the presence of boulder spreads, the upper limits of sediment accumulations and the absence or termination of periglacial features such as blockfields and solifluction lobes (Table 5.1).

Reconstruction of the Younger Dryas Monadhliath Icefield was carried out within *ESRI ArcGIS* using an extrapolative approach based on the geomorphological evidence described in Chapter 4. In order to gain a better estimation of ice-thickness in areas where geomorphological evidence was lacking or ambiguous, two glacier surface profile models (Benn & Hulton, 2010; Ng *et al.,* 2010) were used to identify minimum and maximum boundaries for glacier thickness that could be used to create an 'average thickness' icefield and quantify some of the uncertainty surrounding the thickness of the plateau icefield. This uncertainty was then incorporated into the errors associated with the ELA and palaeoprecipitation calculations.

The systematic geomorphological mapping and sedimentological analysis carried out in Chapter 4 has enabled the identification of a more detailed and consistent relative chronology for deglacial events from the LGM than has previously been recognised. This includes an examination of the relationship between regional ice sheet and local plateau ice during deglaciation from the LGM. The evidence described here suggests that the formation of ice-dammed lakes in the tributary valleys to Strathspey and the Great Glen, caused a retreat of local plateau ice to higher elevations, although some local glaciers remained in contact with the lakes in valleys such as in Glen Mòr and Glen Odhar. Drainage of the ice-dammed lakes, following further retreat of regional ice allowed local ice to readvance at least in some valleys indicating climatic conditions were severe enough after ca. 15.8 to 15.5 ka BP (ice-free conditions in Strathspey) to allow expansion of a plateau icefield centred over the Monadhliath Mountains during this time. An asynchronous expansion of plateau ice is suggested however, based on asynchronous deglaciation of Strathspey and the Great Glen, meaning that Glacial Lake Killin is likely to have formed later than the ice-dammed lakes on the southern side of the plateau. Discrepancies arise in both the northern and southern parts of the study area in that no evidence is found for more extensive pre-Younger Dryas glacier limits in some northern valleys, whilst clear evidence exists in others, suggesting a different ice configuration at this time compared to during the Younger Dryas.

Equilibrium line altitudes were calculated for the Younger Dryas Monadhliath Icefield and the majority of outlet glaciers using the AABR, AAR and AWMA methods. An ELA for the 'average' Monadhliath Icefield was calculated at 714 ± 25 m using an AABR of 1.9 ± 0.81, which is considered the most representative for mid-latitude glaciers (Rea, 2009). ELAs calculated using the 1.9 ± 0.81 AABR for outlet glaciers ranged from 560 ± 20 m in the northwest to 814 ± 8 m in the southeast and showed a significant rise in ELAs from west to east across the region. Palaeoprecipitation at the 1.9 AABR ELAs was examined using the Ohmura *et al.* (1992) and Golledge *et al*. (2010) precipitation-temperature relationships and was calculated at 1829 ± 491 mm a^{-1} (Ohmura *et al.,* 1992), 1809 ± 592 mm a^{-1}, 1292 ± 480 mm a^{-1}

and 1034 ± 424 mm a^{-1} (Golledge *et al.*, 2010, summer, neutral and winter types respectively) for the 714 m ELA of the whole icefield, using a mean July sea-level temperature of 8.5 ± 0.3° C. Palaeoprecipitation amounts within major outlet valleys decreased considerably from west to east, in correspondence with the rise in ELAs in the same direction. As a result, palaeoprecipitation varied between 2286 ± 617 to 1306 ± 438 mma^{-1} in the northwest at an ELA of 570 m and 1493 ± 588 to 853 ± 422 mma^{-1} in the southeast at an ELA of 816 m for the Golledge *et al.* (2010) summer and winter precipitation types respectively. The implications of these calculations for regional palaeoclimate will be discussed in Section 6.2.

A detailed examination of glacier thermal regime and recessional moraine patterns and spacing suggests that the slope of the underlying topography had a large influence on the dynamics of the Monadhliath Icefield. The gradient of the bed topography had a significant influence on the thermal regime of outlet glaciers, in that glaciers residing in steeper catchments were more likely to be warm-based due to increased strain heating. Bed slope also exerted a dominant control on glacier retreat dynamics, where moraines were more closely spaced on steeper slopes, owing to a lower corresponding horizontal distance for a specific rise in ELA height compared to on lower gradient slopes where a larger distance generally occurred between moraines. If the gradient became too steep (i.e. over 50%), however, moraines did not occur, suggesting either more continuous glacier retreat on these slopes and a lack of moraine formation, or lower moraine preservation potential.

Valley morphology was also found to exert a large control on glacier thermal regime and glacier retreat dynamics. Larger, deeper valleys were able to accommodate thicker glaciers, which were able to reach pressure melting point due to the greater thickness of ice. The shape of the valley also had a significant influence on glacier retreat dynamics, where initial retreat within wider, flatter valleys was manifest in thinning of the glacier, causing lateral moraine bifurcations before more continuous retreat upvalley. Conversely, initial retreat of glaciers within narrow valleys with steep valley sides was translated to the snout, which retreated first before any overall glacier thinning occurred, causing frontal moraine bifurcations. These changes were identified as being related to differences in the amount of insolation received by glaciers in different valley types due to variations in shading. The size of the plateau catchment area was found to have little influence on the outlet glaciers during the initial stages of retreat, except where the outlet glacier was small and closely connected to the plateau with no steep backwall. These glaciers produced a combination of frontal and lateral moraine bifurcations indicating that the glaciers retreated more steadily through snout retreat and glacier thinning. Section 6.4 will provide further discussion on these findings with respect to our understanding of the plateau icefield landsystem.

An important outcome of the examination of the retreat dynamics of the Younger Dryas Monadhliath Icefield during the later stages of retreat was that many of the calculated ELAs were lower at the final stage at which moraines were produced than at the maximum glacier positions. This is caused by the loss of a large plateau source area, which has affected the area-based ELA calculation and indicates that the true ELA was probably higher due to snow redistribution by wind and shading within topographic lows. Although this phenomenon has been discussed with respect to the disconnection of valley glacier ice from plateau ice (e.g. Rea *et al*., 1999), it has not been observed for outlet glaciers that retreated onto the plateau. This finding will be examined in greater detail within Section 6.4 in terms of the plateau icefield landsystem and the way in which we consider ELAs in this context.

Chapter 6

Younger Dryas Glaciation in the Monadhliath Mountains and Implications for the Plateau Icefield Landsystem

This chapter considers the main findings of this research (Chapters 4 and 5), with respect to previous studies and the wider context. The discussion focuses on glaciation during the Younger Dryas since this provides the most complete record of former glacier limits and glacier retreat dynamics. This record is still fragmentary in some areas, however, owing to differences in thermal regime, and moraine production and preservation differences across the icefield (Section 5.5.1). The chapter is divided into four main sections that will examine the research aims outlined in Chapter 1. Section 6.1 discusses the timing of maximum glaciation during the Younger Dryas in the Monadhliath Mountains. Section 6.2 focuses on the implications of the identification of a Younger Dryas plateau icefield for former climate in the Monadhliath Mountains and the relationship to other areas of Scotland. Section 6.3 briefly assesses potential modern analogues for the Younger Dryas Monadhliath Icefield. The final section, 6.4, assesses how the examination of plateau icefield dynamics in Chapter 5 has added to our understanding of the plateau icefield landsystem, including a discussion on the effect of plateau ice on area-based ELA estimates and the use of area-based ELA calculations in this context.

Using a morphostratigraphical approach, this research has identified the existence of two substantial coalescent plateau icefields in the Monadhliath Mountains during the Younger Dryas (Section 5.2), which had a combined area of 280 km^2. The reconstructed icefield coincidentally provides a close match in terms of eastwards extent to the results of modelling by Golledge *et al*. (2008) (Fig. 6.1). The model does not produce ice flowing into the major outlet valleys of the Findhorn and Killin, but does indicate that modelled climatic conditions were severe enough over the western and central plateau areas of the Monadhliath Mountains to support the growth of plateau ice. Interestingly, the model does not predict growth of plateau ice further east than the head of the Dulnain catchment, in agreement with the Younger Dryas limits identified in this research. In the west, the model was unable to reproduce the empirical limits of the West Highlands Ice Cap, since it could not replicate ice-dammed lake formation in Glen Spean, Glen Roy and Glen Gloy. Golledge *et al.* (2008) suggest that the Monadhliath Icefield would have remained separate from the main West Highlands Ice Cap because of these lakes, and this ice configuration agrees well with the empirical field evidence presented here.

In the absence of any published dates in the region at present, the assignment of this period of plateau icefield glaciation to the Younger Dryas is still subject to verification through absolute dating techniques. As shown in other dated areas (e.g. Lukas & Bradwell, 2010; Finlayson *et*

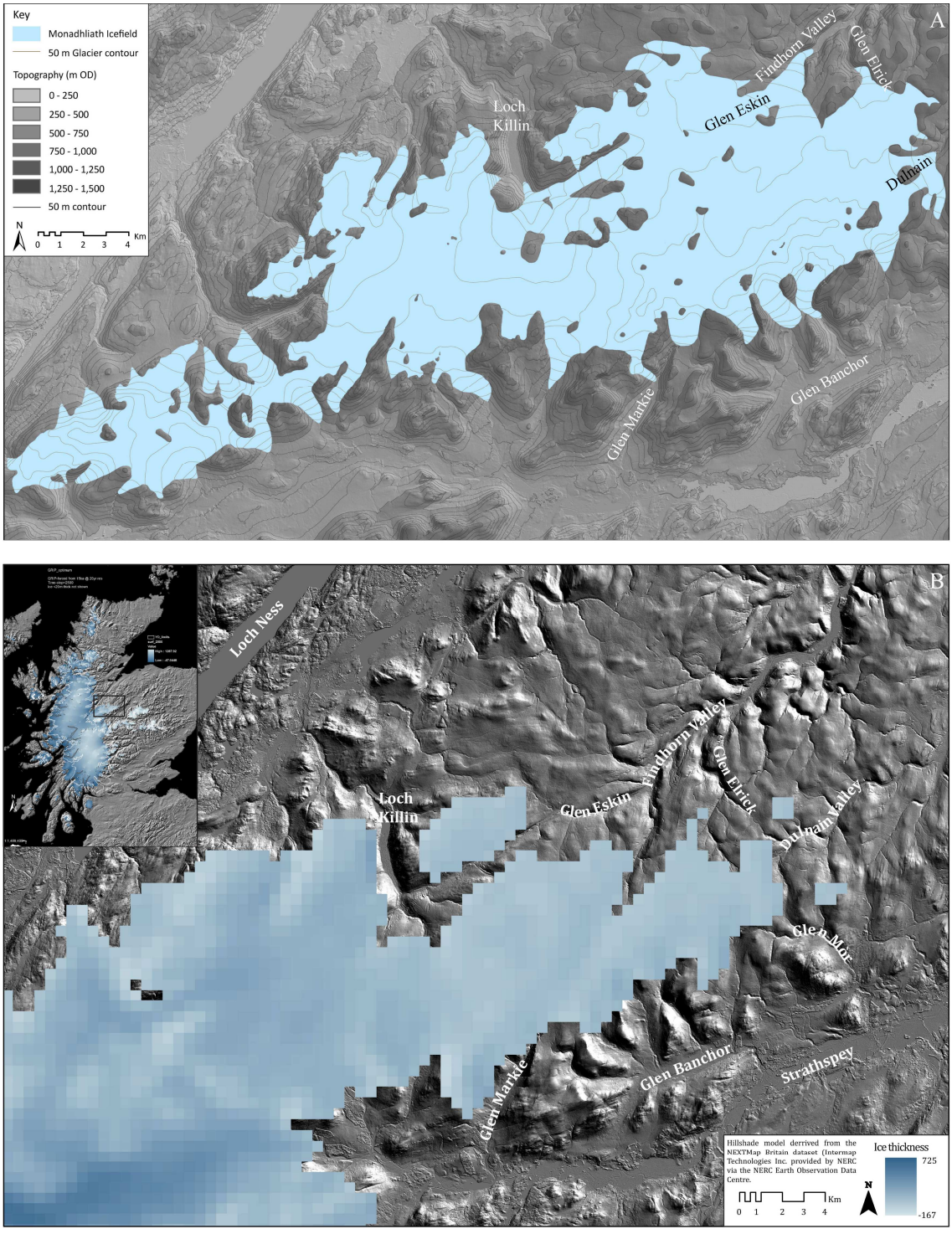

Figure 6.1. Comparison between A) the reconstruction of the Younger Dryas Monadhliath Icefield presented in this research based on empirical evidence and B) modelled Younger Dryas ice extent in the Monadhliath Mountains for an 'optimum' fit model of Younger Dryas ice in Scotland, constrained by empirical evidence from elsewhere in Scotland. Fig. 6.1B adapted from Golledge *et al.* (2008).

al., 2011), however, a morphostratigraphical approach can provide a robust method for identifying the presence of Younger Dryas ice in the first instance. The identification and reconstruction of a Younger Dryas icefield in this research therefore provides a substantial step forward in our understanding of glacier growth and extent during the Younger Dryas in this region of the Scottish Highlands. Further discussion on the timing of maximum glacial extent,

the implications for regional palaeoclimate and the contribution to the plateau icefield landsystem are discussed below and within Sections 6.1 to 6.4.

6.1 Timing of Maximum Glacial Extent

The majority of research relating to the timing of Younger Dryas glaciation in Scotland suggests that glaciers reached their maximum extents in the mid-part of the stadial (e.g. Benn *et al.*, 1992; Benn & Ballantyne, 2005; Golledge *et al*., 2007; Ballantyne, 2012). On the Isle of Skye, Benn *et al*. (1992) suggested that high precipitation and cold temperatures in the early part of the Younger Dryas allowed glaciers to reach their maximum positions early on, before increased aridity caused early deglaciation to begin in the mid to late part of the stadial, well before temperatures rose significantly. This argument is supported by the modelling experiments of Golledge *et al.* (2008) that also indicate glacier growth was fastest during the early part of the stadial. In addition, palaeotemperature estimates from chironomids indicate a cooler first half to the stadial, which also supports these findings (Fig. 2.3). However, recent research from Loch Lomond and Lochaber indicates that the glaciers that dammed Glacial Lake Blane and the lakes in Glen Roy, Glen Spean and Glen Gloy did not reach their maximum limits until late in the stadial (Fabel *et al.*, 2010; Palmer *et al.*, 2010, 2012; MacLeod *et al*., 2011). This evidence is based predominantly on high resolution varve chronologies from sediments deposited within the lakes, which are constrained chronostratigraphically; radiocarbon dates indicate that the formation of Glacial Lake Blane occurred around 12.0 ka BP, with lake drainage between ca. 11.76 to 11.47 ka BP (MacLeod *et al*., 2011), whilst SED ages from Glen Roy constrain the abandonment of the 325 m shoreline to between 11.5 ± 1.1 to 11.9 ± 1.5 ka BP (Fabel *et al*., 2010), with the onset of lake development at ca.12.2 ka BP (Palmer *et al*., 2010).

The research presented here is able to add to this debate based upon the stratigraphical correlation of the western part of the Monadhliath Icefield with the Glen Roy ice-dammed lakes. From arguments made in Section 5.2, Younger Dryas glacier limits were identified at the head of Glen Turret, where glaciolacustrine ice contact fans demonstrate that these glaciers were in contact with the 350 m level lake. The placement of the Younger Dryas limit here, and the subsequent overriding of the Teanga Bige fan following lake drainage, implies that these glaciers reached their maximum extent towards the end of the stadial. This highlights the importance of identifying the correct position of the Younger Dryas limit in this valley, since placement of the limit at the Turret Fan would suggest an early advance of the Turret Glacier, which then retreated to the 350 m position later in the stadial either due to climate forcing or increasing lake levels in Glen Roy. Arguments made in Section 5.2.2 provide convincing evidence that the Younger Dryas limit(s) should be placed at the head of Glen Turret, rather

than at the Turret Fan, therefore implying that the Monadhliath Icefield reached its maximum position in the latter part of GS-1 after 12.2 ka BP (Palmer *et al*., 2010). The presence of moraines on top of the Teanga Bige fan signify that a small advance of the Teanga Bige Glacier occurred following lake drainage between ca. 11.5 and 11.9 ka BP (Fabel *et al.*, 2010) (Sections 2.3.3 & 4.1.6), indicating that small advances were able to occur even in this later part of the stadial. A change from a calving to terrestrial ice margin may have also had a substantial effect on glacier dynamics here, however (e.g. Reitner, 2007).

In the rest of the Monadhliath Mountains, recessional moraine patterns indicate that the glaciers also retreated in an oscillatory fashion, remaining close to equilibrium (Section 5.5.2). In a number of valleys the largest moraines are often found inside the outermost moraines and major river terraces are also observed to start just inside the outermost moraines (see Appendix II). In other valleys, the boundaries between periglacial and glaciogenic evidence are not exact, where thick talus deposits drape the outermost moraines. Whilst the extended talus slopes could simply reflect post depositional movement due to gravity, this potentially indicates that periglacial conditions were still severe enough to allow the formation of periglacial features inside the maximum limits. These factors and the lack of significant end moraines in most valleys signify that many of the outlet glaciers may not have remained at their maximum positions for very long, retreating slightly and stabilising for longer further upvalley. This supports evidence from elsewhere in Scotland for a two phased-Younger Dryas advance, where the maximum glacier positions were reached at a short-lived earlier stage, then retreated slightly before stabilising or re-advancing to a less extensive position (e.g. Sisson, 1974b; Peacock *et al*., 1989; Merritt *et al*., 2003b).

This evidence suggests that an initial advance occurred earlier in the Younger Dryas, which seemingly conflicts with the evidence found in Glen Roy. This inconsistency is resolved here by suggesting that a short-lived early- to mid-stade initial glacier advance was succeeded by retreat over a small distance followed by glacier stabilisation, where higher precipitation levels and proximity to the West Highlands Ice Cap allowed the western part of the icefield to maintain an extensive position for longer, into the latter part of the stadial. Asynchronous deglaciation of the Monadhliath Icefield is also suggested by the results of modelling by Golledge *et al*. (2008), which indicates that ice may have remained relatively extensive in the western Monadhliath Mountains until 12.3 to 12.2 ka BP, even though it is predicted to have disappeared from the eastern Monadhliath Mountains by 12.5 to 12.4 ka BP. Evidence for a two-phased advance is not present in all valleys, suggesting the possibility of an asynchronous ice advance in the region as well as during retreat. This could potentially be a result of different glacier advance and retreat dynamics due to valley and plateau morphology (Section 5.5.2).

There is clearly still a large amount of uncertainty regarding the timing of the maximum extent of Younger Dryas glaciation in the Monadhliath Mountains and further constraint through absolute dating is required.

6.2 Regional Palaeoclimatic Inferences

Table 6.1 compares the palaeoprecipitation at sea level calculated for the Monadhliath Icefield with sea level equivalent palaeoprecipitation values for published ELAs of other Younger Dryas ice masses in Scotland, which were recalculated here using identical methods to those described in Section 5.4. The effects of glacier cooling on air temperatures were not accounted for here due to difficulties in quantifying the amount of cooling that would have occurred (Section 5.4.2), and therefore precipitation totals should be considered maximum values.

The precipitation levels calculated for the Monadhliath Icefield fit well within the overall Younger Dryas precipitation pattern in Scotland, showing slightly less precipitation in the Monadhliath Mountains compared to Creag Meagaidh and Drumochter to the south-west and south, respectively (Benn & Ballantyne, 2005; Finlayson, 2006), but possessing significantly more precipitation than in the Gaick, the southeast Grampians and the Cairngorm Mountains. Palaeoprecipitation values calculated for individual outlet glaciers (Table 5.6) reveal that there was a marked contrast between precipitation amounts in the west and east of the Monadhliath massif, ranging between 1185 ± 434 mma^{-1} in the west for the north-facing Lagan a' Bhainne Glacier and 674 ± 382 mma^{-1} for the Markie Glacier in south-eastern part of the plateau at sea level for the Golledge *et al.* (2010) neutral precipitation type. From these results, the plateau can be divided into three sectors; western, central and eastern. Average precipitation is 1082 mm a^{-1} in the western sector, 914 mma^{-1} in the central sector and 747 mma^{-1} in the eastern sector. The values calculated for the western sector are very similar to those calculated for Creag Meagaidh and Drumochter, showing strong consistency across studies in the western part of the field area (Benn & Ballantyne, 2005; Finlayson, 2006) (Table 6.1). The marked decrease in precipitation amounts eastwards across the Monadhliath massif is also reflected by the significantly lower precipitation values in the Cairngorm Mountains and the southeast Grampians (Sissons, 1974b, 1979e; Sissons & Sutherland, 1976) where precipitation totals calculated for the eastern sector of Monadhliath Mountains are very similar to that of the Gaick Plateau and southeast Grampians. In this respect, the neutral precipitation value at sea level of 474 ± 343 mma^{-1} for the Cairngorm Mountains seems anomalously low.

These results indicate that the Monadhliath Mountains were situated at a central point between significantly wetter conditions to the west and significantly drier conditions in the east, accounting for the strong precipitation gradient across the region. This is manifest in a step-wise

decrease in precipitation from west to east, as exemplified by the division of the region into three sectors, with the greatest decrease in precipitation levels from the western to central parts of the study area. Factors such as redistribution of snow by wind and internal glacier dynamics, which could have been affected by differences in topography and catchment area size, may also have played a role in creating the 'stepped' rise in ELAs from west to east (Fig. 5.9), which in turn has dictated the reconstructed precipitation pattern.

Table 6.1 indicates that the assertion made by Golledge *et al*. (2010) that the Younger Dryas climate in Scotland was more arid than currently recognised using the Ohmura *et al.* (1992) relationship is highly dependent on the degree of seasonal bias that occurred. The severity of precipitation seasonality therefore needs to be better understood in order to advance our understanding of the degree of aridity in Scotland during the Younger Dryas compared to at present (as also shown in Table 6.1).

Recent research suggests that extensive sea ice developed in the North Atlantic and extended to the south of the British Isles during the colder, early part of the Younger Dryas Stadial. This sea ice diverted storm tracks south of the sea-ice margin and towards continental Europe, generating a more stable, arid environment in Scotland and Norway (Isarin *et al*., 1998; Isarin & Rensen, 1999; Bakke *et al*., 2009; Golledge *et al*., 2010; Palmer *et al*., 2012). Increasing temperatures in the latter part of the stadial are thought to have caused the break-up of this sea ice and allowed storm tracks to move further northwards across Scotland and northern Norway, the frequency of which was controlled by the fluctuating sea-ice margin (Bakke *et al*., 2009). These changes in sea-ice extent suggest that during the early part of the stadial winter precipitation was likely to be suppressed due to extensive sea ice and also possibly reduced during the summer months as well. In the latter part of the stadial, however, the increase in the number of storm tracks passing over Scotland would have led to increased precipitation in potentially both the summer and winter months (Palmer *et al*., 2012). Seasonality bias would have had a large effect on the precipitation totals required to sustain glaciers during the Younger Dryas, but at present there are large uncertainties surrounding the degree to which a bias towards summer precipitation occurred (Section 5.4.2). Given these uncertainties, Golledge *et al.* (2010) considered the summer and winter precipitation types produced from the model to be maximum and minimum bracketing values for a likely range of precipitation (Fig. 6.2). This figure indicates much greater aridity in Scotland than has previously been suggested using the Ohmura *et al.* (1992) relationship due to both the incorporation of seasonality bias and the inclusion of the effects of glacier cooling on air temperatures at the ELA by over 2° C (Fig. 6.2).

Table 6.1. Annual precipitation values for Younger Dryas sites in Scotland, arranged from west to east, based on published ELAs, but calculated using the methods described in Section 5.4. The table includes the Monadhliath Icefield and average values for the western, central and eastern sectors. The table also includes modern precipitation data where already published, alongside previously published inferences about Younger Dryas climate and inferences made using the summer and neutral type (Golledge *et al*., 2010) precipitation levels calculated here. Modern precipitation data in the Monadhliath Mountains is shown in more detail in Table 6.2.

Ice Mass	Author	ELA (m)	ELA Method	Precipitation at Sea Level (mma^{-1})				Present day ppt at sea level (mma^{-1})	Climate (previously published)	Climate using summer type ppt	Climate using neutral type ppt
				Ohmura *et al.* (1992)	Golledge *et al.* (2010)						
					Summer type ppt	Neutral type ppt	Winter type ppt				
Uig, Lewis	Ballantyne (2006)	212	AABR (1.8)	2754 ± 349	3216 ± 421	2297 ± 358	1838 ± 327		wet		
Harris	Ballantyne (2007b)	204	AABR (1.8)	2786 ± 349	3259 ± 421	2328 ± 358	1862 ± 326	1885	wet	wet	wet
Skye	Ballantyne (1989)	319	AWMA	2353 ± 355	2675 ± 427	1911 ± 362	1529 ± 330		arid/ap		
Rhum	Ballantyne & Wain-Hobson (1980)	357	AWMA	2221 ± 356	2500 ± 426	1786 ± 363	1429 ± 330				
Mull	Ballantyne (2002a)	250	AABR (1.8)	2605 ± 351	3016 ± 424	2154 ± 360	1723 ± 328	2260	wet	wet	ap
Arran	Ballantyne (2007a)	371	AABR (1.8)	2174 ± 357	2437 ± 428	1741 ± 363	1393 ± 330	2005	arid/ap	wet/ap	ap/arid
Hoy, Orkney	Ballantyne et al. (2007)	141	AABR (1.8)	3046 ± 344	3615 ± 416	2582 ± 354	2066 ± 323				
NW Highlands	Lukas & Bradwell (2010)	339	AABR (1.8)	2283 ± 356	2582 ± 427	1844 ± 362	1475 ± 330	1863	wet	wet	ap
Beinn Dearg	Finlayson et al. (2011)	576	AABR (1.8)	1562 ± 360	1639 ± 425	1171 ± 361	937 ± 329				
Creag Meagaidh	Finlayson (2006)	625	AABR (1.8)	1436 ± 360	1478 ± 423	1056 ± 360	845 ± 328	1303	wet/ap	ap	arid/ap
Monadhliath		**714**	**AABR (1.9)**	**1224 ± 409**	**1211 ± 480**	**865 ± 400**	**692 ± 360**	**1354**		**ap**	**arid**
Western		610	AABR (1.9)	1465	1515	1082	866	1867		arid	arid
Central		705	AABR (1.9)	1279	1280	914	731	1131		ap/arid	arid
Eastern		777	AABR (1.9)	1088	1043	747	596	1064		ap	arid
Drumochter	Benn & Ballantyne (2005)	626	AABR (1.8)	1434 ± 360	1475 ± 423	1054 ± 359	843 ± 328	1337	ap	ap	ap/arid
Gaick	Sissons (1974b)	787	AWMA	1066 ± 358	1016 ± 311	726 ± 279	581 ± 263	1215	arid	ap	arid
SE Grampians	Sissons & Sutherland (1976)	790	AWMA	1060 ± 358	1008 ± 413	720 ± 352	576 ± 322		arid/ap		
Cairngorms	Sissons (1979e)	942	AWMA	773 ± 353	663 ± 401	474 ± 343	379 ± 315		arid		

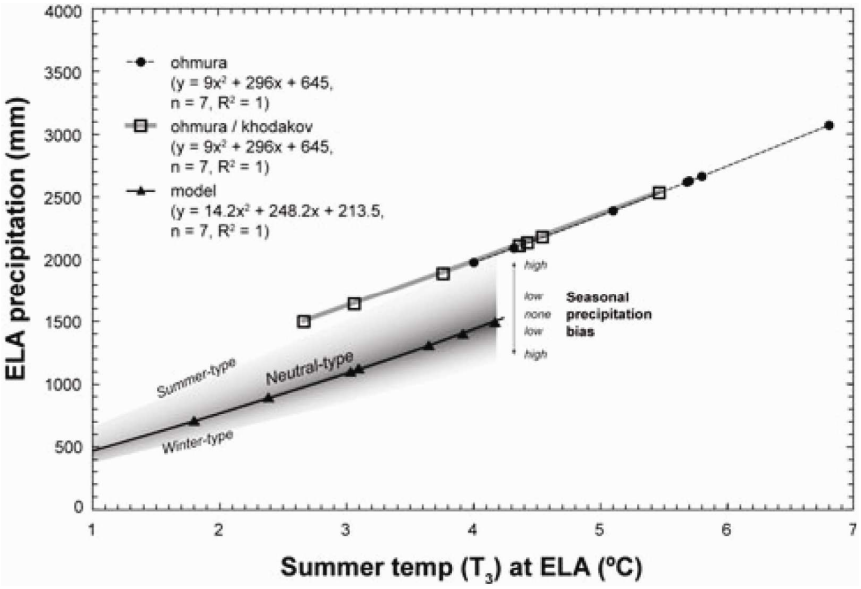

Figure 6.2. Comparison of different precipitation-temperature relationships for Scottish Younger Dryas sites (Drumochter, Benn & Ballantyne, 2005; West Highlands, Golledge, 2007; Harris, Ballantyne, 2007a; Arran, Ballantyne, 2006; Mull, Ballantyne, 2002a) in order from left to right), where the black circles represent the Ohmura *et al*. (1992) relationship, the squares represent the Ohmura *et al*. (1992) relationship that has been corrected for by glacier cooling using a function by Khodakov (1975) and the black triangles represent the Golledge *et al*. (2010) P/T function, with shaded areas illustrating the effects of seasonality. Taken from Golledge *et al.* (2010, p. 766).

Given that Khodakov (1975) suggested a 1.6-1.9° C decrease in temperatures for a glacier of 10 to 20 km in length, much larger than most glaciers in the Monadhliath Mountains, the use of a summer temperature at sea level value of 6.4° C (Golledge, 2008; Finlayson *et al*., 2011), as used in Figure 6.1 (Golledge *et al.*, 2010), to account for the effects of glacier cooling seems excessively low for the current research. Indeed, precipitation values calculated for the Monadhliath Icefield using a 6.4° C summer sea level temperature value (Table 5.6), were between 963 and 550 mma^{-1} at the 714 m ELA for the Golledge *et al*. (2010) summer and winter precipitation types, respectively, which are of a similar magnitude to modern arid polar regions such as central Spitsbergen (500 to 700 mma^{-1} at ca. 500 to 700 m asl.; Humlum, 2002). These calculations show the potentially significant effect that air temperature cooling by glaciers might have on the amount of precipitation required at the ELA. At present there are still large uncertainties surrounding the magnitude of this effect, adding to further uncertainties surrounding precipitation levels calculated for Younger Dryas ice masses in Scotland.

Taking into consideration the effects of winter sea ice formation during a large proportion of the Younger Dryas, a neutral to summer precipitation bias is probably most appropriate for considering the precipitation values in Table 6.1. However, given that the effects of air temperature cooling by glaciers are not accounted for here, Younger Dryas precipitation is likely to have therefore been closer to the neutral seasonality values reported here. The following discussion is therefore centred on these neutral precipitation values.

Average precipitation for ten years (2000 to 2009 inclusive) was acquired for three sites in the Monadhliath Mountains and is shown in Table 6.2. This modern data also shows a significant decrease in precipitation across the Monadhliath Mountains, varying from 2112 mma^{-1} at Braeroy Lodge (220 m OD; NN 336 914) in the west to 1317 mma^{-1} and 1325 mma^{-1} further east at the Spey Dam (270 m OD; NN 582 973) and Coignafearn Lodge (390 m OD; NH 710 179) respectively. This modern data displays a stronger precipitation gradient across the Monadhliath massif than that of the precipitation reconstructed during the Younger Dryas. As a result, although all modern precipitation values are higher than the calculated Younger Dryas neutral type precipitation values, the greatest difference occurs in the west, where modern precipitation is 800 mma^{-1} higher than neutral type precipitation calculated for the Younger Dryas. A potential explanation for this is that a significant amount of snow that fell in the western Monadhliath Mountains was re-distributed further east by a prevailing westerly wind, as has been suggested for the Beinn Dearg Ice Cap (Finlayson *et al*., 2011) and the Northwest Highlands Ice Cap (Lukas & Bradwell, 2010), meaning that greater precipitation levels may have occurred in this area than is reflected in the glacier ELAs.

Table 6.2. A) Modern precipitation data averaged over a 10 year period between 2000 and 2009 for three Met Office weather stations in the eastern, central and western sectors of the Monadhliath Mountains. B) Average Younger Dryas precipitation, calculated using the Golledge *et al.* (2010) precipitation-temperature function, is included below for the western, central and eastern sectors for each corresponding weather station for comparison. Modern precipitation data provided by the British Atmospheric Data Centre (NERC, 2012) and was verified using the FetchClimate (2012) web application.

A	Modern PPT (2000-2009)	Braeroy (mma^{-1})	Spey Dam (mma^{-1})	Coignafearn (mma^{-1})	Regional Average (mma^{-1})
	Average	2112	1317	1325	1585
	Altitude	220	270	390	
	PPT Sea level	1867	1131	1064	1354
B	**Younger Dryas PPT**	**Western (mma^{-1})**	**Central (mma^{-1})**	**Eastern (mma^{-1})**	**Monadhliath Icefield (mma^{-1})**
	Summer	1515	1280	1043	1211
	Neutral	1082	914	747	865
	Winter	866	731	596	692

The palaeoprecipitation values calculated in Section 5.4 therefore indicate that the climate of the Monadhliath Mountains was probably more arid than at present, with a strong precipitation gradient across the plateau apparent in much higher precipitation levels in the west compared to the east that was potentially slightly lower than the precipitation gradient that occurs in the region today. There are still, however, large uncertainties regarding seasonality bias, the effect of air temperature cooling by glaciers and other assumptions that are made in the current precipitation calculation method (Section 5.4.2), which need to be constrained further in order to make more confident assertions about past climate in Scotland using this approach.

6.3 An Assessment of Modern Analogues for the Monadhliath Icefield

Modern glacial environments can provide an important means of assessing glacier processes and dynamics in formerly glaciated regions (e.g. Evans *et al.,* 1999; Benn & Clapperton, 2000; Evans & Twigg, 2002; Benn *et al.*, 2003; Glasser & Hambrey, 2003; Benn & Lukas, 2006; Evans, 2009, 2011). Modern analogues can also be used as an alternative way to examine palaeoclimate in an area of former glaciation by assessing the association of thermal regime and glacier dynamics with climate (e.g. Hambrey *et al*., 1997; Bennett *et al*., 1998; Evans et al., 1999; Benn & Clapperton, 2000; Benn & Lukas, 2006). Thermal regime is usually associated with climate in that cold-based glaciers tend to occur in polar regions, whilst warm-based glaciers occur in more temperate to tropical zones. However, as demonstrated in Section 5.5, a range of thermal regimes can occur across an ice mass such as a plateau icefield, owing to differences in bed-topography and glacier thickness. In other areas of Scotland, landform-sediment assemblages relating to both temperate and polythermal glacial environments have been identified within the Younger Dryas palaeoglacial record, and as a consequence a number of currently glaciated regions have previously been suggested as modern analogues for Scotland, including the European Alps (e.g. Charlesworth, 1955; Bennett & Boulton, 1993a), Iceland (Eyles, 1983; Bennett & Boulton, 1993a), Norway (Benn & Lukas, 2006) and Svalbard (Hambrey *et al*., 1997; Bennett *et al*., 1998).

In the Monadhliath Mountains a range of thermal regimes was identified, varying between cold-based and warm-based ice, with many glaciers lying on a continuum between the two, and indicating polythermal conditions across the icefield as a whole (Section 5.5). Polythermal glaciers are currently recognised in Iceland (e.g. Þórisjökull, Rea & Evans, 2003; Tungnafellsjökull, Evans, 2010) and Norway (e.g. Jiek'kevárri, Øksfjordjókelen, Rea & Evans, 2003), whilst those in the Canadian Arctic are predominantly cold-based (Ó Cofaigh *et al*., 2003; Rea & Evans, 2003). Plateau icefields in Norway are characterised by generally cold-based plateau areas and wet-based outlet glaciers, although ice-moulded bedrock, striations and moraines have been found on some recently deglaciated plateau areas, suggesting that some areas of the plateau are also able to reach pressure melting point (Rea *et al.,* 1998; Evans & Rea, 2003). In Iceland, detailed geomorphological and sedimentological analysis by Evans (2010) at Tungnafellsjökull in the arid interior of Iceland demonstrated evidence for a frozen glacier margin, at otherwise wet-based outlet glaciers, which had reached pressure melting point following strain heating at the plateau margins. Since a frozen glacier margin is argued not to have been a dominant feature of predominantly wet-based outlet glaciers in the Monadhliath Mountains, based on clast morphological analysis (Sections 4.2.6 and 5.5.1), the Monadhliath Icefield is suggested to have been most similar to modern plateau icefields in Norway, although Icelandic plateau icefields cannot be entirely ruled out at this stage. This agrees with the

argument by Benn and Lukas (2006) that Younger Dryas glaciers in the Northwest Highlands were most similar to modern glaciers in Norway.

6.4 Insights from the Monadhliath Mountains into Plateau Icefield Landsystems

Previous research on plateau icefields has focussed predominantly on the geomorphological evidence that can be used to identify the existence of former plateau ice, differences in thermal regime (e.g. Gellatly *et al*., 1988; Dyke, 1993; Rea *et al*., 1996, 1998; McDougall, 2001; Evans *et al*., 2002, 2006a) and the effect that the presence of plateau ice has on the ELA (e.g. Rea *et al*., 1999) (Section 2.4). However, research on the dynamics of plateau icefields, particularly during retreat, is very limited at present and restricted to a few studies on spatial and temporal changes in thermal regime (Dyke, 1993; Fjellanger *et al*., 2006), debris transport pathways (Evans, 2010) and predictions about the future survival of modern plateau icefields (e.g. Nesje *et al*., 2008; Giesen & Oerlemans, 2010). There is currently no research that deals with the retreat dynamics of plateau icefields in any detail in terms of the interaction between local and regional ice during ice sheet deglaciation, factors that influence differences in retreat patterns between outlet valleys and how the ice mass behaves during the final stages of retreat once it is constrained to the plateau.

The palaeoglacial record in the Monadhliath Mountains provides a rare opportunity to examine the dynamics of a plateau icefield during both ice sheet retreat and retreat of an independent plateau icefield. The interaction between regional and local ice at the end of the Dimlington Stadial is discussed in Section 5.3 and therefore this section focuses of the retreat dynamics of Monadhliath Icefield during the Younger Dryas. This research is able to add a new dimension to the current landsystem model though detailed analysis of the retreat dynamics of the Monadhliath Icefield, which has demonstrated that bed slope angles and outlet valley morphology have the most influence on the patterns and spacing of recessional moraines (Section 5.5). The following sections provide details on these factors alongside a further discussion on the effect of plateau ice on area-based ELA calculations and implications for their use in a plateau icefield setting.

Plateau icefield retreat dynamics

A conceptual model is presented in Figure 6.3 to show the role of outlet valley morphology on thermal regime and glacier retreat dynamics, which are manifest in the geomorphology that remains after ice retreat. Whilst climate exerts a large control on glacier thermal regime, the results of this research found that the size of the outlet valley and the gradient of the valley floor also have a strong influence on the thermal regime of individual outlet glaciers, causing a mosaic of thermal regimes both spatially and temporally across the icefield (Section 5.5). These

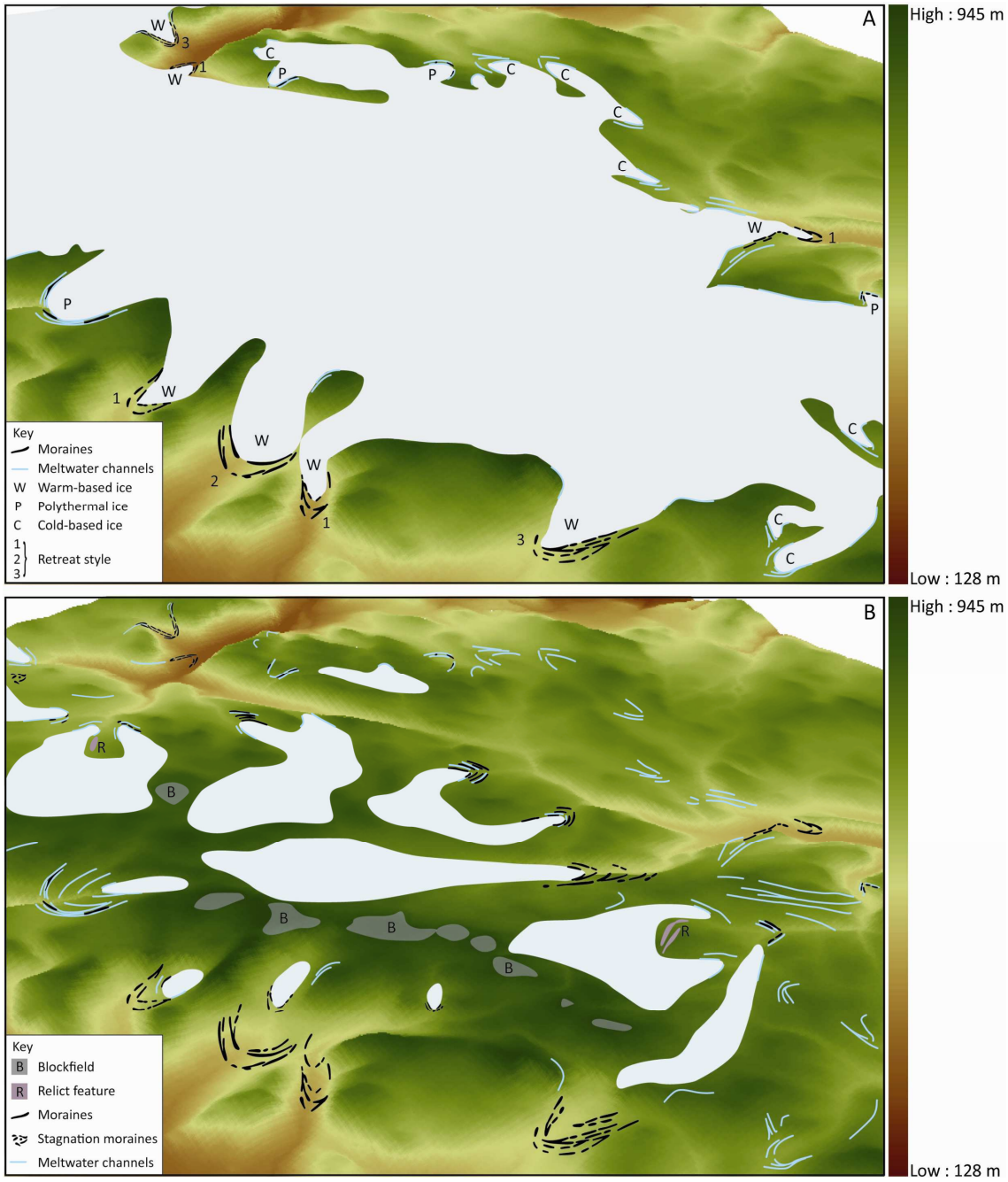

Figure 6.3. Conceptual diagram of a polythermal plateau icefield landsystem illustrating the different types of geomorphological signature that can occur on plateau icefields due to thermal regime. A) At the maximum extent, warm-based outlet glaciers (W) will deposit recessional moraines, cold-based outlet glaciers (C) will produce a network of ice-marginal meltwater channels, and a combination of both features will occur at polythermal outlet glaciers (P), representing a continuum between cold-based and warm-based ice. The type of retreat style based on valley morphology is also shown, where (1) depicts a retreat style dominated by frontal moraine bifurcations within narrow valleys, (2) represents retreat within wider, often flatter valleys, in which lateral moraine bifurcations occur and (3) occurs within valleys that are more closely connected to the plateau, producing a more even response to retreat, manifest in both lateral and frontal moraine bifurcations. B) During recession, the plateau icefield will break up into smaller outlet lobes that retreat into small proto-valleys on the plateau. Recessional moraines, stagnation moraines and ice-marginal meltwater channels are formed on the plateau at this stage of retreat, dependant on whether the outlet glaciers are warm-based and continue to retreat actively. Blockfields and other relict features such as older glaciogenic landforms are often revealed following plateau icefield retreat, where they have survived beneath cold-based ice.

differences in thermal regime have a large influence over the types of landforms produced, where a continuum was identified between the thin, low gradient, cold-based outlet glaciers, for which former ice-marginal positions were marked only by ice-marginal meltwater channels, to thick, warm-based outlet glaciers that deposited densely spaced sequences of recessional moraines.

Previous studies have also highlighted the polythermal nature of many plateau icefields (e.g. Dyke, 1993; McDougall, 1998, 2001; Rea & Evans, 2003; Evans, 2010). The most detailed of this is by Evans (2010) who investigated the effect of thermal regime on debris transport pathways on Tungnafellsjökull in Iceland. However, in spite of the clear relationship between glacier size and thermal regime (e.g. Skidmore & Sharp, 1999; Ó Cofaigh *et al*., 2003), no studies have explicitly made the link between outlet valley morphology and thermal regime in a plateau icefield landsystem, focussing instead on the contrasts in thermal regime between ice on the plateau and that in the outlet valleys (e.g. Dyke, 1993; Evans, 2010). The research presented here provides the first examination of the effect of valley morphology and glacier size on thermal regime in a plateau icefield setting.

Figure 6.3A also depicts the different styles of retreat identified for outlet glaciers that were predominantly warm-based. As discussed in Section 5.5, the spacing of chains of recessional moraines within each outlet valley is closely related to the type of moraine bifurcation that occurred, both of which are strongly controlled by valley morphology. Three types of retreat were identified due to the dominance of lateral or frontal moraine bifurcations, with the third type being a combination of both. This is the only study of its kind that has established such a clear link between valley morphology and recessional moraine patterns, particularly with respect to plateau icefield dynamics.

Figure 6.3B illustrates the break up of the icefield into smaller outlet glaciers that reside in small proto-valleys on the plateau. The diagram illustrates that whilst some glaciers continue to retreat actively, depositing moraines on the plateau, others are cold-based, forming only ice-marginal meltwater channels, a small number stagnate and others leave very little record of their existence. The figure also indicates that areas of blockfield and older glaciogenic features can emerge unmodified from beneath the retreating icefield.

The model shown in Figure 6.3 is based on the analysis of the dynamics of the Monadhliath Icefield, but is likely to be applicable to other polythermal plateau icefields, such as other former plateau icefields in the UK and modern plateau icefields in mid-latitude areas such as Norway and Iceland, which are recognised as potential modern analogues for the former

Monadhliath Icefield (Section 6.3). Since the model is based on the geomorphological signature of a range of thermal regimes it is not as applicable to the plateau icefield landsystem in high latitudes, such as in Arctic Canada, where cold-based conditions dominate and fewer recessional moraines are formed. Since the influence of plateau ice was found to be minimal on outlet glacier dynamics in comparison to valley morphology and the valley floor gradient, the model is also in part highly applicable to the dynamics of valley glaciers in terms of the effect of outlet glacier size on thermal regime and the influence of valley morphology and slope on retreat dynamics and moraine spacing, providing a more quantitative approach to general statements made by Lukas and Benn (2006).

ELAs on plateau icefields and implications for palaeoclimate reconstructions

The capacity of plateau ice to significantly raise outlet glacier ELAs is discussed in detail by Rea *et al*. (1999) and in Section 2.4. This has important implications for palaeoclimate reconstructions in areas where plateau ice could have been present. A further two aspects of this influence of plateau ice on glacier ELAs were brought to light during analysis in this research, by the way in which area-based ELA estimates will be affected. Firstly area-based ELA calculations for the maximum plateau icefield reconstruction were higher than those calculated for the minimum reconstruction due to the greater extent and higher altitude of the plateau ice surface in the maximum reconstruction. Secondly, a number of area-based ELAs calculated for the final stage of active outlet glacier retreat were lower than the apparent ELAs of the respective outlet glaciers at their maximum extent (Section 5.5.2).

The calculation of a higher apparent ELA for the maximum thickness glacier reconstruction meant that calculated palaeoprecipitation for the maximum reconstruction was lower than that for the minimum reconstruction. This initially seems counterintuitive, since, simplistically, more precipitation should be expected for an icefield with a greater volume of ice. This indicates that our current understanding of the relationship between temperature and precipitation at the ELA and/or the current area-based method for calculating ELAs and palaeoprecipitation could be too simplistic for a complex system such as a plateau icefield.

At present the relationship devised by Ohmura *et al.* (1992) entails that, as air temperatures rise, the amount of precipitation required to maintain a glacier at a particular ELA will also increase. Since air temperatures are higher at lower altitudes, higher precipitation levels are required near sea level in order to sustain glaciation compared to higher altitudes within the same region (Benn & Evans, 2010). A number of uncertainties are already recognised in the method currently used to calculate palaeoprecipitation and are discussed in Section 5.4. Most notable and relevant to the current discussion are the values used for the adiabatic lapse rates, the effect

of air temperature cooling by glaciers and the effects of snow redistribution by wind. Wet adiabatic lapse rates, i.e. the rates at which temperature decreases with altitude, have a significant effect on the amount of precipitation reconstructed at the ELA, which varies greatly between the lower (0.006°C m^{-1}) and upper (0.007°C m^{-1}) boundaries used in this research and therefore introduces a large uncertainty to the palaeoprecipitation calculations. The use of this range in itself is also full of uncertainty (Section 5.3.2). In a plateau icefield landsystem, in particular, these rates may not be linear, as is usually assumed, due to large differences in glacier areas at different altitudes, which is likely to be interlinked with the intensity of localised air temperature cooling by the glacier. The effects of snow redistribution are also likely to be more prominent on plateau icefields than on valleys glaciers, where snow is likely to be blown from the plateau into the surrounding valleys. This could mean that a large amount of precipitation falling on the plateau could be redistributed to lower altitudes, causing a thinner icefield. Both glacial air temperature cooling and snow redistribution are difficult to quantify and were therefore not accounted for in this research adding further uncertainty to the palaeoprecipitation values calculated (Sections 5.4 and 6.1.2). However, whilst these uncertainties are clearly significant, they are unlikely to fully explain the inverse relationship between plateau ice thickness and precipitation, which is ultimately linked to the altitude of the equilibrium line.

The way in which ELA estimates are calculated at present, using an area-based approach, such as the AABR, means that the presence of ice at a higher altitude will result in a higher ELA. In a plateau icefield, the large proportion of ice at higher altitudes will therefore significantly raise the apparent ELA. The key questions are therefore 1) how representative is an ELA calculated through an area-based method for describing the proportions of the accumulation and ablation areas for a plateau icefield, and 2) what effect do internal glacier dynamics have on a true ELA that may or may not be represented using an area-based approach?

The surface profile of cold-based ice usually has a greater curvature than warm-based ice, as a result of it being less viscous (higher *C* value; Ng *et al*., 2010; Section 5.2.1), implying that plateau ice would potentially be thicker if the icefield was cold-based. This is supported by the fact that ice velocities would be lower and there would therefore be a slower rate of movement of ice from the plateau into the outlet glaciers. Conversely, lower glacier profiles are usually associated with glacier sliding (e.g. van der Veen, 1999), which could result in a thinner plateau icefield, with a faster draw down of ice into the outlet valleys. Using an area-based ELA method, this would cause a lower apparent ELA and therefore higher precipitation levels to be calculated for a thinner icefield compared to a thicker icefield that would have a higher apparent ELA and lower precipitation levels, as was calculated for the minimum and maximum icefield

reconstructions in this research. This follows, since the presence of cold-based plateau ice would imply lower air temperatures and therefore less precipitation would be required to sustain the icefield. The question is, however, whether this is what the differences between the minimum and maximum reconstructions in this research are actually reflecting. In this research the wet adiabatic lapse rates were varied so that the lowest air temperatures were associated with the thickest icefield and vice versa, so that the minimum and maximum precipitation boundaries could be established. A similar, although less extreme scenario would also occur, however, if the same air temperature had been used for both reconstructions. This is perhaps therefore a question that can only be answered through glacier mass-balance and flow velocity modelling, due to the complexity surrounding the plateau icefield system.

The second aspect of the influence of plateau ice on ELAs was found in the lowering of apparent area-based ELAs for some outlet glaciers during the final stages of retreat. This situation has previously been observed where a steep backwall separates the outlet valley and the plateau, causing a disconnection between plateau ice and the outlet glacier (e.g. Rea *et al*., 1999). In this case, outlet glaciers can be sustained below the regional ELA by snow redistribution and ice avalanching from the plateau, which provides an area of accumulation for a glacier that would otherwise be completely in the ablation zone (Rea *et al*., 1999). Whilst this scenario was found to have occurred at three outlet glaciers during retreat of the Monadhliath Icefield, a further six outlet glaciers retreated onto the plateau, but also exhibited a lowering of their area-based ELA estimates (Section 5.5.2; Table 5.7), due to a loss of plateau ice, which has never been reported in the literature before.

Recent modelling of the Norwegian plateau icefield, Hardangerjøkulen, indicates that if sufficient warming occurs within the next five years, the climate-driven ELA of the icefield will rise above the icefield surface, leaving no accumulation area (Giesen & Oerlemans, 2010). Once this has occurred, the icefield is predicted to break up into several smaller outlet glaciers, thinning into the topographic lows on the plateau where ice is thickest, over a period of approximately 85 years.

Whilst a similar ice configuration is depicted by the break up of the Monadhliath Icefield into small outlet glaciers in topographic lows on the plateau (Fig. 5.20), the presence of moraines delineating the former margin of these glaciers indicates that these glaciers were able to still behave actively. This suggests that retreat was punctuated by stillstands or minor advances in order to deposit the moraines. Since an either positive or zero mass balance is required to achieve an advance or stillstand, respectively, each final stage outlet glacier must have still had an accumulation zone during times of moraine production and therefore the ELA was still

located on the glacier surface, contradictory to the modelled output by Giesen and Oerlemans (2010) and as calculated in Table 5.7. As argued in Section 5.5.2, reasons for the survival of these ice-masses may be because of redistribution of snow by wind and enhanced shading within the topographic lows on the plateau. Another possible reason for this phenomenon could be that the break up of plateau ice into smaller ice masses gave rise to a non-climatic stillstand or readvance, since smaller ice masses are less prone to rapid retreat (Greene, 1992; Lukas, 2007b) and this is a factor that needs to be explored further in terms of the relationship of the final retreat stage moraines to ice mass break up.

In order to provide further understanding on this issue, changes in the climate-driven ELA are considered over a longer time period. Figure 6.4 shows how a range of climate-driven ELA values might be associated with an outlet glacier on the plateau over a 10 to 50 year period. The figure shows that the true ELA may have been located above the glacier for the majority of this time, but short-lived fluctuations in climate could have caused the ELA to lower onto the glacier surface, which would allow minor advances or stillstands to occur during an overall pattern of retreat. This model highlights some of the assumptions that are made about ELA estimates used in palaeo-glacier reconstructions, such as that the ELA is a steady-state ELA, when a large

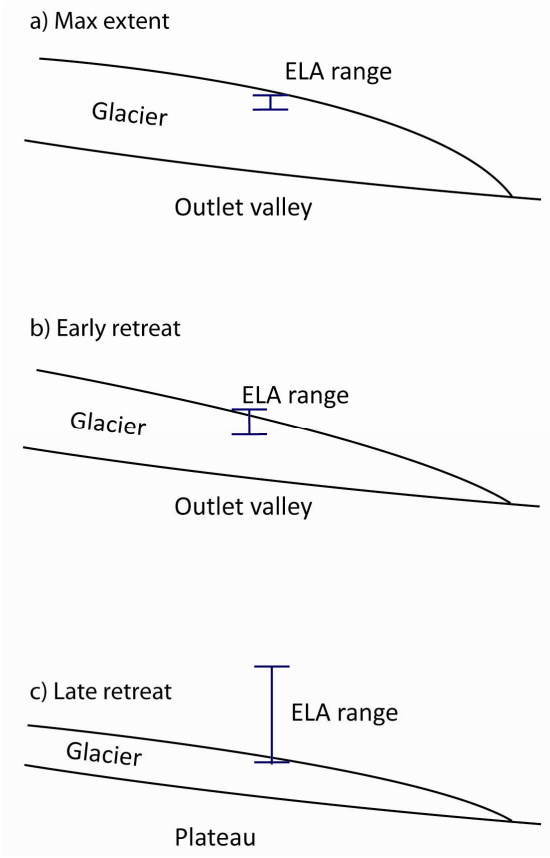

Figure 6.4. Illustrative diagram showing how an ELA associated with a glacier of an approximately similar size may fluctuate over a number of years a) when the glacier is at its maximum extent, b) during early retreat, and c) during late retreat.

proportion of reconstructed glaciers may not have been in equilibrium with the climate. In the case of the reconstructed final stage glaciers in this research, they would have been predominantly retreating, but punctuated by small advances or stillstands. Therefore, whether the apparent ELAs calculated in Table 5.7 are at all representative, is uncertain. This exercise into changes in ELAs during retreat highlights the need for a greater understanding of marginal ice-mass dynamics during retreat, particularly as part of a plateau icefield where retreat is onto an area of relative flat topography and small ice-masses therefore have little altitudinal difference between their accumulation and ablation zones.

6.5 Chapter Summary

This chapter provides a discussion on the main research findings in this thesis. The findings relate predominantly to Younger Dryas glaciation in the Monadhliath Mountains and the plateau icefield landsystem. A two-phased advance is recognised in a number of valleys in the study area, in accordance with other research in Scotland (e.g. Merritt *et al*., 2003b), which indicate that the Monadhliath Icefield initially advanced earlier in the Younger Dryas stadial. However, it is argued here that more favourable conditions in the west allowed glaciers in this area to maintain a maximum position for longer into the latter part of the stadial, due to the association of Younger Dryas limits in the head of Glen Turret with the Glen Roy ice-dammed lakes, for which evidence indicates a late stadial formation (e.g. Fabel *et al*., 2010; Palmer *et al*., 2010, 2012; McLeod *et al*., 2011).

Palaeoprecipitation calculated for the Monadhliath Icefield and individual outlet glaciers fits well with the palaeoprecipitation values calculated for neighbouring ice masses such as Creag Meagaidh, Drumochter, the Gaick Plateau and the southeast Grampians, with a large reduction in precipitation from west to east across the Monadhliath massif. A comparison of Younger Dryas and modern precipitation values is highly dependent on the degree of seasonality bias that occurred and the amounts of air temperature cooling by glaciers. Seasonality bias is likely to have been somewhere between the neutral and summer precipitation boundaries established by Golledge *et al*. (2010) due to the formation of winter sea ice in the North Atlantic during at least the first half of the Younger Dryas (e.g. Isarin *et al*., 1998; Isarin & Rensen, 1999). Using this argument, but also taking into consideration glacial air temperature cooling, which was not quantified in the precipitation calculations presented here, a neutral precipitation bias is suggested as the most appropriate calculation. These precipitation values indicate that the climate in the Monadhliath Mountains during the Younger Dryas was more arid than at present, with the greatest comparative aridity in the west owing to a stronger modern precipitation gradient than during the Younger Dryas.

The final section of this chapter examined the contribution of the research to the plateau icefield landsystem and developed a conceptual model for plateau icefield dynamics during retreat. The section included an assessment of the use of area-based ELAs for calculating precipitation from a plateau icefield and area-based ELA changes that occur during plateau icefield retreat. The discussion highlights the difficulty involved in quantifying the interactions between temperature, precipitation, snow redistribution by wind and internal glacier dynamics. Glacier mass-balance and flow velocity modelling are suggested as a means to examine these issues further and provide an avenue for future research on plateau icefield landsystems (Section 7.5).

Chapter 7

Summary and Conclusions

Chapter 7 summarises the research carried out in this thesis under four key themes that answer the research aims and objectives outlined in Chapter 1. The four themes are: 1) the production of a systematic glacial geomorphological map of the Monadhliath Mountains, 2) the identification of a relative chronology for glacial events in the Monadhliath Mountains, 3) Younger Dryas plateau icefield reconstruction and palaeoclimatic implications and 4) the contribution of this research to the plateau icefield landsystem. These aspects of the research and their implications are summarised in sections 7.1 to 7.4. The scope for future research is discussed within Section 7.5 and the thesis is concluded in Section 7.6.

7.1 Production of a Systematic Glacial Geomorphological Map of the Monadhliath Mountains

Summary

The Monadhliath Mountains are a region in which very little research has previously been conducted and the palaeoglaciological record is relatively unknown. The fragmented nature of the limited previous research has hindered a regional assessment of LGIT glacier fluctuations and the development of a detailed regional chronology. Geomorphological mapping was used as the primary tool in this research to record and assess geomorphological evidence in the study area. Three approaches to mapping were used: field mapping and mapping from aerial photographs and NEXTMap DEMs. Mapping from all three approaches was combined alongside sedimentological information, where available, to produce a systematic glacial geomorphological map of the region (Appendix II). This geomorphological map reveals that a large number of the valleys in the Monadhliath Mountains are dominated by moraines and ice-marginal meltwater channels, alongside other features such as talus slopes, debris cones, ice-contact fans, major river terraces and glaciolacustrine deltas and fans. Geomorphological features on the central plateau area are comparatively sparse, although some moraines and meltwater channels are found in addition to areas of blockfield, solifluction lobes and frost-shattered bedrock on the higher summits.

Implications

The regional assessment of geomorphological evidence carried out in this research has revealed an abundance of glaciogenic features in the Monadhliath Mountains relating to the LGIT, many of which had not previously been recorded. This map therefore provides the first complete documentation of the palaeoglacial record of the Monadhliath Mountains. The systematic approach used to map the region as a whole has allowed the subsequent development of a

regional relative chronology, reconstruction of the maximum extent of prominent ice masses, investigation of the implications for regional palaeoclimate and an examination of the dynamics of the reconstructed ice masses.

7.2 Identification of a Relative Chronology for Glacial Events in the Monadhliath Mountains

Summary

In the absence of any published dates in the majority of the region, a morphostratigraphic approach (*cf.* Lukas, 2006) was used to identify a relative chronology for glacial events in the region. This approach identified two major phases of plateau icefield glaciation following regional ice retreat from the LGM. The first is argued to have occurred during the final stages of ice sheet decay towards the end of GS-2, when continued retreat of regional ice from the area allowed an independent plateau icefield, centred over the Monadhliath Mountains to regain dominance. This is suggested to have occurred soon after drainage of a series of ice-dammed lakes that formed in the lower parts of the southeastern Monadhliath tributaries during regional ice retreat in the Spey Valley. Evidence for this readvance is manifest in the deposition of moraines overlying debris flow deposits relating to an ice-dammed lake within Glen Mòr and prominent end moraines at the mouths of Gleann Lochain and Gleann Madagain. Other moraines from this time period occur in the majority of valleys that emanate from the central Monadhliath plateau, but are most prominent in the southern tributary valleys. There are no clear end moraines in these valleys and it is therefore unknown whether a readvance occurred across the whole icefield, or whether the moraines in some valleys document retreat of local ice towards the plateau only, following separation from regional ice in Strathspey.

The possibility of an asynchronous advance and/or retreat of this icefield is highlighted by the succession of events in Glen Killin, which also record the formation of a large ice-dammed lake, Glacial Lake Killin, during retreat of a regional ice lobe within the Great Glen. Current understanding of the retreat patterns of the Scottish Ice Sheet in eastern Scotland between 16 and 15 ka BP indicates that the Great Glen deglaciated later than Strathspey, implying that Glacial Lake Killin formed later than the ice-dammed lakes in the southeast of the Monadhliath Mountains. At its maximum level (642 m), Glacial Lake Killin submerged the most northerly parts of the plateau, resulting in the formation of a Gilbert-type delta on the plateau above Glen Eich and the deposition of a thick succession of subaqueous debris flows as part of a grounding-line fan within Glen Odhar. These sediments indicate the continued presence of plateau ice in the area, but the extensive nature of the lake implies that local glacier ice would have been very restricted to the higher parts of the plateau in the northern Monadhliath Mountains. At this time, the Findhorn Valley, which served as a drainage route for Glacial Lake Killin, was already

ice-free. The absence of evidence for more extensive local ice in Glen Killin at the end of GS-2 in comparison to the evidence for it in most other valleys also suggests that the configuration of the icefield during this time was different to that reconstructed for a later icefield advance.

This later advance was assigned to the Younger Dryas using morphostratigraphy, supported by an association with dated former lake shorelines within Glen Roy (Fabel *et al*., 2010), unpublished SED dates from Glen Banchor (D.M. Gheorghiu & D. Fabel, pers. comm., 2011) and modelling by Golledge *et al.* (2008). Identification of the maximum limits of ice during the Younger Dryas revealed that two coalescent plateau icefields were present in the region during the Younger Dryas, centred on the Carn Dearg - Poll-gormack plateau in the west and the central plateau of the Monadhliath Mountains in the remainder of the study area, with the eastern-most limits in the upper parts of the Findhorn and Dulnain catchments. The connection of the maximum limits of the icefield in Glen Turret with the 350 m ice-dammed lake in this valley indicates that the icefield reached its maximum position in the latter half of the Younger Dryas based on dates for the final abandonment of the shorelines at ca. 11.5 to 11.9 ka BP and the formation of the Glen Roy lakes at ca. 12.2 ka BP (Fabel *et al*., 2010; Palmer *et al*., 2010, 2012). This contradicts modelling of Younger Dryas ice masses by Golledge *et al*. (2008), which predicts that plateau ice in the Monadhliath Mountains reached its maximum extent by 12.7 ka BP. In other parts of the study area, evidence for a two-phased Younger Dryas advance is recognised, whereby the lack of clear end moraines and the development of some river terraces inside the outermost Younger Dryas moraines indicates that glaciers did not remain at their maximum positions for very long, retreating and stabilising further upvalley, where more prominent moraines were deposited. This implies an early advance during the Younger Dryas in order to allow time for stabilisation further upvalley, again contradicting the evidence within Glen Turret. To resolve this issue, it is suggested that the Monadhliath Icefield reached its maximum position earlier in the stadial, in accordance with the Golledge *et al*. (2008) model, but that more favourable conditions in the west, associated with the advance of the West Highlands Ice Cap, then allowed the western outlet valleys to remain at or near their maximum positions for longer into the latter part of the Younger Dryas Stadial, whilst glacier retreat had already begun further east.

Implications

Evidence for the formation of ice-dammed lakes within a number of valleys to the north and south of the Monadhliath massif and the deposition of extensive lateral moraines on the northern side of the Spey Valley indicates that retreat of regional ice within Strathspey and the Great Glen was oscillatory and punctuated by advances and stillstands. In Strathspey, the research presented here can be correlated to that reported from Raitts Burn (Phillips & Auton,

2000) and the northern Cairngorms (Everest & Golledge, 2004; Everest & Kubik, 2006) and supports a major stillstand of up to 1000 years in this region immediately prior to 15.8 to 15.5 ka. BP. In Glen Killin, geomorphological and sedimentary evidence presented here indicates that a major advance occurred during ice sheet retreat, which allowed regional ice to advance into the Fechlin-Killin valley and dam local drainage. This finding supports evidence in Strathspey that ice sheet retreat was disrupted by major stillstands and advances. This research provides the first examination of the relationship between ice sheet retreat patterns to the north and south of the Monadhliath Mountains, indicating that the formation of ice-dammed lakes in the region may have occurred asynchronously. Absolute dating is now required to examine the temporal relationship further (Section 7.5).

The recognition that a substantial plateau icefield existed in the Monadhliath Mountains during both the later stages of ice retreat from the LGM and during the Younger Dryas has important implications for both our understanding of the glacial history of the region and the plateau icefield landsystem. Firstly evidence for a local glacier advance following ice-dammed lake drainage in several of the southeastern valleys indicates that climatic conditions were severe enough to allow a local icefield to advance and regain dominance following regional ice retreat. In terms of the plateau icefield landsystem, this research provides one of the first examinations of the relationship between plateau ice and regional ice during deglaciation. The research indicates that during deglaciation a combination of unzipping of local and regional ice occurred in some valleys, whilst the development of ice-dammed lakes forced local ice to retreat more rapidly in others. Asynchronous retreat of regional ice most likely caused asynchronous patterns of plateau icefield advance and retreat, where early disappearance of regional ice allowed the local plateau ice to readvance in several valleys, whilst its continued presence elsewhere prohibited a subsequent plateau icefield advance.

Secondly, the identification of a Younger Dryas plateau icefield in the Monadhliath Mountains adds significantly to knowledge on the extent of Younger Dryas glaciation in the UK, has important implications for climate in the region (Section 7.3) and allowed an examination of plateau icefield retreat dynamics (Section 7.4). The geomorphological evidence relating to this time indicates a two-phased advance similar to that identified in other areas (e.g. Peacock *et al*., 1989; Merritt *et al*., 2003b), indicative of an initial advance early in the Younger Dryas, but also suggests that glaciers in the west remained at their maximum position until the latter part of the stadial, corresponding with recent research by Palmer *et al.* (2010, 2012) and MacLeod *et al.* (2011) and adding further information to this debate.

7.3 Younger Dryas Plateau Icefield Reconstruction and Palaeoclimatic Implications

Summary

A Younger Dryas plateau icefield was reconstructed from limits identified through morphostratigraphy. Establishing the upper limit of many of the outlet glaciers and ice on the plateau was, however, hindered by a lack of geomorphological evidence in a number of areas. A glaciological approach was therefore taken to develop realistic upper and lower boundaries for plateau ice thickness, using two surface profile models devised by Benn and Hulton (2010) and Ng *et al.* (2010). This resulted in the production of a maximum, minimum and 'average' icefield reconstruction. ELAs were calculated for the average icefield using the AABR, AAR and AWMA methods in order to allow comparison with previous studies. The AABR has been suggested as the most representative method (Benn & Gemmell, 1997; Rea, 2009) and calculations using this method, with a balance ratio of 1.9 ± 0.81 for mid-latitude glaciers (Rea, 2009), produced an ELA for the average Monadhliath Icefield of 714 ± 25, where the errors incorporated the ELAs calculated for the minimum and maximum reconstructions. ELAs were calculated for outlet glaciers that spanned four or more 50 m contour intervals and the results demonstrate a significant rise in ELAs from west to east, dividing the study area into a western, central and eastern sector, ranging from 560 ± 20 m in the west to 816 ± 24 m in the east.

Palaeoprecipitation was calculated using these ELA values and two different precipitation-temperature relationships. The first, established by Ohmura *et al*. (1992), has been used extensively to calculate precipitation at the ELA of other former ice masses in Scotland, whilst the second has recently been advocated by Golledge *et al*. (2010), specifically for use in Scotland, in order to alleviate problems with the use of a global dataset and to account for potential seasonality bias in precipitation due to the presence of sea ice in the North Atlantic during the Younger Dryas (Isarin *et al*., 1998; Isarin & Rensen, 1999). Calculations using these methods yielded precipitation values of 1829 ± 491 mma^{-1}, 1809 ± 592 mma^{-1}, 1292 ± 480 mma^{-1} and 1034 ± 424 mma^{-1} for the Ohmura *et al*. (1992) relationship and Golledge *et al*. (2010) summer, neutral and winter precipitation types, respectively, at the 714 m ELA, using a mean July temperature of 8.5 ± 0.3°C. Taking into consideration the effect of winter sea ice in the North Atlantic on seasonality bias and the fact that air temperature cooling by the icefield was not accounted for in these figures, the neutral precipitation type value of 1292 ± 480 mma^{-1} is favoured here. Calculation of precipitation values for major outlet glaciers revealed a significant precipitation gradient from west to east across the area, where precipitation levels were considerably reduced in the east.

Implications

Previous research in the Monadhliath Mountains indicated the presence of a few small valley glaciers only during the Younger Dryas (e.g. Young, 1978; Sissons, 1979d; Auton, 1998), suggesting that conditions were too arid in the Monadhliath Mountains to support any substantial glaciation in the region during this time (Sissons, 1979d; Sutherland, 1984). There have been no formal reconstructions of these ice masses and therefore the current research provides the first reconstruction of a Younger Dryas ice mass in region, demonstrating that two coalescent plateau icefields occurred during this time, with a combined area of 280 km^2. The current research highlights the importance of recognising evidence for the existence of plateau icefields, since this is probably a major reason why the Younger Dryas Monadhliath Icefield has not been identified before.

Recognition of this icefield has important implications for the understanding of Younger Dryas climate in the region. Comparison with ice mass reconstructions in neighbouring areas indicates that precipitation in the western sector of the Monadhliath Mountains was of a similar magnitude to that in Creag Meagaidh (Finlayson, 2006) and Drumochter (Benn & Ballantyne, 2005), whilst that in the eastern sector was similar to the central and southeast Grampians (Sissons, 1974b, 1979e; Sissons & Sutherland, 1976). Comparison with modern precipitation data from the study area reveals that the precipitation gradient across the Monadhliath massif during the Younger Dryas was not as strong as it is at present. A possible explanation for this is that a significant proportion of snow that fell in the western sector during the Younger Dryas was redistributed further east by wind, causing an apparent reduction in the strength of the precipitation gradient indicated by the glacier ELAs. Comparison with the modern precipitation data also suggests that the climate in the Monadhliath Mountains during the Younger Dryas was either similar to present or slightly more arid depending on the degree of precipitation seasonality. Using a neutral precipitation type, as favoured here, the climate is concluded to have been comparatively more arid than at present. Comparison with modern glacial environments indicates that Norwegian plateau icefields may provide the most suitable modern analogues for the Monadhliath Icefield.

7.4 Contribution to the Plateau Icefield Landsystem

Summary

A detailed examination of outlet valley retreat patterns and the former thermal regime of the Younger Dryas Monadhliath Icefield was undertaken based on geomorphological and sedimentary evidence found in the study area. This research found that valley morphology and the slope of the bed were important factors for determining the thermal regime of the outlet glaciers and the dynamics of these glaciers during retreat. A range of geomorphological evidence was observed in the outlet valleys in the study area, which was interpreted to be related to differences in thermal

regime; seventeen outlet valleys contained closely spaced moraines, which were interpreted to have been deposited by warm-based outlet glaciers, twenty-three were dominated by ice-marginal meltwater channels indicative of cold-based glacier conditions; and the remaining thirteen were dominated by ice-marginal channels, but contained some moraines and were therefore interpreted to lie on a continuum between cold-based and warm-based glacier ice. The spatial distribution of the different thermal regimes was strongly associated with outlet valley size and gradient, where warm-based glaciers were located in larger outlet valleys, often with steeper backwalls, which enabled the ice to reach pressure melting point through a combination of strain heating and greater ice thickness. Conversely, outlet glaciers located within gently sloping valleys that had little altitudinal difference with the plateau were cold-based.

Valley morphology and the slope of the valley floor also had a significant influence on the patterns of retreat within the outlet valleys. Three styles of retreat were identified based on the spacing of moraines using a 'barcode' approach (*cf.* Lukas & Benn, 2006), which were linked to the type of moraine bifurcation style and the valley morphology. Retreat type 1 occurred in narrow valleys with steep backwalls, where initial retreat of the glacier resulted in a retreat of the glacier snout, causing frontal moraine bifurcations and closely spaced frontal moraines. Retreat type 2 occurred in wide valleys, with gentle gradients, in which retreat occurred initially through glacier thinning causing lateral moraine bifurcations and closely spaced lateral moraines, but fewer moraines across the valley centre line. Retreat type 3 occurred in valleys that contained small outlet valley glaciers that were closely connected to plateau ice. This allowed simultaneous retreat of the glacier terminus and the lateral margins, resulting in both lateral and frontal moraine bifurcations and more evenly distributed moraines across the valley centre line. Further examination of glacier retreat onto the plateau revealed that moraines were more closely spaced on steeper slopes up to a gradient of approximately 50%, beyond which either moraines no longer formed or were not preserved. An important finding from this assessment was that the size of the plateau catchment area had little effect on the retreat dynamics of the outlet glaciers and on the patterns of ice retreat on the plateau, where valley and plateau morphology and bed gradient had a far greater influence.

Area-based 'ELAs' of outlet glaciers at the final stage of active retreat were calculated as an exercise to examine the change in apparent ELA during retreat and the influence of plateau ice on these ELAs. These apparent ELAs cannot be considered as true ELAs, however, since the final stage glaciers were not in climatic equilibrium during this time. A number of the area-based ELAs of the final stage outlet glaciers were calculated as significantly lower than the area-based ELA estimates calculated for the glacier's maximum extent due to a significant loss in plateau area. For three glaciers, this was due to a disconnection from the plateau and these glaciers were

probably able to survive due to snow redistribution and ice avalanching from the plateau and increased shading by a steep valley backwall, meaning that the true ELA was actually much higher (*cf.* Rea *et al*., 1999). Area-based ELAs were also found to be significantly lower for a number of outlet glaciers that retreated onto the plateau into small proto-valleys, again due to a significant loss in area of plateau ice. In order to explain continued active retreat of the glacier in these areas, the climate-driven ELA was considered over a 10 to 50 year period, where for the majority of that time it would be located above the outlet glacier, as modelled by Giesen and Oerlemans (2010). Fluctuations in climate over this time period would cause an occasional lowering of this true ELA onto the glacier surface and allow the plateau ice to advance slightly and deposit a moraine. This suggests that the outlet glaciers were able to respond fairly rapidly to climate fluctuations during this stage of retreat, which may have been a function of size.

An additional factor associated with area-based ELA calculations was also highlighted by the maximum and minimum plateau icefield reconstructions, for which a higher apparent ELA was calculated for the maximum reconstruction. This led to lower precipitation values being calculated for the maximum reconstruction than for the minimum reconstruction, which seemed counter-intuitive. The discrepancy can be explained by differences in the dynamics of the plateau icefield, where a thinner plateau icefield might be expected if plateau ice was warm-based, leading to greater ice velocities and draw-down of ice into the outlet valleys, which would therefore require higher precipitation in order to keep the system in equilibrium. However, since these differences in apparent ELAs and precipitation values will occur using the same temperatures, it suggests that some of assumptions made in methods currently used to calculate area-based ELAs and corresponding palaeoprecipitiation values may not hold true in a plateau icefield landsystem, due to the greater complexities of the system compared to a valley glacier.

Implications

This research provides the first detailed study on the factors that influence thermal regime and glacier retreat patterns in a plateau icefield setting. Although other studies have made the link between outlet glacier size and thermal regime (e.g. Skidmore & Sharp, 1999; Ó Cofaigh *et al*., 2003), this association has not been exclusively made for plateau icefields, where research has tended to focus on the differences between the thermal regime on the plateau and in the outlet valleys (e.g. Dyke, 1993; Rea & Evans, 2003). Nonetheless, the identification of a polythermal plateau icefield in the Monadhliath Mountains adds to a growing body of research that has observed spatial and temporal changes in thermal regime across both modern and palaeo-plateau icefields (e.g. Gellatly *et al*., 1988; Dyke, 1993; Rea *et al*., 1998; McDougall, 2001; Rea & Evans, 2003; Evans, 2010).

In combination with the spatial distribution of thermal regime, the analysis of former outlet glacier retreat patterns at warm-based outlet glaciers has enabled the development of a new conceptual model for the plateau icefield landsystem, which adds to the current model created by Rea and Evans (2003). The original model focuses predominantly on the geomorphological evidence that can be used to identify a plateau icefield landsystem and therefore the conceptual model presented here further adds to our understanding of plateau icefields, by incorporating the influence of valley morphology and slope gradient on plateau icefield retreat patterns. The resulting modified model also shows the break up of the plateau icefield into smaller outlet glaciers, some of which became disconnected from the plateau within corries. The examination of changes in area-based glacier ELA estimates from the maximum extent to final stage of active retreat questions how representative an area-based ELA estimate is for a plateau icefield and emphasises the transient nature of the true ELA during retreat, highlighting the need for a greater understanding of the dynamics of marginal ice masses (see Section 7.5).

7.5 Future Work

The current research has identified a large scope for future research in the field area and on plateau icefield landsystems. The following points outline the key areas for further work.

- The research presented here has established a comprehensive relative chronology for glacial events within the study area during the LGIT. This relative chronology now provides a framework for glaciogenic features to be dated through methods such as surface exposure dating (SED) and optically stimulated luminescence (OSL). The relative chronology, in combination with the geomorphological map, will enable key landforms to be targeted, for example, moraines found immediately inside and outside the Younger Dryas limits identified here and the glaciolacustrine sediments found in the Glen Banchor tributaries and Glen Killin.

- There is scope for further work on deciphering the dominance of plateau and regional ice during retreat from the LGM. This is partly linked to the need for absolute dating in the region, which should help to further constrain the timing of events during this period. This includes further information on the early deglaciation of eastern areas such as the Findhorn Valley and the timing of the advance of local plateau ice in the southeastern corner of the Monadhliath Mountains and its correlation with events in the northern part of the study area. However, insights are also likely to be gained from a further examination of geomorphological and sedimentological evidence in Glen Killin and its vicinity in order to establish a greater understanding of the configuration of the regional ice lobe that advanced into the Fechlin-Killin valley and its relationship to local plateau

ice during this time. For example, lithological analysis on clasts within the subaqueous debris flow deposits in Glen Odhar may provide information on whether the sediments were sourced by local or regional ice.

- The availability of sections within the field area, particularly within moraines was very limited and restricted the amount of sedimentological work that could be undertaken in this research. However, sections within moraines were observed in Corrie Yairack and Coire nam Beith that were not examined in this research due to time constraints. It is perceived that a detailed investigation of the sediments within these sections will provide further information on the processes of moraine formation and debris transport pathways in the region, which can be linked to glacier dynamics, such as thermal regime.

- 3D modelling of glacier mass balance and flow velocities would greatly enhance and add to the work carried out on glacier retreat patterns and thermal regime for the Younger Dryas Monadhliath Icefield (e.g. Carr & Coleman, 2007; Golledge, *et al*., 2008; Carr *et al*., 2010; Finlayson *et al*., 2011). 3D modelling could provide further understanding of the effects of valley morphology on the different retreat patterns identified in this research by replicating recessional moraine sequences to elucidate controls on moraine formation. The modelling could also be used to examine the climatic factors that would lead to active glacier retreat, including evidence for a short-lived maximum extent and an assessment of the scope for an asynchronous advance and retreat of the icefield.

- The research presented here identified an interesting aspect of plateau icefield ELAs relating to plateau icefield thickness, whereby higher apparent ELAs were calculated for icefields with thicker plateau ice, which resulted in lower amounts of precipitation being calculated at this ELA. This requires further examination, either through 3D modelling or observations on modern icefields, in order to ascertain whether this phenomenon can be explained by glacier dynamics or whether the current methods of calculating area-based ELAs produce unrealistic values for plateau icefields.

- The results of this research indicate that small ice masses were able to continue to retreat actively during the later stages of ice retreat, partly due to snow redistribution by wind and enhanced shading in these areas, despite their true ELAs probably lying above the glacier surface the majority of the time. This finding highlights the need for a greater understanding of the behaviour of small, marginal ice masses, particularly on plateau areas where the glaciers cover a very small altitudinal range. Observations on modern plateau icefields, such as Hardangerjøkulen in Norway, where the climate-driven ELA is

predicted to rise above the plateau surface in the next five years (Giesen & Oerlemans, 2010), alongside 3D modelling, would provide a means of investigating this aspect further.

7.6 Conclusion

The research presented in this thesis provides the first systematic mapping of the glacial geomorphology of the Monadhliath Mountains. The results of this mapping were used to identify a comprehensive relative chronology of glacial events in the region during the LGIT. This research identified that regional ice in the Spey Valley and the Great Glen retreated from the LGM in an oscillatory manner, punctuated by stillstands and advances, which caused damming of local drainage in the tributary valleys to the north and south of the Monadhliath Mountains. Two phases of local plateau icefield glaciation were identified, the first relating to a renewed dominance of local plateau ice following the retreat of regional ice from the area and the second relating to glaciation during the Younger Dryas.

Reconstruction of a 280 km^2 Younger Dryas Monadhliath Icefield allowed ELAs and palaeoprecipitation in the region to be calculated, allowing comparison with other areas of Scotland. The results indicate that a strong precipitation gradient occurred across the region, with comparatively wetter conditions in the west than in the east, reflecting overall trends found during the Younger Dryas in Scotland. Comparison with modern precipitation values, however, indicates that the gradient was not as strong during the Younger Dryas as at present, possibly due to redistribution of snow across the plateau from west to east, causing a dampening of the precipitation gradient reflected in the glacier ELAs. Depending on the level of precipitation seasonality during the Younger Dryas, the results indicate that the Monadhliath Mountains were more arid than at present.

The detailed geomorphological mapping undertaken in this research also allowed an examination of the retreat dynamics of the Younger Dryas Monadhliath Icefield, focussing on the thermal regime of the icefield and the spacing of moraines in the outlet valleys and on the plateau. The geomorphological evidence indicates that the icefield was polythermal and retreat dynamics of the outlet glaciers were predominantly influenced by valley morphology and bed gradient rather than the size of the glacier or plateau catchment area. This research provides the first study of its kind on the factors that influence plateau icefield retreat dynamics and adds further detail to the conceptual model of the plateau icefield landsystem.

References

Aber, J.S., Marzolff, I., Ries, J.B. 2010. *Small-format aerial photography: principles, techniques and geoscience applications*. Elsevier, Amsterdam, 266p.

Agassiz, L. 1840. On glaciers, and the evidence of their having once existed in Scotland, Ireland and England. *Proceedings of the Geological Society of London* 3: 327-332.

Anderson, D.E. 1997. Younger Dryas research and its implications for understanding abrupt climate change. *Progress in Physical Geography* 21: 230-249.

André, M.-F. 2003. Do periglacial landscapes evolve under periglacial conditions? *Geomorphology* 52: 149-164.

Atkins, C.B., Dickinson, W.W. 2007. Landscape modification by meltwater channels at margins of cold-based glaciers, Dry Valleys, Antarctica. *Boreas* 36: 47-55.

Auton, C.A. 1998. *Aspects of the Quaternary Geology of 1:50 000 Sheet 74W (Tomatin).* British Geological Survey, Technical Report WA/98/21.

Auton, C.A. 1990. The Middle Findhorn Valley. In: Auton, C.A., Firth, C.R., Merritt, J.W., (eds.). *Beauly to Nairn: Field Guide*. Quaternary Research Association, London, pp. 74-96.

Bakke, J., Dahl, S.O. Paasche, Ø., Løvlie, R., Nesje, A. 2005a. Glacier fluctuations, equilibrium-line altitudes and palaeoclimate in Lyngen, northern Norway, during the Lateglacial and Holocene. *The Holocene* 15: 518-540.

Bakke, J., Lie, Ø. Nesje, A., Dahl, S.O., Paasche, Ø. 2005b. Utilizing physical sediment variability in glacier-fed lakes for continuous glacier reconstructions during the Holocene, northern Folgefonna, western Norway. *The Holocene* 15: 161-176.

Bakke, J., Lie, O., Heegaard, E., Dokken, T., Haug, G., Birks, H.H., Dulski, P., Nilsen, T. 2009, Rapid oceanic and atmospheric changes during the Younger Dryas cold period. *Nature Geoscience* 2: 1-4.

Ballantyne, C.K. 1982. Aggregate clast form characteristics of deposits near the margins of four glaciers in the Jotunheimen massif, Norway. *Norsk Geografisk Tiddskift* 36: 103-113.

Ballantyne, C.K. 1984. The Late Devensian periglaciation of upland Scotland. *Quaternary Science Reviews* 3: 311-343.

Ballantyne, C.K. 1988. Ice-sheet moraines in southern Skye. *Scottish Journal of Geology* 24: 301-304.

Ballantyne, C.K. 1989. The Loch Lomond Readvance on the Isles of Skye, Scotland: glacier reconstruction and palaeoclimatic implications. *Journal of Quaternary Science* 4: 95-108.

Ballantyne, C.K. 1990. The Holocene glacial history of Lyngshalvöya, northern Norway: chronology and climatic implications. *Boreas* 19: 93-117.

Ballantyne, C.K. 1991. Holocene geomorphic activity in the Scottish Highlands. *Scottish Geographical Magazine* 107: 84-98.

Ballantyne, C.K. 1997. Periglacial trimlines in the Scottish Highlands. *Quaternary International* 38-9: 119-136.

Ballantyne, C.K. 1998. Age and significance of mountain-top detritus. *Permafrost and Periglacial Processes* 9: 327-345.

Ballantyne C.K. 2002a. The Loch Lomond Readvance on the Isle of Mull, Scotland: glacier reconstruction and palaeoclimatic implications. *Journal of Quaternary Science* 17: 759-771.

Ballantyne, C.K. 2002b. Paraglacial geomorphology. *Quaternary Science Reviews* 21: 1935-2017.

Ballantyne, C.K. 2002c. A general model of paraglacial landscape response. *The Holocene* 12: 371-376.

Ballantyne, C.K. 2006. Loch Lomond Stadial Glaciers in the Uig Hills, Western Lewis, Scotland. *Scottish Geographical Journal* 122: 256-273.

Ballantyne, C.K. 2007a. The Loch Lomond readvance on North Arran, Scotland: Glacier reconstruction and palaeoclimatic implications. *Journal of Quaternary Science* 22: 343-359.

Ballantyne, C.K. 2007b. Loch Lomond Stadial glaciers in North Harris, Outer Hebrides, North-West Scotland: glacier reconstruction and palaeoclimatic implications. *Quaternary Science Reviews* 26: 3134-3149.

Ballantyne, C.K. 2008. After the ice: Holocene geomorphic activity in the Scottish Highlands. *Scottish Geographical Journal* 124: 8-52.

Ballantyne, C.K. 2010a. Extent and deglacial chronology of the last British-Irish Ice Sheet: implications of exposure dating using cosmogenic isotopes. *Journal of Quaternary Science* 25: 515-534.

Ballantyne, C.K. 2010b. A general model of autochthonous blockfield evolution. *Permafrost and Periglacial Processes* 21: 289-300.

Ballantyne, C.K. 2012. Chronology of glaciation and deglaciation during the Loch Lomon (Younger Dryas) Stade in the Scottish Highlands: implications of recalibrated ^{10}Be exposure ages. *Boreas* 10.1111/j.1502-3885.2012.00253.x.

Ballantyne, C.K., Benn, D.I. 1994. Paraglacial slope adjustment during deglaciation and resedimentation following glacier retreat, Fåbergstølsdalen, Norway. . *Arctic and Alpine Research* 26: 255-269.

Ballantyne, C.K., Hall, A.M. 2008. The altitude of the last ice sheet in Caithness and east Sutherland, northern Scotland. *Scottish Journal of Geology* 44: 169-181.

Ballantyne, C.K., Harris, C. 1994. *The Periglaciation of Great Britain*. Cambridge University Press, Cambridge.

Ballantyne, C.K., Stone, J.O. 2011. Did large ice caps persist on low ground in north-west Scotland during the Lateglacial Interstade? *Journal of Quaternary Science*. DOI: 10.1002/jqs.1544.

Ballantyne C.K., Wain-Hobson T. 1980. The Loch Lomond Advance on the Island of Rhum. *Scottish Journal of Geology* 16: 1-10.

Ballantyne, C.K., Whittington, G.W. 1999. Late Holocene alluvial fan formation and floodplain incision, Central Grampian Highlands, Scotland. *Journal of Quaternary Science* 14: 651-671.

Ballantyne, C.K., Hall, A.M., Phillips, W., Binnie, S., Kubik, P.W. 2007. Age and significance of former low-altitude corrie glaciers on Hoy, Orkney Islands. *Scottish Journal of Geology* 43: 107-114.

Ballantyne, C.K., McCarroll, D., Nesje, A., Dahl, S.O. 1997. Periglacial trimlines, former nunataks and the altitude of the last ice sheet in Wester Ross, northwest Scotland. *Journal of Quaternary Science* 12: 225-238.

Ballantyne, C.K. McCarroll, D., Nesje, A., Dahl, S.O., Stone, J.O. 1998. The last ice sheet in north-west Scotland: reconstruction and implications. *Quaternary Science Reviews* 17: 1149-1184.

Barrow, G., Hinxman, L.W., Cunningham Craig, E.H., Kynaston, H. 1913. *The geology of Upper Strathspey, Gaick, and the Forest of Atholl*. Memoir of the Geological Survey, Scotland, Sheet 64 (Scotland). HMSO, Edinburgh.

Benediktsson, I.O., Moller, P., Ingolfsson, O., van der Meer, J.J.M., Kjaer, K.H., Kruger, J. 2008. Instantaneous end moraine and sediment wedge formation during the 1890 glacier surge of Bruarjokull, Iceland. *Quaternary Science Reviews* 27: 209-234.

Benn, D.I. 1989. Controls on sedimentation in a Late Devensian ice-dammed lake, Achnasheen, Scotland. *Boreas* 18: 31-42.

Benn, D.I. 1992. The genesis and significance of hummocky moraine – evidence from the Isle of Skye, Scotland. *Quaternary Science Reviews* 11: 781-799.

Benn, D.I. 1994. Fabric shape and the interpretation of sedimentary fabric data. *Journal of Sedimentary Research* A64: 910-915.

Benn, D.I. 1995. Fabric signature of till deformation, Breidamekurjokull, Iceland. *Sedimentology* 42: 735-747.

Benn, D.I. 1996. Subglacial and subaqueous processes near a glacier grounding line: Sedimentological evidence from a former ice-dammed lake, Achnasheen Scotland. *Boreas* 25: 23-36.

Benn, D.I. 2004a. Clast Morphology. In: Evans, D.J.A., Benn, D.I., (eds.). *A Practical Guide to the Study of Glacial Sediments*. Arnold, London, pp. 78-92.

Benn, D.I. 2004b. Macrofabric. In: Evans, D.J.A., Benn, D.I., (eds.). *A Practical Guide to the Study of Glacial Sediments*. Arnold, London, pp. 92-114

Benn, D.I., Ballantyne, C.K. 1993. The description and representation of clast shape. *Earth Surface Processes and Landforms* 18: 665-672.

Benn, D.I., Ballantyne, C.K. 1994. Reconstructing the transport history of glaciogenic sediments - a new approach based on the co-variance of clast form indexes. *Sedimentary Geology* 91: 215-227.

Benn, D.I., Ballantyne, C.K. 2005. Palaeoclimatic reconstruction from loch Lomond Readvance glaciers in the West Drumochter Hills, Scotland. *Journal of Quaternary Science* 20: 577-592.

Benn, D.I., Clapperton, C.E. 2000. Glacial sediment-landform associations and palaeoclimate during the last glaciation, Strait of Magellan Strait, Chile. *Quaternary Research* 54: 13-23.

Benn, D.I., Evans, D.J.A. 1993. Glaciomarine deltaic deposition and ice-marginal tectonics: the "Loch Don Sand Moraine", Isle of Mull, Scotland. *Journal of Quaternary Science* 8: 279-291.

Benn, D.I., Evans, D.J.A. 1996. The interpretation and classification of subglacially-deformed materials. *Quaternary Science Reviews* 15: 23-52.

Benn, D.I., Evans, D.J.A. 2008. A Younger Dryas ice cap to the north of Glen Roy: a new perspective on the origin of the Turret Fan. In: Palmer, A.P., Lowe, J.J., Rose, J., (eds.). *The Quaternary of Glen Roy and Vicinity: Field Guide*. Quaternary Research Association, London, pp. 158-161.

Benn, D.I., Evans, D.J.A. 2010. *Glaciers and Glaciation*. Hodder Education, London. 2nd Edition.

Benn, D.I., Gemmell., A.M.D. 1997. Calculating equilibrium line altitudes of former glaciers by the balance ratio method: a new computer spreadsheet. *Glacial Geology and Geomorphology*. http://ggg.ac.uk/ggg/papers/full/1997/tn011997/tn01.html

Benn, D.I., Hulton, N.R.J. 2010. An Excel™ spreadsheet program for reconstructing the surface profile of former mountain glaciers and ice caps. *Computers & Geosciences* 36: 605-610.

Benn D.I., Lehmkuhl, F. 2000. Mass balance and equilibrium-line altitudes of glaciers in high-mountain environments. Conference on Late Quaternary Glaciation and Palaeoclimate of the Tiberan Plateau and Bordering Mountains. *Quaternary International* 65-66: 15-29.

Benn, D.I., Lukas, S., 2006. Younger Dryas glacial landsystems in North West Scotland: An assessment of modern analogues and palaeoclimatic implications. *Quaternary Science Reviews* 25: 2390-2408.

Benn, D.I., Evans, D.J.A., Phillips, E.R., Hiemstra, J.F., Walden, J., Hoey, T.B. 2004. The research project - a case study of Quaternary glacial sediments. In: Evans, D.J.A., Benn, D.I., (eds.). *A Practical Guide to the Study of Glacial Sediments*. Arnold, London, pp. 209-234.

Benn, D.I., Kirkbride, M.P., Owen, L.A., Brazier, V. 2003. Glaciated Valley Landsystems. In: Evans, D.J.A., (ed.). *Glacial Landsystems.* Arnold, London, pp. 372 -405.

Benn, D.I., Lowe, J.J., Walker, M.J.C. 1992. Glacier response to climatic change during the Loch Lomond Stadial and Early Flandrian – geomorphological and palynological evidence from the Isle of Skye, Scotland. *Journal of Quaternary Science* 7: 125-144.

Benn, D. I., Owen, L. A., Osmaston, H.A., Seltzer, G.O., Porter, S.C., Mark, B. 2005. Reconstruction of equilibrium-line altitudes for tropical and sub-tropical glaciers. *Quaternary International* 138-139: 8-21.

Bennett, M.R., 1996, Landform-sediment distributions within the northern part of the Younger Dryas highland ice-field, Scotland. *Scottish Journal of Geology* 32: 97-105.

Bennett, M.R. 1999. Paraglacial and periglacial slope adjustment of a degraded lateral moraine in Glen Torridon. *Scottish Journal of Geology*. 35: 79-83.

Bennett, M.R., Boulton, G.S. 1993a. A reinterpretation of Scottish 'hummocky moraine' and its significance for the deglaciation of the Scottish Highlands during the Younger Dryas or Loch Lomond Stadial. *Geological Magazine* 130: 301-318.

Bennett, M.R., Boulton, G.S. 1993b. Deglaciation of the Younger Dryas or Loch-Lomond Stadial ice-field in the northern Highlands, Scotland. *Journal of Quaternary Science* 8: 133-145.

Bennett, M.R., Hambrey, M.J., Huddart, D. Glasser, N.F. 1998. Glacial thrusting and moraine-mound formation in Svalbard and Britain: the example of Coire a' Cheud-chnoic (Valley of Hundred Hills), Torridon Scotland. *Quaternary Proceedings* 6:17-34.

Bennett, M.R., Huddart, D., Thomas, G.S.P. 2002. Facies architecture within a regional glaciolacustrine basin: Copper river, Alaska. *Quaternary Science Reviews* 21: 2237 – 2279.

Bennett, M.R., Waller, R.I., Glasser, N.F., Hambrey, M.J., Huddart, D. 1999. Glacigenic clast fabrics: genetic fingerprint or wishful thinking? *Journal of Quaternary Science* 14: 125-135.

Björck, S., Bennike, O. Rosén, P. Andresen, C.S., Bohncke, S., Kaas, E., Conley, D. 2002. Anomalously mild Younger Dryas summer conditions in southern Greenland. *Geology* 30: 427-430.

Borgström, I. 1999. Basal ice temperatures during late Weichselian deglaciation: Comparison of landform assemblages in west-central Sweden. *Annals of Glaciology* 28: 9-15.

Boulton, G.S., Clark, C.D. 1990. A highly mobile Laurentide ice sheet revealed by satellite images of glacial lineations. *Nature* 346: 813-817.

Boulton, G.S., Eyles, C.H. 1979. Sedimentation by valley glaciers: a model and genetic classification. In: Schluchter, C., (ed.). *Moraines and Varves*. Balkema, Rotterdam, p. 11-23.

Boulton, G.S., Dobbie, K.E., Zatsepin, S. 2001. Sediment deformation beneath glaciers and its coupling to the subglacial hydraulic system. *Quaternary International* 86: 3-28.

Boulton, G.S., Jones, A., Clayton, K., Kenning, M. 1977. A British ice sheet model and patterns of glacial erosion and deposition in Britain. In: Shotton, F.W., (ed.). *British Quaternary Studies: Recent Advances.* Oxford University Press, Oxford, pp. 231-246.

Boulton, G.S., Smith, G.D., Jones, A.S., Newsome, J. 1985. Glacial geology and glaciology of the last mid-latitude ice sheets. *Journal of the Geological Society of London* 142: 447-474.

Bradwell, T. 2006. The Loch Lomond Stadial Glaciation in Assynt: A Reappraisal. *Scottish Geographical Journal* 122: 274 - 292.

Bradwell, T., Stoker, M., Krabbendarn, M. 2008. Megagrooves and streamlined bedrock in NW Scotland: The role of ice streams in landscape evolution. *Geomorphology* 97: 135-156.

Bradwell, T., Stoker, M., Larter, R. 2007. Geomorphological signature and flow dynamics of The Minch palaeo-ice stream, northwest Scotland. *Journal of Quaternary Science* 22: 609-617.

Braithwaite, R.J. 1980. On glacier energy balance, ablation and air temperature. *Journal of Glaciology* 27: 381-391.

Braithwaite, R.J. 2008. Temperature and precipitation climate at the equilibrium line altitude of glaciers expressed by the degree-day factor for snow melting. *Journal of Glaciology* 54: 437-444.

Brazier, V., Gordon, J.E., Kirkbride, M.P., Sugden, D.E. 1996. The Late Devensian ice sheet and glaciers in the Cairngorm Mountains. In: Glasser, N.F., Bennett, M.R., (eds.). *The Quaternary of the Cairngorms: Field Guide.* Quaternary Research Association, London, pp. 28-53.

Brazier, V., Kirkbride, M.P., Gordon, J.E., 1998. Active ice-sheet deglaciation and ice-dammed lakes in the northern Cairngorm Mountains, Scotland. *Boreas* 27: 297-310.

Bridgland, D.R., Westaway, R. 2008. Climatically controlled river terrace staircases: A worldwide Quaternary phenomenon. *Geomorphology* 98: 285-315.

British Atmospheric Data Centre (NERC). https://badc.nerc.ac.uk/home/ Accessed 17/02/2012.

British Geological Survey. 2004**.** *Tomatin Sheet 74W (Scotland) Bedrock and Superficial Deposits*. 1: 50 000 Series. British Geological Survey, Edinburgh.

Brook, M.S., Paine, S. 2011. Ablation of ice-cored moraine in a humid, maritime climate: Fox Glacier, New Zealand. *Geografiska Annaler: Series A, Physical Geography*. DOI: 10/111/j.1468-0459.2011.00442.x

Brooks, S.J., Birks, H.J.B. 2000. Chironomid-inferred Late-glacial air temperatures at Whitrig Bog, south-east Scotland. *Journal of Quaternary Science* 15: 759-764.

Brooks, S.J., Birks, H.J.B. 2001. Chironomid-inferred air temperatures from Lateglacial and Holocene sites in north-west Europe: progress and problems. *Quaternary Science Reviews* 20: 1723-1741.

Brown, I.M. 1993. Pattern of deglaciation of the last (Late Devensian) Scottish ice sheet: evidence from ice-marginal deposits in the Dee valley, north-east Scotland. *Journal of Quaternary Science* 8: 235-250.

Brown, V.H. 2009. *Reconstructing Loch Lomond Stadial Glaciers and Climate in the south-west English Lake District*. Unpublished MSc thesis, University of Durham.

Brown, V.H., Evans, D.J.A., Evans, I.S. 2011. The Glacial Geomorphology and Surficial Geology of the South-West English Lake District. *Journal of Maps* v2011: 221-243.

Campbell, J.B. 2002. *Introduction to remote sensing*. 3rd edition. Taylor and Francis, London.

Carr, S.J., Coleman, C.G. 2007. An improved technique for the reconstruction of former glacier mass-balance and dynamics. *Geomorphology* 92: 76-90.

Carr, S.J., Lukas, S., Mills, S.C. 2010. Glacier reconstruction and mass balance modelling as a geomorphic and palaeoclimatic tool. *Earth Surface Processes and Landforms* 35: 1103-1115.

Channel Coastal Observatory. 2011. *Southeast Regional Coastal Monitoring Programme: Digital Aerial Photos*. http://www.channelcoast.org/southeast/survey_techniques/airborne_remote_sensing_topographic_surveys/?link=digital_aerial_photos.html. Accessed 6/11/2011.

Charlesworth, J.K. 1955. The Late-glacial history of the Highlands and islands of Scotland. *Transactions of the Royal Society of Edinburgh* 62: 769-933.

Cheel, R.J., Rust, B.R. 1982. Coarse grained facies of glaciomarine deposits near Ottawa, Canada. In: Davidson-Arnott, R., Nickling, W., Fahey, B.D., (eds.). *Research in Glaciofluvial and Glaciolacustrine Systems*. Geobooks, Norwich, pp. 279-295.

Chen, C., Rose, J., 2008, Assessment of remote sensed imagery on the analysis of landforms in Glen Roy. In: Palmer, A.P., Lowe, J.J., Rose, J., (eds.). *The Quaternary of Glen Roy and Vicinity: Field Guide*. Quaternary Research Association, London, pp. 36-45.

Church, M., Gilbert, R. 1975. Proglacial fluvial and lacustrine sediments. In :Jopling, A.V., McDonald, B.C., (eds.). *Glaciofluvial and Glaciolacustrine Sedimentation*. SEPM, Special Publication 23: 22-100.

Clapperton, C.M., Sugden, D.E. 1977. The Late Devensian glaciation of north east Scotland. In: Gray, J.M., Lowe, J.J., (eds.). *Studies in the Scottish Lateglacial Environment*. Pergamon, Oxford, pp. 1-14.

Clapperton, C.M., Gunson, A.R., Sugden, D.E. 1975. Loch Lomond Readvance in the eastern Cairngorms. *Nature* 253: 710-712.

Clark, C.D. 1997. Reconstructing the evolutionary dynamics of former ice sheets using multi-temporal evidence, remote sensing and GIS. *Quaternary Science Reviews* 16: 1067-1092.

Clark, C.D., Meehan, R.T. 2001. Subglacial bedform geomorphology of the Irish Ice Sheet reveals major configuration changes during growth and decay. *Journal of Quaternary Science* 16: 483-496.

Clark, C.D., Evans, D.J.A., Khatwa, A., Bradwell, T., Jordan, C.J., Marsh, S.H., Mitchell, W.A., Bateman, M.D. 2004. Map and GIS database of landforms and features related to the last British Ice Sheet. *Boreas* 33: 359-375.

Clark, C.D., Greenwood, S.L., Evans, D.J.A. 2006. Palaeoglaciology of the last British-Irish ice sheet: challenges and some recent developments. In: Knight, P., (ed.). *Glacier Science and Environmental Change*. Blackwell, Oxford, pp. 248-264.

Clark C.D., Hughes, A.L.C., Greenwood, S.L. Jordan C., Sejrup, H.P. 2010. Pattern and timing of retreat of the last British-Irish Ice Sheet. *Quaternary Science Reviews*. http://dx.doi.org/10.1016/j.quascirev.2010.07.019

Clark, C.D., Knight, J.K., Gray, J.T. Geomorphological reconstruction of the Labrador Sector of the Laurentide Ice Sheet. *Quaternary Science Reviews* 19: 1343-1366.

Close, M.H. 1867. Notes on the general glaciation of Ireland. *Journal of the Royal Geographical Society of London Dublin* 1: 207-242.

Coleman, C.G., Carr, S.J. 2008. Complex relationships between Younger Dryas glacial, periglacial and paraglacial landforms, Brecon Beacons, South Wales. *Proceedings of the Geologists' Association* 119: 259-276.

Collinson, J.D., Thompson, D.B. 1989. *Sedimentary Structures*. Unwin Hyman, London.

Coope GR, Rose J. 2008. Palaeotemperatures and palaeoenvironments during the Younger Dryas: arthropod evidence from Croftamie at the type area of the Loch Lomond Readvance, and significance for the timing of glacier expansion during the Lateglacial period in Scotland. *Scottish Journal of Geology* 44: 43–49.

Curry, A.M. 2000. Holocene reworking of drift-mantled hillslopes in the Scottish Highlands. *Journal of Quaternary Science* 15: 529-41.

Dahl, R. 1966. Block fields, weathering pits and tor-like forms in the Narvik Mountains, Nordland, Norway. *Geografiska Annaler* 46A: 55-85.

Dahl S.O, Nesje A. 1996. A new approach to calculating Holocene winter precipitation by combining glacier equilibrium-line altitudes and pine-tree limits: case study from Hardangerjøkulen, central southern Norway. *The Holocene* 6: 381-398.

Dahl S.O, Nesje A, Ovstedal J. 1997. Cirque glaciers as evidence for a thin Younger Dryas ice sheet in east-central southern Norway. *Boreas* 26: 161–180.

Dorling, D., Fairbairn, D. 1997. *Mapping: ways of representing the world*. Prentice Hall, Harlow, 184 p.

Dowdeswell, J.A., Sharp, M.J. 1986. Characterization of pebble fabrics in modern terrestrial glacigenic sediments. *Sedimentology* 33: 699-710.

Dowman, I., Balan, P., Renner K., Fischer, P. 2003. *An Evaluation of Nextmap Terrain Data in the Context of UK National Datasets*. Report to Getmapping, University College London.

Duyster, J. 2011. *Stereo32 version 1.0.3*. Ruhr University Bochum, Germany. http://www.ruhr-uni-bochum.de/hardrock/downloads.html. Downloaded 07/11/2011.

Dyke, A.S. 1993. Landscapes of cold-centred Late Wisconsinan ice caps, Arctic Canada. *Progress in Physical Geography* 17: 223-247.

England, J. 1986. Glacial erosion of a high arctic valley. *Journal of Glaciology* 32: 60-64.

Evans, D.J.A. 1990. The effect of glacier morphology on surficial geology and glacial stratigraphy in a high arctic mountainous terrain. *Zeitschrift für Geomorphologie* 43: 481-503.

Evans, D.J.A. 2009. Controlled moraines: origins, characteristics and palaeoglaciological implications. *Quaternary Science Reviews* 28: 183-208

Evans, D.J.A. 2010. Controlled moraine development and debris transport pathways in polythermal plateau icefields: examples from Tungnafellsjökull, Iceland. *Earth Surface Processes and Landforms* 35: 1430-1444.

Evans, D.J.A. 2011. Glacial landsystems of Satujökull, Iceland: A modern analogue for glacial landsystem overprinting by mountain icecaps. *Geomorphology* 129: 225-237.

Evans, D.J.A., Benn, D.I. 2004. *A Practical Guide to the Study of Glacial Sediments*. London, Arnold.

Evans, D.J.A., Hiemstra, J.F. 2005. Till deposition by glacier submarginal, incremental thickening. *Earth Surface Processes and Landforms* 30: 1633-1662.

Evans, D.J.A., Rea, B.R. 2003. Surging Glacier Landsystem. In: Evans, D.J.A., (ed.). *Glacial Landsystems*. Arnold, London, pp. 259-288.

Evans, D.J.A., Thomson, S.A. 2010. Glacial sediments and landforms of Holderness, eastern England: A glacial depositional model for the North Sea Lobe of the British-Irish Ice Sheet. *Earth Science Reviews* 101: 147-189.

Evans, D.J.A., Twigg, D.R. 2002. The active temperate glacial landsystem: a model based on Breidamerkurjökull and Fjallsjökull, Iceland. *Quaternary Science Reviews* 21: 2143-2177.

Evans, D.J.A., Clark, C. D., Mitchell, W.A. 2005. The last British Ice Sheet: A review of the evidence utilised in the compilation of the Glacial Map of Britain. *Earth Science Reviews* 70: 253-312.

Evans, D.J.A., Hiemstra, J.F., Ó Cofaigh, C. 2007. An assessment of clast macrofabrics in glacigenic sediments based on A/B plane data. *Geografiska Annaler* 89A: 103-120.

Evans, D.J.A., Lemmen, D.S., Rea, B.R. 1999. Glacial landsystems of the southwest Laurentide Ice Sheet: modern Icelandic analogues. *Journal of Quaternary Science* 14: 673-691.

Evans, D.J.A, Livingstone, S.J., Vieli, A. Ó Cofaigh, C. 2009. The palaeoglaciology of the central sector of the British and Irish Ice Sheet: reconciling glacial geomorphology and preliminary ice sheet modelling. *Quaternary Science Reviews* 28: 739-757.

Evans, D.J.A., Nelson, C.D., Webb, C. 2010b. An assessment of fluting and "till esker" formation on the foreland of Sandfellsjökull, Iceland. *Geomorphology* 114: 453-465.

Evans, D.J.A., Phillips, E.R., Hiemstra, J.F., Auton, C.A. 2006b. Subglacial till: formation, sedimentary characteristics and classification. *Earth Science Reviews* 78: 115-176.

Evans, D.J.A., Rea, B.R., Benn, D.I. 1998. Subglacial deformation and bedrock plucking in areas of hard bedrock. *Glacial Geology and Geomorphology* v. rp04/1998 - http://ggg.qub.ac.uk/ggg/papers/full/1998/rp041998/rp04.html.

Evans, D.J.A., Rea, B.R., Hansom, J.D., Whalley, W.B. 2002. Geomorphology and style of plateau icefield deglaciation in fjord terrains: the example of Troms-Finnmark, north Norway. *Journal of Quaternary Science* 17: 221-239.

Evans, D.J.A., Shulmeister, J., Hyatt, O. 2010a. Sedimentology of latero-frontal moraines and fans on the west coast of South Island, New Zealand. *Quaternary Science Reviews* 29: 3790-3811.

Evans, D. J. A., Twigg, D.R., Shand, M. 2006a. Surficial geology and geomorphology of the þórisjökull plateau icefield, west-central Iceland. *Journal of Maps* v2006: 17-29.

Evans I.S. 2006. Local aspect asymmetry of mountain glaciation: a global survey of consistency of favoured directions for glacier numbers and altitudes. *Geomorphology* 73: 166–184.

Everest, J., Kubik, P. 2006. The deglaciation of eastern Scotland: cosmogenic ^{10}Be evidence for a Lateglacial stillstand. *Journal of Quaternary Science* 21: 95-104.

Everest, J.D., Golledge, N.R. 2004. Dating deglaciation in Strath Spey and the Cairngorm Mountains. In: Lukas, S., Merritt, J.W., Mitchell, W.A., (eds.). *The Quaternary of the Central Grampian Highlands: Field Guide*. Quaternary Research Association, London, pp. 50-57.

Eyles, N. 1983. Modern Icelandic glaciers as depositional models for 'hummocky moraine' in the Scottish Highlands. In: Evenson, E.B., Schlüchter, C., Rabassa, J., (eds.). *Tills and Related Deposits*. Balkema, Rotterdam, pp. 47-59.

Eyles, N., Eyles, C.H., Miall, A.D. 1983. Lithofacies types and vertical profile models: an alternative approach to the description and environmental interpretation of glacial diamict and diamictite sequences. *Sedimentology* 30: 393-410.

Eyles, N., Eyles, C.H., McCabe, A.M. 1988. Late Pleistocene subaerial debris-flow facies of the Bow Valley, near Banff, Canadian Rocky Mountains. *Sedimentology* 35: 465-480.

Fabel, D., Small, D., Miguens-Rodriguez, M., Freeman, S.P.H.T. 2010. Cosmogenic nuclide exposure ages from the Parallel Roads of Glen Roy, Scotland. *Journal of Quaternary Science* 25: 597-603.

FetchClimate. 2012. http://fetchclimate.cloudapp.net/ Accessed 21/03/12.

Finlayson, A.G. 2006. Glacial Geomorphology of the Creag Meagaidh Massif, Western Grampian Highlands: implications for local glaciation and palaeoclimate during the Loch Lomond Stadial. *Scottish Geographical Journal* 122: 293-307.

Finlayson, A., Bradwell, T., Gollege, N., Merritt, J. 2007. Morphology and significance of transverse ridges (De Geer moraines) adjacent to the Moray Firth, NE Scotland. *Scottish Geographical Journal* 123: 257 - 270.

Finlayson, A., Golledge, N., Bradwell, T., Fabel, D. 2011. Evolution of a Lateglacial mountain ice cap in northern Scotland. *Boreas* 40: 536-554

Fjellanger, J., Sørbel, L., Linge, H., Brook, E.J., Raisbeck, G.M., Yiou, F. 2006. Glacial survival of blockfields on the Varanger Peninsula, northern Norway. *Geomorphology* 82: 255-272.

Furbish, D.J., Andrews, J.T. 1984. The use of hypsometry to indicate long-term stability and response of valleys glaciers to changes in mass transfer. *Journal of Glaciology* 30: 199-211.

Gellatly, A.F., Gordon, J.E., Whalley, W.B., Hansom, J.D. 1988. Thermal regime and geomorphology of plateau ice caps in northern Norway: observations and implications. *Geology* 16: 983-986.

Gibson, P.J. 2000. *Introductory Remote Sensing: Principles and concepts*. Routledge, London, 184p.

Gibson, P.J., Power, C.H. 2000. *Introductory Remote Sensing: Digital image processing and applications*. Routledge, London, 249 p.

Giesen, R.H., Oerlemans, J. 2010. Response of the ice cap Hardangerjøkulen in southern Norway to the 20th and 21st century climates. *The Cryosphere* 4: 191-213.

Glasser, N.F., Hambrey, M.J. 2003. Ice-marginal terrestrial landsystems: Svalbard polythermal glaciers. In: Evans, D.J.A., (ed.). *Glacial Landsystems*. Arnold, London, pp. 65-88.

Goehring, B.M., Brook, E.J. Linge, H., Raisbeck, G.M., Yiou, F. 2008. Beryllium-10 exposure ages of erratic boulders in southern Norway and implications for the history of the Fennoscandian Ice Sheet. *Quaternary Science Reviews* 27: 320-336.

Golledge, N.R. 2006. The Loch Lomond Stadial glaciation south of Rannoch Moor: new evidence and palaeoglaciological insights. *Scottish Geographical Journal* 122: 326-343.

Golledge, N.R. 2007. An ice cap landsystem for palaeoglaciological reconstructions: characterizing the Younger Dryas in western Scotland. *Quaternary Science Reviews* 26: 213-229.

Golledge, N.R. 2008. *Glacial geology and glaciology of the Younger Dryas ice cap in Scotland*. Unpublished PhD thesis, University of Edinburgh.

Golledge N.R. 2010. Glaciation of Scotland during the Younger Dryas stadial: a review. *Journal of Quaternary Science* 25: 550-566.

Golledge, N.R., Hubbard, A. 2005. Evaluating Younger Dryas glacier reconstructions in part of the western Scottish Highlands: a combined empirical and theoretical approach. *Boreas* 34: 274-286.

Golledge, N.R., Hubbard, A., Bradwell, T. 2010. Influence of seasonality on glacier mass balance, and implications for palaeoclimate reconstructions. *Climate Dynamics* 30: 757-700.

Golledge, N.R., Hubbard, A., Sugden, D.E., 2008. High-resolution numerical simulation of Younger Dyras glaciation in Scotland. *Quaternary Science Reviews* 27: 888-904.

Goodchild, J.G. 1875. The glacial phenomena of the Eden Valley and the western part of the Yorkshire-dale District. *Quarterly Journal of the Geological Society of London* 31: 55-99.

Graham, D.J., Midgley, N.G. 2000. Graphical representation of clast shape using triangular diagrams: an Excel spreadsheet method. *Earth Surface Processes and Landforms* 25: 1473-1477.

Gray, J.M. 1982. The last glaciers (Loch Lomond Advance) in Snowdonia, N. Wales: *Geological Journal* 17: 111-133.

Gray, J.M., Coxon, P. 1991. The Loch Lomond Stadial glaciation in Britain and Ireland. In: Ehlers, J., Gibbard, P.L., Rose, J., (eds.). *Glacial deposits in Great Britain and Ireland.* Balkema, Rotterdam, pp. 89-105.

Greene, D.R. 1992. Topography and former Scottish tidewater glacier. *Scottish Geographical Magazine* 108: 164-171.

Greenwood, S.L., Clark, C.D. 2008. Subglacial bedforms of the Irish Ice Sheet. *Journal of Maps* v2008: 332-357.

Greenwood, S.L., Clark, C.D., Hughes, A.L.C., 2007. Formalising an inversion methodology for reconstructing ice sheet retreat patterns from meltwater channels: application to the British Ice Sheet. *Journal of Quaternary Science* 22: 637-645.

Gurnell, A.M., Edwards, P.J., Petts, G.E., Ward, J.V. 1999. A conceptual model for alpine proglacial river channel evolution under changing climatic conditions. *Catena* 38: 223-242.

Hall, A.M., Glasser, N.F. 2003. Reconstructing the basal thermal regime of an ice stream in a landscape of selective linear erosion: Glen Avon, Cairngorm Mountains, Scotland. *Boreas* 32: 191-208.

Hambrey, M.J., Huddart, D., Bennett, M.R., Glasser, N.F. 1997. Genesis of 'hummocky moraines' by thrusting in glacier ice: Evidence from Svalbard and Britain. *Journal of the Geological Society* 154: 623-632.

Hart, J.K. 1994. Till fabric associated with deformable beds. *Earth Surface Processes and Landforms* 19: 15-32.

Haselock, P.J., Leslie, A.G. 1992. Polyphase deformation in Grampian Group rocks of the Monadhliath defined by a ground magnetic survey. *Scottish Journal of Geology* 28: 81-87.

Haselock, P.J., Winchester, J.A., Whittles, K.H. 1982. The stratigraphy and structure of the southern Monadhliath Mountains between Loch Killin and upper Glen Roy. *Scottish Journal of Geology* 18: 275-290.

Hättestrand, C., Stroeven, A.P. 2002. A relict landscape in the centre of Fennoscandian glaciation: Geomorphological evidence of minimal Quaternary erosion. *Geomorphology* 44: 127-143.

Hicock, S.R., Dreimanis, A. 1992. Deformation till in the Great Lakes region: implications for rapid flow along the south-central margin of the Laurentide Ice Sheet. *Canadian Journal of Earth Sciences* 29: 1565-1579.

Hiemstra, J.F., Rijsdijk, K.F., Shakesby, R.A., McCarroll, D. 2009. Reinterpreting Rotherslade, Gower Peninsula: implications for Last Glacial ice limits and Quaternary stratigraphy of the British Isles. *Journal of Quaternary Science* 24: 399-410.

Highton, A.J. Hyslop, E.K., Noble, S.J. 1999. U-Pb geochronology of migmatisation in the Northern Central Highlands: evidence for pre-Caledonian (Neoproterozoic) tectonometamorphism in the Grampain Block, Scotland. *Journal of the Geological Society, London* 156: 1195-1204.

Hinchcliffe, S., Ballantyne, C.K., Walden, J. 1998. The structure and sedimentology of relict talus, Trotternish, northern Skye, Scotland. *Earth Surface Processes and Landforms* 23: 545–60.

Hinxman, L.W., Anderson, E.M. 1915. *The geology of Mid-Strathspey and Strathdearn, including the country between Kingussie and Grantown.* Memoir of the Geological Survey, Scotland, Sheet 74 (Scotland). HMSO, Edinburgh.

Hinxman, L.W., Carruthers, R.G., MacGregor, M. 1923. *The Geology of Corrour and the Moor of Rannoch. Memoir of the Geological Survey, Scotland*. HMSO, Edinburgh.

Hiscott, R.N., Aksu, A.E., Mudie, P.J., Parsons, D.F. 2001. A 340,000 year record of ice rafting, palaeoclimatic fluctuations, and shelf-crossing glacial advances in the southwestern Labrador Sea. *Global and Planetary Change* 28: 227-240.

Hockey, B. 1970. An improved co-ordinate system for particle shape representation. *Journal of Sedimentary Petrology* 40: 1054-1056.

Hofmann, H.J. 1994. Grain-shape indexes and isometric graphs. *Journal of Sedimentary Research A* 64: 916-920.

Hollingworth, S.E. 1931. The glaciation of western Edenside and adjoining areas and the drumlins of Edenside and the Solway Basin. *Quarterly Journal of the Geological Society of London* 87: 281-359.

Holmes, G. 1984. *Rock-slope failure in parts of the Scottish Highlands*. Unpublished PhD thesis, University of Edinburgh.

Hooyer, T.S., Iverson, N.R. 2000. Clast-fabric development in a shearing granular material: Implications for subglacial till and fault gouge. *Geological Society of America Bulletin* 112: 683-692.

Hornung, J.J., Asprion, U., Winsemann, J. 2007. Jet-efflux deposits of a subaqueous ice-contact fan, glacial Lake Rinteln, northwestern Germany. *Sedimentary Geology* 193: 167-92.

Hubbard, A., 1999. High-resolution modelling of the advance of the Younger Dryas ice sheet and it climate in Scotland. *Quaternary Research* 52: 27-43.

Hubbard, B., Glasser, N.F. 2005. *Field Techniques in Glaciology and Glacial Geomorphology*. John Wiley & Sons Ltd, Chichester.

Huddart, D. 1999. Supraglacial trough fills, southern Scotland: origins and implications for deglacial processes. *Glacial Geology and Geomorphology*. http://boris.qub.ac.uk/ggg/papers/full/1999/rp041999/rp04.html

Hughes, A.L.C., Clark, C.D., Jordan, C.J. 2010. Subglacial bedforms of the last British Ice Sheet. *Journal of Maps* v2010: 543-563.

Hughes, M.L., McDowell, P.F., Marcus, W.A. 2006. Accuracy assessment of georectified aerial photographs: Implications for measuring lateral channel movement in a GIS. *Geomorphology* 74: 1-16.

Hughes, P.D. 2002. Loch Lomond Stadial glaciers in the Aran and Arenig Mountains, North Wales, Great Britain. *Geological Journal* 37: 9-15.

Hughes, P.D. 2010. Geomorphology and Quaternary stratigraphy: The roles of morpho-, litho-, and allostratigraphy *Geomorphology* 123: 189-199.

Hughes, P.D., Braithwaite, R.J. 2008. Application of a degree-day model to reconstruct Pleistocene glacial climates. *Quaternary Research* 69: 110-116.

Humlum, O. 2002. Modelling late 20th-century precipitation in Nordenskiöld Land, Svalbard by geomorphic means. *Norsk Geografisk Tidsskrift* 56: 96-103.

Intermap Technologies. 2004. *Product Handbook and Quick Start Guide: Version 3.3*. Intermap, Englewood, USA.

Isarin, R.F.B., Rensen, H. 1999. Reconstructing and modelling late Weischelian climates: the Younger Dryas in Europe as a case study. *Earth Science Reviews* 48: 1-38.

Isarin, R.F.B., Rensen, H., Vandenberghe, J. 1998. The impact of the North Atlantic Ocean on the Younger Dryas climate in north western and central Europe. *Journal of Quaternary Science* 13: 447-454.

Iturrizaga, L. 2008. Post-sedimentary Transformation of Lateral Moraines – the Tributary Tongue Basins of the Kvíárjökull (Iceland). *Journal of Mountain Science* 5: 1-16.

Jackson, L.E.J., MacDonald, G.M., Wilson, M.C. 1982. Paraglacial origin for terraced river sediments in Bow Valley, Alberta. *Canadian Journal of Earth Sciences* 19: 2219-2231.

Jamieson, T.F. 1863. On the parallel roads of Glen Roy and their place in the history of the glacial period. *Journal of the Geological Society of London* 19: 235-259.

Jansson, K.N. 2005. Map of the glacial geomorphology of north-central Québec-Labrador, Canada. *Journal of Maps* v2005: 46-55.

Jarman, D. 2006. Large rock slope failures in the Highlands of Scotland: Characterisation, causes and spatial distribution. *Engineering Geology* 83: 161-182.

Jiskoot, H., Curran, C.J., Tesler, D.L., Shenton, L.R. 2009. Changes in Clemenceau Icefield and Chaba Group glaciers, Canada, related to hypsometry, tributary detachment, length-slope and area-aspect relations. *Annals of Glaciology* 50: 133- 143.

Johnsen, T.F., Brennand, T.A. 2000. The environment in and around ice-dammed lakes in the moderately high relief setting of the southern Canadian Cordillera. *Boreas* 35: 106-125.

Johnson-Ferguson, I. 2004. *Glacial-lacustrine sediments and landforms in Glen Turret, western Scotland*. Unpublished BSc dissertation, University of St Andrews.

Jost, A., Lunt, D., Kageyama, M., Abe-Ouchi, A., Peyron, O, Valdes, P.J., Ramstein, G. 2005. High-resolutions simulations of the last glacial maximum climate over Europe: a solution to discrepancies with continental palaeoclimate reconstructions? *Climate Dynamics* 24: 577-590.

Kaser G, Osmaston H.A. 2002. *Tropical Glaciers*. Cambridge University Press: Cambridge, UK.

Kellerer-Pirklbauer, A. 2008. The supraglacial debris system at the Pasterze glacier, Austria: Spatial distribution, characteristics and transport of debris. *Zeitschrift für Geomorphologie* 52: 3-25.

Kendall, P.F. 1902. A system of glacier lakes in the Cleveland Hills. *Quarterly Journal of the Geological Society of London* 58: 471-571.

Khodakov, V.G. 1975. Glaciers as water resource indicators of the glacial areas of the USSR. In: Proceedings of the Moscow Snow and Ice Symposium, August 1971. *International Association of Hydrological Sciences* 104: 22-29.

Kirkbride, M.P., Brazier, V. 1998. A critical evaluation of the use of glacier chronologies in climatic reconstruction, with reference to New Zealand. *Quaternary Proceedings* 6: 55-64.

Kjær, K.H., Sultan, L., Kruger, J., Schomacker, A. 2004. Architecture and sedimentation of outwash fans in front of the Myrdalsjokull ice cap, Iceland. *Sedimentary Geology* 172: 139-163.

Kleman, J. 1994. Preservation of landforms under ice sheets and ice caps. *Geomorphology* 9: 19-32.

Kleman, J., Stroeven, A.P., Lundqvist, J. 2008. Patterns of Quaternary ice sheet erosion and deposition in Fennoscandia. *Geomorphology* 97: 73-90.

Knighton, A.D. 1998. *Fluvial Forms and Processes - a new perspective.* Arnold, London, 383 p.

Krüger, J., Kjær, K.H. 1999. A data chart for field description and genetic interpretation of glacial diamicts and associated sediments – with examples from Greenland, Iceland and Denmark. *Boreas* 28: 386-402.

Krumbein, W.C. 1941. Measurement and geological significance of shape and roundness of sedimentary particles. *Journal of Sedimentary Petrology* 11: 64-72.

Krzyszkowski, D. 2002. Sedimentary successions in ice-marginal fans of the Late Saalian glaciation, southwestern Poland. *Sedimentary Geology* 149: 93-109.

Krzyszkowski, D. & Zielinski, T. 2002: The Pleistocene end moraine fans: controls on their sedimentation and location. *Sedimentary Geology* 149: 73-92.

Larsen, N.K., Piotrowski, J.A. 2003. Fabric pattern in a basal till succession and its significance for reconstructing subglacial processes. *Journal of Sedimentary Research* 73: 725-734.

Lawson, D.E. 1982. Moblisation, movement and deposition of sub-aerial sediment flows, Matanuska Glacier, Alaska. *Journal of Geology* 90: 279-300.

Lawson, D.E. 1989. Glacigenic resedimentation: classification, concepts and application to mass-movement processes and deposits. In: Goldthwait, R.P., Matsch, C.L., (eds.). *Genetic Classification of Glacigenic Environments: Processes, Dynamics and Sediments*. Butterworth-Heinemann, Oxford, pp. 337-363.

Letreguilly, A., Reynaud, L. 1989. Spatial patterns of mass balance fluctuations of North American glaciers. *Journal of Glaciology* 35: 163-168.

Li, D., Yi, C., Ma, B., Wang, P., Ma, C., Cheng, G. 2006. Fabric analysis of till clasts in the upper Urumqi River, Tian Shan, China. *Quaternary International* 154-155: 19-25.

Liestøl, O. 1967. Storbreen Glacier in Jotunheimen, Norway. *Norsk Polarinstitutt Skrifter* 14: 1-63.

Lillesand, T.M., Kiefer, R.W., Chipman, J.W. 2008. *Remote Sensing and Image Interpretation*, Sixth Edition, John Wiley & Sons, Hoboken, USA, 756 p.

Livingstone, S.J., Evans, D.J.A., Ó Cofaigh, C. 2010b. Re-advance of Scottish Ice into the Solway Lowlands (Cumbria, UK) during the Main Late Devensian deglaciation. *Quaternary Science Reviews* 29: 2544-2570.

Livingstone, S.J., Evans, D.J.A., Ó Cofaigh, C., Davies, B.J., Merritt, J.W., Huddart, D., Mitchell, W.A., Roberts, D.H., Yorke, L. 2012. Glaciodynamics of the central sector of the last British–Irish Ice Sheet in Northern England. *Earth-Science Reviews* 111: 25-55.

Livingstone, S.J., Evans, D.J.A., Ó Cofaigh, C., Hopkins, J. 2010c. The Brampton Kame Belt and Pennine Escarpment meltwater channel system (Cumbria, UK): Morphology, Sedimentology and Formation. *Proceedings of the Geologists Association* 121: 423-443.

Livingstone, S.J., Ó Cofaigh, C., Evans, D.J.A. 2008. The glacial geomorphology of the central sector of the British-Irish Ice Sheet. *Journal of Maps* v2008: 358-377.

Livingstone, S.J., Ó Cofaigh, C., Evans, D.J.A. 2010a. A major ice drainage pathway of the last British-Irish Ice Sheet: the Tyne Gap, northern England. *Journal of Quaternary Science* 25: 354-370.

Livingstone, S.J., Ó Cofaigh, C., Evans, D.J.A., Palmer, A. 2010d. Sedimentary evidence for a major glacial oscillation and proglacial lake formation in the Solway Lowlands (Cumbria, UK) during Late Devensian deglaciation. *Boreas* 39: 505-527.

Locke, W.W. 1995. Modelling of icecap glaciation of the northern Rocky Mountains of Montana. *Geomorphology* 14: 123-130.

Lovell, H., Stokes, C. R., Bentley, M. J. 2011. A glacial geomorphological map of the Seno Skyring-Seno Otway-Strait of Magellan region, southernmost Patagonia. *Journal of Maps* v2011: 318-339.

Lowe, J.J., Cairns, P. 1991. Pollen-stratigraphic evidence for the deglaciation and lake drainage chronology of the Glen Roy-Glen Spean area. *Scottish Journal of Geology* 27: 41-56.

Lowe, J.J., Walker, M.J.C. 1997. *Reconstructing Quaternary Environments*. Pearson, Harlow.

Lowe, J.J., Rasmussen, S.O., Björck, S., Hoek, W.Z., Steffensen, J.P., Walker, M.J.C., Yu, Z.C., the INTIMATE group. 2008. Synchronisation of palaeoenvironmental events in the North Atlantic region during the Last Termination: a revised protocol recommended by the INTIMATE group. *Quaternary Science Reviews* 27: 6-17.

Lowick, S. 2005. *The application of optically stimulated luminescence to the dating of glacial sediments in the Northwest Highlands of Scotland.* Unpublished MSc thesis, Royal Holloway, University of London.

Lukas, S., 2003. Scottish Landform Example No. 31. The moraines around the Pass of Drumochter. *Scottish Geographical Journal* 119: 383-393.

Lukas, S. 2005a. *Younger Dryas moraines in the NW Highlands of Scotland: genesis, significance and potential modern analogues.* Unpublished PhD thesis, University of St Andrews.

Lukas, S. 2005b. A test of the englacial thrusting hypothesis of 'hummocky' moraine formation: case studies from the northwest Highlands, Scotland. *Boreas* 34: 287-307.

Lukas, S.L., 2006, Morphostratigraphic principles in glacier reconstruction - a perspective from the British Younger Dryas. *Progress in Physical Geography* 30: 719-736.

Lukas, S. 2007a. 'A test of the englacial thrusting hypothesis of 'hummocky' moraine formation: case studies from the northwest Highlands, Scotland.': reply to comments. *Boreas* 36: 108-113.

Lukas, S., 2007b. Early-Holocene glacier fluctuations in Krundalen, south central Norway: palaeo-glacier dynamics and palaeoclimate. *The Holocene* 17: 585-598.

Lukas, S., 2011. Younger Dryas. In: Singh, V., Singh, P., Haritashya, U.K., (eds.). *Encyclopaedia of Snow, Ice and Glaciers*. Springer, Heidelberg, pp. 1229-1232.

Lukas, S. 2012. Processes of annual moraine formation at a temperate alpine valley glacier: insights into glacier dynamics and climatic controls. *Boreas*, in press.

Lukas, S., Benn, D.I. 2006. Retreat dynamics of Younger Dryas glacier in the far NW Scottish Highlands reconstructed from moraine sequences. *Scottish Geographical Journal* 122: 308-325.

Lukas, S., Bradwell, T., 2010. Reconstruction of a Lateglacial (Younger Dryas) mountain ice field in Sutherland, NW Scotland, and its palaeoclimatic implications. *Journal of Quaternary Science* 25: 567-580.

Lukas, S., Lukas, T, 2006a. A glacial geological and geomorphological map of the far NW Highlands, Scotland. Part 1. *Journal of Maps* v2006: 43-55.

Lukas, S., Lukas, T, 2006b. A glacial geological and geomorphological map of the far NW Highlands, Scotland. Part 2. *Journal of Maps* v2006: 56-58.

Lukas, S., Sass, O. 2011: The formation of Alpine lateral moraines inferred from sedimentology and radar reflection patterns - a case study from Gornergletscher, Switzerland. *Geological Society of London Special Publications*, in press.

Lukas, S., Coray, S., Graf, A., Schlüchter, C. In press. The influence of clast lithology and fluvial reworking on the reliability of clast shape measurements in glacial environments – a case study from a temperate Alpine glacier. In: Bridgland, D.R., (ed.). *Clast lithological analysis. Technical Guide*. Quaternary Research Association, London.

Lukas, S., Graf, A., Coray, S., Schlüchter, C. 2012. Genesis, stability and preservation potential of large lateral moraines of Alpine valley glaciers - towards a unifying theory based on Findelengletscher, Switzerland. *Quaternary Science Reviews*, in press.

Lunkka, J.P., Gibbard, P.L., 1996. Ice-marginal sedimentation and its implications for ice-lobe deglaciation patterns in the Baltic region: Pohjankangas, western Finland. *Journal of Quaternary Science* 11: 377-388.

MacLeod, A., Palmer, A.P., Lowe, J.J., Rose, J., Bryant, C., Merritt, J.W. 2011. Timing of glacier response to Younger Dryas climatic cooling in Scotland. *Global and Planetary Change* 79: 264-274.

Macpherson, J. 1978. Pollen chronology of the Glen Roy - Loch Laggan proglacial lake drainage. *Scottish Journal of Geology* 14: 125-139.

Maddy, D., Lewis, S.G., Scaife, R.G., Bowen, D.Q., Coope, G.R., Green, C.P., Hardaker, T., Keen, D.H., Rees-Jones, J., Parfitt, S., Scott, K. 1998. The Upper Pleistocene deposits at Cassington, near Oxford, England. *Journal of Quaternary Science* 13: 205-231.

Madgett, P.A., Catt, J.A. 1978. Petrography, stratigraphy and weathering of Late Pleistocene tills in East Yorkshire, Lincolnshire and North Norfolk. *Proceedings of the Yorkshire Geological Society* 42: 55-108.

Maizels, J.K. 1993. Lithofacies variations within sandur deposits: the role of runoff regime, flow dynamics and sediment supply characteristics. *Sedimentary Geology* 85: 299-325.

Manley, G. 1955. On the occurrence of ice-domes and permanently snow-covered summits. *Journal of Glaciology* 2: 453-456.

Mark, D.M. 1973. Analysis of axial orientation data, including till fabrics. *Geological Society of America Bulletin* 84: 1369-1374.

Mark, D.M. 1974. On the interpretation of till fabrics. *Geology* 2: 101-104.

Marquette, G.C., Gray, J.T., Gosse, J.C., Courchesne, F., Stockli, L., Macpherson, G., Finkel, R. 2004. Felsenmeer persistence under non-erosive ice in the Torngat and Kaumajet mountains. Québec and Labrador, as determined by soil weathering and cosmogenic nuclide exposure dating. *Canadian Journal of Earth Sciences* 41: 19-38.

McCarroll, D., Rijsdijk, K.F. 2003. Deformation styles as a key for interpreting glacial depositional environments. *Journal of Quaternary Science* 18: 473-489.

McCormack, D.C., Irving, D.H.B., Brocklehurst, S.H., Rarity, F. 2008. Glacial geomorphological mapping of Coire Mhic Fhearchair, NW Scotland: The contribution of a high-resolution ground based LiDAR survey. *Journal of Maps* v2008: 315-331.

McDougall, D.A. 1998. *Loch Lomond Stadial Plateau Icefields in the Lake District, Northwest England.* Unpublished PhD thesis, University of Glasgow.

McDougall, D.A. 2001. The geomorphological impact of Loch Lomond (Younger Dryas) Stadial plateau icefields in the central Lake District, northwest England. *Journal of Quaternary Science* 16: 531-543.

Merritt, J.W., Auton, C.A., Connell, E.R., Hall, A.M., Peacock, J.D. 2003a. *Late Cainozoic geology and landscape evolution of north-east Scotland.* Memoir of the British Geological Survey, Sheets 66E, 67, 76E, 77, 86E, 87W, 87E, 95, 96W, 96E and 97 Scotland. British Geological Survey, Edinburgh, pp. 1655–1680.

Merritt, J. W., Auton, C. A., Firth, C. R. 1995. Ice-proximal glaciomarine sedimentation and sea-level change in the Inverness area, Scotland: a review of the deglaciation of a major ice stream of the British Late Devensian Ice Sheet. *Quaternary Science Reviews* 14: 289-329.

Merritt, J.W., Coope, G.R.,Walker, M.J.C. 2003b. The Torrie Lateglacial organic site and Auchenlaich pit, Callander. In: Evans, D.J.A., (ed.). *The Quaternary of the Western Highland Boundary: Field Guide.* Quaternary Research Association, London pp. 126-133.

Miall, A.D. 1977. A review of the braided river depositional environment. *Earth Science Reviews* 13: 1-62.

Miall, A.D. 1985. Architectural-element analysis: a new method of facies analysis applied to fluvial deposits. *Earth Science Reviews* 22: 261-308.

Midgley, N.G., Glasser, N.F., Hambrey, M.J. 2007. Sedimentology, structural characteristics and morphology of a Neoglacial high-Arctic moraine-mound complex: Midre Lovénbreen, Svalbard. In: Hambrey, M.J., Christoffersen, P., Glasser, N.F., Hubbard, B., (eds.). *Glacial sedimentary processes and products*. Blackwell, London, pp. 11-22.

Mills, S.C., Grab, S.W., Carr, S.J. 2009. Recognition and palaeoclimatic implications of late Quaternary niche glaciation in eastern Lesotho. *Journal of Quaternary Science* 24: 647-663.

Mitchell, W.A. 1991. Geomorphological Mapping: an introduction. In: Mitchell, W.A., (ed.). *Quaternary of the Western Pennines: Field Guide*. Quaternary Research Association, London, pp. 19-23.

Mitchell, W.A.,Riley, J.M. 2006. Drumlin map of the Western Pennines and southern Vale of Eden, Northern England, UK. *Journal of Maps* v2006: 10-16.

Morgan, J.L., Gergel, S.E., Coops, N.C. 2010. Aerial Photography: A Rapidly Evolving Tool for Ecological Management. *BioScience* 60: 47-59.

Müller, H.-N., Kerschner, H., Küttel, M., 1983. The Val de Nendaz (Valais, Switzerland). A type locality for the Egesen advnace and the Daun advance in the western Alps. In: Schroeder-Lanz, H., (ed.). *Late- and postglacial oscillations of glaciers: glacial and periglacial forms*. Balkema, Rotterdam, pp. 73-82.

Murton, J.B., Belshaw, R.K. 2011. A conceptual model of valley incision, planation and terrace formation during cold and arid permafrost conditions of Pleistocene southern England. *Quaternary Research* 75: 385-394.

Nemec, W. 1990. Aspects of Sediment movement on steep delta slopes. In: Colella, A., Prior, D., (eds.). *Coarse Grained Deltas*. International Association of Sedimentologists, Special Publication 10: 29-73.

Nemec, W., Lønne, I., Blikra, L. 1999. The Kregnes moraine in Gauldalen, west-central Norway: anatomy of a Younger Dryas proglacial delta in a palaeofjord basin. *Boreas* 28: 454-476.

NEODC. 2012. *NERC Earth Observation Data Centre*. http://badc.nerc.ac.uk/view/neodc.nerc.ac.uk__ATOM__dataent_11658383444211836. Accessed 2008 to 2012.

Nesje, A., 1989. The geographical and altitudinal distribution of blockfields in southern Norway and its significance to the Pleistocene ice sheets. *Zeitschrift Fur Geomorphologie, Supplementband* 72: 41-53.

Nesje, A., Bakke, J., Dahl, S.O., Lie, Ø., Matthews, J.A. 2008. Norwegian mountain glaciers in the past present and future. *Global and Planetary Change* 60: 10-27.

Ng, F.S.L., Barr, I.D., Clark, C.D. 2010. Using the surface profiles of modern ice masses to inform palaeo-glacier reconstructions. *Quaternary Science Reviews* 29: 3240-3255.

Nye, J.F. 1951. The flow of glaciers and ice-sheets as a problem in plasticity. *Proceedings of the Royal Society of London, Series A* 207: 554-572.

Nye, J.F. 1952. The mechanics of glacier flow. *Journal of Glaciology* 2: 82-93.

Ó Cofaigh, C., Evans, D.J.A., England, J. 2003. Ice-marginal terrestrial landsystems: sub-polar glacier margins of the Canadian and Greenland high Arctic. In: Evans, D.J.A., (ed.). *Glacial Landsystems*. London, Arnold, pp. 44-64.

Ó Cofaigh, C., Lemmen, D.S., Evans, D.J.A., Bednarski, J. 1999. Glacial landform-sediment assemblages in the Canadian High Arctic and their implications for late Quaternary glaciation. *Annals of Glaciology* 28: 195-201.

Ó Cofaigh, C. Evans, D.J.A., Hiemstra, J.F. 2011. Formation of a stratified subglacial 'till' assemblage by ice-marginal thrusting and glacier overriding. *Boreas* 40: 1-14.

Oerlemans, J. 2001. *Glaciers and Climate Change*. Balkema, Lisse.

Ohmura A., Kasser, P., Funk, M. 1992. Climate at the equilibrium line of glaciers. *Journal of Glaciology* 38: 397 – 411.

Osmaston, H. 2005. Estimates of glacier equilibrium line altitudes by the Area x Altitude, the Area x Altitude Balance Ratio and the Area x Altitude Balance Index methods and their validation. *Quaternary International* 138-139: 22-31.

Ottesen, D., Dowdeswell, J.A. 2006. Assemblages of submarine landforms produced by tidewater glaciers in Svalbard. *Journal of Geophysical Research* 111: F01016. DOI:10.1029/2005JF000330.

Ottesen, D., Dowdeswell, J.A., Benn, D.I., Kristensen, L., Christiansen, H.H., Christensen, O., Hansen, L., Lebesbye, E., Forwick, M., Vorren, T.O. 2008. Submarine landforms characteristic of glacier surges in two Spitsbergen fjords. *Quaternary Science Reviews* 27: 1583-1599.

Owen, L.A. 1994. Glacial and non-glacial diamictons in the Karakoram Mountains and Western Himalayas. In: Warren, W.P., Croot, D.G., (eds.). *The Formation and Deformation of Glacial Deposits*. Balkema, Rotterdam, pp. 9-28.

Owen, L.A. 1989. Terraces, uplift and climate in the Karakorum Mountains, Northern Pakistan: Karakorum intermontane basin evolution. *Zeitschrift für Geomorphologie, Supplementband* 76: 117-146.

Paasche, Ø., Strømsøe, J.R., Dahl, S.O., Linge, H. 2006. Weathering characteristics of arctic islands in northern Norway. *Geomorphology* 82: 430-452.

Palmer, A.P. 2008. Developing a varve chronology for the Spean-Roy lakes: the Lochaber Master Varve Chronology (LMVC). In: Palmer, A.P., Lowe, J.J., Rose, J., (eds.). *The Quaternary of Glen Roy and Vicinity: Field Guide*. Quaternary Research Association, London, pp. 139-149.

Palmer, A.P., Lowe, J.J., Rose, J. 2008. *The Quaternary of Glen Roy and Vicinity: Field Guide*. Quaternary Research Association, London, 224 p.

Palmer, A.P., Rose, J., Lowe, J.J., MacLeod, A. 2010. Annually resolved events of Younger Dryas glaciation in Lochaber (Glen Roy and Glen Spean), western Scottish Highlands. *Journal of Quaternary Science* 25: 581-596.

Palmer, A.P., Rose, J., Rasmussen, S.O. 2012. Evidence for phase-locked changes in climate between Scotland and Greenland during GS-1 (Younger Dryas) using micromorphology of glaciolacustrine varves from Glen Roy. *Quaternary Science Reviews* 36: 114-123.

Peach, B.N. 1909. Boulder distribution from Lennoxtown, Scotland. *Geological Magazine* 46: 26-31.

Peach, B.N., Horne, J. 1881. The glaciation of Caithness. *Proceedings of the Royal Society of Edinburgh* 6: 316-352.

Peacock, J.D. 1970. Glacial geology of the Lochy-Spean area. *Bulletin of the Geological Survey of Great Britain* 31: 185-98.

Peacock, J.D. 1986. Alluvial fans and outwash in upper Glen Roy. *Scottish Journal of Geology* 33: 347-366.

Peacock, J.D. 1999. The Pre-Windermere Interstadial (Late Devensian) raised marine strata of eastern Scotland and their microfauna: a review. *Quaternary Science Reviews* 18: 1655-1680.

Peacock, J.D. 2009. The QRA 2008 field guide to the Quaternary of Glen Roy and vicinity: a discussion. *Quaternary Newsletter* 118: 1-7.

Peacock, J.D., Cornish, R. 1989. *Glen Roy Area – Field Guide.* Quaternary Research Association, Cambridge, 69p.

Peacock, J.D., Harkness, D.D., Housley, R.A., Little, J.A., Paul, M.A. 1989. Radiocarbon ages for a glaciomarine bed associated with the maximum extent of the Loch Lomond Readvance in west Benderloch, Argyll. *Scottish Journal of Geology* 25: 69-79.

Peacock, J.D., Wilkinson, I.P. 1995. Appendix 1. Kessock Biostratigraphy. In: Merritt, J.W. Auton, C.A. Firth, C.R. 1995. Ice-proximal glaciomarine sedimentation and sea-level change in the Inverness area, Scotland: a review of the deglaciation of a major ice stream of the British late Devensian ice-sheet. *Quaternary Science Reviews* 14: 289-329.

Pennington, W., Haworth, E.Y., Bonny, A.P., Lishman, J.P. 1972. Lake sediments in northern Scotland. *Philosophical Transactions of the Royal Society* 24B: 191-294.

Phillips, E. R., Auton, C. A. 2000. Micromorphological evidence for polyphase deformation of glaciolacustrine sediments from Strathspey, Scotland. In: Maltman, A.J., Hubbard, B., Hambrey, M.J., (eds.). *Deformation of Glacial Materials*. Geological Society of London, Special Publications 176: 279-292.

Phillips, E.R., Key, R.M. 1992. Porphyroblast-fabric relationships: an example from the Appin Group in the Glen Roy area. *Scottish Journal of Geology* 28: 89-101.

Phillips, E.R., Clark, G.C., Smith D.I. 1993. Mineralogy, petrology and microfabric analysis of the Eilrig Shear Zone, Fort Augustus, Scotland. *Scottish Journal of Geology* 29: 143-158.

Phillips, E.R., Evans, D.J.A., Auton, C.A. 2002. Polyphase deformation at an oscillating ice margin following the Loch Lomond Readvance, central Scotland, UK. *Sedimentary Geology* 149: 157-182.

Phillips, E.R., Merritt, J.W., Auton, C.A., Golledge, N.R. 2007. Microstructures in subglacial and proglacial sediments: understanding faults, folds and fabrics, and the influence of water on the style of deformation. *Quaternary Science Reviews* 26: 1499-1528.

Phillips, W.M., Hall, A.M., Ballantyne, C.K., Binnie, S. 2008. Extent of the last ice sheet in northern Scotland tested with cosmogenic ^{10}Be exposure ages. *Journal of Quaternary Science* 23: 101-107.

Phillips, W.M., Hall, A.M., Mottram, R., Fifield, L.K., Sugden, D.E. 2006. Cosmogenic 10Be and 26Al exposure ages of tors and erratics, Cairngorm Mountains, Scotland: Timescales for the development of a classic landscape of selective linear glacial erosion. *Geomorphology* 73: 222-245.

Plassen, L. Vorren, T.O., Forwick, M. 2004. Integrated acoustic and coring investigation of glacigenic deposits in Spitsbergen fjords. *Polar Research* 23: 89-110.

Porter, S.C. 1975. Equilibrium line altitudes of late Quaternary glaciers in Southern Alps, New Zealand. *Quaternary Research* 5: 27-47.

Postma, G. 1986. Depositional architecture and facies of river and fan deltas: a synthesis. In: Oti, M.N., Postma, G., (eds.). *Geology of Deltas*. Balkema, Rotterdam, pp. 3-16.

Postma, G. 1990. Depositional architecture and facies of river and fan deltas: a synthesis. In: Colella, A., Prior, D.B., (eds.). *Coarse-Grained Deltas*. Blackwell, Oxford. International Association of Sedimentologists, Special Publication 10: 13-27.

Powell, R.D. 2003. Subaquatic landsystems: fjords. In: Evans, D.J.A., (ed.). *Glacial Landsystems.* Hodder Arnold, London, pp. 313 - 347.

Powers, M.C. 1953. A new roundness scale for sedimentary particles. *Journal of Sedimentary Petrology* 23: 117-119.

Prestwich, J. 1879. On the Origin of the Parallel Roads of Lochaber and Their Bearing on Other Phenomena of the Glacial Period. *Philosophical Transactions of the Royal Society of London* 170: 663-672.

Raistrick, A. 1933. The glacial and post-glacial periods in West Yorkshire. *Proceedings of the Geologists' Association* 44: 263-269.

Rasmussen, S.O., Andersen, K.K., Svensson, A.M., Steffensen, J.P., Vinther, B.M., Clausen, H.B., Siggaard-Andersen, M-L., Larsen, L.B., Dahl-Jensen, D., Bigler, M., Rothlisberger, R., Fischer, H., Goto-Azuma, K., Hansson, M.E., Ruth, U. 2006. A new Greenland ice core chronology for the last glacial termination. *Journal of Geophysical Research* 111: D6102. DOI:10.1029/2005JD006079.

Rea, B.R. 2009. Defining modern day Area-Altitude Balance Ratios (AABRs) and their use in glacier-climate reconstructions. *Quaternary Science Reviews* 28: 237-248.

Rea, B.R., Evans, D.J.A. 2003. Plateau Icefield Landsystems. In: Evans, D.J.A., (ed.). *Glacial Landsystems.* Hodder Arnold, London, pp. 407 – 431.

Rea, B.R., Evans, D.J.A. 2007. Quantifying climate and glacier mass balance in north Norway during the YD. *Palaeogeography, Palaeoclimatology, Palaeoecology* 246: 307-330.

Rea, B.R., Walley, B.W., Dixon, T., Gordon, J.E. 1999. Plateau icefields as contributing areas to valley glaciers and the potential impact on reconstructed ELAs: a case study from the Lyngen Alps, North Norway. *Annals of Glaciology* 28: 97-102.

Rea, B.R., Walley, B.W., Evans, D.J.A., Gordon, J.E., McDougall, D.A. 1998. Plateau Icefields: Geomorphology and Dynamics. *Quaternary Proceedings* 6: 35 - 54.

Rea, B.R., Walley, B.W., Rainey, M.M., Gordon, J.E. 1996. Blockfields, old or new? Evidence and implications from some plateaus in northern Norway. *Geomorphology* 15: 109-121.

Reinardy, B.T.I., Lukas, S. 2009. A comparison of the sedimentary signature of ice-contact sedimentation and deformation at macro- and micro-scale: a case study from NW Scotland. *Sedimentary Geology* 221**:** 87-98.

Reinick, H.E., Singh, I.B. 1975. *Depositional Sedimentary Environments*. Springer, Berlin, 439p.

Reitner, J.M. 2007. Glacial dynamics at the beginning of Termination I in the Eastern Alps and their stratigraphic implications. *Quaternary International* 164-165: 64-84.

Robertson, S., Smith, M. 1999. The significance of the Geal Charn-Ossian Steep Belt in basin development in the Central Scottish Highlands. *Journal of the Geological Society of London* 156: 1175-1182.

Robinson, M., Ballantyne, C.K. 1979. Evidence for a glacial readvance pre-dating the Loch Lomond Advance in Wester Ross. *Scottish Journal of Geology* 15: 271-277.

Rose, J., Letzer, J.M. 1977. Superimposed drumlins. *Journal of Glaciology* 18: 471-480.

Rose, J., Smith, M.J. 2008. Glacial geomorphological maps of the Glasgow region, western central Scotland. *Journal of Maps* v2008: 399-416.

Russell, A.J., Marren, P.M. 1998. A Younger Dryas (Loch Lomond Stadial) jökulhlaup deposit, Fort Augustus, Scotland. *Boreas* 27: 231-242.

Sahlin, E.A.U., Glasser, N.F. 2008. A geomorphological map of Cadair Idris, Wales. *Journal of Maps* v2008: 299-314.

Salt, K.E., Evans, D.J.A. 2004. Superimposed subglacially streamlined landforms of southwest Scotland. *Scottish Geographical Journal* 120: 133-147.

Savigear, R.A.G. 1965. A Technique of Morphological Mapping. *Annals of the Association of American Geographers* 55: 514-538.

Schilling, D.H., Hollin, J.T. 1981. Numerical reconstructions of valley glaciers and small ice caps. In: Hughes, T.J., (ed.). *The Last Great Ice Sheets*. Wiley, New York, pp. 207-220.

Sharp, M.J. 1984. Annual moraine ridges at Skàlafellsjökull, south-east Iceland. *Journal of Glaciology* 30: 82-93.

Singh, P. Kumar, N., Arora, M. 2000. Degree-day factors for snow and ice for Dokriani Glacier, Garhwal Himalayas. *Journal of Hydrology* 235: 1-11.

Sissons, J.B. 1967. *The Evolution of Scotland's Scenery*. Oliver & Boyd, Edinburgh, 259p.

Sissons, J.B. 1972. The last glaciers in the south-east Grampians. *Scottish Geographical Magazine* 89: 138-139.

Sissons, J.B. 1974a. The Quaternary in Scotland: a review. *Scottish Journal of Geology* 10: 311-337.

Sissons, J.B. 1974b. A Late-glacial ice cap in the central Grampians, Scotland. *Transactions of the Institute of British Geographers*. 62: 95-114.

Sissons, J.B. 1974c. Late glacial site in the central Grampian Highlands. *Nature* 249: 822-824.

Sissons, J. B. 1977a. *The Parallel Roads of Glen Roy*. Nature Conservancy Council, London. 12p.

Sissons J.B. 1977b. The Loch Lomond Readvance in the northern mainland of Scotland. In: Gray J.M., Lowe J.J., (eds.). *Studies in the Scottish Lateglacial Environment*. Pergamon Press, Oxford, pp. 45-49.

Sissons, J.B. 1978. The parallel roads of Glen Roy and adjacent glens, Scotland. *Boreas* 7: 229-244.

Sissons, J.B. 1979a. The limit of the Loch Lomond Advance in Glen Roy and vicinity. *Scottish Journal of Geology* 15: 31-42.

Sissons, J.B. 1979b. The Later Lakes and Associated Fluvial Terraces of Glen Roy, Glen Spean and Vicinity. *Transactions of the Institute of British Geographers* 4: 12-29.

Sissons, J.B. 1979c. Catastrophic lake drainage in Glen Spean and the Great Glen, Scotland. *Journal of the Geological Society of London* 136: 215-224.

Sissons, J.B. 1979d. Loch Lomond Stadial in the British Isles. *Nature* 280: 199-203.

Sissons, J.B. 1979e. Loch Lomond advance in the Cairngorm Mountains. *Scottish Geographical Magazine* 95: 66-82.

Sissons, J.B. 1980. The Loch Lomond Advance in the Lake District, northern England. *Transactions of the Royal Society of Edinburgh: Earth Sciences* 71: 13-27.

Sissons, J.B. 1981a. Ice-Dammed Lakes in Glen Roy and Vicinity: A Summary. In: Neale, J., Flenley, J. (eds.). *The Quaternary in Britain*. Pergamon Press, Oxford, pp. 174-183.

Sissons, J.B. 1981b. The last Scottish ice sheet: facts and speculative discussion. *Boreas* 10: 1-17.

Sissons, J.B. 1983. Quaternary. In: Craig, G.Y., (ed.). *The Geology of Scotland*. Scottish Academic Press, Edinburgh, 2nd Edition, pp. 399-424.

Sissons, J.B., Cornish, R. 1982. Rapid localised glacio-isostatic uplift at Glen Roy, Scotland. *Nature* 297:213-214.

Sissons, J.B. Cornish, R. 1983. Fluvial landforms associated with ice-dammed lake drainage in upper Glen Roy, Scotland. *Proceedings of the Geologists Association* 94: 45-52.

Sissons, J.B., Grant, A.J.H. 1972. The last glaciers in the Lochnagar area, Aberdeenshire. *Scottish Journal of Geology* 8: 85-93.

Sissons, J.B., Sutherland, D.G. 1976. Climatic inferences from former glaciers in the south-east Grampian Highlands, Scotland. *Journal of Glaciology* 17: 325-346.

Sissons, J.B., Walker, M.J.C. 1974. Late glacial site in central Grampian Highlands. *Nature* 249: 822-824.

Sissons, J.B., Lowe, J.J. Thompson, K.S. Walker, M.J.C. 1973. Loch Lomond readvance in Grampian Highlands of Scotland. *Nature-Physical Science* 244: 75-77.

Skidmore, M.L., Sharp, M.J. 1999. Drainage system behaviour of a high arctic polythermal glacier. *Annals of Glaciology* 28: 209-215.

Small, R.J. 1983. Lateral moraines of Glacier De Tsidjiore Nouve: form, development and implications. *Journal of Glaciology* 29: 250-259.

Smith, J.S. 1966. Morainic limits and their relationship to raised shorelines in the East Scottish Highlands. *Transactions of the Institute of British Geographers* 39: 61-64.

Smith, M., Robertson, S., Rollin, K.E. 1999. Rift basin architecture and stratigraphical implications for basement-cover relationships in the Neoproterozoic Grampian Group of the Scottish Caledonides. *Journal of the Geological Society of London* 156: 1163-1173.

Smith, M.J., Clark, C.D. 2005. Methods and visulisation of digital elevation models for landform mapping. *Earth Surface Processes and Landforms* 30: 885 - 900.

Smith, M.J., Wise, S.M. 2007. Problems of bias in mapping linear landforms from satellite imagery. *International Journal of Applied Earth Observation and Geoinformation* 9: 65-78.

Smith, M.J., Rose, J., Booth, S. 2006. Geomorphological mapping of glacial landforms from remotely sensed data: An evaluation of the principal data sources and an assessment of their quality. *Geomorphology* 76: 148-165.

Sneed, E.D., Folk, R.L. 1958. Pebbles in the Lower Colorado River, Texas, a study in clast morphogenesis. *Journal of Geology* 66: 114-150.

Stephenson, D., Gould, D. 1995. *British Regional Geology: The Grampian Highlands*. British Geological Survey, Nottingham. 4th Edition.

Stoker et al. 2009

Stokes, C.R., Clark, C.D. 2004. Evolution of late glacial ice-marginal lakes on the northwestern Canadian Shield and their influence on the location of the Dubawnt Lake palaeo-ice stream. *Palaeogeography, Palaeoclimatology, Palaeoecology* 215: 155-171.

Stokes, C.R., Lian, O.B., Tulaczyk, S., Clark, C.D. 2008. Superimposition of ribbed moraines on a palaeo-ice-stream bed: implications for ice stream dynamics and shutdown. *Earth Surface Processes and Landforms* 33: 593-609.

Strachan, R.A., Smith, M., Harris, A.L., Fettes, D.J. 2002. The Northern Highland and Grampian Terranes. In: Trewin, N.H., (ed.). *The Geology of Scotland*. The Geological Society, London. 4th Edition, pp. 87-147.

Stroeven, A.P., Fabel, D., Hättestrand, C., Harbor, J. 2002. A relict landscape in the centre of Fennoscandian glaciation: cosmogenic radionuclide evidence of tors preserved through multiple glacial cycles. *Geomorphology* 44: 145-154.

Sugden, D. E. 1968. The Selectivity of Glacial Erosion in the Cairngorm Mountains, Scotland. *Transactions of the Institute of British Geographers* 45: 79-92.

Sugden, D.E., Balco, G., Cowdery, S.G., Stone, J.O., Sass III, L.C. 2005. Selective glacial erosion and weathering zones in the coastal mountains of Marie Byrd Land, Antarctica. *Geomorphology* 67: 317-334.

Sumner, P.D., Meiklejohn, K.I. 2004. On the development of autochthonous blockfields in the grey basalts of sub-Antarctic Marion Island. *Polar Geography* 28: 120-132.

Sutherland, D.G. 1984. The Quaternary deposits and landforms of Scotland and the neighbouring shelves: a review. *Quaternary Science Reviews* 3: 157-254.

Syverson, K.M., Mickelson, D.M. 2009. Origin and significance of lateral meltwater channels formed along a temperate glacier margin, Glacier Bay, Alaska. *Boreas* 38: 132-145.

Tarasov, L., Peltier, W.R. 2005. Arctic freshwater forcing of the Younger Dryas cold reversal. *Nature* 435: 662-665.

Thomas, G.S.P., Montague, E. 1997. The morphology, stratigraphy and sedimentology of the Carstairs esker, Scotland, UK. *Quaternary Science Reviews* 16: 661-674.

Thorp, P.W. 1986. A mountain icefield of Loch Lomond Stadial age, western Grampians, Scotland. *Boreas* 15: 83-97.

Torsnes, I., Rye, N., Nesje, A. 1993. Modern and Little Ice Age equilibrium line altitudes on outlet valley glaciers from Jostedalsbreen, Western Norway – an evaluation of different approaches to their calculation. *Arctic and Alpine Research* 25: 106-116.

Trelea, M. 2008. *Reconstruction of the Younger Dryas glaciation in the Monadhliath Mountains.* Unpublished MSc thesis, University of Edinburgh.

Trotter, F.M. 1929. The glaciation of the eastern Edenside, the Alston Block and the Carlisle Plain. *Quarterly Journal of the Geological Society of London* 88: 549-607.

Turner, A.J., Woodward, J., Dunning, S.A., Shine, A.J., Stokes, C.R., Cofaigh, C.Ó. 2012. Geophysical surveys of the sediments of Loch Ness, Scotland: implications for the deglaciation of the Moray Firth Ice Stream, British–Irish Ice Sheet. J*ournal of Quaternary Science* 27: 221-232

van der Veen, C.J. 1999. *Fundamentals of Glacier Dynamics*. Balkema, Rotterdam, 462p.

van der Wateren, F.M. 2003. Ice-marginal terrestrial landsystems: southern Scandinavia ice sheet margin. In: Evans, D.J.A., (ed.). *Glacial Landsystems*. Arnold, London, pp. 166-203.

Vieira, G. 2008. Combined numerical and geomorphological reconstruction of the Serra da Estrela plateau icefield, Portugal. *Geomorphology* 97: 190-207.

Walker M.J.C. 1975. Late Glacial and Early Postglacial environment history of the central Grampian Highlands, Scotland. *Journal of Biogeography* 2: 265-284.

Whalley, W.B., Gordon, J.E., Thompson, D.L. 1981. Periglacial features on the margins of a receeding plateau ice cap, Lyngen, North Norway. *Journal of Glaciology* 27: 492-496.

Whalley, W.B., Rea, B.R., Rainey, M.M. 2004. Weathering, blockfields and fracture systems and the implications for long-term landscape formation: some evidence from Lyngen and Öksfjordjokelen areas in north Norway. *Polar Geography* 28: 93-119.

Whalley, W.B., Rea, B.R., Rainey, M.M., McAlister, J.J. 1997. Rock weathering in blockfields: some preliminary data from mountain plateaus in North Norway. *Geological Society of London, Special Publication* 120: 133-145.

Wilson, G.V., Edwards, W., Knox, J., Jones, R.C.B., Stephens, J.V. 1935. *The geology of the Orkneys*. HMSO, Edinburgh.

Wilson, S.B., Evans, D.J.A. 2000. Coire a' Cheud-chnoic, the 'hummocky moraine' of Glen Torridon. *Scottish Geographical Journal* 116: 149-158.

Winsemann, J., Asprion, U., Meyer, T. 2007b. Lake-level control on ice-margin subaqueous fans, glacial Lake Rinteln, Northwest Germany. In: Hambrey, M.J., Christoffersen, P., Glasser, N.F., Hubbard, B., (eds.). *Glacial Processes and Products*. International Association of Sedimentologists, Special Publication 39: 121-148.

Winsemann, J., Asprion, U., Meyer, T., Schramm, C. 2007a. Facies characteristics of Middle Pleistocene (Saalian) ice-margin subaqueous fan and delta deposits, glacial Lake Leine, NW Germany. *Sedimentary Geology* 193: 105-129.

Winsemann, J., Hornung, J.J. Meinsen, J., Asprion, U., Polom, U., Brandes, C., BußMann, M., Weber, C. 2009. Anatomy of asubaqueous ice-contact fan and delta complex, Middle Pleistocene, North-west Germany. *Sedimentology* 56: 1041-1076.

Young, J.A.T. 1977. Glacial geomorphology of the Dulnain valley, Inverness-shire. Scottish *Journal of Geology* 13: 59-74.

Young, J.A.T. 1978. The landforms of the upper Strathspey. *Scottish Geographical Magazine* 94: 76-94.

Zielinski, T. & van Loon, A.J. 2000: Subaerial terminoglacial fans III: overview of sedimentary characteristics and depositional model. *Geologie en Mijnbouw* 79: 93–107.

Appendix I

A Map of Place Names In The Study Area

Appendix II

THE GLACIAL GEOMORPHOLOGY OF THE MONADHLIATH MOUNTAINS

Clare M. Boston

School of Geography, Queen Mary University of London, Mile End Road, London, E1 4NS

Legend

- Younger Dryas moraines
- Pre-Younger Dryas moraines
- Stagnation moraines
- Gullied glaciogenic material
- Solifluction lobe
- Blockfield
- Bedrock at or near surface (frost-shattered)
- Bedrock outcrop
- Rock slope failure (RSF)
- RSF scarp
- Debris cone
- Alluvial fan
- River terrace
- Terrace
- Glaciolacustrine sediments
- Ice-contact fan
- Lake
- Stream
- Ice-marginal meltwater channel
- Lake overflow channel
- Convex break in slope
- Concave break in slope
- Steep bedrock
- Talus slope
- Upper limit of sediment (drift limit)
- Former shoreline
- 500 50 m contours

N

0 1 2 Km

Contours derived from NEXTMap Britain (Intermap Technologies Inc. provided by NERC via the NERC Earth Observation Data Centre)

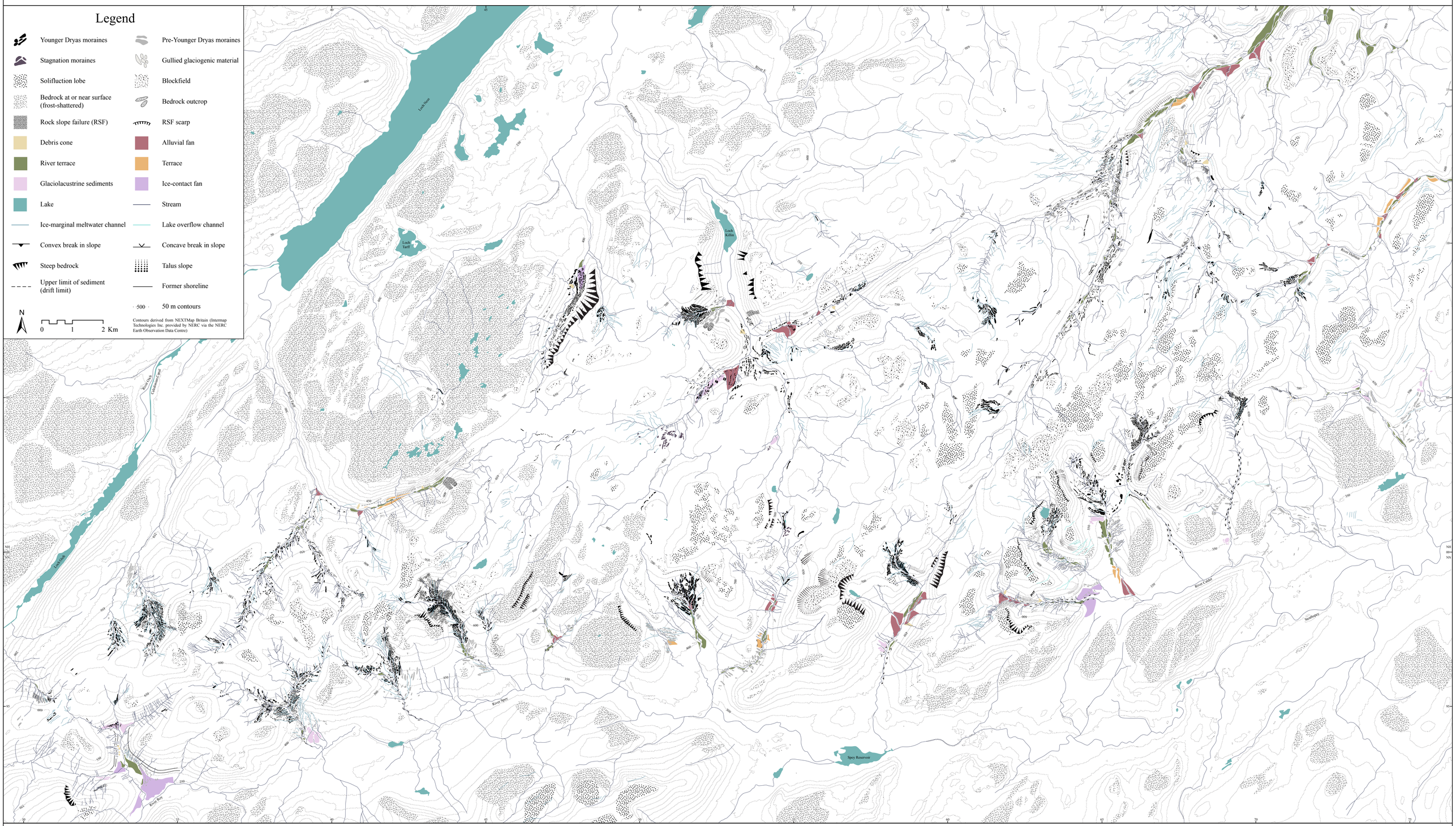

Clare Mary Boston. A Lateglacial plateau icefield in the Monadhliath Mountains, Scotland: reconstruction, dynamics and palaeoclimatic implications. Appendix II, part of a thesis submitted for the degree of Doctor of Philosophy in Geography, Queen Mary University of London. 2012.

NATURAL ENVIRONMENT RESEARCH COUNCIL